

FLOW PATTERNS AND EVAPORATION  
IN COCURRENT SPRAY-DRYERS

A thesis presented for the degree of  
Doctor of Philosophy in Chemical Engineering  
in the University of Canterbury,  
Christchurch, New Zealand.

by

Pham Quang Tuan

1975

ENGINEERING  
LIBRARY

~~TP~~  
TP  
363  
.P534  
1975

### ACKNOWLEDGMENTS

My sincere thanks to Dr. R.B. Keey for his patient guidance throughout this project.

Many persons from this and other departments are to be thanked for their help and advice, particularly Mr. C. Campbell and Mr. N. Foot of the Chemical Engineering technical staff. Thanks are due to Mrs. Levicky for her careful typing.

The author received a Colombo Plan scholarship while undertaking this project. The Spray-Drying project was financially supported by the New Zealand Dairy Research Institute.

I am grateful to Mrs. T.S. McMillan for her cups of tea and encouragement during the past seven years.

## CONTENTS

	<u>Page</u>
SUMMARY . . . . .	1
INTRODUCTION . . . . .	3
<u>Part One: Equipment</u>	
Chapter 1: THE SPRAY DRYER . . . . .	5
<u>Part Two: Residence Times and Flow Patterns</u>	
Chapter 2: TRACER KINETICS : BACKGROUND AND THEORY . . .	29
Chapter 3: AIR RESIDENCE TIME DISTRIBUTION AND AIR FLOW PATTERN . . . . .	70
Chapter 4: SPRAY RESIDENCE TIME DISTRIBUTION AND SPRAY FLOW PATTERN . . . . .	124
<u>Part Three: Evaporation and Drying</u>	
Chapter 5: TRANSPORT PHENOMENA FOR SINGLE DROPLETS . .	155
Chapter 6: SPRAY DRYER DESIGN AND PERFORMANCE . . . . .	191
CONCLUSION . . . . .	264
REFERENCES . . . . .	265

## Appendices

Appendix A: DATA AND SEMI-PROCESSED RESULTS

Appendix B: MISCELLANEOUS EXPERIMENTS

- I. Drop sizes from a pneumatic atomiser.
- II. Atomiser air flow area and air flow rate measurements.
- III. Suspended-drop drying tests with a zinc-oxide slurry.
- IV. An attempted simultaneous measurement of evaporation and residence time.

Appendix C: OPERATING PROCEDURES FOR THE TWO-STAGE SPRAY DRYER

Appendix D: COMPUTER PROGRAM FOR SPRAY EVAPORATION CALCULATION IN  
A COCURRENT SPRAY DRYER.



### SUMMARY

A cocurrent two-stage spray dryer was designed and built, and its performance investigated by means of residence time distribution (R.T.D.) analysis for both the continuous phase and the dispersed phase. Analytical methods using transfer functions were developed and found to be very useful in interpreting the data obtained.

In the present equipment the flow pattern of the drying gas was found by these methods to consist of a well-mixed zone and a plug-flow zone in series. The presence of a pneumatic nozzle had a very large effect on the flow pattern in the chamber, in spite of the small atomising air rate used. The Craya-Curtet number  $C_t$  (the square root of the drying air momentum / atomising air momentum ratio) correlated this effect well, the atomising air stream becoming dominant as  $C_t$  becomes somewhat less than one, a result already found in other contexts. An interesting phenomenon is the existence of a minimum dispersion point at  $C_t \approx 0.25$ . All these results were confirmed by hot-wire anemometry and flow visualisation with smoke.

The droplet-phase R.T.D. yielded some useful information on the degree of entrainment of droplets into the air stream. This entrainment could be correlated by a newly derived parameter involving the Lagrangian scale of turbulence, the intensity of fluid turbulence and the inertia of the droplet to velocity fluctuations in the fluid.

Finally a method of performance prediction for cocurrent spray dryers was developed, using a stepwise computation and paying special attention to the jet zone and the effect of solute or suspended solids in the feed. The predictions of the method agree well with existing data, but also pointed out the need for more experiments on the drying

of single droplets of industrially important materials. Methods for taking R.T.D. effects into account were discussed and illustrated.

## INTRODUCTION

Spray drying is the process whereby a solid-liquid mixture is atomised and brought into contact with a hot gas to yield a dried powder. The atomisation increases greatly the surface/volume ratio of the mixture, enabling the drying to take place in a very short time, typically of order 2 - 20 s. The process is thus particularly suitable for heat-sensitive products or when the solubility of the product must be large. In New Zealand spray drying is of particular importance in view of the large scale production of milk powder.

Although the process of spray drying has existed for more than a hundred years and considerable research has been done on it, (M5,M7,M8, L6,B17) the design and performance prediction of spray dryers in practice are still mostly a matter of empiricism. The process is simple in principle, but a large number of parameters can affect the results. Furthermore, the design pattern varies greatly from dryer to dryer and a different approach may be preferable in each case.

Some of the basic investigations of heat, mass and momentum transfer and of turbulence effects have previously been carried out in this department (B17). It seemed logical that the next step should be to move closer to an industrial type situation, and to study the performance of a realistic spray dryer. Therefore this work consisted of three parts:

- 1) The design and construction of a spray dryer (chapter 1).
- 2) The investigation of both continuous and dispersed-phase flow patterns, using residence-time distributions with some new developments in transfer-function analysis (chapters 2, 3 and 4). From the data obtained, insights can be gained on how to improve the design of this and similar models or to optimise their operation.

3) The development of a method of evaporation prediction in this type of spray dryer (chapters 5 and 6).

## CHAPTER 1.

### THE SPRAY DRYER

#### Chapter contents:

#### I. DESIGN CONSIDERATIONS

#### II. DESCRIPTION OF INSTALLATION

##### 1. General layout.

##### 2. Individual items:

1. The 1st-stage drying chamber.
2. The feed system.
3. The 2nd-stage dryer.
4. The rotary valve.
5. Powder collection equipments.
6. Air flow, heating, humidifying and temperature control.

##### 3. Monitoring equipment:

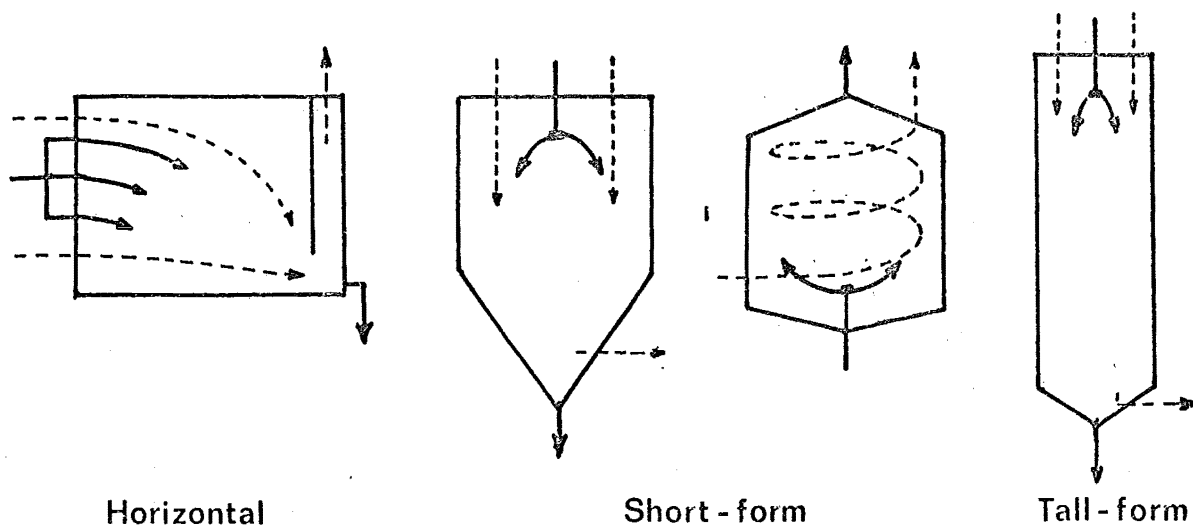
1. Flow measurements.
2. Temperature measurements.
3. Humidity measurements.

## I. DESIGN CONSIDERATIONS

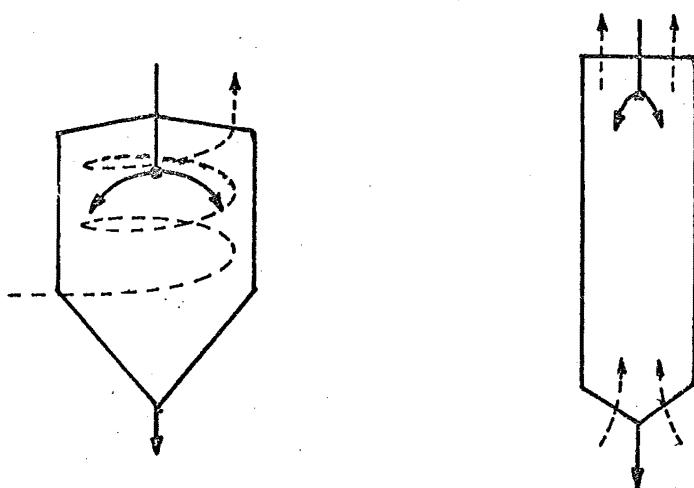
Industrial spray dryers come in a great diversity of sizes, shapes, flow and atomising arrangements. The general geometry varies from squat-looking chambers with a 1/1 length-to-diameter (or height-to-width) ratio to tall-form dryers with a 4/1 ratio. Flow regimes may be cocurrent, countercurrent, crossflow or mixed, dominantly axial or tangential, horizontal or vertical, upward or downward (figure 1). Atomising can be done with rotary atomisers (discs, cups or vaned wheels), pressure nozzles, pneumatic nozzles (with external or internal mixing) or a combination of these (figure 2). Atomisers can be positioned at the top, at the bottom or on the side walls of the drying chamber.

Experimental workers, on the other hand, tend to work with chambers having a high length-to-diameter ratio, typically 10/1 or more, using cocurrent flow with a nozzle atomiser on top. This set-up allows easy control of the flow pattern and precise measurements of the temperature, humidity, evaporation and other profiles. One such dryer has been built and studied in this department<sup>(B17)</sup>.

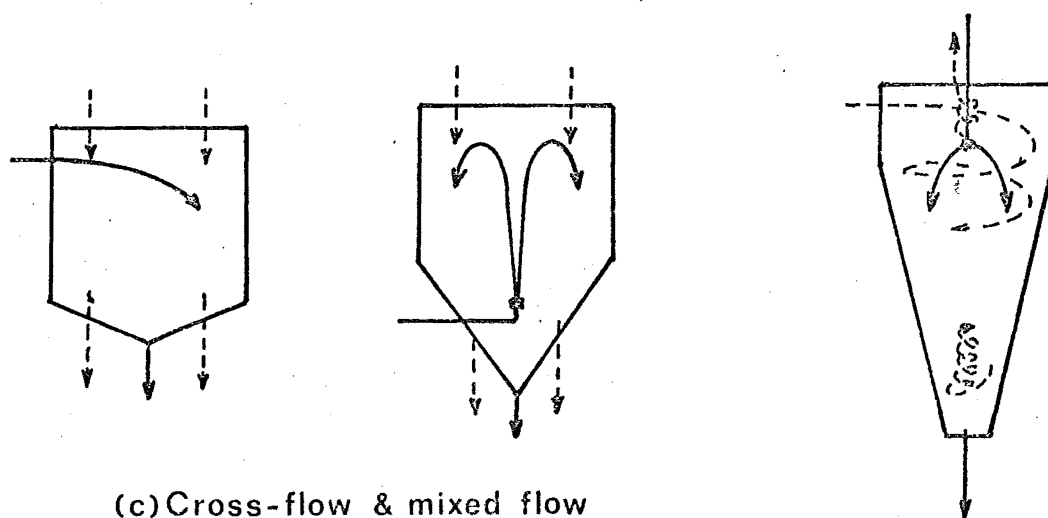
Therefore, for the present work, a compromise has been made in building a drying chamber which would not deviate too much from the geometry of industrial installations, and yet would enable the flow pattern to be easily controlled should such a need arise. The result is a tall-form (5/1 length-to-diameter ratio) dryer with downward cocurrent flow, a central nozzle atomiser and axially directed air inlets. From an economic point of view, cocurrent flow does not maximise thermal or volumetric efficiency, but it gives good control of the product quality since hot inlet air does not come into contact with dry product. Hence this kind of flow is particularly suitable



(a) Cocurrent flow



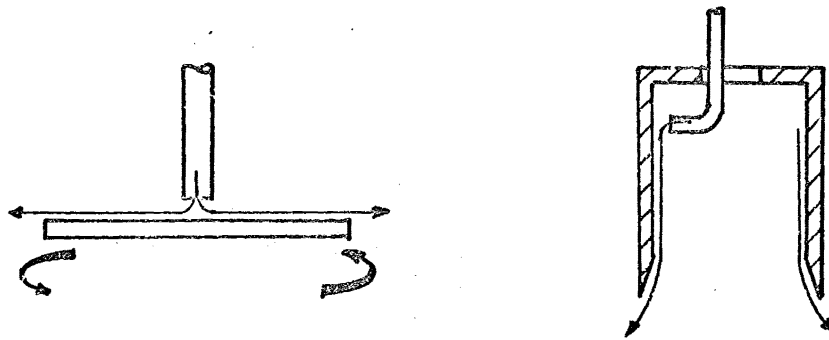
(b) Countercurrent flow



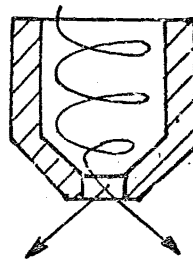
(c) Cross-flow &amp; mixed flow

-----> Gas                      —————> Feed or product

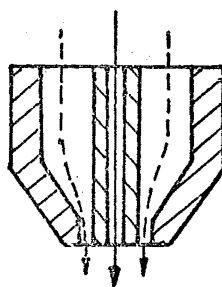
FIGURE 1.1: GEOMETRY OF INDUSTRIAL SPRAY DRYERS  
(H5, M5, M8)



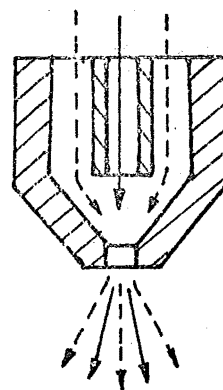
(a) Rotary



(b) Pressure



External mixing



Internal mixing

(c) Pneumatic or twin-fluid

—————→ Feed      - - - - - → Atomising gas

FIGURE 1.2: BASIC ATOMISER TYPES



for heat-sensitive products such as foodstuffs.

To improve the performance of the unit, a second stage pneumatic dryer has been added. Such a configuration has been suggested before (D9) and used in the dairy industry (B2). Apart from being volumetrically more efficient than a single big drying chamber, it may also give better product quality, as the almost dry powder can be dried more gently in the cooler 2nd stage.

General quantitative specifications for the design of the equipment are as follows:

- First-stage air velocity: 0.1 - 3.0 m/s,  
inlet air temperature: up to 250°C.
- Second-stage air velocity: 5. - 25. m/s,  
inlet air temperature: up to 150°C.
- Estimated maximum droplet size: 150 µm.

## II. DESCRIPTION OF INSTALLATION

### II.1 General layout

The flow diagram of the installation is shown in figure 3. The main part of the air from the blower goes through the heaters, but some of it bypasses the heaters and cools the bus bars of the electric air heating elements. The two streams merge again and go to the first stage.

After the first stage, the air is separated from the products by a cyclone, goes to a cooler-scrubber and discharges to the atmosphere. The product collected by the cyclone is transferred pneumatically by a rotary valve to the 2nd stage.

The 2nd stage, a pneumatic dryer, is fed with hot air from the heaters mentioned earlier and cold air directly from the blower, in a

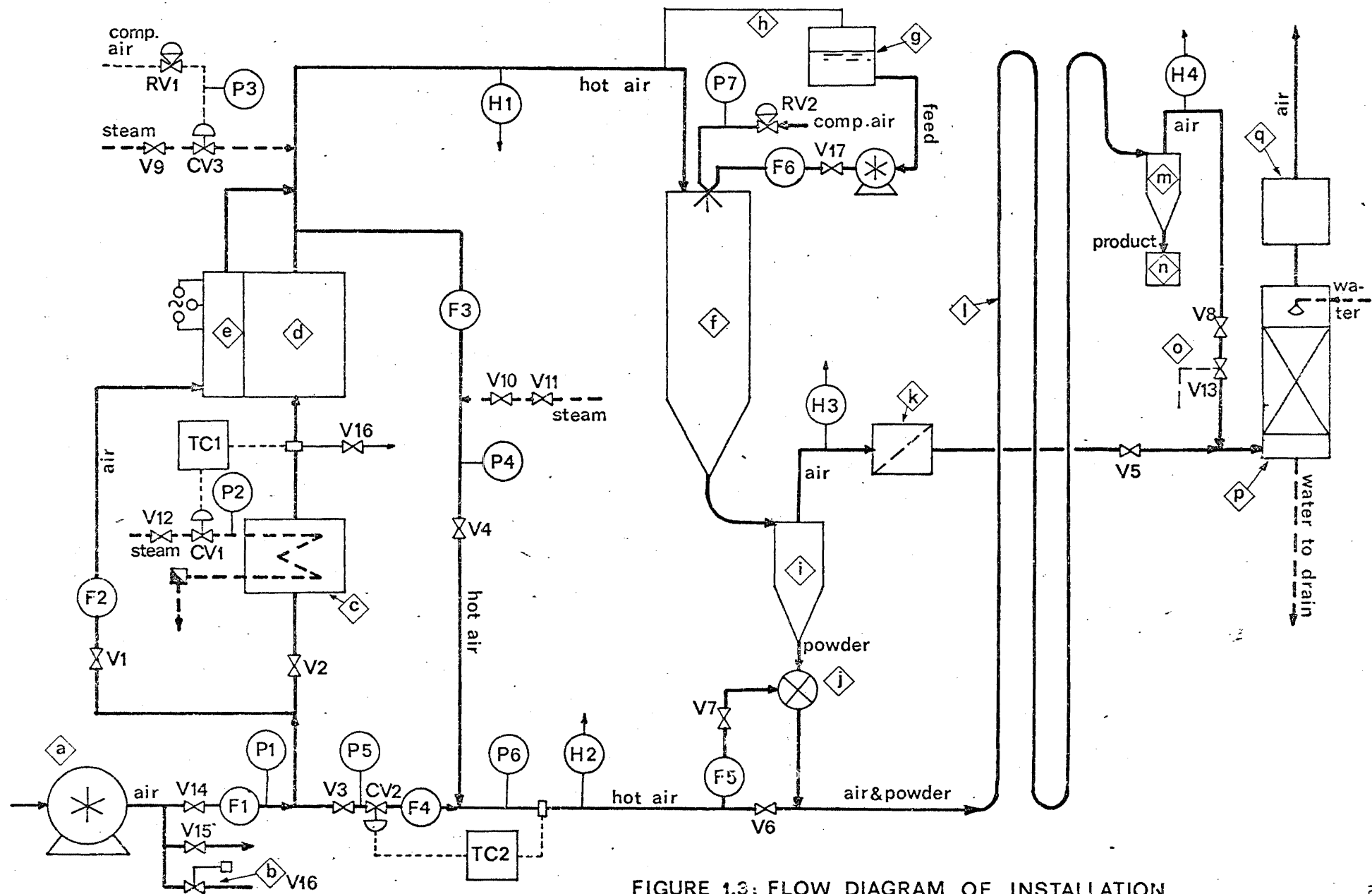


FIGURE 1.3: FLOW DIAGRAM OF INSTALLATION

Legend for Figures 1.3 and 1.4

- (a) Blower.
- (b) Relief valve, set at 24 k Pa.
- (c) Steam heater.
- (d) Electric heater.
- (e) Busbar box.
- (f) First-stage drying chamber.
- (g) Feed tank.
- (h) Pressure-equalising line.
- (i) First-stage cyclone.
- (j) Rotary valve.
- (k) Filter bag.
- (l) Second-stage pneumatic dryer.
- (m) Second-stage cyclone.
- (n) Product receiver.
- (o) Intermittent, automatically operated butterfly valve.
- (p) Cooler-scrubber.
- (q) De-entrainer.

CV Control valve. CV3 is a pneumatically operated valve.

F Flowmeter. F1 and F2 are Pitot tube<sup>s</sup>, the rest are rotameters.

H Humidity probe. H1 and H2 are LiCl cells; H3 and H4 are wet-and-dry-bulb psychrometers.

P Pressure tapping.

RV Regulating valve.

TA Air temperature point thermocouples. TA1 & TA2, TA8 & TA9 are wet-and-dry-bulb psychrometers.

TC Temperature controller.

TW Wall temperature point (thermocouples brazen onto wall).

Figure 3 only:

———— Drying air, feed or product.

- - - - - Service line.

- - - - - Control line.

ratio adjusted to give the correct inlet temperature. At the end of this stage a cyclone finally separates out the product, and the air goes to the cooler-scrubber.

For the set-up to work properly, pressure balance between the two stages must be maintained (for example, if the pressure drop through the 1st stage is too low, the hot air would be at low pressure and unable to flow into the 2nd stage). This is obtained by manipulating the valves V1, V2, V3, V4 and especially the butterfly valve V5 (see figure 3). Fine control is given by the control valve CV2.

Figures 4 and 5 are an isometric sketch and a photograph of the set-up (except the blower). For further details on the operating procedures the reader is referred to Appendix C.

## II.2 Individual items

### II.2.1 The first-stage drying chamber (figure 6)

The column is 400 mm diameter by 2 m long, with a conical bottom 550 mm long, made of mild steel, later hot dip galvanised. The air inlet, consisting of four elliptical parts surrounding the nozzle, was designed to give easy access to the atomiser, rather than controlled plug flow. In such a design, the sudden expansion of air around the nozzle would give good spray-air mixing at the cost of some backmix being present.

### II.2.2 The feed system

In the present work, two pneumatic nozzles with external mixing were used, henceforth referred to as no.1 and no.2 nozzles respectively. Their description and performance characteristics are shown in figure 7 and table 1. The "effective" air-flow areas and the discharge

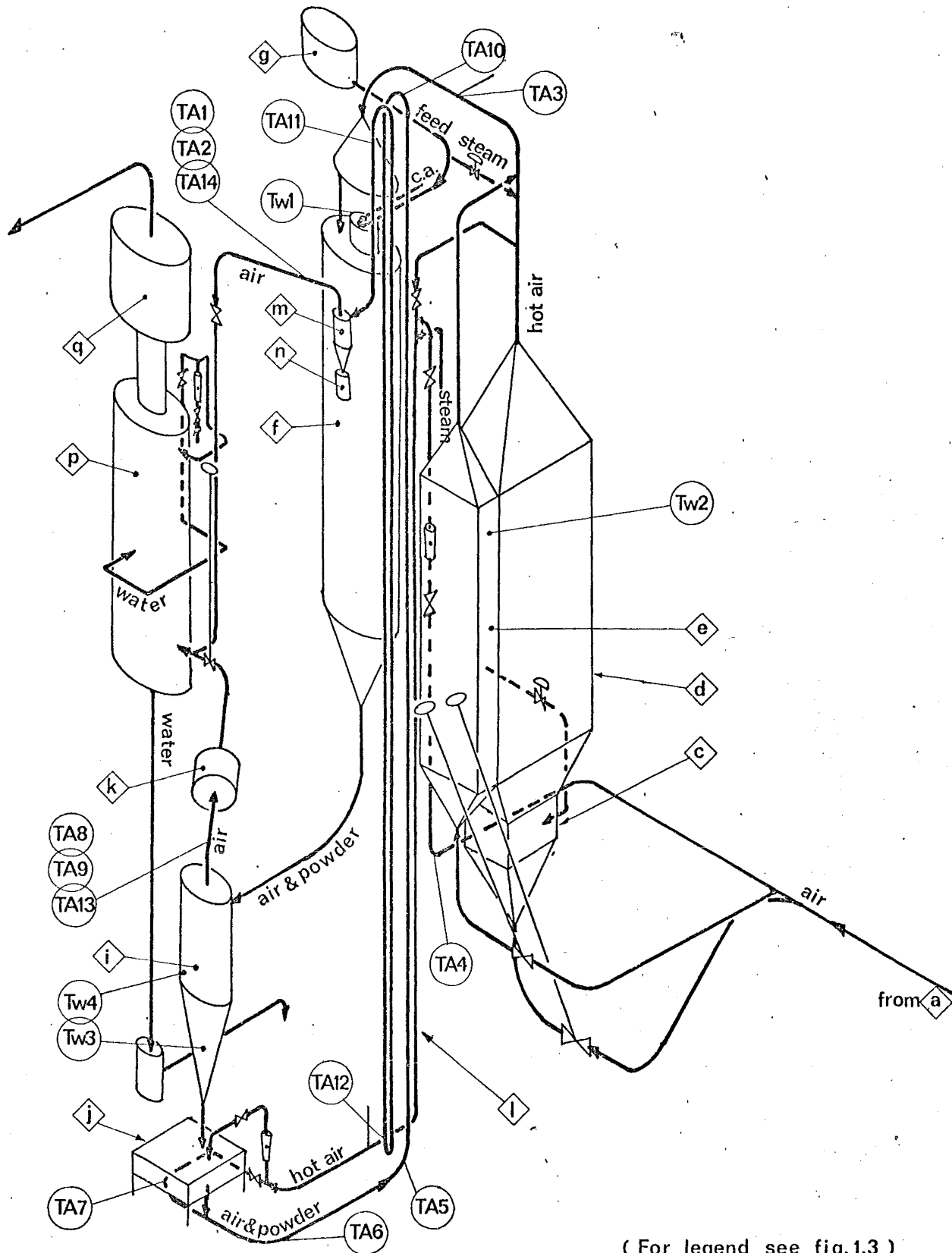


FIGURE 1.4: ISOMETRIC DIAGRAM OF INSTALLATION

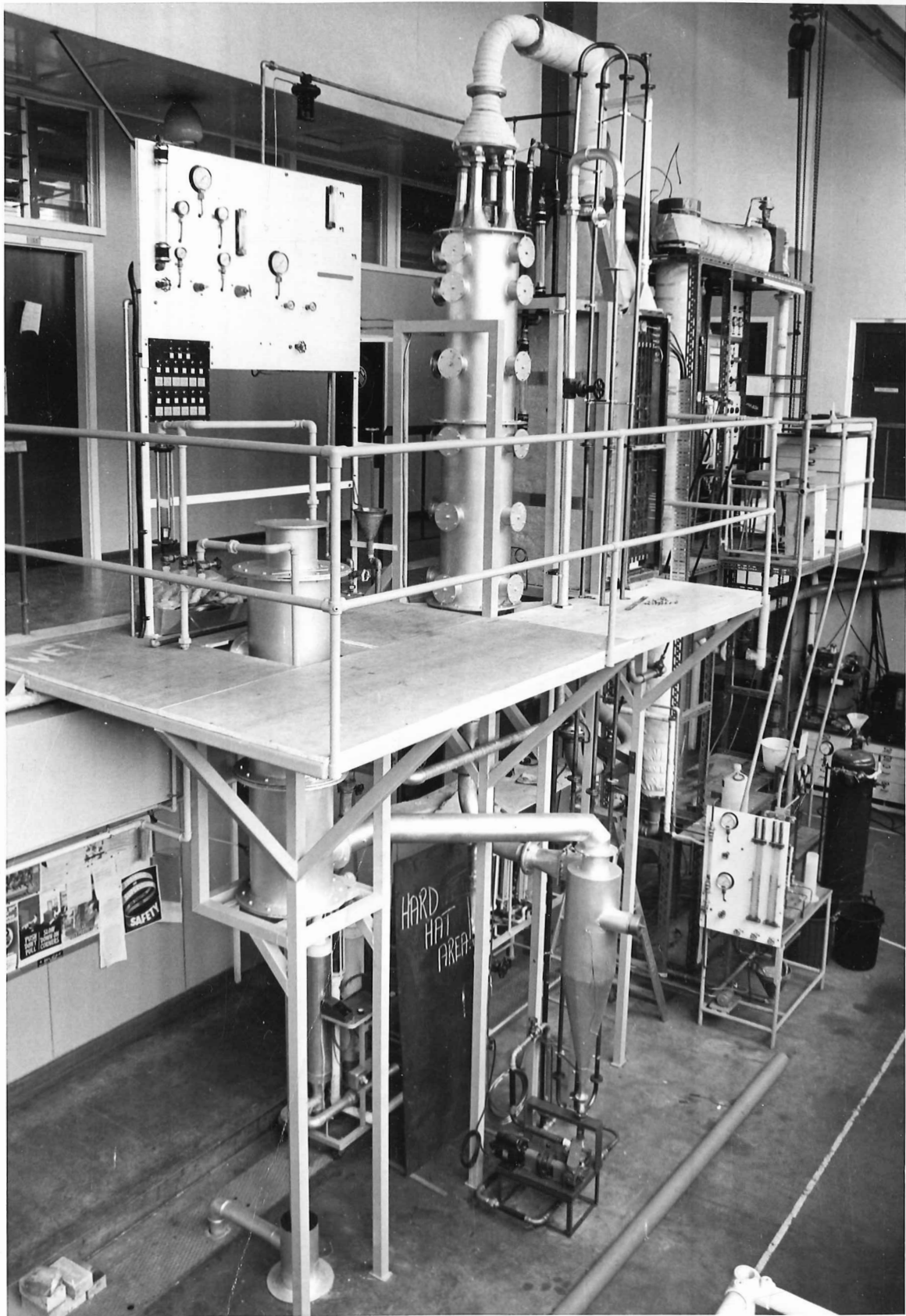
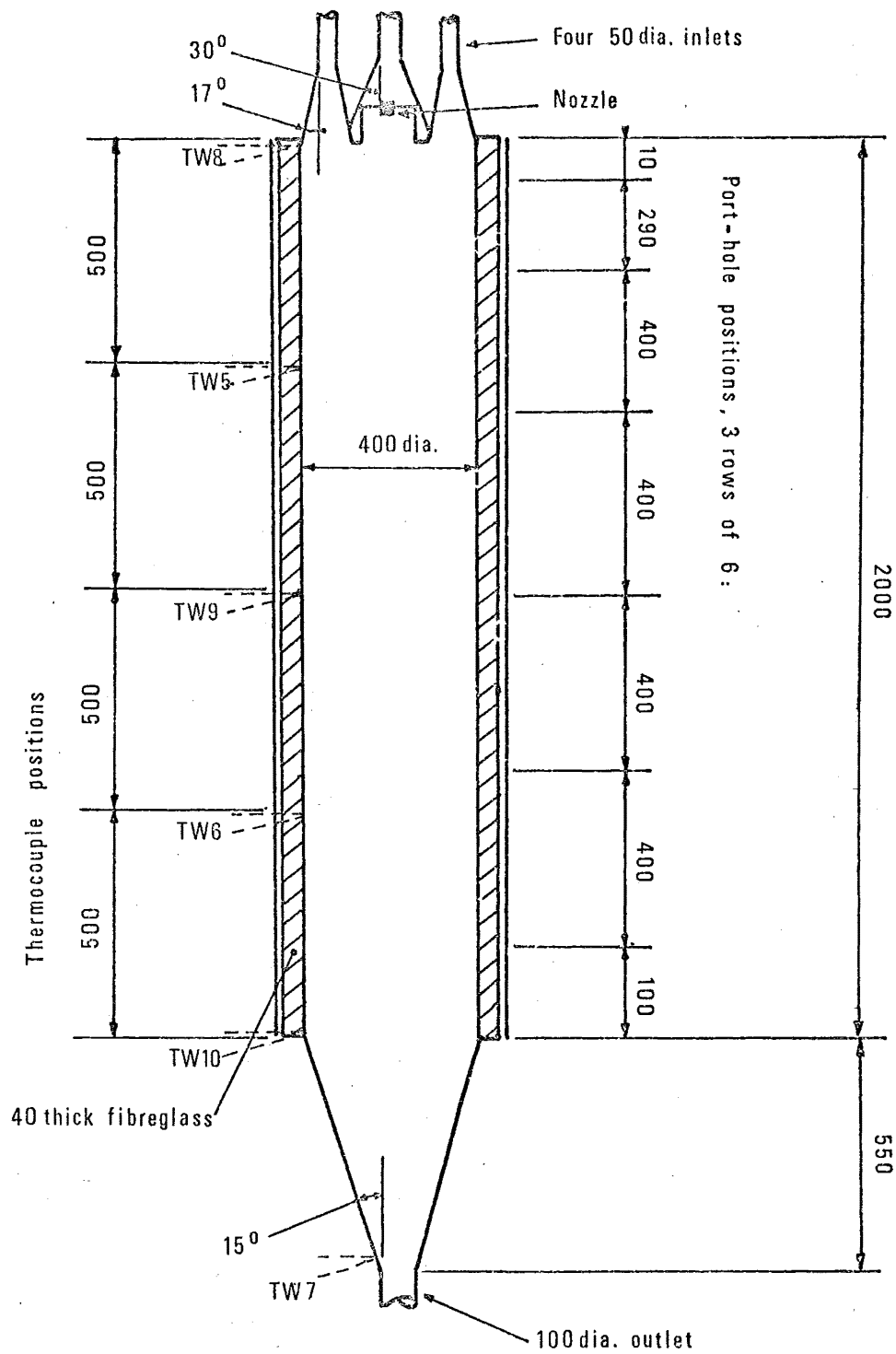


FIGURE 1.5



TW : see fig.1.3

All dimensions in mm

Cross-section area .126 m<sup>2</sup>

Volume .274 m<sup>3</sup>

FIGURE 1.6: FIRST-STAGE DRYING CHAMBER

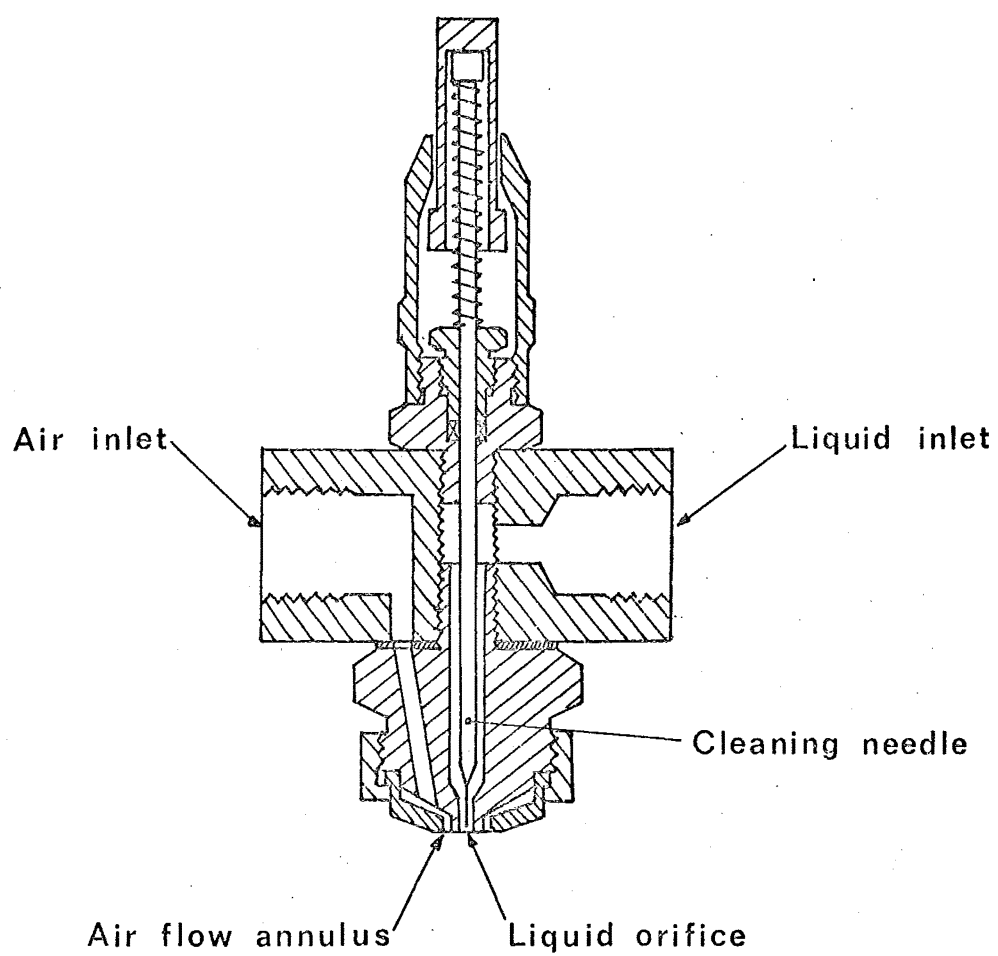


FIGURE 1.7: ATOMISER USED IN THIS WORK



TABLE 1.1

Description and performance characteristic of atomisers used

Identification in this work	No.1	No.2
Manufacturer	Spraying Systems Co. (U.S.A.)	
Type	Pneumatic, round spray, siphon or gravity feed	
Manufacturer's catalog no.	1/4 JCO set-up 1A	1/4 JCO set-up 2
Liquid orifice diameter (nominal)	0.406 mm	0.711 mm
Air annulus inner dia. (nominal)	1.27 mm	1.27 mm
Air annulus outer dia. (nominal)	1.626 mm	1.778 mm
Effective air flow area (measured)	1.4 mm <sup>2</sup>	2.3 mm <sup>2</sup>
Discharge coefficient (measured)	5.66 x 10 <sup>-9</sup> kg/s Pa	3.42 x 10 <sup>-9</sup> kg/s Pa

NB. The discharge coefficient  $C_N$  is defined by

$$C_N \equiv \frac{\text{Air mass rate at room temperature}}{\text{Absolute upstream pressure } P_a}$$

$$P_a \geq 1.9 \times 10^5 \text{ Pa}$$

(isentropic flow equation)

coefficients were not calculated from the manufacturer's data but determined from discharge experiments (see Appendix B.II).

Initially the liquid was fed under a gravity head of 0 to 600 mm, with the feed container sitting on a movable platform and connected to the column by a pressure equalising line (figure 3). However, this set-up was inadequate to control the flow, so a peristaltic pump (no internal moving part) with variable speed, in series with a restriction valve, were added to the line. When working with slurries, a solenoid-operated cleaning needle clears the orifice regularly with an adjustable period of 1 to 5 seconds, the solenoid circuit being actuated by a small electric motor.

#### II.2.3 The second-stage dryer

The 2nd stage is a pneumatic dryer 1 inch (25.4 mm) I.D., 18 m long (but can be reduced to 6 m by re-connecting), made of 9 sections of mild steel tubing. The stream flows up 6 m, then either goes to a cyclone or flows into a U-tube for another 12 m before reaching the cyclone. Lagging consists of 25 mm of fibreglass preformed sections.

A major problem in commissioning the plant was the deposition of powder on the walls and especially at the bends, gradually clogging up this pneumatic stage. In fact, industrial practice recommends against such small pipes and tight bends as used in the present equipment (E3, S18). However, after several trials, the following measures were successful in preventing clogging and ensuring a 99% recovery of slightly moist zinc-oxide powder:

- (1) The use of glass bends with a 120 mm bend radius;
- (2) The use of pneumatic vibrators at the bends with a frequency of about 400 Hz;

- (3) Installation of a butterfly valve downstream of the cyclone which opens and closes intermittently with a period of about 2 s. This valve was actuated by an automatically operated solenoid.

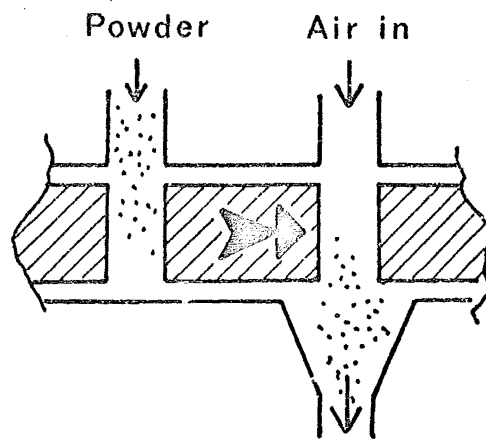
#### II.2.4 The rotary valve

This is an essential piece of equipment in a two-stage installation, transferring the powder from one stream to another. Although several types are commercially available, none would handle small-sized (1 in. inlet/outlet) equipment. Hence a rotary valve was designed and built, with the help of Mr. C. Campbell of this department, to the following criteria:

- (1) To be suitable for 1 in. (25.4 mm) diameter inlet/outlet;
- (2) To ensure an even flow of powder, with a minimum of intermittence of discharge;
- (3) To reduce hold-up time to a minimum;
- (4) To minimise contact between powder and wall.

The principle of operation and sketch of the valve are shown in figure 8. The rotor, revolving about a vertical axis, contains 6 vertical cylindrical holes 25.4 mm in diameter.

Each hole passes under the inlet, when some powder falls into it, then over the outlet when the powder is blown out under air pressure. The speed of the rotor is adjusted to a value of about 100-120 rpm to ensure that the powder does not reach the bottom of the hole before it is blown out. Sealing was ensured by pads of P.T.F.E. around the holes in the stationary part, and good contact between the P.T.F.E. surfaces and the stainless steel rotor maintained by spring-loading the top of the assembly.



Principle of operation

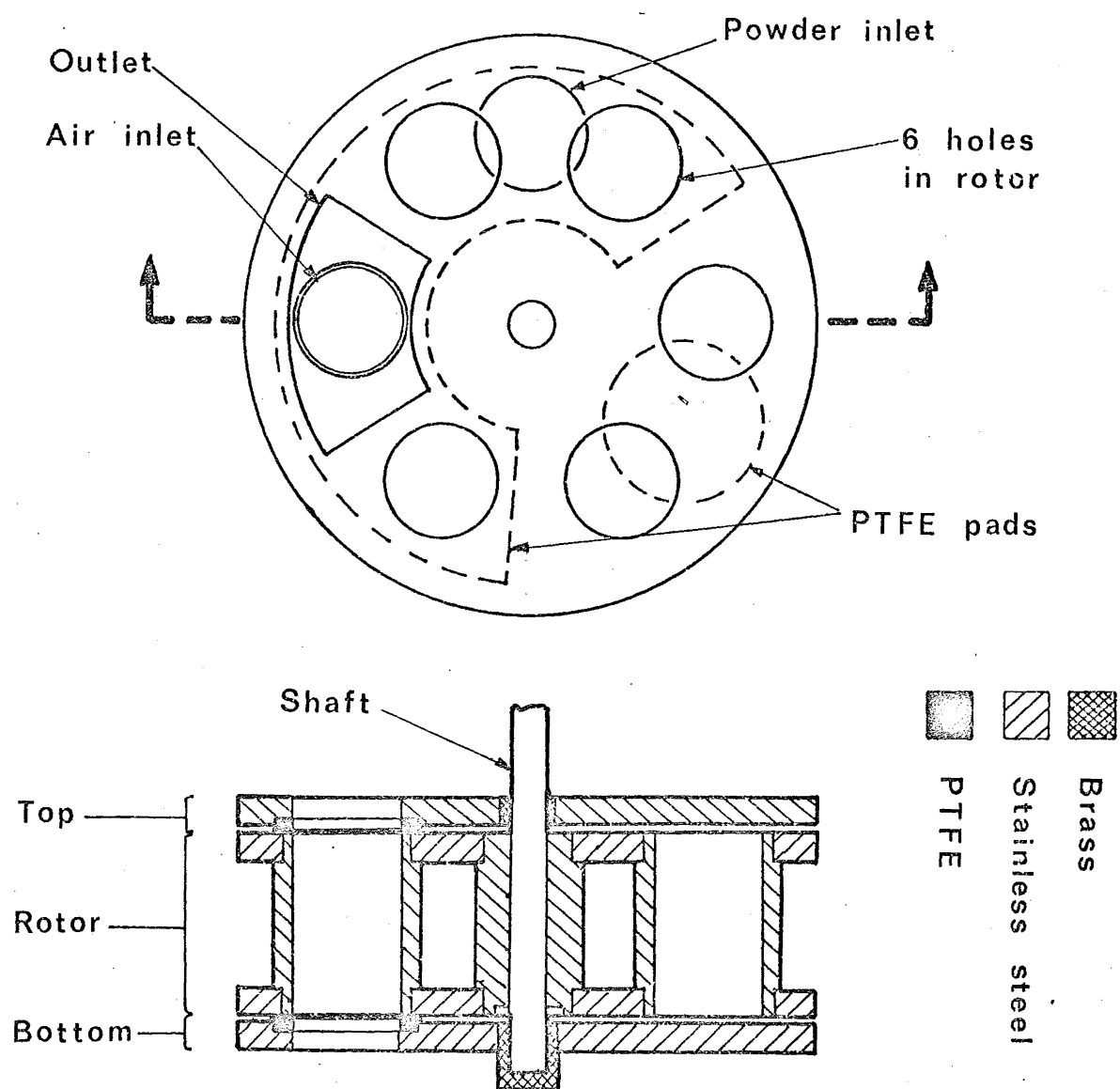


FIGURE 1.8: THE ROTARY VALVE

## II.2.5 Powder collection equipment

The product is collected at the outlet of the 1st stage by either of two cyclones (the smaller can be used for air velocities up to 1.5 m/s in the spray dryer, the larger for higher air rates). These cyclones are of Stairmand's "high-efficiency" type (figure 9a), with diameters of 300 mm and 165 mm respectively. A pneumatic vibrator is used to prevent powder build-up on the wall. A 160 mm diameter bag filter can be installed near the cyclone outlet to remove the finer particles.

For the 2nd stage, a 150 mm diameter Stairmand-type cyclone made of glass was used.

The cooler-scrubber (figure 9b) at the end of the air-flow line consists of a 400 mm diameter column with two grid plates which are stacked with Pall rings to a height of 150 mm to increase contact at low air rate. It was designed for a maximum air rate of 0.43 kg/s and a maximum water rate of 2 kg/s (at low air rate).

## II.2.6 Air flow, heating, humidifying and temperature control

A Rootes blower with a maximum capacity of  $0.56 \text{ m}^3/\text{s}$  (700 scfm) at  $24 \text{ kN/m}^2$  (3.5 psig) was used to generate air flow. A gear-box and bypass system enable the flow to be varied from zero to the maximum flow. On top gear the pulsation frequency of the blower is 24 Hz, on third gear it is 13.5 Hz.

Heating the air is done in two stages: a steam heater (maximum power 49 KW at 480 kPa (70 psig) steam pressure) heats the air up to  $115\text{--}138^\circ\text{C}$ , then further heating is done by an electric heater with  $39 \times 1.25 \text{ KW}$  elements with mild steel sheaths and fins (maximum allowable temperature:  $430^\circ\text{C}$ ), installed in 3 banks in a staggered configuration and connected to a 3-phase 220 V power supply.

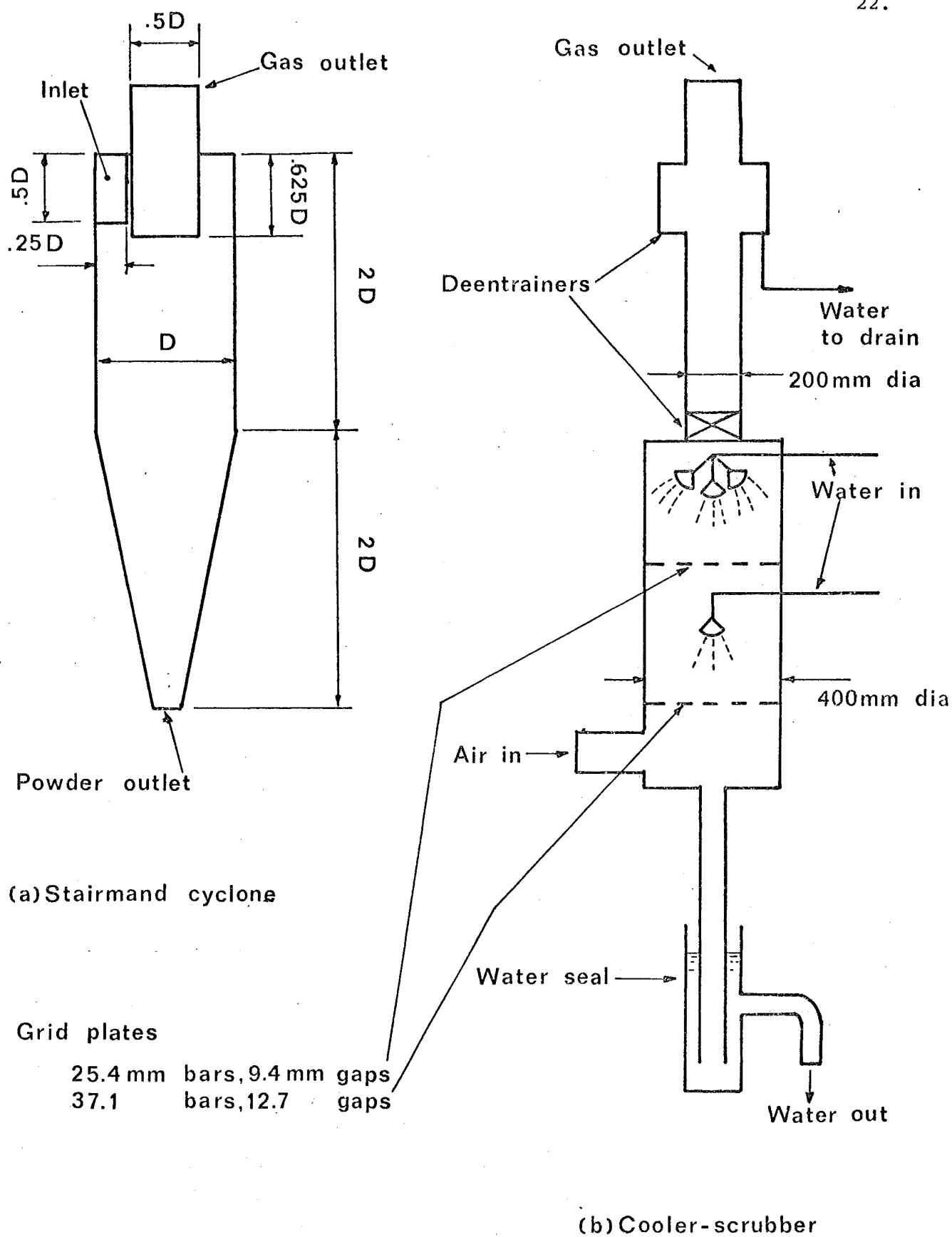


FIGURE 1.9: SEPARATION EQUIPMENT

A flow sensor automatically triggers the switching-off of the current whenever the flow is stopped, and a micro-switch performs the same function whenever the lid of the connection box is opened. The connection box (containing 6 bus bars and small connectors) is cooled with a bypass air stream (figure 3). Groups of 3 elements (one in each phase) can be disconnected at will to adjust the heat input.

Temperature control in the first stage is done by controlling the steam pressure in the steam heater with a pneumatically operated proportional controller and an electrically actuated valve.

The valve has 12.7 mm ( $\frac{1}{2}$  in.) inlet/outlet and a valve coefficient of  $C_v = 4.0$ , where  $C_v$  is defined as the number of US gpm of water discharged through a wide open valve with a 1 psi pressure drop through it (S17). This arrangement keeps the inlet temperature constant to within  $\pm 1^\circ\text{C}$ .

In the second stage, temperature control is done by varying the cold air stream into this stage with a pneumatic controller and electrically operated valve, the valve having a  $C_v$  coefficient of 2.5.

Humidifying steam to the first stage is controlled by a pneumatically actuated valve, but the pneumatic pressure is set manually on a pressure regulator. A globe valve controls humidifying-steam flow to the second stage.

## II.3 Monitoring equipment

II.3.1 Flow measurement. Total flow to both stages is measured with a pitot tube placed in the 100 mm (4 in.) diameter inlet line on a long straight section. Flow-profile measurements were done to correlate the velocity along the axis to the mean velocity according to the method outlined in (P6), and results are shown in figure 10. Flow

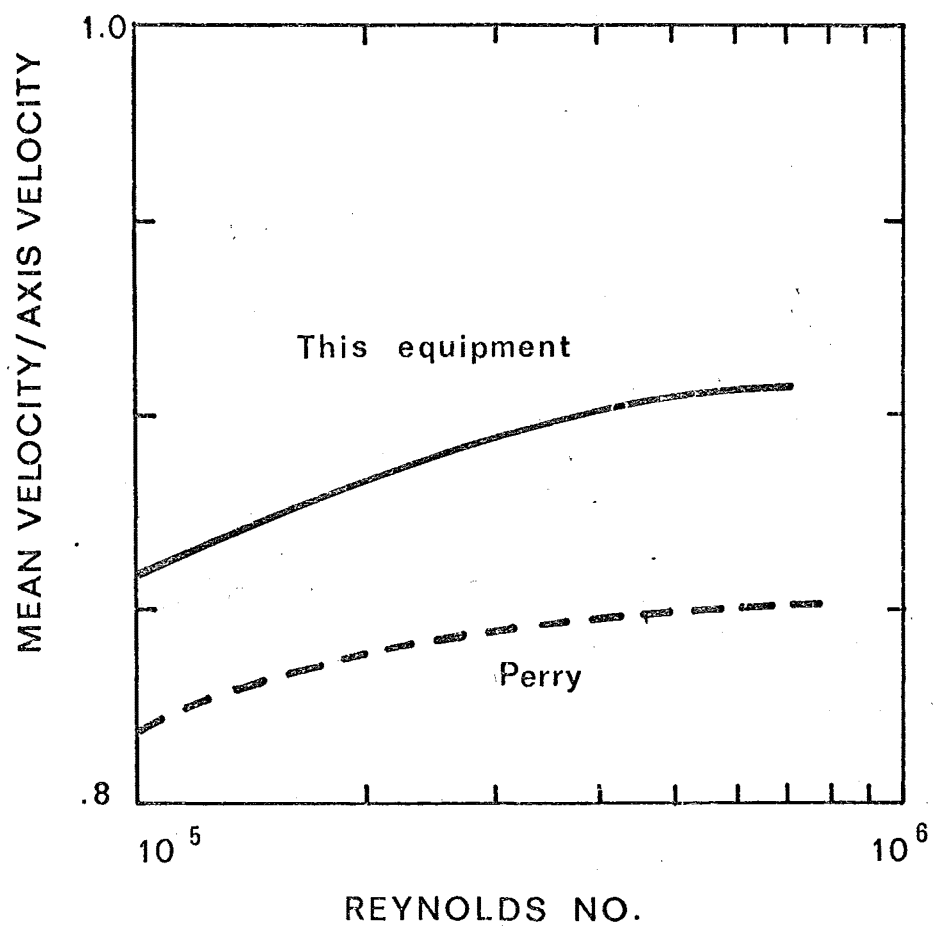


FIGURE 1.10 : MEAN/AXIS VELOCITY RATIO IN  
100MM DIAMETER AIR INLET PIPE



through the busbar box is also monitored with a Pitot tube in the 25.4 mm diameter inlet line.

Second-stage air flow, hot and cold, and liquid feed rates are measured with rotameters.

### II.3.2 Temperature measurements

Thermometer and (copper-constantan) thermocouple junction positions are shown in figures 4 and 6. For wall-temperature measurements the thermocouples are welded on, while for air-temperature measurements they are placed in a 6 mm I.D. radiation shield and a flow of air is drawn through the shield over the junction (this current of air is also used to measure humidity). A Phillips 12-point recorder with a maximum sensitivity of 2 mV f.s.d. is used to record thermocouple voltages.

### II.3.3 Humidity measurements

The humidity of inlet air to each stage is measured with a Lithium-chloride cell (K3) (Phillips type PR 6010 H). This instrument measures directly the dew-point which is related to the absolute humidity of the air. The characteristics of the sensor are shown in table 2.

For the outlet streams, miniature wet-and-dry-bulb psychrometers were specially made, with the advice of Dr. P.E. Doe of Tasmania University (figure 11). Calibration of this instrument was done on a stream of air of known humidity, and the following correction to the indicated wet bulb temperature must be applied:

$$T_{sm}^* - T_{st}^* = 0.06 (T - T_{st}^*) \pm 15\%$$

where  $T_{sm}^*$  and  $T_{st}^*$  are the measured and "true" wet-bulb temperatures respectively, and  $T$  is the air temperature. The "wet bulb" must be kept clean by frequent washing, for example before each run.

TABLE 1.2

LiCl Dew-point probe characteristics  
(Manufacturer's values)

Air temperature range:  $-30^{\circ}\text{C}$  to  $+100^{\circ}\text{C}$

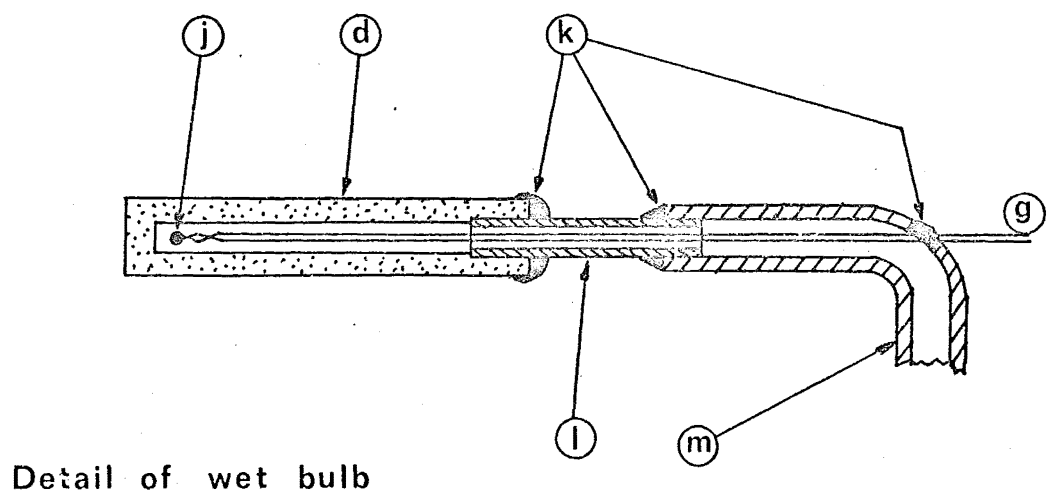
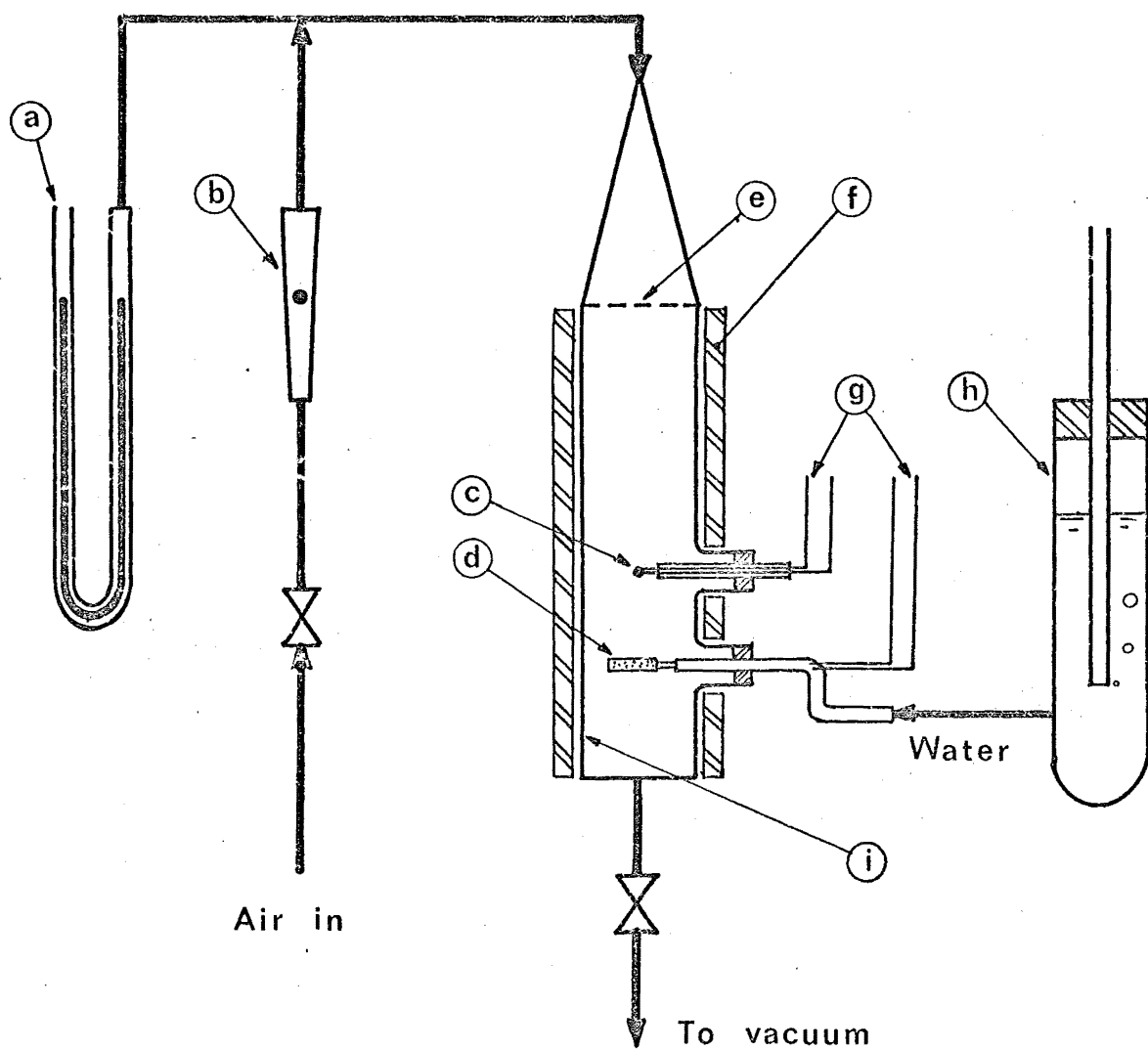
Dew-point range:  $-30^{\circ}\text{C}$  to  $+60^{\circ}\text{C}$

Air velocity: recommended: 0 m/s  
maximum: 0.5 m/s

Accuracy:  $\pm 1^{\circ}\text{C}$  Dew-point.

Calibration curve:

Dew-point / $^{\circ}\text{C}$	Resistance/ $\Omega$
0	113.67
5	116.38
10	119.09
15	121.81
20	124.51
25	127.53
30	130.55
35	133.57
40	136.49
45	138.91
50	141.33
55	143.75
60	146.16



Detail of wet bulb

FIGURE 1.11: PSYCHROMETER

Legend for Figure 1.11

- (a) Mercury manometer.
- (b) Rotameter.
- (c) Dry-bulb thermocouple junction.
- (d) Wet-bulb, made of Vyon porous plastic, 3 mm O.D., 1.5 mm I.D., 20 mm long, bonded to drawn glass tubing (l) below under low heat, then glued with Araldite.
- (e) Filter gauze.
- (f) Aluminium foil - fibreglass - aluminium foil lagging.
- (g) 32-gauge (0.274 mm diameter) Copper-Constantan thermocouple wires with fibreglass insulation. For wet-bulb, wires are insulated with varnish.
- (h) "Minsky" constant-level water-feed bottle.
- (i) Glass tube.
- (j) Wet-bulb thermocouple junction.
- (k) Araldite glue.
- (l) 2 mm O.D. drawn glass tubing.
- (m) 4 mm O.D. glass tubing.

## CHAPTER 2.

### TRACER KINETICS; BACKGROUND AND THEORY

#### Chapter contents:

##### INTRODUCTION

#### I. FUNDAMENTALS OF TRACER KINETICS

1. Basic quantities and concepts
  1. Holding time and reduced time
  2. Age distributions
  3. Ideal response curves
  4. End conditions
  5. Moments of the C-curve
  6. Transfer functions
  7. Frequency response & Fourier transforms
2. Flow modeling
  1. Basic components
  2. Mixed models
  3. Stochastic models
3. Flow patterns, mixedness and conversions

#### II. EXPERIMENTAL MODELING AND PARAMETER FINDING METHODS

1. Methods of tracer injection
  1. Delta pulse input
  2. Step input
  3. Sine input
  4. Random pulse input
  5. Injection of reactants
2. Methods of processing response data
  1. Analysis of moments
  2. Frequency analysis
  3. Transfer function methods
  4. Curve-fitting in the time domain
  5. Miscellaneous methods

### III. TRANSFER FUNCTION METHODS

1. Introduction
2. Basic quantities and relationships
  1. Definitions
  2. Calculation of the U-functions
  3. Properties of the U-functions
3. Applications to particular cases
  1. A.D.P.F.
  2. Tanks-in-series-and-plug-flow
  3. Diminishing backmix flow:
    1. Construction of model
    2. Properties of model
    3. Parameter finding
  4. Backflow cell model
  5. Second order model.

### IV. CONCLUSION

### NOTATION

## INTRODUCTION

Tracer kinetics provide a method of flow investigation whereby some small quantity of an easily detectable substance is injected into the inlet of a flow system (pipe or vessel) and the concentration monitored at the outlet. In this way information is gained about what is happening inside the system, information which can be used to improve the design and operation of the equipment, to set up an optimal control system, or to predict how the equipment will respond to external manipulations.

The use of tracer kinetics is becoming increasingly popular, one of the reasons being its experimental simplicity. The basic concepts have evolved in the 1950's with the work of Danckwerts <sup>(D1)</sup>, Levenspiel, Bishoff, Avis and others, and have been summarised by Levenspiel <sup>(L6, L7)</sup>. More recent advances have been reviewed elsewhere. <sup>(H11, H12, S6, B21)</sup>

In this chapter, we shall first describe the basic concepts and methods of tracer kinetics, then develop one class of methods in particular, those involving Laplace Transforms, for use in subsequent work.

### I. FUNDAMENTALS OF TRACER KINETICS

#### I.1 Basic quantities and concepts

##### I.1.1 Holding time and reduced time.

For the flow of a fluid through a vessel the holding time or space time  $\tau$  is defined by

$$\tau \equiv V/v \quad (2.1)$$

where  $V$  is the vessel volume and  $v$  the volumetric flow rate of the fluid calculated at its inlet density. In subsequent discussion we shall assume the fluid density to be constant, hence  $\tau$  is also the mean residence time.

The reduced time  $\theta$  is defined by

$$\theta \equiv t/\tau \quad (2.2)$$

### I.1.2 Age distribution curves

Age distributions can be defined in terms of either  $\theta$  or  $t$  :

(a) The internal age distribution of fluid in the vessel:

$I \, d\theta \equiv$  fraction of fluid inside the vessel having an age (past stay time) between  $\theta$  and  $\theta+d\theta$ .

$I_t \, dt \equiv$  fraction of fluid inside the vessel having an age between  $t$  and  $t+dt$ .

(b) The exit age distribution, or residence time distribution function (R.T.D.):

$E \, d\theta \equiv$  fraction of fluid in the exit stream having spent a time between  $\theta$  and  $\theta+d\theta$  in the vessel.

$E_t \, dt =$  fraction of fluid in the exit stream having spent a time between  $t$  and  $t+dt$  in the vessel.

Since these curves are normalised

$$\int_0^{\infty} E \, d\theta = \int_0^{\infty} E_t \, dt = 1 \quad (2.3)$$

$$\int_0^{\infty} I \, d\theta = \int_0^{\infty} I_t \, dt = 1 \quad (2.4)$$

### I.1.3 Ideal response curves

Age distributions are somewhat abstract concepts. In practice information about them can be obtained by injecting a tracer at the inlet of the vessel and measuring the response curve at the outlet. Two idealised injection patterns are useful for theoretical considerations:



(a) The Impulse-response or C-curve

Suppose a  $\delta$ -pulse is injected at time  $t = 0$ , the total amount of tracer used being  $\Delta$ . Then

$C d\theta \equiv$  fraction of  $\Delta$  present in the exit stream between  $\theta$  and  $\theta+d\theta$

$C_t dt \equiv$  fraction of  $\Delta$  present in the exit stream between  $t$  and  $t+dt$ .

(b) The step-response or F-curve

Suppose the inlet concentration of tracer is suddenly increased from 0 to  $c_o$ . Then

$$F \equiv c/c_o$$

$$F_t \equiv c/c_o$$

where  $c_o$  is the concentration of tracer in the exit stream at time  $t$  or  $\theta$ .

The relationships between the dimensional and dimensionless forms of the age distributions and ideal response curves are listed below:

$$E(\theta) = \tau E_t(t) \quad (2.5)$$

$$I(\theta) = \tau I_t(t) \quad (2.6)$$

$$C(\theta) = \tau C_t(t) \quad (2.7)$$

$$F(\theta) = F_t(t) \quad (2.8)$$

where  $t = \tau\theta$ .

I.1.4 End conditions

Vessels can be open-ended (open) or close-ended (close). In the latter case the flow into and out of the vessel is by bulk movement only, while in the former diffusion can also occur at the inlet and outlet. For example, if the vessel is close-ended, it is clear that  $C = E$ . But if it is open-ended, a  $\delta$ -pulse injection does not result in a  $\delta$ -pulse inlet concentration; back-diffusion up the inlet

stream occurs and the inlet concentration will be non-zero at  $t > 0$ .

Hence  $C \neq E$ , and in fact  $E$  and  $I$  lose their significance because molecules are moving in and out of the vessel more than once.

The following relationships can be proved<sup>(L6)</sup>:

(a) For all end conditions:

$$F = \int_0^{\infty} C \, d\theta \quad ; \quad C = \frac{dF}{d\theta} \quad (2.9)$$

(b) For closed vessels:

$$C = E \quad (2.10)$$

$$I + F = 1 \quad (2.11)$$

#### I.1.5 Moments of the C-curve

The first moment of the C-curve is defined by

$$M_1 = \bar{\theta} \equiv \int_0^{\infty} C \theta \, d\theta \quad (2.12)$$

$$M_{t1} = \bar{t} \equiv \int_0^{\infty} C_t \, t \, dt \quad (2.13)$$

$$\text{hence } \bar{\theta} = \bar{t}/\tau \quad (2.14)$$

The second moment with respect to the time origin is defined

by:

$$M'_2 \equiv \int_0^{\infty} C \, \theta^2 \, d\theta \quad (2.15)$$

$$M'_{t2} \equiv \int_0^{\infty} C_t \, t^2 \, dt \quad (2.16)$$

hence

$$M'_2 = (M'_{t2})^2 / \tau^2 \quad (2.17)$$

The second moment can also be defined with respect to the first, in which case it is a measure of the spread of the C-curve:

$$M_2 = \sigma^2 \equiv \int_0^{\infty} C(\theta - \bar{\theta})^2 d\theta \quad (2.18)$$

$$M_{t2} = \sigma_t^2 \equiv \int_0^{\infty} C_t(t - \bar{t})^2 dt \quad (2.19)$$

hence

$$\sigma^2 = \sigma_t^2 / \tau^2 \quad (2.20)$$

$$\sigma^2 = M_2' - \bar{\theta}^2 \quad (2.21)$$

For closed vessels

$$\bar{\theta} = 1 \quad (2.22)$$

$$\text{or } \bar{t} = \tau \quad (2.23)$$

For open vessels this will not necessarily be so; because of diffusion at the inlet and/or outlet, the effective volume holding the tracer will include elements in the inlet and/or outlet lines, and will be greater than the actual vessel volume, so that

$$\bar{\theta} > 1$$

$$\text{or } \bar{t} > \tau$$

#### I.1.6 Transfer Functions

By the convolution theorem<sup>(K12)</sup>, any system with linear properties (i.e. where the total response to several stimuli is equal to the sum of the responses to each) will have a characteristic transfer function

$$\mathcal{F}(s) \equiv \bar{c}_o(s) / \bar{c}_i(s) \quad (2.24)$$

where  $\bar{c}_o(s)$  is the Laplace Transform of the outlet stream tracer concentration, and  $\bar{c}_i(s)$  that of the inlet stream concentration.  $s$  is the Laplace-transform parameter.

Since the Laplace transform of the  $\delta$ -pulse is 1 for all  $s$ , we have for close-ended systems:

$$\mathcal{F}(s) = \bar{C}_t(s) = \bar{C}(\tau s) . \quad (2.25)$$

From its definition<sup>(K12)</sup>,

$$\bar{f}(s) \equiv \int_{-\infty}^{\infty} f(t) \exp(-ts) dt , \quad (2.26)$$

it can be seen that the Laplace transform is a moment-generating function, i.e.

$$M'_{tk} = (-1)^k \mathcal{F}^{(k)}(0) \quad (2.27)$$

where  $M'_{tk}$  is the  $k$ -th moment of the  $C_t$ -curve with respect to the origin.

This provides a convenient method for calculating these moments even

when the  $C$ -curve cannot be explicitly expressed<sup>(V1)</sup>. Equation 27

holds strictly for closed vessels only. For open vessels the

left-hand side must be replaced by the difference in the  $k$ -th

moments of the outlet and inlet concentration curves.

### I.1.7 Frequency response and Fourier transforms

The response of a linear system to a sinusoidal input is characterised by an amplitude ratio  $A$  and a phase-lag angle  $\psi$ , both functions of the frequency  $\omega$ .

$A(\omega)$  and  $\psi(\omega)$  can be found directly using sinusoidal inputs.

More conveniently they can be found either from data or from theory by the equation

$$\mathcal{F}(i\omega) = A \exp(-i\psi) \quad (2.28)$$

where  $\mathcal{F}(i\omega)$  is the Laplace transform with the imaginary argument

$i\omega$ , or Fourier-transform transfer function, and  $i = \sqrt{-1}$ .

A useful property of the Fourier transform is that a further Fourier transformation gives back the original function:

$$\begin{aligned} \text{if } Y(\omega) &= \int_{-\infty}^{\infty} z(t) \exp(i\omega t) dt \\ \text{then } z(t) &= \frac{1}{2\pi} \int_{-\infty}^{\infty} Y(\omega) \exp(-i\omega t) d\omega \end{aligned} \quad (2.29)$$

Hence the C-curve can be obtained from the frequency response. This property is used in the deconvolution of the response curve, where the response to a random pulse is used to calculate the frequency response and from this the C-curve (C4).

## I.2 Flow modeling

### I.2.1 Basic components of flow modeling

In modeling a flow system one usually constructs a network of basic units, the most common of which are described below:

(a) The stirred tank or backmix vessel: this is the "most mixed" flow unit, characterised by a uniform concentration of tracer in the whole vessel. It is a one-parameter model, with the parameter  $\tau$ .

(b) The plug-flow vessel: this is the "least mixed" flow unit, also a single parameter model characterised by  $\tau$ . The flow in it is parallel without backmix. All molecules in the exit stream have spent exactly  $\tau$  seconds in the vessel.

(c) The axially-dispersed plug-flow vessel (ADPF): the flow is subject to axial dispersion of Fick's law type:

$$u \frac{\partial c_A}{\partial x} + \frac{\partial c_A}{\partial t} - \mathcal{D} \frac{\partial^2 c_A}{\partial x^2} = 0 \quad (2.30)$$

where  $c_A$  is any concentration,  $u$  the fluid mean velocity,  $x$  the axial distance and  $\mathcal{D}$  the dispersion coefficient.

In dimensionless terms

$$\frac{\partial c_A}{\partial \xi} + \frac{\partial c_A}{\partial \theta} - \frac{1}{Pe} \frac{\partial^2 c_A}{\partial \xi^2} = 0 \quad (2.31)$$

where

$$\xi = x/L$$

$$\theta = ut/L = t/\tau$$

$$Pe = uL/D$$

and  $L$  is the vessel length.

This model is intermediate between the previous two (which are its extreme cases). It is characterised by two parameters,  $\tau$  and  $Pe$ . Its behaviour further depends on end conditions and has been the subject of a large amount of work. (A6, B11, B12, L5, P7, T3, V1, O1)

(d) Deadwater: deadwater occupies vessel space, but does not participate in the flow, hence it reduces the effective volume and the first moment of the C-curve:

$$\bar{t} < \tau$$

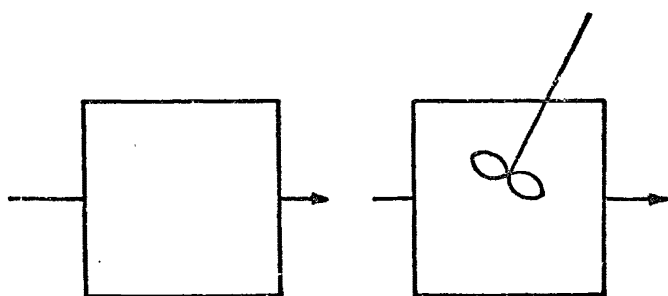
$$\bar{\theta} < 1.$$

In some recent work<sup>(B21)</sup>, the slow mass interchange between the deadwater region and the rest of the system has been studied.

The symbols for these flow units are shown in figure 1, and the properties of the first three in Table 1.

### I.2.2 Mixed models

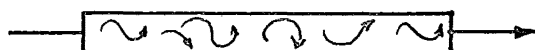
An example of a mixed model is shown in figure 1(e). The properties of a composite model can be deduced from those of elementary units according to the rules laid out in Table 2. In this table  $f_j$  is the fraction of fluid entering the  $j$ -th stream in a parallel flow network.  $M'_{tk}$  is the  $k$ -th moment with respect to the origin.



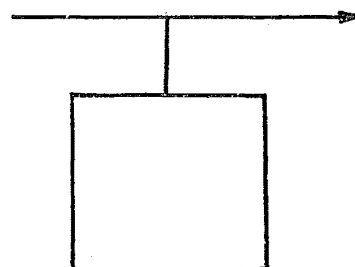
(a) Stirred tanks



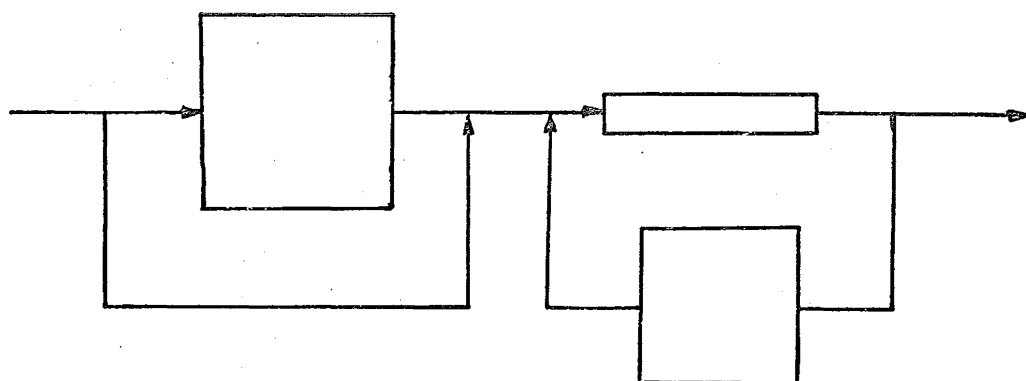
(b) Plug-flow



(c) Axially dispersed plug-flow



(d) Deadwater



(e) A mixed model

FIGURE 2.1: SYMBOLS OF FLOW MODELS

TABLE 2.1

Properties of the elementary flow units1. Stirred tank:

$$F = 1 - I = 1 - \exp(-\theta) \quad (2.32)$$

$$C = E = \exp(-\theta) \quad (2.33)$$

$$\bar{\theta} = 1 \quad (2.34)$$

$$\sigma^2 = 1 \quad (2.35)$$

$$\mathcal{F}(s) = 1/(1+\tau s) \quad (2.36)$$

$$A = 1/\sqrt{1 + \tau^2 \omega^2} \quad (2.37)$$

$$\tan \psi = -\tau \omega \quad (2.38)$$

2. Plug flow:

$$F = 1 - I = H(1) \quad \text{where } H = \text{unit step function} \quad (2.39)$$

$$C = E = \delta(1), \text{ the unit pulse} \quad (2.40)$$

$$\bar{\theta} = 1 \quad (2.41)$$

$$\sigma^2 = 0 \quad (2.42)$$

$$\mathcal{F}(s) = \exp(-\tau s) \quad (2.43)$$

$$A = 1 \quad (2.44)$$

$$\psi = -\tau \omega \quad (2.45)$$

(continued)



TABLE 2.1 (continued)

3. A.D.P.F.:(a) open-ended vessel:

$$C = \frac{1}{2} \sqrt{\frac{Pe}{\pi\theta}} \exp \left\{ -\frac{Pe(1-\theta)^2}{4\theta} \right\} \quad (2.46)$$

$$\bar{\theta} = 1 + 2/Pe \quad (2.47)$$

$$\sigma^2 = 2/Pe + 8/Pe^2 \quad (2.48)$$

$$\Delta\sigma^2 = 2/Pe \quad (2.48b)$$

$$\mathfrak{J}(s) = \exp \left\{ \frac{Pe}{2} \left( 1 - \sqrt{1 + \frac{4\tau s}{Pe}} \right) \right\} \quad (2.49)$$

$$A = \exp \left\{ \frac{Pe}{2} \left( 1 - \sqrt{\frac{a+1}{2}} \right) \right\} \quad (2.50)$$

$$\psi = -\frac{Pe}{2} \sqrt{\frac{a-1}{2}} \quad (2.51)$$

$$\text{where } a = \sqrt{1 + (4\tau\omega/Pe)^2}$$

(b) close-ended vessels:

$$\bar{\theta} = 1 \quad (2.52)$$

$$\sigma^2 = 2/Pe - 2\{1 - \exp(-Pe)\} / Pe^2 \quad (2.53)$$

$$\mathfrak{J}(s) = \frac{2b \exp\{Pe(1+b)/2\}}{b-1 + (b+1) \exp(bPe)} \quad (2.54)$$

$$\text{where } b = \sqrt{1 + 4\tau s/Pe}$$

(c) open-closed or closed-open vessel:

$$\bar{\theta} = 1 + Pe \quad (2.55)$$

$$\sigma^2 = 2/Pe + 3/Pe^2 \quad (2.56)$$

See Reference (V1) for further properties.

TABLE 2.2

Rules for calculating the properties of mixed models

	Closed vessels in parallel	Closed vessels in series
(a) E, C curves	$C = \sum_j f_j C_j$	$C = \int_{-\infty}^{\theta} C_1 (\xi - \theta) C_2 (\xi) d\xi$
(b) Moments	$M'_{tk} = \sum_j f_j M'_{tkj}$	$\bar{t} = \sum_j \bar{t}_j$ $\sigma_j^2 = \sum_j \sigma_{tj}^2$
(c) Transfer functions	$\mathcal{F}(s) = \sum_j f_j \mathcal{F}_j(s)$	$\mathcal{F}(s) = \prod_j \mathcal{F}_j(s)$
(d) Frequency response	-	$A = \prod_j A_j$ $\psi = \sum_j \psi_j$

### I.2.3 Stochastic models

In some systems the flow may switch repeatedly from one pattern to another. Such non-stationary behaviour is frequently caused by turbulence, when eddies detach from obstacles or flows separate from boundaries.

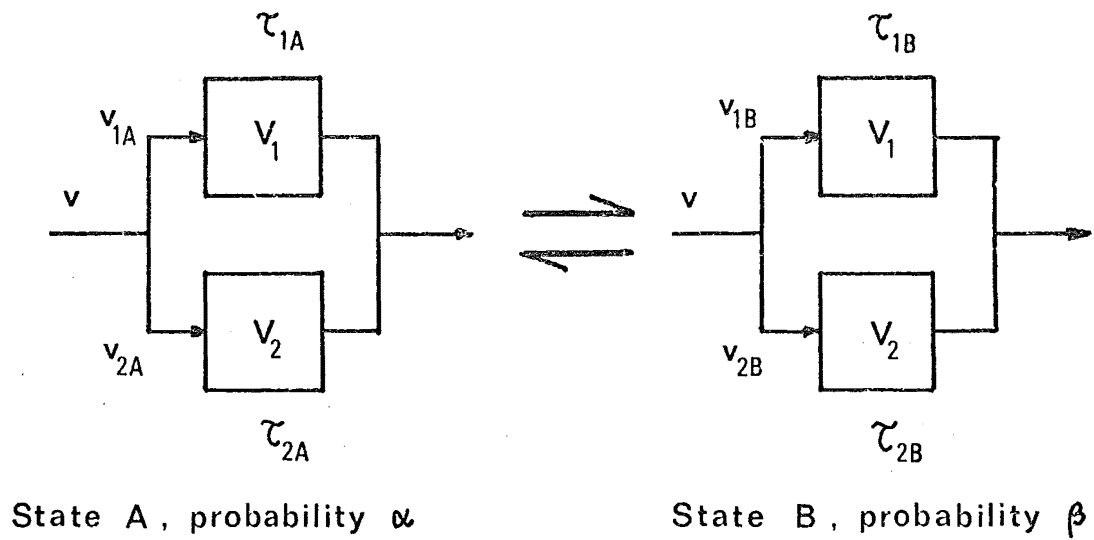
Krambeck et al. (K10, S6) introduced the concept of stochastic models to deal with non-stationary flows. Their models assume a network of tanks, each with a given volume, interconnected by flows which can take certain sets of values or "states" (say A, B ...), each state having a constant (ergodic) probability, say  $\alpha$ ,  $\beta$ ... (fig.2a).

For such models the C-curves will change from experiment to experiment, unless the switching rate is infinitely fast. If we average out a large number of experimental C-curves, the result will be the same as that of an "equivalent" deterministic model where the flow is split into several parallel streams, a fraction  $\alpha$  of the flow going to the configuration corresponding to state A, and so on (fig. 2b).

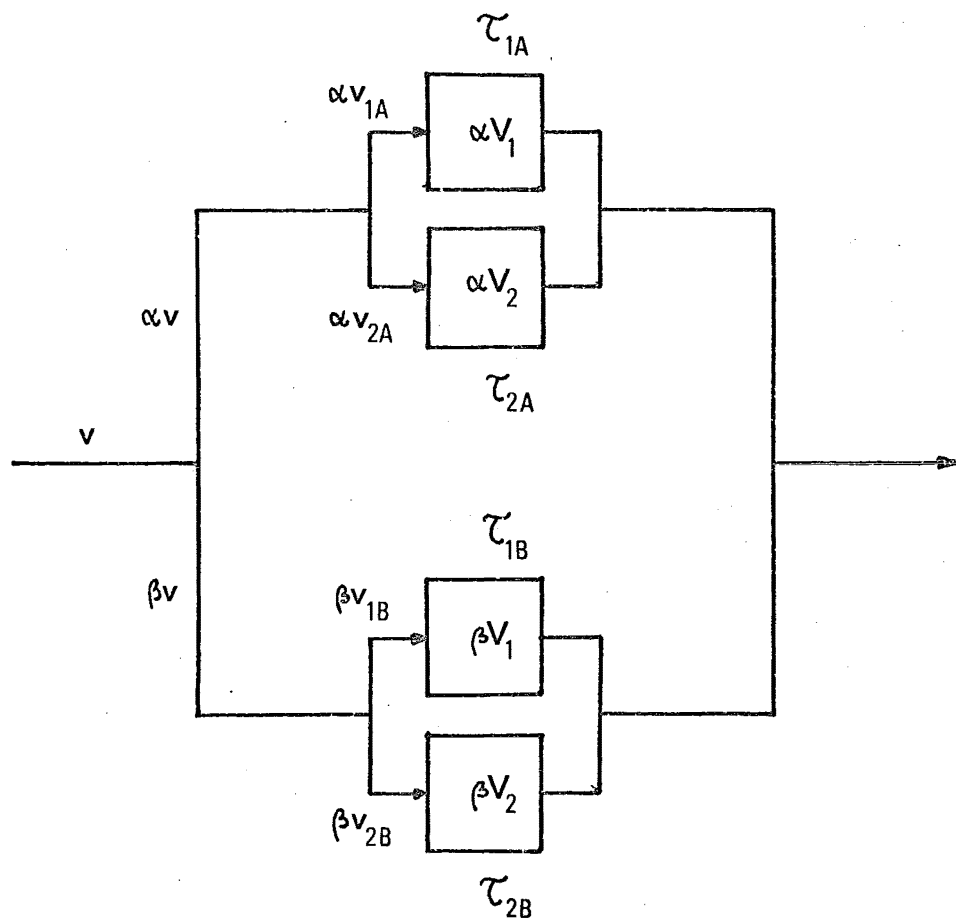
The difference between the stochastic model and the equivalent deterministic model is however shown up in the spread of the C-curve values at each instant in time, which is a function of the switching rate and the fluctuation magnitude. At the moment this subject is still at an embryonic stage.

### I.3 Flow patterns, mixedness and conversion

The residence time distribution by itself is insufficient to characterise a flow system; the mixedness must also be specified. The degree and scale of mixedness are closely related to the flow pattern.



(a) Stochastic model



(b) Deterministic model

FIGURE 2.2: A STOCHASTIC MODEL AND ITS DETERMINISTIC EQUIVALENT

A system will have the maximum degree of mixedness for a given R.T.D. if molecules that have the same life expectation in the vessel will mix with each other as early as possible <sup>(Z1)</sup>. Two systems with the same R.T.D. but different flow patterns (hence different degrees of mixing) are shown in figure 3.

Where the scale of mixedness is concerned the system may be macromixed or micromixed. A macromixed fluid (or macrofluid) flows as large aggregates (compared to molecular size), each retaining its own identity - for example, swarms of non-interacting particles, droplets or bubbles. In a micromixed fluid, on the other hand, molecules mingle with each other and lose their identities <sup>(D2)</sup>.

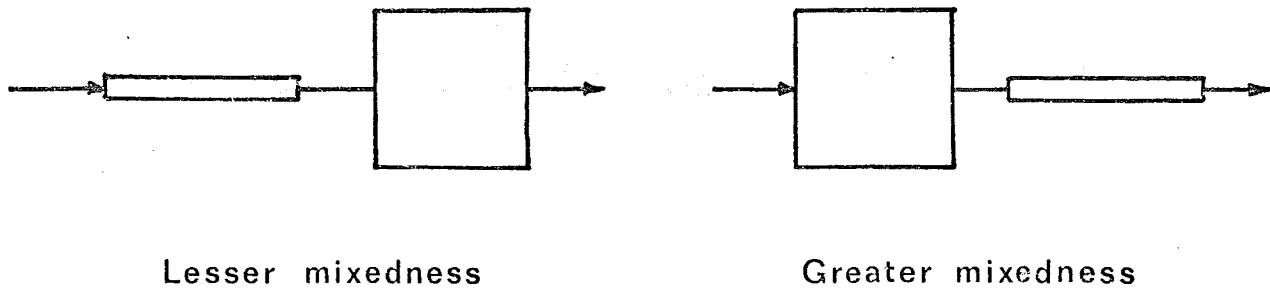
The conversion of chemical reactions depends on both the degrees and scale of mixedness <sup>(L6)</sup>. For reaction with order smaller than unity, the conversion is least with macromixing and minimum mixedness. For reactions with order larger than unity, the effect is reversed. Only when the order is one (linear reaction) is the conversion independent of the mixedness and the flow pattern.

A macrofluid can be said also to have a minimum degree of mixedness. The conversion in a macromixed system is independent of the flow pattern and is given by

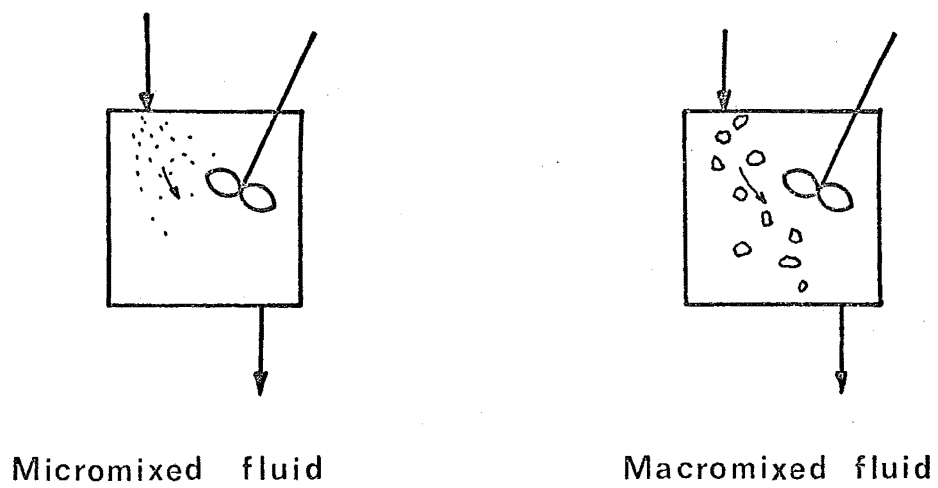
$$X = \int_0^{\infty} X_b E_t dt \quad (2.57)$$

where  $X$  is the fraction of initial reactant remaining in the outlet stream, and  $X_b$  the fraction of reactant remaining at time  $t$  in a batch reactor.

Most tracer experiments will provide information on residence-time distributions, but not on mixedness or flow patterns. The foregoing considerations point to the limitations of such methods.



(a) Degree of mixedness



(b) Scale of mixedness

FIGURE 2.3: MIXEDNESS

## II. EXPERIMENTAL MODELING AND PARAMETER FINDING METHODS

In a tracer kinetics experiment the tracer must first be injected in any of several ways, then the data obtained must be processed in some way. Thus a two-way classification of methods suggests itself (Table 3).

### II.1 Methods of tracer injection

II.1.1 Delta-pulse input: When possible this is the most desirable type of input. From a time-domain point of view, its zero spread enables an accurate measurement of the spread due to the system itself to be made. From a frequency-domain point of view, a delta-pulse has a large content of all frequencies, thus enabling a large range of  $\omega$  to be investigated. Its disadvantages are that it may disturb the flow, and is difficult to administer.

The result of a delta-pulse input is a directly-obtained C-curve, on which a direct curve-fit in the time domain against a theoretical C-curve, an analysis of moments, or a Laplace-transform analysis can be performed. Alternatively it can be Fourier-transformed and undergo a frequency analysis, a quick and economical procedure if fast Fourier transformations are used <sup>(W6)</sup>. Finally an integration will give the F-curve, hence all methods applicable to the F-curve can also be used here.

II.1.2 Step input: Step inputs do not give as much information as pulse inputs, but in some particular cases they may be useful alternatives (see section II.2.5).

II.1.3 Sinusoidal input: although this type of input gives the frequency response directly, it is time-consuming and difficult to perform, hence it is little used in practice.

II.1.4 Random or imperfect pulse input: This is the next best thing to the delta-pulse. It is easy to administer and is probably the most widely used method of injection. Moment analysis and Laplace transform methods are readily applicable to the data obtained. Frequency analysis can also be done after a Fourier transformation has given the amplitude ratios and phase angles. Curve fits to theoretical models can be done in the time domain, either before deconvolution or after (the deconvolution being achieved by a double Fourier transform).

The pulse must be measured both at the inlet and at the outlet. It should be kept as narrow as possible for the reasons already outlined (section II.1.1).

II.1.5 Injection of reactants: This is a recent development<sup>(Pl)</sup> whereby a reactant with order different from unity is injected either as a steady stream or as a pulse, and the outlet concentration measured. This method can discriminate between several flow patterns or degrees of mixedness for a given R.T.D. . Parimi and Harris<sup>(Pl)</sup> used it successfully to distinguish between the two flow patterns shown in figure 3(a). They also stated that a pulse input gives better discrimination than a steady injection. Data processing was by curve-fit in the time domain.



TABLE 2.3

Classification of tracer kinetics methods

	<u>Data processing:</u>			
	Moments analysis	Frequency analysis	Laplace Transform	Time domain curve fit
<u>Tracer input:</u>				
$\delta$ -pulse	Y	Y	Y	Y
Step input	N	Y	Y	Y
Sine input	N	Y	Y	N
Random pulse	Y	Y	Y	Y
Reactants	N	N	N	Y

Y : possible combination

N : impossible combination.

II.2 Methods of processing the response dataII.2.1 Analysis of moments (L6)

The moments of a C-curve or the differences in the moments of the input and output curves are usually expressible in terms of the model parameters (see for example Table 1). Hence by comparing the experimental moments to the theoretical ones, these parameters can be evaluated. Although simple to apply, the method of moments suffers from several disadvantages:

- (1) There is no guarantee that the model used is valid.
- (2) If the response curve has a long tail, large errors will be involved in calculating the higher moments. Levenspiel<sup>(L6)</sup> suggested cutting off the tail at  $t=3\tau$ . Jagota et al.<sup>(J1)</sup> proposed an iterative tail-cutting technique. Neither method has much theoretical justification.

- (3) Because of the errors involved in the higher moments it is inadvisable to go beyond the second moment, hence models with more than 2 parameters cannot usually be evaluated.

### II.2.2 Frequency analysis

For some of the simple systems the frequency response follows simple equations which enable the parameters to be found graphically. For example, in the case of the two-tanks-in-series (second order) model it can be shown that

$$(\tan \psi) = -(T_1 + T_2)\omega \quad (2.58)$$

$$\left(\frac{1}{A^2} - 1\right) \frac{1}{\omega^2} = (T_1^2 + T_2^2) \omega^2 + (T_1^2 + T_2^2) \quad (2.59)$$

where  $T_1$  and  $T_2$  are the holding times of the tanks.

These two equations can be plotted as straight lines, the slopes and intercepts of which then give  $T_1$  and  $T_2$  after some manipulation.

Similarly, the the single-tank-and-plug model:

$$\frac{1}{A^2} = 1 + T_t^2 \omega^2 \quad (2.60)$$

where  $T_t$  is the space time of the tank.

For the n-equal-tanks-in-series model:

$$\frac{d(\omega^2)}{d(\ln A)} = -\left(\frac{2}{n}\right) \omega^2 = \frac{2n}{\tau^2} \quad (2.61)$$

where  $\tau$  is the total space time.

For the axial dispersion model with open ends (see Table 1):

$$\ln A = \frac{Pe}{2} + \left(\frac{Pe \tau}{2}\right) \left(\frac{\omega}{\psi}\right) \quad (2.62)$$

A more orthodox and generally useful method, and one widely used in automatic control works, is to perform a curve-fit in the frequency domain<sup>(C4)</sup>. From Parseval's theorem (see for example Ref.(D4)), it can be shown that a curve-fit, by minimisation of squared errors in the frequency domain, is equivalent to a similar procedure in the time domain:

$$\int_0^{\infty} |\mathcal{F}_t(i\omega) - \mathcal{F}_e(i\omega)|^2 d\omega = \pi_0 \int_0^{\infty} [C_{tt}(t) - C_{te}(t)]^2 dt \quad (2.63)$$

where  $\mathcal{F}_t(i\omega)$  and  $\mathcal{F}_e(i\omega)$  are the theoretical and experimental Fourier-transform transfer functions, and  $C_{tt}(t)$  and  $C_{te}(t)$  are the theoretical and experimental  $C_t$  curves respectively. By minimising the left-hand side with a numerical procedure, the right-hand side is also minimised.

Although very flexible, this method, like any other curve-fit, does not guarantee the validity of the model. Any number of model parameters can be introduced but one cannot be sure that these parameters have any physical meaning.

### II.2.3 Methods using Laplace Transform Transfer functions

Conceivably a theoretical L.T. Transfer function can be curve-fitted to the experimental one, as is done for the Fourier-transform transfer function. In practice this has not been done because no relationship has yet been found between the errors in the L.T. domain and those in the time domain<sup>(H11)</sup>.

Recently, Michelsen and Østergaard<sup>(M12, M13, O1)</sup> introduced methods whereby the Transfer function and its derivatives are manipulated to enable the parameters of the axially dispersed plug flow model to be found graphically. As the author has applied these methods to other models for use in subsequent parts of this work, they will be the subject of the third part of this chapter.

#### II.2.4 Curve-fitting in the time domain

The response to any non-periodic input can be fitted to a model curve by an error minimisation procedure (R9). Although very flexible, this method does not guarantee the validity of the model and this must be confirmed by other means. If an inordinate number of parameters are used, the hill-climbing procedure may end up at local minima which are quite far from the true minimum error. In general no more than 5 or 6 parameters should be used, although a 12-parameter model has been curve-fitted elsewhere on a counter-current spray dryer, without very much success (B9).

#### II.2.5 Miscellaneous methods

For some simple models the C or F curves follow simple equations from which the parameters can be found graphically. For example,  $\ln C_t$  or  $\ln (1-F_t)$  for a single tank can be plotted against time (equations 32, 33) to give a straight line with slope  $-1/\tau$ .

For the ADPF with large  $Pe$ , the  $C_t$ -curve tends to a normal distribution with mean  $\bar{t}$  and standard deviation  $\sigma_t$ . Hence the F-curve can be plotted on probability graph paper,  $\bar{t}$  and  $\sigma_t$  calculated, and  $\tau$  and  $Pe$  deduced (L6).

### III. RESPONSE-CURVE PROCESSING BY TRANSFER FUNCTIONS

#### III.1 Introduction

The use of transfer functions with a real argument offers many attractive features:

(1) Laplace transforms have been used extensively in other fields, and comprehensive reviews and tables are available for consultation.

(2) Experimental transfer functions can be obtained from almost any type of tracer injection, provided the inlet concentration curve is known.

(3) The Laplace transform weights down the response curve by a factor  $\exp(-st)$ , which tends to zero as  $t$  tends to infinity. Hence tailing effects, which account for large errors in many cases, are reduced. This offers a definite advantage over, say, the method of moments.

(4) The Laplace transformation is an integration procedure which tends to average out fast random fluctuations, so that only the main features of the response curve remain.

(5) In addition, the approach followed here involves a graphic procedure which enables the validity of the model to be evaluated, something which is not possible in curve-fitting procedures or moment analysis. In transfer-function methods, a valid model shows up as a straight line on a graph.

On the debit side, transfer-function methods as described here are not as flexible as curve-fitting methods. Only methods with no more than 3 or 4 parameters can be evaluated. For the relatively simple situation arising in the present work (Chapter 1) this is not a serious restriction.

For these reasons, transfer-function methods, which were originally introduced by Michelsen and Østergaard (M12, M13, O1) to treat the ADPF, will be generalised for use with several other models of interest to the present work. One of these was specially developed to account for gradual change in the turbulent mixing pattern. Only the graphical version of those authors' method will be followed, for the reasons already mentioned.

### III.2 Basic quantities and relationships

#### III.2.1 Definitions

From now on the non-normalised transfer function  $\mathcal{F}^*(s)$  will be used. It is defined by:

$$\mathcal{F}^*(s) \equiv K \bar{C}_O(s) / \bar{C}_i(s) \quad (2.64)$$

where K is an arbitrary proportionality constant. Its introduction facilitates the experimental procedure, as in many practical situations only the relative change in the tracer concentration and not its absolute value can be measured.

The following three functions were introduced by Michelsen and Østergaard:

$$U_0 \equiv \ln \mathcal{F}^* = \ln \mathcal{F} + \ln K \quad (2.65)$$

$$U_1 \equiv -U_0' = -\mathcal{F}' / \mathcal{F} \quad (2.66)$$

$$U_2 \equiv -U_1' = \mathcal{F}'' / \mathcal{F} - (\mathcal{F}' / \mathcal{F})^2 \quad (2.67)$$

where ' denotes a derivative with respect to s. The asterisk has been dispensed with in equations 66 and 67 because the constant K drops out during differentiation.

#### III.2.2 Calculation of the U-functions

$U_0$ ,  $U_1$ ,  $U_2$  are functions of s. If a theoretical model is being considered, they can be derived directly from the theoretical function via equations 65 to 67.

If they are to be found from experimental data, numerical differentiation can be avoided by the use of the following relationships<sup>(M12)</sup>, which can be proved by substituting the defining equation of the transfer function into 65, 66, 67:

$$U_0 = [\ln \{ \mathcal{M}_0(s) \}]_i^0 \quad (2.68)$$

$$U_1 = \left[ \frac{\mathcal{M}_1(s)}{\mathcal{M}_0(s)} \right]_i^0 \quad (2.69)$$

$$U_2 = \left[ \frac{\mathcal{M}_2(s)}{\mathcal{M}_0(s)} - \left\{ \frac{\mathcal{M}_1(s)}{\mathcal{M}_0(s)} \right\}^2 \right]_i^0 \quad (2.70)$$

where  $[\ ]_i^0$  denotes the difference between the vessel outlet and inlet values, and  $\mathcal{M}_n(s)$  is the n-th moment of the weighted concentration curve:

$$\mathcal{M}_n(s) \equiv \int_0^{\infty} c_A \exp(-st) \cdot t^n \cdot dt \quad (2.70b)$$

where  $c_A$  is the tracer concentration in arbitrary units.

### III.2.3 Properties of the U-functions

From equations 68 to 70, some insight into the significance of the U-functions can be gained. When  $s = 0$ ,  $\mathcal{M}_n(0)$  is the (unnormalised) n-th moment of the concentration curve with respect to the origin. Hence  $U_0(0)$  is the logarithm of the ratio of the areas under the inlet and outlet concentration curves respectively,  $U_1(0)$  the difference between the mean response times (or first moments) of these concentration curves, and  $U_2(0)$  the difference between the variances of these concentration curves:

$$U_1(0) = \bar{t}_o - \bar{t}_i \quad (2.71)$$

$$U_2(0) = \sigma_{to}^2 - \sigma_{ti}^2 \quad (2.72)$$

For closed vessels,

$$U_1(0) = \bar{t} \quad (2.73)$$

$$U_2(0) = \sigma_t^2 \quad (2.74)$$

where  $\bar{t}$  and  $\sigma_t^2$  are the moments of the  $C_t$ -curve. Equations 71 to 74 are also useful for the analysis of moments.

From the properties of the transfer function (Table 2), it can be shown that the U-functions of a system of closed vessels in series are the sums of the individual U-functions:

$$U_0 = \sum_j U_{0j} \quad (2.75)$$

$$U_1 = \sum_j U_{1j} \quad (2.76)$$

$$U_2 = \sum_j U_{2j} \quad (2.77)$$

For example, the addition of a plug-flow element  $[ \mathcal{J}(s) = \exp(-T_p s) ]$  to a system will contribute a further term  $(-T_p s)$  to  $U_0$ , a term  $T_p$  to  $U_1$ , but will not affect  $U_2$ .

### III.3 Application of transfer function methods to particular cases

#### III.3.1 ADPF model: (M13)

From equation 49 for the transfer function of the ADPF with open ends, one obtains:

$$U_0 = \frac{Pe}{2} \left( 1 - \sqrt{1 + \frac{4s\tau}{Pe}} \right) + \ln K \quad (2.78)$$

$$U_1 = \frac{\tau}{\sqrt{1 + 4s\tau/Pe}} \quad (2.79)$$

from which

$$\frac{1}{U_1^2} = \frac{4}{\tau Pe} \cdot s + \frac{1}{\tau^2} \quad (2.80)$$

Thus, if the model is valid,  $1/U_1^2$  when plotted against  $s$  will give a straight line, and  $\tau$  and  $Pe$  can be calculated from its slope and its intercept.

Michelsen and Østergaard made a noise sensitivity analysis for this model. If the errors are randomly distributed on both sides of the response curve and if the mean fluctuation amplitude does not



change with time, then the recommended range of  $st$  values to minimise the errors in  $Pe$  should be in the vicinity of 1. However, the choice of  $s$ -values must obviously depend on the situation: if, for example, there is some uncertainty in the base line and tailing effects are serious, then larger values of  $st$  should be used.

### III.3.2 Tanks-in-series-and-plug-flow model (figure 4b)

The A.D.P.F. model assumes an equal degree of dispersion or backmix throughout the vessel. Another situation may arise whereby all the backmixing takes place in one part of the vessel (say the entrance zone), while for the remainder plug flow dominates. In this case the model shown in figure 4(b) is applicable.

The equal-tanks-in-series by itself is a common substitute for the A.D.P.F. For a given total tank time  $T_t$  the degree of backmixing varies inversely with the number  $n$  of tanks:

$$\sigma_t^2 = \frac{T_t^2}{n} \quad (2.81)$$

The C-curve for the present model is given by:

$$C_t = \frac{n^n}{T_t^n \Gamma(n)} (t-T_p)^{n-1} \exp[-n(t-T_p)/T_t] \quad (2.82)$$

where  $\Gamma$  is the gamma function.

The transfer function is given by:

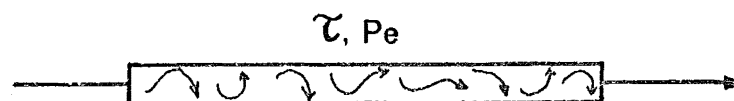
$$\mathcal{J}^*(s) = \frac{K \exp(-T_p s)}{(1+T_t s/n)^n} \quad (2.83)$$

from which

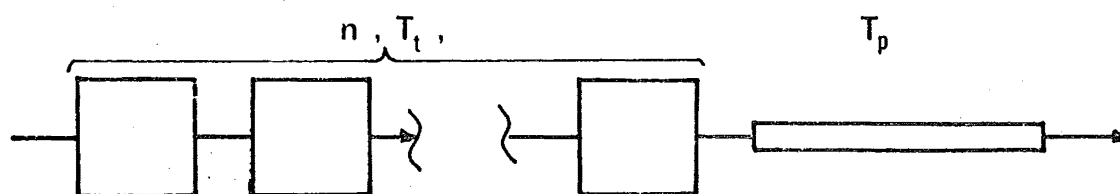
$$U_0 = -n \ln(1+T_t s/n) - T_p s + \ln K \quad (2.84)$$

$$U_1 = \frac{n}{n/T_t + s} + T_p \quad (2.85)$$

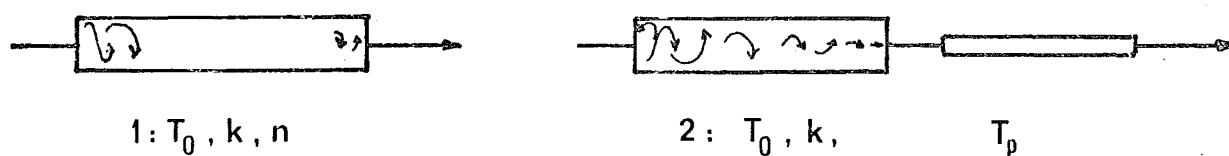
$$U_2 = \frac{n}{(n/T_t + s)^2} \quad (2.86)$$



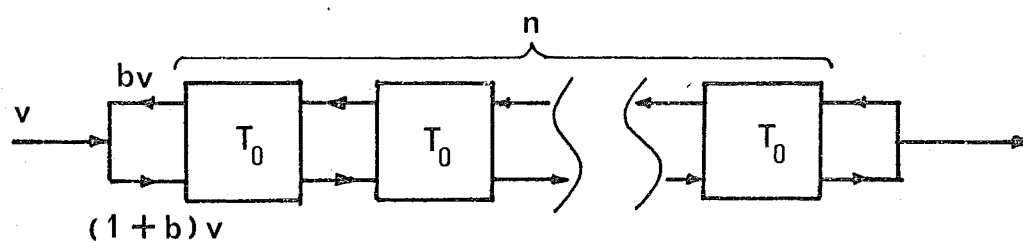
(a) A.D.P.F.



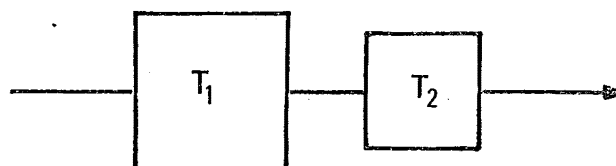
(b) Tanks in series &amp; plug-flow



(c) Diminishing backmix flow



(d) Backflow cells



(e) Second-order system

FIGURE 2.4: MODELS STUDIED BY TRANSFER FUNCTION METHODS

Since this is a three-parameter model, at least two equations must be plotted to find  $T_t$ ,  $T_p$  and  $n$ . From equation 85 and 86 one gets:

$$\frac{1}{\sqrt{U_2}} = \frac{\sqrt{n}}{T_t} + \frac{s}{\sqrt{n}} = Y_1 + S_1 s \quad (2.87)$$

$$\frac{U_1}{\sqrt{U_2}} = \sqrt{n} \left(1 + \frac{T_p}{T_t}\right) + \left(\frac{T_p}{\sqrt{n}}\right) s = Y_2 + S_2 s \quad (2.88)$$

These equations give two slopes ( $S_1$ ,  $S_2$ ) and two intercepts ( $Y_1$ ,  $Y_2$ ) for calculating three quantities. There is thus a redundancy which can provide a further check on the validity of the model. For example, a possible combination may be:

$$n = 1/S_1^2 \quad (2.89)$$

$$T_t = 1/(S_1 Y_1) \quad (2.90)$$

$$T_p = S_2/S_1 \quad (2.91)$$

$$= Y_2/Y_1 - 1/(S_1 Y_1) \quad (2.92)$$

### III.3.3 Diminishing backmix model

#### III.3.3.1 Construction of the model

The previous model assumes that the flow changes suddenly from a backmix regime to a plug-flow regime. It is desirable to have an alternative model whereby the degree of backmixing gradually decreases, and such a model will now be constructed.

We first consider a series of tanks, the sizes of which decrease in a geometric series (figure 5).

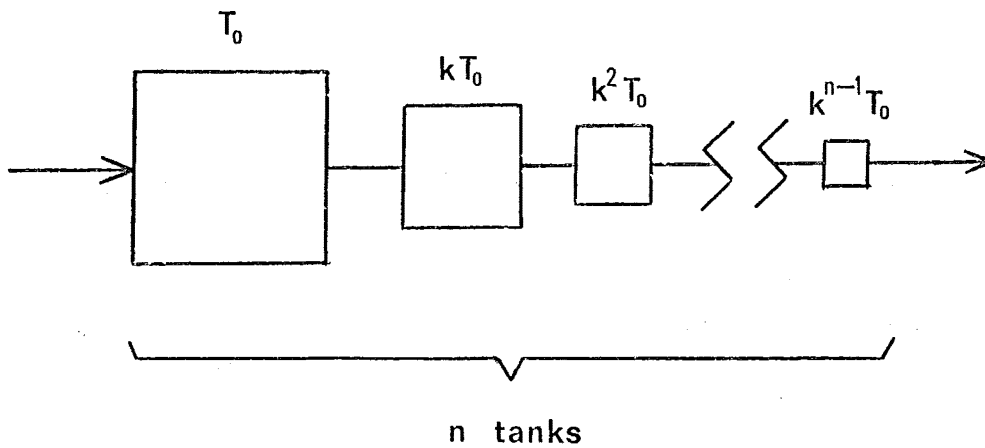


FIGURE 2.5: SERIES OF DIMINISHING TANKS

The transfer- and U-functions of this system are:

$$\mathcal{J}^*(s) = K \prod_{j=0}^{n-1} \frac{1}{1 + k^j T_0 s} \quad (2.93)$$

$$U_0 = \ln K + \sum_{j=0}^{n-1} \ln(1 + k^j T_0 s) \quad (2.94)$$

$$U_1 = T_0 \sum_{j=0}^{n-1} \frac{k^j}{1 + k^j T_0 s} \quad (2.95)$$

$$U_2 = T_0^2 \sum_{j=0}^{n-1} \frac{k^{2j}}{1 + k^j T_0 s} \quad (2.96)$$

where  $T_0$  is the holding time of the first tank,  $n$  the number of tanks and  $k$  the ratio between successive tank times.

By analogy with equations 94 to 96 the diminishing backmix model will now be defined by the following equations:

$$U_0 = \int_0^n \ln(1 + k^z T_0 s) dz + \ln K \quad (2.97)$$

$$\begin{aligned} U_1 &= T_0 \int_0^n \frac{k^z}{1+k^z T_0 s} dz \\ &= -\frac{1}{s \ln k} \ln \left( \frac{1+T_0 s}{1+T_0 k^n s} \right) \end{aligned} \quad (2.98)$$

$$\begin{aligned} U_2 &= T_0^2 \int_0^n \frac{k^{2z}}{1+k^z T_0 s} dz \\ &= \frac{T_0 (k^n - 1)}{s \ln k (1+T_0 s) (1+T_0 k^n s)} + \frac{1}{s^2 \ln k} \ln \left( \frac{1+T_0 k^n s}{1+T_0 s} \right) \end{aligned} \quad (2.99)$$

### III.3.3.2 Properties of the model:

For the present model  $U_0$ ,  $\mathcal{F}(s)$  and the C-curve cannot be expressed algebraically.  $T_0$ ,  $k$  and  $n$  have lost their original meaning in figure 5, but are still measures of the original degree of backmixing, the rate of decrease of backmixing and the total vessel size respectively.

This model is close-ended and the holding time  $\tau$  is equal to the first moment  $\bar{t}$  of the C-curve:

$$\begin{aligned} \tau = \bar{t} &= U_1(0) \\ &= \frac{T_0 (1-k^n)}{-\ln k} \end{aligned} \quad (2.100)$$

by taking the limit of equation 98 as  $s \rightarrow 0$ .

The maximum possible value of  $\tau$  or  $\bar{t}$  is obtained by letting  $n \rightarrow \infty$ :

$$\tau_m = \bar{t}_m = \frac{T_0}{-\ln k} \quad (2.101)$$

The variance of the C-curve is

$$\begin{aligned}\sigma_t^2 &= U_2(0) \\ &= \frac{T_o^2 (1-k^{2n})}{-2 \ln k}\end{aligned}\quad (2.102)$$

$$\sigma^2 = \sigma_t^2 / \tau^2 = \frac{-\ln k \cdot (1+k^n)}{2(1-k^n)} \quad (2.103)$$

As  $n \rightarrow \infty$ ,  $\sigma^2 \rightarrow -(\ln k) / 2$ .

### III.3.3.3 Parameter finding

Two cases will be considered: in the first one, the end of the vessel is reached while there is still some backmixing; in the second one, backmixing decreases to zero with the last part of the vessel occupied by plug flow.

#### (a) No plug-flow zone (figure 4(c1))

$U_o$ ,  $U_1$ ,  $U_2$  are given by equations 97 to 99. This is a three-parameter model ( $T_o$ ,  $k$ ,  $n$ ). From 98 and 99:

$$\left[ \left( s + \frac{1}{T_o} \right) (U_1 - sU_2) \right]^{-1} = \left( \frac{-\ln k}{1-k^n} \right) - \left( \frac{T_o k^n \ln k}{1-k^n} \right) s \quad (2.104)$$

$T_o$  can be adjusted until equation 104 gives the best straight line, then  $k$  and  $n$  can be estimated from the slope and the intercept of the plot.

#### (b) Decreasing backmix zone followed by plug-flow (figure 4c2)

The U-functions can be found by letting  $n \rightarrow \infty$  in equations 97 to 99 and adding a term for the plug-flow part:

$$U_0 = - \int_0^{\infty} \ln(1 + k^n T_0 s) \, dn - T_p s + \ln k \quad (2.105)$$

$$U_1 = \frac{-\ln(1+T_0 s)}{s \ln k} + T_p \quad (2.106)$$

$$U_2 = \frac{-\ln(1+T_0 s)}{s^2 \ln k} - \frac{T_0}{s \ln k \cdot (1+T_0 s)} \quad (2.107)$$

$U_0$  can also be written as the integral of  $U_1$ , in the form:

$$U_0 = \frac{1}{\ln k} \int_0^{T_0 s} \frac{\ln(z+k)}{z} \, dz - T_p s + \ln k \quad (2.108)$$

The integral is the dilogarithmic function, which has been investigated and tabulated elsewhere<sup>(A4)</sup>.

This is again a three-parameter model ( $T_0$ ,  $k$ ,  $T_p$ ). The parameters can be found by plotting

$$\frac{1}{U_1 - T_p - sU_2} = (-\ln k)s - \frac{\ln k}{T_0} \quad (2.109)$$

(an equation obtained by combining 106 and 107), with various  $T_p$ , until the best straight line is obtained, then calculate  $k$  and  $T_0$  from the slope and the intercept. A first estimate of  $T_p$  is easily obtainable by visual examination of the response curve.

### III.3.4 Backflow cell model (Figure 4d)

This model consists of a series of equal-size stirred tanks with backward as well as forward flow. It has been used to represent the behaviour of systems wherein mixing occurs as a result of turbulent eddying, such as packed beds<sup>(S3)</sup>. Its established properties are listed below:

$$\bar{t} = \tau = n T_o \quad (2.110)$$

where  $n$  is the number of cells and  $T_o$  the holding time per cell for all passes (i.e. the cell volume divided by the net flow through the system)

$$\sigma^2 = \sigma_t^2 / \tau^2 = \frac{1+2b}{n} - \frac{2b(1+b)[1-(\frac{b}{1+b})^n]}{n^2} \quad (2.111)$$

where  $b$  is the backward flow rate as a fraction of the net flow rate into (or out of) the system.

For  $n \gg 1$ ,

$$\sigma^2 \approx \frac{1+2b}{n} \quad (2.112)$$

The transfer function, neglecting recycling effects at the inlet, is given by:

$$\mathcal{F}^*(s) = K \left\{ \frac{1}{2b} (1 + 2b + T_o s - \sqrt{1 + 2T_o s(1+2b) + T_o^2 s^2}) \right\}^n \quad (2.113)$$

from which

$$U_o = \ln K + n \ln(1+2b+T_o s - \sqrt{1 + 2T_o s(1+2b) + T_o^2 s^2}) - n \ln(2b) \quad (2.114)$$

$$U_1 = \frac{n T_o}{\sqrt{1 + 2(1+2b) T_o s + T_o^2 s^2}} \quad (2.115)$$

$$U_2 = \frac{n T_o^2 (1+2b+T_o s)}{(1 + 2(1+2b) T_o s + T_o^2 s^2)^{3/2}} \quad (2.116)$$

After rearrangement, equations 115 and 116 give:

$$\frac{U_2}{U_1^3} = \frac{s}{n^2} + \frac{1+2b}{T_o n^2} \quad (2.117)$$

$$\frac{1}{U_1^2} \left(1 - \frac{U_2 s}{U_1}\right) = \left(\frac{1+2b}{T_o n^2}\right) s + \frac{1}{T_o n^2} \quad (2.118)$$

which can be plotted for parameter finding in the usual manner.

Note the redundancy (two slopes plus two intercepts, three unknowns)



which allows the validity of the model to be checked as in the case of the tanks-in-series-and-plug-flow model.

The model can be extended to include a plug flow  $T_p$  in series. Equations 117 and 118 can still be used to find the parameters, except that  $U_1$  must be replaced by  $(U_1 - T_p)$  where  $T_p$  is adjusted to give the best straight lines.

### III.3.5 Second-order model (figure 4e)

This model, consisting of two stirred tanks in series (with holding times  $T_1$  and  $T_2$  respectively), is frequently mentioned in the literature, especially in the field of automatic control, and will be studied briefly here. It can be shown that:

$$\mathcal{J}^*(s) = \frac{K}{(T_1 s + 1)(T_2 s + 1)} \quad (2.119)$$

$$U_0 = \ln(T_1 s + 1) - \ln(T_2 s + 1) + \ln K \quad (2.120)$$

$$U_1 = \frac{T_1}{1 + T_1 s} + \frac{T_2}{1 + T_2 s} \quad (2.121)$$

$$U_2 = \frac{T_1^2}{(1 + T_1 s)^2} + \frac{T_2^2}{(1 + T_2 s)^2} \quad (2.122)$$

The C-curve is given by:

$$C_t = \frac{\exp(-t/T_1) - \exp(-t/T_2)}{T_1 - T_2} \quad (2.123)$$

For parameter finding, equations 121 and 122 give:

$$\left( \frac{2}{U_1^2 - U_2} - s^2 \right) = \frac{T_1 + T_2}{T_1 T_2} s + \frac{1}{T_1 T_2} \quad (2.124)$$

which can be plotted as a straight line. If a plug flow element  $T_p$  is present,  $U_1$  must be replaced by  $(U_1 - T_p)$ , and  $T_p$  can be adjusted

to give the best straight line in the usual manner.

#### IV      CONCLUSION

It can be seen that, although Transfer-function methods are not applicable to all possible models, they can incorporate up to four parameters. The models developed in this chapter were considered because they appeared relevant to the present equipment; no doubt other models can be investigated on this line.

For models that are not amenable to the graphical methods just described, the transfer- and U-functions can still be a useful way to minimise tailing problems<sup>(M12, M13)</sup>.

The use of transfer-function methods will be illustrated in the next two chapters.

NOTATION FOR CHAPTER 2

- $A$  amplitude ratio, [ - ]  
 $b$  recycle ratio in backflow cell model, [ - ]  
 $c$  concentration in arbitrary units  
 $C$  impulse response in terms of reduced time  $\theta$ , [ - ]  
 $C_t$  impulse response in terms of time  $t$ , [  $s^{-1}$  ]  
 $D$  axial dispersion coefficient, [  $m^2/s$  ]  
 $E$  exit age distribution in terms of reduced time  $\theta$ , [ - ]  
 $E_t$  exit age distribution in terms of time  $t$ , [  $s^{-1}$  ]  
 $f_j$  fraction of total flow going to the  $j$ -th branch in a parallel arrangement, [ - ]  
 $F$  step response in terms of  $\theta$ , [ - ]  
 $F_t$  step response in terms of  $t$ , [ - ]  
 $\mathcal{F}$  normalised transfer function, [ - ]  
 $\mathcal{F}^*$  unnormalised transfer function, in arbitrary units.  
 $H(t)$  unit step function, [ - ]  
 $i$   $\sqrt{-1}$   
 $I$  internal age distribution in terms of  $\theta$ , [ - ]  
 $I_t$  internal age distribution in terms of  $t$ , [ - ]  
 $k$  parameter in diminishing backmix model, [ - ]  
 $K$  proportionality constant of transfer function in arbitrary units.  
 $L$  length of vessel, [  $m$  ]  
 $M_n$   $n$ -th moment of  $C$ -curve, [ - ]  
 $M_{tn}$   $n$ -th moment of  $C_t$ -curve, [  $s^n$  ]  
 $M'_n$   $n$ -th moment of  $C$ -curve about origin, [ - ]  
 $M'_{tn}$   $n$ -th moment of  $C_t$ -curve about origin, [  $s^n$  ]  
 $\mu_n(s)$   $n$ -th moment of the weighted concentration curve about the origin (equation 2.70b), [  $s^{n+1}$   $\times$  concentration unit ]

(Notation for Chapter 2, cont.)

$n$	number of tanks in multi-tank models, [ - ]
	parameter in diminishing backmix model, [ - ]
$s$	Laplace transform parameter, [ $s^{-1}$ ]
$S$	slope of a straight line, [variable units]
$t$	time, [ s ]
$\bar{t}$	first moment of the $C_t$ -curve, [ s ]
$\bar{t}_o$	first moment of the outlet concentration curve, [ s ]
$\bar{t}_i$	first moment of the inlet concentration curve, [ s ]
$T$	holding time of a flow component, [ s ]
$T_t$	holding time of a stirred tank, [ s ]
$T_p$	holding time of a plug-flow component [ s ]
$T_o$	parameter in dimishing backmix model, [ s ]
$u$	fluid velocity, [ m/s ]
$U_o$	function defined by eqn.65, [ - ]
$U_i$	function defined by eqn.66, [ s ]
$U_2$	function defined by eqn.67, [ $s^2$ ]
$v$	volumetric flow through system, [ $m^3/s$ ]
$V$	vessel volume, [ $m^3$ ]
$x$	axial distance, [ m ]
$X$	fraction of reactant unconverted, [ - ]
$X_b$	fraction unconverted in a batch reactor at time $t$ , [ - ]
$Y$	intercept of a straight line on the ordinate axis.

(Notation for Chapter 2, cont.)

$\alpha, \beta$	probabilities associated with flow states A,B respectively in stochastic models, [ - ]
$\delta(t)$	unit impulse function, [ - ]
$\xi$	dimensionless distance, $x/L$ , [ - ]
$\psi$	phase angle in radian, [ - ]
$\pi$	3.14159 ...
$\sigma^2$	second moment of C-curve about $\bar{\theta}$ , [ - ]
$\sigma_t^2$	second moment of $C_t$ -curve about $\bar{t}$ , [ s <sup>2</sup> ]
$\theta$	reduced time, $t/\tau$ , [ - ]
$\bar{\theta}$	first moment of C-curve, [ - ]
$\tau$	holding time or space time, $V/v$ or $L/u$ , [ s ]
$\omega$	angular frequency, [radian/s]

#### Dimensionless numbers

Pe Peclet number,  $uL/D$

#### Superscript

' differentiation  
 - Laplace transform

#### Subscript

A any substance  
 A,B states of a stochastic process  
 i inlet of vessel  
 j j-th vessel (in series flow)  
   j-th branch (in parallel flow)  
 o outlet of vessel

### CHAPTER 3

#### AIR RESIDENCE TIME DISTRIBUTION AND

#### AIR-FLOW PATTERN

##### I. INTRODUCTION

##### II. THEORETICAL BACKGROUND

1. Drying air-flow pattern.
2. Interaction between atomising air and drying air.
3. Expected atomising air R.T.D.

##### III. EXPERIMENTAL DETAILS

1. Tracer kinetics equipment.
2. Velocity and turbulence measurement.

##### IV. EXPERIMENTS CARRIED OUT

##### V. RESULTS AND DISCUSSION

1. Results of R.T.D. measurement.
  1. Response curves.
  2. Moment analysis.
  3. Transfer function analysis.
  4. Convolution of response curves.
  5. Influence of air velocity.
  6. Influence of atomising air rate.
  7. Comparison of atomising and drying air R.T.D's.
2. Velocity and turbulence measurements
3. Flow visualisation results

##### VI. CONCLUSION

##### NOTATION

## I. INTRODUCTION

The performance of a spray dryer is strongly dependent on the flow and mixing patterns of both phases. Previously most information on the air-flow pattern has been obtained from either visual tests or velocity measurements. Residence-time distribution (R.T.D.) tests are attractive alternative studies because of their simplicity and easy practicability in industrial situations. R.T.D. data also lend themselves readily to the quantification of mixing phenomena and of the non-ideality of flow patterns.

Previous works on the R.T.D. of the air in spray dryers are few: one can quote Paris et al.<sup>(P2)</sup>, Place et al.<sup>(P9)</sup> and some unpublished research of industrial workers<sup>(B9)</sup>. In the present work, an attempt will be made to model both the drying air stream and the atomising air jet in the existing dryer, using a random pulse injection combined with Laplace transform and other data processing techniques described in the last chapter. The changes in the behaviour of the column with changes in drying air and atomising air rates will be studied. R.T.D. modeling will be checked with velocity measurements and results from smoke tests. From the data obtained it is hoped that some general remarks on the design and operation of spray dryers can be made.

## II. THEORETICAL BACKGROUND

The theoretical background of R.T.D. modeling in general has been described in the last chapter. Before describing the experiment and its results, however, some speculations will be made on what can be expected concerning the air-flow pattern.

## II.1 Drying air-flow pattern

If entrance effects can be neglected in the drying chamber, axially dispersed plug-flow (A.D.P.F.) will take place at least in part of the dryer. Taylor<sup>(T 3)</sup> derived theoretical expressions for the axial dispersion in infinite pipes. His results can be written as:

$$(a) \text{ Streamline flow: } Pe_D = 192 Sc Re, \quad Re < 2400 \quad (3.1)$$

$$(b) \text{ Turbulent flow: } Pe_D \approx \log_{10} Re - .87, \quad 2400 < Re < 10^6 \quad (3.2)$$

where  $Re$  is the Reynolds number based on the pipe diameter,  $Pe_D$  the Peclet number also based on the pipe diameter, and  $Sc$  the Schmidt number of the fluid. In practice equation 1 has been verified, but equation 2 tends to give high Peclet numbers compared to experimental results<sup>(L6)</sup>, although the trend ( $Pe_D$  increasing with measured Reynolds number) is correct.

Taylor's results, being based on infinite pipes, are not directly applicable to the present equipment, but can serve as a basis for comparison. When the vessel length is finite, entrance and exit effects will modify the flow and turbulence profiles. The use of a closed-ended ADPF model does not improve the situation because of the magnitude of the turbulence changes, and an open-ended ADPF model will serve just as well.

A more realistic model should take into account the change in the turbulence pattern along the vessel. The change may be sudden, as in the tanks-in-series-and-plug-flow (TSPF) model or the second-order and plug flow model, or it may be gradual, in which case the diminishing-backmix model with or without plug flow would be a better approximation (see chapter 2, figure 4c). On the other hand, the backflow-cell model is also a good candidate for describing the large structure of turbulence.



Some insight into the hydrodynamic situation can be obtained by considering the drying chamber, with its sudden expansion at the inlet end, as a jet-stirred vessel, which has been studied before.<sup>(S9,W7,W8)</sup>

In fairly squat vessels (length to diameter ratio  $\leq 3$ ) with a small central orifice at each end through which fluid is injected and withdrawn, the model in figure 1b has been found to apply. Sinclair and McNaughton<sup>(S9)</sup> gave the following expressions for its parameters:

$$T_t/\tau = 1 \quad (3.3)$$

$$p = \frac{2r_o}{k_e L} \quad (3.4)$$

$$\frac{T_p}{\tau} = \frac{k_e L r_o}{D^2} \quad (3.5)$$

where  $\tau$  is the holding time and  $k_e$  is a constant characterising the rate of entrainment of air into the jet, and  $k_e$  has the value of 0.23 for air (Chapter 6, eqn.31).

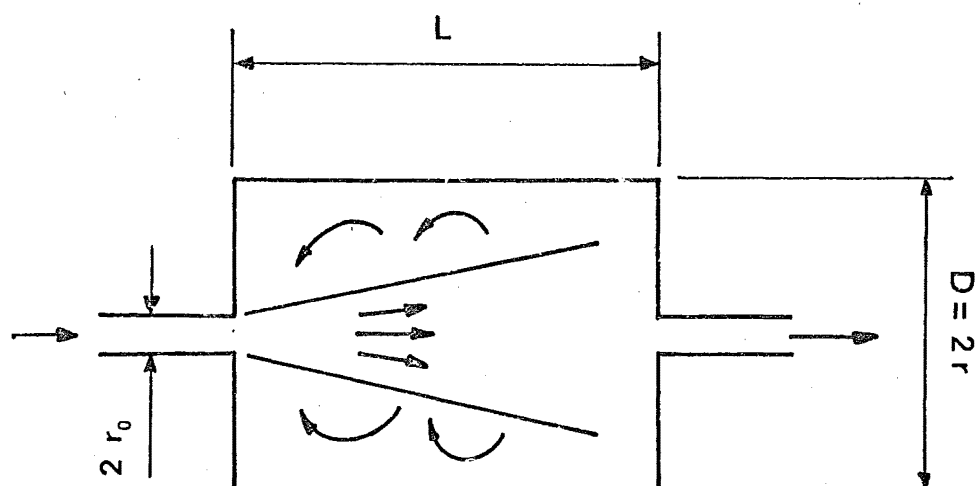
If this model applies to the spray dryer as a whole ( $L = 2200$  mm,  $D = 400$  mm,  $r_o = 25.4$  mm), then from those equations:

$$p = .1$$

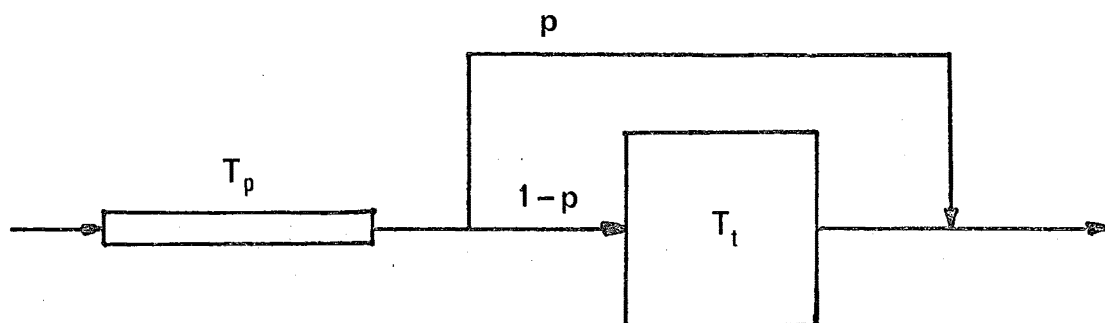
$$T_p/\tau = .08$$

i.e. the whole chamber behaves almost as a single stirred tank.

On the other hand the flow may also settle down to a plug flow pattern before the end of the vessel is reached, in which case  $T_p$  will increase. Furthermore the single-tank approximation would not strictly hold for the high  $r_o/r$  ratio ( $1/8$ ) that is the case on this equipment.



(a) Jet-stirred vessel



(b) Model

FIGURE 3.1: JET-STIRRED VESSEL &amp; MODEL

## II.2 Interaction between the atomising air flow and the drying air stream

Consider first a small jet (representing the atomising air) injected into an external parallel cocurrent stream of air (figure 2). The flow of such a system is governed by the Craya-Curtet number:<sup>(B7,C9,M15)</sup>

$$Ct = \left[ \frac{r_o^2 (u_o^2 - u^2) + u^2 r^2 / 2}{v_t^2 / (\pi r)^2} - \frac{1}{2} \right]^{-1/2} \quad (3.6)$$

It has been found experimentally that if  $Ct < .75$ , recirculation will take place (figure 2c). For the spray drying chamber and nozzle being considered,

$$u/u_o \approx 10^{-3} \quad (3.7)$$

$$r_o/r \approx 10^{-3} \quad (3.8)$$

$$v_t \approx \pi r^2 u \quad (3.9)$$

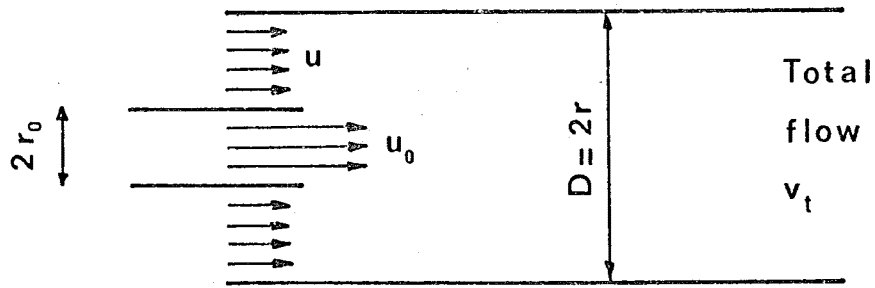
hence

$$Ct \approx \frac{ru}{r_o u_o} \quad (3.10)$$

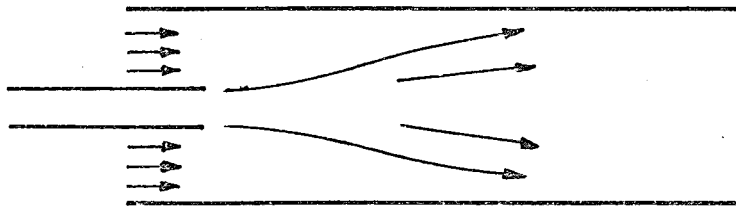
(the square root of a momentum ratio)

Hence in the present case  $Ct$  is proportional to the flow ratio of the drying air to the atomising air. As can be seen from equations 7, 8 and 10,  $Ct$  is of order one and recirculation due to the nozzle may or may not occur.

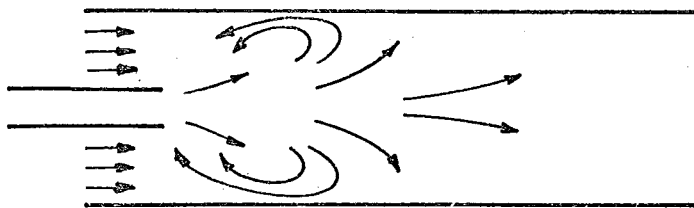
In the actual situation, the external (drying air) flow will not be parallel because of entrance effects. However the previous results may be generalised by saying that the jet effect will become dominant and have an important influence on the drying air flow for small Craya-Curtet numbers (large atomising air rate to drying air rate ratios).



(a)



(b) No recirculation



(c) Recirculation

FIGURE 3.2 : JET IN COCURRENT DUCTED FLOW

### II.3 Expected atomising air R.T.D.

Will the mean residence time of the jet of atomising air be greatly different from that of the drying air ? To predict this, one has to explore the dynamics of jet motion. This subject will be considered in more detail in Chapter 6. For the moment, the following results will be assumed for an air jet into which a tracer of concentration  $c$  is injected <sup>(A3)</sup> (Figure 3) :

$$\begin{aligned} c &= c_m \left[ 1 - \left( \frac{y}{r_j} \right)^{1.5} \right], \quad y < r_j \\ &= 0, \quad y > r_j \end{aligned} \quad (3.11)$$

$$c_m = \frac{9 r_o c_o}{x - 8r_o} \approx \frac{9 r_o c_o}{x} \quad (3.12)$$

$$r_j = 0.22 (x - 8r_o) \approx 0.22 x \quad (3.13)$$

where  $c_m$  is the axis value of the tracer concentration at  $x$  metres from the orifice and  $c_o$  its value at the orifice.

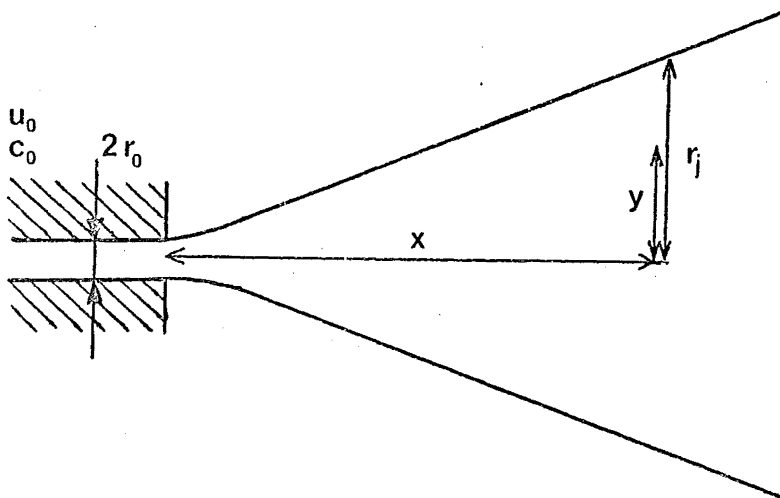


FIGURE 3.3 : SUBMERGED JET

The total amount of tracer in the jet from  $x = 0$  to  $x$  is:

$$m = \int_{x=0}^x \int_{y=0}^{r_j} c(2\pi y) dy dx$$

which, on substituting in equations 11, 12 and 13, gives

$$m = 0.093 \pi r_o^2 c_o x^2 \quad (3.14)$$

The rate of tracer injection is

$$\dot{m} = \pi r_o^2 u_o c_o \quad (3.15)$$

Hence the mean residence time in the jet for the tracer is

$$\tau_{jo} = m/\dot{m} = \frac{0.093 x^2}{u_o r_o} \quad (3.16)$$

The mean velocity of the tracer in the jet is

$$u_j = dx/d\tau_{jo} = \frac{u_o r_o}{0.186 x} \quad (3.17)$$

If the jet is injected into a stream with velocity  $u$ , the two velocities can be superimposed. Hence the mean residence time of the tracer between  $x = 0$  and  $x = L$  is:

$$\begin{aligned} \tau_j &= \int_0^L \frac{dx}{u+u_j} \\ &= \frac{L}{u} - \frac{u_o r_o}{0.186 u^2} \ln\left(1 + \frac{0.186 u L}{u_o r_o}\right) \end{aligned} \quad (3.18)$$

Without the jet, the mean residence time of a tracer in the stream would be  $L/u = \tau$ . Hence the ratio between the mean residence time of the jet and that of the main stream is:

$$\frac{\tau_j}{\tau} = 1 = \frac{\ln(1+\beta)}{\beta} \quad (3.19)$$

where

$$\beta = \frac{0.186 Lu}{u_o r_o} \quad (3.19b)$$

In the present equipment,

$$L = 2200 \text{ mm}$$

$$r_o = 0.9 \text{ mm}$$

$$u_o \approx 350 \text{ m/s}$$

$$u \approx 0.1 \text{ m/s to } 2 \text{ m/s}$$

hence

$$\beta = 0.13 \text{ to } 2.6$$

$$\tau_j/\tau = 0.06 \text{ to } 0.74 .$$

So if the external flow is non-turbulent and parallel, the jet mean residence time can be appreciably lower than the external flow residence time, especially as the external velocity decreases.

Whether this is the case or not in a real situation depends on how the turbulence in the external (drying) air affects the jet:

if the jet is broken up early, then the two R.T.D. will become closer.

### III. EXPERIMENTAL DETAILS

#### III.1 Tracer kinetics apparatus

(a) Pulse injection: The tracer used is Freon-12 (dichloro-difluoromethane,  $\text{CCl}_2\text{F}_2$ ) which is supplied in liquified form in cans under a vapour pressure of 550 kPa at  $20^\circ\text{C}$ . For the drying air, injection is done through a solenoid valve modified to give a narrow pulse (figure 4a). When the valve opens, the pressure on its downstream side increases and a "puff" of Freon is injected into the stream. However, the reverse flow from the air stream to the vacuum is quickly re-established, thus ensuring that the Freon pulse is of short duration. The injection pattern has been found to be highly reproducible, as

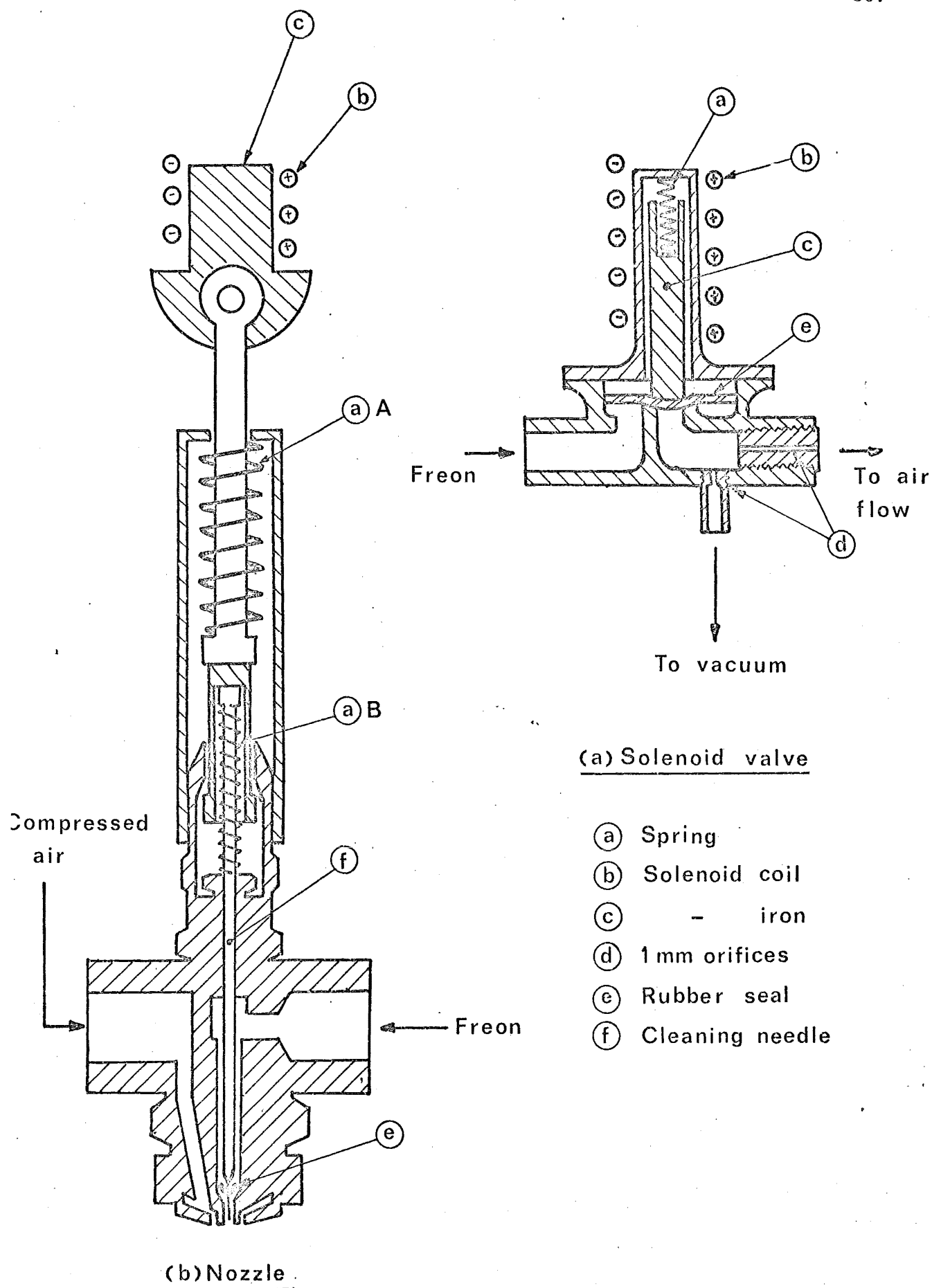


FIGURE 3.4: FREON INJECTION



evidenced by concentration measurements a short distance from the injection point.

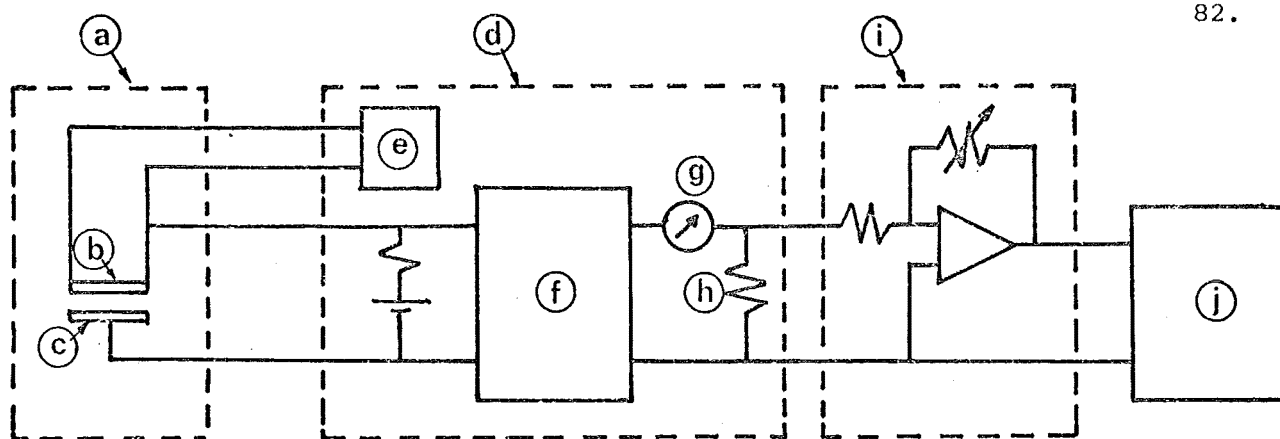
The injection system for the atomising air is shown in figure 4b. The liquid inlet is connected to the Freon and the liquid orifice is normally closed by the cleaning needle with a rubber gasket, the needle being held down by a strong spring A. When the solenoid is activated, it counteracts this spring, and a weak spring B pushes up the needle to let through a pulse of Freon.

The solenoids are activated by a unit pulse generator (manufacturer: General Radio; type: 1217-B) operating through a relay. This relay also sends a pulse to the recorder to mark the injection time (figure 6). The pulse duration can be varied from 1  $\mu$ s to 1 s, but in practice pulses of 10 to 60 milliseconds were used.

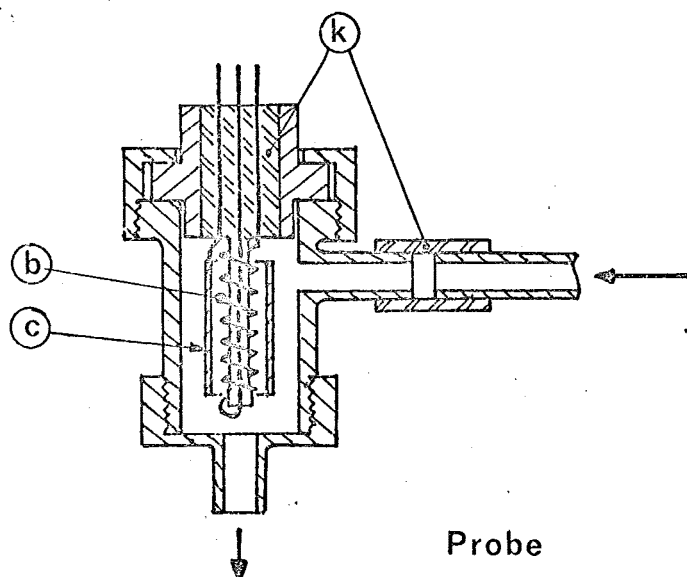
(b) Pulse detection: a Dynavac leak detector (manufacturer: Dynavac High Vacuum Ltd (Australia); type HLD1) is used to monitor the Freon concentration in the air. An air stream is withdrawn from the flow and passes over the probe, which consists of a red-hot platinum anode and a cathode (figure 5). Small amounts of halogen vapour in the air will markedly increase the positive ion emission of the platinum wire, causing a current to flow. The signal is then amplified and fed to a recorder.

The recorder used is a six-channel galvanometric fast-response recorder (manufacturer: Honeywell; type: Visicorder model 1406), which uses beams of ultraviolet light to write on photosensitive paper. It has a maximum chart speed of 635 mm/s (25 in/s) and the frequency response amplitude ratio remains flat to  $\pm 10\%$  up to 200 Hz.

The air flow past the probe is kept constant at about 70 cm<sup>3</sup>/s.



Circuit diagram



Probe

FIGURE 3.5: FREON DETECTION

- a Probe
- b Pt anode
- c Cathode
- d Control box
- e Heating supply
- f Cathode follower
- g Galvanometer
- h 500Ω resistor
- i Operational amplifier
- j Recorder
- k Insulator

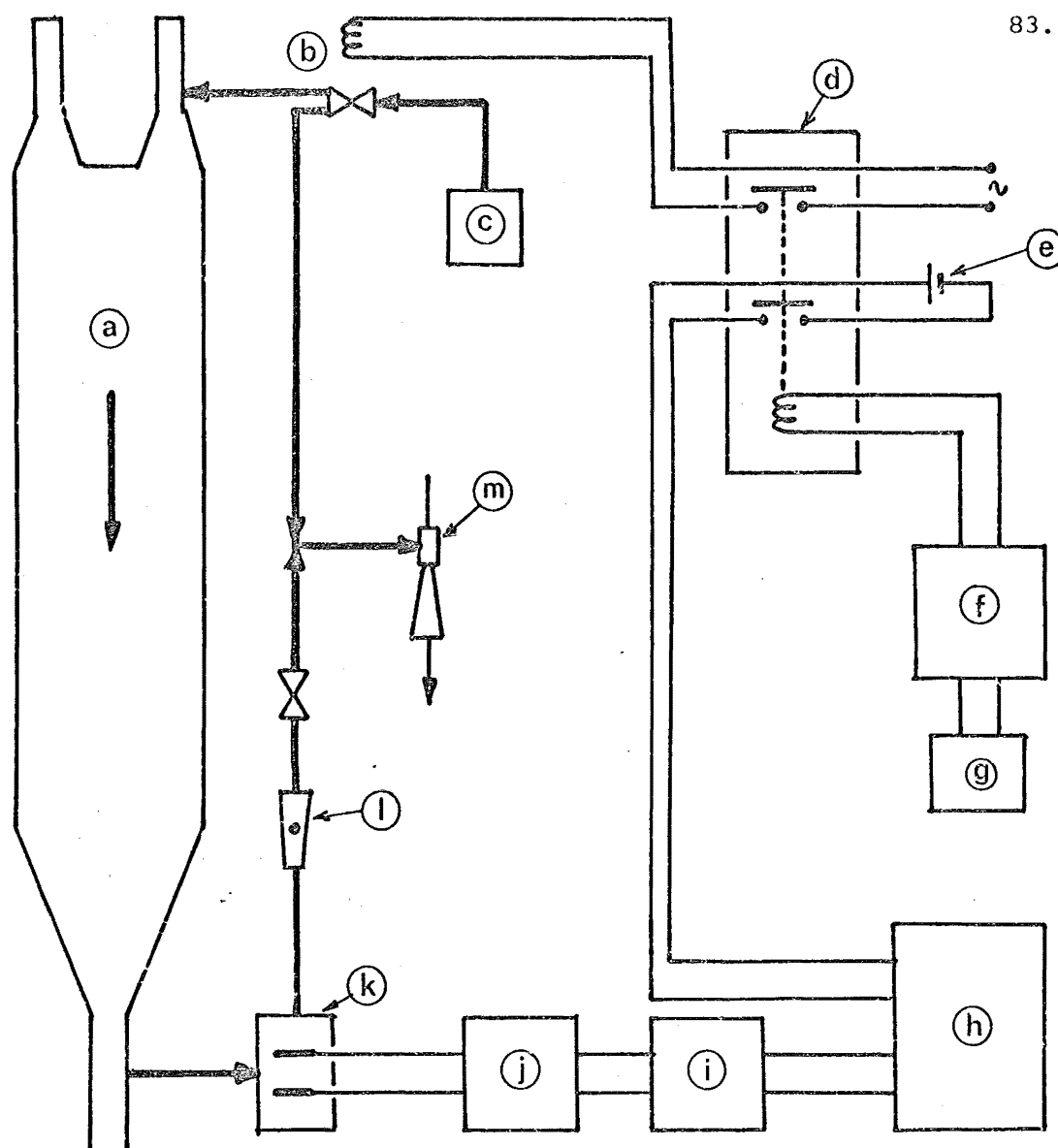


FIGURE 3.6: BLOCK DIAGRAM , AIR RTD EQUIPMENT

- a Dryer
- b Solenoid valve, n.c.
- c Freon
- d Relay box
- e 1.5V cell
- f Unit pulse generator
- g Trigger
- h Multichannel recorder
- i Operational amplifier
- j Dynavac control box
- k Probe
- l Rotameter
- m Water ejector

The total volume of the tubing between the sampling point and the probe, plus that of the probe housing, is estimated to be  $12 \text{ cm}^3$ . Thus the detection system has a time constant of about  $12/70 = 0.17 \text{ s}$ , which is small compared to that of the column (1 to 30 s).

Since the total transfer function of the system between the injection point and the recorder is the product of the transfer function of the drying chamber and that of the detecting system (the latter including the probe housing and all the electronic equipment up to the recorder), the response curve of this detecting system is mathematically equivalent to the "inlet concentration curve" as defined in Chapter 2. It can be measured simply by sampling the air a short distance (5 cm) below the Freon injection point. This was done and the curve obtained was highly reproducible, being independent of the column operating conditions.

### III.2 Velocity and turbulence measurement

A DISA constant-temperature hot-wire anemometer (figure 7) was used to measure the velocity and turbulent profiles in the column. The probes (type DISA 55A22) are made of  $5 \mu\text{m}$  diameter  $\times$  1.2 mm platinum-coated tungsten wire having a resistance of  $3.6 \pm .6 \text{ ohms}$  at  $20^\circ\text{C}$ .

(a) Mean velocity measurement: Detailed descriptions of the theory of hot-wire anemometry can be found elsewhere<sup>(H13)</sup>. In the present work the following equation, based on King's law or Kramer's law, will be used:

$$V^2 - V_0^2 = B\bar{u} \quad (3.20)$$

where  $V$  is the d.c. voltsge across the bridge containing the probe,  $V_0$  its value in quiescent fluid,  $\bar{u}$  the mean fluid velocity and  $B$  is a constant depending on the wire, the fluid and the overheating ratio  $\alpha$ :

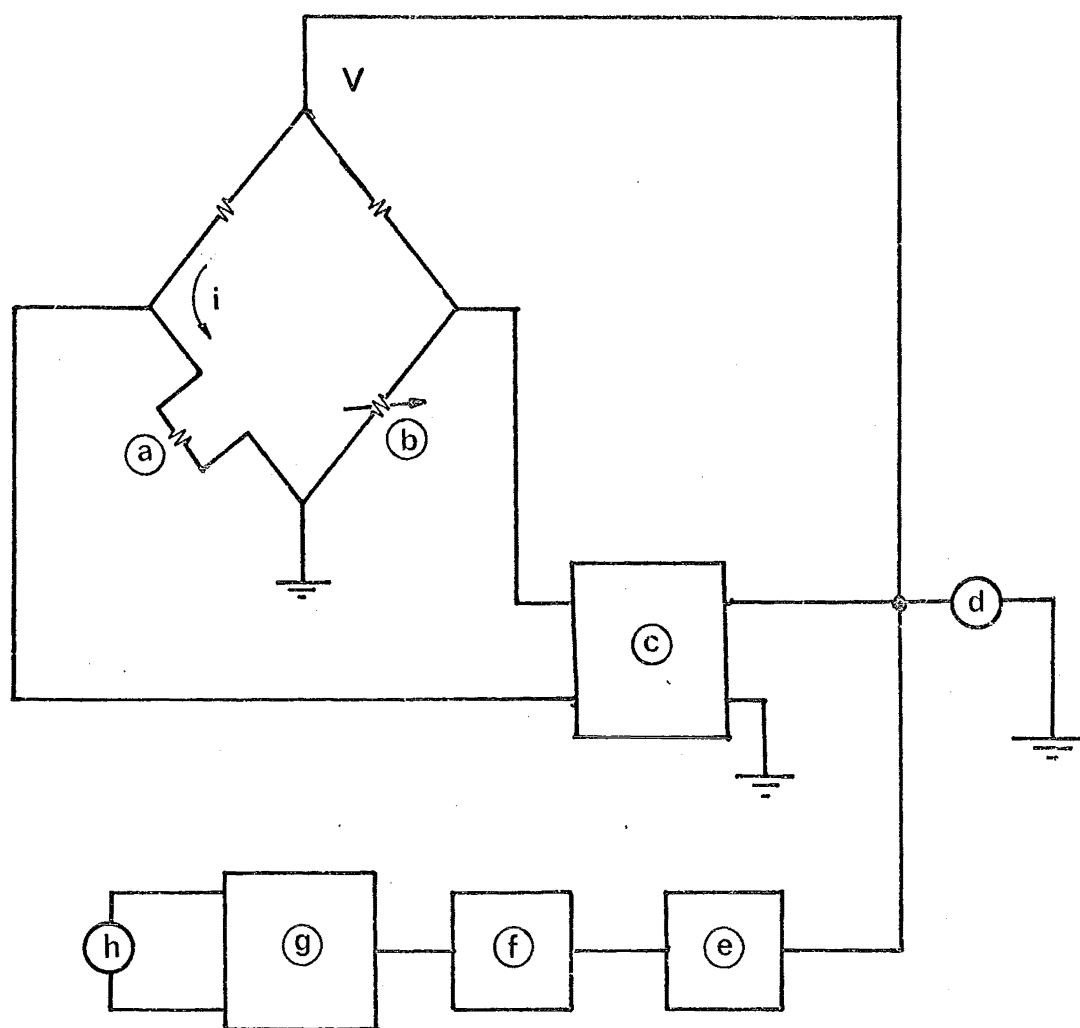


FIGURE 3.7: BLOCK DIAGRAM, HOT-WIRE ANEMOMETER

- a Hot-wire probe
- b Decade resistors
- c Amplifier with transconductance  $g_{tr}$
- d D.c. voltmeter
- e High-pass filter
- f Low-pass filter
- g A.c. amplifier
- h A.c. voltmeter

$$\alpha \equiv (R - R_c) / R_c \quad (3.21)$$

$R$  is the hot wire resistance and  $R_c$  the cold wire resistance, i.e. measured at the fluid temperature.

Several probes were used as they break now and then. For each  $B$  was determined by calibrating the probe in a wind tunnel against a pitot tube. A typical value is  $B = 9.6 \text{ V}^2/\text{m}^2 \text{ s}^{-1/2}$ .

Because of eddies in the air stream, the velocity fluctuates and the d.c. voltage  $V$  cannot be read directly. Instead  $V$  was integrated over an interval of 30 to 120 seconds by means of an electronic integrator.

(b) Turbulence measurement: The relative turbulence intensity,  $u'/\bar{u}$ , where  $u'$  is the root-mean-square turbulent velocity component perpendicular to the wire, can be found by <sup>(D6)</sup>:

$$\frac{u'}{\bar{u}} = \frac{4VV'}{V^2 - V_0^2}$$

where  $V'$  is the rms value of the fluctuations in  $V$ .

The instrument has a high-pass filter ( $5$  to  $10^3$  Hz) and a low-pass filter ( $10^3$  to  $10^5$  Hz) which can be used to give a stepwise spectrum of turbulence. When doing this, the frequency response of the system must be taken into account. A Bode diagram is given by the manufacturer <sup>(D6)</sup> for a particular wire at a few sets of operating conditions. To extrapolate to other situations the following equation <sup>(H13)</sup> can be used:

$$\tau_w \propto \frac{\alpha}{R_o i^2 (1 + 2\alpha R g_{tr})} \quad (3.22)$$

where  $\tau_w$  is the time constant of the anemometer,  $R_o$  is the resistance of the probe at a certain reference temperature,  $i$  the d.c. current through the wire and  $g_{tr}$  the a.c. transconductance of the amplifiers

in the instrument. On the present instrument  $g_{tr} \approx 8$  mho's,  $R \approx 5$  ohms, so that equation (22) simplifies to

$$\begin{aligned} \tau_w &\propto \frac{1}{R_o i^2 R g_{tr}} \\ &\propto \frac{1}{R_o i^2 R} \end{aligned} \quad (3.23)$$

Also on this instrument

$$i = \frac{V}{R+100\Omega} = \frac{\sqrt{V_o^2 + B\sqrt{u}}}{R+100\Omega} \quad (3.24)$$

where  $100\Omega$  is the resistance in series with the hot wire in the bridge circuit of the anemometer (figure 7). Hence,

$$\tau_w \propto \frac{(100\Omega + R)^2}{R_o R (V_o^2 + B\sqrt{u})} \quad (3.25)$$

#### IV. EXPERIMENTS CARRIED OUT

R.T.D. measurements were carried out at 28 drying air-flow rates, but only on 6 of these were the R.T.D. of the atomising gas investigated. The drying air velocity in the chamber varied from 0.055 m/s to 2.2 m/s, the drying air flow rate from  $6.9 \times 10^{-3} \text{ m}^3/\text{s}$  to  $0.276 \text{ m}^3/\text{s}$  (as calculated from the residence-time data). The drying air was not heated, but due to compression its temperature may go up to  $38^\circ\text{C}$  at the higher flow rates.

Nozzle no.2 (Chapter 1, Table 1) was used in all runs except run 1, where nozzle no.1 was used. The atomising air pressure varied from 0 to 380 kPa gauge, and its discharge rate from 0 to  $1.65 \times 10^{-3} \text{ kg/s}$  or  $1.27 \times 10^{-3} \text{ m}^3/\text{s}$  at standard conditions (graphs of atomising air rates can be found in Appendix B.II). No liquid feed was atomised in any run. Since the momentum of the liquid is

negligible when compared with that of the atomising gas (in ordinary operation the two flows are of similar magnitude but the liquid velocity is at most 4 m/s as compared with nearly sonic velocity for the air), it can be assumed that the presence of a liquid flow would not significantly affect the results of the present experiments.

On four runs (runs 5, 9, 14 and 17 in Table 1) velocity and turbulence profiles were measured at the top, middle and bottom of the vessel. The influence of the atomising air jet on the velocity profile and the turbulence spectrum was also investigated (run 17).

A summary of the experiments carried out is shown in Table 1. Henceforth the runs will be referred to by their number in this table and an index denoting the nozzle pressure. For example, run 20b is that done at a drying air velocity of 1.22 m/s and a nozzle pressure of 70 kPa above atmospheric pressure.



TABLE 3.1Operating conditions in air R.T.D. experiments

Run	Air vel./ms <sup>-1</sup>	Whether atomising R.T.D. measured	Atomising pressures used / kPa				
			a	b	c	d	e
1	.055	Y	0	140	205	275	380
2	.055	Y	0	70	180	275	380
3	.077		0	-			
4	.127		0	-			
5	.135		0	69	138	207	345
6	.144	Y	0	69	180	275	380
7	.183		0	-			
8	.23		0	-			
9	.24		0	69	138	207	345
10	.29	Y	0	69	180	275	380
11	.31		0	-			
12	.41		0	-			
13	.45		0	-			
14	.54		0	69	138	207	345
15	.57		0	-			
16	.61	Y	0	69	180	275	380
17	.69		0	69	138	207	345
18	.73		0	-			
19	.95		0	-			
20	1.22	Y	0	69	180	275	380
21	1.27		0	69	138	207	345
22	1.32		0	-			
23	1.57		0	-			
24	1.59		0	-			
25	1.80		0	-			
26	2.16		0	-			
27	2.2		0	-			
28	2.2		0	-			

N.B. Nozzle 2 used in all runs except run 1.

Y = yes.

## V. RESULTS AND DISCUSSIONS

### V.1 Results of R.T.D. measurements

A summary of all the results can be found in Appendix A. All runs were repeated at least once and the average results ( $\bar{t}$ ,  $\sigma^2$ ,  $Pe$  and other parameters) tabulated. In the following section only typical samples will be described and discussed. As there is no qualitative difference between the drying air R.T.D. and the atomising air R.T.D., only the former will be discussed until section V.1.7.

#### V.1.1 Response curves

Some response curves for a medium air flow rate with various atomising pressures are given in Figure 8. There appears to be no qualitative difference between runs done at different drying air rates. At low air rates the base line ( $c = 0$ ) may shift during a run, by as much as 1.5% of the peak value. An exponential decay curve was fitted to the tail of each curve above 3 times the first moment.

Visual examination of the curves show the following points:

- (1) There is a noticeable plug flow section where  $c = 0$ .
- (2) There is as expected a significant effect of the atomising air rate on the drying air R.T.D. This effect will be studied in detail later.

(3) On some of the runs a bypass is observable, as shown by a sharp peak early in the response curve.

(4) There is either some recycling, or non-stationary behaviour, or both, as evidenced by the oscillations in the response. This effect is particularly noticeable at low air velocities (below 0.2 m/s in the column), which is not surprising since the flow always tends to be unstable at or near the transition point (at a velocity of 0.1 m/s, the Reynolds number of the column would be about 3000).

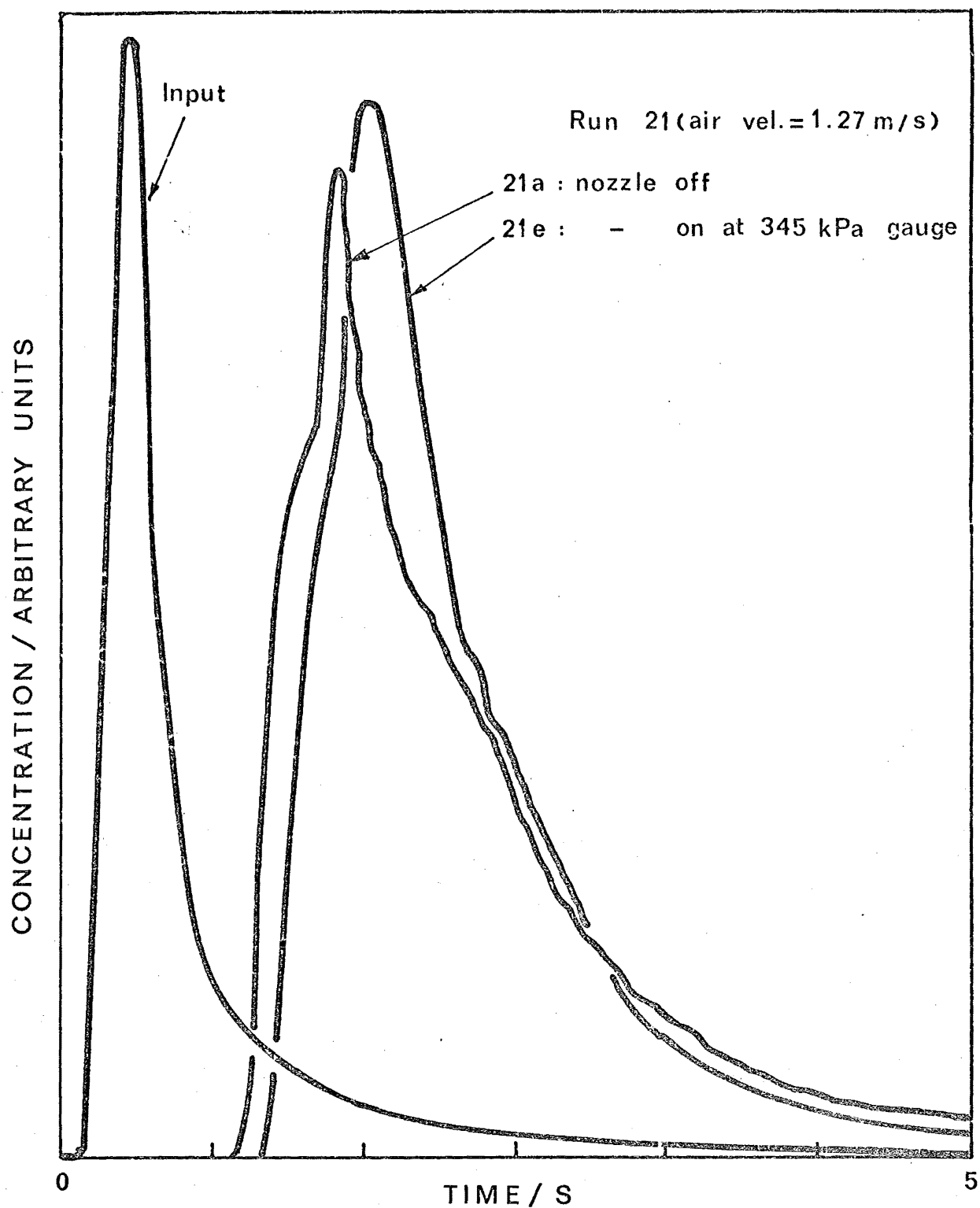


FIGURE 3.8: CONCENTRATION CURVES, DRYING AIR

### V.1.2 Moment analysis

Due to the long tail of both the input and output concentration curves, and the uncertainty in the baseline, it is difficult to apply the method of moments rigorously. The iterative truncation method suggested by Jagota et al.<sup>(J1)</sup> was tried on run 24: the input curve is cut off at an arbitrary time  $t_1$ ; the output curve is cut off at  $t_2^{(1)}$ , and the residence time  $\bar{t}^{(1)}$  is calculated. Then the output curve is truncated at  $t_2^{(2)} = t_1 + \bar{t}^{(1)}$  and a new mean residence time  $\bar{t}^{(2)}$  is found, and so on until  $\bar{t}^{(n)} = t_2^{(n)} - t_1$ . The results are strongly dependent on  $t_1$ :

$$\text{For } t_1 = 5\text{s} , \quad \bar{t} = 1.33 \text{ s}$$

$$\sigma^2 = 0.132$$

$$\text{For } t_1 = 7\text{s} , \quad \bar{t} = 1.43 \text{ s}$$

$$\sigma^2 = 0.249$$

This is not surprising since the truncation method described here cuts off the output concentration curve too early, where it still has a significant value. For the same reason this method invariably gives low values of  $\bar{t}$  and  $\sigma^2$  compared with any of the transfer function methods. The second moment is especially sensitive to changes in  $t_1$ .

### V.1.3 Transfer-function analysis

The models listed in figure 4 of Chapter 2 were tried on the response curves, using the transfer-function methods described in that chapter. Complete results are shown in Appendix A.

#### (a) The axially dispersed plug flow (A.D.P.F.) model:

$U_1^{-2}$  was plotted against  $s$  according to equation 80 of chapter 2, as shown in figure 9. For a true A.D.P.F., the plot should be linear.

It can be seen that this is not the case here. If, nevertheless, the

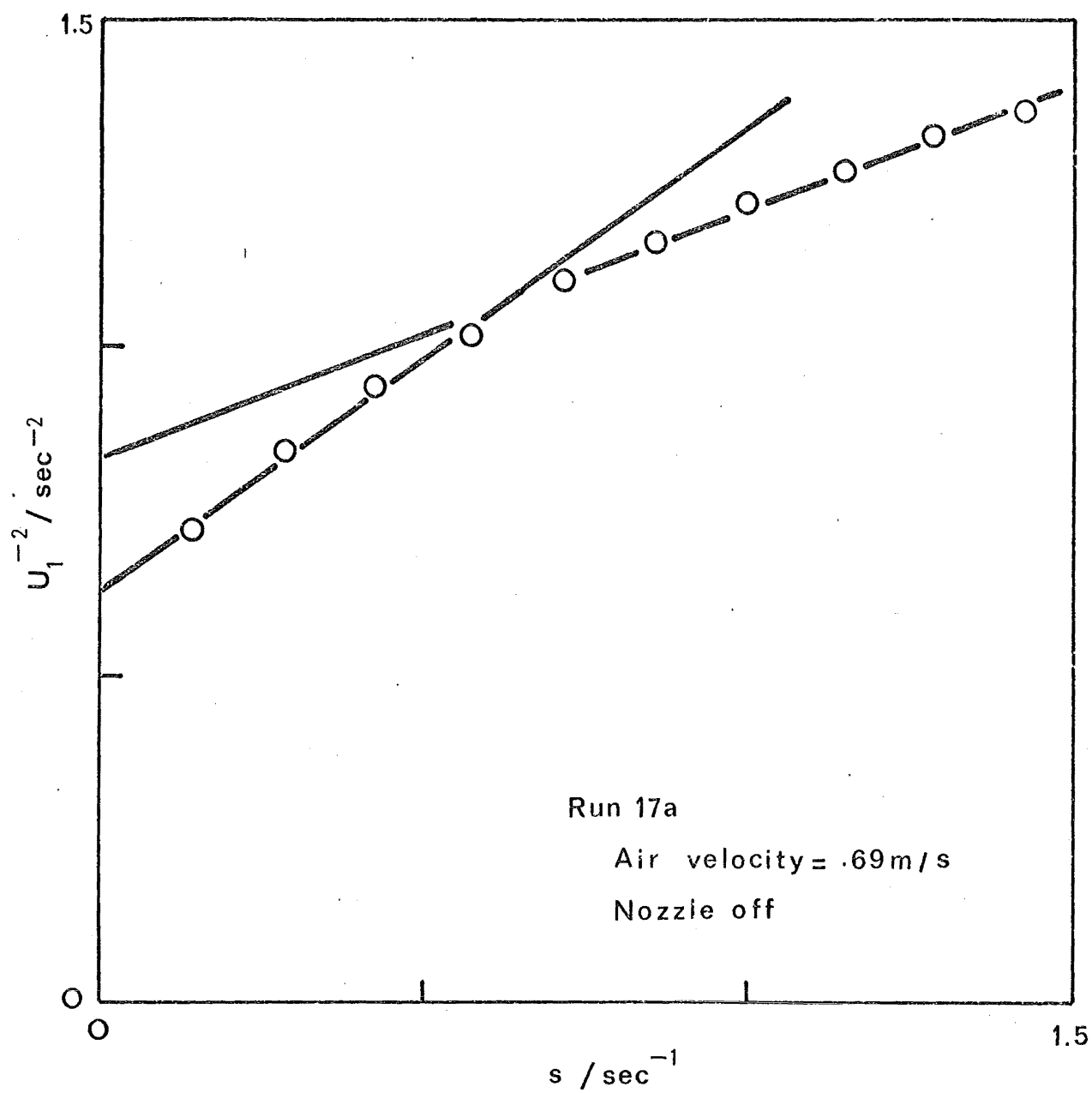


FIGURE 3.9: TRANSFER-FUNCTION ANALYSIS, DRYING AIR;  
ADPF MODEL

model is fitted to the data, a straight line can be drawn through the first 4 points ( $st \approx .5$  to 2) or through the remaining points ( $st \approx 2-5$ ) and the differences will give an estimate of the errors involved. Since  $\tau$  is the inverse square root of the intercept, the error in  $\tau$  is not too large ( $\pm 7\%$  for the case shown) but the error in  $Pe$  is usually much higher ( $\pm 20\%$ ). For the results shown in Appendix A, a range  $st = 0.5 - 2$  were used following Michelson and Østergaard's recommendation<sup>(M13)</sup>.

The curvature of the  $U_1^{-2}$  plots is always negative (concave down), i.e.  $U_1$  decreases with increasing  $s$  more slowly than for true A.D.P.F. flow. This would indicate that there is a plug flow region  $T_p$  in the system (or at least a region with low dispersion coefficient), since  $U_1(s) + T_p$  decreases relatively more slowly than  $U_1(s)$  alone (see Chapter 2, section III.2.3).

Although the model is not strictly valid, it is the only two-parameter model attempted and can still be a useful characterisation of the average degree of backmix in the column.

(b) The second-order-and-plug-flow model (S.O.P.F.)

$\{2/[(U_1 - T_p)^2 - U_2] - s^2\}$  was plotted against  $s$  (Chapter 2, eqn.124) as shown in figure 10. The plug-flow time was measured directly from the response curve. The calculated values of the tank times are 4.54 s and 0.11 s, so that the vessel behaves almost as a single tank with plug-flow in series. However, the graph is not linear and errors in the slope and the intercept are very large (the intercept may be as low as 0, in which case the tank times would be infinite). It was concluded that this model is not useful to the present arrangement.

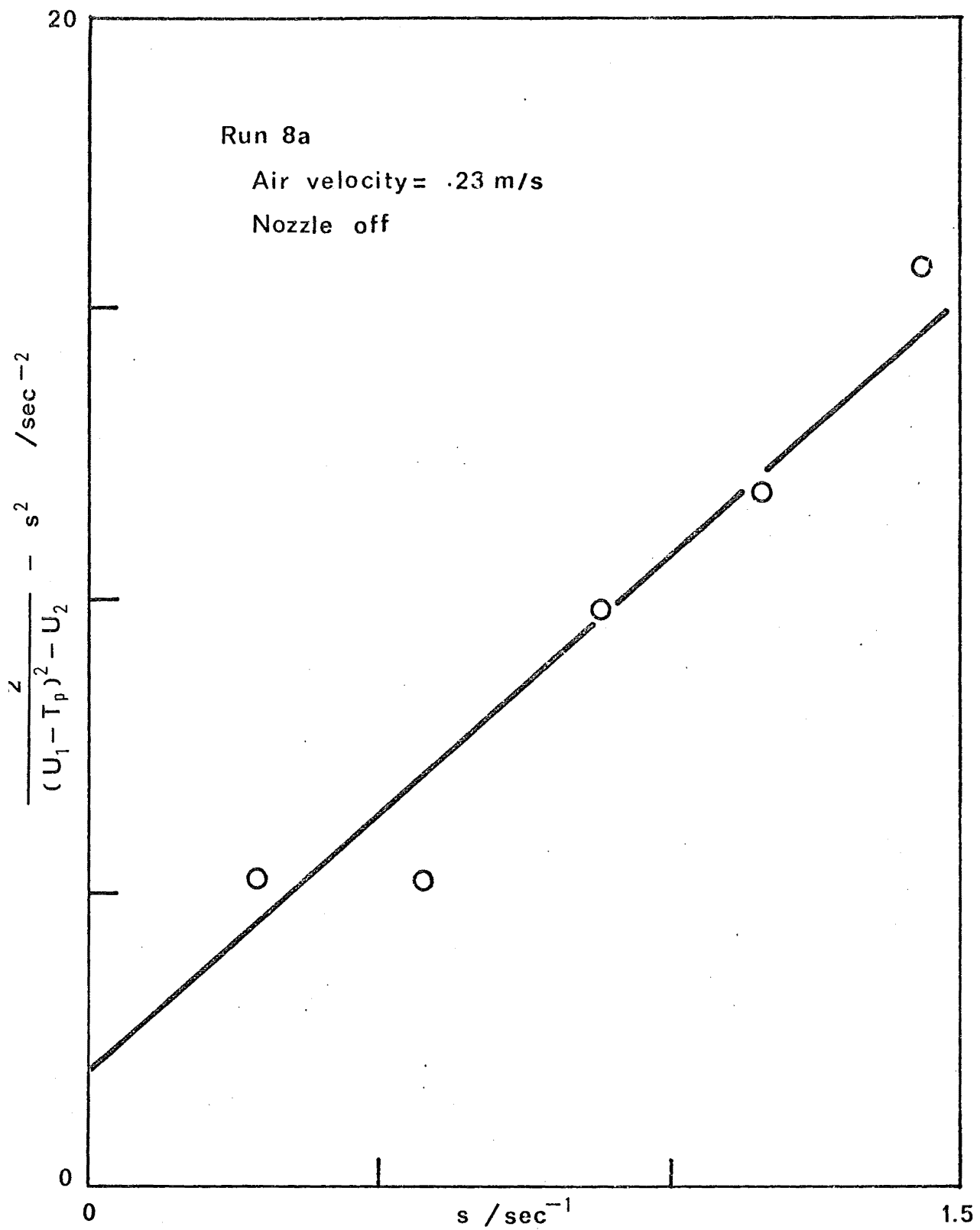


FIGURE 3.10 : TRANSFER-FUNCTION ANALYSIS, DRYING AIR, SOPF MODEL

(c) The tanks-in-series-and-plug-flow (T.S.P.F.) model:

Typical plots of  $U_2^{-1/2}$  and  $U_1/\sqrt{U_2}$  against  $s$  (Chapter 2, equations 87,88) are shown in figure 11. These plots are not straight below  $s = 2$ , but are quite linear above this value. In the time domain this means that the model would predict accurately the response curve at small or negative  $t-T_p$  but would be wrong in the tail region.

At low air rates almost all plots have a positive curvature (concave up) at low  $s$ , i.e. as  $s$  decreases,  $U_2$  increases more slowly than expected for a TSPF model, which would be the case if the tail is smaller than expected. The trend is reversed at high drying air rates. The latter case is probably due to the presence of a deadwater region (a steady eddy) which exchanges tracer slowly with the rest of the vessel. This would not be surprising since at high velocities the jets from the inlets would be more pronounced and able to form a steady eddy near the top of the column. At low velocities, because of the unsteadiness of the flow, no durable eddy can be formed.

It was stated in Chapter 2 that one of the parameters, for example the plug flow time  $T_p$ , can be calculated in two ways (Chapter 2, equations 91 and 92), thus giving a check on the validity of the model. This was done on all runs and typical results are shown in Table 2. It can be seen that the two equations are in agreement to within 0.8%. For all other runs the discrepancies are below 2%.

TABLE 3.2

Plug-flow time of T.S.P.F. model, calculated by two methods

Run	$T_p/s$ (eqn.2.91)	$T_p/s$ (eqn. 2.92)
10a	3.41	3.40
10b	3.30	3.29
10c	2.94	2.92
10d	2.44	2.44
10e	2.40	2.38



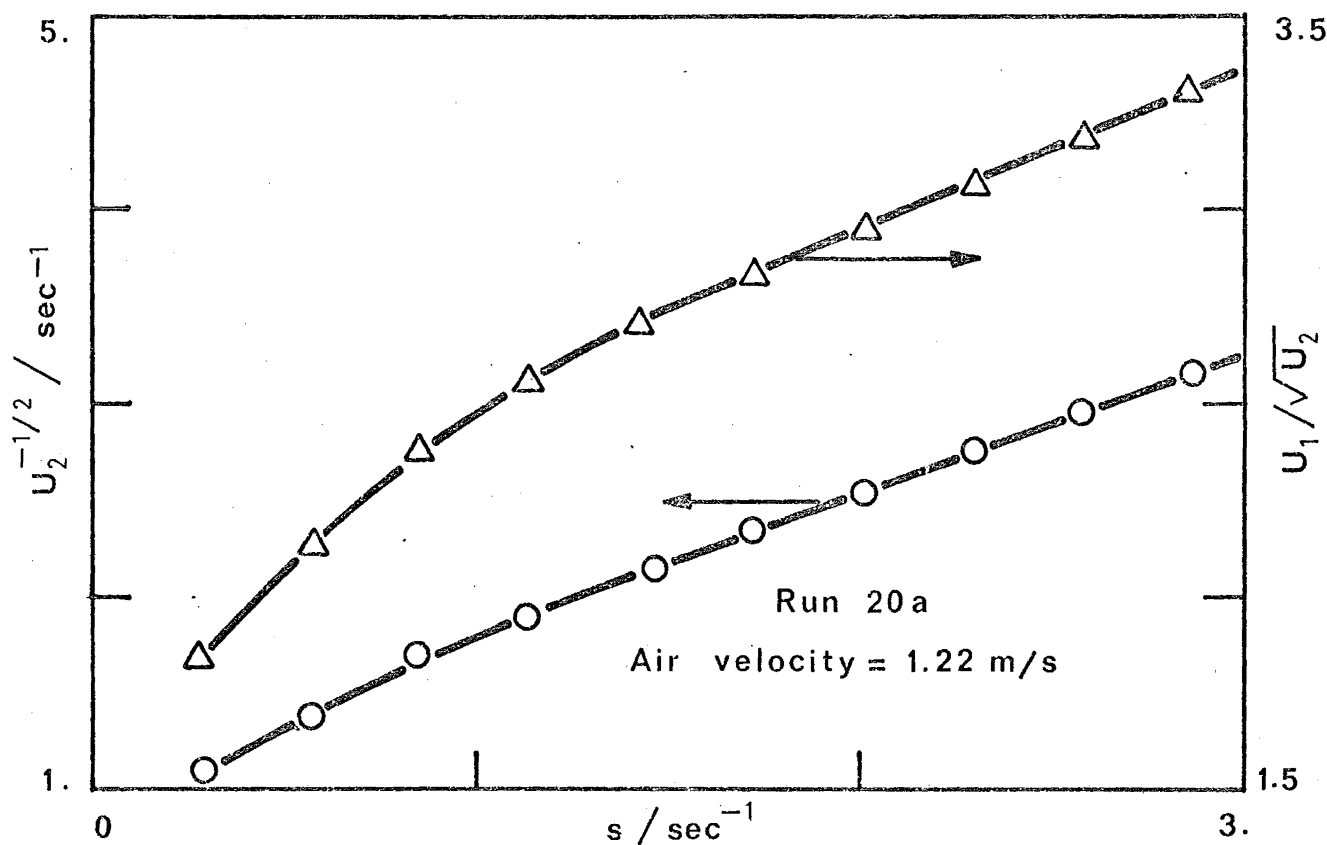
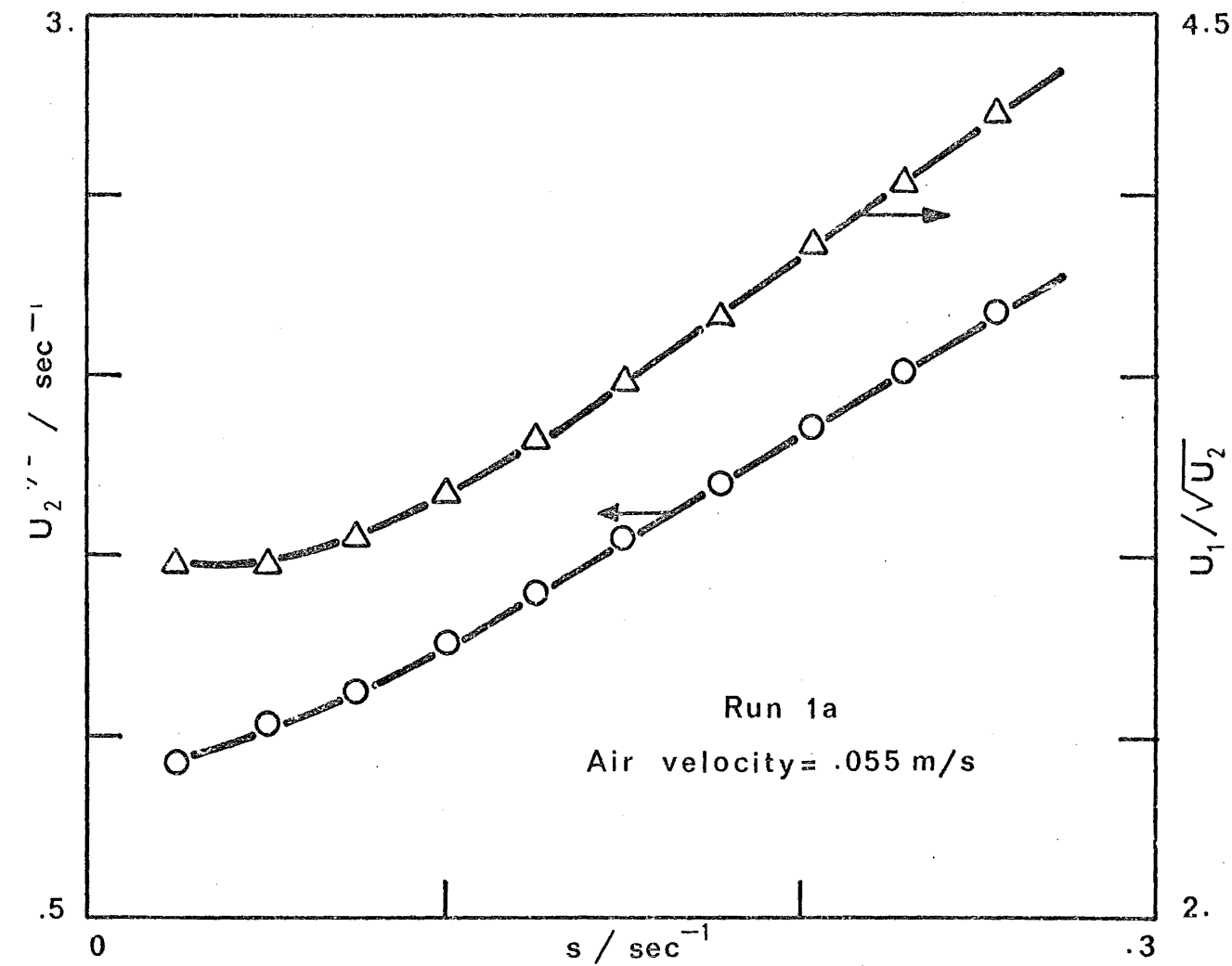


FIGURE 3.11: TRANSFER-FUNCTION ANALYSIS, DRYING AIR, TSPF MODEL

The calculated values of  $T_p$  are plotted in figure 12 against its measured values (on the concentration curves) for a number of runs. The agreement is satisfactory with an error of less than 10% in most cases, the measured values themselves being subjected to errors of 5 or 10% due to the gradual rise of the concentration curves. It is noticed that the larger discrepancies in figure 12 occur when the nozzle is turned on, indicating that the atomising jet tends to disrupt the clear two-zone separation.

In conclusion, it can be said that several facts tend to confirm the T.S.P.F. as a valid model, except possibly for the presence of a deadwater region. It would be interesting to compare the total residence time  $\tau$  as predicted by the A.D.P.F. and the T.S.P.F. models (Table 3). At low air velocities the latter model predicts higher residence time than the former, while the reverse is the case at higher air velocities. This would be explained by the presence of the deadwater region mentioned earlier at high velocities.

TABLE 3.3

Comparison of total residence times according to  
the A.D.P.F. and the T.S.P.F  
models.

Run	$\tau$ (A.D.P.F.) / s	$\tau$ (T.S.P.F.) / s
5a	16.3	17.6
9a	8.9	9.1
14a	4.0	3.9
17a	3.17	3.02
21a	1.73	1.70

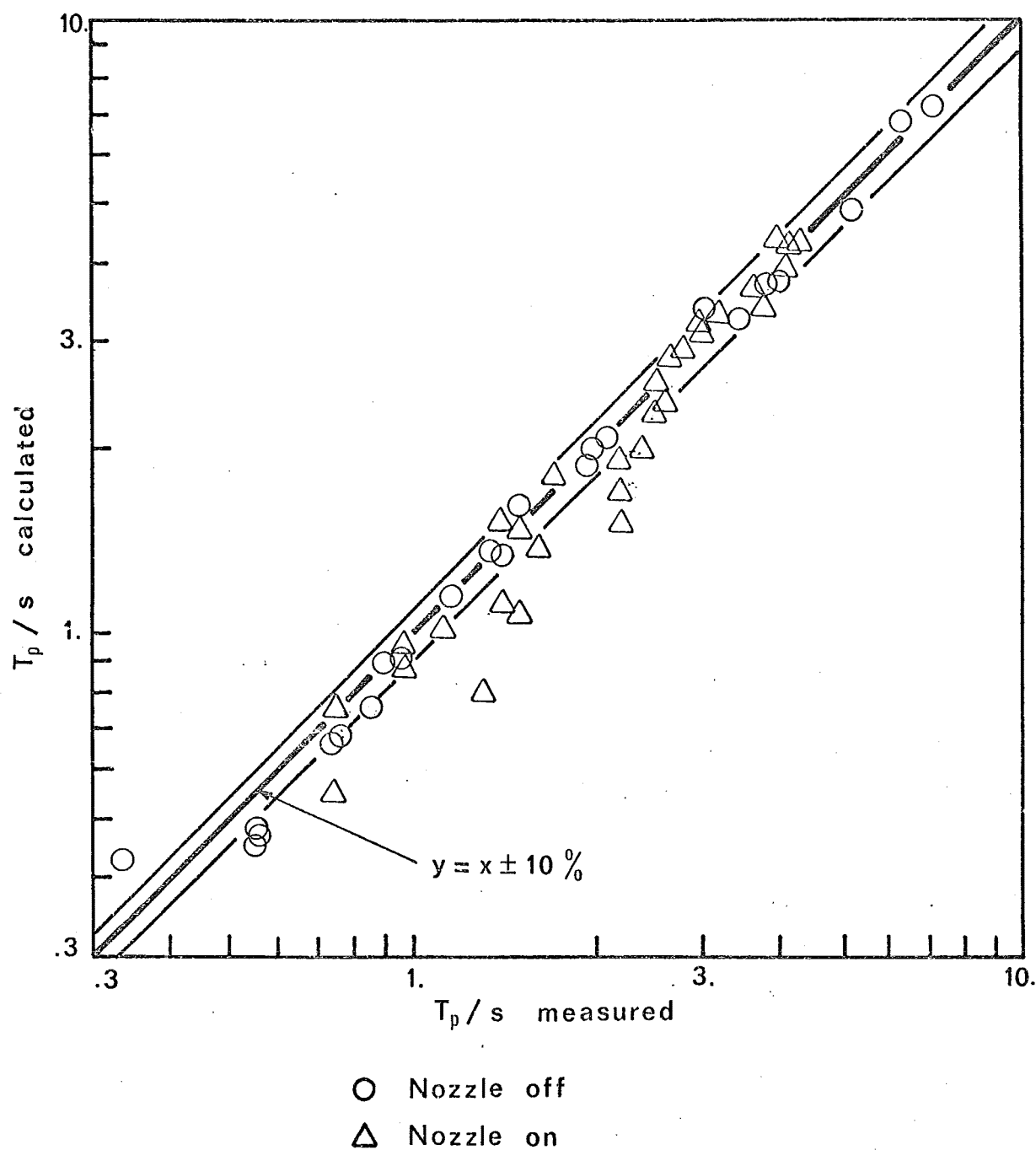


FIGURE 3.12 : CALCULATED VS MEASURED PLUG-FLOW TIME IN TSPF MODEL , DRYING AIR

(d) The dimishing-backmix model (D.B.M)

The D.B.M. model without plug flow was evaluated by plotting equation 104 of Chapter 2 (figure 13). The parameter  $T_0$  must be varied until the best straight line, as measured by the correlation coefficient, is obtained. (This was done automatically with a golden section subroutine on a computer.) Because one parameter is adjusted the method almost always gives good straight lines, but impossible values of the parameters result:  $T_0$  is found in many cases to be negative and  $k$  may be larger than unity. This clearly shows that the model must be ruled out.

The D.B.M. model with plug-flow (Chapter 2, equation 109) gives good results at high air flow rates (air velocities in excess of 0.3 m/s in the dryer) but fails at low air rates. Where it is applicable, the decay parameter  $k$  varies from 0.9 to 0.1 ( $k = 1$  corresponds to pure plug flow), but no trend can be discerned as to the influence of either the drying air rate or the atomising air rate.

Since no significant improvement over the T.S.P.F. model can be found in spite of an extra adjustable parameter, the D.B.M. model was not subsequently used to characterise the flow although it still cannot be ruled out as a valid representation of the flow pattern, at least at high air velocities.

(e) The backflow-cell model with plug-flow in series (B.C.P.F.):

Equations 117 and 118 of Chapter 2 were plotted with  $U_1$  replaced by  $U_1 - T_p$ , where  $T_p$  is adjusted to give the best straight line (figure 14). The range  $st \approx 1$  to 5 was used as consistent results could not be obtained in the lower  $st$  range (the results in that case being too sensitive to  $st$ ). For the runs so analysed (Appendix 1) the values of the recycle  $b$  are small and distributed on both sides of

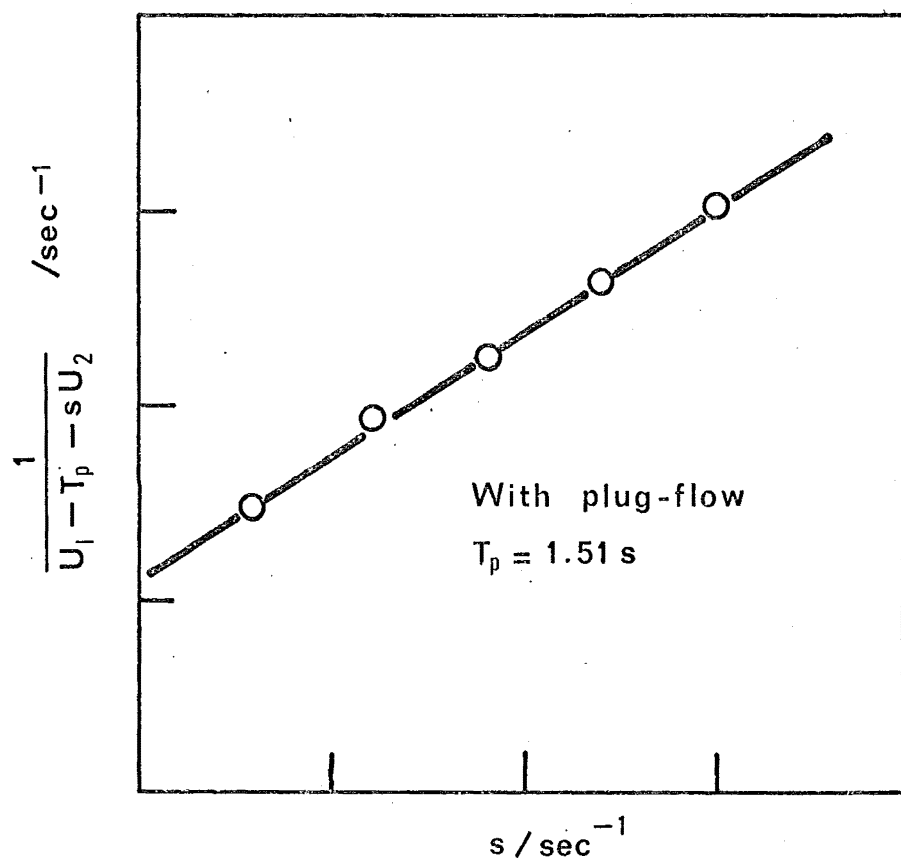
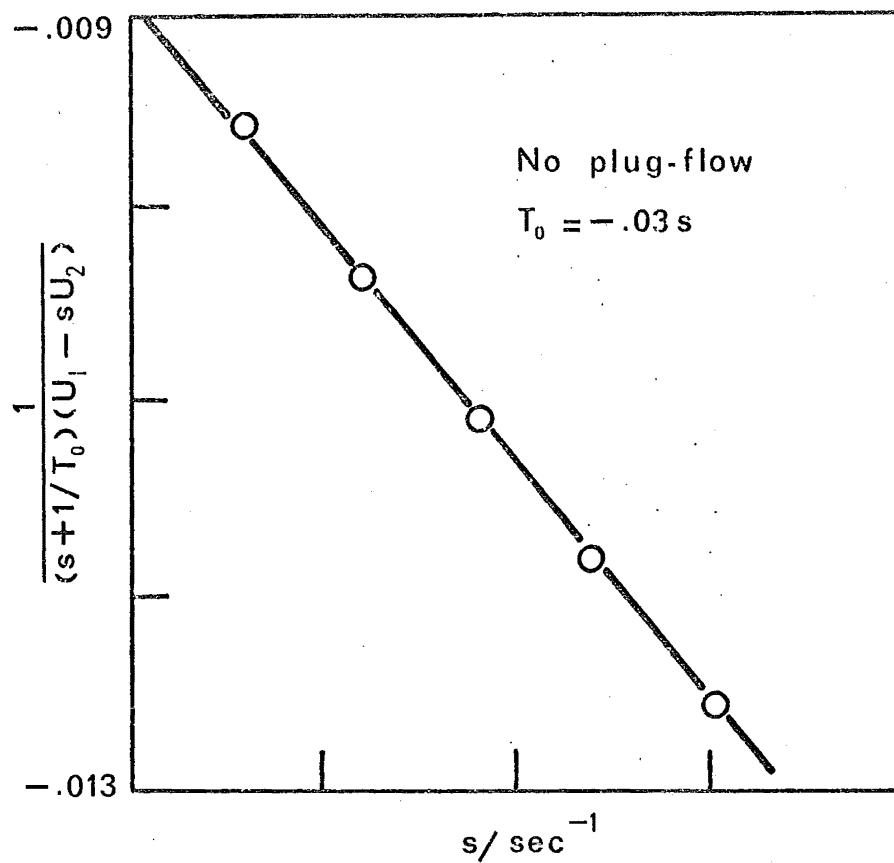


FIGURE 3.13: TRANSFER-FUNCTION ANALYSIS ,  
 DRYING AIR , DBM MODEL

Run 16a , air velocity = .61 m/s

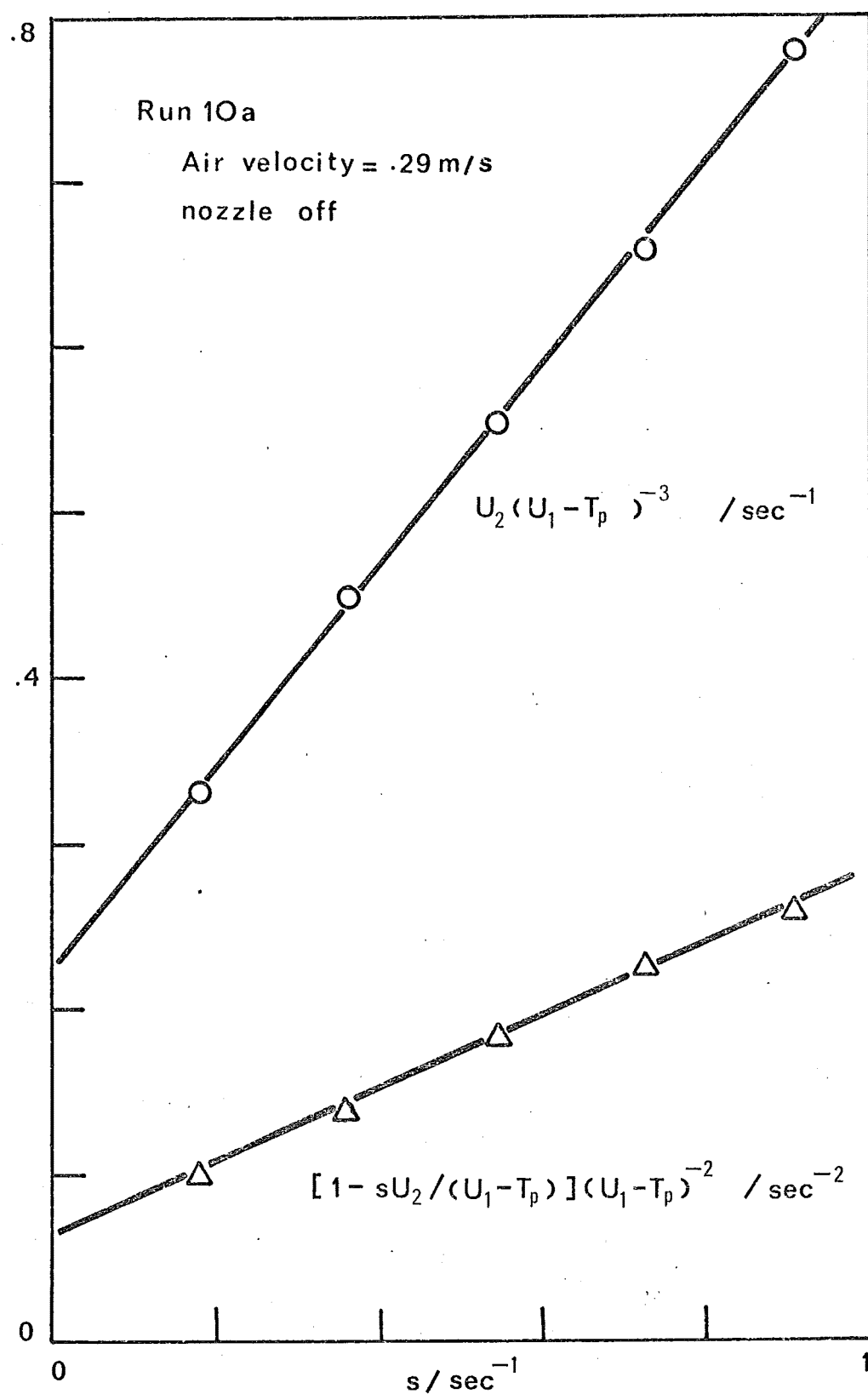


FIGURE 3.14: TRANSFER-FUNCTION ANALYSIS, DRYING AIR, BCPF MODEL

zero. Furthermore they are very sensitive to changes in  $T_p$ , a 5% difference in the latter causing in some cases a 0.2 change in  $b$ . A negative  $b$  indicates bypass, while  $b = 0$  corresponds of course to the T.S.P.F. model. Therefore it was concluded that it is unnecessary to bring in the extra parameter  $b$ , and the T.S.P.F. model is sufficient.

#### V.1.4 Convolution of the response curves.

For the A.D.P.F., T.S.P.F. and S.O.P.F. models, the impulse response (C-) curves are expressible analytically and can be convolved with the input concentration curve to give a predicted outlet response curve. Typical results for the first two models are shown in figure 15. The parameters for each model have been found by transfer-function methods. The results confirm what has been found by transfer function analysis, that the T.S.P.F. is the most accurate representation of the two.

#### V.1.5 Influence of the air velocity on the mixing pattern

(a) Average dispersion: It has already been pointed out that the Peclet number is a measure of the inverse of the average degree of backmixing or dispersion. In figure 16,  $Pe$  is plotted against the mean air velocity in the column,  $u$ , where  $u$  is found by dividing the length of the chamber by the holding time according to the T.S.P.F. model. Also plotted are Taylor's prediction (section II.1) and other workers' data for infinitely long pipes (L6).

The average degree of backmix is nearly insensitive to the air velocity,  $Pe$  has a mean value of 13.9. It may be thought that due to entrance effects  $Pe$  would be much lower than for infinite pipes. However this is not the case, the column Peclet number being slightly

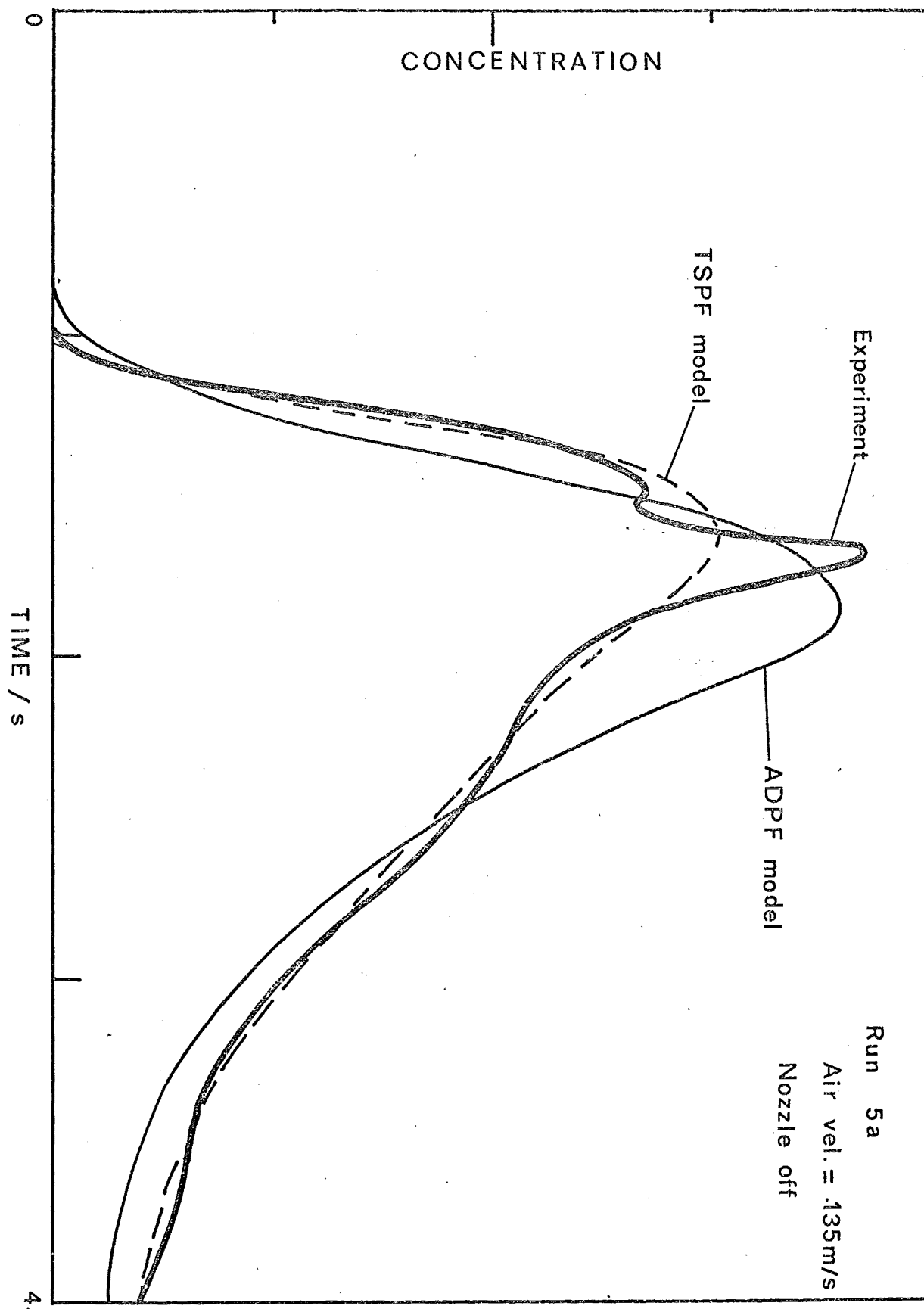


FIGURE 3.15: CONVOLUTION OF DRYING AIR RESPONSE



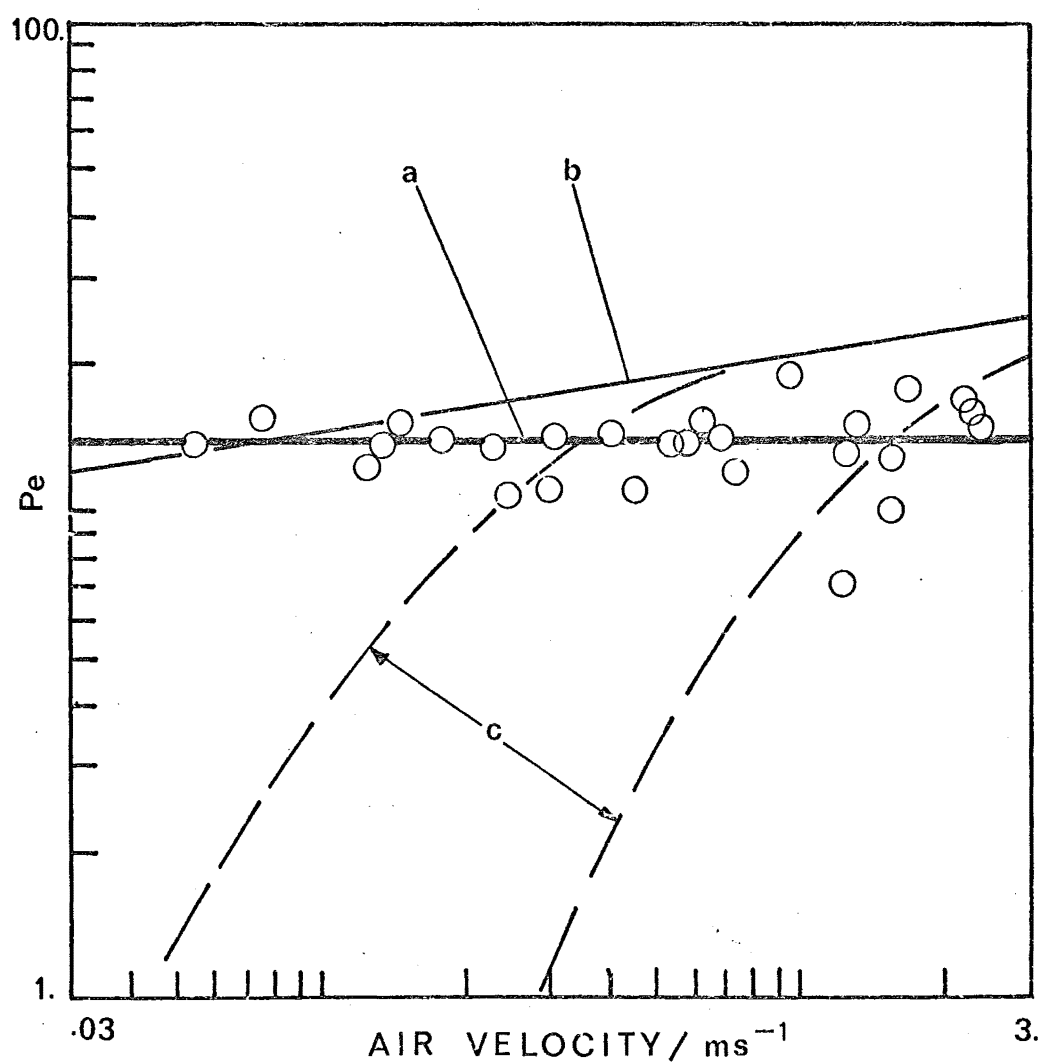


FIGURE 3.16: DEPENDENCE OF DRYING AIR-FLOW PECLET NO. ON AIR VELOCITY IN CHAMBER

- (a) This equipment (nozzle off)
- (b) Taylor's equation,  $\infty$  pipes
- (c) Previous data,  $\infty$  pipes

lower than Taylor's prediction but higher than experimental infinite pipe values. The explanation is that when using the transfer function method one takes  $st \approx 0.5 - 2$  so that less weight has been given to the tail, and the effect of any deadwater region exchanging slowly with the main flow has been minimised. Moment analysis and other standard methods can be considered as special cases of transfer function methods, with  $st = 0$ .

(b) T.S.P.F. model parameters: The number of tanks,  $n$ , and the relative plug flow time,  $T_p/\tau$ , are plotted against  $u$  in figure 17.  $n$  varies from 1 to 3 with an average of 1.9. No influence of  $u$  can be observed on  $n$ .

The fractional values of this parameter may be difficult to relate to physical reality. Stokes and Nauman (S19) interpreted this as a series of tanks with some bypassing. The appearance of the response curve and the results of the backflow-cell model (negative recycle ratios  $b$ ) seem to confirm this. Another explanation may be that the flow is stochastic (Chapter 2, section I.2.3) and the value obtained for  $n$  is simply an average of several flow states.

$T_p/\tau$  has an average value of 0.45. It appears to increase slightly as the velocity increases, to a maximum near  $u \approx 1$  m/s, then decrease again. Perhaps at low velocities the flow is inherently unstable, being near the transition point (see section IV.1.1), while at very high velocities the momentum of the "jets" of air from the inlet carries them further down and extends the stirred zone.

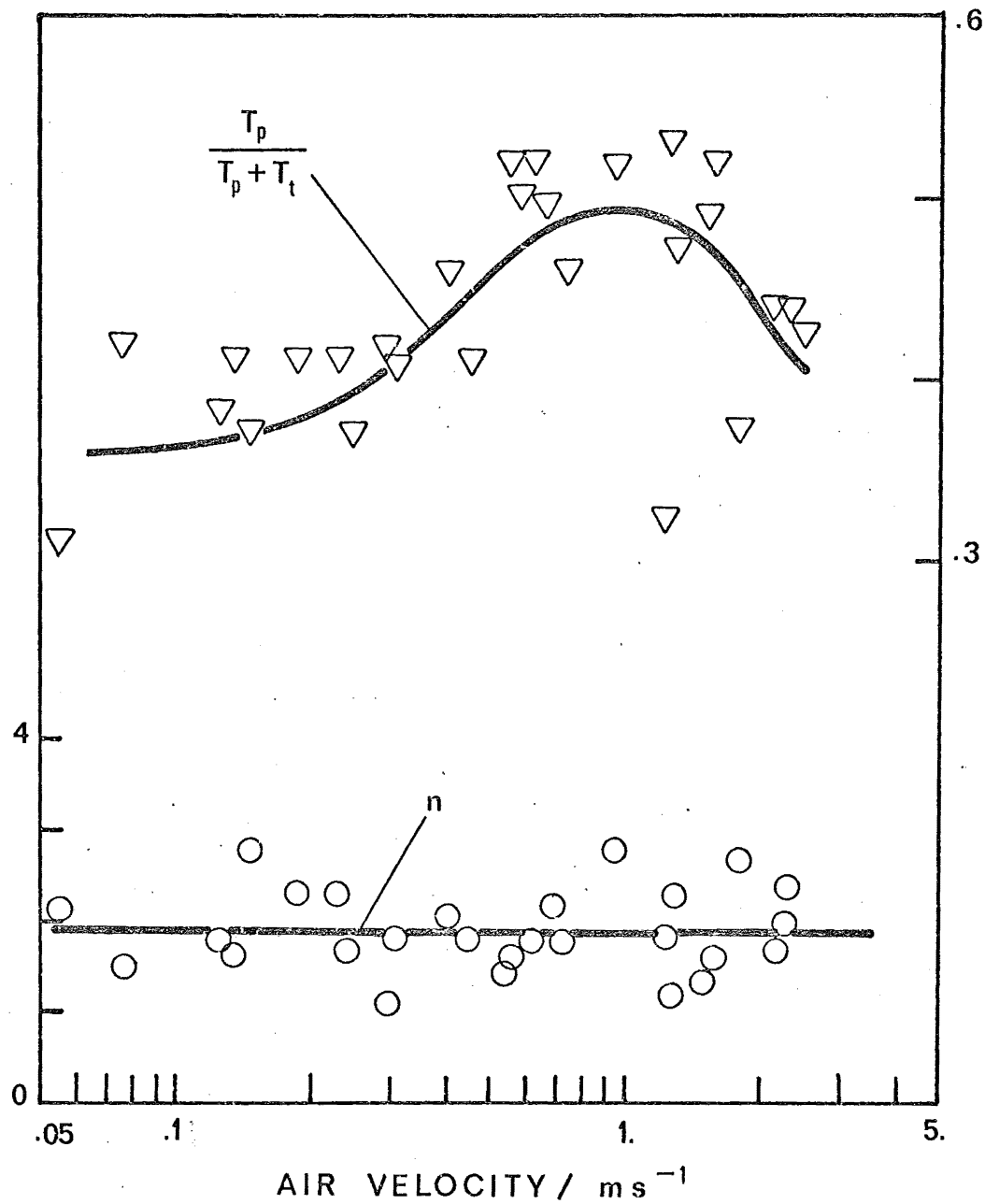


FIGURE 3.17: DEPENDENCE OF TSPF PARAMETERS ON AIR VELOCITY IN CHAMBER

### V.1.6 Influence of the atomising air flow rate on the backmixing pattern

When the atomising air is turned on, a surprising effect is noticed: the Peclet number at first climbs sharply, sometimes to a value as high as 100, then decreases again to below its initial value. In figure 18,  $Pe/Pe_0$  is plotted against  $R_u$ , where  $Pe_0$  is the Peclet number at zero atomising air flow and  $R_u$  is the ratio of atomising air flow to main air flow.  $Pe/Pe_0$  reaches a maximum of 2.4 at  $R_u = 0.018$ .

How can the introduction of a disturbance drastically decrease the dispersion? To find an answer, the T.S.P.F. parameters were plotted against  $R_u$  (figure 19). It can be seen that both  $n$  and  $T_p/\tau$  have a maximum, although each takes place at a slightly different point:

$R_u = 0.018$  for  $n$ ,  $R_u = 0.012$  for  $T_p/\tau$ . Since the relative dispersion of this model is given by: (Chapter 2, section III.2.3)

$$\begin{aligned}\sigma^2 &= U_2(0) / [U_1(0)]^2 \\ &= \frac{(1 - T_p/\tau)^2}{n}\end{aligned}\tag{3.25}$$

this would explain the trend in figure 17; the backmix region near the entrance is first broken up into small eddies which therefore decay more rapidly. However, as the atomising air rate increases further, it creates more turbulence and disturbance, and  $Pe$  decreases again (figure 20).

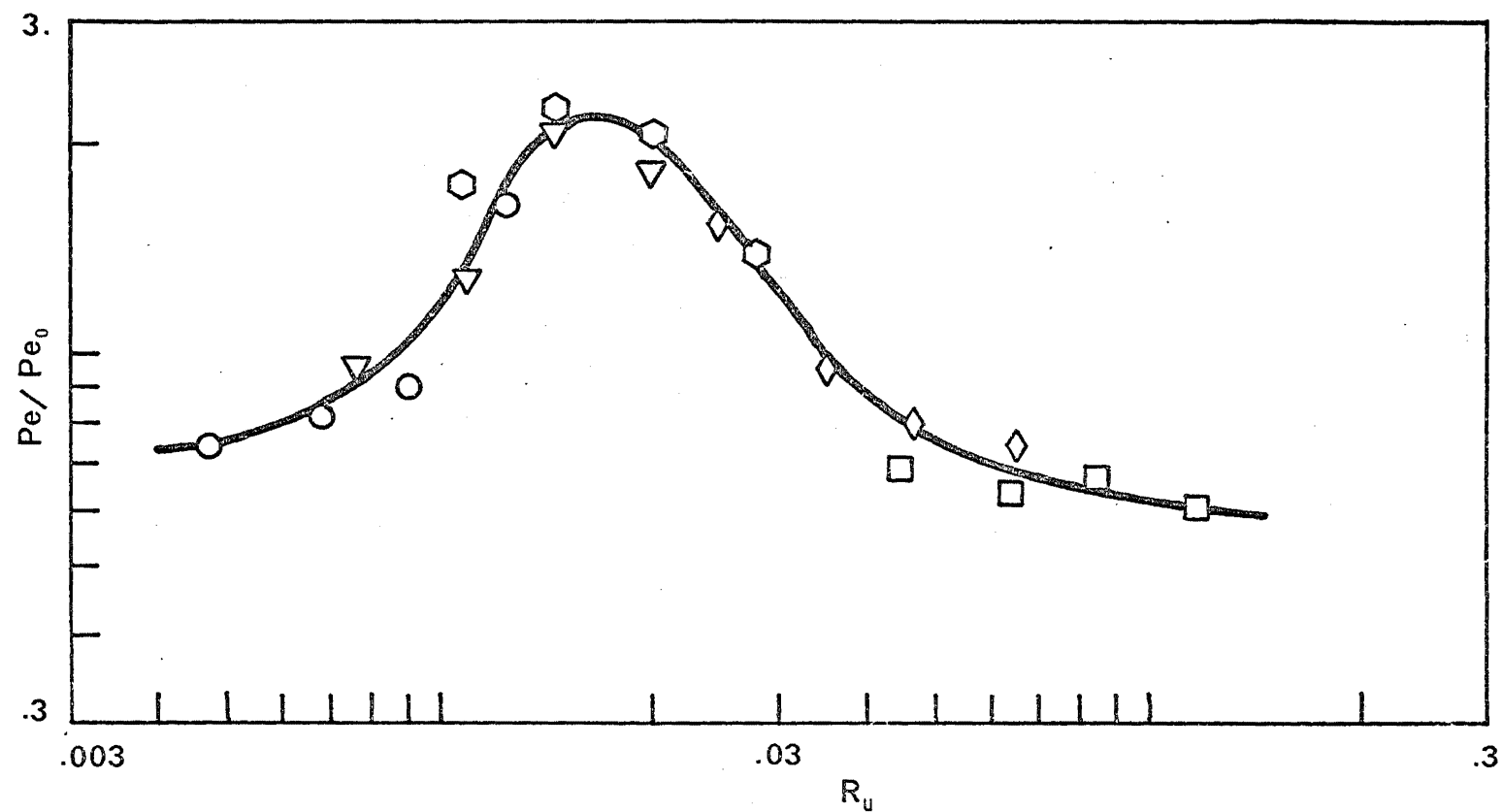


FIGURE 3.18: DEPENDENCE OF PECLET NO. ON THE AIR RATE RATIO  $R_u$

	Run	Air velocity/ms <sup>-1</sup>
□	5	.135
◇	9	.244
◻	14	.54
▽	17	.69
○	21	1.27

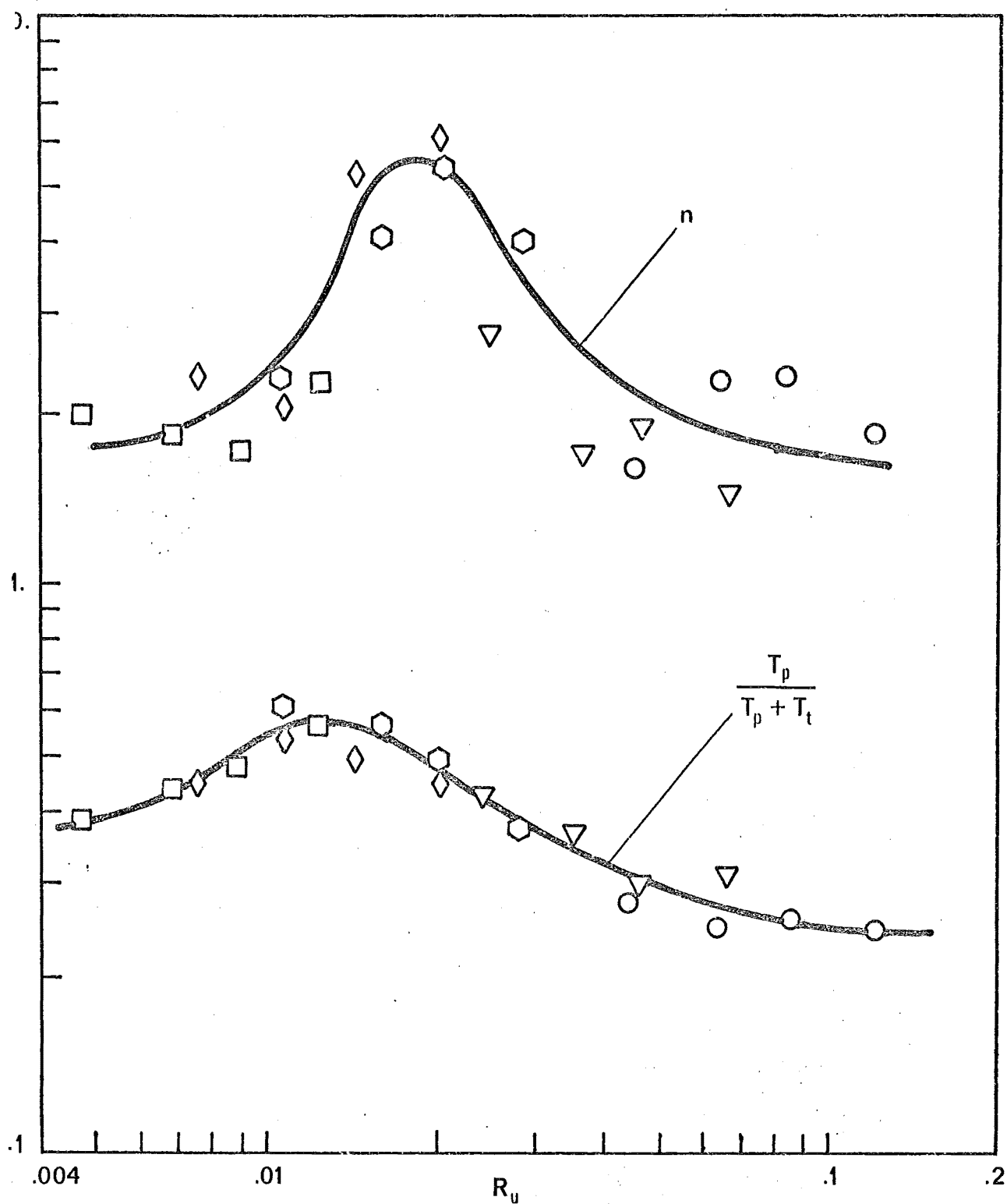


FIGURE 3.19: DEPENDENCE OF TSPF PARAMETERS ON THE AIR RATE RATIO  $R_u$

	Run	Air velocity /ms <sup>-1</sup>
○	5	.135
▽	9	.244
⬡	14	.54
◇	17	.69
□	21	1.27

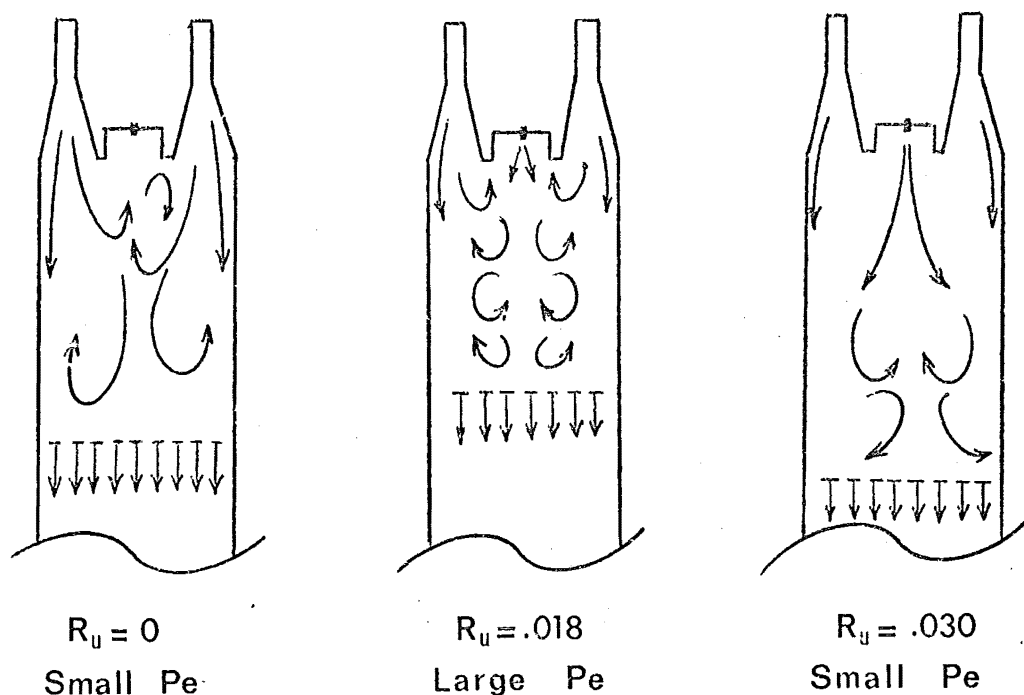


FIGURE 3.20 : PROPOSED EXPLANATION OF  
EFFECT OF JET ON BACKMIXING

The Craya-Curtet number at the minimum backmix point is (equation 10)

$$Ct = \frac{ru}{r_o u_o} = \frac{r_o}{R_u r_u} = 0.25 .$$

The theory outlined in section II predicts a noticeable effect of the atomising jet as  $Ct < 0.75$ . In figure 19,  $n$  and  $T_p/T$  start to rise at  $R_u = 0.006 \pm 0.001$ , i.e.  $Ct = 0.74 \pm .15$ . In view of the difference in geometries between the idealised model (figure 2) and the actual equipment, the agreement is surprisingly good.

### V.1.7 Comparison of the drying air and the atomising air R.T.D.

So far only the drying air R.T.D has been described. This is because there is no qualitative difference between the R.T.D. of the two streams, both being best described by the T.S.P.F. model. A quantitative comparison of the mean residence time  $\tau$  and the degree of backmix (as measured by  $Pe$ ) is shown in Table 4. Because of fluctuations between runs at different  $R_u$  values, no influence of the latter has been observed, and only the mean results for all atomising air pressures have been tabulated.

Both the  $\tau$ - and  $Pe$ -ratios are close to unity, and no trend can be observed as to the influence of the air velocity  $u$ . The residence time of the atomising air is slightly below that of the drying air, indicating that a jet zone does exist for the former, but only for a short distance ( $0.15 \times 2200 \text{ mm} = 300 \text{ mm}$  at the most for run 10); certainly the range of  $\tau$ -ratios (0.06 - 0.74) predicted by equation 19 is not to be found here.

In conclusion it can be said that the two streams merge quite early and become indistinguishable. The fluctuations in the value of the two ratios are much larger at low air rates, suggesting again the non-stationary nature of the flow in that range.

TABLE 3.4

Comparison of atomising air and drying air R.T.D's.

Run	$\tau$ ratio atom./drying	$Pe$ ratio atom./drying
1	$0.88 \pm .20$	$1.00 \pm .30$
2	$1.00 \pm .10$	$0.89 \pm .15$
6	$0.98 \pm .06$	$0.80 \pm .12$
10	$0.85 \pm .02$	$1.03 \pm .20$
16	$0.98 \pm .18$	$0.94 \pm .08$
20	$0.94 \pm .10$	$1.26 \pm .06$



## V.2 Velocity and turbulence measurements

The velocity and turbulence profiles, both radial and longitudinal, were measured for runs 5, 9, 14, 17, 21. There is no qualitative difference between them, and since run 14 straddles the minimum dispersion point, its results will be shown here.

The profiles were measured at 5 sections. At each section 24 points were probed, the DC voltage being integrated three times for 20 to 30 seconds each. The diameter traversed is at an angle of  $12^\circ$  with the air inlets, i.e. almost directly below them. Three runs were made, at  $R_u = 0, 0.016$  (near the minimum dispersion point) and 0.030 respectively.

Mean velocity profiles are shown in figure 21. The results are of limited accuracy due to the following factors:

(1) The non-parallel nature of the flow: the probes used were inadequate to discriminate effectively the component of flow being measured from other components. Also, the direction of the flow can only be guessed at.

(2) The influence of turbulence on the mean reading: when the turbulent component  $u'$  is small, its effect can be corrected for by (H13):

$$\bar{u}_m \approx \bar{u} \left( 1 - \frac{1}{4} \frac{u_1'^2}{\bar{u}^2} + \frac{1}{2} \frac{u_2'^2}{\bar{u}^2} \right) \quad (3.27)$$

where  $\bar{u}_m$  is the measured value of  $\bar{u}$ , and the subscripts 1 and 2 denote the components parallel to and perpendicular to the main flow direction respectively. However, in this experiment  $u_1'/\bar{u}$  is very large (up to 50%),  $u_2'$  is not known, the flow being anisotropic, and so the correlation cannot be made. Therefore the uncorrected values have been plotted on an arbitrary scale to give a qualitative picture of the flow.

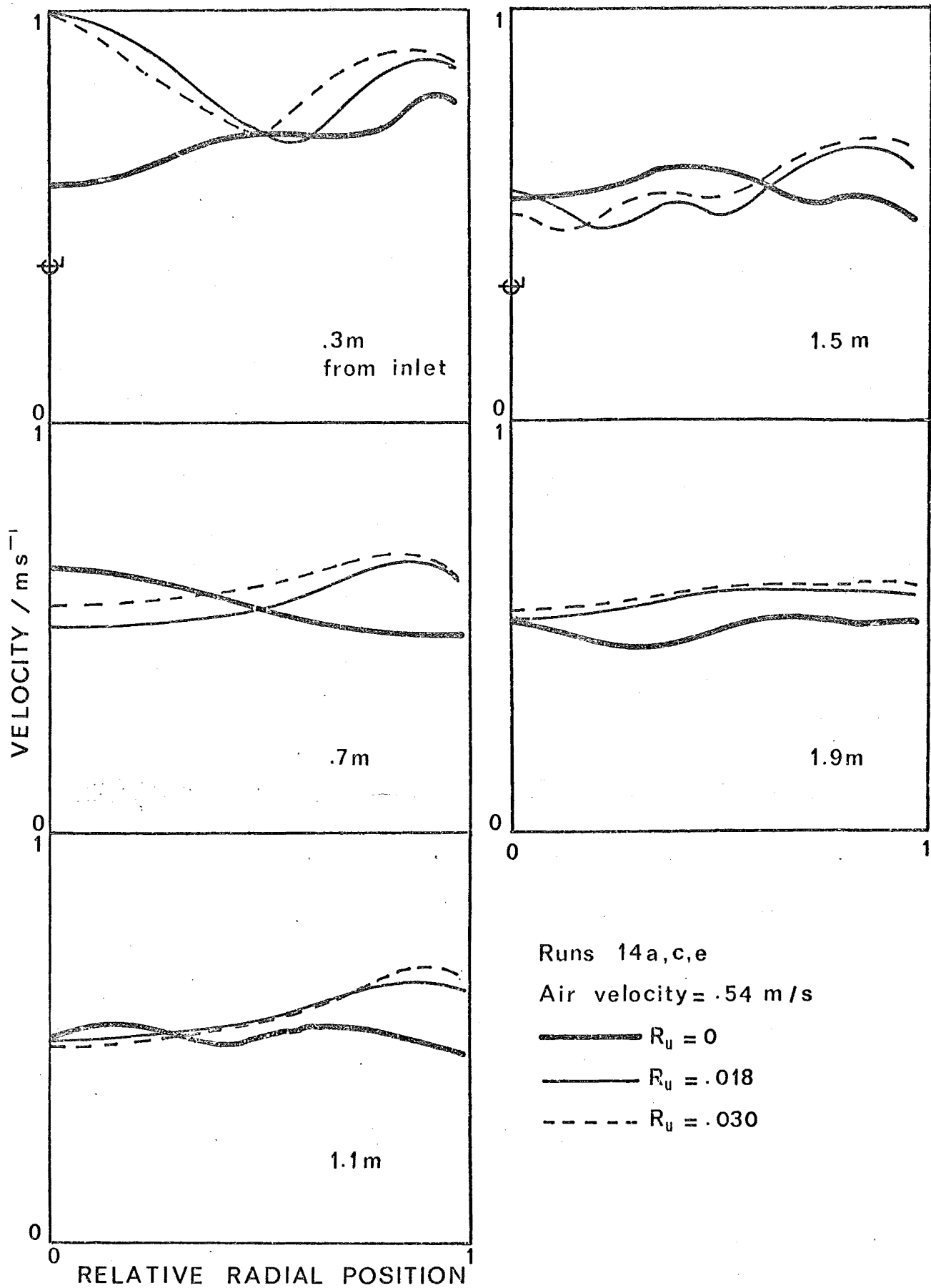


FIGURE 3.21: AIR VELOCITY PROFILES

Without the jet, a complex eddy system can be seen, extending far down the column. The jet reverses the flow profile drastically in the upper part of the column. However, a nearly two-fold increase of the atomising air rate makes little further difference to the profiles.

The spectra of turbulence for the 3 runs (again on an arbitrary scale) at a distance of 1.9 m from the inlet is shown in figure 22b. The spectra have been corrected for the frequency response of the instrument using graph 22a, which has been obtained by the method of section III.2. Similar spectra have been measured at 1.1 m from the inlet: at that point (not shown here) the three spectra are almost identical. Hence figure 22b shows that in run 14c the turbulence has decayed quicker than either in run 14a or run 14e. The small structures of turbulence are in all cases very close.

The longitudinal turbulence intensity profiles are plotted in figure 23.  $\bar{u}/u'$  has been plotted in order to correlate the decay process as described by Taylor<sup>(T2, B10)</sup>. The turbulence decays slowly in the first 50-60% of the chamber, then much more quickly in the remaining 40-50%. This division corresponds quite accurately to that of the T.S.P.F. model. In the plug-flow part the energy input due to the stirring action of the entering air has stopped, so the decay must be more rapid. The presence of the atomising air jet accelerates the decay of turbulence, as seen by the steeper slopes of curves c and e in figure 23, presumably because it breaks up the eddy pattern near the entrance and decreases the scale of turbulence, hence increasing the energy dissipation<sup>(H13)</sup>. There is considerable uncertainty in curve 14c, indicating that the flow and decay pattern may be complex at the minimum dispersion point, a fact also borne out by R.T.D. analysis.

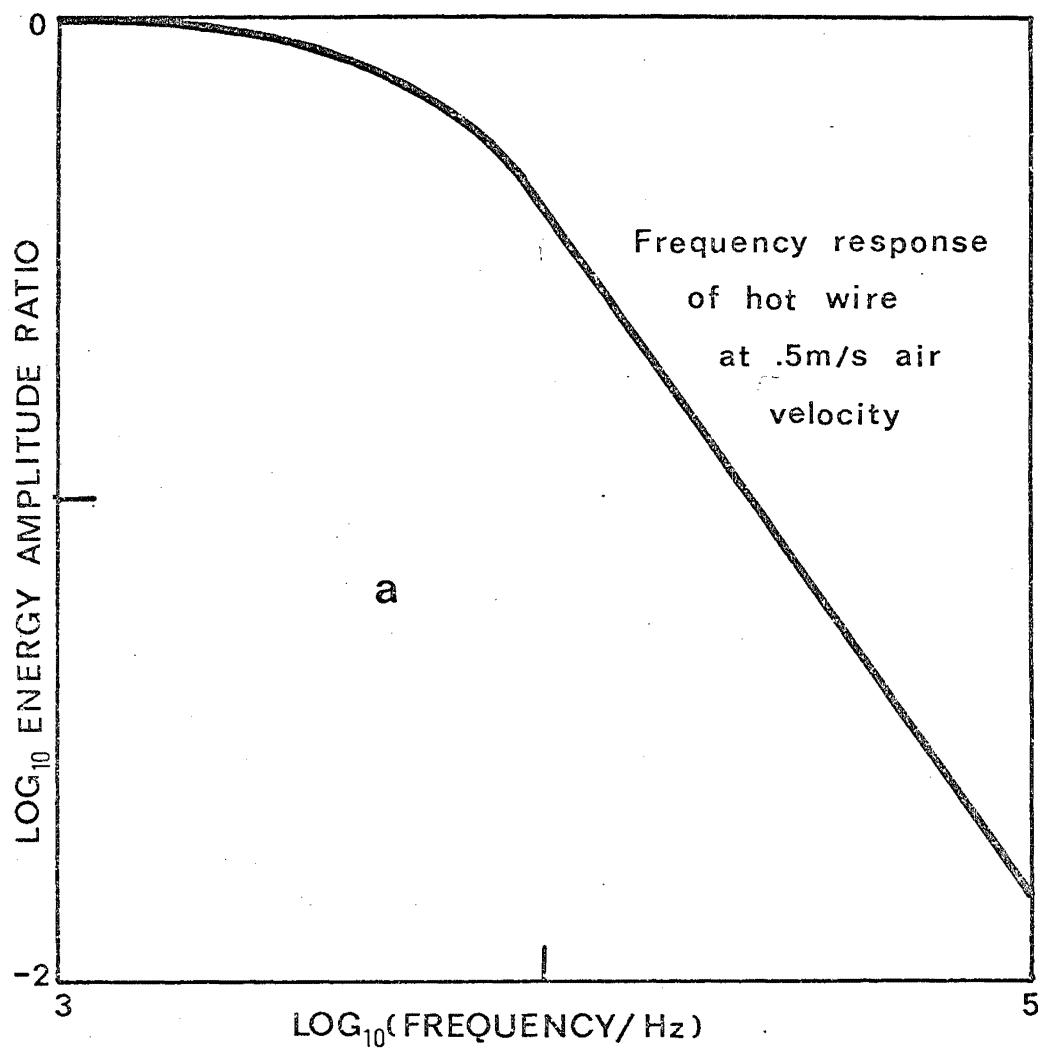
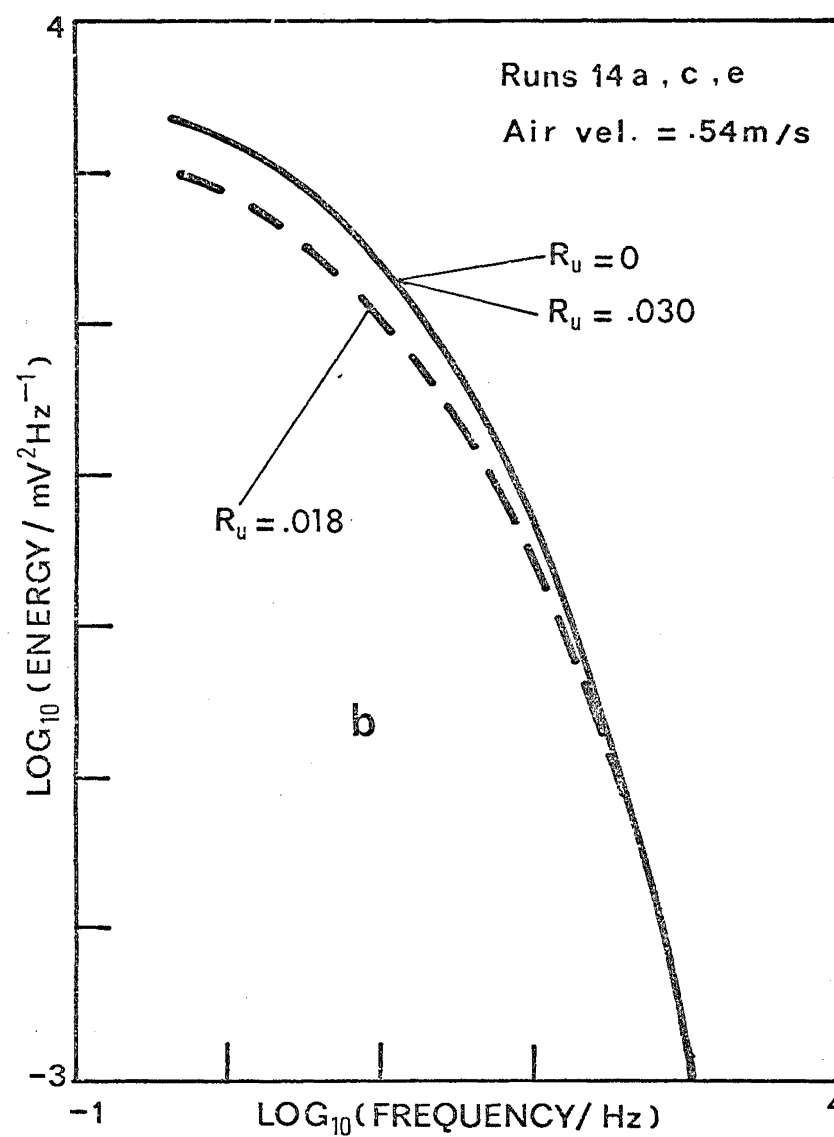


FIGURE 3.22: TURBULENCE SPECTRA



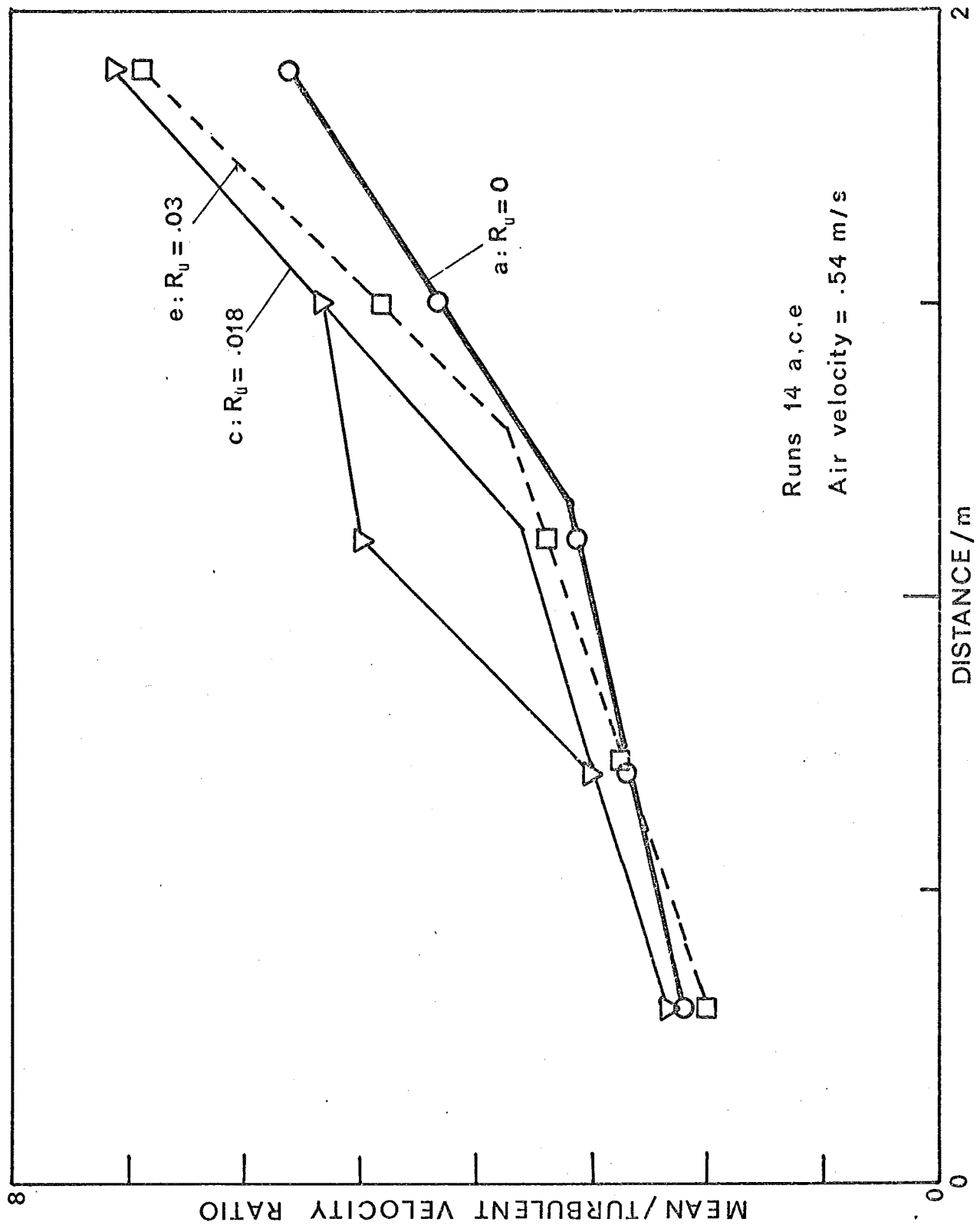


FIGURE 3.23: LONGITUDINAL TURBULENCE PROFILES

### V.3 Flow visualisation results

More recently, smoke tests have been made by Uru<sup>(U2)</sup> on a similar 400 mm diameter column made of Perspex. He found two quite distinct regions in the chamber, - a well-mixed zone occupying the upper half approximately, and a parallel-flow zone, - the two zones being separated by a stable interface. He also found that the length of the plug-flow zone increases to a maximum then decreases again as the air velocity increases (figure 19). Thus the results of the transfer-function analysis are again confirmed.

## VI. CONCLUSION

The transfer-function methods described in Chapter 2 are a promising way to process R.T.D. data. From simple and fast experiments valuable information can be obtained about the flow pattern in a vessel: backmix, bypass, recycle, plug-flow and non-stationarity can be detected. The analytical procedure used minimises tailing effects and does not require absolute values of concentrations to be known, so that sophisticated detection equipment is not necessary. The procedure dispenses with multivariable curve-fitting and gives direct visual information on the validity of the model used. Some care must be exerted in choosing the appropriate range of  $s$ ; although a range  $s\tau = 0.5 - 2$  was recommended by Michelsen and Østergaard<sup>(M12, M13)</sup>, when a plug-flow region  $T_p$  is present, clearly a more appropriate range would be  $s(\tau - T_p) = 0.5 - 2$ .

For the spray dryer in question, the flow has been found to consist of a well-mixed zone (about two equal tanks in series, with a small amount of recycling and bypassing) in the upper half approximately, and a parallel-flow zone in the lower half. The flow is highly

unstable at low air rates, in the transition Reynolds number zone ( $u < 0.3$  m/s). The atomising air jet has a large effect on the flow pattern, the degree of backmix in the vessel being governed by the Craya-Curtet number  $Ct$ . Minimum backmix occurs at  $Ct \approx 0.25$ . The atomising air and the drying air appear in all cases to merge almost immediately upon entry.

This column and inlet design therefore offers desirable features from the process point of view, ensuring that the droplets and the air are well mixed immediately and thus increasing the evaporation (see Chapter 6), but then reverting to parallel flow in the lower part, where the particles are nearly dry and could be easily damaged by heat. This in turn suggests that if the problem of wall deposition can somehow be overcome, drying chambers with larger  $L/D$  ratios still would be desirable, especially for heat-sensitive products, as they would have a relatively longer plug-flow zone.

For spray dryers of this type, the most stable operating range would be:

(1) air velocity  $\approx 0.5$  m/s - 1 m/s ( $Re = 1.5 \times 10^4 - 3 \times 10^4$ ), where the plug flow zone has a maximum length and does not appear to fluctuate (figure 17).

(2)  $Ct$  (= column radius x mean velocity / nozzle radius x atomising air velocity)  $\ll 0.25$  or  $Ct > 0.74$ , in which regions the flow pattern would not be too sensitive to small changes in the nozzle operating conditions, thus making process control easier. Only if it is essential to keep axial dispersion to a minimum, or when the atomising and drying air flow rates are not expected to fluctuate, should the region  $Ct \approx 0.25$  be used.

The results obtained in this chapter may also be applied to another type of spray dryer (K9) where a secondary air stream is

directed on the spray emerging from a pressure or rotary atomiser, thus ensuring good mixing. This arrangement, known as the "Czech concept", has been reported to increase the performance considerably. In this type of spray dryer, the air flow will also be influenced by a Craya-Curtet number based on the ratio between the primary and the secondary air flows.



NOTATION FOR CHAPTER 3

$b$	recycle parameter in backflow-cell model, [ - ]
$B$	anemometer wire constant, [ $\text{V}^2 \text{s}^{\frac{1}{2}} \text{m}^{-\frac{1}{2}}$ ]
$c$	concentration of a tracer, [ $\text{kg/m}^3$ ]
$c_m$	concentration of tracer at the jet axis, [ $\text{kg/m}^3$ ]
$c_o$	concentration of tracer at the jet orifice, [ $\text{kg/m}^3$ ]
$D$	vessel diameter, [ m ]
$g_{tr}$	(a.c.) transconductance of anemometer amplifier, [ $\Omega^{-1}$ ]
$i$	current through anemometer probe, [ A ]
$k_e$	entrainment constant of a jet, [ - ]
$k$	decay coefficient, diminishing backmix model.
$L$	vessel length, [ m ]
$m$	mass, for example of tracer, [ kg ]
$\dot{m}$	mass injection rate, [ $\text{kg s}^{-1}$ ]
$n$	number of tanks, [ - ]
$p$	bypass parameter in jet-stirred tank, [ - ]
$r$	vessel radius, $D/2$ , [ m ]
$r_o$	jet orifice radius or inlet radius, [ m ]
$r_j$	jet boundary radius, [ m ]
$R_u$	atomising air to drying air rate ratio, [ - ]
$R$	hot wire resistance, [ $\Omega$ ]
$R_c$	cold wire (at fluid temperature) resistance [ $\Omega$ ]
$R_o$	wire resistance at reference temperature, [ $\Omega$ ]
$s$	Laplace transform parameter, [ $\text{s}^{-1}$ ]
$t$	time, [ s ]
$\bar{t}$	difference in first moments between outlet and inlet concentration curves, [ s ]

(Notation for Chapter 3, cont.)

- $T_o$  time parameter in diminishing backmix model, [ s ]  
 $T_p$  plug-flow time, [ s ]  
 $T_t$  total tank time, [ s ]  
 $u$  air velocity, or drying air velocity, [ m/s ]  
 $u'$  turbulent r.m.s. velocity, [ m/s ]  
 $\bar{u}$  mean air velocity, [ m/s ]  
 $u_j$  effective jet carrying velocity, [ m/s ]  
 $u_o$  jet orifice velocity, [ m/s ]  
 $U_1, U_2$  functions of  $s$  defined in Chapter 2.  
 $v_t$  total fluid volumetric flow rate, [ m<sup>3</sup>/s ]  
 $V$  d.c. voltage, [ V ]  
 $V'$  root-mean-square a.c. voltage, [ V ]  
 $V_o$  d.c. voltage across the hot wire anemometer bridge at zero fluid velocity, [ V ]  
 $x$  axial distance, [ m ]  
 $y$  radial distance, [ m ]  
 $\alpha$  hot wire overheating ratio,  $(R-R_c) / R_c$ , [ - ]  
 $\beta$  defined by equation 19b, [ - ]  
 $\pi = 3.14159$ .  
 $\sigma^2$  difference in the 2nd moments of the outlet and inlet concentration curves divided by the squared difference in the 1st moments, [ - ]  
 $\tau$  holding time of vessel, [ s ]  
 $\tau_w$  anemometer time constant, [ s ]

(Notation for Chapter 3, cont.)

Dimensionless numbers:

Ct Craya-Curtet number (equation 6)

Pe Peclet number,  $Lu/D$  where  $D$  is the axial dispersion coefficient.

$Pe_D$  Peclet number based on diameter,  $Pe D/L$ .

Re Reynolds number,  $Du/\nu$  where  $\nu$  is the kinematic viscosity.

Sc Schmidt number,  $\nu/D_m$  where  $D_m$  is the diffusion coefficient.

## CHAPTER 4

### SPRAY RESIDENCE TIME DISTRIBUTION AND FLOW PATTERN

#### Chapter contents:

##### INTRODUCTION

#### I. THEORY

1. Turbulence, entrainment and R.T.D.
2. Structure of turbulence in present equipment

#### II. EXPERIMENTAL DETAILS

1. Material sprayed
2. Spray R.T.D. equipment and methods
  1. Tracer and tracer injection
  2. Droplet sampling equipment
  3. Triggering and timing circuitry
  4. Radioactivity measurement
3. Droplet size measurement

#### III. EXPERIMENTS PERFORMED

#### IV. RESULTS AND DISCUSSION

1. Droplet sizes
2. Entrainment parameters
3. Droplet R.T.D.
  1. Input pulses
  2. Output pulses
  3. Transfer-function analysis
  4. Variation of dispersion
  5. Degree of entrainment

#### V. CONCLUSION

#### NOTATION

## INTRODUCTION

To date the author knows of only two attempts to measure the disperse-phase residence time distribution in a spray dryer, both unpublished<sup>(C2, B9)</sup>. This may seem surprising, because information on this subject should be valuable for the determination of the air-spray mixing pattern and the degree of evaporation. Only if the spray R.T.D. is known can the performance of a dryer be accurately predicted (see Chapter 6). The reason for this lack of information is undoubtedly the experimental difficulties involved in sampling the dispersed phase at short time intervals and in detecting minute quantities of tracer. This chapter describes one such experiment using a radioactive tracer, as well as some speculative arguments concerning the degree of entrainment undergone by the droplets or particles, which may be useful in devising further experiments.

### I. THEORY

#### I.1 Turbulence, entrainment and residence time distributions

"Entrainment" is the degree to which the particle motion tends to follow the fluid motion. Depending on the inertia of the particle, the viscosity of the fluid and the turbulence pattern of the fluid flow, the particles may either display plug-flow characteristics or have exactly the same R.T.D. as the fluid, but most often in spray-drying chambers an intermediate case will occur.

The effect of turbulence on the R.T.D. of a particle cloud is twofold: first, by imposing random motions on the particles, it will increase the axial and radial dispersion of the cloud; secondly, the drag and hence the settling velocity and mean residence time of the cloud will also be affected.

(a) Effect of turbulence or particle dispersion: According to the classical theory of turbulent diffusion (H13, F4, T2), the turbulent diffusivity of a cloud of particles,  $\mathcal{D}_p$ , is related to its root-mean-square velocity fluctuation  $u'_p$  and its Lagrangian time scale  $t_{Lp}$  by

$$\mathcal{D}_p = u_p'^2 t_{Lp} \quad (4.1)$$

As the particle inertia increases,  $u'_p$  decreases but  $t_{Lp}$  will change in an indeterminate manner. Soo and Perkins<sup>(S15)</sup> both predicted that  $\mathcal{D}_p$  will decrease with increasing particle inertia. Lilly<sup>(L9)</sup> carried out experiments with very small and very large particles and found that  $\mathcal{D}_p$  is equal to the fluid turbulent diffusivity in one case, and to zero in the other. This would seem to confirm Soo's and Perkins' theories, except that these are based on the assumption of very small particles which always stay within an eddy. Thus the state of the theory is still inadequate for calculating the dispersion of particles in a turbulent fluid.

(b) Effect of turbulence on the mean settling velocity: In Chapter 5 a review of this effect will be carried out, and it will be seen that in general an increase in the mean drag force will result from turbulence. Two effects (in gas-solid systems) are involved:

(1) A "Basset force" due to unsteady state of the flow field. In gas-solid systems, this force becomes important only at high energy dissipations<sup>(B1)</sup>. Its magnitude cannot at present be predicted theoretically.

(2) An increase in the "effective" relative velocity  $u_{Re}$ .  $u_{Re}$ , which determines the Reynolds number and hence the drag coefficient  $c_D$ , is a combination of the mean relative velocity  $\bar{u}_R$  and the

turbulent relative velocity  $u'_R$ . Since

$$\bar{F}_{Di} \propto c_D |u_{Re}| \bar{u}_{Ri}$$

where  $\bar{F}_{Di}$  is the mean drag force and  $i$  denotes the  $i$ -th direction, an increase in  $u_{Re}$  will in general result in an increase in  $c_D |u_{Re}|$  except in Stokes's regime, and thus an increase in  $\bar{F}_{Di}$ .

A quantitative criterion to determine the importance of this second effect will now be derived. Since the Basset force usually varies qualitatively in the same way as the increased effective relative velocity effect, this criterion will not be adversely affected by Basset forces. It will be assumed that:

(1) Turbulence effects are still slight,  $u'_R \ll \bar{u}_R$  and  $\bar{u}_R \approx u_t$  where  $u_t$  is the terminal velocity of the particle in quiescent fluid.

(2) The mean and turbulent relative velocities can be combined vectorially:

$$u_{Re} = \sqrt{\bar{u}_R^2 + u_R'^2} \quad (4.2)$$

$$\approx \sqrt{u_t^2 + u_R'^2} \quad (4.3)$$

For small values of  $u'_R$  as assumed before, the relative increase in the mean drag force  $\bar{F}_D = c_D u_{Re} u_t$  will be:

$$R_D \approx \frac{u'_R}{c_D u_{Re} u_t} \cdot \frac{d(c_D u_{Re} u_t)}{d(u'_R)} \quad (4.4)$$

Let

$$c_D = a Re^{-n} \quad (4.5)$$

$$= b (u_t^2 + u_R'^2)^{-n/2} \quad (4.6)$$

where  $n$  has a local value on the drag curve corresponding to a relative velocity between  $u_t$  and  $\sqrt{u_t^2 + u_R'^2}$  ( $n=1$  for Stokes's regime,  $n=0$  for Newton's law region).

From equations 6 and 4 :

$$R_D = \frac{(1-n) u_R'^2}{u_t^2 + u_R'^2} \quad (4.7)$$

There remains to evaluate  $u_R'$ . Friedlander<sup>(F6)</sup> showed that:

$$\frac{u_R'^2}{u_t^2} = 1 - \frac{u_p'^2}{u_t^2} = \frac{1}{1 + t_L/t_p} \quad (4.8)$$

where  $u'$  is the turbulent fluid velocity,  $t_L$  the fluid Lagrangian time scale, and  $t_p$  the particle time constant, defined in Stokes's regime by:

$$t_L \equiv \rho_p D_p^2 / (18 \mu_f) \quad (4.9)$$

Friedlander results will be generalised to large particles by the use of a redefined time constant (see Chapter 5) :

$$t_p \equiv \frac{4\rho_p D_p}{3\rho_f c_D |\bar{u}_R|} \quad (4.10)$$

From the assumption of low turbulent relative velocity,

$$t_p \approx t_{pt} = \frac{4\rho_p D_p}{3\rho_f c_{Dt} u_t} \quad (4.11)$$

where  $c_{Dt}$  is the terminal drag coefficient, and  $t_{pt}$  is independent of the turbulence.

Hence equation (8) becomes:

$$R_D = \frac{1-n}{1 + \frac{u_t^2 (1 + t_L/t_{pt})}{u_R'^2}} \quad (4.12)$$

For small particles, when Stokes's regime prevails,  $n=1$ ,  $R_D=0$  until  $\sqrt{u_t^2 + u_R'^2}$  is large enough to make  $n$  differ significantly from 1.



When the assumption  $u'_R \ll u_t$  does not hold, and Basset forces come into play,  $R_D$  is no longer a relative increase in drag force, but its value would hopefully provide some indication of how complete entrainment is. A more rigorous parameter could be derived, but it would still be based on untested theories and a detailed knowledge of the structure of turbulence, and may not be worth the effort.

## I.2 The structure of turbulence in the present equipment

In order to apply equation (12)  $t_L$  must be known. In liquids it can sometimes be measured directly by high speed photography of neutrally buoyant particles (L8, K14). Alternatively,  $u'$  and  $\mathcal{D}_t$  (the diffusivity of a solute) can be measured separately and  $t_L$  calculated from an equation similar to (1).

There are, however, approximate relationships relating  $t_L$  to more conveniently measurable or calculable turbulence parameters such as  $u'$ ,  $\epsilon$  (the energy dissipation rate per unit mass),  $\lambda_g$  (the Eulerian lateral microscale) or  $L_f$  (the Eulerian longitudinal macroscale). From the definition of  $\epsilon$  and  $\lambda_g$  it can be shown that:

$$\epsilon = 15 \nu u'^2 / \lambda_g \quad (4.13)$$

where  $\nu$  is the fluid kinematic viscosity. For high turbulence Reynolds numbers  $Re_\lambda \equiv u' \lambda_g / \nu$  (dominant inertial effects), Corrsin<sup>(C7)</sup> showed that:

$$\frac{\lambda_g}{\lambda_L} \approx 5.4 \rho Re_\lambda^{-1/2} \quad (4.14)$$

$$\frac{\lambda_L}{u' t_L} \approx 3 Re_\lambda^{-1/2} \quad (4.15)$$

where  $\lambda_L$  is the Lagrangian microscale, from which:

$$t_L = K_L u'^2 / \epsilon \quad (4.16)$$

and  $K_L \approx 0.9$ .

Levins and Glastonbury<sup>(L8)</sup> found experimentally that  $K_L \approx 0.6$ . Other investigators found it equal to 0.7<sup>(A2)</sup>, 0.33<sup>(T4)</sup>, while Hinze<sup>(H13)</sup> established that it must be of order 1. Therefore an average value  $K_L \approx 0.7$  seems reasonable:

$$t_L \approx 0.7 u'^2 / \varepsilon \quad (4.17)$$

In the present equipment  $\varepsilon$  can be calculated as follows: the upper 55% of the drying chamber, up to  $x = 1.2$  m, can be considered as a jet stirred tank (see Chapter 3), receiving energy from the entering air which is at a velocity of  $64 \bar{u}$  in the inlet pipes, where  $\bar{u}$  is the mean air velocity in the dryer, and dissipating this energy within its volume. By means of an energy balance, it is easy to show that:

$$\varepsilon \approx \frac{1700 \bar{u}^3}{L_1} \quad (4.18)$$

where  $L_1 = 1$  m, from which

$$t_L \approx \frac{0.7 u'^2 L_1}{1700 \bar{u}^3} = \frac{4 \times 10^{-4} I L_1}{\bar{u}} \quad (4.19)$$

where  $I \equiv (u'/\bar{u})^2$  is the relative intensity of turbulence.

## II. EXPERIMENTAL DETAILS

### II.1 Material sprayed

In order to minimise and monitor any evaporation, a saturated solution of sodium chloride with traces of sodium dichromate - sodium hydroxide corrosion inhibitor was used in all runs. Microscopic examination of the droplets collected at the outlet showed no crystallisation, except for run E3 (Table 1) and hence it can be assumed that evaporation can be ignored except in that run.

## II.2 Spray R.T.D. equipment and methods

### II.2.1 Tracer and tracer injection

Carbon-14 in the form of a solution of sodium bicarbonate was used as a tracer. The solution is saturated with sodium chloride to avoid disturbing the feed properties. An amount of 10 - 50  $\mu$ l of the solution, which has a specific activity of 1 mc/ml, was injected per pulse by means of a solenoid-operated 100  $\mu$ l microsyringe (Figure 1). The nozzle was modified to permit the insertion of the syringe needle to within 5 mm of the nozzle orifice.

### II.2.2 Droplet sampling equipment

The sampling equipment is shown in Figure 2. It consists of 40 brass cells, 6.35 mm diameter x 9.5 mm, placed at 8 mm centerline intervals in a half-cylindrical holder, and shielded by a 21 mm O.D. brass tube with a single 6.35 mm diameter hole at the top centre. The cell-holder has side grooves so that it can be guided along by pins in the shield. Each cell is covered by a slightly concave pad of Whatman glass filter paper, the purpose of which will be made clear later. As the cell holder moves, the cells pass successively under the hole in the shield, collecting each a small quantity of droplets on the filter paper.

The holder and cell assembly is pulled by a flexible cable wound on a 25.4 mm diameter spool, through a flexible-casing-type transmission. The spool is driven by a 1/4 HP motor acting through a reducing gearbox, and a continuously variable speed ratio gearbox, so that the spool speed varies from 0.2 to 1.8 turns/second and the cable speed from 16 to 145 mm/s approximately.

In order to have a degree of control on the size range of the

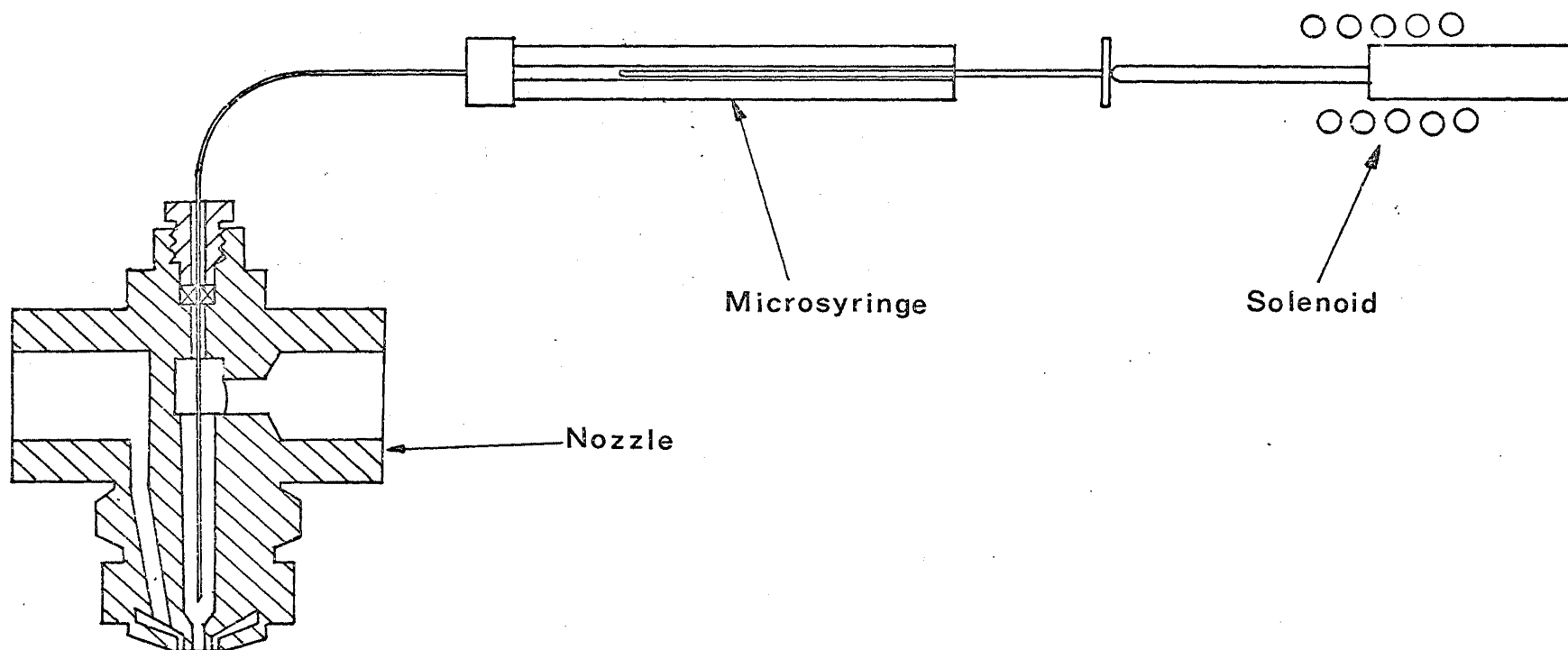


FIGURE 4.1 : LIQUID TRACER INJECTION EQUIPMENT

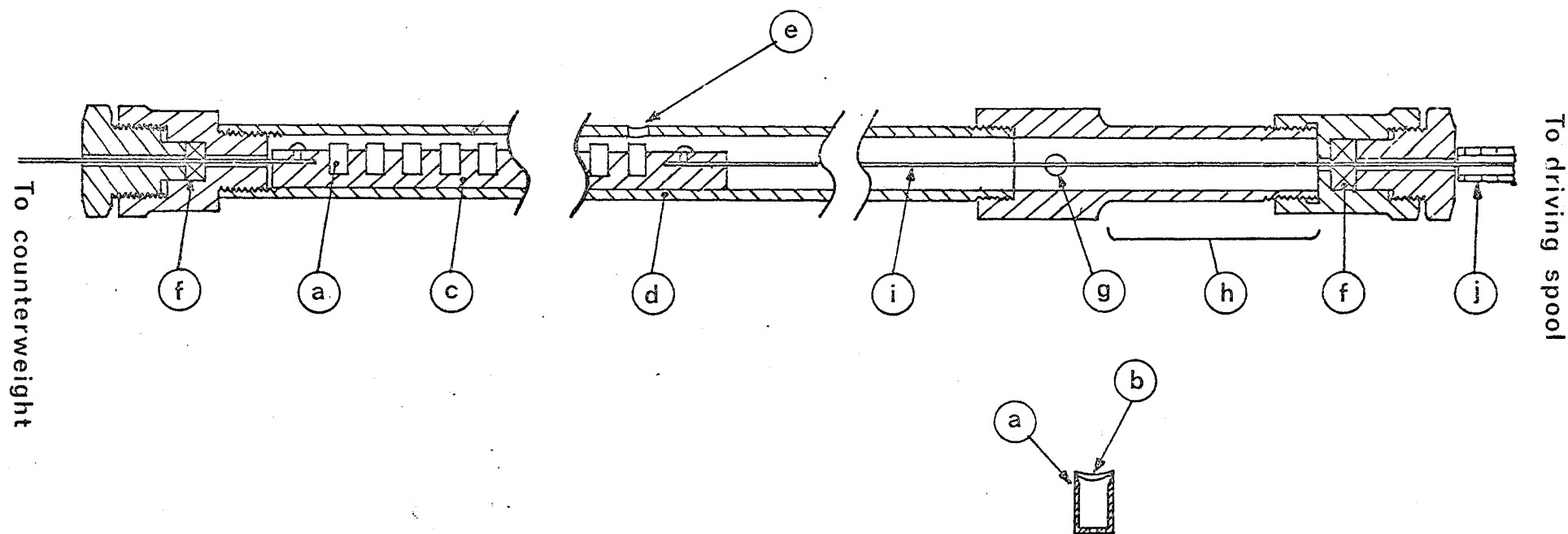


FIGURE 4.2: TRAVELING DROPLET CATCHER

- a Collecting cell
- b Glass filter paper
- c Cell holder
- d Shield
- e 6.4 mm hole
- f Packing
- g Perspex window for photoswitch
- h Stopping length
- i Cable
- j Flexible casing

droplets collected, the velocity of the air past the cylindrical droplet catcher is controlled by a funnel placed just above the catcher. The sizes of the funnels are given in Table 1.

### II.2.3 Triggering and timing circuitry

A scaler counting in hundredths of a second determines the travel time of the cell holder between two given points, from a starting point to a photoelectric switch consisting of a beam of light shining on a CdS photoconductive cell. The circuit for triggering the injection, the sampler and the timer and stopping the last two is shown in Figure 3. As switch S.1 closes, it triggers the microsyringe solenoid and the motor, at the same time sending a "start" pulse to the scaler. When the photoelectric switch (CdS cell) is cut off, it activates relay R1 which opens switch S.3, stopping the motor, and closes S.2, sending a "stop" pulse to the scaler. The variation in the travel time for a given speed setting is less than  $\pm 0.5\%$ . The start of the motor can, however, be delayed manually by opening the switch S.4.

### II.2.4 Radioactivity measurement

The pads of glass filter paper impregnated with radioactive material are each put in a counting vial with 10 ml of scintillant and 2.5 ml of water. The scintillant used consists of 67 % by volume of Triton X-100 and 33% of toluene, the toluene having been premixed with 0.4% 2-5 diphenyloxazole (P.P.O) and 0.01% 1,4-bis(5-phenyloxazol-2-yl)benzene (P.O.P.O.P.). This mixture was introduced by Patterson and Greene<sup>(P5)</sup> and has been highly commended for  $^{14}\text{C}$  counting<sup>(R2)</sup>. It has a complex phase diagram when mixed with water, first forming a clear solution, then an unstable suspension,

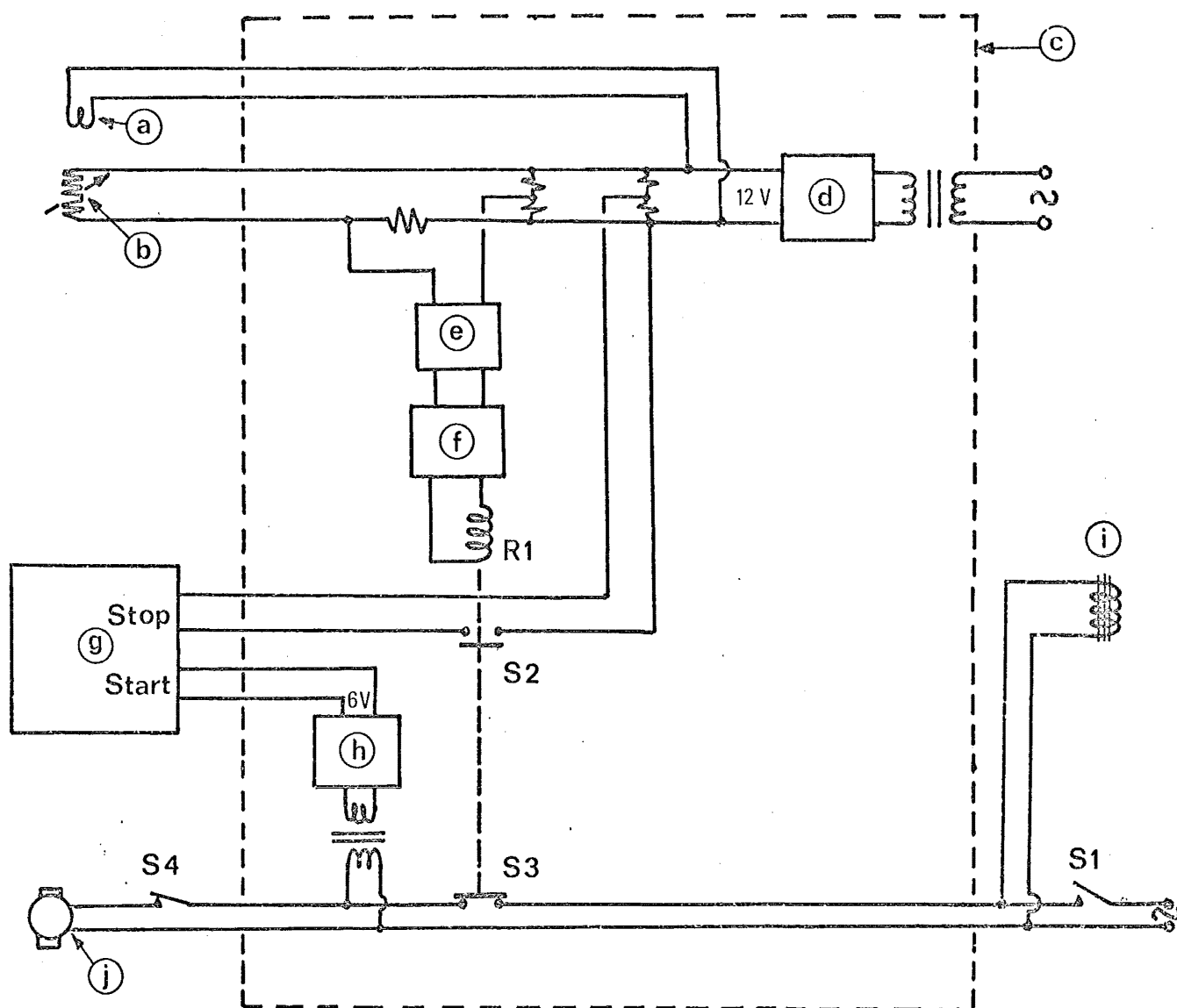


FIGURE 4.3 : TRIGGERING & TIMING CIRCUIT FOR SPRAY RTD MEASUREMENT

- a 12V bulb
- b CdS cell
- c Control box
- d Rectifier
- e Amplifier
- f Emitter follower
- g Scaler
- h Rectifier
- i Microsyringe solenoid
- j Droplet catcher motor

then a stable emulsion, and finally another unstable suspension as the water content increases. At the proportions given earlier the mixture is in the stable emulsion phase.

Each vial is vigorously shaken with a mechanical shaker for about two minutes, at the end of which the glass filter paper is disintegrated and suspended in the emulsion, thus achieving maximum dispersion of  $^{14}\text{C}$  in the scintillant. The vials are then counted for  $\beta$ -radiation in a Unilux III automatic scintillation counter with two channels and coincidence circuit to eliminate background noise. The counting efficiency of each sample is determined by the channel ratio method and is about 80-90% for most vials. Detailed descriptions of the theory and practice of scintillation counting and other methods of radiation detection have been made by Price (Pl0, Pl1).

The standard deviation of a radioactivity count is equal to the square root of the total number of pulses counted. In this experiment the counting time was set to give a standard deviation of about 0.2% for the most active samples, i.e. a total count of about  $2.5 \times 10^5$  pulses for these samples.

The vials were reused after being rinsed successively in methanol (using equipment similar to the one described by Harris and Friedman<sup>(H4)</sup>) and water, soaked for 24 hours in a 3% solution of Decon-90, and rinsed again with water. The background counts of the vials were checked before each run and were always insignificant compared with the activities measured. The brass cells were cleaned in a similar manner to the vials.

### II.3 Droplet size measurement

For size measurements the droplets were collected in a rectangular perspex cell, 6.35 mm wide x 60 mm long, shielded in a hollow brass



cylinder of the same size as the travelling droplet catcher shield, and placed in the same position. The shield has a 6.35 mm wide slot which when passing over the cell (by a rotation of the shield) allows some droplets to fall in.

The cell contains a collecting fluid consisting of Shell Carnae-69 oil, which has been used by several other investigators<sup>(F2, R8, S13)</sup>. Within one minute of sampling the droplets were photographed under microscope at a magnification of 60, together with an eyepiece grid which had previously been calibrated against a stage micrometer. After enlargement, the final magnification was 110. More details about the microphotography technique can be found in references (R8) and (S13).

The droplets were then counted and sized with a perspex grid divided into 9 size ranges (2, 4, 5.7, 8, 11.3, 15.5, 18.9, 22.6 and 27 mm). Between 1800 and 6000 droplets were counted for each run.

### III. EXPERIMENTS PERFORMED

Liquid R.T.D. measurements were carried out at drying air rates corresponding to runs 1, 2, 6, 10, 16 and 20 of Table 3.1, Chapter 3. A summary of the operating conditions is shown in Table 1 below, together with the mass-median drop size results  $D_m$  for easy reference. It can be seen that 3 sets of nozzle operating conditions were used, giving a small droplet size range (run A1), a medium size range (run A2) and a large size range respectively (runs A3 to E3).

For each set of nozzle operating conditions, the "input concentration curve" was found by placing the droplet catcher 150 mm below the nozzle. This point is within the jet zone of the nozzle, where velocities are high, hence the shape of the concentration curve depends only on the tracer injection method and not on the drop size.

TABLE 4.1

Operating conditions for the spray R.T.D. experiments

Run No.	Corresponding air RTD run	Drying air velocity /ms <sup>-1</sup>	Funnel outlet dia. /mm	Nozzle no.	Atomising pressure /kPa	Feed rate	Sampling time interval /s	D <sub>m</sub> /μm
A1	1 & 2	0.055	25.4	1	380	0.21	0.514	15
A2	1 & 2	0.055	25.4	2	180	0.58	0.514	41
A3	1 & 2	0.055	25.4	2	180	1.33	0.514	90
B3	6	0.144	36.	2	180	1.33	0.513	125
C3	10	0.29	51.	2	180	1.33	0.513	63
D3	16	0.61	72.	2	180	1.33	0.355	94
E3	20	1.22	102.	2	180	1.33	0.208	(93)

For each of the runs listed, the funnel was installed, a small Pitot tube was placed under it at the spot where the travelling droplet catcher would be, then the air flow rate was adjusted to give a Pitot tube reading of  $36 \pm 2$  mm of water (4.8 kPa) corresponding to a velocity reading of 24 m/s. Then the Pitot tube was removed and the travelling droplet catcher was inserted. In this manner the impact efficiencies for the droplets are kept at the same value from run to run.

When residence times are high (runs A, B, C, D) each concentration curve must be measured in two or three overlapping segments. For each segment, 2 to 4 runs were done and measured separately. Each of these runs may consist of 1 to 25 samplings, in order to collect enough droplets in each cell to minimise random errors. The higher the air flow rate, the more samplings are needed to compensate for the small collecting cell area/total flow area ratio and the reduced cell exposure time.

#### IV. RESULTS AND DISCUSSION

##### IV.1 Droplet sizes

Droplet sizes results are shown in Table 2. For run E3 no measurement was taken because the flow past the collecting cell was extremely unstable, and droplets tended to come in dense swarms and merge on impact with the collecting fluid. An average value of the results of other runs (A3 to D3),  $D_m = 93 \mu\text{m}$ , will be used for subsequent calculations.

TABLE 4.2

Droplet size results

Run \ Size/ $\mu\text{m}$	Number of droplets									$D_m/\mu\text{m}$
	5 to 9	9 to 25.5	25.5 - 43	43 - 61	61 - 86	86 - 119	119- 154	154- 186	186- 223	
A1	3265	70	0	0	0	0	0	0	0	15
A2	2757	434	98	26	2	0	0	0	0	41
A3	955	385	183	115	62	19	5	1	0	90
B3	1848	455	189	130	94	30	17	8	3	125
C3	1929	428	137	74	15	6	0	0	0	63
D3	4546	2037	679	467	271	70	28	9	0	94

##### IV.2 Entrainment parameters

The parameters  $u_t$ ,  $n$ ,  $t_{pt}$ ,  $R_D$  and others related to entrainment are shown in Table 3 for later reference. The fluid turbulent velocity  $u'$  cannot be determined accurately, as it varies considerably within the well mixed zone, and a mean value  $u'/u = 0.4$  ( $I = 0.16$ ) was used for all runs.

The value of  $n$  was taken at a mean value of the Reynolds number between  $u_t$  and  $\sqrt{u_t^2 + u_R'^2}$ . It was determined from the equation:

$$c_D = \frac{24(1 + 0.1 \text{ Re})}{\text{Re}} \quad (4.20)$$

which describes the drag curve between  $\text{Re} = 0.4$  and  $\text{Re} = 2$  (Chapter 5).

From this equation,

$$\begin{aligned} n &\equiv - \frac{d(\ln c_D)}{d(\ln \text{Re})} \\ &= \frac{1}{1 + 0.1 \text{ Re}} \end{aligned} \quad (4.21)$$

TABLE 4.3

Entrainment parameters

Run	$D_m/\mu\text{m}$	$u_t/\text{ms}^{-1}$	$t_{pt}/\text{s}$	$\bar{u}/\text{ms}^{-1}$	$u'/\text{ms}^{-1}$	$t_L/\text{s}$	$u_R'/\text{ms}^{-1}$	$n$	$R_D$
A1	15	0.007	$7 \times 10^{-5}$	0.055	0.022	$1.2 \times 10^{-3}$	0.005	1.0	0
A2	41	0.05	$5.5 \times 10^{-4}$	0.055	0.022	$1.2 \times 10^{-3}$	0.012	0.9993	$4. \times 10^{-5}$
A3	90	0.22	$2.2 \times 10^{-2}$	0.055	0.022	$1.2 \times 10^{-3}$	0.021	0.88	0.001
B3	125	0.37	$3.8 \times 10^{-2}$	0.144	0.058	$4.4 \times 10^{-4}$	0.058	0.76	0.006
C3	63	0.12	$1. \times 10^{-2}$	0.29	0.12	$2.2 \times 10^{-4}$	0.12	0.943	0.028
D3	94	0.23	$2.3 \times 10^{-2}$	0.61	0.24	$1.0 \times 10^{-4}$	0.24	0.85	0.08
E3	(93)	(0.23)	$(2.3 \times 10^{-2})$	1.22	0.49	$5.2 \times 10^{-5}$	0.49	0.81	0.16

### IV.3 Droplet residence time distribution

#### IV.3.1 Input pulses

The input pulses for nozzle operating conditions no.2 (run A2) and no.3 (runs A3-E3) were found to be virtually perfect  $\delta$ -pulses, dropping to near zero as early as the second cell ( $t = 0.066$  s).

The input pulse for nozzle operating condition no.1 (run A1) has a first moment of  $0.58 \pm .03$  s and a second moment of  $0.29 \pm .07$  s<sup>2</sup>, which are low compared to the moments of the outlet concentration curve (21 s and 71 s<sup>2</sup> respectively).

#### IV.3.2 Output pulses

All the averaged output pulses are plotted in Figure 4. Numerical data can be found in Appendix A. The atomising air R.T.D.s under the same operating conditions are also plotted for comparison.

An outstanding feature is the large and often regular fluctuations present in most curves. In run A1 for example, these fluctuations have a period of about 7 s. Several factors may have caused these fluctuations:

- (1) Radiation counting errors.
- (2) The small number of the droplets collected in each cell.
- (3) Eddies or instability in the droplet flow.

Factor (1) may be discounted, the counting procedure having been checked by repeated measurement, and the counting times being large enough to keep the errors below 1% in most cells.

Factor (2) is due to the fact that quantities, and not concentrations, of tracer are measured. Hence the apparent "concentrations" depend in fact on the number of droplets collected in each cell. This number is calculated to be between 750 and 7200 droplets for each point on the curve. Assuming that this quantity follows a Poisson distribution,

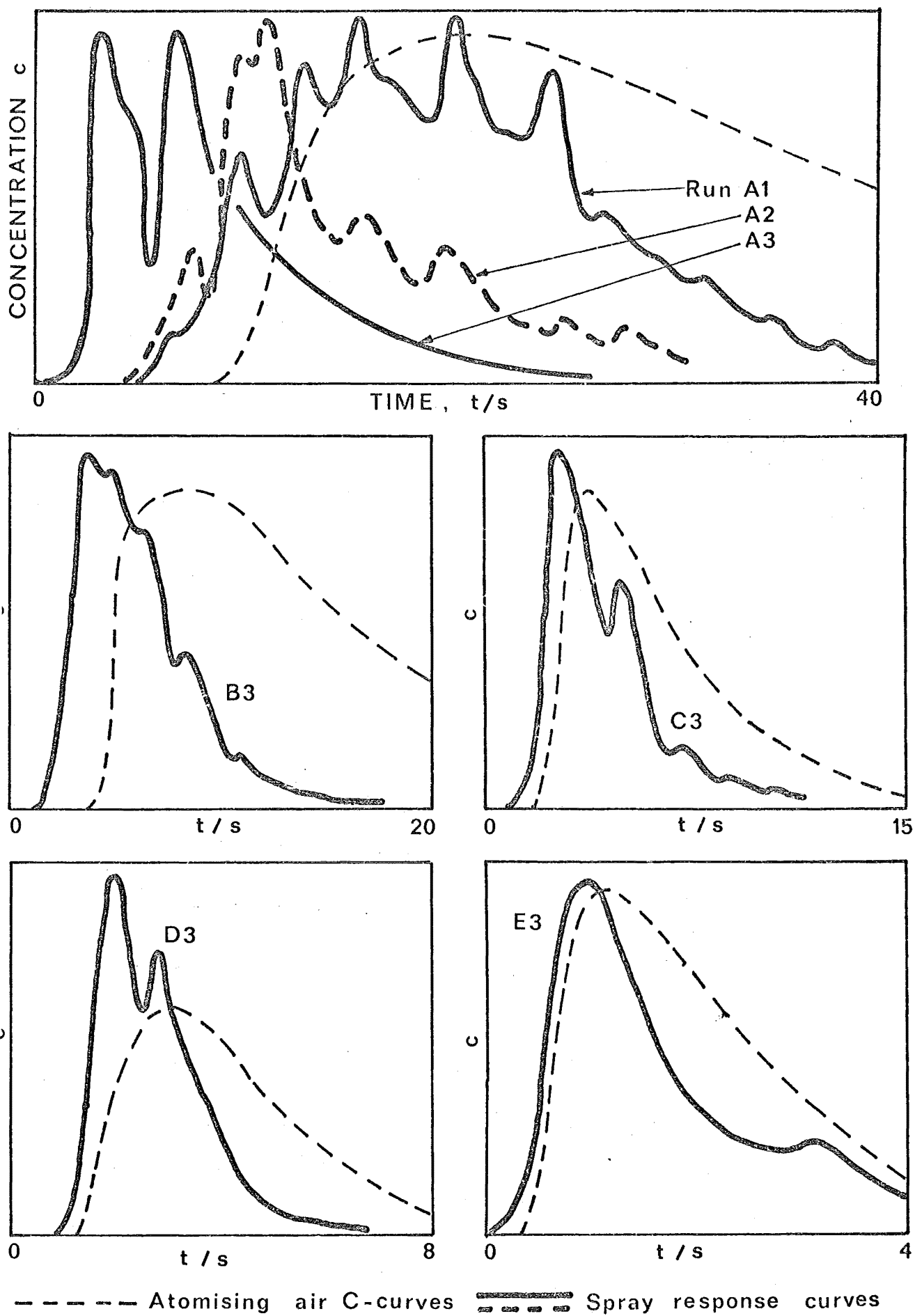


FIGURE 4.4: SPRAY OUTLET TRACER CONCENTRATION CURVES

the standard deviation would then be 3.5% to 1% (the upper limit applies to run E3, the lower to run A1). Although fairly large, this error can only explain the random fluctuations from cell to cell and not the slow and systematic fluctuations observed, each of which may encompass more than 10 cells.

Therefore it must be concluded that either true eddying or unsteady state is occurring in the flow of the droplets, especially at fine and medium droplet sizes (runs A1, A2).

Run A3 (low air velocity, large droplet sizes) shows a pronounced bimodal (two peak) response curve, peaking at 3.6 and 6.7 s respectively. Run A2 (medium droplet sizes) shows the same feature although less markedly. The first peak is probably due to a bypass, the momentum of the larger droplets carrying them right through the well mixed zone. Less heavy droplets, or those on the boundary of the jet, are caught in the air turbulence and slowed down. At higher air velocities, the response curve is generally unimodal, indicating that no significant bypassing occurs.

#### IV.3.3 Transfer function analysis

Only the axially-dispersed plug flow (A.D.P.F.) and the tanks-in-series-and-plug-flow (T.S.P.F.) models were analysed (Table 4), since the lack of accuracy does not justify models with more parameters.

The graphs for the transfer function analysis are shown for all runs in Figure 5. It can be seen that the T.S.P.F. model is not as good as the A.D.P.F., probably because of the lower degree of turbulent motion undergone by the droplets, as well as to the velocity distribution of the droplets resulting from the drop size distribution (section IV.3.4).

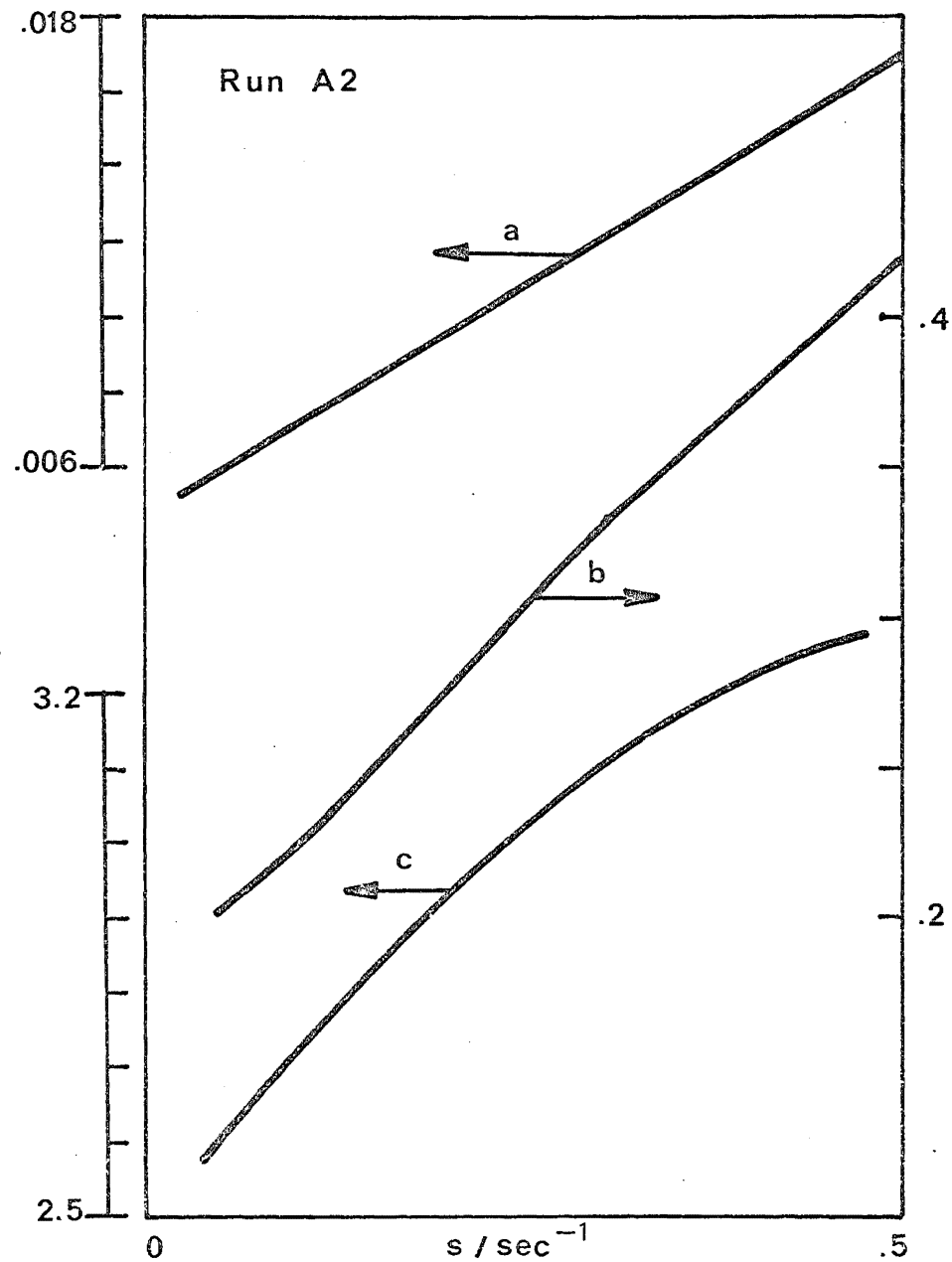
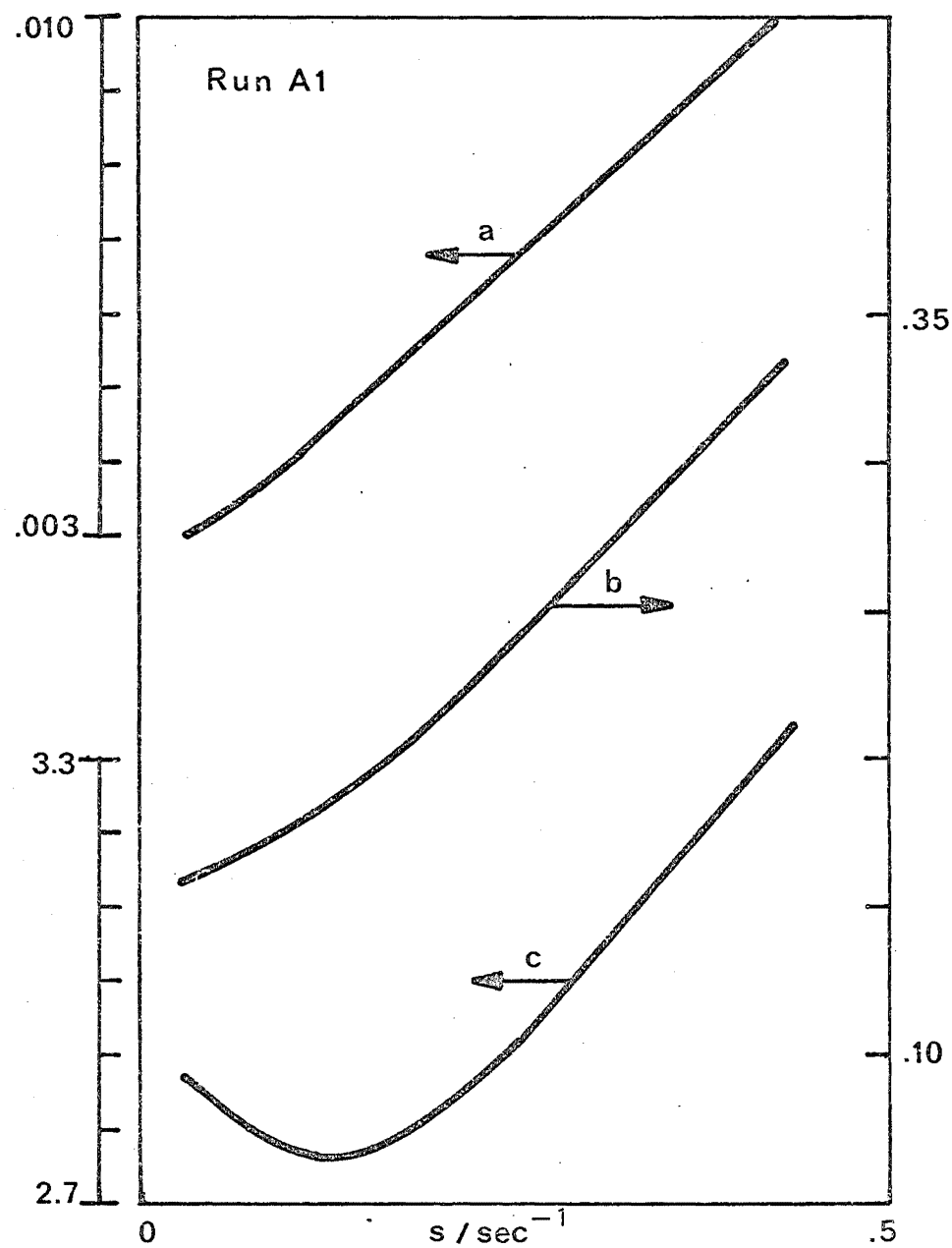


FIGURE 4.5 : TRANSFER-FUNCTION ANALYSIS FOR SPRAY RTD, ADPF & TSPF MODELS



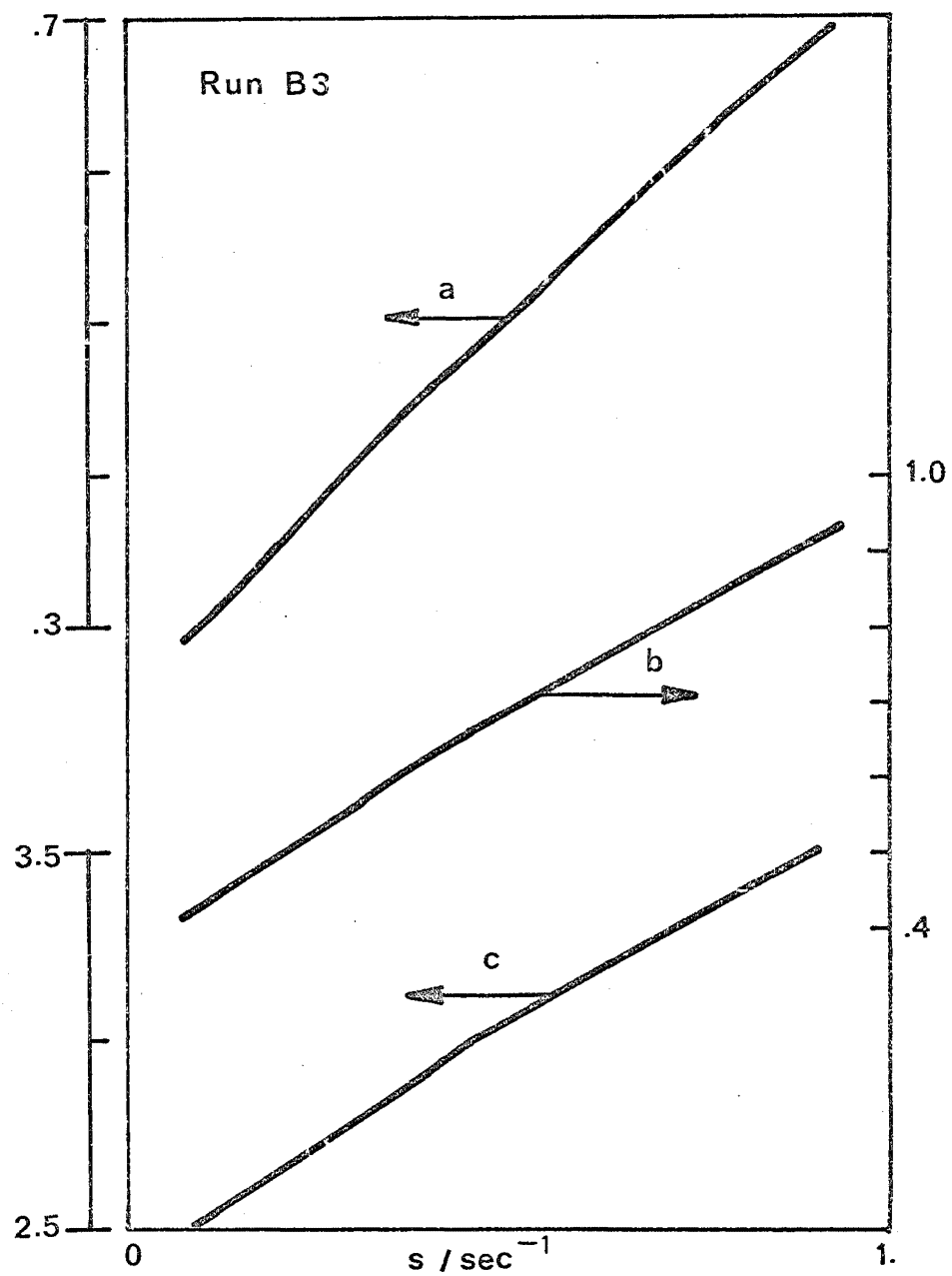
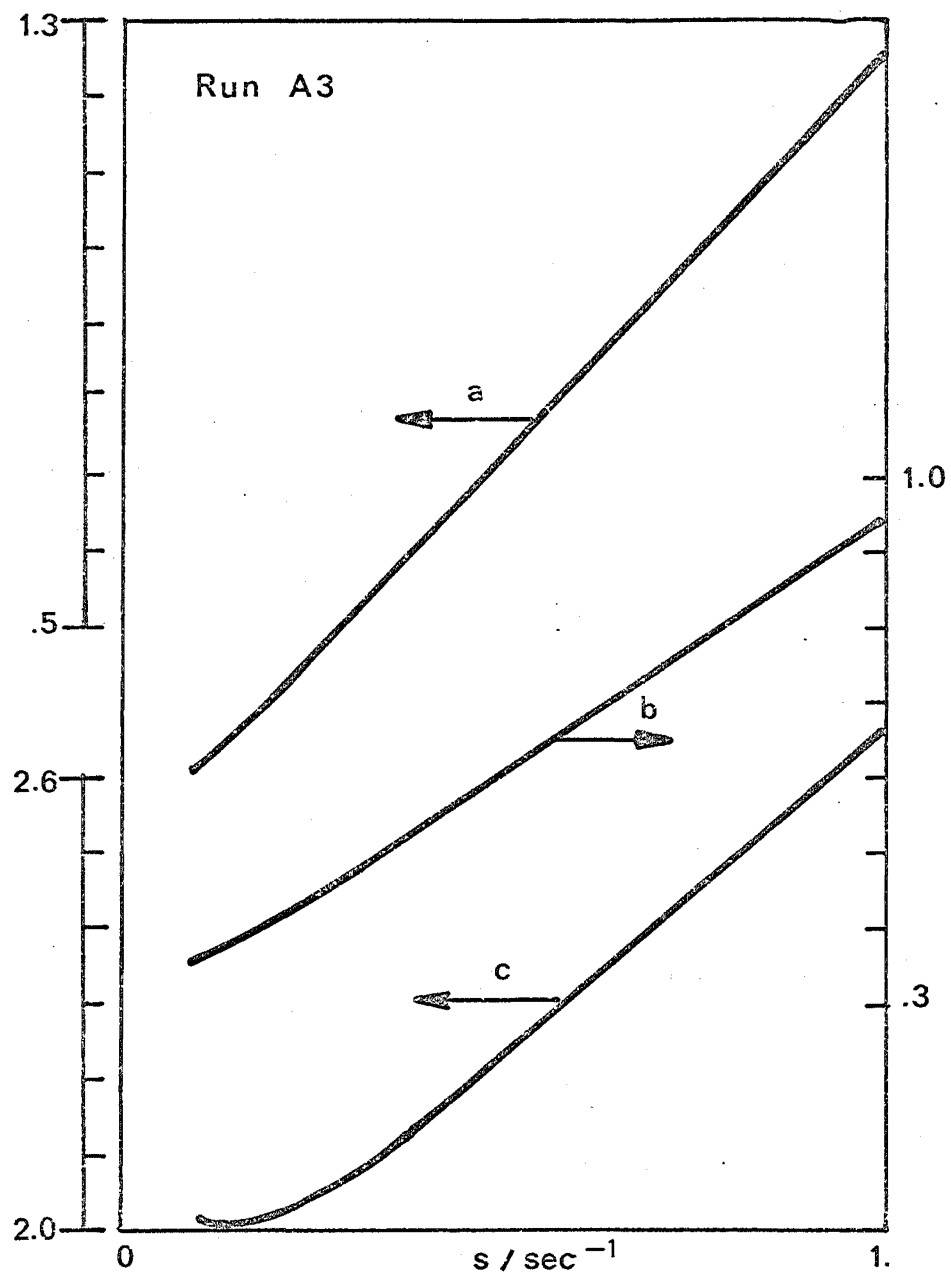


FIGURE 4.5 (cont)

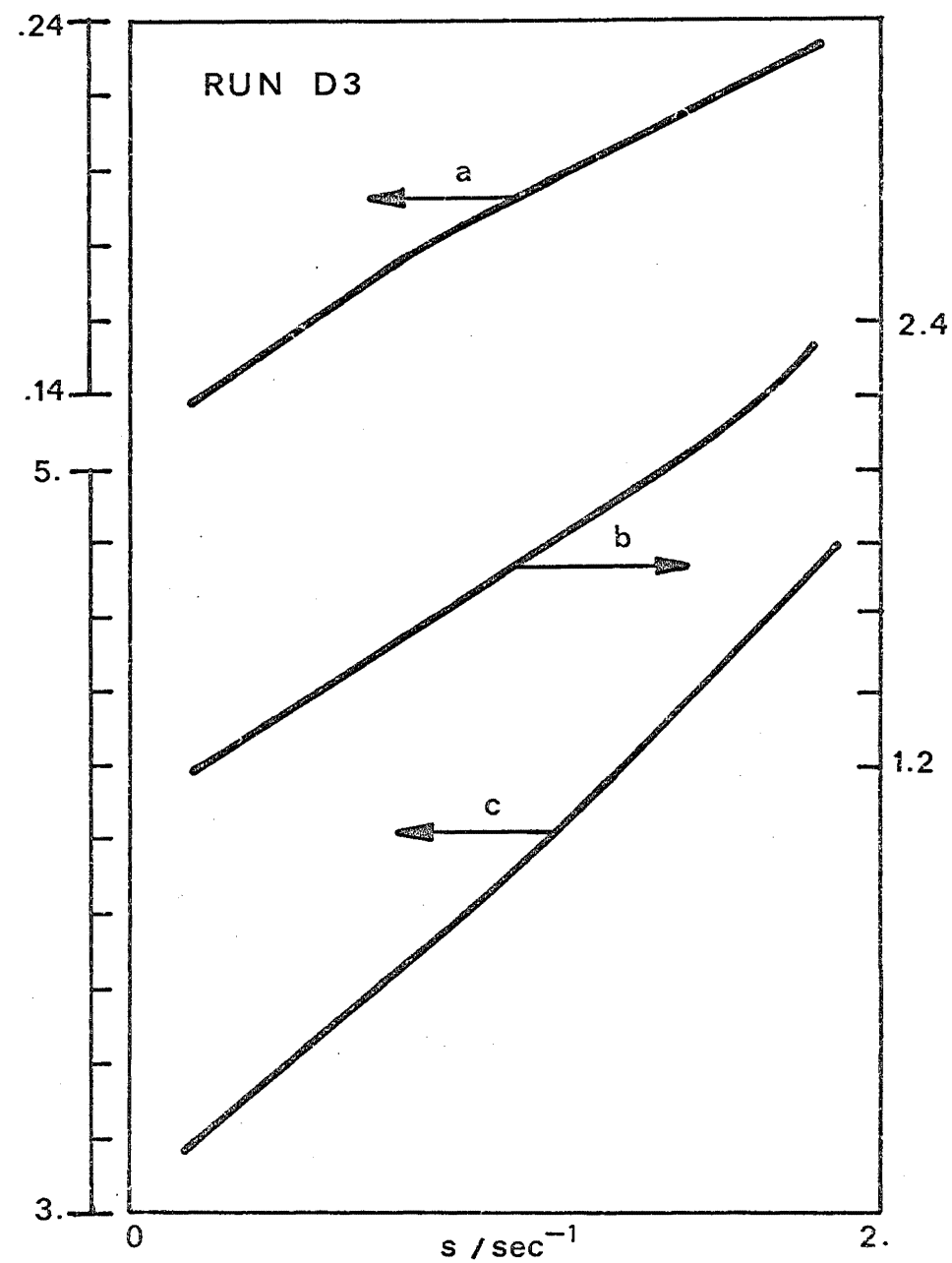
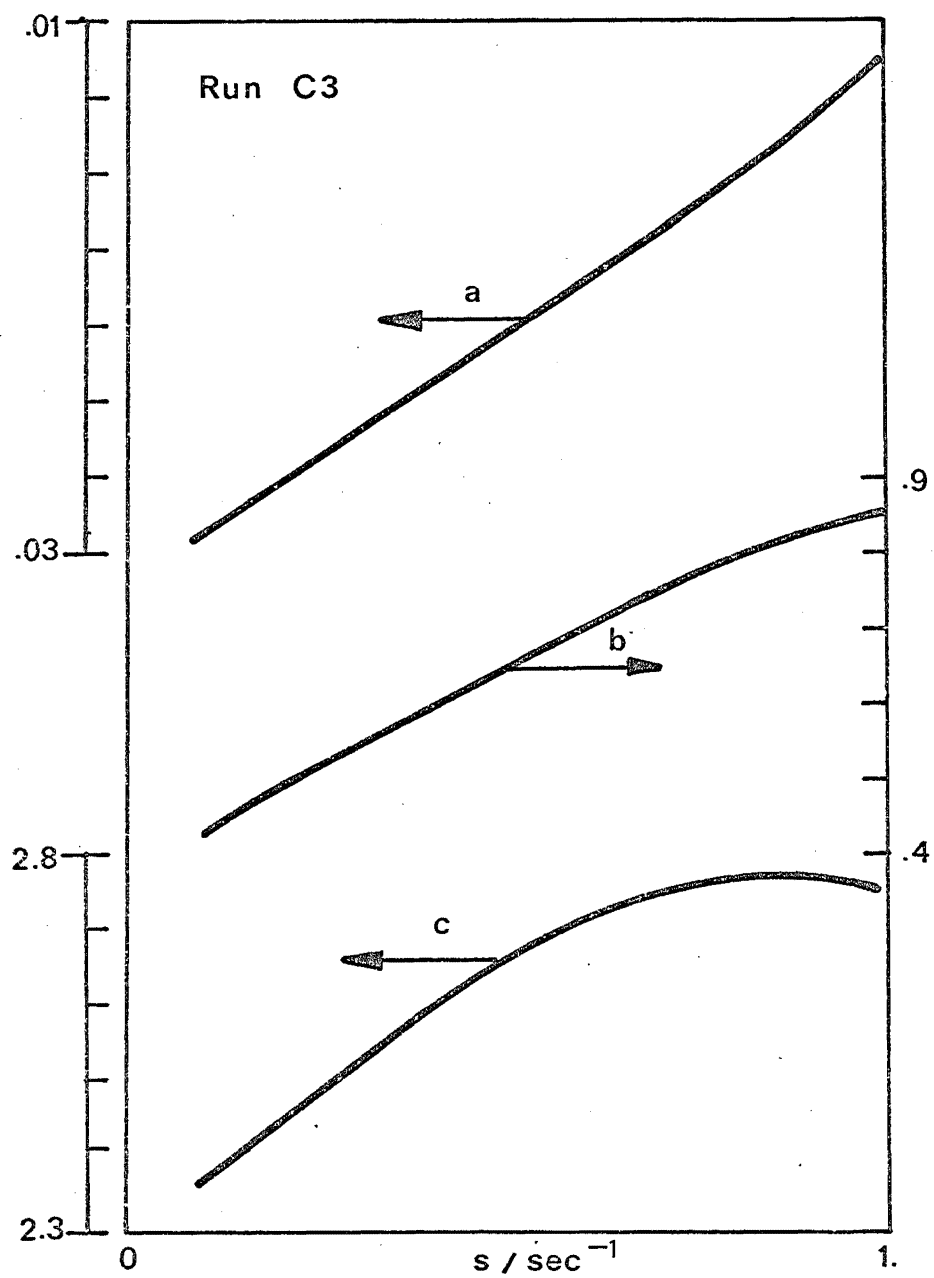


FIGURE 4.5 (cont.)

Curves:

(a)  $1/U_1^2$  in  $\text{sec}^{-2}$ ,  
ADPF model

(b)  $1/\sqrt{U_2}$  in  $\text{sec}^{-1}$ ,  
TSPF model

(c)  $U_1/\sqrt{U_2}$  in  $\text{sec}^{-1}$ ,  
TSPF model

FIGURE 4.5 (cont.)

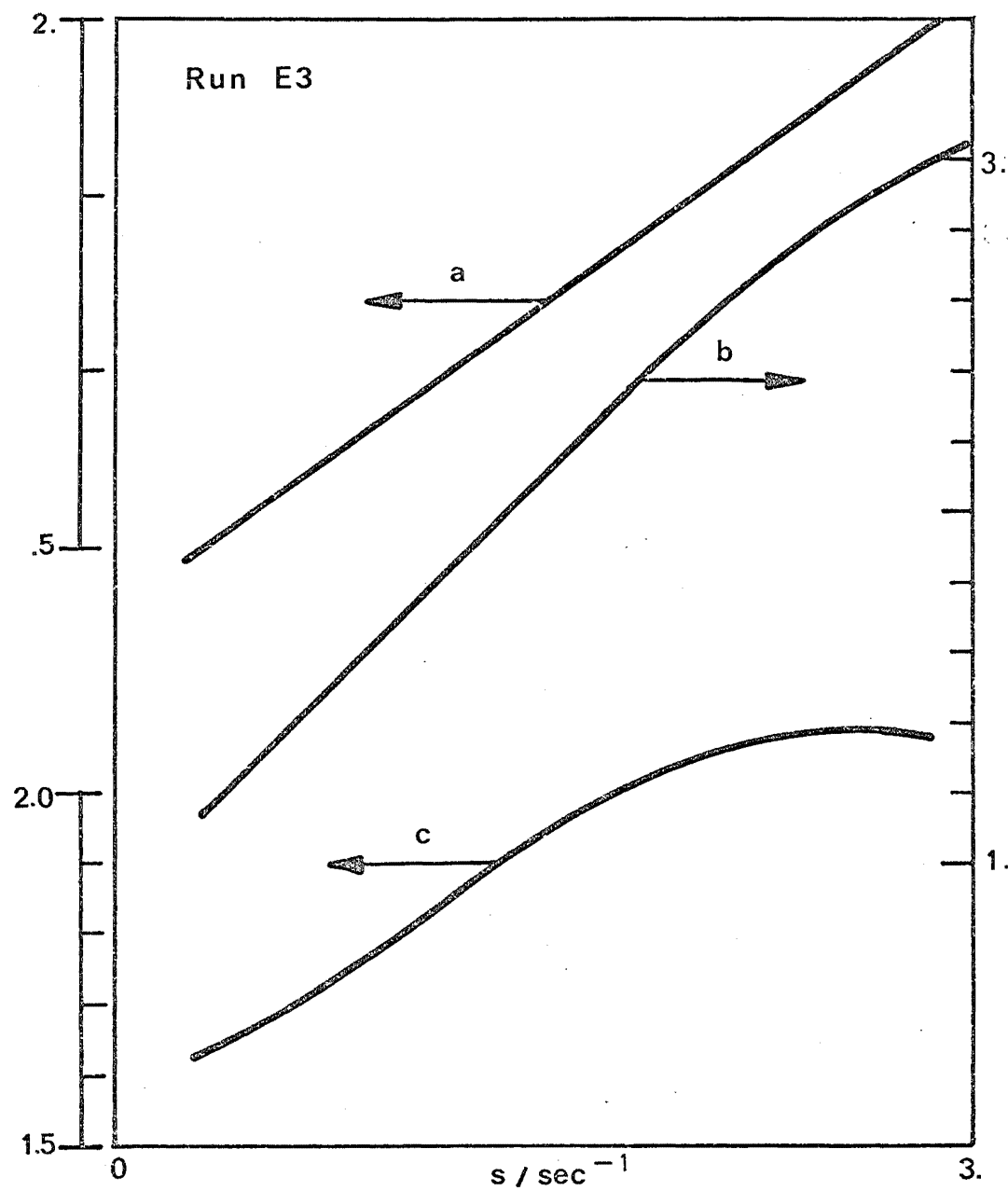


TABLE 4.4

Transfer function analysis of droplet R.T.D.

Run	A.D.P.F.		T.S.P.F.		
	$\tau/s$	Pe	n	$T_t/s$	$T_p/s$
A1	20.5	11.8	3.76	17.4	4.12
A2	14.4	11.3	4.42	11.2	2.7
A3	6.9	5.75	2.15	5.64	1.28
B3	6.36	11.9	2.82	4.32	2.00
C3	6.16	9.65	4.76	5.12	0.75
D3	2.81	21.2	2.14	1.42	1.43
E3	1.74	3.96	2.15	1.32	2.27

IV.3.4 Variation of dispersion with the operating conditions

The interpretation of the Peclet number is complicated by the existence of a size spectrum rather than a single size. Each response curve is thus a superimposition of many possibly different curves, one for each size. Only at very high entrainments will these curves tend to the same.

In run D3 the Peclet number is at a maximum; this occurs at an atomising air rate / drying air rate ratio  $R_u = 0.019$ , which is near the minimum dispersion point (maximum Pe) for the air flow as well.

#### IV.3.5 Degree of entrainment

In Table 5 the "predicted" and measured values of the droplet mean residence time,  $\tau_{Dp}$  and  $\tau_{Dm}$ , and the atomising air mean residence time,  $\tau_A$ , are tabulated against the entrainment parameter  $R_D$ . The "predicted" values  $\tau_{Dp}$  were based on the free fall of a particle with diameter  $D_m$  with no acceleration or turbulence effect. It can be seen that  $\tau_{Dm}$  starts to deviate significantly from  $\tau_{Dp}$  and to tend to  $\tau_A$  from run C3 onwards, at  $R_D \approx 0.03$ . An exception is run D3, where the measured and predicted values  $\tau_{Dm}$  and  $\tau_{Dp}$  are much closer than expected. This run is at the minimum dispersion point, where the air-flow pattern and turbulence structure are profoundly altered (Chapter 3), so that  $R_D$  may have been overestimated. Also, the droplet flow in this regime may have been confined to a thin core where low turbulence prevails, since it has been found that the air flow is close to the plug flow regime.

TABLE 4.5

Droplet and air mean residence times

Run	$R_D$	$\tau_{Dp}/s$	$\tau_{Dm}/s$	$\tau_A/s$	$\frac{\tau_{Dm} - \tau_{Dp}}{\tau_A - \tau_{Dp}}$
A1	0	28.3	20.5	31.1	- 1.6
A2	$4 \times 10^{-5}$	17.5	14.4	29.1	- 0.27
A3	$1 \times 10^{-3}$	7.4	6.9	29.1	- 0.2
B3	$6 \times 10^{-3}$	4.24	6.4	14.8	0.2
C3	$2.8 \times 10^{-2}$	4.8	6.2	6.54	0.8
D3	$8 \times 10^{-2}$	2.63	2.8	3.62	0.2
E3	0.16	1.36	1.74	1.59	1.7

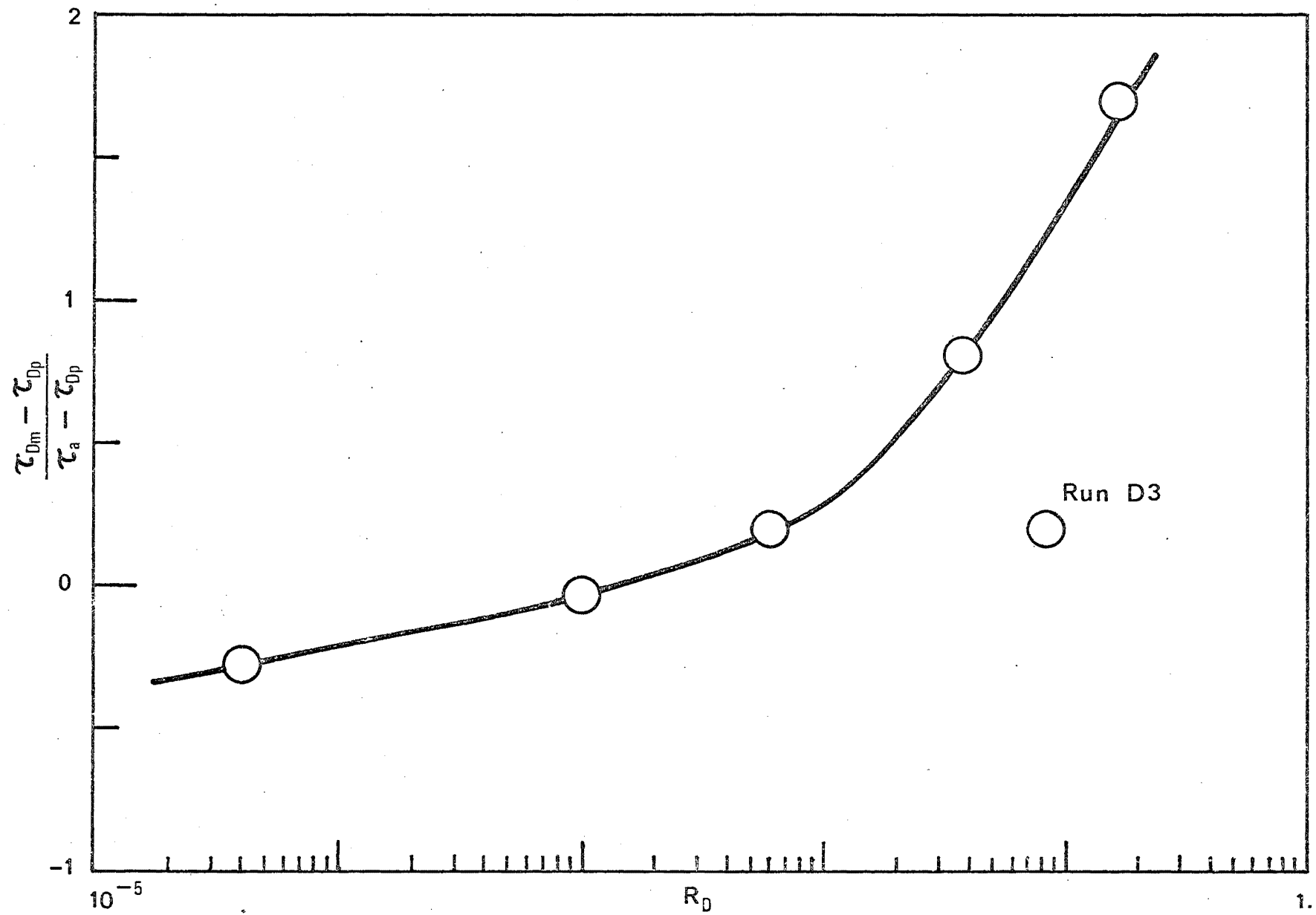


FIGURE 4.6: EFFECT OF THE ENTRAINMENT PARAMETER  $R_D$   
 (see errata at front)

A measure of the degree of entrainment is the fractional approach to the air mean residence time  $R_t$ :

$$R_t \equiv \frac{\tau_{Dm} - \tau_{Dp}}{\tau_A - \tau_{Dp}} \quad (4.22)$$

This parameter is tabulated in Table 5 and plotted against  $R_D$  in figure 6. It should theoretically range between 0 and 1, but due to the approximations made (replacement of the size spectrum by a single size, neglect of the jet zone and of any bypassing, neglect of the effect of the liquid flow at the nozzle on the atomising air flow pattern), values outside this range are found.

In spite of this, there is a visible correlation between  $R_D$  and  $R_t$ , except for run D3 at the minimum dispersion point. The  $R_t$  curve climbs steeply after  $R_D \approx 5 \times 10^{-3}$ , indicating that turbulence effects, possibly Basset forces, and entrainment become rapidly important from that value onwards.

## V. CONCLUSION

On the operation and design of cocurrent spray dryers the following recommendations can be made after examining the results from the present experiment :

(1) It is desirable to promote a high degree of turbulence near the atomiser, in order to disperse the droplets into the air flow and avoid bypassing. For this purpose, a high air inlet velocity may be necessary and can be obtained by forcing the drying air to come in as jets, for example. Alternatively a secondary air stream can be made to impinge on the spray, as in the new Czech-type spray dryers<sup>(K9)</sup>.

(2) When pneumatic or possibly pressure atomisers are used, the

minimum dispersion point ( $Ct \approx 0.25$ ,  $R_u \approx 0.018$ ) is to be avoided, as bypassing of the whole spray (i.e. insufficient mixing) may occur.

(3) Operating at high air turbulence and entrainment ( $R_t \gg 0.005$ ) increases the drag force and hence should also increase the heat and mass transfer rate, a factor which may improve product quality or at least go some way towards counteracting the adverse effect of backmixing.  $R_D$  seems to be a convenient and useful parameter for measuring this effect, but more experimental data would be desirable in order to confirm this.

Quantitatively the results of this experiment are not as rigorous as may be hoped for, and are difficult to interpret because of the existence of a size spectrum. The experiment is of an exploratory nature and many improvements are possible. In particular, the addition of a cascade impactor, such as the one described by May<sup>(M9)</sup>, to the design of the travelling droplet catcher in order to single out a certain size may yield useful results.



NOTATION FOR CHAPTER 4

$c_D$	drag coefficient, [ - ]
$D_m$	mass-median diameter, [ m ]
$\mathcal{D}_t$	turbulent diffusivity of fluid, [ m <sup>2</sup> /s ]
$\mathcal{D}_p$	turbulent diffusivity of particles or droplets, [ m <sup>2</sup> /s ]
$F_D$	drag force, [ N ]
$I$	relative turbulent intensity, $(u'/\bar{u})^2$ , [ - ]
$K_L$	$t_L \epsilon / u'^2$ , [ - ]
$n$	$d(\ln c_D) / d(Re)$ , [ - ]
$R_D$	entrainment parameter, equation 12, [ - ]
$R_t$	fractional approach of liquid residence time to air residence time, $(\tau_{Dm} - \tau_{Dp}) / (\tau_A - \tau_{Dp})$ , [ - ]
$R_u$	atomising air/drying air flow rate ratio, [ - ]
$s$	Laplace transform parameter, [ s <sup>-1</sup> ]
$T_p$	plug flow time, [ s ]
$T_t$	total tank time, [ s ]
$t_L$	Lagrangian time scale of fluid turbulence, [ s ]
$t_{Lp}$	Lagrangian time scale of particle turbulence, [ s ]
$t_p$	particle time constant (equation 10), [ s ]
$t_{pt}$	value of $t_p$ at terminal velocity in quiescent air, [ s ]
$\bar{u}$	mean air velocity, [ m/s ]
$u'$	root-mean-square turbulent air velocity, [ m/s ]
$u'_p$	root-mean-square turbulent particle velocity, [ m/s ]
$\bar{u}_R$	mean relative velocity, [ m/s ]
$u'_R$	root-mean-square turbulent relative velocity, [ m/s ]
$u_{Re}$	effective relative velocity, [ m/s ]
$u_t$	terminal velocity of particle in quiescent air, [ m/s ]
$U_o, U_1, U_2$	functions of the transfer function as defined in Chapter 2.

(Notation for Chapter 4, cont.)

$\epsilon$	turbulent energy dissipation per unit mass, $[ \text{m}^2/\text{s}^3 ]$
$\nu$	fluid kinematic viscosity, $[ \text{m}^2/\text{s} ]$
$\lambda_g$	Eulerian lateral microscale of turbulence, $[ \text{m} ]$
$\lambda_L$	Lagrangian microscale of turbulence, $[ \text{m} ]$
$\tau$	mean residence time, or parameter in the A.D.P.F. model, $[ \text{s} ]$
$\tau_A$	atomising air mean residence time, $[ \text{s} ]$
$\tau_{Dm}$	measured droplet mean residence time, $[ \text{s} ]$
$\tau_{Dp}$	predicted droplet mean residence time based on zero turbulence, $[ \text{s} ]$

#### Dimensionless numbers

$Ct$	Craya-Curtet number = (vessel radius x drying air velocity)/ (nozzle radius x atomising air velocity)
$Pe$	Peclet number for A.D.P.F. model
$Re$	(particle) Reynolds number

CHAPTER 5TRANSPORT PHENOMENA FOR SINGLE DROPLETSChapter contents:INTRODUCTIONI. BASIC EQUATIONS OF TRANSFER

1. Heat and mass transfer
2. Momentum transfer

II. VARIOUS INFLUENCES ON PARTICLE-FLUID TRANSFER PHENOMENA

1. Effect of mass flux on heat transfer
2. Effect of free convection
3. Effect of radiation
  - (a) Particle in a dilute cloud
  - (b) Particle in a dense cloud
4. Effect of turbulence
  1. On momentum transfer
  2. On heat and mass transfer
5. Effect of droplet sensible heat
6. Presence of solids
  1. Particle formation
  2. Drying behaviour
7. Drop mechanics

## NOTATION

## INTRODUCTION

A detailed knowledge of transfer phenomena to single droplets is a starting point to any study of spray evaporation. Extensive reviews have been done elsewhere on this subject (M6,M8,S3,B17,F8) and we shall not attempt to repeat them, but simply to summarise the most significant results to serve as a basis for the next chapter. Some aspects, however, have not received much attention before and will be dealt with in more detail.

### I. BASIC EQUATIONS OF TRANSFER

#### I.1 Mass and heat transfer

For a spherical body in an infinite quiescent fluid it can be shown analytically that<sup>(L1)</sup>:

$$Nu = 2 \quad (5.1a)$$

$$Sh = 2 \quad (5.1b)$$

When the particle and the fluid are in relative motion, it can be expected from dimensional analysis that:

$$Nu = Nu (Re, Pr) \quad (5.2a)$$

$$Sh = Sh (Re, Sc) \quad (5.2b)$$

and much work has been done to determine the actual form of these equations. (A5,F7,E1,G2,H22,J2,M1,P4,P12,R3,R4,W3) The most widely accepted form is that due to Frössling<sup>(F7)</sup>:

$$Nu = 2 + \beta Re^{\frac{1}{2}} Pr^{1/3} \quad (5.3a)$$

$$Sh = 2 + \beta Re^{\frac{1}{2}} Sc^{1/3} \quad (5.3b)$$

Values of  $\beta$  found experimentally range from 0.52 to 0.72<sup>(B16, P12)</sup> except for a value of 0.95 found by Garner and Suckling<sup>(G4)</sup> for solid spheres in liquids. The most widely quoted value, and the one used

in this work because of its intermediate value and the close resemblance between the experimental condition and the spray drying situation (droplets in air), is that due to Ranz and Marshall<sup>(R4)</sup>:

$$\beta = 0.6 . \quad (5.3b)$$

These authors also pointed out that in evaluating the dimensionless numbers, the average film properties (at a temperature and concentration equal to the arithmetic mean between the surface and bulk fluid values) should be used. Some care must be exercised in defining Nu when the mass transfer has an important effect on the heat transfer. Equations 3a and 3b can be rewritten in terms of the heat transfer rate  $q$  and mass transfer rate  $\dot{m}$  as:

$$q = \pi k_f D_p (T_\infty - T_s) (2 + 0.6 Re^{\frac{1}{2}} Pr^{1/3}) \quad (5.4a)$$

$$\dot{m} = \pi \mathcal{D}_{AB} D_p \left( \frac{c_{A\infty} - c_{As}}{x_{BM}} \right) (2 + 0.6 Re^{\frac{1}{2}} Sc^{1/3}) \quad (5.4b)$$

where  $D_p$  is the particle diameter,  $k_f$  the gas thermal conductivity,  $\mathcal{D}_{AB}$  the diffusion coefficient,  $T_\infty$  and  $T_s$  the fluid and surface temperatures,  $c_{A\infty}$  and  $c_{As}$  the fluid and surface (mass-) concentration of the transferred substance, and  $x_{BM}$  the log-mean mole fraction of the non-transferred substances between infinity and surface. At steady state, equations 4a and 4b are coupled by the heat balance:

$$q = - \lambda \dot{m} \quad (5.5)$$

and the equilibrium curve:

$$c_{As} = c_{As}^* (T_s) \quad (5.6)$$

so that the system of equations (4a, 4b, 5, 6) can be solved for  $q$ ,  $\dot{m}$ ,  $T_s$  and  $c_{As}$  when the other variables are known.

For the water-air system

$$Pr \approx Sc \quad (5.7)$$

or

$$\frac{k_f}{\phi_{AB} c_{pf} \rho_f} \approx 1 \quad (5.8)$$

where  $c_{pf}$  and  $\rho_f$  are the specific heat and density of the fluid, hence equations 4a and 4b can be reduced to:

$$\frac{T_\infty - T_s}{Y_\infty - Y_s} \approx - \frac{\lambda}{c_{pf}} = \frac{T_\infty - T_s^*}{Y_\infty - Y_s^*} \quad (5.9)$$

that is, the surface temperature and humidity ( $Y_s = c_{As}/(\rho_f - c_{As})$ ) are equal to the adiabatic saturation temperature  $T_s^*$  and humidity  $Y_s^*$  respectively, and independent of Re. Equations 4a, 4b and 5 can now be reduced to:

$$\dot{m} = - \frac{\pi k_f D_p (T_\infty - T_s^*)}{\lambda} (2 + 0.6 Re^{1/2} Pr^{1/3}) \quad (5.10)$$

(one equation in one unknown,  $\dot{m}$ ) .

If the particle is a spherical droplet of pure liquid, the rate of shrinking can be easily derived from equation 10:

$$\frac{d(D_p^2)}{dt} = - \frac{4k_f (T_\infty - T_s^*)}{\rho_p \lambda} (2 + 0.6 Re^{1/2} Nu^{1/3}) \quad (5.11)$$

For the quiescent-fluid case (equation 1) this reduces to:

$$\frac{d D_p}{dt} = - \frac{4 k_f (T_\infty - T_s^*)}{\rho_p \lambda} \frac{1}{D_p} \quad (5.12a)$$

or

$$\frac{d(D_p^2)}{dt} = \text{constant} \quad (5.12b)$$

an equation extensively used in the spray drying literature.

Finally, if one puts  $E$  = fractional evaporation, equation 10 becomes:

$$\frac{dE}{dt} = \frac{\pi k_{fp}^D (T_\infty - T_s^*)}{\lambda m_o} (2 + 0.6 Re^{1/2} Pr^{1/3}) \quad (5.13)$$

for a pure water droplet, where  $m_o$  is the initial droplet mass. If the droplet contains solids

$$\frac{dE}{dt} = \frac{\pi k_{fp}^D (T_\infty - T_s^*)}{\lambda m_o w_{lo}} (2 + 0.6 Re^{1/2} Pr^{1/3}) \quad (5.13a)$$

where  $w_{lo}$  is the initial solid mass fraction.

## I.2 Momentum transfer

The drag coefficient

$$c_D = \frac{\text{drag force}}{\text{inertial stress} \times \text{projected area}} \quad (5.14)$$

has been plotted for solid spherical particles by Lapple and Shepherd<sup>(L2)</sup>. This "standard drag curve" has won universal acceptance and still serves as a basis for subsequent modifications due to deformation, deviations from sphericity, turbulence and other effects<sup>(T5, T6)</sup>.

For low Reynolds numbers ( $Re < .1$ ) the flow around a sphere is laminar and  $c_D$  is given by Stokes's equation:

$$c_D = \frac{24}{Re} \quad (5.15)$$

For higher Reynolds numbers, many equations have been proposed, both theoretical (H2, H3, H8, K2) and empirical (B6, C5, D5, G4, H6, I1, K1, S3, S12, U1).

Apart from Ingbo<sup>(I1)</sup>, most of the latter are simply attempts to approximate the standard drag curve by algebraic equations. After investigating several of these, the author found that the following

segmentwise approximation gives the best fit ( $\pm 4\%$  up to  $Re = 5000$ ) :

$$c_D = 24/Re \quad Re \leq .4 \quad (5.16a)$$

$$= \frac{24}{Re} (1 + 0.1 Re), \quad .4 < Re \leq 2. \quad (5.16b)$$

$$= \frac{24}{Re} (1 + 0.15 Re^{.687}) + \frac{0.42}{1 + 4.25 \times 10^4 Re^{-1.16}} \quad (5.16c)$$

$$2 < Re \leq 5000$$

The second equation is similar to Oseen's equation<sup>(O.2)</sup>, the third is Schiller and Naumann's equation<sup>(S2)</sup> with an extra term by Clift and Gauvin<sup>(C5)</sup>.

Lapple and Shepherd<sup>(L2)</sup> have also derived general equations for the motion of particles in several cases of interest, while Sjetnitzer<sup>(S11)</sup> considered cases where the particles are shrinking during motion.

In many cases, the droplet or particle will travel at its terminal velocity  $u_t$  with respect to the gas. If Stokes's equation applies, then  $u_t$  is given by:

$$u_t = \frac{D_p^2 (\rho_p - \rho_f) g}{18 \mu_f} \quad (5.17)$$

where  $g$  is the acceleration of gravity and  $\mu_f$  the fluid viscosity. Outside the laminar regime  $u_t$  is usually computed numerically<sup>(P6)</sup>. However, Smith<sup>(S12, B17)</sup> has derived the following equation which can be used for  $u_t$  :

$$c_D = \frac{576}{\Pi} + \frac{32}{\Pi^{.39}} + \frac{1}{1.8 + 758 \Pi^{-.36}} \quad (5.18)$$

where  $\Pi = c_D Re^2$



$$\Pi = \Pi_t = \frac{4 g \rho_f D_p^3 (\rho_p - \rho_f)}{3 \mu_f^2} \quad (5.19)$$

at the terminal velocity  $(P6)$ . This equation has been found by the author to apply in the range  $\Pi > 10$ . For  $\Pi \leq 10$ , equation 17 can be used (Table 1).

$\Pi_t$  is a measure of the relative importance of the gravitational and drag forces acting on a particle at settling velocity. It has been found (D7, H14) that water droplets with diameters less than about 40  $\mu\text{m}$  will follow the motion of the surrounding air stream. In terms of  $\Pi_t$  the condition for complete entrainment can thus be stated:

$$\Pi_t < 4 \quad (5.20)$$

TABLE 5.1

Terminal coefficients by Stokes's and Smith's equations

Re	$\Pi = c_D R_e^2$		$c_D$	
		Experiment	Stokes	Smith
.1	2.4	240.	240.	
.3	7.2	80.	80.	
.7	17.9	36.5	32.1	42.5
2	57.6	16.6	10.0	16.6
10	410.	4.1		4.5
200	$3.1 \times 10^4$	.77		.64
1000	$4.6 \times 10^5$	.46		.31
3000	$3.6 \times 10^6$	.40		.28
7000	$1.9 \times 10^7$	.39		.32
20000	$1.8 \times 10^8$	.45		.40

## II. VARIOUS INFLUENCES ON PARTICLE-FLUID TRANSFER PHENOMENA

### II.1 Effect of mass flux on heat transfer:

In simultaneous heat and mass transfer, some heat is transported by convection as well as conduction, the transferred matter taking up or releasing some of the heat as it goes through a thermal gradient. In this case, care must be exercised in defining the heat transfer coefficients  $h$  and the Nusselt number  $Nu = h D_p / k_f$ .

The commonest practice is to define  $h$  and  $Nu$  as "apparent" transfer coefficients:

$$h \equiv \frac{q_s}{T_\infty - T_s} \quad (5.21)$$

where  $q_s$  is the heat transferred to the particle surface. The total heat lost (gained) by the surroundings will be greater (less), due to heat being used in heating (cooling) the evaporating (condensing) vapour. Thus defined,  $h$  and  $Nu$  differ from the "true" or zero-mass-flux values  $h_o$ ,  $Nu_o$  by a factor

$$f_{Nu} \equiv \frac{Nu}{Nu_o} = \frac{h}{h_o}.$$

When mass is being transferred from the particle to its surroundings,  $f_{Nu}$  will always be less than 1. The governing parameter here is Spalding's number:

$$B \equiv \frac{c_{pv} (T_\infty - T_s)}{\lambda} \quad (5.22)$$

Several relationships have been proposed, among them:

(a) The film theory<sup>(S16, R4)</sup>:

$$f_{Nu} = \frac{\ln(1+B)}{B} \quad (5.23)$$

(b) The laminar boundary layer theory <sup>(E2)</sup>:

$$f_{\text{Nu}} = \frac{1}{1+B} \quad (5.24)$$

(c) The slow-viscous flow theory <sup>(E2)</sup>:

$$f_{\text{Nu}} = (1 + B/2)^{-1} \quad (5.25)$$

(d) Hoffmann and Ross's boundary layer theory <sup>(H17)</sup>:

$$f_{\text{Nu}} = (1 + B)^{-.6} \quad (5.26)$$

A comparison of the predictions of these equations for the water air system is shown in Table 2. Equation 24 seems to be the most widely accepted in spray drying situations <sup>(K3)</sup>.

TABLE 5.2

Predictions of mass flux effect on heat transfer for  
air-water systems.

$\Delta T/K$	50	100	150	200
$1 - B$	.021	.042	.063	.085
$1 - \ln(1+B)/B$	.011	.021	.032	.041
$1 - (1+B)^{-1}$	.021	.040	.059	.079
$1 - (1+B/2)^{-1}$	.010	.021	.040	.059
$1 - (1+B)^{-.6}$	.013	.024	.036	.048

## II.2 Effect of free convection

Free convection adds another component to the relative velocity. Fuchs <sup>(F8)</sup> proposed that in Ranz and Marshall's equation 3,  $Re$  should be replaced by  $Re = \sqrt{Gr}$ .

## II.3 Effect of Radiation

### (a) Particle in a dilute cloud:

A single particle at temperature  $T_p$  in an infinitely large vessel with wall temperature  $T_w$  will receive a radiant heat rate:

$$q_R = \sigma \pi D_p^2 \alpha_p (T_w^4 - T_p^4) \quad (5.27)$$

where  $\alpha_p$  is the particle absorptivity and  $\sigma$  is Stefan-Boltzmann's constant. For liquid droplets the prediction of  $\alpha_p$  is very difficult. Multiple reflections, refractions and absorptions inside the droplet must be considered <sup>(H21)</sup>. If the droplet contains solids as well, the problem becomes intractable, and  $\alpha_p$  must be determined experimentally. A discussion of the importance of radiation in spray drying can be found in reference H15.

When gas radiation is also important, equation 27 can no longer be used because of interaction between wall, gas and particles, each of which emits and transmits or reflects radiation simultaneously. According to Hottel and Sarofim <sup>(H21)</sup>, we can define a net leaving flux or radiosity density  $W$ , which is the sum of transmitted, reflected and emitted radiant energy per unit solid angle (steradian) at each point. The manner in which  $W$  can be calculated for any system has been described by Hottel and Sarofim <sup>(H21)</sup> and applied to spray drying chambers by Hoffmann and Gauvin <sup>(H15, H16)</sup>. Briefly, it consists of subdividing the system into elements of surface and volume

which are assumed to be at uniform temperatures. The radiant transfer to a particle is then given by

$$q_R = \pi D_p^2 \frac{\alpha_p}{1 - \alpha_p} (W - \sigma T_p^4) \quad (5.28)$$

(b) Particle in a dense cloud

For particles in a dense cloud gas radiation may not be important because of the short mean beam length between particles. On the other hand, particles now tend to shield each other from the wall, so that a wall-particle view factor  $S_{wp}$  must be introduced into equation 27:

$$q_R = \sigma \pi D_p^2 \alpha_p S_{wp} (T_w^4 - T_p^4) \quad (5.29)$$

$S_{wp}$  takes into account directly-received as well as reflected radiation. The rest of this section will be devoted to the calculation of this factor  $S_{wp}$ , which has received little attention so far. We first consider the cloud absorptivity  $\alpha_c$ , which is the fraction of light impinging on the cloud absorbed by it.  $\alpha_c$  has been related to  $\alpha_p$  by: <sup>(P6)</sup>

$$\alpha_c = 1 - \exp(-K_e L_b \alpha_p) \quad (5.30)$$

where  $K_e$  is the "extinction coefficient" of the cloud, or projected particle area ( $\pi D_p^2/4$  per particle) per unit cloud volume, and  $L_b$  is the mean beam length, defined as the length of a parallel beam after which the same fraction of the original light has been intercepted as in the actual situation. For  $\alpha_p < 1$  this equation is in error, as it implies that reflected light continues to travel in the same direction as before. We shall therefore try to derive a more accurate expression.

Consider a beam of light of intensity  $I_0$  falling on the cloud (Figure 1). For each increment of distance  $dx$  a fraction  $K_e dx$  of the light is intercepted, hence the intensity  $I$  of the beam is



decreasing at a rate:

$$\frac{dI}{I} = K_e dx \quad . \quad (5.31)$$

Hence, by integrating (31) from 0 to  $L_b$  :

$$\text{Unintercepted light} = I_o \exp(-K_e L_b) \quad (5.32)$$

$$\text{First-time intercepted light} = I_o (1 - \exp(-K_e L_b)) \quad (5.33)$$

Of the first-time intercepted light, a fraction  $\alpha_p$  is absorbed and  $(1 - \alpha_p)$  is reflected:

$$\text{First absorption} = I_o \{1 - \exp(-K_e L_b)\} \alpha_p \quad (5.34)$$

$$\text{First reflection} = I_o \{1 - \exp(-K_e L_b)\} (1 - \alpha_p) \quad (5.35)$$

The light from the first reflection travels another mean beam length  $L'_b$  ( $\neq L_b$ ) before reaching the cloud boundary. Along similar lines of reasoning it can be seen that:

$$\begin{aligned} \text{Second-time intercepted light} &= \text{1st reflection} \times (1 - \exp(-K_e L'_b)) \\ &= I_o \{1 - \exp(-K_e L_b)\} (1 - \alpha_p) \{1 - \exp(-K_e L'_b)\} \end{aligned} \quad (5.36)$$

$$\begin{aligned} \text{Second-time absorbed light} &= \text{2nd time intercepted light} \times \alpha_p \\ &= I_o \{1 - \exp(-K_e L_b)\} (1 - \alpha_p) \{1 - \exp(-K_e L'_b)\} \alpha_p \end{aligned} \quad (5.37)$$

By comparing equations 37 and 34 we see that the ratio between successive absorptions is:

$$r = (1 - \alpha_p) \{1 - \exp(-K_e L'_b)\} \quad , \quad (5.38)$$

and we can assume this ratio to remain constant since after the second, third ... reflections the mean beam length for the reflected light to travel before it reaches the cloud boundary remains constant at  $L'_b$  .

To find the total absorption, we sum up the successive absorptions (which form a geometric series):

$$\begin{aligned} \text{Total absorption} &= \text{1st absorption} \times \sum_{j=0}^{\infty} r^j \\ &= I_0 \frac{\alpha_p (1 - \exp(-K_e L_b))}{1 - (1 - \alpha_p) (1 - \exp(-K_e L'_b))} \end{aligned} \quad (5.39)$$

Since  $\alpha_p$  is the fraction of  $I_0$  which is absorbed,

$$\alpha_c = \frac{\alpha_p (1 - \exp(-K_e L_b))}{1 - (1 - \alpha_p) (1 - \exp(-K_e L'_b))} \quad (5.40)$$

Now the mean beam length from boundary to boundary  $L_b$  is twice the mean beam length from boundary to particle  $L'_b$  :

$$L_b = 2L'_b \quad (5.41)$$

hence equation 40 becomes:

$$\alpha_c = \frac{\alpha_p \{1 - \exp(-K_e L_b)\}}{1 - (1 - \alpha_p) \{1 - \exp(-K_e L_b/2)\}} \quad (5.42)$$

Equation 42 enables the wall-to-cloud radiation transfer  $q_{w \rightarrow c}$  to be calculated by the standard equation<sup>(H21)</sup>:

$$q_{w \rightarrow c} = \frac{\sigma A_c}{1/\alpha_c + 1/\alpha_w - 1} (T_w^4 - T_p^4) \quad (5.43)$$

where  $A_c$  is the cloud outside area which is also the wall area of the chamber and  $\alpha_w$  is the chamber wall emissivity.

We now put

$$q_{w \rightarrow c} = q_R V_c n \quad (5.44)$$

where  $q_R$  is the radiation to one particle,  $V_c$  the cloud or vessel volume,  $n$  the number of particles per unit cloud volume. Substituting equations 43 and 29 into 44, we get:

$$S_{wp} = \frac{A_c}{(1/\alpha_c + 1/\alpha_w - 1) V_c n \pi D_p^2 \alpha_p} \quad (5.45)$$



But  $A_c/V_c \equiv 4D_h$  where  $D_h$  is the hydraulic diameter of the cloud or vessel, and  $n\pi D_p^2 \equiv 4K_e$ , hence equation 45 becomes:

$$S_{wp} = \left[ \alpha_p (K_e D_h) (1/\alpha_c + 1/\alpha_w - 1) \right]^{-1} \quad (5.46)$$

where  $\alpha_c$  is given by equation 42.

There now remains to estimate the mean beam length  $L_b$  in equation 42. In gas radiation  $L_b$  is defined by:

(5.47)

Absorption through  $L_b \approx$  Absorption by given volume and shape of gas. Hottel (H20) showed that for this approximate equation to hold to a few per cent it is sufficient to take  $L_b \approx 0.9 D_h$ . But in our case, due to the presence of reflections, this approximate definition may lead to error. So we define  $L_b$  by the exact form of equation 47, which can be written as: (H20)

$$\exp(-K_e L_b) = \frac{2\pi \int \exp(-K_e x) \text{ (View angle factor) } d \text{ (solid angle)}}{2\pi \int \text{ (view angle factor) } d \text{ (solid angle)}} \quad (5.47b)$$

where  $x$  is the boundary-to-boundary distance in a certain direction. Ways of determining these integrals are described in reference H21. The only case in which equation 47 can be expressed analytically is that of a spherical cloud (chamber):

$$K_e L_b = - \ln \left\{ \frac{8}{9(K_e D_h)^2} \left[ 1 - \left( 1 + \frac{3}{2} K_e D_h \right) \exp \left( -\frac{3}{2} K_e D_h \right) \right] \right\} \quad (5.48)$$

However, numerical integration of equation 47 shows that  $K_e L_b$  varies with  $K_e D_h$  in almost exactly the same ways for infinite cylinders (Table 3). Hence equation 48 can be used for both, and also for any intermediate geometry.

TABLE 5.3Mean beam lengths of spheres and infinite cylinders

$K_e D_h$	$K_e L_b$	
	sphere	cylinder
0.2	.198	.195
1.	.93	.91
3.	2.4	2.3
5.	3.4	3.4
10.	4.7	4.8
100.	9.3	9.4

Note:

$D_h$  = cylinder diameter  
 $= \frac{2}{3} \times$  sphere diameter

TABLE 5.4Wall-particle view factor predictions

$\alpha_p$	$K_e D_h$	$S_{wp}$	
		present method	equation 30
.1	1.	.91	.86
	2.	.85	.82
	5.	.72	.72
	10.	.53	.59
.5	1.	.74	.72
	2.	.58	.59
	5.	.33	.36
.8	1.	.65	.64
	2.	.46	.48
	5.	.23	.24

To sum up our results so far: we use equation 48 to calculate  $L_b$ , equation 42 to calculate  $\alpha_c$ , equation 46 to calculate  $S_{wp}$ , and equation 29 to evaluate the wall-to-particle radiation.

When  $K_e D_h \rightarrow 0$  (very dilute cloud),

$$K_e L_b \rightarrow K_e D_h \quad (\text{from eqn.48})$$

$$\alpha_c \rightarrow \alpha_p K_e D_h \quad (\text{from eqn 42})$$

$$S_{wp} \rightarrow 1 \quad (\text{from eqn. 46}), \text{ as expected.}$$

Exactly the same result applies when  $\alpha_p \rightarrow 0$ , which means that if the particles are highly reflecting, the multiple reflections compensate for the intercepted light.

Table 4 gives some values of  $S_{wp}$  as calculated by the present method (equations 48, 42, 46, 29) and also by a combination of eqns.30 and 46 (in eqn.30 we use  $L_b = 0.9 D_h$  as recommended in the literature). As expected, when  $\alpha_p$  is small and  $K_e D_h$  not large, equation 30 leads to a low value of  $S_{wp}$  because it fails to take multiple reflections into account, while when  $K_e D_h$  is large, it predicts a high  $S_{wp}$  because it overestimates the mean beam length and neglects the light bouncing off the cloud at an early stage. However, in most cases the errors are not large and unless a great accuracy is required equation 30 would be adequate.

The equations derived for  $\alpha_c$  can also be quite useful in estimating the radiosity  $W$  in dense cloud situations, whence an accurate calculation of the wall-to-particle radiation is facilitated (equation 28), even when the wall temperature is not uniform as assumed in equation 29.

#### II.4 Influence of turbulence

The effect of turbulence on transfer phenomena in particle-fluid systems has been the subject of a vast amount of works. Several approaches have been tried and results are often contradictory.

In the field of momentum transfer, theoretical<sup>(B1,F6,L8,S14,S15)</sup> as well as experimental<sup>(K14,B1,L9,T6)</sup> studies are numerous. Some of the latter show that the drag force is increased by turbulence<sup>(U1)</sup>, while others show a decrease<sup>(T6,C5)</sup>, and some find no effect<sup>(B17)</sup>. Theoretical analysis, on the other hand, shows that the drag can be either increased or decreased depending on the pattern of turbulence, although an increase is the more common case. All theoretical works point to the important influence of scales of turbulence, while many experimental investigations either found no scale effects or simply ignore them.

A similar situation exists in the field of mass and heat transfer. Here again theoretical analysis points to a turbulence-scale effect<sup>(K13,L8)</sup>. While some experimental studies demonstrate this<sup>(G7,H7,K13,R3)</sup>, others show that turbulence intensity is the only factor<sup>(G2,L3,M2)</sup>, and some do not find any effect at all<sup>(D7,B15)</sup>. The lack of a unified approach to the correlation of results poses a handicap to an attempt to compare them: while some workers present the turbulence effect as empirical factors to be inserted into the transfer equations (eq.2)<sup>(G2,G7,H7)</sup>, others keep these equations unchanged, but introduce extra components in the Reynolds number, attributed to turbulence<sup>(L8,K13)</sup>.

Many of the experimental works have been done on large, fixed spheres, hence the results may not be directly applicable to spray-drying situations. Studies on the separation of the boundary layer and the interaction of turbulence with the wake suffer particularly

in this respect. Torobin and Gauvin (T6) did extensive work on free-falling spheres, but these are fairly large (1.5 mm - 3 mm). The main effect they found was the earlier occurrence of the critical Reynolds number  $Re_c$ , at which the drag coefficient  $c_D$  suddenly falls off to below 0.3. In turbulent flow  $Re_c$  occurs at 500-5000 (instead of  $4 \times 10^5$  for the standard drag curve) for  $u'_f/u_R = 0.1$  to  $0.4$ , where  $u'_f$  is the turbulent component of the fluid velocity. In spray drying, particle sizes are usually below 300  $\mu\text{m}$  for which  $\Pi$  (as defined in equation 19) is  $\approx 1000$  and  $Re \approx 20$  at the terminal velocity, hence this effect will not be important.

Comprehensive reviews of turbulence effects can be found in reference B17, T5, G2, F9. In the absence of definitive results, the theoretical approach of Friedlander (F6) and Levins and Glastonbury (L8) will be followed: first, evaluate the momentum transfer and relative turbulent velocities, then use them as a basis for calculating the added mass and heat transfer, according to standard relationships. This approach is deemed suitable for the low Reynolds number and small particle sizes encountered in spray-drying practice.

#### II.4.1 Effect of turbulence on momentum transfer:

##### (a) Force balance on the particle:

Most theoretical studies of particle motion in turbulent fields start from Tchen's equation (S15) which states that:

$$\begin{aligned} \text{Net force on particle} = & \text{Drag} + \text{Pressure gradient effect} \\ & + \text{added mass effect} + \text{Basset force} \\ & + \text{Body force} \end{aligned} \quad (5.49)$$

As Bailey (B1) pointed out, the effect of turbulence is mainly due to changes in the first and fourth terms of the right-hand side.

Added mass effects can be neglected in solid-gas systems. The Basset force constitutes a resistance to the unsteady state of the flow field. It can be neglected if

$$D_p \sqrt{\frac{\pi \rho_f}{2 \mu_f \tau}} < 1 \quad (5.50)$$

where  $\tau$  is the period of the oscillation. For large particles at high energy dissipation (low  $\tau$ ) this term can be quite large, especially when the fluid is a liquid, but it must usually be determined experimentally.

The effect of turbulence on the first term (drag force) can be easily explained qualitatively. Since

$$F_D = a \text{Re}^b \quad (5.51)$$

where  $b > 1$  (except in Stokes's regime) and  $F_D$  is the drag force, if  $\text{Re}$  is oscillating about a mean value  $\overline{\text{Re}}$ , we have:

$$\overline{F_D} = (\overline{a \text{Re}^b}) > a \overline{\text{Re}}^b \quad (5.52)$$

hence the mean drag force is increased with respect to the steady-state case. Quantitatively the effect is more difficult to calculate. The author suggests a vectorial addition of the average and turbulent components of velocity in calculating  $c_D$  and  $F_D$  :

$$\text{Re}_e = \sqrt{\overline{u_R}^2 + u_R'^2} \quad (5.53)$$

$$c_D = c_D(\text{Re}_e)$$

$$F_{Di} = \frac{1}{2} c_D \frac{\pi D^2}{4} \left( \sqrt{\overline{u_R}^2 + u_R'^2} \right) \overline{u_{Ri}} \quad (5.54)$$

where  $\overline{u_R}$  is the mean relative velocity,  $u_R'$  the root-mean-square turbulent relative velocity and  $i$  refers to the  $i$ -th direction.

(b) Effect of turbulence on relative motion:

Ignoring all terms on the right of equation 49 except the drag force, we have:

$$\rho_p \cdot \frac{\pi D_p^3}{6} \cdot \frac{du_R}{dt} = - \frac{1}{2} \cdot \frac{\pi D_p^2}{4} \cdot c_D \rho_f |u_R| u_R \quad (5.55)$$

or

$$\frac{du_R}{dt} = - \frac{u_R}{t_p} \quad (5.56)$$

where  $t_p$  is the particle time constant:

$$t_p = \frac{4 \rho_p D_p}{3 \rho_f c_D |u_R|} \quad (5.57)$$

For Stokes's regime, this becomes:

$$t_p = \frac{\rho_p D_p^2}{18 \mu_f} \quad (5.58)$$

$t_p$  is the ratio of the inertia of the particle to the drag force acting on it, and is a measure of how fast it can respond to velocity fluctuations in the fluid.

In Stokes's regime, Friedlander showed that

$$\frac{u_R'^2}{u_f'^2} = \frac{1}{1 + t_L/t_p} \quad (5.59)$$

where  $u'$  is the rms turbulent fluid velocity and  $t_L$  the Lagrangian time scale of turbulence. We shall assume that this result also holds in the turbulent regime, with  $t_p$  given by equation 57.

#### II.4.2 Effect of Turbulence on heat and mass transfer

In a turbulent field, heat and mass transfers are enhanced by two effects: the turbulent relative velocity  $u'_R$  and the turbulent velocity gradient. <sup>(L8)</sup> The latter has been found to be important in stirred vessel, especially at high energy dissipation rate, but it has not been correlated for gas-solids systems. Levins and Glastonbury suggest that in calculating the effective Reynolds number, the turbulent and average components of velocity should be added vectorially (equation 53). Then Nu and Sh can be calculated by standard relationships.

#### II.5 Effect of droplet sensible heat

When the droplet is not at the equilibrium surface temperature, some heat goes to heating or cooling it, so that the heat balance (equation 5) becomes:

$$q = -\lambda \dot{m} + c_{pp} m \frac{dT_p}{dt} \quad (5.60)$$

where  $c_{pp}$  is the particle specific heat,  $m$  its mass, and  $T_p$  its mean temperature. Usually the sensible heat term has a magnitude nearly two orders below that of the heat of evaporation term <sup>(K4)</sup> and can be ignored.

One case when the sensible heat is important is near the atomiser orifice, when the droplets are still essentially at the feed temperature which can be substantially higher than adiabatic saturation point (this is usually done purposely to accelerate the evaporation). The transfer equations 4a, 4b now become:

$$q' = \pi k_f D_p (T_\infty - T_p) (2 + 0.6 Re^{1/2} Pr^{1/3}) \quad (5.61)$$



$$\dot{m}' = - \pi D_{AB} D_p \frac{c_{Ap}^* - c_{A\infty}}{x'_{BM}} (2 + 0.6 Re^{1/2} Sc^{1/3}) \quad (5.62)$$

where  $c_{Ap}^*$  is the vapour mass concentration in equilibrium with  $T_p$  and the dash refers to non-steady state ( $T_p \neq T_s^*$ ) conditions.

In computations it will be convenient to express  $q'$ ,  $\dot{m}'$  in terms of the steady-state values  $q$ ,  $\dot{m}$ , when the droplet is at adiabatic saturation conditions  $T_s^*$ ,  $c_{As}^*$  (or  $T_s^*$ ,  $y_s^*$ ). For this we introduce the correction factors  $S_m$ ,  $S_h$ :

$$S_m \equiv \frac{\dot{m}'}{\dot{m}} = \frac{c_{Ap}^* - c_{A\infty}}{c_{As}^* - c_{A\infty}} \cdot \frac{x_{BM}}{x'_{BM}} \quad (5.63)$$

$$S_h \equiv \frac{q'}{q} = \frac{T_\infty - T_p}{T_\infty - T_s^*} \quad (5.64)$$

The rate of decrease of the droplet temperature can be obtained from equations 60, 63 and 64:

$$\frac{dT_p}{dt} = \frac{S_q q + \lambda S_m \dot{m}}{c_{pp} m} \quad (5.65)$$

$q$  and  $\dot{m}$  are the (hypothetical) steady-state transfer rates (for  $T_p = T_s^*$ ).

But

$$\lambda \dot{m} = - q \quad (5.5)$$

hence

$$\frac{dT_p}{dt} = \left( \frac{S_q - S_m}{c_{pp} m} \right) q = \left( \frac{S_m - S_q}{\lambda c_{pp} m} \right) \dot{m} \quad (5.66)$$

In terms of the fractional evaporation  $E$

$$m = m_o (1 - w_{lo} E) \quad (5.67)$$

$$\dot{m} = m_o w_{lo} \frac{dE}{dt} \quad (5.68)$$

where  $w_{lo}$  is the initial liquid mass fraction,

hence equation 66 becomes:

$$\frac{dT_p}{dE} = \frac{(S_q - S_m) w_{lo}}{\lambda c_{pp} (1 - w_{lo} E)} \quad (5.69)$$

an equation independent of time  $t$ .

## II.6 Presence of solids

The manner in which solids affect the evaporation behaviour depends on what form the solid-liquid dispersion takes: a suspension, a colloidal dispersion, a solution, or a combination of the three. Once the droplet has consolidated, the microstructure and hygroscopic properties of the solid will determine the subsequent drying pattern.

### II.6.1 Particle formation

In the first stages of evaporation, the droplet shrinks freely as does a pure liquid droplet. In some cases crystals may form at various places <sup>(C3)</sup>, in others a flexible membrane may form on the surface (for example with emulsions such as milk), but these at first do not hinder the shrinking.

At a certain value of the (dry basis) moisture content  $X_{cr}$ , the droplet rather suddenly forms a crust (figure 2). This moisture content  $X_{cr}$  is strongly dependent on the initial moisture content  $X_o$ , as shown in figure 3 for two slurries (experimental details for the present work on zinc oxide slurry can be found in Appendix B.III). For a short time, surface-tension forces cause a temporary shrinking of the particle, at the moment when the moisture is in a pendular state, i.e. forms wedges between solid elements. This can be observed in figure 2. The value of  $X_{cr}$  probably also depends on the drying rate, but little work has been done on this.

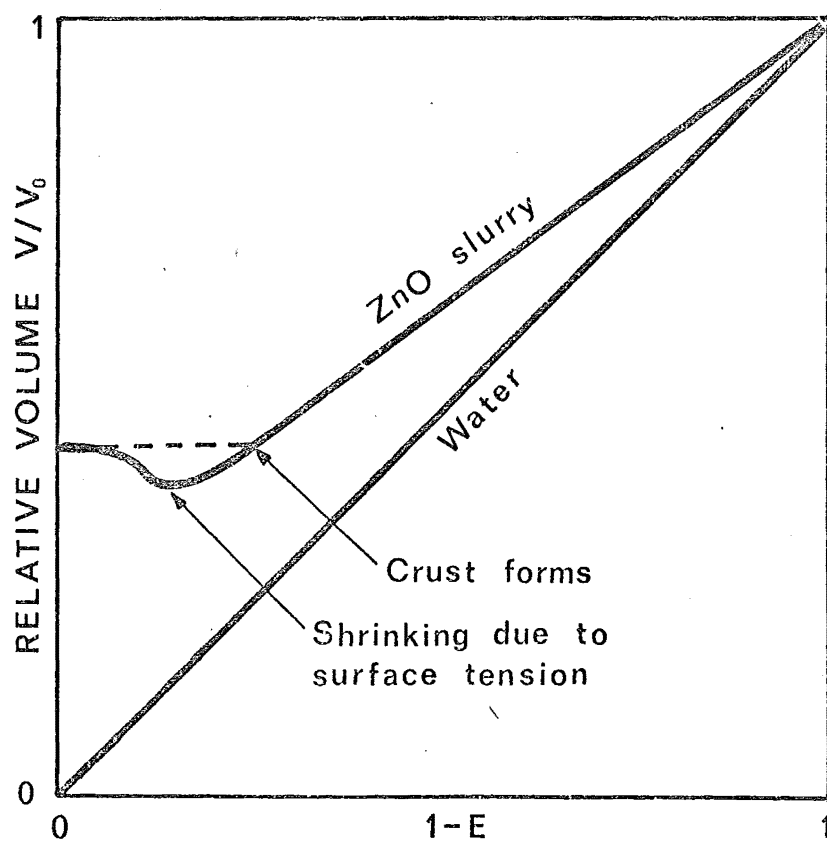


FIGURE 5.2 : SHRINKING OF A DROPLET  
OF ZINC OXIDE SLURRY

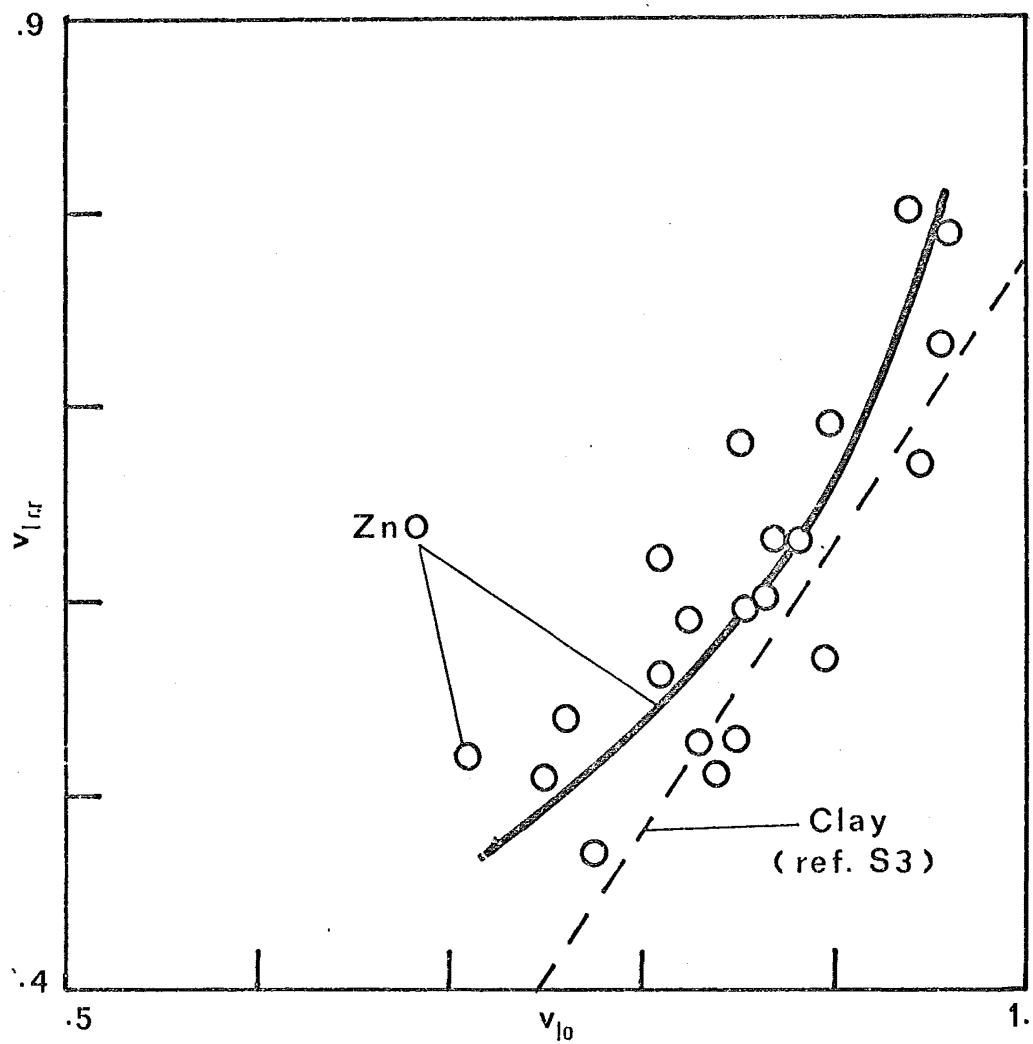


FIGURE 5.3: DEPENDENCE OF CRITICAL LIQUID VOLUME FRACTION ON INITIAL VOLUME FRACTION FOR SLURRIES

Once the crust has formed, it can either remain unchanged (rigid porous crust) or undergo deformations (C3, P8). If the drying air is above boiling point, the particle may inflate, fracture, explode, or fracture and collapse repeatedly due to the bubbling inside it. If the air is below boiling point, fracture, collapse or shrivelling may occur.

## II.6.2 Drying behaviour

### (a) Prior to particle consolidation:

Suspensions of solids do not have any effect in the stage before consolidation. Colloidal emulsions may form a membrane which hinders evaporation at an early stage, as data on milk demonstrate (T7, C1). True solutions will lower the vapour pressure at the surface, and thus lessen the evaporation (Henry or Raoult's law). This effect depends on the surface concentration of the solute,  $c_R$ , but the relationship of this concentration to the mean concentration  $\bar{c}$  is unclear. If evaporation is fast and diffusion in the liquid slow,  $c_R$  will be close to its saturation value  $c_s$ . In the opposite case, or when there is internal convection,  $c_R \approx \bar{c}$ . Approximate theoretical solutions have been obtained (C3, S3) but experimental results (C3, R4, S3) are inconclusive, and both limiting cases as well as variations between them have been observed, depending on the material tested, the initial mean solid concentration, the rate of evaporation, and other process conditions.

### (b) After particle consolidation:

Drying behaviour differs markedly for porous and non-porous materials, and for hygroscopic and non-hygroscopic ones (K3). In non-porous materials, moisture migrates by diffusion and an analytical treatment is relatively easy (B10). For non-hygroscopic, capillary-porous

materials, the drying pattern has been studied analytically by Keey and Suzuki (K4) for example, and for hygroscopic capillary-porous materials Berger and Pei (B8) have done a numerical study. Out of their results the following general conclusion can be drawn, that the relative drying rate  $f_d$ ,

$$f_d \equiv \frac{\text{evaporation from particle}}{\text{evaporation from liquid droplet}} \quad (5.70)$$

at any particular instant depends on the moisture profile in the particle, which in turn depends on the following factors:

(1) External factors:

- The Biot number for heat transfer:  $Bi_h \equiv \frac{hD_p}{k_p}$
- The Biot number for mass transfer:  $Bi_m = \frac{k_c D_p}{\kappa_p}$

where  $h$  and  $k_c$  are the heat and mass transfer coefficients,  $k_p$  the particle thermal conductivity and  $\kappa_p$  the thermal diffusivity of the solid.

(2) Internal factors:

- The sorption curve.
  - Luikov number for liquid movement in the particle:  $Lu_\ell = \frac{\mathcal{D}_\ell}{\kappa_p}$
  - Luikov number for vapour diffusion in the particle:  $Lu_v = \frac{\mathcal{D}_v}{\kappa_p}$
- where  $\mathcal{D}_\ell$  and  $\mathcal{D}_v$  are the diffusivities of the liquid and vapour within the particle.

(3) History: the past history of drying, - for example the mean rate of evaporation and the initial moisture, - determines the moisture profile.

In practical terms, the foregoing influences can be summed up in the equation:

$$f_d = f_d(D_p, X_o, \bar{X}, X, \text{material}) \quad (5.71)$$

where  $\bar{X}$  is the mean evaporation rate up to the moment the relative drying rate falls to  $f$ . The actual form of the function  $f$  must usually be determined experimentally for each material.

Hypothetical drying curves to illustrate the various drying period for the general case are shown in figure 4. The shapes of the final falling rate period are taken from reference K3.

## II.7 Drop mechanics

A liquid droplet behaves differently from a solid particle because it is subject to distortion, oscillations and internal circulation. These phenomena have been studied by Garner and Lane (G5), Hughes and Gilliland (H23) and others.

Using dimensional analysis, the factors governing distortion and oscillations have been shown to be the Reynolds number  $Re$  and the surface tension number  $Su \equiv \sigma \rho_c D_p / \mu_c^2$ , where  $\sigma$  is the interfacial tension and the subscript  $c$  refers to the continuous phase. At terminal velocity these two terms can be combined into the Bond number,

$$Bo = g(\rho_d - \rho_c) D_p^2 / \sigma, \text{ where } \rho_d \text{ is the disperse phase density.}$$

The oscillation frequency  $n$  is governed by Lamb's equation:

$$n = \sqrt{\frac{8\sigma}{2\pi m}} \quad (5.72)$$

where  $m$  is the mass of the droplet. Internal circulation is a function of  $Re$ ,  $Su$  and the viscosity ratio  $\mu_c / \mu_d$ .

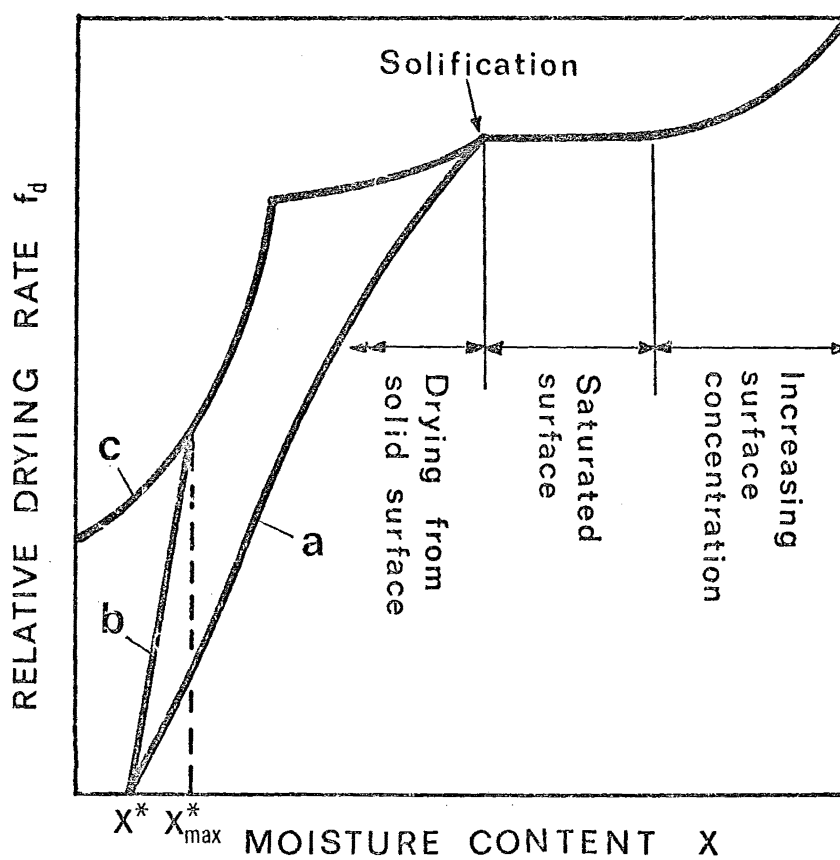


FIGURE 5.4: DRYING CURVE OF DROPLETS CONTAINING SOLIDS

- (a) hygroscopic non-porous solid
- (b) hygroscopic porous solid
- (c) non-hygroscopic capillary-porous solid



The effects of these phenomena are:

(a) Reduction of drag coefficient: Bond and Newton <sup>(B13)</sup> showed theoretically that for creeping flow the terminal velocity is increased by a factor

$$K = \frac{1 + \mu_c/\mu_d}{1 + 2\mu_c/3\mu_d} \quad (5.73)$$

Ingebo <sup>(I 1)</sup> found that droplets accelerated in air streams obey the equation:

$$c_D = 27 \text{ Re}^{-.84} \quad (5.74)$$

which gives a lower drag coefficient than the standard drag curve for the range studied. However, he was working with clouds of droplets, which could have some effect on the apparent drag due to droplet interaction. Brehaut <sup>(B17)</sup>, on the other hand, found no evidence of the effect of internal circulation.

(b) Changes in the solute concentration profile: Internal circulation, by mixing the contents of the drop, bring the surface solute concentration closer to the mean concentration. This will increase the mass transfer rate <sup>(G5, P12)</sup>, retard the formation of a crust <sup>(S3)</sup> and diminish the thermal degradation of the final product. Evidences of this effect in industrial spray dryers <sup>(S1)</sup> are, however, scant and inconclusive, in view of the high viscosities of the materials sprayed.

(c) Splitting of drops: When the oscillation amplitude is too large, the droplet will break up <sup>(H10)</sup>. The parameters governing this phenomenon are  $Su$ ,  $\mu_c/\mu_d$  and the Weber number  $We \equiv \tau D_p/\sigma$ , where  $\tau$  is the shear stress. In a turbulent field it can be deduced that splitting occurs when

$$D_p \left( \frac{\rho_c}{\sigma} \right)^{3/5} \epsilon^{2/5}$$

reaches a certain critical value, a result which has been experimentally verified. Here  $\epsilon$  is the energy dissipation rate per unit mass.

The presence of solute even in small quantities will alter  $\mu_d$  and  $\sigma$  greatly, and often inhibit the behaviour mentioned above.

NOTATION FOR CHAPTER 5

$c$	concentration, $[ \text{kg/m}^2 ]$
$c_D$	drag coefficient, $[ - ]$
$c_p$	specific heat, $[ \text{J/kg K} ]$
$D_p$	particle or droplet diameter, $[ \text{m} ]$
$D_h$	$4 \times \text{Volume} / \text{Area} = \text{hydraulic diameter}$ , $[ \text{m} ]$
$\mathcal{D}_{AB}$	diffusivity, $[ \text{m}^2/\text{s} ]$
$E$	fractional evaporation, $[ - ]$
$F$	$1-E = \text{fraction unevaporated}$ , $[ - ]$
$f_d$	dimensionless or relative drying rate (eqn.70), $[ - ]$
$F_D$	drag force, $[ \text{N} ]$
$g$	gravitational acceleration, $[ \text{m}^2/\text{s} ]$
$h$	heat transfer coefficient, $[ \text{W/K m}^2 ]$
$h_o$	heat transfer coefficient at zero mass flux, $[ \text{W/K m}^2 ]$
$I$	intensity of light, $[ \text{W/m}^2 ]$
$k$	thermal conductivity, $[ \text{W/mK} ]$
$K_e$	extinction coefficient, or projected particle area per unit cloud volume, $[ \text{m}^{-1} ]$
$k_c$	mass transfer coefficient, $[ \text{m/s} ]$
$L_b$	mean beam length, boundary to boundary (eqn.47), $[ \text{m} ]$
$L'_b$	mean beam length, particle to boundary, $[ \text{m} ]$
$m$	particle or droplet mass, $[ \text{kg} ]$
$\dot{m}$	mass transfer rate, $[ \text{kg/s} ]$
$n$	frequency of oscillation, $[ \text{s}^{-1} ]$
$q$	heat transfer rate to particle or droplet, $[ \text{W} ]$
$q_R$	" " " " " " " by radiation, $[ \text{W} ]$
$q_{w \rightarrow c}$	net radiation from wall to cloud of particles, $[ \text{W} ]$

Notation for Chapter 5 cont.

$S$	view factor in radiation, [ - ]
$S_R$	relative heat transfer rate when droplet is overheated, (section II.5), [ - ]
$S_m$	relative mass transfer rate when droplet is overheated, (section II.5), [ - ]
$t$	time, [ s ]
$t_p$	particle time constant, [ s ]
$t_L$	Langrangian time scale of turbulence, [ s ]
$u$	velocity [ m/s ]
$u_R$	relative velocity between particle and fluid, [ m/s ]
$u'$	turbulent rms velocity, [ m/s ]
$V_c$	cloud or chamber volume, [ m <sup>3</sup> ]
$v_l$	volume fraction of liquid in liquid-solid dispersion, [ - ]
$w_l, w_s$	liquid, solid mass fraction, [ - ]
$x$	distance, [ m ]
$x$	mole fraction, [ - ]
$X$	dry basis moisture content [ - ]
$X_{cr}$	dry basis moisture content at droplet solidification, [ - ]
$y$	air humidity dry basis, [ - ]
$\alpha$	emissivity or absorptivity of radiation, [ - ]
$\beta$	$(Nu-2)/Re^{1/2}Pr^{1/3}$ or $(Sh-2)/Re^{1/2}Sc^{1/3}$ , [ - ]
$\epsilon$	turbulent energy dissipation rate per unit mass, [ W/kg ]
$\kappa$	heat diffusivity, [ m <sup>2</sup> /s ]
$\lambda$	latent heat of evaporation, [ J/kg ]
$\mu$	viscosity, [ kg/ms ]
$\nu$	kinematic viscosity, [ m <sup>2</sup> /s ]
$\pi$	3.14159...
$\Pi$	$c_D Re^2$ , [ - ]

Notation for Chapter 5 cont.

$\rho$  density,  $[ \text{kg/m}^3 ]$

$\sigma$  surface tension,  $[ \text{N/m} ]$

$\sigma$  Stefan-Boltzmann's constant,  $[ \text{W/m}^2\text{K}^4 ]$

$\tau$  shear stress,  $[ \text{N/m}^2 ]$

Dimensionless numbers

$B \quad \frac{C_{pv} \Delta T}{\lambda} = \text{Spalding's number}$

$Bi_h \quad \frac{hD_p}{k_p} = \text{Biot's number for heat transfer}$

$Bi_m \quad \frac{k_c D_p}{K_p} = \text{Biot's number for mass transfer}$

$Bo \quad \frac{g \Delta \rho D_p^2}{\sigma} = \text{Bond number}$

$Lu \quad \frac{\mathcal{D}}{K} = \text{Luikov number}$

$Nu \quad \frac{hD_p}{k_f} = \text{Nusselt number}$

$Nu_o \quad \text{Nu at zero mass flux}$

$Pr \quad \frac{\mu_f c_{pf}}{k_f} = \text{Prandtl number}$

$Re \quad \frac{D_p u_{Rf} \rho_f}{\mu_f} = \text{Reynolds number}$

$Sc \quad \frac{v_f}{\mathcal{D}_{AB}} = \text{Schmidt number}$

$Sh \quad \frac{k_c D_p}{\mathcal{D}_{AB}} = \text{Sherwood number}$

Notation for Chapter 5 cont.

$$\text{Su} \quad \frac{\sigma \rho_c D_p}{\mu_c^2} = \text{Surface tension group}$$

$$\text{We} \quad \frac{\tau D_p}{\sigma} = \text{Weber number}$$

$$\text{Wt} \quad \frac{g(\rho_d - \rho_c) D_p^2}{\sigma} = \text{Weight group}$$

Subscripts

a	air
c	continuous phase
c	cloud
cr	critical, at droplet solidification
d	dispersed phase
f	fluid
g	gas
i	in the i-th direction
l	liquid
p	particle, droplet
R	relative (velocity)
R	at droplet radius or surface
s	solid
s	surface
t	terminal
v	vapour
w	wall
w→c	wall to cloud
wp	wall to particle (view factor)
o	initial (at t=0 or x=0)
∞	at infinite distance, in the surroundings

Superscripts

*	equilibrium, saturation
'	turbulent (rms)
-	mean
·	rate of change

## CHAPTER 6

### SPRAY DRYER DESIGN AND PERFORMANCE

#### Chapter contents:

#### INTRODUCTION

#### I. REVIEW OF CALCULATION METHODS

1. Empirical and semi-empirical
2. Analytical:    1. Single droplet  
                      2. Whole spectrum
3. Numerical

#### II. A NUMERICAL SIMULATION OF SPRAY EVAPORATION

1. Theoretical basis:    1. Hydrodynamics: the jet zone.  
                              2. Basic Transfer equations.  
                              3. Miscellaneous effects.  
                              4. Miscellaneous equations.
2. Computational problems (flow diagram-convergence problems)
3. Sample calculation, results and discussion
  1. Fine water spray.
  2. Coarse milk spray.

#### III. INFLUENCE OF RESIDENCE TIME DISTRIBUTION

1. Air R.T.D.
2. Liquid R.T.D.:    1. General approach  
                              2. Case of similar R.T.D.s  
                              3. Case of first-order reaction  
                              4. Extended first-order reaction  
                              5. Sample calculation

#### IV. CONCLUSION

#### NOTATION

## INTRODUCTION

The spray drying process consists of three main steps:

1. Atomisation
2. Evaporation and drying
3. Product collection.

This chapter is mainly concerned with the second step, that is: what happens to the droplets once they leave the atomiser and until they emerge from the drying chamber. However, the atomisation process will also often have to be considered, since it supplies the initial conditions of the drying history of the spray.

A short review of available spray-evaporation calculation methods will be carried out, followed by a computer simulation of cocurrent spray dryers with nozzle atomisers. Finally, the influence of air and spray residence time distributions will be discussed.

### I. A REVIEW OF METHODS FOR SPRAY DRYER DESIGN AND PERFORMANCE PREDICTION

Until recently, the state of the art of spray dryer design was, in the words of an engineer in the field, "to build it and make it work". There has been no unified approach and probably never will be, as spray-drying situations vary greatly and the interacting factors are too complex. Most of the methods proposed so far are only tentative and insufficiently proven. A classification of available methods is shown in Table 1.



TABLE 6.1

CLASSIFICATION OF SPRAY-DRYER DESIGN OR PERFORMANCE  
PREDICTION METHODS

---

1. Empirical or semi-empirical methods:

Luikov, Feder, Borde, Dolinsky

2. Analytical methods:

1. Based on one droplet size: Johnstone & Eads, Miesse,  
Sjetnitzer, Gluckert.

2. Based on a size spectrum: Schlünder, Marone, McIlvried & Massoth.

First-order reaction  
methods:

Shapiro & Erickson, Hopkins & Eisenklam,  
Dombrowski & Johns.

3. Numerical (stepwise) methods: Marshall, Dickinson & Marshall,  
Leonchik, Katta & Gauvin,  
Parti & Palancz, Weber & Viehweg.

---

I.1 Empirical and semi-empirical methods

Luikov<sup>(L10)</sup> gave an empirical equation for the volumetric heat transfer coefficient as a function of droplet mean diameter, droplet velocity and other parameters. Turba and Nemeth<sup>(T8)</sup> found that this equation gave a prediction for their spray dryer which was out by a factor of 10.

Feder<sup>(F1)</sup> gave a graphical method based mainly on empirical data. Borde<sup>(B14)</sup> derived a design equation based on dimensional analysis, but did not give any explicit solution. Dolinsky<sup>(D9)</sup> followed a similar approach, but arrived at explicit equations for the dimensions of a dryer with disk atomiser and cocurrent flow of spray and air. He made the assumption that:  $Nu = 2$ .

Due to the diversity of spray drying systems (geometry, operating ranges, feed materials ...) and the numerous simplifying assumptions that must be made in order to arrive at any "general" equation, it can safely be said that the above-mentioned methods are of little practical use, and can at best give some qualitative idea of the effects of some variables.

## I.2 Analytical methods

### I.2.1. Methods which consider one drop size

Several authors have tried to replace the polydisperse spray by a single droplet size, usually the maximum size produced by the atomiser. The equations of motion and evaporation for this size can then be solved, with the initial conditions given by the atomising method used.

Sjetnitzer<sup>(S11)</sup> gave his results as graphs. He assumed constant air conditions, pure liquid droplets, Ranz and Marshall's equation for heat and mass transfer:

$$Nu = 2 + 0.6 Re^{1/2} Pr^{1/3} ,$$

and Ingebo's equation for the drag curve:

$$c_D = 27 Re^{-.84} . \quad (6.1)$$

He also derived<sup>(S10)</sup> an equation for the height of transfer unit of a spray dryer based on some mean evaporative diameter.

Johnstone and Eads<sup>(J3)</sup> derived a relationship for the lifetime of a pure liquid drop. Their assumption of constant relative velocity between drop and gas restricts its usefulness. Miesse<sup>(M14)</sup> solved the equations of motion and evaporation for a pure liquid drop in constant, decelerating and accelerating gas flows. His assumptions were a Stokes flow regime and  $Nu = 2$ .

Schlünder<sup>(S3)</sup> also studied the drying history of individual droplets. Gluckert<sup>(G9)</sup> proposed basing the design of spray dryers on the maximum droplet diameter  $D_m$ , which he took to be:

$$D_m = 3 \bar{D}_{vs}.$$

Using available relationships in the literature for the effect of atomising conditions on the initial droplet sizes and velocities, he arrived at equations for the design of spray dryers with disk, twin-fluid and pressure atomisers.

At first sight it would appear that replacing the spray by a single droplet size is a rather crude assumption. However, as will be seen later, the largest drops are in fact the determining factor for the design and operation of spray dryers in most cases. Thus the foregoing methods can be useful, although for a more accurate calculation one needs to consider further the mechanics of drying; most of the methods so far are only for pure liquids.

### I.2.2. Analytical methods which treat a size spectrum

#### I.2.2.1 General approach:

In the following methods the evaporation of each sized droplet is integrated over the whole size spectrum to yield the total evaporation. Probert<sup>(P13)</sup> was the first to make this approach. Shapiro and Erickson<sup>(S8)</sup> developed a general differential equation for a cloud of particles or droplets undergoing evaporation or combustion and acceleration. By a numerical accounting of droplets with a given size, position and velocity, they showed that:

$$\frac{\partial \mathcal{Q}}{\partial t} + u_p \frac{\partial \mathcal{Q}}{\partial x} + \mathcal{Q} \frac{\partial u_p}{\partial x} = - \mathcal{Q} \left[ \frac{\partial u_p}{\partial x} + \frac{u_p}{A} \frac{dA}{dx} + \frac{\partial \mathcal{R}}{\partial D_p} \right] \quad (6.2)$$

where  $A$  is the flow area of the cloud,  $R$  is the growth rate of the particles ( $R = dD_p/dt$ ),  $g$  is the number-size distribution ( $g = dn/dD_p$ ),  $u_p$  the particle velocity ( $u_p = dx/dt$ ) and  $R$ ,  $u_p$ ,  $g$  are all functions of the diameter  $D_p$ . Williams<sup>(W5)</sup> also gave a similar equation.

By assuming some form of  $R(D_p)$ ,  $u_p(D_p)$  and  $g(D_p)$ , equation 2 can be solved for the entire spray.  $dA/dx$  is generally assumed to be 0, and in most treatments  $du_p/dD_p$  is assumed to be zero also (uniform cloud motion), so that only  $R(D_p)$  and  $g(D_p)$  have to be assumed.

For  $g(D_p)$  being a normal distribution, Schlünder<sup>(S3 § 5.321)</sup> tried several different power laws for the growth rate

$$\frac{dD_p}{dt} \propto D_p^{-\gamma} \quad (6.3)$$

and arrived at semi-analytical expressions for the evaporation history. These are quite complex and make extensive use of uncommon tabulated functions.

Marone<sup>(M4)</sup>, assuming a constant Nusselt number and a Rosin-Rammler size distribution (equation 18), arrived at an integral equation which has to be solved numerically. Yaron and Gal-Or<sup>(Y1)</sup> also made an analytical study of transfer phenomena with size-distributed systems which can be applied to spray drying. One interesting work is that of McIlvried and Massoth<sup>(M10)</sup> who studied a single particle and clouds of solid particles reacting with a gas. The reaction is assumed to be controlled by solid-phase diffusion and the results may be useful for the cases where drying proceeds well into the falling-rate period.

However, due to the complexity of those solutions, several authors have purposely chosen expressions for  $R(D_p)$  and  $g(D_p)$  to get simpler results. The next section examines in some detail a class of methods which may be of particular use when we come to the study of the

effects of deviations from plug-flow and residence time distributions.

#### I.2.2.2 Constant evaporative diameter or first-order reaction methods:

A first-order reaction has a rate equation of the form<sup>(L6)</sup> :

$$-\frac{dc_A}{dt} = k_1(c_A - c_{Ae}) \quad (6.4)$$

where  $c_A$  is the concentration of reactant A,  $c_{Ae}$  its equilibrium value,  $k_1$  the rate constant. This type of reaction is particularly amenable to mathematical treatment. In particular, their yield in a reactor is independent of the actual mixing pattern and depends only on the residence time distribution (RTD) curve  $C(t)$  :

$$\begin{aligned} \frac{c_{A2} - c_{Ae}}{c_{A1} - c_{Ae}} &= \int_0^{\infty} e^{-k_1 t} C(t) dt \\ &= \text{L.T. } \{C(t)\} \end{aligned} \quad (6.5)$$

(neglecting end effects), where  $c_{A2}$  and  $c_{A1}$  are the outlet and inlet values of  $c_A$  respectively, and L.T. is the Laplace Transform.

Because of this mathematical simplicity, many workers have tried to approximate the process of evaporation by a first-order reaction. The reasoning is as follows: as the smaller droplets evaporate very quickly, they soon disappear from the evaporation process and leave behind the larger droplets. Thus, although all droplets are shrinking, their mean evaporative diameter (M.E.D.) and hence their specific (per unit remaining mass) evaporation are constant.

The M.E.D.,  $D_e$ , is the diameter of a pure liquid droplet which has the same evaporation rate  $k_1$  per unit (remaining) liquid mass:

$$k_1 = \frac{(\pi/2) D_e^2 R(D_e)}{(\pi/6) D_e^3} = \frac{\int_0^{\infty} (\pi/2) D_p^2 R(D_p) G(D_p) dD_p}{\int_0^{\infty} (\pi/6) D_p^3 G(D_p) dD_p} \quad (6.6)$$

with  $R(D_p)$  and  $G(D_p)$  defined as in equation 2.

In particular if

$$R(D_p) = -K D_p^{-\gamma} \quad (6.7)$$

then

$$D_e = \left[ \frac{\int_0^\infty D_p^3 g_{dp} dD_p}{\int_0^\infty D_p^{2-\gamma} g_{dp} dD_p} \right]^{\frac{1}{1+\gamma}} = \bar{D}_{3,2-\gamma} \quad (6.8)$$

and

$$k_1 = 3 K D_e^{-(1+\gamma)} \quad (6.9)$$

where  $\bar{D}_{m,n}$  is the m-n mean diameter<sup>(M16)</sup>.

Whether  $k_1$  and  $D_e$  remain constant with time obviously depends on the form of  $R(D_p)$  and  $g_{dp}$ , as can be seen from equation 2. Shapiro and Erickson<sup>(S8)</sup> showed that if

$$g \propto D_p e^{-KD_p^2} \quad (6.10)$$

and

$$R \propto D_p^{-1} \quad (6.11)$$

(the latter equation implying  $Sh = Nu = \text{constant}$ ), then  $D_e$  and  $k_1$  are constant.

Hopkins and Eisenklam<sup>(H19)</sup> extended this method and showed that the same result is obtained whenever

$$g \propto D_p^{n-1} e^{-KD_p^n} \quad (6.12)$$

and

$$R \propto D_p^{1-n} \quad (6.13)$$

This may be shown by solving equation 2. They suggested  $n = 1.55$  for burning oil sprays.

Dombrowski and John<sup>(D11)</sup> used a polynomial form for the size distribution

$$g = a + b D_p^2 + c D_p^5 + d D_p^8 \quad (6.14)$$

and equation 11 for  $\mathcal{Q}$ , and found that  $D_e = \bar{D}_{31}$  remains roughly constant for up to 90% evaporation in pure liquid sprays. In fact they showed that

$$\frac{k_{10}}{k_1} = \left( \frac{D_e}{D_{eo}} \right)^2 = 1.1(1-E)^{0.13} \quad (6.15)$$

where E is the fractional evaporation.

#### Critical examination of the constant M.E.D. methods:

Thus far all these methods have assumed certain forms of the size-distribution equation which are not widely accepted. The most common equations for the size distribution are: <sup>(M16)</sup>

(1) Log-normal (L.N.) distribution:

$$\frac{dv}{d(\ln D_p)} = \frac{1}{\sqrt{2\pi} \sigma_{LN}} \exp \left[ - \frac{(\ln D_p - \mu_{LN})^2}{2\sigma_{LN}^2} \right] \quad (6.16)$$

(2) Root-normal (R.N.) distribution:

$$\frac{dv}{d(\sqrt{D_p})} = \frac{1}{\sqrt{2\pi} \sigma_{RN}} \exp \left[ - \frac{(\sqrt{D_p} - \mu_{RN})^2}{2\sigma_{RN}^2} \right] \quad (6.17)$$

where  $\mu_{LN}, \mu_{RN}, \sigma_{LN}, \sigma_{RN}$  are the means and standard deviation of  $\ln D_p$  and  $\sqrt{D_p}$  respectively, and v is the volume fraction under size  $D_p$ .

(3) Rosin-Rammler (R.R.) distribution:

$$\frac{dv}{dD_p} = K D_p^{\delta-1} \exp \{-a D_p^\delta\} \quad (6.18)$$

(4) Nukiyama-Tasanawa (N.T.) distribution:

$$\frac{dv}{dD_p} = K D_p^5 \exp \{-a D_p^\delta\} \quad (6.19)$$

where  $\delta$  is the dispersion index.

In order to see how the constant M.E.D. assumption holds for these four distributions in the case of constant Nusselt number (equation 11), a numerical computation of the variation of the specific evaporation rate was carried out.  $\sigma_{LN}$ ,  $\sigma_{RN}$  and  $\delta$  for equations 18 and 19 were varied. The procedure followed was a simplified version of Marshall's stepwise method described in the next section, and the results are plotted as  $f_c$  against  $E$ , where:

$$f_c \equiv \frac{k_1}{k_{10}} \equiv \left( \frac{D_e}{D_{eo}} \right)^{-2}.$$

If  $f_c$  is constant, then the M.E.D. is also constant. The results are shown in Figure 1. An alternative approach would be to plot  $\ln F$  against  $t$ , where  $F \equiv 1-E$ , and see if the graph is linear. These plots can be found in reference D5. In practice one would be content with a 10% variation in  $f_c$ .

It can be seen from figure 1 that the constant M.E.D. assumption holds only for a limited range of  $\sigma_{LN}$ ,  $\sigma_{RN}$  or  $\delta$ , and up to a certain value of  $E$ . The values of the dispersion parameters for best approximation are:

N.T. distribution:  $\delta = 1.5 - 1.8$

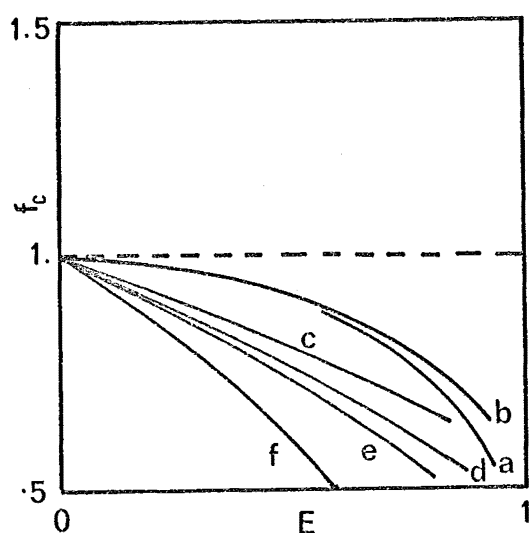
R.R. distribution: none

R.N. distribution:  $\sigma_{RN}/\mu_{RN} = .15 - .17$

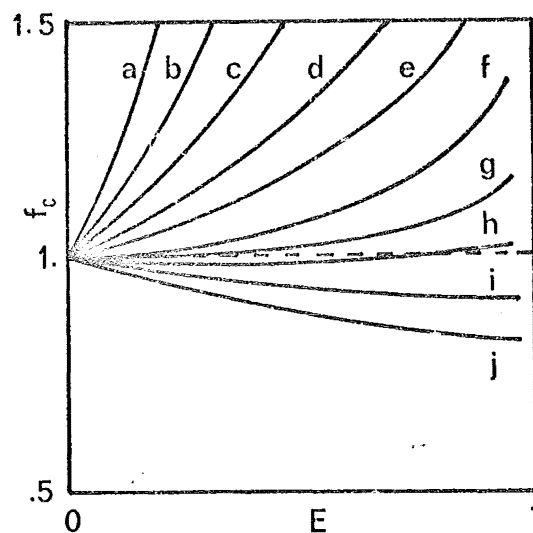
L.N. distribution:  $\sigma_{LN}/\mu_{LN} = .25 - .35$

The presence of solids may or may not have an important effect on the foregoing results, depending on how the material behaves. Two criteria must be considered: whether the solid forms a crust at an early or late stage, and whether it hinders the evaporation by resistance to moisture transfer.

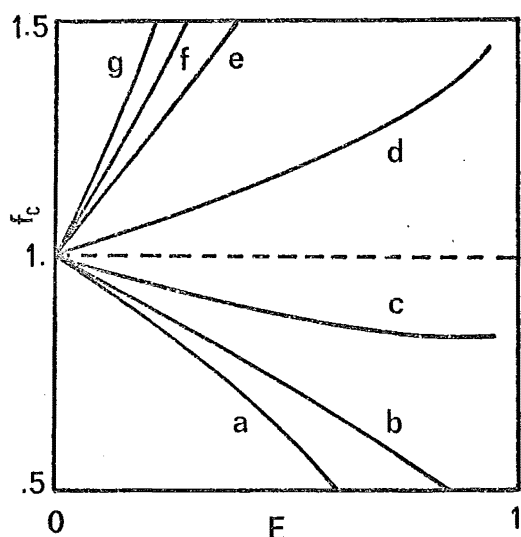




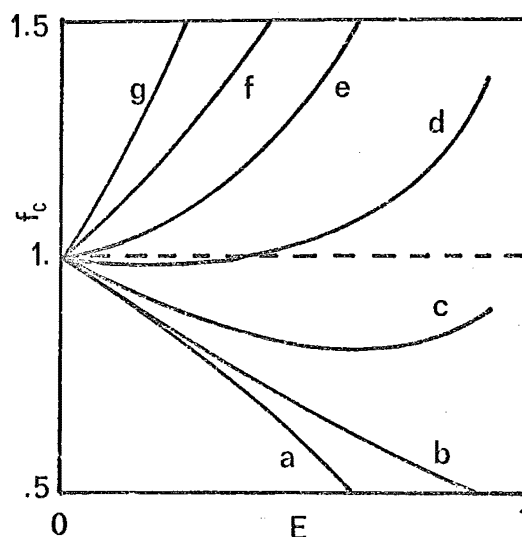
Rosin - Rammler



Nukiyama - Tasanawa



Root-normal



Log - normal

FIGURE 6.1: VARIATION IN SPECIFIC EVAPORATION RATE  
FOR SOME SPRAYS

Rosin-Rammler distribution: value of  $\delta$ :

(a) 2.0 (b) 2.3 (c) 3.2 (d) 3.8 (e) 4.4 (f)  $\infty$  (monodisperse spray).

Nukiyama-Tasanawa distribution: value of  $\delta$  :

(a) 0.2 (b) 0.4 (c) 0.6 (d) 0.8 (e) 1.0 (f) 1.2 (g) 1.4 (h) 1.6  
(i) 1.8 (j) 2.0.

Root-normal distribution: value of  $\sigma_{RN}/\mu_{RN}$  :

(a) 0 (monodisperse spray) (b) 0.10 (c) 0.15 (d) 0.20 (e) 0.25  
(f) 0.30 (g) 0.40.

Log-normal distribution: value of  $\sigma_{LN}/\mu_{LN}$  :

(a) 0 (monodisperse spray) (b) 0.2 (c) 0.3 (d) 0.4 (e) 0.5 (f) 0.6  
(g) 0.8 .

Consider the following extreme cases:

- (1) Immediate forming of crust, no hindering of evaporation (thick slurry of non-hygroscopic coarse-grained material): moisture evaporates from the droplet surface at a constant rate, i.e.  $k_1$  increases with time.
- (2) Immediate forming of crust, appreciable hindering of evaporation: the change in  $k_1$  will depend mainly on the characteristic drying curve of the material, and not on the size distribution. This is an important case in industrial spray drying, but has not received much attention up to now.
- (3) Late forming of crust, late hindering of evaporation: there will be little change in the behaviour of  $f_v$ ,  $D_e$  or  $k_1$  (this has been checked by a numerical calculation similar to the one mentioned earlier).

Apart from the restrictions already mentioned, the usefulness of constant M.E.D. methods is limited by the following underlying assumptions:

- (1) The particles move in a uniform manner, with no differential velocity.
- (2)  $Nu = \text{constant}$  (except in the case of Hopkins and Eisenklam's method).
- (3) Constant drying conditions (this restriction can be waived, but this leads to complex results).
- (4) Little effect of the presence of solids on the evaporation and shrinking of the droplets.
- (5) An infinite maximum droplet size (except in Dombrowski and Johns' method).

Assumptions (1) and (2) mean that these methods apply only to fine sprays, perhaps  $D_{\max} < 40 \mu\text{m}$ .<sup>(D7)</sup> In industry, fine products are often not desirable for reason of coagulability, handling

difficulties and losses. Assumption (4) is similarly unrealistic in most cases. When assumption (5) does not hold and there is a finite maximum diameter, the M.E.D. will decrease more quickly than predicted towards the end of evaporation. Finally, the author has found that many sprays generated by nozzles have a Nukiyama-Tasanawa distribution with  $\delta \approx 0.5$ , for which  $D_e$  does not remain constant.

For these reasons, the methods considered can be used (in the best cases) only in the early stages of evaporation, say for  $E < .8$ . Thus they may be applicable in spray-cooling towers, or perhaps in combustion chambers. In spray drying, one is mainly interested in the later stages, where  $E \approx 1.$ ,  $F \approx 0.$ , and product quality may be quite sensitive to variations in  $F$ . Thus if  $E = .95$ , a 1% error in  $E$  means a 20% error in  $F$ , and no analytical method would be even that accurate.

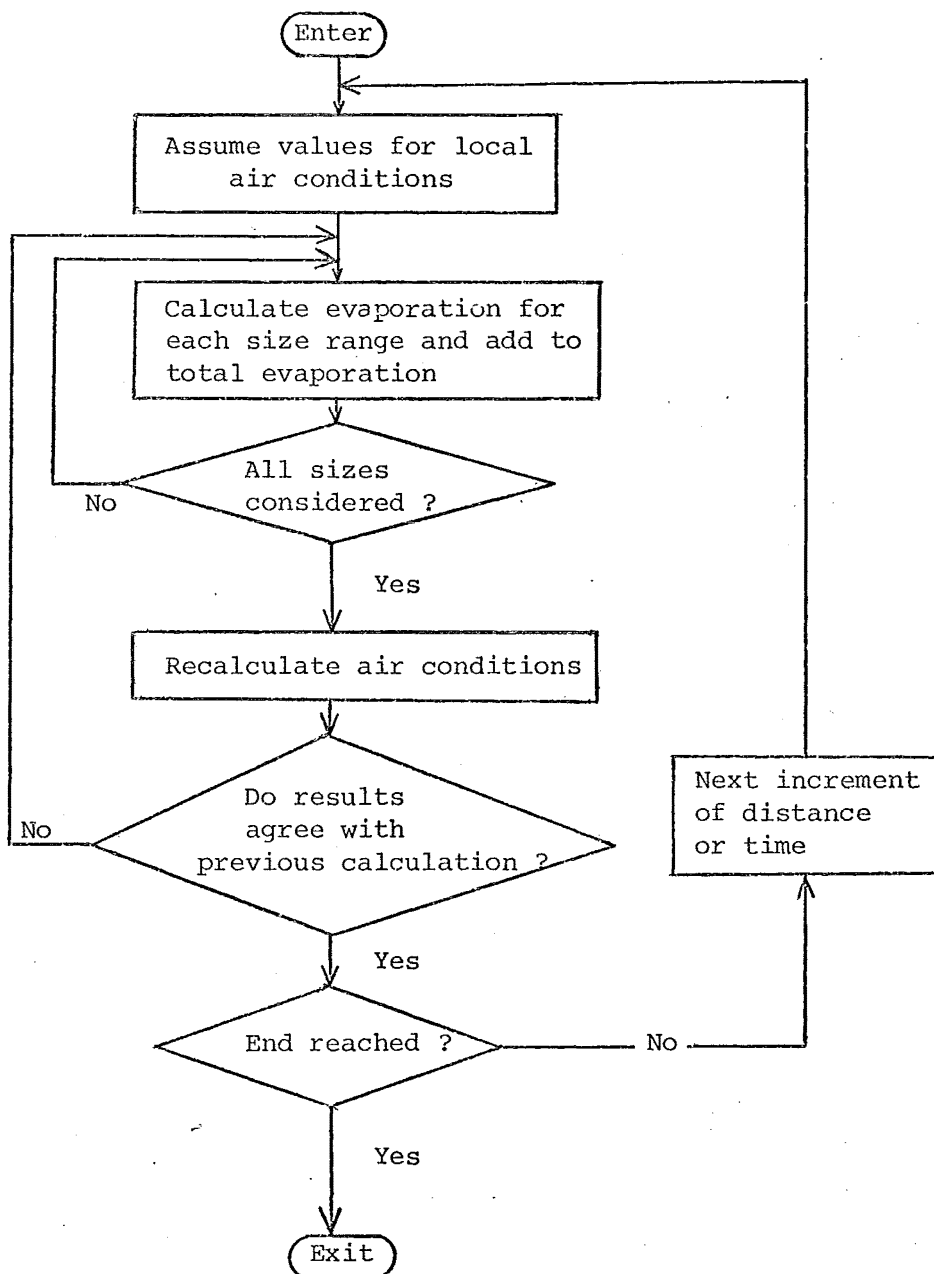
### I.3 Numerical (stepwise) methods

When computers are available, the most obvious approach is to calculate the evaporation of each size range in the spray for a given increment of time or space, sum up over all size ranges to get the total evaporation, and go on to the next increment. Size ranges are based on the initial sizes and not on the instantaneous size, so that each group of droplets is followed throughout its history. When the air-spray rate ratio is small, the evaporation may have an appreciable effect on the air conditions, so an iteration process at each point may be necessary. A simplified flow diagram is shown in figure 2.

Such a method was first proposed by Marshall<sup>(M6)</sup> and used with various modifications by Dickinson and Marshall<sup>(D5)</sup>, Leonchik<sup>(L4)</sup>, Dlouhy and Gauvin<sup>(D7, D8)</sup>, Gauvin and Katta<sup>(K1, G6)</sup>, Hoffmann and Gauvin<sup>(H15)</sup>, Weber, Viehweg and Biess<sup>(V2, W2)</sup>, Parti and Palancz<sup>(P3)</sup>.

Figure 6.2

Simplified flow diagram for stepwise calculation of spray evaporation



Numerical methods are in general very flexible, a great number of influences can be taken into account and, provided the basic assumptions are sound, the results should be fairly accurate<sup>(D7, K1)</sup>. This flexibility should make up for the lack of generality of the results.

One of the most recent programs available is that of Katta and Gauvin who considered short-form spray dryers with tangential air inlet.

In the next section, a program will be developed to consider tall-form cocurrent spray dryers with predominantly axial air inlets.

## II. A NUMERICAL SIMULATION OF SPRAY DRYING

A computer program was written essentially along the lines of Marshall's method (figure 2), but incorporating several factors which may be of importance in industrial situations. The configuration considered is that of a cocurrent tall-form drying chamber, with a pneumatic or pressure atomiser.

### II.1 Theoretical considerations

#### II.1.1 Hydrodynamic profile

##### II.1.1.1 Existence and extent of a jet zone

Visual observations made on our spray dryer as well as those made by others<sup>(G6, K1)</sup> point to the existence of two quite different hydrodynamic zones through which the droplets must travel: a jet zone and a main zone. In the latter, spray-air mixing is complete (to within the limit imposed by the chamber geometry and drying-air flow pattern) and the particles fall at their settling velocities. In the former, the hydrodynamic profile is governed by the characteristics of the nozzle.

In the past, many workers have ignored this zone on the grounds that droplets projected into a slower air flow will be rapidly decelerated to their terminal velocity, as shown by the equations of Lapple and Shepherd<sup>(L2)</sup> and Sjetnitzer<sup>(S11)</sup>. For instance, in the Stokes regime, a particle projected into a quiescent fluid will travel at an exponentially decreasing velocity

$$u_p = u_{po} \exp(-t/t_p) \quad (6.20)$$

where

$$t_p = \rho_p D_p^2 / 18 \mu_a \quad (6.21)$$

For a 40  $\mu\text{m}$  water droplet in air this means that the velocity is halved every 4 ms.

However, we must take into account the fact that a swarm of droplets may travel in a fairly coherent manner, entraining the gas with them, so that they will decelerate much more slowly than a single droplet<sup>(I1, A7)</sup>. Therefore, a closer look into jet dynamics is necessary.

The effects of the jet zone are threefold:

- (1) The relative velocity between droplet and air are higher than in the main zone, due to the larger gas velocity gradient.
- (2) The absolute velocity of the droplets will also be high.
- (3) The confined geometry of the jet, and the limited flow of air in it, will restrict the maximum possible evaporation.

Effect (1) will tend to increase evaporation, while effects (2) and (3) will decrease it.

There is as yet no method for predicting when the jet zone stops and the main zone starts. It may be speculated that this is a function of the momentum of the jet and the turbulent intensity of the surrounding fluid, and thus interpolation between experimental data

may be possible. In the meantime, visual observations must provide the answer.

#### II.1.1.2 Properties of the jet zone

Jet dynamics is an extensive subject<sup>(A3, B19, B3, C9, M11)</sup>. The approach followed here will be a somewhat simplified version of Abramovitz's treatment<sup>(A3)</sup>. The simplest case is that of an axisymmetric, one-phase, incompressible submerged jet (i.e. one that is injected into quiescent fluid) with no initial radial or tangential velocity. This case will be considered first, then modifications made for an industrial situation.

(a) Single-phase submerged jet: A jet can be divided into three regions (Figure 3): an initial region with a diminishing core, a transition region, and a main region which is conical in shape (the last is not to be confused with the "main zone" of the spray dryer mentioned earlier). The first two regions are quite short. In the nomenclature of figure 3:

$$x_1 \approx 8 r_o \quad (6.22)$$

$$x_2 \approx 12.4 r_o \quad (6.23)$$

where  $r_o$  is the orifice radius, so that for our purposes the jet can be considered as consisting of its main region only. Also, the pole of the main region nearly coincides with the orifice:

$$x_o/r_o \approx 0 \quad (6.24)$$

In the main region of the jet (from now on referred to simply as "the jet"), the jet radius  $R_j$  is proportional to the distance from the pole:

$$R_j = 0.22 (x - x_o) \quad (6.25)$$

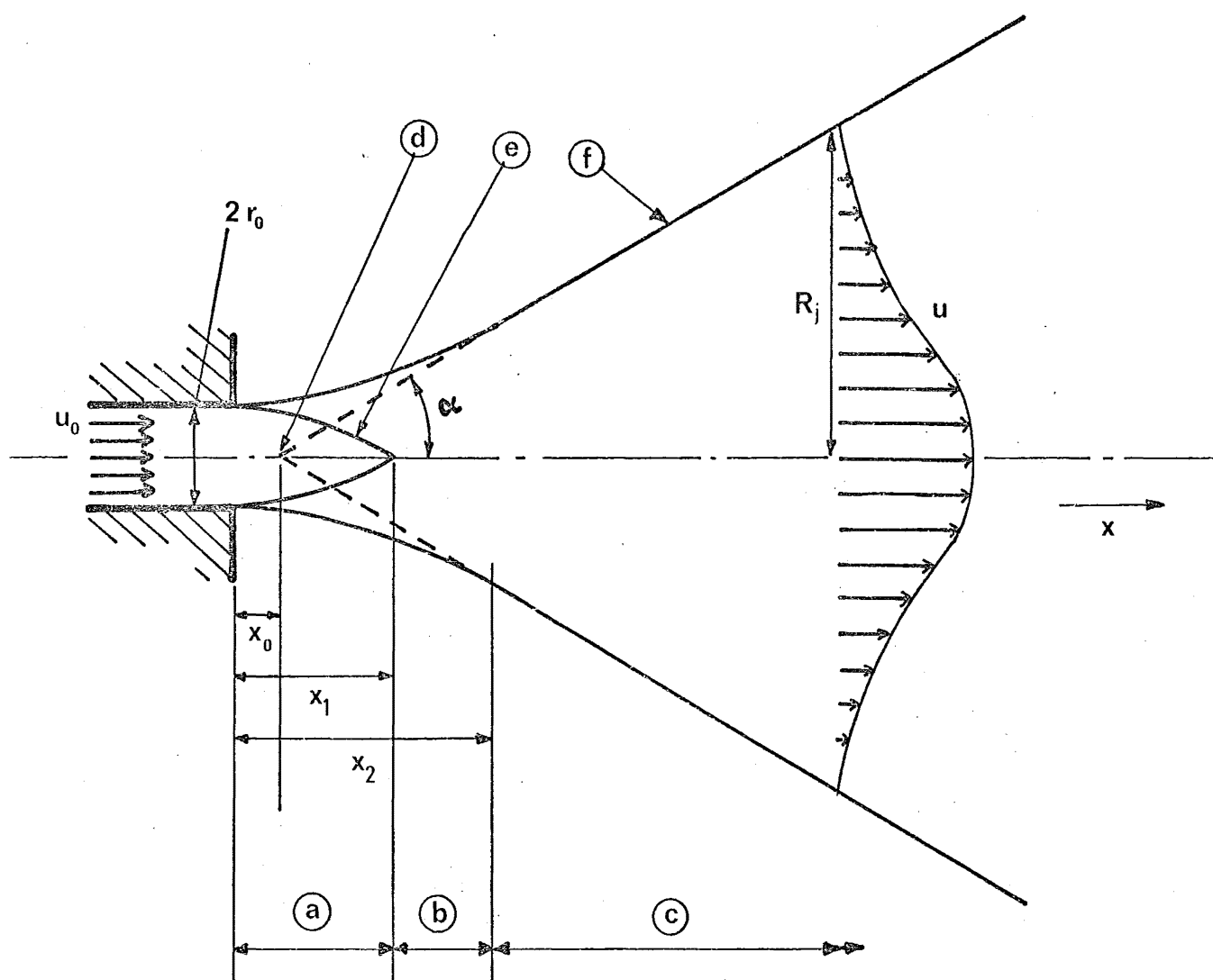


FIGURE 6.3: ONE-PHASE SUBMERGED JET

- (a) Initial region
- (b) Transition region
- (c) Main region
- (d) Pole
- (e) Core
- (f) Boundary of jet



so that the jet is conical and sustends a half angle

$$\alpha = \tan^{-1} 0.22 = 12.4 \text{ deg.} \quad (6.26)$$

The radial velocity profile remains similar at any cross-section, having a bell shape which can be represented either by a Gaussian function or by the formula

$$\frac{u}{u_m} = \left[ 1 - \left( \frac{r}{R_j} \right)^{1.5} \right]^2 \quad (6.27)$$

where  $u_m$  is the (axial) velocity at the jet axis. By conservation of momentum

$$u_m^2 R_j^2 = \text{Constant} \quad (6.28)$$

so that from equation 26

$$\frac{u_m}{u_o} = \frac{12.4 r_o}{x - x_o} \quad (6.29)$$

The rate of air flow in the jet can be found by integrating the velocity over the jet cross-section, which gives:

$$\frac{G}{G_o} = \frac{0.14(x - x_o)}{r_o} \quad (6.30)$$

This is in satisfactory agreement with the empirical equation found by Davies<sup>(D3)</sup>

$$\frac{G}{G_o} = \frac{0.115 x}{r_o} - 1 \quad (6.31)$$

the difference being probably due to the approximate velocity profile used.

The radial temperature profile varies as the square root of the velocity profile:

$$\frac{T - T_\infty}{T_m - T_\infty} = 1 - \left( \frac{r}{R_j} \right)^{1.5} \quad (6.32)$$

where  $T_m$  is the axis temperature and  $T_\infty$  is the surrounding-fluid temperature, and

$$\frac{T_m - T_\infty}{T_o - T_\infty} = \frac{9 r_o}{x - x_o} \quad (6.33)$$

where  $T_o$  is the temperature of the fluid emerging from the orifice.

If there is a tracer gas or a spray in the jet, then their concentration  $c$  will be similar to the temperature profile:

$$\frac{c - c_\infty}{c_m - c_\infty} = 1 - \left( \frac{r}{R_j} \right)^{1.5} \quad (6.34)$$

$$\frac{c_m - c_\infty}{c_o - c_\infty} = \frac{9 r_o}{x - x_o} \quad (6.35)$$

where the suffixes  $m$ ,  $\infty$  and  $o$  refer to the axis, surrounding and orifice values as usual.

(b) Two-fluid jets; This is the case of pneumatic atomising nozzles. The properties of the jet will be modified by the change in mean jet density. The governing parameter here is the liquid-to-gas ratio at the orifice, and an analytical treatment was given by Abramovitz. However, in computer simulation a simpler approach can be made by recalculating the profile numerically: we shall assume a one-phase jet, calculate the momentum transfer between the air and the liquid, and modify the air velocity accordingly.

(c) Liquid jet injected into a gas: This is the case of pressure atomisers. The governing factor is now the liquid/gas density ratio

$$j = \frac{\rho_l}{\rho_g} .$$

Equations 22, 23, 24 must be changed to:

$$\frac{x_1}{r_o} = 24 \quad (6.36)$$

$$\frac{x_2}{r_o} = 10.7 (1.73 \sqrt{j} - 1) \quad (6.37)$$

$$= 500 \quad \text{for water-air sprays} \quad (6.38)$$

$$\frac{x_o}{r_o} = \frac{x_2}{r_o} - 13.6 \sqrt{j} \quad (6.39)$$

$$= 120 \quad \text{for water-air sprays} \quad (6.40)$$

The longitudinal velocity profile (equation 29) now becomes:

$$\frac{u_m}{u_o} = 2.25 j \left( \frac{r_o}{R_j} \right)^2 \left[ \sqrt{1 - 1.5 \left( \frac{R_j}{r_o} \right)^2 / j} - 1 \right] \quad (6.41)$$

where  $R_j$  is given by the implicit equation:

$$\begin{aligned} 0.22 \left( \frac{x-x_o}{r_o} \right) &= \frac{R_j}{r_o} + \sqrt{j} \left\{ \ln \left[ 1.22 \frac{R_j}{r_o \sqrt{j}} + \sqrt{1 + \frac{1.48}{j} \left( \frac{R_j}{r_o} \right)^2} \right] \right. \\ &\quad \left. - 0.25 \tan^{-1} \left[ 1.28 \frac{R_j}{r_o \sqrt{j}} \frac{1 + \frac{1.48}{j} \left( \frac{R_j}{r_o} \right)^2 - 0.24}{\sqrt{1 + \frac{1.48}{j} \left( \frac{R_j}{r_o} \right)^2 + \frac{0.31}{j} \left( \frac{R_j}{r_o} \right)^2}} \right] \right\} \end{aligned} \quad (6.42)$$

At large distances  $x$  this gives a profile similar to that of one phase jets, with a half-angle of 12.4 deg.

The air flow (equation 31) now becomes:

$$G = 1.82 u_o r_o^2 j \rho_g \left[ \sqrt{1 + \frac{1.5}{j} \left( \frac{R_j}{r_o} \right)^2} - 1 \right] \quad (6.43)$$

The longitudinal temperature profile is given by:

$$\frac{T_m - T_\infty}{T_o - T_\infty} = \frac{0.75 u_m/u_o}{1 - 0.6 u_m/u_o} \quad (6.44)$$

and the longitudinal concentration profile by:

$$\frac{c_m - c_\infty}{c_o - c_\infty} = \frac{0.75 u_m/u_o}{1 - 0.6 u_m/u_o} \quad (6.45)$$

instead of eqns. 33 and 35 respectively. The radial profiles of  $u$ ,  $T$  and  $c$  will of course remain the same.

(d) Jets with initial radial or tangential velocity: Pressure nozzles are often designed to give the jet an initial non-axial velocity component so that the jet angle  $\alpha$  may be different from 12.4 deg. For full-cone jets this can be taken into account by applying the momentum conservation equation, eqn. 28, which gives

$$u_m \propto 1/R_j \quad (6.46)$$

and a correction factor can be applied to all the previous equations for the longitudinal profiles of  $u_m$ ,  $T_m$ ,  $c_m$  and  $G$ . In equations 29, 33, 35 and 41, the right-hand side must be divided by  $(\tan \alpha / \tan(12.4 \text{ deg.}))$ , while in equations 30, 31 and 43 the right-hand side must be multiplied by the same factor.

(e) Jets injected into cocurrent streams: If the velocity  $u_\infty$  of the stream is low compared to the orifice velocity, as is usually the case, we can simply replace  $u$  by  $(u - u_\infty)$ ,  $u_m$  by  $(u_m - u_\infty)$  and  $u_o$  by  $(u_o - u_\infty)$  in equations 27, 29, 41. For large mainstream velocities the general profile of the jet will be stretched and more complicated equations arise (A3).

### II.1.1.3 Particle behaviour in jet zone

The gas velocity in a jet is inversely proportional to the distance from the pole. The momentum, heat and mass transfer behaviour of a single liquid droplet in such a flow-field will now be briefly considered. The flow field will be somewhat simplified for the purpose of the present calculations. The equations to be solved are:

- The equation of motion:

$$\frac{du_p}{dx} = - \frac{1}{u_p} \frac{0.75 c_D \rho_a}{D_p \rho_p} |u_p - u_a| (u_p - u_a) \quad (6.47)$$

where  $c_D$  is the drag coefficient,  $u_p$  and  $u_a$  the droplet and air velocities respectively,  $\rho_p$  and  $\rho_a$  the droplet and air densities, and

$$u_a = u_o \frac{x_c}{x + x_c} \quad (6.48)$$

where  $x_c$  is a characteristic length

$$c_D = c_{D_0} (D_p |u_p - u_a| / \nu_a)$$

where  $\nu_a$  is the kinematic viscosity of air.

- The equation of evaporation (Ranz and Marshall type):

$$\frac{dD_p}{dx} = - \frac{2k_a \Delta T}{\rho_p \lambda D_p u_p} \left( 2 + \frac{0.6 Pr^{1/3} D_p^{1/2} |u_p - u_a|^{1/2}}{\nu_a^{1/2}} \right) \quad (6.49)$$

where  $k_a$  is the air thermal conductivity,  $\lambda$  the latent heat of evaporation,  $\Delta T$  the temperature difference between the air and the droplet.

It will be more convenient to write these equations in dimensionless forms :

$$\frac{du_p^*}{dx^*} = -N_2 \frac{c_D}{D_p^* u_p^*} \left| u_p^* - \frac{1}{1+x^*} \right| \left( u_p^* - \frac{1}{1+x^*} \right) \quad (6.50)$$

with

$$c_D = c_D(\text{Re})$$

$$\text{Re} = N_1 D^* \left| u_p^* - \frac{1}{1+x^*} \right|$$

$$\frac{dD_p^*}{dx^*} = \frac{-N_3 (2 + 0.6 \text{Pr}^{1/3} \text{Re}^{1/2})}{D_p^* u_p^*} \quad (6.51)$$

where the dimensionless variables are defined by:

$$D_p^* = D_p / D_{po}$$

$$u_p^* = u_p / u_o$$

$$x^* = x / x_o$$

and the dimensionless groups by:

$$N_1 = D_{po} u_o / \nu_a$$

$$N_2 = 0.75 \rho_a x_c / \rho_p D_{po}$$

$$N_3 = 2 k_a \Delta T x_c / \rho_p \lambda u_o D_{po}^2$$

The initial conditions of this set of equations are:

$$D_p^* = 1 \quad \text{at} \quad x^* = 0 \quad (6.52)$$

and either

$$u_p^* = 1 \quad (6.53)$$

or

$$u_p^* = 0 \quad \text{at} \quad x^* = 0 \quad (6.54)$$

Equation 53 would hold for pressure nozzles, while equation 54 would hold for pneumatic nozzles with external mixing. Pneumatic nozzles with internal mixing present an intermediate behaviour.

The solution to this set of equations was carried out numerically using a fourth-order Runge-Kutta procedure for the air-water system and with the range:

$$N_1 = 10 \text{ to } 10^4$$

$$N_2 = 0.01 \text{ to } 1$$

$$N_3 \rightarrow 0 \quad (\approx 10^{-6})$$

which covers the ranges encountered in a real spray. The reason for the small value of  $N_3$  (the driving-force number) is that, in the region near the nozzle, air entrainment into the jet is limited and the air quickly approaches saturation.

The results are plotted as  $\overline{Nu}$  against  $N_1$  (which is proportional to the air velocity), with  $N_2$  (which is inversely proportional to the droplet diameter) as a parameter, where  $\overline{Nu}$  is the average Nusselt number between  $x^* = 0$  and  $x^* = 50$ , an arbitrarily chosen value (figure 4).

It can be seen that  $\overline{Nu}$  tends to 2 at low  $N_1$  (low air velocity) and tends to vary as  $N_1^{1/2}$  as  $N_1$  becomes large. This can be seen intuitively as follows: from the Ranz-Marshall equation,

$$Nu = 2 + a u_R^{1/2} \quad (6.55)$$

where  $u_R$  is the relative velocity. For a given particle size  $u_R$  can be expected to vary as  $u_a$ .

Hence

$$\begin{aligned} Nu &\approx 2 + b u_a^{1/2} \\ &\approx 2 + c N_1^{1/2} \end{aligned} \quad (6.56)$$

The spatial (per unit distance) heat-transfer rate, on the other hand, is also proportional to the time spent in an interval of distance, hence it is inversely proportional to the particle velocity, and approximately inversely proportional to the air velocity.

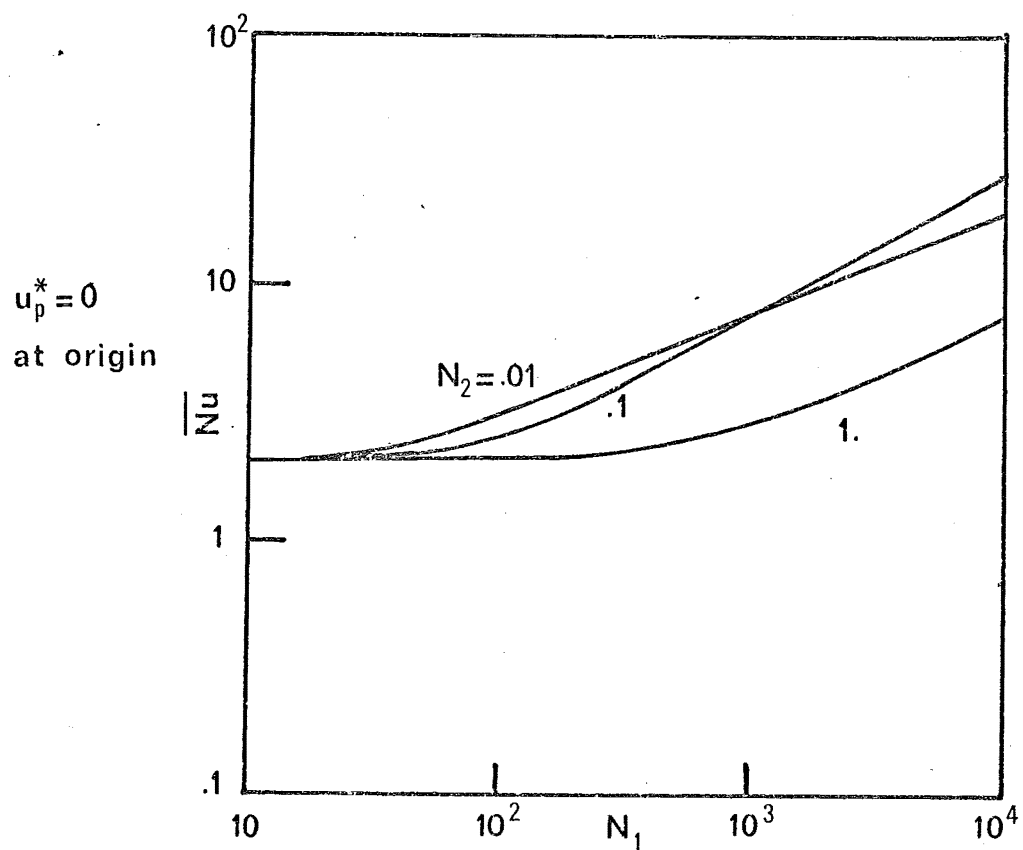
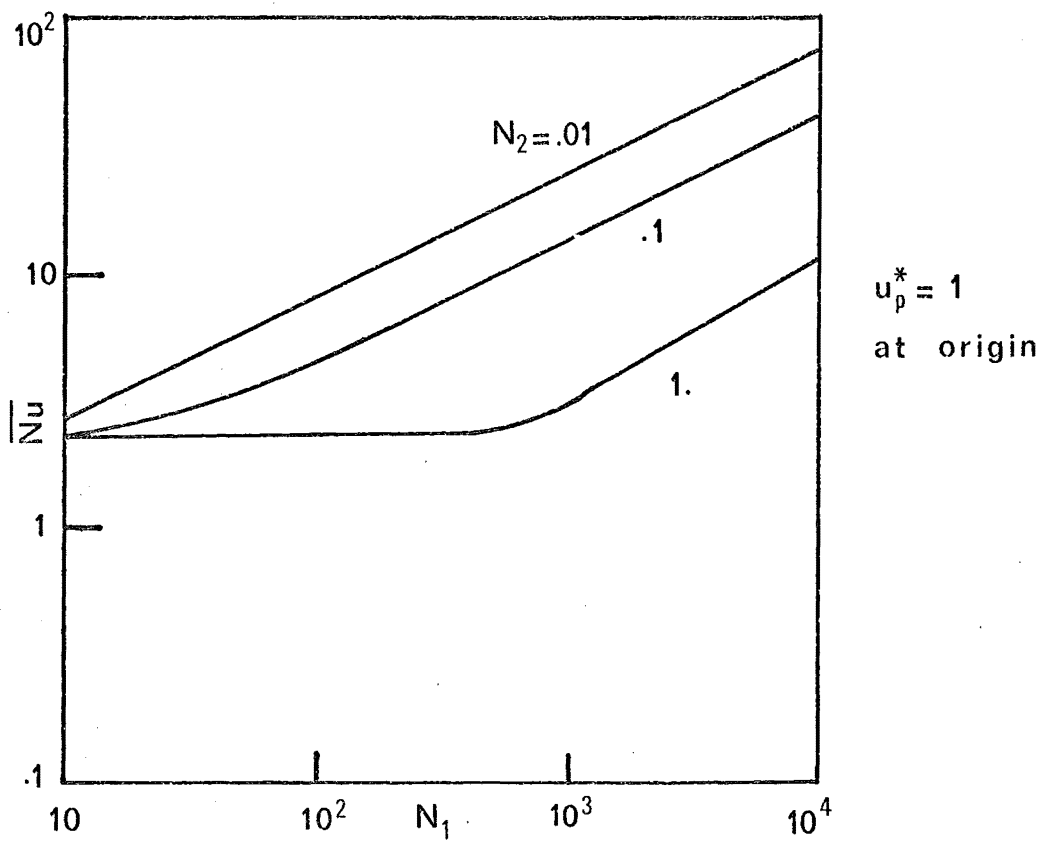


FIGURE 6.4: MEAN NUSSELT NUMBER OF PARTICLE  
IN DECELERATING AIR FLOW



Hence

$$\text{Spatial transfer rate} \propto \frac{Nu}{u_p} = \frac{2}{u_a} + \frac{d}{u_a^{1/2}} \quad (6.57)$$

This result will be useful for averaging the jet profile.

#### II.1.1.4 The averaging of the jet profile

A spray issuing from a nozzle consists of a spectrum of droplet sizes, velocities and directions. Subsequently the droplets will be randomly distributed across the jet and be subjected to different air velocities, temperatures and vapour concentrations. The paths of the particles will contain a random element due to the turbulence of the air. Furthermore, interaction between the jet and the droplets (in the process of heat, mass and momentum transfers) must also be taken into account. Therefore it is impossible to solve the spray evaporation problem by following up each particle rigorously, and even Monte Carlo methods are impracticable, due to the great number of variables involved. The approach followed instead will be:

(1) To replace the bell-shaped velocity, temperature and concentration profiles at each point  $x$  by "equivalent" flat profiles.

(2) To solve the equations of motion and evaporation for each droplet size, basing on these equivalent profiles.

By means of such an averaging procedure, the problem becomes one-dimensional and manageable. The "equivalent" profiles are those which will give the same spatial rate of evaporation as the real profiles.

Since

$$\text{Spatial rate of transfer} \propto (Nu/u_p) \Delta T$$

the equivalent velocity profile must give the first term  $(Nu/u_p)$  and the equivalent temperature profile the second term.

(a) Equivalent velocity profile

Let  $c(\xi)$  be the droplet concentration, where  $\xi = r/R_j$  (in the notation of figure 3).

$$\text{Let } Nu/u_p = f(u_a) \quad (6.58)$$

The equivalent velocity must give rise to the same average  $(Nu/u_p)$ :

$$\int_0^1 (c u_p) \cdot f(u_a) \cdot (\pi \xi d\xi) = f(u_{ae}) \int_0^1 (c u_p) (\pi \xi d\xi) \quad (6.59)$$

where  $u_{ae}$  is the equivalent (air) velocity,  $(c u_p)$  is the flux of particles and  $(\pi \xi d\xi)$  the element of area.

$u_p$  may be assumed to have a similar profile to  $u_a$ :

$$u_p = u_{pm} (1 - \xi^{1.5})^2 \quad (6.60)$$

Also, from equation 34,

$$c = c_m (1 - \xi^{1.5})$$

Substituting these back into equation 59, one gets:

$$\int_0^1 (1 - \xi^{1.5})^3 \xi f(u_a) d\xi = f(u_{ae}) \int_0^1 (1 - \xi^{1.5})^3 \xi d\xi \quad (6.61)$$

From the previous section (equation 57), one has:

$$\frac{Nu}{u_p} = f(u_a) = \frac{a}{u_a} + \frac{b}{u_a^{1/2}}$$

Substituting this into equation 61 and also using equation 27 for  $u_a$ , one finally obtains:

$$\frac{a}{u_m} \int_0^1 (1 - \xi^{1.5}) \xi d\xi + \frac{b}{u_m^{1/2}} \int_0^1 (1 - \xi^{1.5})^2 \xi d\xi = \left( \frac{a}{u_{ae}} + \frac{b}{u_{ae}^{1/2}} \right) \int_0^1 (1 - \xi^{1.5})^3 \xi d\xi$$

or

$$0.214 \frac{a}{u_m} + 0.129 \frac{b}{u_m^{1/2}} = 0.089 \left( \frac{a}{u_{ae}} + \frac{b}{u_{ae}^{1/2}} \right) \quad (6.62)$$

If the first term on each side of equation 62 is dominant, then:

$$u_{ae} = 0.42 u_m \quad (6.63)$$

If the second term is dominant,

$$u_{ae} = 0.48 u_m \quad (6.64)$$

Since the difference is slight, we shall take

$$u_{ae} \approx 0.45 u_m \quad (6.65)$$

(b) Equivalent temperature profile

By similar reasoning:

$$\int_0^1 (c u_p) \Delta T (\pi \xi d \xi) = \Delta T_e \int_0^1 (c u_p) (\pi \xi d \xi)$$

which, on inserting

$$\Delta T = (T_m - T_\infty) (1 - \xi^{1.5}) - (T_p - T_\infty) \quad \text{(from equation 32)}$$

$$c = c_m (1 - \xi^{1.5}) \quad (6.34)$$

and

$$u_p = u_{pm} (1 - \xi^{1.5})^2 \quad (6.60)$$

gives:

$$(T_e - T_\infty) = 0.75 (T_m - T_\infty) \quad (6.67)$$

In summary, we have replaced the real jet by an equivalent jet with the following flat radial profiles:

Air velocity is given by equation 65,

Temperature is given by equation 67,

and in those equation,  $u_m$  and  $T_m$ , the axis velocity and temperature, can be calculated according to the formulae laid out in section II.1.1.2.

### II.1.2 The basic equations of heat and momentum transfer for a single droplet

#### (a) The equation of evaporation

From equation (5.13a) of Chapter 5, it has been established that:

$$\frac{dE}{dt} = \frac{6(2 + .6 Re^{1/2} Pr^{1/3}) D_p k_a \Delta T}{\lambda w_{lo} \rho_{po} D_{po}^3} \quad (6.68)$$

where  $\lambda$  is the latent heat of evaporation,  $w_{lo}$  the initial liquid mass fraction and  $\rho_{po}$  the initial mean droplet density.

When there are differential velocities between the particles themselves and between the particles and the air, it is easier to keep track of the spray as a whole and to set up heat and mass balances if we use the rate of change with respect to distance rather than time.

From

$$d/dt = u_{pi} d/dx$$

we finally have

$$\frac{dE}{dx} = \frac{6(2 + .6 Re^{1/2} Pr^{1/3}) D_p k_a \Delta T}{\lambda w_{lo} \rho_{po} D_{po}^3 u_{pi}} \quad (6.69)$$

where  $u_{pi}$  is the particle velocity in the x-direction.

#### (b) The equation of motion

$$m \frac{du_{pi}}{dt} = \frac{1}{2} c_D \left( \frac{\pi D_p^2}{4} \right) \rho_a |u_p - u_a| (u_{pi} - u_{ai}) + g_i \quad (6.70)$$

where  $g_i$  is the acceleration of gravity in the x-direction (axial direction),  $u_{pi}$  and  $u_{ai}$  the particle and air velocities in the same direction, and  $c_D$  is the drag coefficient.

This can be rewritten as:

$$\frac{d(u_{pi}^2)}{dx} = - \frac{1.5 c_D \rho_a |u_p - u_a| (u_{pi} - u_{ai})}{\rho_p D_{po}} + 2g_i \quad (6.71)$$

where  $\rho_p$  is the particle density.

Equations 69 and 71 are the two basic equations of the simulation program.

### II.1.3 Miscellaneous effects

The methods used in accounting for various influences on droplet behaviour have already been examined in Chapter 5 and will only be briefly recounted here, except for the initial evaporation at the nozzle exit which will be considered in some detail.

#### II.1.3.1 Effect of mass flux on heat transfer:

Equation 5.24 of Chapter 5 will be used.

#### II.1.3.2 Effect of radiation:

Either of two methods can be used:

(a) Mean cloud absorptivity method, using equations 5.48, 42, 46 & 29 of Chapter 5.

(b) Net leaving-flux method, using equation 5.28 of Chapter 5.

#### II.1.3.3 Turbulence effect:

Turbulence causes a turbulent relative velocity  $u'_R$  calculable by equation 5.59 of Chapter 5. This turbulent relative velocity will be added vectorially to the mean relative velocity when calculating the Reynolds number for the drag coefficient and the Nusselt number.

#### II.1.3.4 Presence of solids

The first effect of solids is to reduce the vapour pressure of the evaporating liquid. For computational purpose the relative reduction will be assumed to be constant throughout the evaporation process and can be found experimentally or calculated from Raoult's or Wüllner's law, assuming a saturated solution.

The second effect is crust formation: each droplet is assumed to shrink freely until a solid crust forms at a certain moisture content. Thereafter the diameter is assumed to be constant. Shrivelling, ballooning and explosions will be ignored.

The third effect of solids is to impede the moisture transfer rate to the surface, by the formation of a membrane or a crust.

Let

$$f_d = \frac{\text{drying rate of particle}}{\text{drying rate of liquid droplet of evaporating solution.}}$$

The surface temperature  $T_s$  of the particle will be raised according to:

$$T_a - T_s = f_d (T_a - T_s^*) \quad (6.72)$$

where  $T_s^*$  is the adiabatic saturation temperature of the evaporating solution.

In general,  $f_d$  is a function of the present moisture content, the initial moisture content, the particle diameter and the mean rate of drying in the past history of the particle (these factors all affect the moisture profile in the particle), and the nature of the solid material.

#### II.1.3.5 Droplet sensible heat:

Some of the heat transferred to the particle must be used to raise or lower the particle temperature. As the heat capacity of the droplet is low compared with its latent heat of evaporation, sensible

heat effects will be neglected except in the case of feed overheat.

The effect of the particle temperature  $T_p$  being higher than the adiabatic saturation temperature  $T_s^*$  is to multiply the evaporation rate (based on  $T_s^*$ ) by a factor given in equation 5.63 of Chapter 5. Due to the extra evaporation which takes heat from the particle, its temperature falls at a rate given by equation 5.66 or 5.69 of Chapter 5. Once  $T_p$  has fallen to  $T_s^*$ , sensible-heat effects can be neglected.

#### II.1.3.6 Initial evaporation due to atomising air

In pneumatic atomising, due to the intense mixing at the nozzle orifice, the feed and the atomising air will come to hygrothermal equilibrium upon emerging from the nozzle, and some immediate evaporation will take place.

From figure 5 we can write the mass balance for the amount evaporated:

$$G(y_s^* - y_a) = L w_{lo} E \quad (6.73)$$

and the heat balance:

$$\begin{aligned} & \text{Dry air enthalpy in} + \text{vapour enthalpy in} \\ & + \text{feed enthalpy in} \\ & = \text{Dry air enthalpy out} + \text{vapour enthalpy out} \\ & + \text{feed enthalpy out} . \end{aligned}$$

Assuming that the change in vapour enthalpy is due only to the heat of evaporation of the evaporated vapour, that is, neglecting the sensible heat of the vapour, the heat balance comes to:

$$G c_{pa} T_a + L c_{pf} T_f = G c_{pa} T_s^* + L(1 - w_{lo} E) c_{pf} T_s + L w_{lo} E \lambda \quad (6.74)$$

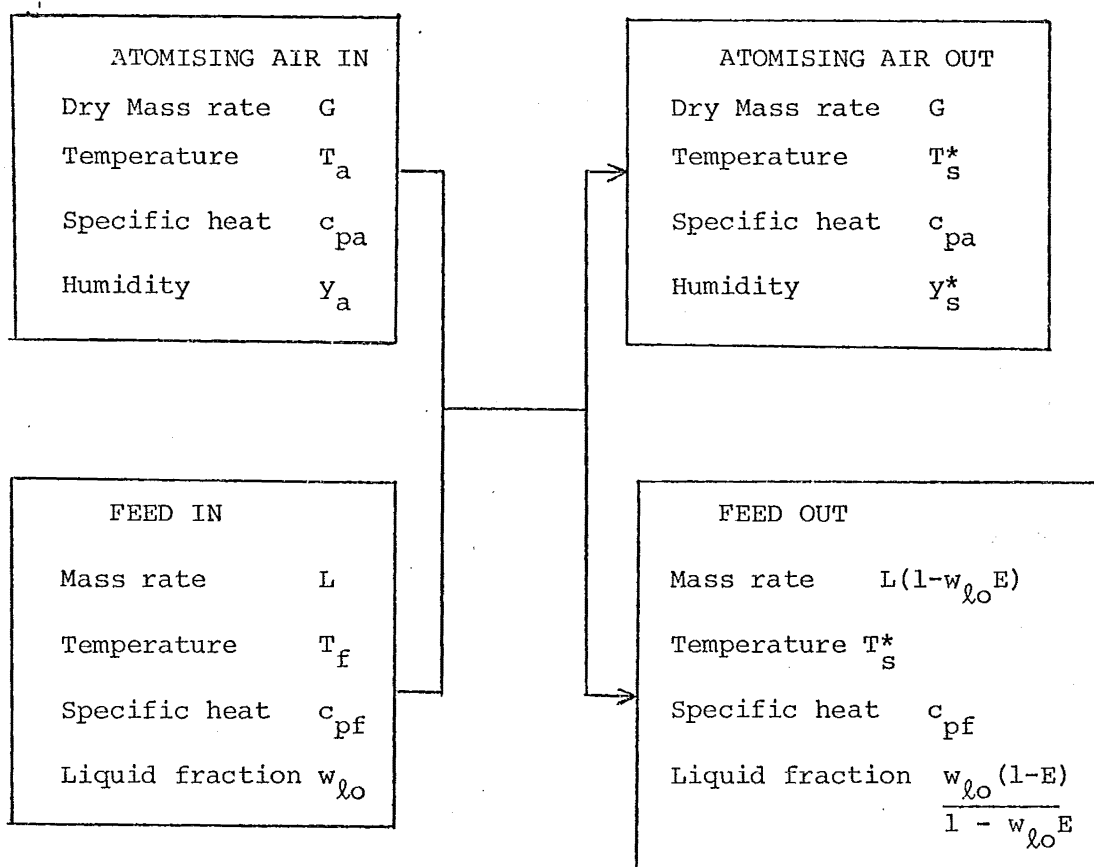
Combining the mass and heat balances we get:

$$T_s^* = T' - K(y_s^* - y_a) \quad (6.75)$$

where  $T' = (G c_{pa} T_a + L c_{pf} T_f) / (G c_{pa} + L c_{pf})$  is the equilibrium temperature in the absence of evaporation, and

Figure 6.5

Mass and heat balance for evaporation at the  
pneumatic nozzle exit



$L$  include solid and liquid flows.



$$K = G\lambda / (Gc_{pa} + Lc_{pf})$$

is the change in the mean temperature of the air-feed system for a unit change in air moisture due to evaporation.

$y_s^*$  and  $T_s^*$  being coupled by the saturation curve, equation 75 can be solved by iteration.

#### II.1.4 Miscellaneous equations

##### II.1.4.1 The standard drag curve

The following segmentwise approximation is used:

$$\begin{aligned} c_D &= \frac{24}{Re} & , \quad Re \leq .4 \\ &= \frac{24}{Re} (1 + .1 Re) & , \quad .4 < Re \leq 2 \\ &= \frac{24}{Re} (1 + .15 Re^{.687}) + \frac{.42}{1 + 4.25 \times 10^{-4} Re^{1.16}} & Re > 2 \end{aligned} \quad (6.76)$$

The last equation is due to Schiller and Naumann and modified by Clift and Gauvin (C5).

##### II.1.4.2 The saturation curve of water and the calculation of adiabatic-saturation conditions.

The saturation curve of water is calculated by a curve-fitted Riedel-Miller-Planck equation (R6)

$$\ln p_w = \frac{-6348.8}{T} + 22.536 - 0.019639 T + 1.301 \times 10^{-5} T^2 \quad (6.77)$$

for  $T = 300 - 380$  K

where  $p_w$  is the partial pressure of water measured in atmospheres.

The adiabatic-saturation temperature and humidity are calculated by the Newton-Raphson iterative method from the equation

$$\frac{y_s^* - y_a}{T_s^* - T_a} = - \frac{c_{ps}}{\lambda} \quad (6.78)$$

where  $c_{ps}$  is the wet air specific heat and  $\lambda$  the latent heat of evaporation, and

$$y_s^* = \frac{0.622 p_w}{1 - p_w} \quad (6.79)$$

#### II.1.4.3 Droplet size distribution

Nukiyama-Tasanawa's equation (eqn. 19) with  $\delta = 0.5$  is recommended:

$$Q = a D_p^2 \exp(-b D_p^{0.5}) \quad (6.80)$$

where

$$b = \sqrt{\frac{\Gamma(12)}{\Gamma(10) \bar{D}_{vs}}} \quad (6.81)$$

$Q$  is the number of droplets between  $D_p$  and  $D_p + dD_p$ , and  $\Gamma$  is the gamma function. A maximum diameter (2.5 to  $3 \bar{D}_{vs}$ ) must be specified.

#### II.1.4.4 Terminal velocity calculations

Where necessary, the terminal drag  $c_{Dt}$  of a particle is calculated by:

$$c_{Dt} = \frac{576}{\Pi} \quad , \quad \Pi \leq 10 \quad (\text{Stokes regime}) \quad (6.82)$$

$$= \frac{574}{\Pi} + \frac{32}{\Pi^{.39}} + \frac{1}{1.8 + 758 \Pi^{-.36}} \quad , \quad \Pi > 10 \quad (6.83)$$

(Smith's equation (S12))

where

$$\Pi = c_{Dt} \text{Re}_t^2 = \frac{4\rho_p g D_p^3}{\rho_a v_a^2}$$

in which  $g$  is the gravitational acceleration,  $v_a$  the air kinematic viscosity,  $D_p$  the particle diameter,  $\rho_a$  and  $\rho_p$  the air and particle densities respectively.

#### II.1.4.5 Air properties

The air density will be assumed to be inversely proportional to the absolute temperature.

The viscosity of the air,  $\mu_a$ , is calculable by the modified Sutherland equation <sup>(K5)</sup>:

$$\mu_a = \frac{1.488 \times 10^{-6} T^{1.5}}{T + 122.1 \exp(-11.5/T)} \quad , \quad (6.84)$$

$$90K < T < 1845K$$

where  $T$  is the absolute temperature in degree K.

The thermal conductivity of air,  $k_a$ , is given by Keyes' equation <sup>(G3)</sup>:

$$k_a = \frac{2.646 \times 10^{-3} T^{1.5}}{T + 245 \exp(-27.6/T)} \quad , \quad (6.85)$$

$$90K < T < 584K$$

## II.2 Computational problems

A simplified flow chart for the calculation has been drawn in figure 2. A more detailed version is now given in figure 6. The actual program written in Fortran can be found in Appendix D.

Since the air properties (density, viscosity, thermal conductivity) and the adiabatic saturation conditions change fairly slowly, their values can be based on the previous point in space. Similar

Figure 6.6 DETAILED FLOW DIAGRAM OF SIMULATION OF COCURRENT SPRAY DRYER.

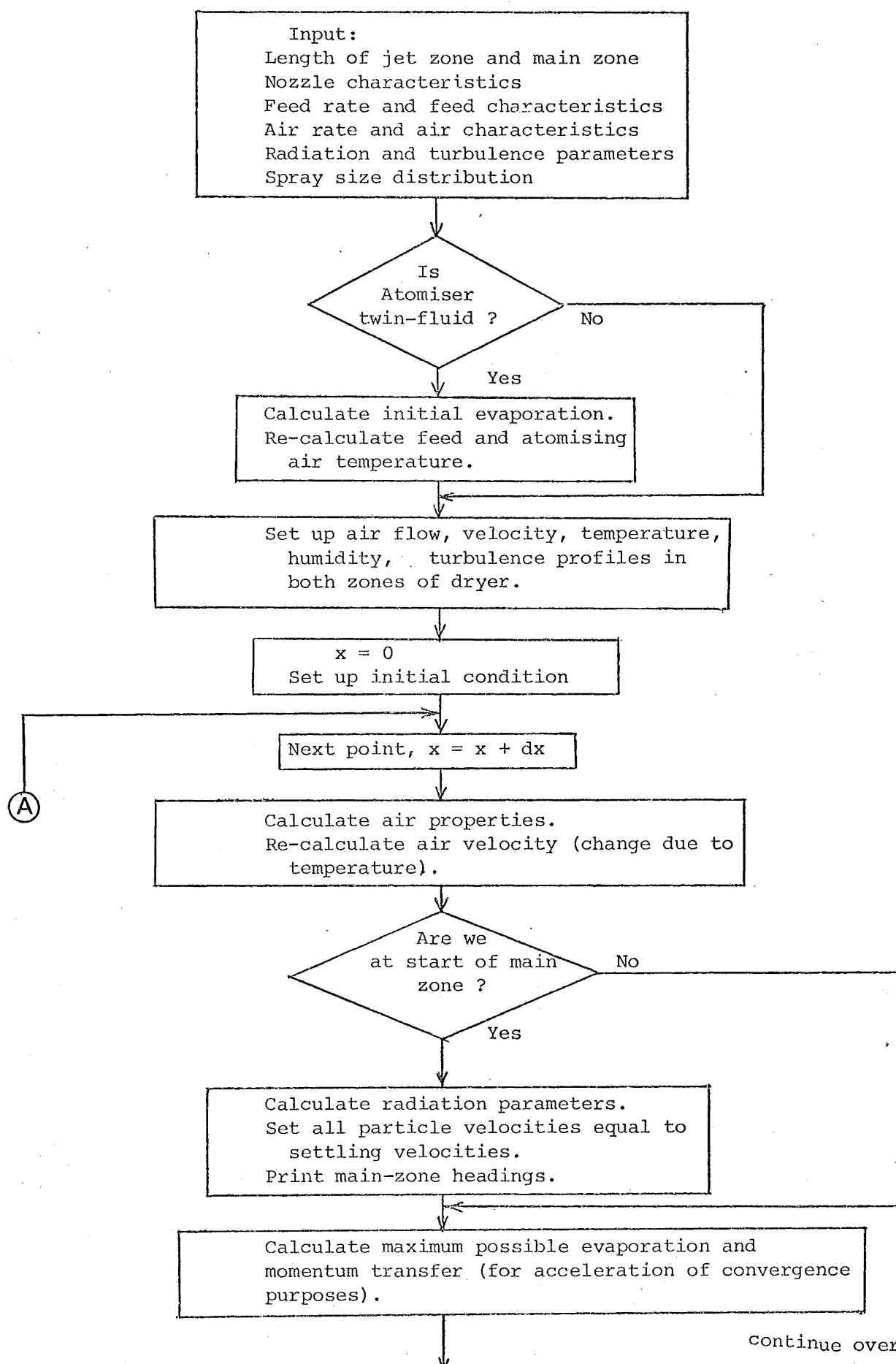
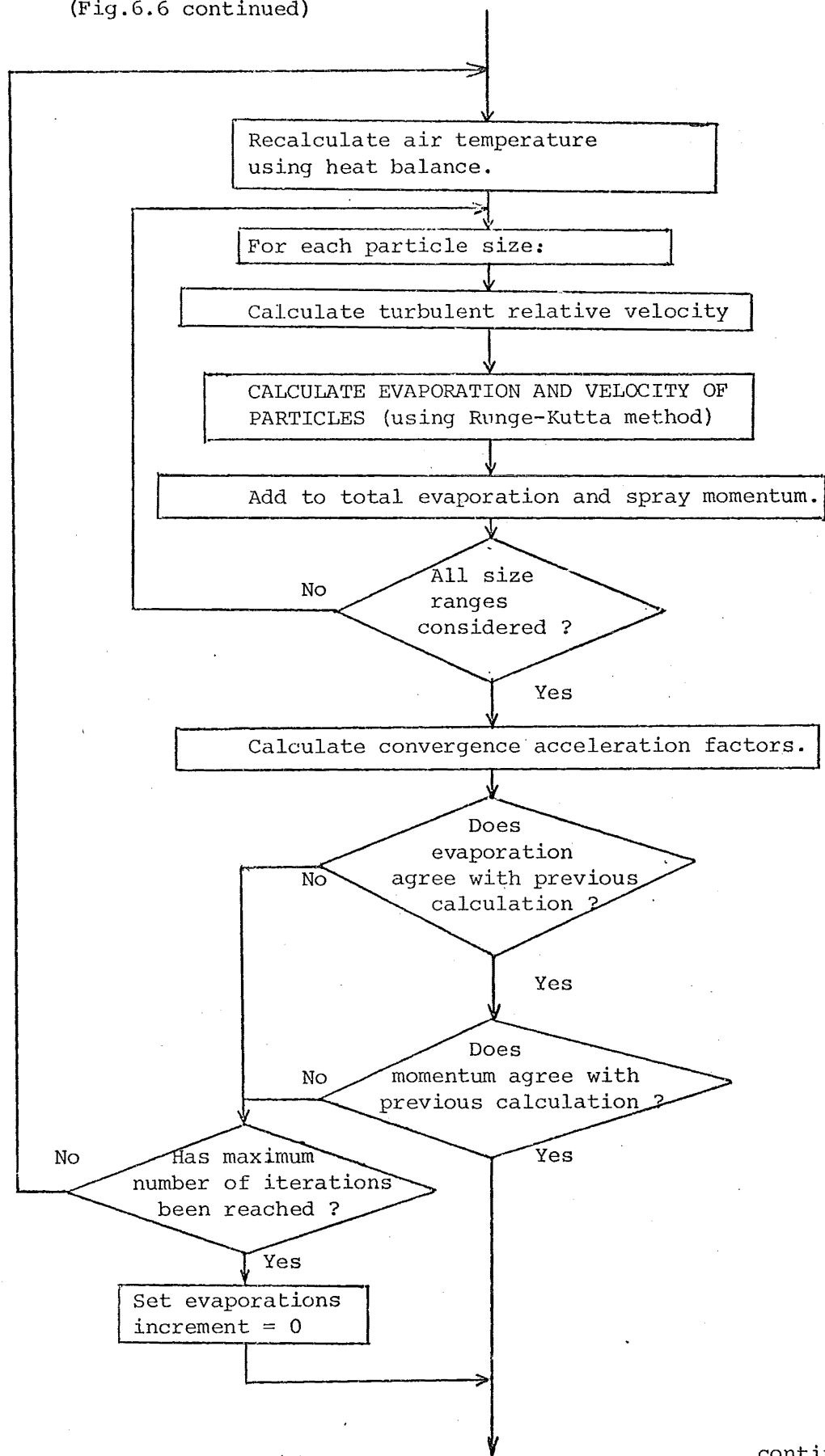
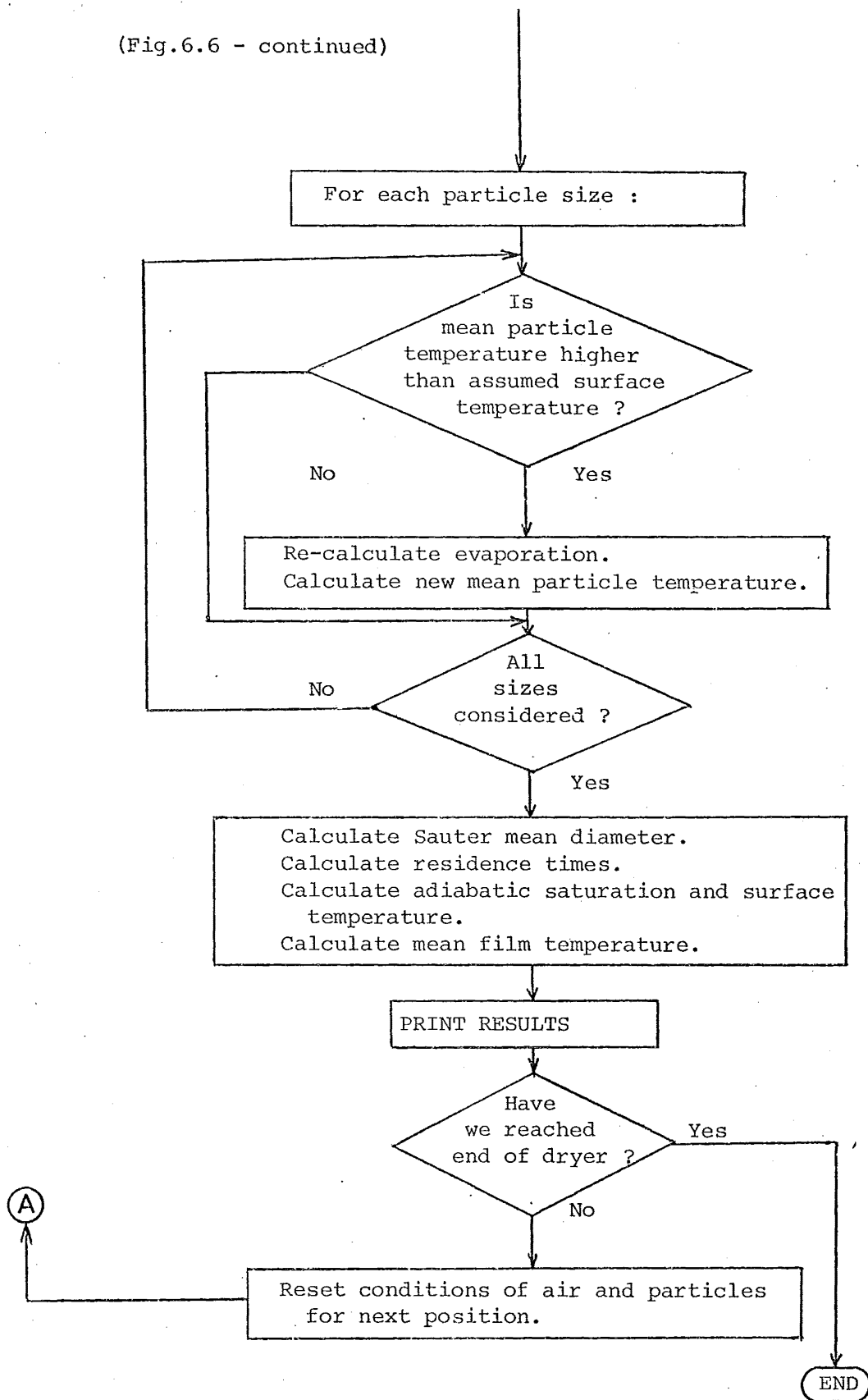


(Fig.6.6 continued)



continue over

(Fig.6.6 - continued)



conditions apply for the droplet surface temperature and relative turbulent motion. As a distance increment is only a few thousandths of the total dryer length, this approximation will not involve large errors.

In the jet zone, a major problem is the convergence of the iteration procedure used in recalculating air conditions and hence evaporation. The problem arises from the high transfer coefficient (due to high relative velocities), rapid change in the air velocity and temperature profiles, and small air flow rate. A small amount of evaporation will cause a major change in air temperature and humidity, hence the iteration becomes easily unstable and must be somehow accelerated. The procedure is outlined in figure 7.

The purpose is to make the new estimate of the fraction evaporated,  $E^{(2)}$ , a certain combination of the previous two estimates  $E^{(0)}$  and  $E^{(1)}$ , which would be as close to the correct value  $E_i$  as possible. Suppose this has been done and  $E^{(2)} = E_i$ .

Consider  $(E_m - E^{(0)})$  to be a measure of the driving force used in the previous calculation, and  $(E_m - E_i)$  to be the "real" driving force. Since the increase in evaporation between the last position and this one is roughly proportional to the driving force, one can write:

$$\frac{\text{Previous estimate of increase in evaporation}}{\text{Previous estimate of driving force}} = \frac{\text{real increase in evaporation}}{\text{real driving force}}$$

$$\frac{E^{(1)} - E_{i-1}}{E_m - E^{(0)}} = \frac{E_i - E_{i-1}}{E_m - E_i} \quad (6.86)$$

or

$$E^{(2)} \approx E_i = \frac{E^{(1)} E_m - E^{(0)} E_{i-1}}{E_m - E_{i-1} + E^{(1)} - E^{(0)}} \quad (6.87)$$

Figure 6.7

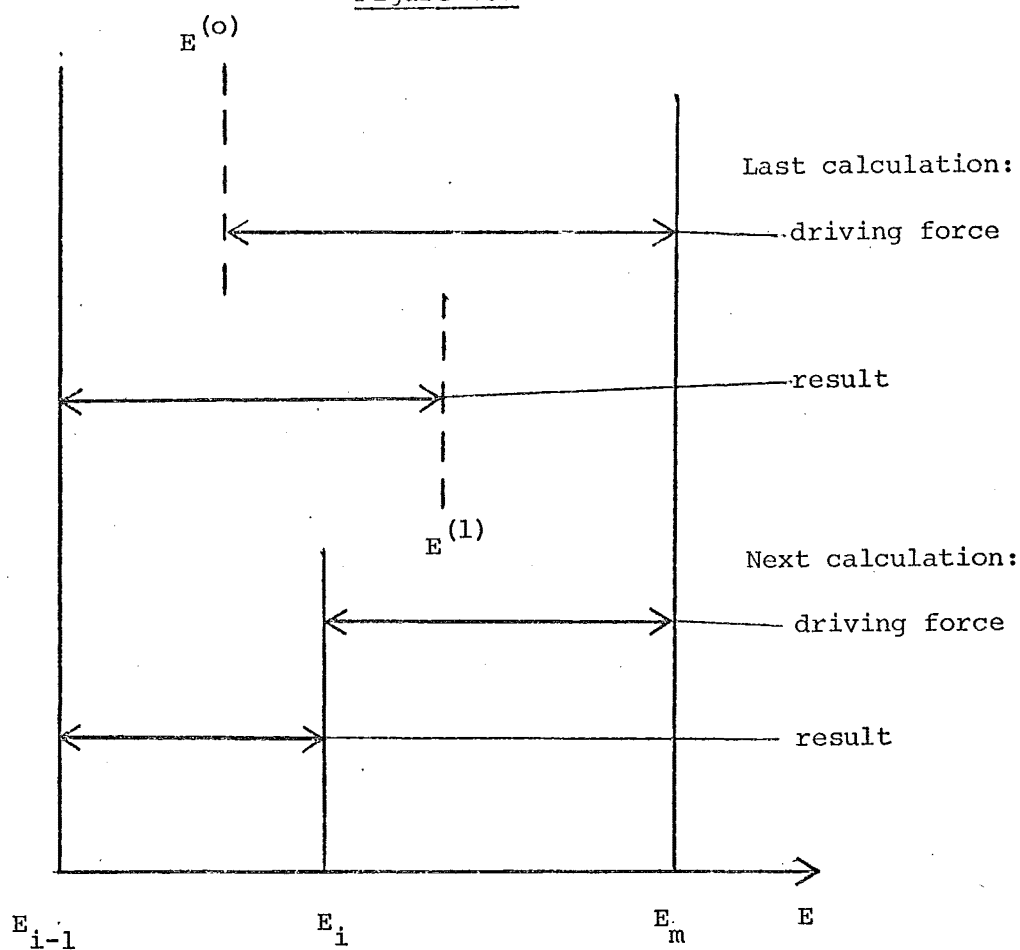


Fig.6.7 Illustration of convergence acceleration scheme for evaporation calculation.

$E_{i-1}$  = evaporation at previous position

$E_i$  = correct value of evaporation at present position

$E_m$  = maximum possible evaporation at present position based on the available air flow

$E^{(0)}$  = a first estimate of  $E_i$

$E^{(1)}$  = a second estimate of  $E_i$ , based on air conditions which result from  $E^{(0)}$ .



which is the combination that we are seeking. A similar equation can be found for momentum transfer.

### II.3 Sample calculations and results

The simulation program was applied to two cases with quite different characteristics: a very fine spray ( $\bar{D}_{vs} = 12 \mu\text{m}$ ) of pure water in a jet-dominated air flow, and a coarse spray ( $\bar{D}_{vs} = 105 \mu\text{m}$ ) of milk in a spray dryer with only a short jet zone. The results will be compared with experimental data available.

#### II.3.1 Evaporation of a fine, pure water spray in a jet zone

##### II.3.1.1 Operating conditions

Manning and Gauvin<sup>(M3)</sup> presented evaporation, temperature, droplet sizes and droplet velocity data in their cocurrent tall-form spray dryer. The air inlet is designed to minimise turbulence and backmixing, and thus it can be assumed that the jet zone extends through the whole zone considered (which is 0.5 m long). This assumption was checked by doing a numerical computation of droplet velocities based on jet-zone characteristics (section II.1.1). The predicted pattern of deceleration agrees satisfactorily with experimental measurements (figure 8).

Manning and Gauvin's run 29 was used for our sample calculation as the data for this run were complete. The input conditions given by them (or calculated from their specifications) are summarised in Table 2. It must be noted that for a pneumatic nozzle with an annular outer air outlet, the outer radius of the air annulus must be used as the "orifice radius",  $r_o$ , mentioned in jet theory.

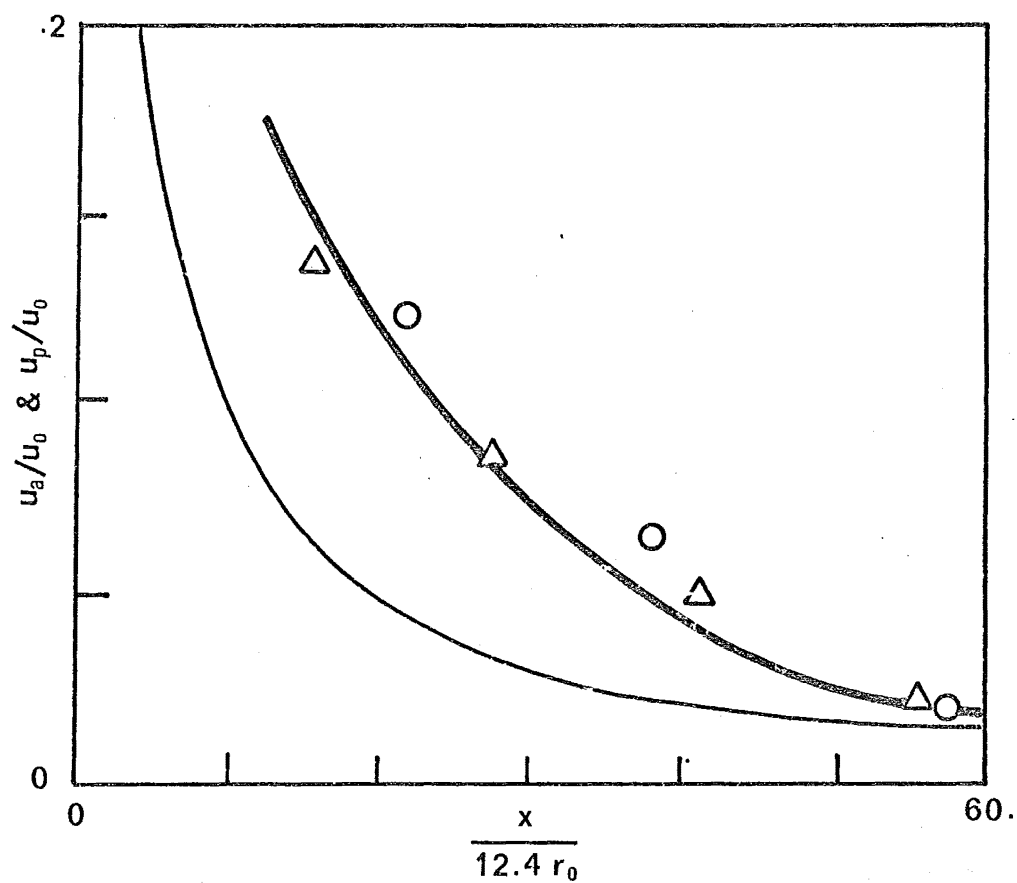


FIGURE 6.8: VELOCITY OF A 40  $\mu\text{m}$  DROPLET IN THE JET ZONE OF A PNEUMATIC NOZZLE (JN12)

- Predicted air velocity
- - - Predicted droplet velocity
- $\Delta$  Data<sup>(M3)</sup> at 173 kPa g. atomising pressure
- $\circ$  Data<sup>(M3)</sup> at 242 kPa g. - - -

TABLE 6.2

Input conditions for sample calculation 1

(pure water, fine spray)

Flow pattern: cocurrent with jet zone characteristics.Nozzle type: pneumatic with internal mixing (Spraying Systems Co. type JN 12)Air orifice radius =  $7.6 \times 10^{-4}$  m.Nozzle operating conditions:Atomising air rate =  $9.1 \times 10^{-4}$  kg/s

Atomising air orifice velocity = 370 m/s

Atomising air temperature = 300 K

Liquid rate =  $5.55 \times 10^{-4}$  kg/s

Liquid temperature = 300 K

Spray half angle = 12.4 deg.

Feed properties: (pure water)Density =  $1 \times 10^3$  kg/m<sup>3</sup>Latent heat of evaporation =  $2.46 \times 10^6$  J/kgSpecific heat =  $4.19 \times 10^3$  J/kg K

Solid mass fraction = 0.

Drying air:Flow rate =  $3.8 \times 10^{-2}$  kg/s

Inlet temperature = 377 K

Inlet humidity = .005 - .01 kg/kg

Turbulence = negligible

Spray size distribution:

Nukiyama-Tasanawa, with dispersion parameter

 $\delta = 0.5$  and $\bar{D}_{vs} = 12 \mu\text{m}$

### II.3.1.2 Results and discussion

The results are plotted in figure 9 together with experimental data.

Agreement is quite good except for  $\bar{D}_{vs}$ , which increases more slowly than was observed. This may be due to the inaccuracy of the size distribution assumed, and also possibly to some inaccuracy in the droplet sampling procedure. The authors used a collection cell method for measuring droplet diameters. If some smaller droplets were not collected, due to their low inertia, and the effect insufficiently accounted for, then the Sauter diameter measured would be higher than the actual value.

In figure 10 is plotted the calculated evaporation when the jet zone stops and the main zone starts at points A, B, C. It can be seen that evaporation in the jet zone is by comparison severely limited, due to the high droplet velocities (hence low residence time) and limited air available. The graph shows the severe errors that would be involved if the jet dynamics were not accounted for.

In figure 11a the air velocity at the orifice is reduced by 33%. Increased residence times give rise to increased evaporation, but the latter increase is slight (3 to 10%), justifying our assumption in averaging equations 63 and 64 for the equivalent velocity. In practice this increase in evaporation will be almost exactly balanced by a decrease due to the reduction in air entrainment (figure 11a). On the other hand, changes in nozzle operating conditions will affect the drop sizes<sup>(K6)</sup>, which will have a very large effect on the performance (figure 11b).

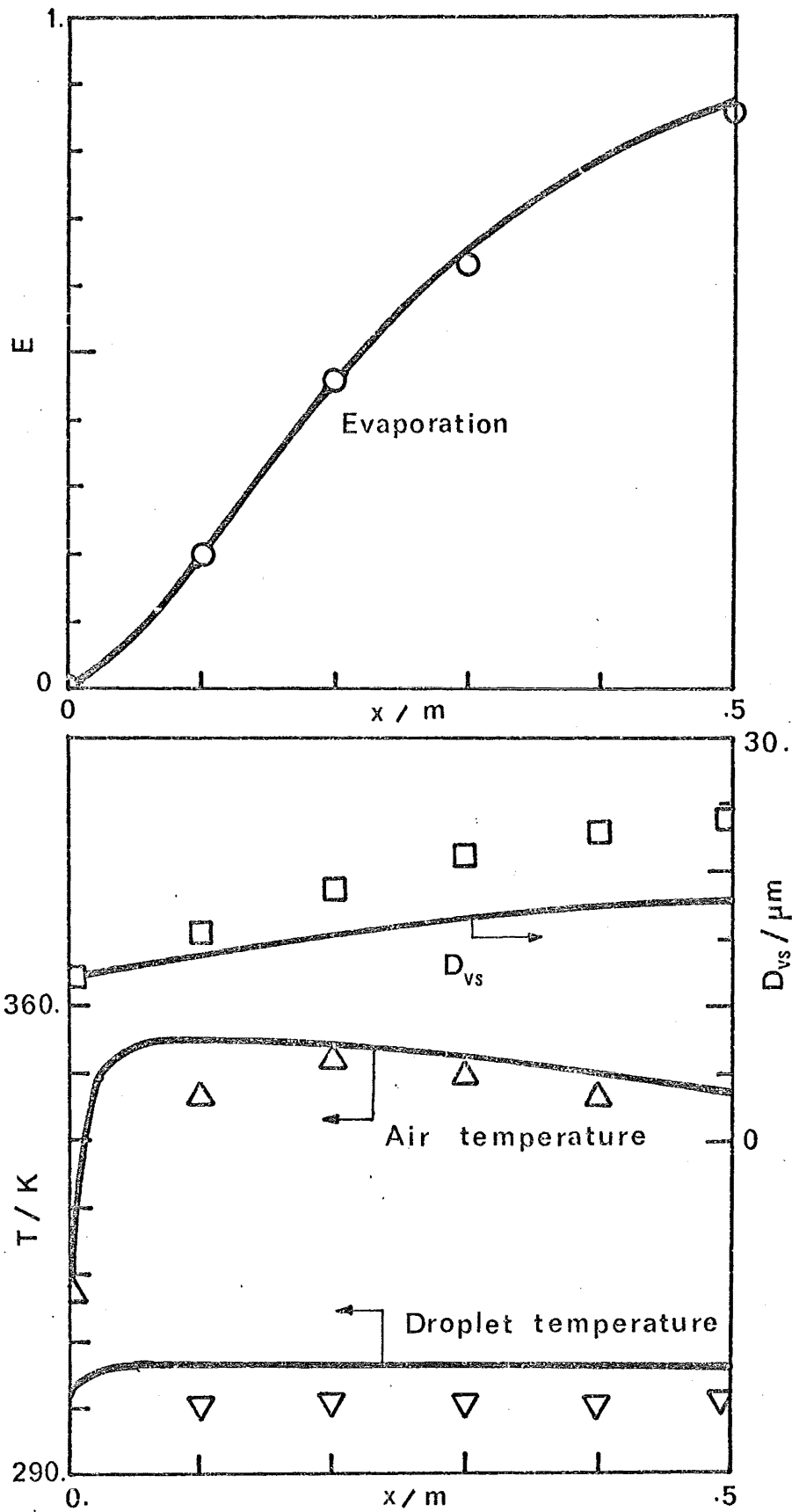


FIGURE 6.9: JET-ZONE EVAPORATION, WATER SPRAY

○ □ △ ▽ Data (M3)  
 — Calculation

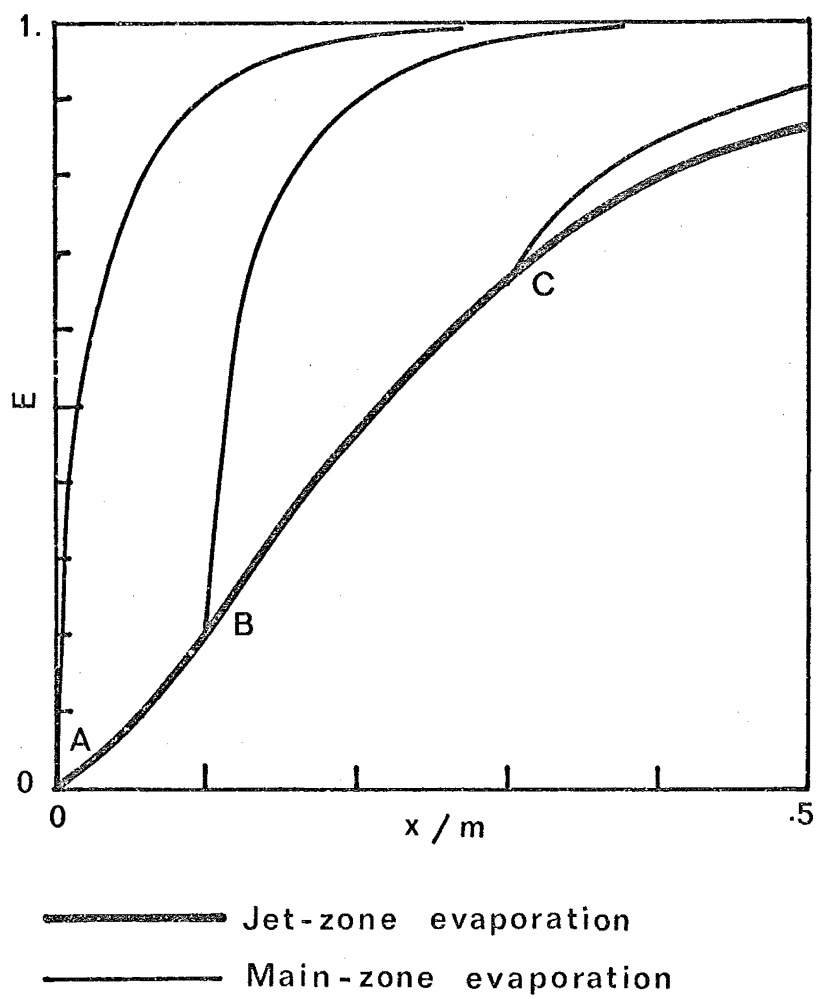


FIGURE 6.10: COMPARISON OF JET- & MAIN-ZONE EVAPORATION

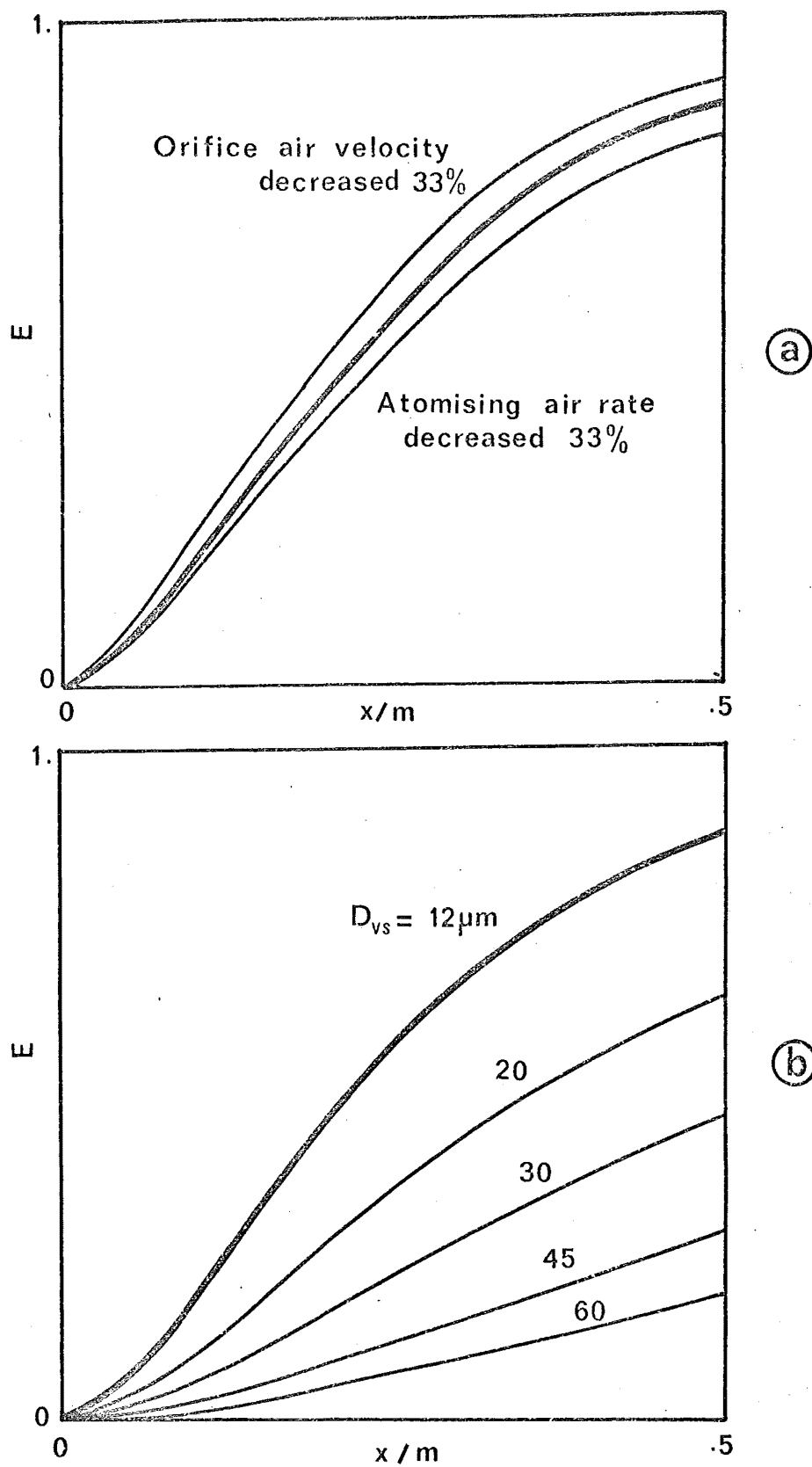


FIGURE 6.11 : EFFECT OF ATOMISING CONDITIONS ON JET-ZONE EVAPORATION

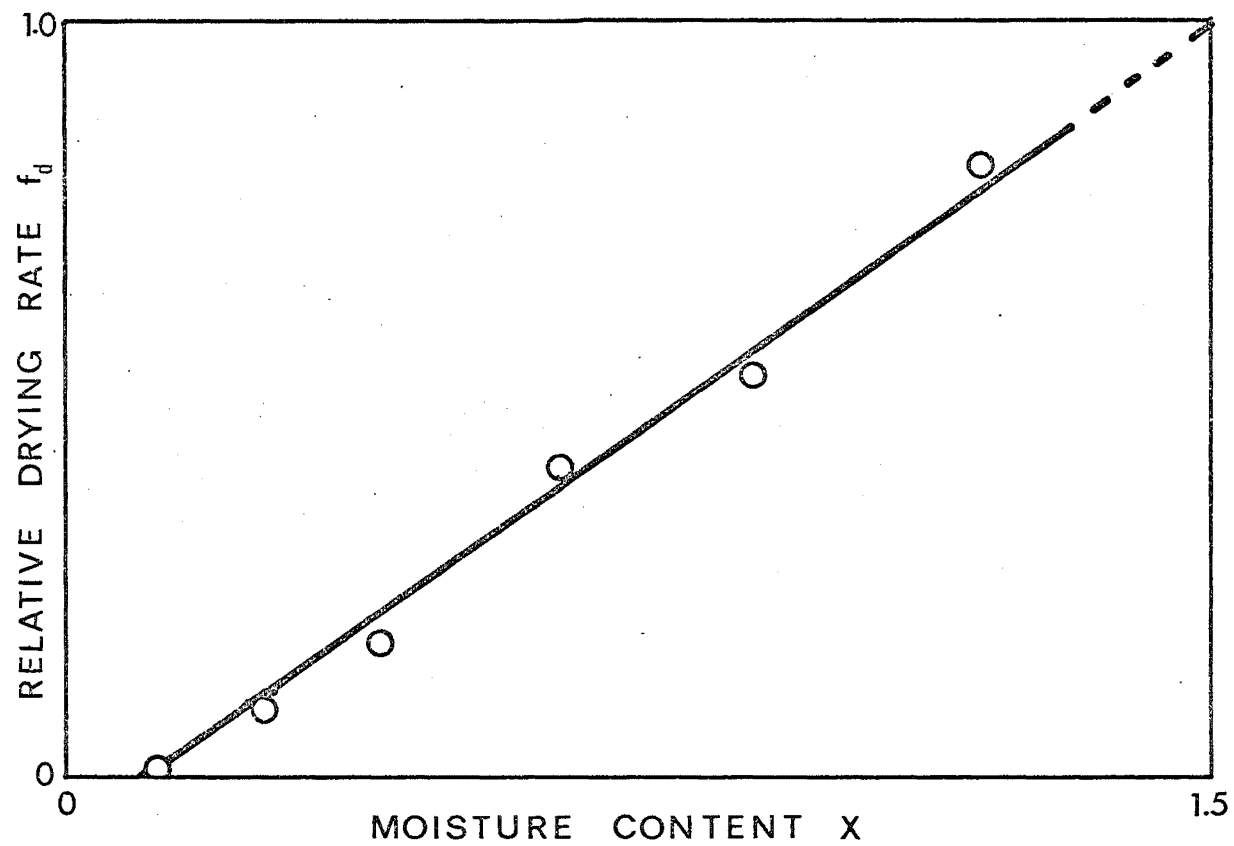
### II.3.2 Evaporation of a coarse spray of skim-milk in a predominantly main zone dryer.

#### II.3.2.1 Operating conditions

The data used in this calculation are based mainly on a skim-milk spray dryer studied by Hayashi<sup>(H5)</sup>, with the difference that his drying chamber is squat (length/diameter ratio = 1) and has nozzles on the wall, while this calculation will assume a purely cocurrent situation. Hayashi's dryer is 8 m tall. It was found that his droplet size distribution data can be fitted very well with the Nukiyama-Tasanawa equation<sup>80</sup>. Further properties of skim-milk and skim-milk powder were taken from Hall and Hendrick<sup>(H1)</sup>, King<sup>(K7, K8)</sup>, Webb and Johnson<sup>(W1)</sup> and Masters<sup>(M8)</sup>. All the quantities used are typical values in the dairy industry. The inputs are summarised in Table 3.

The drying curve of milk droplets was found from the supported drop data of Trommelen and Crosby<sup>(T7)</sup> who plotted drop surface temperature  $T_s$  and fractional evaporation  $E$  against time. From their data the relative drying rate (compared with unhindered evaporation),  $f_d$ , can be found by using equation 72. Trommelen and Crosby's results are re-plotted in figure 12 as a drying curve ( $f_d$  vs  $X$ ) in which  $X$  is the dry basis moisture content. The result is an almost linear falling rate curve starting from the moment drying begins, i.e. even before the crust forms. This conclusion is supported by the work of Campbell-Board<sup>(C1)</sup> who, in similar experiments with reconstituted condensed skim-milk, was unable to find a constant-rate period. A probable explanation for this surprising phenomenon is the early formation of a flexible membrane on the surface of the droplet, which hinders moisture transfer but does not prevent shrinking.





Data from ref. T7 for initial  $X = 1.5$

FIGURE 6.12 : DRYING CURVE FOR SUSPENDED DROP OF MILK

TABLE 6.3

Input conditions for sample calculation 2  
(spray of skim milk)

Air flow pattern: cocurrent, with jet zone from 0 - .5 m,  
transition with linear gradients from .5 - 1 m,  
main zone 1 - 10 m.

Nozzle type: pressure nozzle  
Orifice radius =  $4 \times 10^{-4}$  m

Nozzle operating conditions: Jet half-angle = 38 deg.  
Feed rate = 0.02 kg/s  
Feed temperature = 350 K.

Feed properties:

Solid mass fraction = 0.50  
Solid density =  $1590 \text{ kg/m}^3$   
Liquid density =  $1000 \text{ kg/m}^3$   
Latent heat of vaporisation =  $2.46 \times 10^6 \text{ J/kg}$   
Feed specific heat =  $3950 \text{ J/kg K}$   
Liquid mass fraction at solidification = 0.178  
Drying curve = linear throughout evaporation  
Lowering of vapour pressure due to solutes: negligible  
according to Raoult's law

Drying air flow:

Flow rate = 0.6 kg/s  
Inlet velocity = 2.4 m/s  
Inlet temperature = 400 K  
Inlet humidity = 0.005 kg/kg  
Mean turbulent velocity (assumed) = 0.02 m/s  
Mean Lagrangian scale of turbulence (assumed) = 0.001 s

Radiation parameter:

Tower diameter = 2 m  
Projected particle area/unit volume =  $0.3 \text{ m}^2/\text{m}^3$   
Particle absorptivity = 1  
Stainless steel wall emissivity = .85  
Mean wall radiating temperature = 370 K.

Spray size distribution:

Nukiyama-Tasanawa distribution with parameters  
 $\delta = 0.5$   
 $\bar{D}_{vs} = 105 \text{ } \mu\text{m}$

### II.3.2.2 Results and discussion

The fraction unevaporated  $F = 1-E$  is plotted against distance in figure 13.

#### (a) Comparison with available data:

The calculation gives at 8 m a product unbound moisture content of 1.7%. To this must be added the hygroscopic moisture about 1% at this temperature and humidity <sup>(H1)</sup>, hence the total product moisture is 2.7% which is in reasonable agreement with Hayashi's value of 3.1% for his 8 m chamber.

The outlet air temperature is 362 K which is also in the recommended range (Hayashi's value is 364 K).

However, the calculation assumed a uniform amount of shrinking for all droplet sizes, hence  $\bar{D}_{vs}$  is larger for the feed than for the product:

$$\bar{D}_{vs} \text{ (feed)} = 105 \text{ } \mu\text{m}$$

$$\bar{D}_{vs} \text{ (product)} = 84 \text{ } \mu\text{m}$$

Literature data give the same value of  $\bar{D}_{vs}$  for feed and product, indicating that some puffing has taken place, probably in the lower size range since the specific evaporation in these sizes is most rapid. If that is true, then the overall accuracy of the calculation will not be affected, as will be shown later.

#### (b) Shape of the F-curve and influence of the drying curve of single droplets:

Again it can be seen that the jet zone severely restricts evaporation. From about 5 m the  $(\ln F)$  curve becomes linear with  $x$ . The reason is that all droplets are now almost completely evaporated except the largest ones, which comprise about 30% of the total mass and a much smaller percentage of the total number (table 5). These lie in a fairly narrow size range, have consolidated and fall with constant velocity.

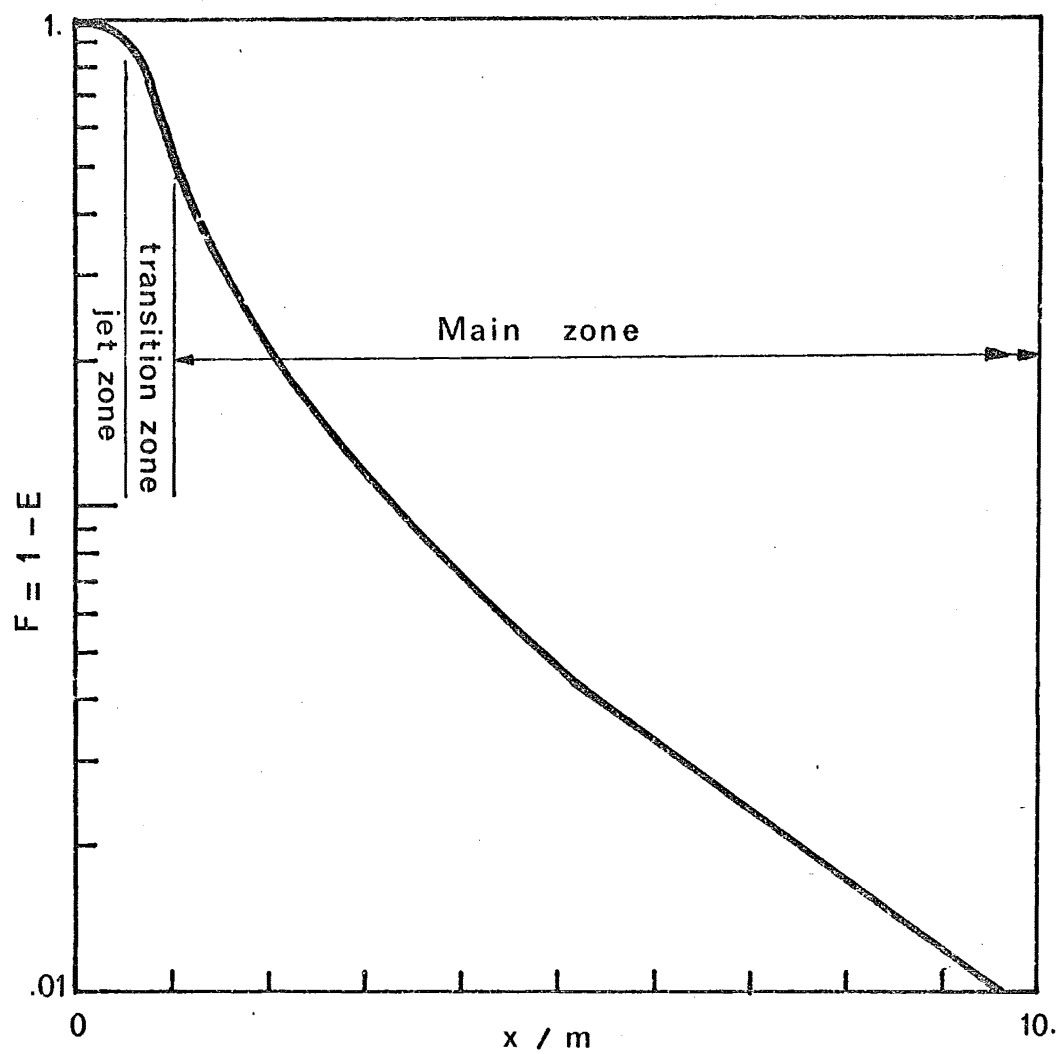


FIGURE 6.13: EVAPORATION CALCULATION  
FOR SKIMMILK

The linearity of the  $\ln F$  vs  $x$  graph is due to our earlier assumption of a linear falling rate, which makes the evaporation process a first-order reaction, provided the diameters are constant (equation 4). Thus the importance of getting an accurate single-droplet drying curve is emphasized.

(c) Importance of the maximum droplet size

The largest droplets are the governing factor in the design and performance of spray dryers. In one calculation in this work, the finest size ranges, up to 130  $\mu\text{m}$  and making up 50% of the spray original mass, are assumed to evaporate completely upon entering the main zone. The drying curves of the larger sizes were found to be almost unaffected by this and, as a result, from the 4 m level downwards the total evaporation curve is almost the same as for a "correct" calculation (Table 4).

TABLE 4

Effect of small droplet evaporation on large droplet behaviour

Initial sizes / $\mu\text{m}$	Fractional evaporation at 4 m	
	Correct calculation	Finer ranges immediately evaporated
0 - 130	1.000	1.000
150 - 170	.959	.957
190 - 210	.843	.838
230 - 250	.713	.708
270 - 290	.598	.594

This suggests that if one wants to avoid a tedious size-by-size calculation, one can simply consider the largest drop size and ignore the rest, an approach followed by Gluckert<sup>(G9)</sup>, Gauvin and Katta<sup>(G6,K1)</sup> and others. However such an approach is justified only if we want a fully dried product. For incompletely dried products the droplets below the maximum size will still have some importance (Table 5).

(d) Sensitivity analysis

The calculation of the milk spray was repeated with variations in each of the main parameters. The effect of turbulence is found to be negligible in this particular case. This is not surprising since the main air velocity is low, and the particles being rather large have high settling velocities (up to .9 m/s), hence  $Re$ ,  $c_D$  and  $Nu$  are little affected by the turbulent relative velocity.

The effect of radiation is also negligible, the reason being that, in milk spray drying, fairly low temperatures are involved.

The strongest influences are those of the drying air rate and inlet air temperature, and the solid content of the feed. These and other effects are plotted in figure 14. It must be kept in mind that the altering of any one operating condition will result in the change of several variables, the effects of which must be added together. For example, if the air temperature is increased, air velocity, wall temperature, heat loss ... will also be changed.

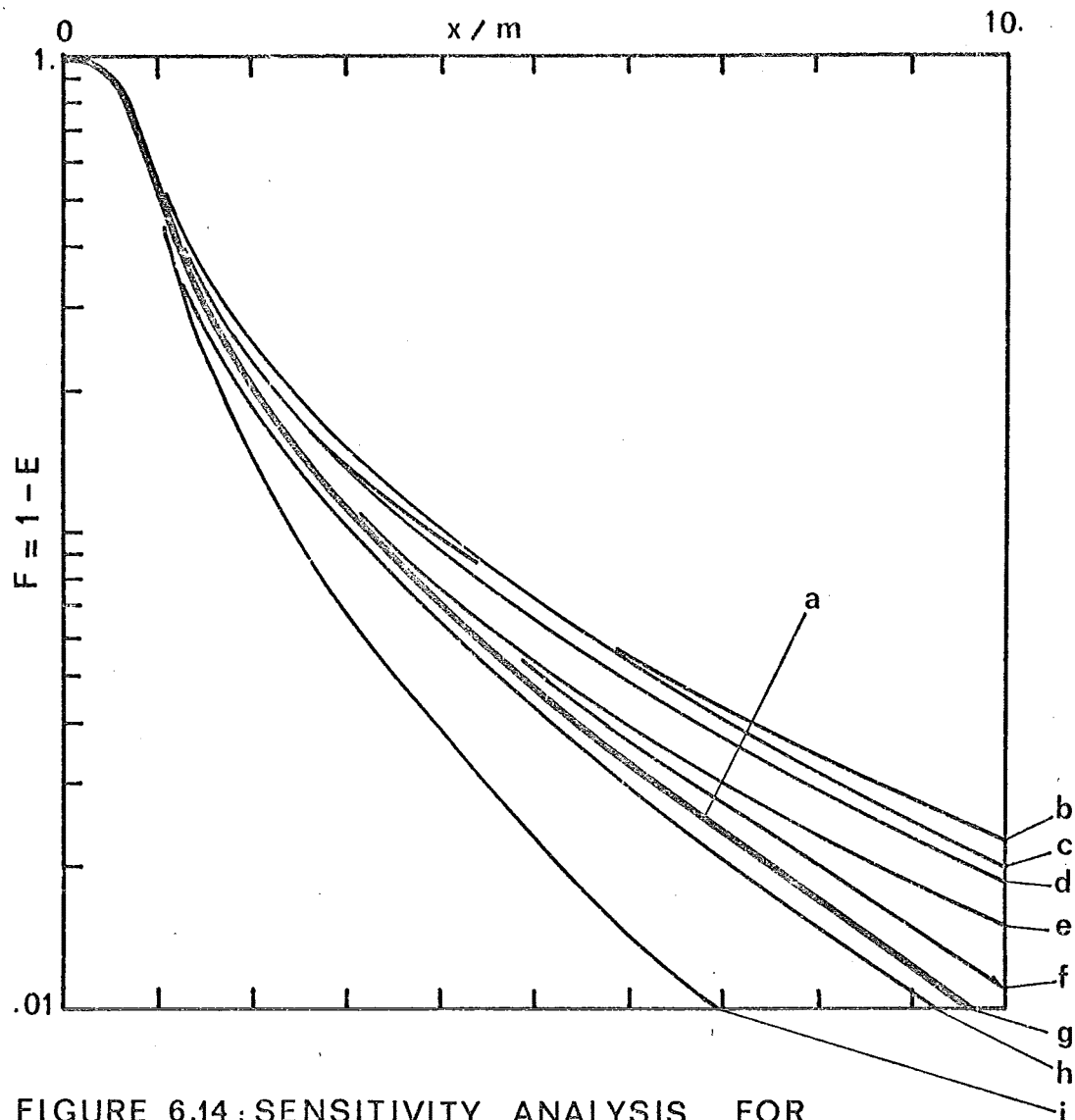


FIGURE 6.14: SENSITIVITY ANALYSIS FOR SKIMMILK EVAPORATION

- (a) Original operating conditions.
- (b) Air flow rate decreased 15%
- (c) Sauter diameter increased 15%
- (d) Solid mass fraction decreased 20%
- (e) 2 K/m air temperature gradient caused by heat loss
- (f) Feed temperature decreased by 40 K
- (g) Turbulence neglected. Also radiation neglected. Also, feed ejection velocity increased 50%.
- (h) Inlet air velocity decreased 15%
- (i) Inlet air temperature increased by 30 K.

### III. INFLUENCE OF RESIDENCE TIME DISTRIBUTION ON EVAPORATION

Most calculation methods, including the simulation in the previous sections, assume a perfectly cocurrent or countercurrent air-spray system. In real spray dryers, deviations from plug-flow for each phase will tend to modify the performance, often in a disfavoured direction.

#### III.1 Influence of air residence time distribution

Using the residence time distribution (R.T.D.) data of the air, one can model the flow pattern in the drying chamber, and hence get a realistic picture of the temperature, velocity and humidity profiles. For example, if the RTD data point to the existence of a well-mixed (stirred tank) zone in the dryer, then the profiles of the air conditions in this zone must be assumed to be uniform instead of varying steadily as in the case of perfect plug flow.

Obviously this cannot be done in a first calculation, as the extent of evaporation and its influence on the air are not yet known. Thus a suggested procedure is:

- (1) Calculate the evaporation based on perfect plug-flow for each phase.
- (2) Modify the air condition profiles according to the evaporation calculated and the actual flow pattern.
- (3) Recalculate the evaporation.
- (4) Repeat steps 2 and 3 if necessary.

Apart from the effect on evaporation, an equally serious consequence of air deviations from plug-flow, especially in cocurrent dryers, is that backmixing may bring hot air into contact with dry particles to damage the product if it is heat sensitive. If sufficiently



accurate information on the drying curve of the material is available, this effect can be studied by calculating the droplet or particle temperature at each point. However, random fluctuations in real systems may make this impossible.

It must also be noted that a model based on RTD data only is not guaranteed to be exact. Its validity will depend on how much is known of the geometry and general behaviour of the system, and it is always desirable to back up the results with other data, such as visualisation or velocity measurements (Chapter 3).

### III.2 Influence of spray R.T.D.

#### III.2.1 General approach

Dispersed-phase R.T.D. data are difficult to obtain and very little work has been done in this field. But theoretically it is easy to predict its influence on evaporation. This is because the dispersed phase is a macromixed system (Chapter 2), that is, its droplets or particles do not remerge and resplit during their travel through the chamber, but remain separate entities. Whereas with micromixed systems the performance depends on the actual flow pattern and the same RTD can give rise to quite different yields (except for first order reactions), the conversion of a macrofluid depends on the RTD only<sup>(L6)</sup>:

$$F_L = \int_0^{\infty} \left( \frac{c_A(t)}{c_{Ao}} \right)_{\text{plug}} C(t) dt = \int_0^{\infty} F(t) C(t) dt \quad (6.88)$$

where  $F_L$  is the fraction unconverted at the outlet,  $C(t)$  the RTD or impulse-response curve, and  $F(t) = \left[ \frac{c_A(t)}{c_{Ao}} \right]_{\text{plug}}$  is the fraction unconverted as a function of residence time in a plug flow (or batch) reactor, which can be calculated readily.

In a spray system the situation is further complicated by the fact that different droplet sizes have different R.T.D.s. Thus, in a rigorous calculation, the fraction unconverted  $f_j$  of each size range must be found separately, then added:

$$F_L = \sum_{j=1}^N \int_0^{\infty} f_j(t) C_j(t) dt = \int_0^{\infty} \int_0^{\infty} f_j(D_{po}, t) C(D_{po}, t) dt dD_{po} \quad (6.89)$$

where the index  $j=1,2,\dots,N$  refers to the  $j$ -th size range. Both  $f_j$  and  $C$  now are functions of initial size as well as of time.

This general equation can be tedious to apply, but in general the smaller droplet sizes can be ignored as they are completely evaporated long before approaching the outlet, as has been shown earlier.

### III.2.2 Geometrically similar R.T.D. curves for all sizes

An interesting case is when the R.T.D. curves of all sizes are similar in shape and have the same amount of relative dispersion, that is, when the ratio of the second moment  $\sigma_t$  and the first moment  $\bar{t}(D_{po})$  are the same:

$$\left[ \frac{\sigma_t}{\bar{t}(D_{po})} \right]_j = \text{constant for all sizes} \quad (6.90)$$

or

$$C_j(D_{po}, \frac{t}{\bar{t}(D_{po})}) = C_j(D_{po}, \theta) = C(\theta), \quad (6.91)$$

all sizes.

For example, all sizes may display dispersed plug-flow behaviour with the same Peclet number.

Equation 89 then can be written as:

$$F_L = \int_0^\infty \left\{ \int_0^\infty f_j(D_{po}, \bar{t}(D_{po}) \cdot \theta) dD_{po} \right\} C(\theta) d\theta \quad (6.92)$$

where  $\theta = t/\bar{t}(D_{po})$  and  $\bar{t}(D_{po})$  is the mean residence time of particles with initial diameter  $D_{po}$ .

Further assuming that the mean velocity  $\bar{u}_p(D_{po})$  of each size is constant through the length  $L$  of the dryer,

i.e.

$$\bar{u}_p(D_{po}) = \frac{L}{\bar{t}(D_{po})} \quad (6.93)$$

then

$$\theta = \frac{t}{\bar{t}(D_{po})} = \frac{t \bar{u}_p(D_{po})}{L} = \frac{x}{L} \quad (6.94)$$

i.e.  $\theta$  in equation 92 is both the relative residence time and the relative distance moved through the dryer. The usefulness of this result is that  $f_j(\theta)$  can now be readily calculated with a simulation.

Equation 92 becomes:

$$F_L = \int_0^\infty \left[ \int_0^\infty f_j(D_{po}, \frac{x}{L}) dD_{po} \right] C(\theta) d\theta \quad (6.95)$$

The term in brackets is simply the conversion of the spray as a whole at the relative position  $x/L$ , which is  $F(x/L)$ .

Hence

$$F_L = \int_0^\infty F(\theta) C(\theta) d\theta \quad (6.96)$$

where  $\theta = x/L$  for  $F$

$= t/\bar{t}$  for  $C$

Equation 96 is similar in form to equation 88 except for the independent variable. In this equation no integration over droplet sizes is necessary.  $F(\theta) = F(x/L)$  is assumed to have been calculated in a simulation or other computation, and  $C(\theta) = C(t/\bar{t})$  is the impulse response curve or RTD curve for any particular size (equation 91).

### III.2.3 First-order reaction assumption

If the evaporation process can be assumed to be of first order,  
i.e.

$$-\frac{dF}{dx} = k_1'' F \quad (6.97)$$

or

$$-\frac{dF}{d\theta} = k_1' F \quad (6.98)$$

then

$$F = F_e \exp(-k_1' \theta) \quad (6.99)$$

and the right-hand side of equation 96 is simply the product of  $F_e$  and the transfer function of the spray. In these equations,  $k_1''$  and  $k_1'$  have been defined as the specific rate of evaporation with respect to distance rather than time, because when there is relative motion between particles no common time base can be found. Also, in the simulation program,  $F$  is calculated as a function of distance.

The first-order reaction assumption can be used in two important cases:

(a) The constant mean-evaporative-diameter case:

This case has been extensively examined in section II.1.2 and no more will be said here.

(b) The linear drying rate case:

The first-order reaction approximation will hold if the following conditions are fulfilled:

- (1) The particles are falling at constant velocity;
- (2) They have consolidated and stopped shrinking;
- (3) They have entered a region in the drying curve where the relative drying rate varies linearly with the moisture content, i.e.

$$-\frac{dF}{dt} = k_1 F \quad (6.100)$$

- (4) Evaporation is confined to a narrow size range.

Then it can easily be seen that equations 97, 98 will hold. Although the conditions quoted seem restrictive, they probably often occur in practice, as can be seen from the sample calculation on a milk spray (figures 12, 13, 16 and Table 5).

#### III.2.4 Extended first-order reaction method

By assuming a first-order reaction, we replaced the exact equation 96

$$F_L = \int_0^{\infty} F(\theta) C(\theta) d\theta$$

by the equation

$$F_L = \int_0^{\infty} F_e \exp(-k'_1 \theta) \cdot C(\theta) d\theta \quad (6.101)$$

so that the error involved is

$$\Delta F_L = \int_0^{\infty} [F(\theta) - F_e \exp(-k'_1 \theta)] C(\theta) d\theta \quad (6.102)$$

Usually  $F_e$  and  $k'_1$  are taken to fit the evaporation curve  $F(\theta)$  towards the outlet of the dryer ( $\theta \rightarrow 1$ ), where  $C(\theta)$  is large. Hopefully the term in brackets in equation 102 is important only at low  $\theta$ , when  $C(\theta)$  in turn becomes small, and thus the error will be small.

When this is not the case, as when  $C(\theta)$  has a large dispersion and remains high for small  $\theta$ , then the accuracy of the calculation can be improved by writing:

$$F(\theta) = F_1 \exp(-k'_1 \theta) + F_2 \exp(-k'_2 \theta) + \dots \quad (6.103)$$

where  $F_i$  and  $k'_i$ ,  $i = 1$  to  $N$ , are chosen to give the best fit, especially near  $\theta = 1$ .

Then equation 101 can be extended to:

$$F_L = \sum_{i=1}^N F_i \int_0^{\infty} \exp(-k'_i \theta) C(\theta) d\theta \quad (6.104)$$

which is a weighted sum of transfer functions.

Equation 103 may in fact come up quite often in cocurrent spray drying, one of the terms being due to the mean evaporative diameter remaining approximately constant, and another term being due to the linearity of the final period drying curve (the two cases examined in the last section). The former would be dominant in the early period of drying, while the latter would be dominant in the final period.

For example, the  $F(\theta)$  curve for the sample calculation for skim-milk can be very accurately represented in the main zone by:

$$F(\theta) = 0.36 \exp[-1.31(x-1)] + 0.17 \exp[-.33(x-1)] \quad (6.105)$$

as evidenced by figure 15. Note that in this case the constant M.E.D. assumption does not depend on the assumption of zero relative velocity between the particles, provided the evaporation rate is based on distance rather than time.

### III.2.5 Sample calculation of R.T.D. effect

As an example we shall take the spray of milk studied earlier. Data for the calculations are summarised in Table 5 and figure 16, where apart from the R.T.D. characteristics all the information has been obtained from the computer simulation. Equation 105 (figure 15) must also be noted.

From Table 5 it can be seen that evaporation is controlled by size ranges 10 to 14 ( $D_p = 200-300 \mu\text{m}$ ), which display similar RTD curves (axially dispersed plug flow with a Peclet number of 36), and have a roughly constant velocity in the whole of the dryer main zone (figure 16a). Hence the conditions for equation 96 have been fulfilled.

From figure 16 the particle residence times in the jet and transition zones are very low, so that only the main zone needs to be considered. In equation 96 and subsequent equations we shall take

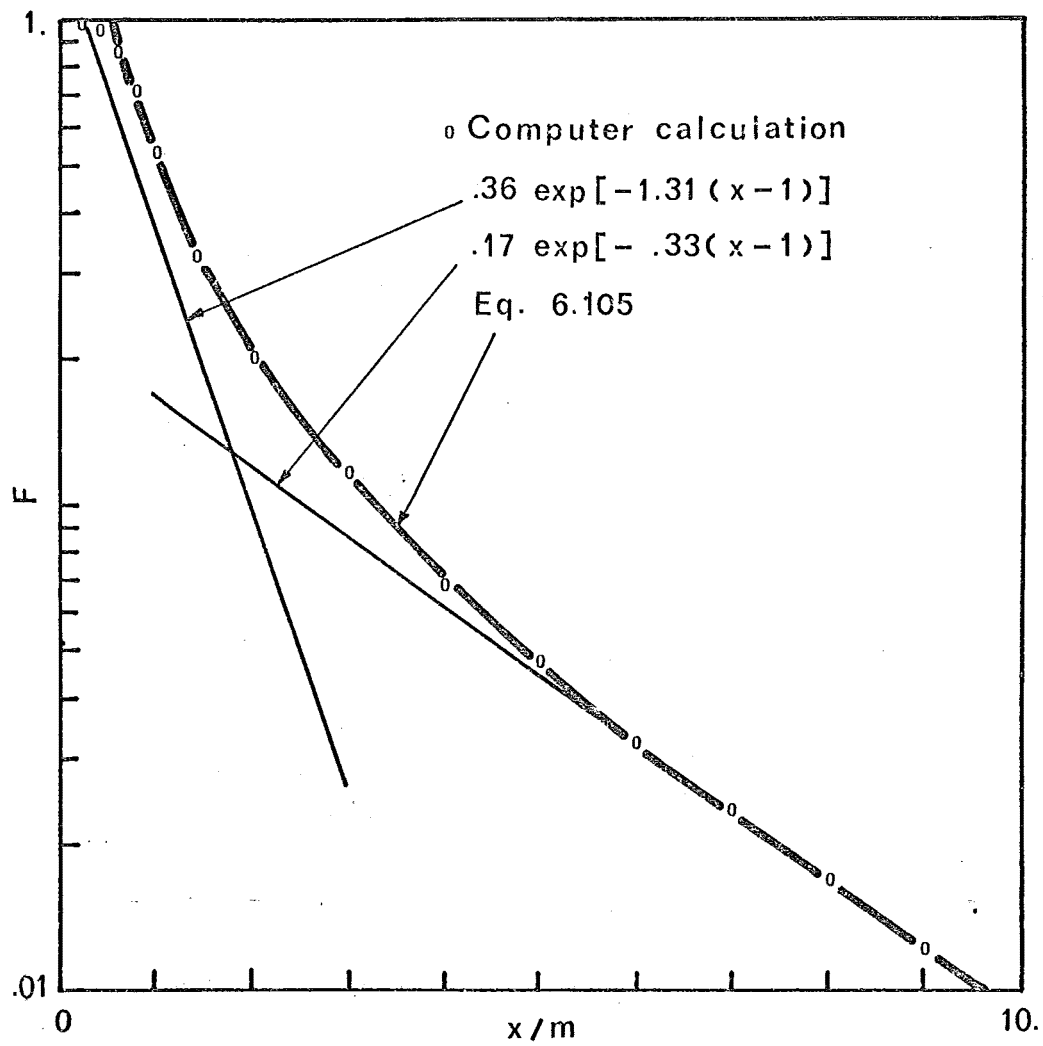


FIGURE 6.15: EVAPORATION OF SKIMMILK SPRAY  
AS A SUM OF FIRST-ORDER REACTIONS

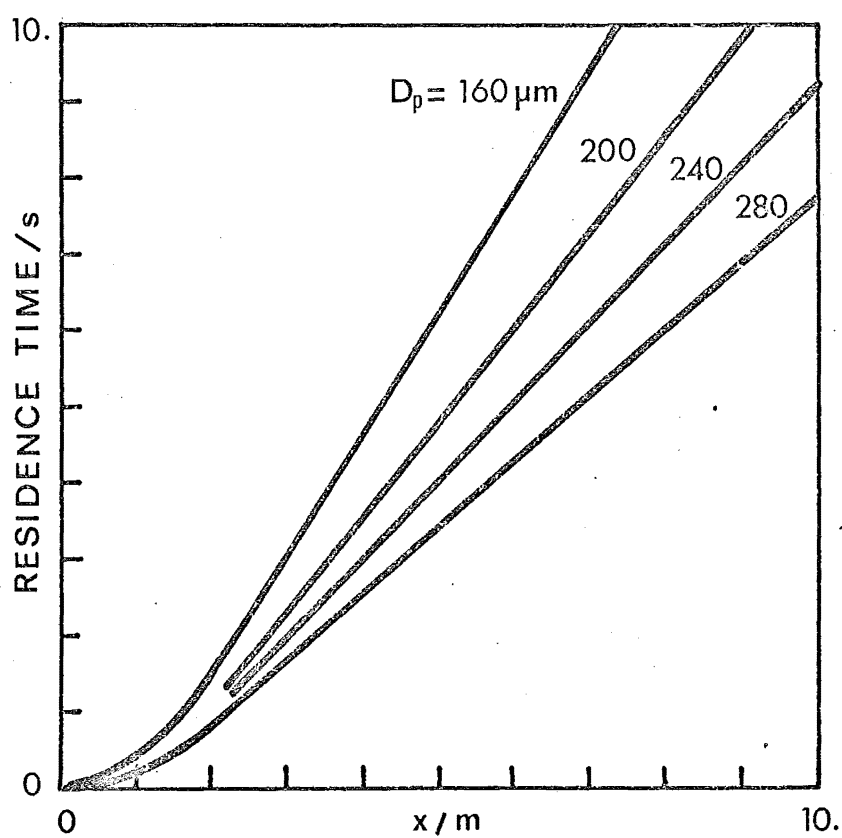
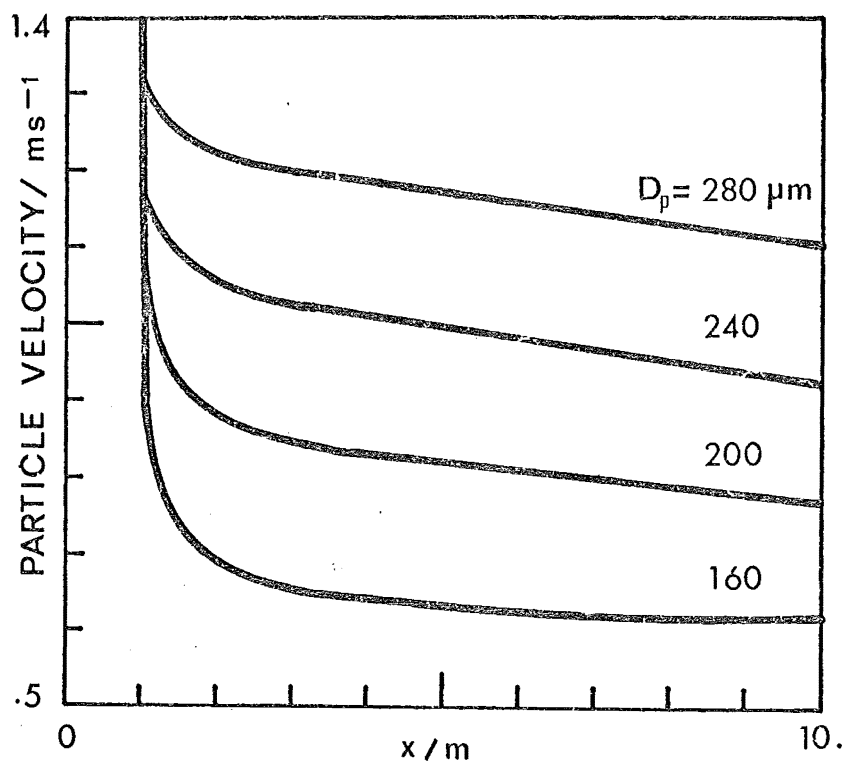


FIGURE 6.16: PARTICLE VELOCITY & RESIDENCE TIME  
IN SAMPLE CALCULATION



TABLE 6.5

Input conditions for calculation of effect of spray R.T.D.  
on evaporation of milk

Dryer length: 8 m

Fraction unevaporated at outlet for pure plug-flow: 0.0170

Length of jet zone: 1 m

Spray R.T.D.: Axially dispersed plug-flow for each size group,  
 with Peclet numbers given below.

Size group no.	Diameter $\mu\text{m}$	Initial mass fraction of total spray $V_j$	Fraction unevaporated $f_j$	$V_j f_j$	Pe
1 - 7	0 - 150	.6083	0	0	-
8	150-170	.0930	0	0	-
9	170-190	.0783	.0016	$1.3 \times 10^{-4}$	36
10	190-210	.0647	.0077	$5.0 \times 10^{-4}$	36
11	210-230	.0526	.0215	$1.13 \times 10^{-3}$	36
12	230-250	.0421	.0446	$3.19 \times 10^{-3}$	36
13	250-270	.0337	.0757	$2.55 \times 10^{-3}$	36
14	270-290	.0268	.1127	$3.02 \times 10^{-3}$	36

$\theta$  as the relative distance into the main zone:

$$\theta = \frac{x - L_j}{L_m}$$

where  $L_j = 1$  m is the length of the jet and transition zone, and  $L_m = 7$  m is the length of the main zone.

Because the velocities of the particles are fairly constant,  $\theta$  is also equal to  $t/\bar{t}(D_{po})$  for any size  $D_{po}$ , and the impulse response curve in terms of  $\theta$  for any size is: (L5)

$$C(\theta) = \frac{1}{2} \sqrt{\frac{Pe}{\pi\theta}} \exp \left\{ -\frac{Pe(1-\theta)^2}{4\theta} \right\} \quad (6.106)$$

for which the transfer function is:

$$\mathcal{F}(s) = \exp \left[ \frac{Pe}{2} \left( 1 - \sqrt{1 + \frac{4sT}{Re}} \right) \right] \quad (6.107)$$

Substituting equations 106 and 107 into 104, we finally obtain for the fraction unevaporated  $F_L$ :

$$\begin{aligned} F_L &= .36 \exp \left[ \frac{Pe}{2} \left( 1 - \sqrt{1 + \frac{4 \times 9.2}{Pe}} \right) \right] \\ &\quad + .17 \exp \left[ \frac{Pe}{2} \left( 1 - \sqrt{1 + \frac{4 \times 2.3}{Pe}} \right) \right] \\ &= .0005 + .0192 \\ &= .0197 \end{aligned}$$

as compared with  $F_L = .0170$  for the perfect plug-flow case (figure 13).

#### IV. CONCLUSION

In this chapter it has been shown that, due to the great number of factors affecting the spray drying process, analytical methods are usually inadequate for predicting the performance of industrial spray

dryers. The suggested procedure is first to do a numerical (stepwise) calculation, assuming perfect plug-flow regime, then correct for residence-time-distribution effects. A computer program was written to carry out the first step for cocurrent systems, but accounting for residence-time-distribution effects is possible only in some cases.

The jet zone near the nozzle and the size of the largest droplets were shown to be important factors in limiting the performance of a dryer. But, above all, because in industrial situations one usually goes far into the falling rate period of the droplets, research into the drying curve of droplets of various materials seems to be of great importance before more accurate predictions can be made.

NOTATION FOR CHAPTER 6

- $A$  area,  $[m^2]$   
 $c$  concentration,  $[kg/m^3]$   
 $C(t)$  impulse response curve,  $[s^{-1}]$   
 $C(\theta)$  impulse response curve as function of dimensionless time,  $[-]$   
 $c_D$  drag coefficient of particle,  $[-]$   
 $c_p$  specific heat,  $[J/kg\ K]$   
 $D$  diameter,  $[m]$   
 $D_e$  mean evaporative or equivalent diameter,  $[m]$   
 $D_h$  hydraulic diameter of vessel =  $4 \times \text{volume/area}$ ,  $[m]$   
 $\bar{D}_{m,n}$  m-n mean diameter,  $[m]$   
 $D_{vs}$  3-2 or Sauter or surface-volume mean diameter,  $[m]$   
 $D_m$  maximum diameter,  $[m]$   
 $\mathcal{D}$  diffusion coefficient,  $[m^2/s]$   
 $\mathcal{D}_t$  turbulent dispersion coefficient,  $[m^2/s]$   
 $E$  fractional evaporation,  $[-]$   
 $F$  fraction unevaporated ( $=1-E$ ), or more generally fraction unreacted,  $[-]$   
 $f_c$  ratio of present to initial specific evaporation rate,  $[-]$   
 $f_d$  relative drying rate (compared to constant rate period),  $[-]$   
 $f_j$  fraction unevaporated or unreacted for a particular size group,  $[-]$   
 $\mathcal{F}(s)$  Transfer function,  $[-]$   
 $G$  gas flow rate,  $[kg/s]$   
 $g$  gravitational acceleration,  $[m/s^2]$   
 $g$  number size distribution =  $dn/dD_p$ ,  $[m^{-1}]$   
 $h$  heat transfer coefficient,  $[W/Km^2]$   
 $j$  liquid/gas density ratio =  $\rho_l/\rho_g$ ,  $[-]$

(Notation for Chapter 6, cont.)

$k_a$	air thermal conductivity, [ W/mK ]
$k_1$	specific (per unit remaining mass) rate of conversion (or evaporation) = reaction rate constant for first-order reactions, [ s <sup>-1</sup> ]
$k_1'$	first-order reaction rate constant or specific rate of conversion, in terms of dimensionless time or distance, [ - ]
$k_1''$	first order reaction rate constant or specific rate of conversion (or evaporation) in terms of distance = $k_1/\text{velocity}$ , [ m <sup>-1</sup> ]
$k_e$	extinction coefficient, or projected particle area per unit particle cloud volume, [ m <sup>-1</sup> ]
$L$	liquid or feed flow rate, [ kg/s ]
$L_b$	mean beam length, [ m ]
$n$	fraction of total number of particles under size $D_p$ , [ - ]
$p_w$	water vapour partial pressure in atmosphere.
$q$	heat transfer rate, [ W ]
$q_R$	heat transfer rate by radiation, [ W ]
$R_j$	jet radius, [ m ]
$R_s$	factor to account for feed overheat effect on evaporation, [ - ]
$r$	radial position, [ m ]
$r_o$	orifice radius, [ m ]
$\mathcal{R}$	rate of growth of droplet = $dd_p/dt$ , [ m/s ]
$s$	Laplace Transform parameter, [ s <sup>-1</sup> ]
$S$	shape or view factor in radiation, [ - ]
$T$	temperature, [ K ]
$T_s$	surface temperature, [ K ]
$T_s^*$	adiabatic saturation temperature, [ K ]
$t$	time, [ s ]
$\bar{t}$	mean residence time, [ s ]
$t_p$	particle time constant, [ s ]

## (Notation for Chapter 6, cont.)

$u$	velocity, [ m/s ]
$u_R$	relative velocity between particle and fluid, [ m/s ]
$u_o$	orifice velocity of air in pneumatic nozzles, of feed in pressure nozzle, [ m/s ]
$u_a'$	air turbulent velocity, [ m/s ]
$u_R'$	turbulent relative velocity, [ m/s ]
$V$	volume, [ m <sup>3</sup> ]
$v$	volume fraction of particles under a size $D_p$ , [ - ]
$w$	mass fraction, [ - ]
$X$	dry basis moisture content, [ - ]
$x$	distance from nozzle, [ m ]
$x_1, x_2, x_3$	lengths defined in figure 3, [ m ]
$y$	air humidity, dry basis, [ - ]
$y_s$	surface humidity, dry basis, [ - ]
$y_s^*$	adiabatic saturation humidity, dry basis, [ - ]
$\alpha$	jet half-angle, [ degree ]
$\delta$	dispersion index in size distributions, [ - ]
$\lambda$	latent heat of evaporation, [ J/kg ]
$\mu_z$	mean value of variable $z$ .
$\mu$	viscosity, [ N s/m <sup>2</sup> ]
$\nu$	kinematic viscosity [ m <sup>2</sup> /s ]
$\xi$	dimensionless radial position, [ - ]
$\pi$	3.14159 ...
$\Pi$	$c_D Re^2$ , [ - ]
$\rho$	density, [ kg/m <sup>3</sup> ]
$\sigma_z$	standard deviation of variable $z$ .
$\tau$	time parameter, [ s ]
$\theta$	dimensionless time or distance, [ - ]

(Notation for Chapter 6, cont.)

Dimensionless Groups:

$B = C_{pm} \Delta T / \lambda$  , Spalding number.

$N_1$  ,  $N_2$  ,  $N_3$  : as defined on page 214.

$Nu = h D_p / k_a$  , Nusselt number.

$Sh = k_c D_p / \mathcal{D}$  , Sherwood number.

$Pr = \nu_a G_a / k_a$  , Prandtl number.

$Sc = \nu / \mathcal{D}$  , Schmidt number.

$Pe = u L / \mathcal{D}_t$  , Peclet number.

Subscripts:

Superscripts:

a	air	*	equilibrium or saturation
c	cloud	*	dimensionless
e	equivalent, equilibrium		
f	fluid, feed		
g	gas		
i	in the i-th direction		
j	referring to size group j		
ℓ	liquid		
L	at end of chamber		
m	maximum, axis value (in a jet), mixture		
p	particle or droplet		
s	solid, surface		
t	terminal (velocity)		
w	wall		
o	initial (at $t = 0$ or at $x = 0$ )		
∞	at infinite distance, in surrounding		

### CONCLUSION

In the second part of this work (Chapters 2, 3, 4) the residence-time distribution approach using transfer-function analysis has been found to be a powerful way of investigating flow patterns, and thus of improving spray-dryer design and operation. The methods and results described may be of more general usefulness in the study of process equipment, especially those concerning the transfer-function analysis, the correlation of droplet entrainment, and mixing phenomena in a vessel with a sudden inlet expansion or with a secondary jet.

The evaporation prediction method described in the third part (Chapters 5 and 6) has been shown to be capable of great flexibility and accuracy. However, it also pointed out the necessity of obtaining more data on the evaporation of single droplets of the materials to be dried, and this would seem to be one of the most useful areas of research for some time to come.



# REFERENCES

- A. (A1) Abdul-Rahman Y.A.K., Crosby E.J., Bradley R.L., J.Dairy Sci. 54, 1111 (1971).
- (A2) Abrahamson J., (Department of Chemical Engineering, University of Canterbury) "Collision rate of small particles in a vigorously turbulent fluid", to be published.
- (A3) Abramovich G.N., "The Theory of Turbulent Jets", M.I.T.Press, Cambridge, Mass. (1963).
- (A4) Abramowitz M., Segun A., "Handbook of Mathematical Functions", Dover, N.Y. (1964).
- (A5) Ahmadzadeh J., Harker J.H., Trans.Inst.Ch.Eng. 52, 108 (1974).
- (A6) Aris R., Chem.Eng. 9, 266 (1959).
- (A7) Arrowsmith A., Foster P.J., Chem.Eng.J. 5, 243 (1973).
- B. (B1) Bailey J.E., Chem.Eng.Sci. 29, 767 (1974).
- (B2) Baldwin A.J., Symp. on Spray Dried Milk Powders, Palmerston North, Summary of Proceedings, New Zealand Dairy Research Institute, p.67 (1973).
- (B3) Barchilon M., Curtet R., Trans. A.S.M.E. 86, 777 (1964).
- (B4) Batchelor G.K., "The Theory of Homogeneous Turbulence", Cambridge University Press (1953).
- (B5) Baxter J.A., Fanning L.E., Swartz H.A., Int.J. Appl. Radiation & Isotope, 15, 415 (1964).
- (B6) Beard K.V., Pruppacher H.R., J. Atm.Sci. 26, 1066 (1969).
- (B7) Becker H.A., Hottel H.C., Williams G.C., 9th Symp. on Combustion Proc. Academic Press, p.7 (1963).
- (B8) Berger D., Pei D.C.T., Int.J. Heat Mass Tr. 16, 293 (1973).
- (B9) Bessant D.J., Lake G., unpublished (1975).
- (B10) Bird R.B., Stewart W.E., Lightfoot E.N., "Transport Phenomena", J. Wiley & Sons, N.Y. (1960).

- (B11) Bischoff K.B., Chem.Eng.Sci.12, 69 (1960).
- (B12) Bischoff K.B., Levenspiel O., Chem.Eng.Sci.17, 245 (1962).
- (B13) Bond W.N., Newton D.A., Phil.Mag. 4, 889 (1927); 5, 794 (1928).
- (B14) Borde I.I., Proc. 2nd All-Soviet Union Conference on Heat & Mass Transfer, Rand Report R-451-PR, Vol.5, 649 (1964).
- (B15) Bose A.K., Pei D.C., Can.J.Ch.E. 42, 259 (1962).
- (B16) Brauer H., "Stoff Austausch einschliesslich chemischer Reaktionen", Verlag Sauerländer, Aarau (1971).
- (B17) Brehaut W.J., "Evaporating Drops and Sprays in Turbulent Air Streams", Ph.D. Thesis, Chem. Engineering Dept., University of Canterbury, New Zealand (1969).
- (B18) Brehaut W.J., Keey R.B., Zdravotní Technika a Vzduchotechnika 16, no.2, 75 (1973).
- (B19) Briffa F.E.J., Dombrowski N., A.I. Ch.E.J. 12, 708 (1966).
- (B20) Buffham B.A., Kropholler H.W., Chem.Eng.Sci. 28, 1081 (1973).
- (B21) Burghart A., Lipowska L., Intern.Chem.Eng. 13, 227 (1973).

- C. (C1) Campbell-Board M., B.E. Project Report, Dept. of Chem.Eng., University of Canterbury, New Zealand (1975).
- (C2) Chan M., research report, Dept. of Chem. Eng., University of Canterbury, New Zealand (1971).
- (C3) Charlesworth D.H., Marshall W.R., A.I.Ch.E.J. 6, 9 (1960).
- (C4) Clements W.C., "Computer Programs for Chemical Engineering Education", vol.2, p.296 (1972).
- (C5) Clift R., Gauvin W.H., "Chemeca '70", part 1, 14 (1970).
- (C6) Clift R., Gauvin W.H., Can.J.Chem.Eng. 49, 439 (1971).
- (C7) Corrsin S., J. Atm.Sci. 20, 115 (1963).
- (C8) Curtet R., Combustion and Flame 2, 383 (1958).
- (C9) Curtet R., Ricou F.P., Trans. A.S.M.E. 86, 765 (1964).

- D. (D1) Dankwerts P.V., Chem.Eng.Sci. 2, 1 (1953).
- (D2) Dankwerts P.V., Chem.Eng.Sci. 8, 93 (1958).
- (D3) Davies J.T., "Turbulence Phenomena", Academic Press, N.Y. (1972).
- (D4) Davies W.D.T., "System Identification for self-adaptive control", Wiley Inter-Science, London (1970).
- (D5) Dickenson D.R., Marshall W.R., A.I. Ch.E.J. 14, 541 (1968).
- (D6) D.I.S.A. Elektronik A/S, "DISA Constant Temperature Anemometer Instruction Manual" (1966).
- (D7) Dlouhy J., Gauvin W.H., Can.J.Chem.Eng. 38, 113 (1960).
- (D8) Dlouhy, J., Gauvin W.H., A.I.Ch.E.J. 6, 29 (1960).
- (D9) Dolinsky A.A., Proc.2nd All-Soviet Union Conference on Heat & Mass Transfer, Rand Report R-451-PR, vol.5, 666 (1964).
- (D10) Dombrowski N., "Spray Drying", in "Biochemical and Biological Engineering Science", Blakeborough N. ed., vol.2, p.209, Academic Press, N.Y. (1968).
- (D11) Dombrowski N., Johns W.R., "Spray-drier design", Dept.of Chem.Eng., Imperial College, London.
- E. (E1) Eastop T.D., Smith C., Trans.Inst.Chem.Eng. 50, 26 (1972).
- (E2) Eisenklam P., Arunachalam S.A., Weston J.A., 11-th Internat.Symp. on Combustion, 715 (1967).
- (E3) Engineering Equipment Users' Association, "Pneumatic Handling of Powdered Materials", Constable & Co.Pub., London (1963).
- F. (F1) Feder A., Chem.Eng. 66, 159 (21/9/1959).
- (F2) Fraser R.P., Eisenklam P., Trans.Inst.Chem.Eng. 34, 294 (1956).
- (F3) Fraser R.P., Dombrowski N., John W.R., Brit.Chem.Eng. 8, 390 (1963).
- (F4) Frenkiel F.N., "Advances in Applied Mechanics", Vol.3, p.61, Academic Press, N.Y. (1953).
- (F5) Friedlander S.K., A.I.Ch.E.J. 3, 43 (1957).
- (F6) Friedlander S.K., A.I.Ch.E.J. 3, 381 (1957).

- (F7) Frössling N., Beitr. Geophys. 52, 170 (1938).
- (F8) Fuchs N.A., "Evaporation and Droplet Growth in Gaseous Media", Pergamon Press, N.Y. (1959).
- (F9) Fuchs N., "Mechanics of Aerosols", Pergamon Press, Oxford (1964).
- G. (G1) Gal G., Am.Inst.Aeronautic & Astronautic J. 8, 814 (1970).
- (G2) Galloway T.R., Sage B.H., Intern. J. Heat Mass Tr., 7, 1283 (1964).
- (G3) Galloway T.R., Sage B.H., A.I.Ch.E.J. 18, 287 (1972).
- (G4) Garner F.H., Suckling R.D., A.I.Ch.E.J. 4, 114 (1958).
- (G5) Garner F.H., Lane J.J., Trans.Inst.Chem.Eng. 37, 162 (1959).
- (G6) Gauvin W.H., Katta S., Knelman F.H. (McGill University), to be published.
- (G7) Gibert H., Angelino H., Can.J.Chem.Eng. 51, 319 (1973).
- (G8) Glassman I., Bonilla C.F., Chem.Eng.Prog. Symposium Series, vol.49, no.5 (1953).
- (G9) Gluckert F.A., A.I. Ch.E.J. 8, 460 (1962).
- H. (H1) Hall C.W., Hendrick T.I., "Drying of Milk and Milk Products", 2nd ed., Avi Pub.Co., Westport, Connecticut, U.S.A. (1971).
- (H2) Hamielec A.E., Johnson A.I., Can.J.Chem.Eng. 40, 41 (1962).
- (H3) Hamielec A.E., Hoffman T.W., Ross L.L., A.I.Ch.E.J. 13 (1967).
- (H4) Harris J.E., Friedman L., Anal.Biochem.30, 199 (1969).
- (H5) Hayashi H., "Studies on Spray Drying Mechanisms of Milk Powder", Snow Brand Milk Product (1962).
- (H6) Hedley A.B., Arrowsmith A., Foster P.J., Chemeca '70, part 6, p.51 (1970).
- (H7) Hegge Zignen B.G. van der, Appl. Sci.Res. 7A, 205 (1958).
- (H8) Hetsroni G., Haber S., Rheol.Acta 9, 488 (1970).
- (H9) Hilsenrath J., Touloukian Y.S., Trans.A.S.M.E. 76, 976 (1954).
- (H10) Hinze J.O., A.E.Ch.E.J. 1, 289 (1955).

- (H11) Himmelblau D.M., Bischoff K.B., "Process Analysis and Simulation, Deterministic Systems", J. Wiley & Sons, N.Y. (1968).
- (H12) Himmelblau D.M., "Process Analysis by Statistical Methods", J. Wiley & Sons, N.Y. (1970).
- (H13) Hinze J.O., "Turbulence", McGraw Hill, N.Y. (1959).
- (H14) Hoffmann T.W., Gauvin W.H., Can.J.Chem.Eng. 38, 129 (1960).
- (H15) Hoffmann T.W., Gauvin W.H., Can.J.Chem.Eng. 39, 179 (1961).
- (H16) Hoffmann T.W., Gauvin W.H., Can.J.Chem.Eng. 40, 110 (1962).
- (H17) Hoffmann T.W., Ross L.L., Intern.J.Heat Mass Tr., 15, 599 (1972).
- (H18) Hopkins M.J., Sheppard A.J., Eisenklam P., Chem.Eng.Sci. 24, 1131, (1969).
- (H19) Hopkins M.J., Eisenklam P., Chemeca '70, 91 (1970).
- (H20) Hottel H.C., Trans.A.I.Ch.E. 19, 173 (1927).
- (H21) Hottel H.C., Sarofim A.F., "Radiative Transfer", McGraw Hill, N.Y. (1967).
- (H22) Hsu N.T., Sato K., Sage B.H., Ind.Eng.Chem. 46, 870 (1954).
- (H23) Hughes R.R., Gilliland E.R., Chem.Eng. Prog. 48, 497 (1952).
- I. (I 1) Ingebo R.D., N.A.C.A.Tech.Note 2368 (1951).
- J. (J1) Jagota A.K., Rhodes E., Scott D.S., Can.J.Chem.Eng. 51, 393 (1973).
- (J2) Jenson V.G., Horton T.R., Wearing J.R., Trans.Inst.Chem.Eng. 46, T177 (1968).
- (J3) Johnstone H.F., Eads D.K., Ind.Eng.Chem. 42, 2293 (1950).
- K. (K1) Katta S., Gauvin W.H., A.I.Ch.E.J. 21, 143 (1975).
- (K2) Kawaguti M., Rept.Inst.Sci. Tokyo, 2, 66 (1948).
- (K3) Keey R.B., "Drying, Principles and Practice", Pergamon Press, Oxford (1972).
- (K4) Keey R.B., Suzuki M., Intern.J.Heat Mass Tr. 17, 1455 (1974).
- (K5) Keyes F.G., Trans. A.S.M.E. 73, 589 (1951).

- (K6) Kim K.Y., Marshall W.R., A.I.Ch.E.J. 17, 575 (1971).
- (K7) King N., Dairy Sci.Abstr. 27, 91 (1965).
- (K8) King N., Dairy Sci.Abstr. 28, 105 (1966).
- (K9) Kolář S., Zdravotní Technika a Vzduchotechnika 15, no.1, 7 (1972).
- (K10) Krambeck F.J., Katz S., Strumar R., Ind.Eng.Chem.Fund. 6, 276 (1967).
- (K11) Kreith F., "Principles of Heat Transfer", 2nd ed., International Textbook Co., London (1965).
- (K12) Kreyszig E., "Advanced Engineering Mathematics", 2nd ed., J.Wiley & Sons, N.Y. (1967).
- (K13) Kuboi R., Komasaawa I., Otake T., Chem.Eng.Sci. 29, 651 (1974).
- (K14) Kuboi, Komasaawa I., Otake T., Isawa M., Chem.Eng.Sci. 29, 659 (1974).
- L. (L1) Langmuir I., Phys.Rev. 12, 368 (1918).
- (L2) Lapple C.E., Shepherd C.B., Ind.Eng.Chem. 32, 605 (1940).
- (L3) Lavender W.J., Pei D.C.T., Internat. J. Heat Mass Tr. 10, 529 (1967).
- (L4) Leonchik B.I., Proc. 2nd All-Soviet Union Conference on Heat & Mass Transfer, Rand Report R-451-PR, vol.5, 656 (1964).
- (L5) Levenspiel O., Smith W.K., Chem.Eng.Sci. 6, 227 (1957).
- (L6) Levenspiel O., "Chemical Reaction Engineering", J. Wiley & Sons, N.Y. (1962).
- (L7) Levenspiel O., Bischoff K.B., "Advances in Chemical Engineering", vol.4, 95 (1963).
- (L8) Levins D.M., Glastonbury J.R., Trans.Inst.Chem.Eng. 50, 32, 132 (1972).
- (L9) Lilly G.P., Ind. Eng.Chem.Fund. 12, 268 (1973).
- (L10) Luikov M.V., "Szuska Raszpileniyem", Moszkva, Pischepromizdat (1955).
- M. (M1) Maisel D.S., Sherwood T.R., Chem.Eng.Prog. 46, 131 (1950).
- (M2) Maisel D.S., Sherwood T.R., Chem.Eng.Prog. 46, 172 (1950).
- (M3) Manning W.P., Gauvin W.H., A.I.Ch.E.J. 6, 184 (1960).
- (M4) Marone I.Ya., Theoretical Foundations of Chem.Eng. 5, English transl. p.546 (1971).

- (M5) Marshall W.R., "Atomisation and Spray Drying", Chem.Eng.Prog. Monograph Series, vol.50, no.2 (1954).
- (M6) Marshall W.R., Trans.A.S.M.E. 77, 1377 (1955).
- (M7) Masters K., Ind.Eng.Chem. 60, no.10, 53 (1968).
- (M8) Masters K., "Spray Drying", Leonard Hill, London (1972).
- (M9) May K.R., J.Scientific Instruments 22, 187 (1945).
- (M10) McIllvried H.G., Massoth F.E., Ind. Eng.Chem.Fund. 12, 225 (1975).
- (M11) McQuaid J., Wright W., Internat.J.Heat Mass Tr. 17, 341 (1974).
- (M12) Michelsen M.L., Østergaard K., Chem.Eng.J. 1, 37 (1970).
- (M13) Michelsen M.L., Østergaard K., Chem.Eng.Sci. 25, 583 (1970).
- (M14) Miesse C.C., Jet Propulsion 24, p.237 (1954).
- (M15) Moeller W.G., Dealy J.M., Can.J.Chem.Eng. 48, 356 (1970).
- (M16) Mugele R.A., Evans H.D., Ind.Eng.Chem. 43, 1317 (1951).
- (M17) Mugele R.A., A.I.Ch.E.J. 6, 3 (1960).
- N. (N1) Nukiyama S., Tasanawa Y., Trans.Soc.Mech.Eng. Japan, 5, no.18, 63 (1938).
- O. (O 1) Østergaard K., Michelsen M.L., Can.J.Chem.Eng. 47, 107 (1969).
- (O2) Oseen C.W., Arkiv.Mat.Astron.Fysik 6 no.29 (1911); 7 no.1 (1911); 9 no.16 (1913).
- P. (P1) Parimi K., Harris T.R., Can.J.Chem.Eng. 53, 175 (1975).
- (P2) Paris J.R., Ross P.N., Dastur S.P., Morris R.L., Ind.Eng.Chem.Process Design & Development 10, no.2, 157 (1971).
- (P3) Parti M., Paláncz B., Chem.Eng.Sci. 29, 355 (1974).
- (P4) Pasternak I.S., Gauvin W.H., Can.J.Chem.Eng. 38, 35 (1960).
- (P5) Patterson M.S., Greene R.C., Anal.Chem. 37, 854 (1965).
- (P6) Perry J.H. ed., "Chemical Engineers' Handbook", 4th edn., McGraw Hill N.Y. (1963).
- (P7) Pigford R.L., Pyle C., Ind.Eng.Chem. 43, 1649 (1951).

- (P8) Pisecky J., The World Galaxy no.5 (Nov.1974).
- (P9) Place G., Ridgway K., Danckwerts P.P., Trans.Inst.Chem.Eng.37, 268 (1959).
- (P.10) Price W.J., "Nuclear Radiation Detection", 2nd ed. McGraw Hill, N.Y. (1964).
- (P11) Price L.W., Laboratory Practice (1973), pp.27,110,181,277,352,417, 480,571 (1973).
- (P12) Pritchard C.L., Biswas S.K., Brit.Chem.Eng. 12, 879 (1967).
- (P13) Probert R.P., Phil.Mag. 37, 94 (1946).
- R (R1) Radiochemical Centre, Amersham, "The Radiochemical Manual", 2nd edn. (1966).
- (R2) Radiochemical Centre, Amersham, "Sample preparation for liquid scintillation counting", review no.6 (1971).
- (R3) Raithby G.D., Eckert E.R., Internat. J. Heat Mass Tr. 11, 1233 (1968).
- (R4) Ranz W.E., Marshall W.R., Chem.Eng.Prog. 48, 141 and 173 (1952).
- (R5) Ranz W.E., Trans.A.S.M.E. 78, 909 (1956).
- (R6) Reid R.C., Sherwood T.K., "The Properties of gases and liquids", 2nd edn., McGraw Hill, N.Y. (1966).
- (R7) Rietema K., Chem.Eng.Sci. 8, 103 (1956).
- (R8) Robertson G.J., B.E. Project Report, Dept. of Chem.Eng., University of Canterbury, New Zealand (1967).
- (R9) Rosenbrock H.H., Storey C., "Computational Techniques for Chemical Engineers", Pergamon Press, N.Y. (1966).
- S. (S1) Sanderson W.E., Symposium on Spray Dried Milk Powders, Palmerston North, Summary of Proceedings, N.Z. Dairy Research Inst.(1973)
- (S2) Schiller L., Nauman A.Z., Ver.deut.Ing. 77, 318 (1933).
- (S3) Schlünder E.U., "Über die Trocknung ruhender Einzeltropfen und fallender Sprühnebel", Ph.D. Dissertation, Technischer Hochschule, Darmstadt (1962).



- (S4) Schlünder E.U., Internat.J.Heat Mass Tr. 7, 49 (1964).
- (S5) Schwartzberg H.G., Treybal R.E., Ind.Eng.Chem.Fund. 7, 6 (1968).
- (S6) Seinfeld J.H., Lapidus L., "Mathematical Methods in Chemical Engineering", vol.3, Prentice Hall, N.J. (1974).
- (S7) Schlien D.J., Corrsin S., J.Fluid Mech. 62, 255 (1974).
- (S8) Shapiro A.H., Erickson A.J., Trans.A.S.M.E. 775 (1957).
- (S9) Sinclair C.G., McNaughton K.J., Can.J.Chem.Eng. 48, 411 (1970).
- (S10) Sjenitzer F., Chem.Eng.Sci. 1, 101 (1952).
- (S11) Sjenitzer F., Chem.Eng.Sci. 17, 309 (1962).
- (S12) Smith S.C.J., unpublished work, Dept.of Chem.Eng., University of Canterbury, New Zealand.
- (S13) Son N.T., B.E. Project report, Dept. of Chem.Eng., Univ. of Canterbury, New Zealand (1968).
- (S14) Soo S.L., Chem.Eng.Sci. 5, 57 (1956).
- (S15) Soo S.L., "Fluid Dynamics of Multiphase Systems", Blaisdell Pub.Co., Waltham, Mass., U.S.A. (1967).
- (S16) Spalding D.B., Proc.Roy.Soc. A221, 78 (1954).
- (S17) Spink L.K., "Principles and Practice of Flowmeter Engineering", 9th ed., Foxboro (1967).
- (S18) Stoess H.A., "Pneumatic Conveying", Wiley-Interscience, N.Y. (1970).
- (S19) Stokes R.L., Nauman E.B., Can.J.Chem.Eng. 48, 723 (1970).
- T. (T1) Tate, R.W., Marshall W.R., Chem.Eng.Prog. 49, 169 (1953).
- (T2) Taylor G.I., Proc.Roy.Soc. S151, 421, 478 (1935).
- (T3) Taylor G.I., Proc.Roy.Soc. 223A, 446 (1954).
- (T4) Tennekes H., Lumley J.L., "A First Course in Turbulence", M.I.T. Press, Mass., U.S.A. (1972).
- (T5) Torobin L.B., Gauvin W.H., Can.J.Chem.Eng. 37, 129,167,224;  
38, 142,189; 39, 113 (1959-1961).
- (T6) Torobin L.B., Gauvin W.H., A.I.Ch.E.J. 7, 615 (1961).

- (T7) Trommelen A.M., Crosby E.J., A.I.Ch.E.J. 16, 857 (1970).
- (T8) Turba J., Nemeth J., Brit.Chem.Eng. 9, 157 (1964).
- U. (U1) Uhlherr P.H.T., Sinclair C.G., "Chemeca '70", part 1, p.1 (1970).
- (U2) Uru W., B.E. Project Report, Dept. of Chem.Eng., University of Canterbury, New Zealand (1975).
- V. (V1) Van der Laan E.T., Chem.Eng.Sci. 7, 187 (1957).
- (V2) Viehweg H., Biess G., Weber B., Chem. Techn. 20, 620 (1968).
- W (W1) Webb B.H., Johnson A.H., "Fundamentals of Dairy Chemistry", AVI (1965).
- (W2) Weber B., Viehweg H., Chem.Techn. 22, 599 (1970).
- (W3) Whittaker S., A.I.Ch.E.J. 18, 361 (1972).
- (W4) Wiggs L.D., J.Inst.Fuel 37, 500 (1964).
- (W5) Williams A., Oxidation & Combustion Reviews 3, 1 (1968).
- (W6) Wilson G., B.E. Project Report, Dept. of Chem.Eng., University of Canterbury, New Zealand (1974).
- (W7) Wood T., Chem.Eng.Sci. 23, 783 (1968).
- (W8) Wood T., Hop N.H., Proceedings 5th Australasian Conference on Hydraulics and Fluid Mechanics, vol.1, 360 (1974).
- Y. (Y1) Yaron I., Gal-Or B., Internat.J.Heat Mass Tr. 14, 727 (1971).
- Z. (Z1) Zwietering T.N., Chem.Eng.Sci. 11, 1 (1959).



APPENDIX ADATA AND RESULTS OF RESIDENCETIME DISTRIBUTION (R.T.D.) EXPERIMENTSContents

<u>Table A1</u>	Input concentration curves for drying and atomising air R.T.D.
<u>Table A2</u>	Output concentration curves for drying air R.T.D.
<u>Table A3</u>	Output concentration curves for atomising air R.T.D.
<u>Table A4</u>	U-functions for drying air R.T.D.
<u>Table A5</u>	U-functions for atomising air R.T.D.
<u>Table A6</u>	Moment analysis of drying air R.T.D.
<u>Table A7</u>	Transfer-function analysis (A.D.P.F. and T.S.P.F. models) of drying air R.T.D.
<u>Table A8</u>	Transfer-function analysis (A.D.P.F. and T.S.P.F. models) of atomising air R.T.D.
<u>Table A9</u>	Transfer-function analysis (D.B.M. and B.C.P.F. models) of drying air R.T.D.
<u>Table A10</u>	Output concentration curves for spray R.T.D.
<u>Table A11</u>	U-functions for spray R.T.D.
<u>Table A12</u>	Moment analysis and transfer-function analysis (A.D.P.F. and T.S.P.F. models) of spray R.T.D.

Table A1: Input concentration curves for drying and atomising air R.T.D.

AIR RTD INPUT CONCENTRATION CURVE NO. 11

APPLIES TO RUNS 5

TIME= 0.10 SECONDS TO 30.00 SECONDS IN INTERVALS OF 0.10 SECONDS

[illegible]

AIR RTD INPUT CONCENTRATION CURVE NO. 12

APPLIES TO RUNS 9

TIME= 0.05 SECONDS TO 15.00 SECONDS IN INTERVALS OF 0.05 SECONDS

[illegible]

AIR RTD INPUT CONCENTRATION CURVE NO. 13

APPLIES TO RUNS 3,4,7,8,11-15,17-19,21-28

TIME= 0.02 SECONDS TO 6.00 SECONDS IN INTERVALS OF 0.02 SECONDS

[illegible]

AIR RTD INPUT CONCENTRATION CURVE NO. 14

APPLIES TO RUNS 1,2,6,10,16,20

TIME= 0.02 SECONDS TO 6.00 SECONDS IN INTERVALS OF 0.02 SECONDS

[illegible]

Table A2: Output concentration curves for drying air R.T.D.

RUN	1A	SUBRUN 1				DT=	0.50SECS(1ST 4 LINES)				THEN	5.00SECS(LAST 2 LINES)											
	0	0	0	0	0	0	0	0	0	0	0	0	0	0	0	0	0	0	0	0	0		
	0	8	21	59	215	489	882	973	990	930	796	811	807	784	742	747	731	694	634	669	699		
	839	828	367	893	905	903	891	893	907	936	938	936	928	914	907	903	902	903	903	903	903		
	871	858	839	815	785	780	774	769	764	737	710	683	656	645	624	591	548	531	516	504	494		
	419	258	197	151	116	88	63	52	39	30	23	17	13	10	8	6	4	3	2	2	1		
	0	0	0	0	0	0	0	0	0	0	0	0	0	0	0	0	0	0	0	0	0		
RUN	1A	SUBRUN 2				DT=	0.50SECS(1ST 4 LINES)				THEN	5.00SECS(LAST 2 LINES)											
	0	0	0	0	0	0	0	0	0	0	0	0	0	0	0	0	0	0	0	0	0		
	0	0	0	94	185	274	360	402	412	391	340	358	391	440	505	519	587	710	886	928	959		
	947	917	921	928	937	948	942	938	937	938	938	938	938	938	935	928	915	897	903	897	877		
	845	858	855	837	804	808	794	761	711	689	670	653	639	622	608	596	557	587	587	587	587		
	391	278	213	163	125	95	73	56	43	33	25	19	14	11	8	6	5	3	2	2	1		
	0	0	0	0	0	0	0	0	0	0	0	0	0	0	0	0	0	0	0	0	0		
RUN	1B	SUBRUN 1				DT=	0.50SECS(1ST 4 LINES)				THEN	5.00SECS(LAST 2 LINES)											
	0	0	0	0	0	0	0	0	0	0	0	0	0	0	0	0	0	32	86	99	121		
	294	333	363	359	398	480	606	649	693	736	779	816	849	877	901	931	953	966	970	981	987		
	981	970	964	953	938	918	920	918	912	901	907	901	881	849	838	831	829	831	823	814	805		
	727	697	675	662	658	649	641	632	623	615	606	597	589	580	571	563	554	545	537	528	519		
	242	329	274	228	190	158	132	110	91	76	63	53	44	36	30	25	21	17	14	12	10		
	4	3	2	2	1	1	1	1	0	0	0	0	0	0	0	0	0	0	0	0	0		
RUN	1B	SUBRUN 2				DT=	0.50SECS(1ST 4 LINES)				THEN	5.00SECS(LAST 2 LINES)											
	0	0	0	0	0	0	0	0	0	0	0	0	0	0	0	0	0	32	86	99	121		
	294	333	363	359	398	480	606	649	693	736	779	816	849	877	901	931	953	966	970	981	987		
	981	970	964	953	938	918	920	918	912	901	907	901	881	849	838	831	829	831	823	814	805		
	727	697	675	662	658	649	641	632	623	615	606	597	589	580	571	563	554	545	537	528	519		
	242	329	274	228	190	158	132	110	91	76	63	53	44	36	30	25	21	17	14	12	10		
	4	3	2	2	1	1	1	1	0	0	0	0	0	0	0	0	0	0	0	0	0		
RUN	1C	SUBRUN 1				DT=	0.50SECS(1ST 4 LINES)				THEN	5.00SECS(LAST 2 LINES)											
	0	0	0	0	0	0	0	0	0	0	0	0	0	0	0	0	0	14	39	63	98		
	274	335	411	426	450	485	529	588	646	705	764	789	813	838	862	883	901	917	931	948	960		
	985	970	966	960	952	940	940	940	940	940	918	901	889	882	874	862	845	823	812	803	797		
	725	710	695	681	666	656	646	637	627	623	617	608	597	589	578	564	548	546	539	526	509		
	401	343	288	242	204	171	144	121	102	85	72	60	51	42	36	30	25	21	18	15	12		
	5	4	3	3	2	2	1	1	1	1	0	0	0	0	0	0	0	0	0	0	0		
RUN	1C	SUBRUN 2				DT=	0.50SECS(1ST 4 LINES)				THEN	5.00SECS(LAST 2 LINES)											
	0	0	0	0	0	0	0	0	0	0	0	0	0	0	0	0	0	14	39	63	98		
	274	335	411	426	450	485	529	588	646	705	764	789	813	838	862	883	901	917	931	948	960		
	985	970	966	960	952	940	940	940	940	940	918	901	889	882	874	862	845	823	812	803	797		
	725	710	695	681	666	656	646	637	627	623	617	608	597	589	578	564	548	546	539	526	509		
	401	343	288	242	204	171	144	121	102	85	72	60	51	42	36	30	25	21	18	15	12		
	5	4	3	3	2	2	1	1	1	1	0	0	0	0	0	0	0	0	0	0	0		
RUN	1D	SUBRUN 1				DT=	0.50SECS(1ST 4 LINES)				THEN	5.00SECS(LAST 2 LINES)											
	0	0	0	0	0	0	0	0	0	0	0	0	0	0	3	10	119	210	282	336	454		
	788	801	799	787	788	803	830	816	809	811	820	842	862	879	894	900	915	937	967	972	978		
	976	978	989	988	974	946	926	915	911	915	882	862	855	862	858	851	842	830	826	820	811		
	715	706	694	679	662	642	631	627	631	625	620	615	610	604	599	594	589	583	578	573	567		
	399	347	289	241	200	167	139	116	96	80	67	56	46	38	32	27	22	18	15	13	10		
	4	3	3	2	2	1	1	1	1	0	0	0	0	0	0	0	0	0	0	0	0		
RUN	1D	SUBRUN 2				DT=	0.50SECS(1ST 4 LINES)				THEN	5.00SECS(LAST 2 LINES)											
	0	0	0	0	0	0	0	0	0	0	0	0	0	0	3	10	119	210	282	336	454		
	788	801	799	787	788	803	830	816	809	811	820	842	862	879	894	900	915	937	967	972	978		
	976	978	989	988	974	946	926	915	911	915	882	862	855	862	858	851	842	830	826	820	811		
	715	706	694	679	662	642	631	627	631	625	620	615	610	604	599	594	589	583	578	573	567		
	399	347	289	241	200	167	139	116	96	80	67	56	46	38	32	27	22	18	15	13	10		
	4	3	3	2	2	1	1	1	1	0	0	0	0	0	0	0	0	0	0	0	0		
RUN	1E	SUBRUN 1				DT=	0.50SECS(1ST 4 LINES)				THEN	5.00SECS(LAST 2 LINES)											
	0	0	0	0	0	0	0	0	0	0	0	0	0	0	22	73	149	249	344	433	510		
	791	850	895	923	941	946	941	946	952	958	964	978	987	989	987	971	964	965	975	977	975		
	938	918	913	906	896	883	868	849	827	803	799	791	781	769	763	757	751	746	740	734	728		
	677	664	654	647	642	639	631	616	596	594	585	571	550	538	528	520	516	499	482	464	447		
	344	275	227	187	154	127	105	86	71	59	48	40	33	27	22	18	15	12	10	8	7		
	2	2	1	1	1	1	0	0	0	0	0	0	0	0	0	0	0	0	0	0	0		
RUN	1E	SUBRUN 2				DT=	0.50SECS(1ST 4 LINES)				THEN	5.00SECS(LAST 2 LINES)											
	0	0	0	0	0	0	0	0	0	0	0	0	0	7	19	37	59	114	159	194	219		
	428	485	548	586	628	675	728	731	748	776	817	850	877	900	917	933	947	958	967	980	987		
	983	977	981	977	966	947	942	937	932	927	921	907	886	857	840	827	820	817	820	817	810		
	758	741	728	716	708	689	668	644	618	595	578	566	558	558	558	558	558	559	558	554	548		
	408	339	279	230	190	157	129	106	88	72	59	49	40	33	27	22	18	15	12	10	8		
	3	2	2	1	1	1	1	0	0	0	0	0	0	0	0	0	0	0	0	0	0		



Table A2 (continued)

[illegible]





Table A2 (continued)

RUN	9A	, SUBRUN 1				, DT=	0.05SECS(1ST 4 LINES)				THEN	0.50SECS(LAST 2 LINES)															
	0	0	0	0	0	0	0	0	0	0	0	0	0	0	0	0	0	0	0	0	0	0	0	0	0		
	0	0	0	0	0	0	0	0	0	0	0	0	0	0	0	0	0	0	0	0	0	0	0	0	0		
	0	0	0	0	0	0	0	0	0	0	0	0	0	0	0	0	0	0	0	0	0	0	0	0	0		
	105	141	183	229	280	329	373	414	450	482	510	534	553	569	580	595	609	621	631	640	646	651	654	655	655		
	674	720	866	970	987	955	834	797	747	716	632	545	486	436	390	349	319	290	255	224	199	184	167	153	144		
	132	123	113	105	98	90	86	80	76	71	67	63	61	57	55	51	48	46	44	40	38	36	34	32	28		
RUN	9A	, SUBRUN 2				, DT=	0.05SECS(1ST 4 LINES)				THEN	0.50SECS(LAST 2 LINES)															
	0	0	0	0	0	0	0	0	0	0	0	0	0	0	0	0	0	0	0	0	0	0	0	0	0		
	0	0	0	0	0	0	0	0	0	0	0	0	0	0	0	0	0	0	0	0	0	0	0	0	0		
	0	0	0	0	0	0	0	0	0	0	0	0	0	0	0	0	0	0	0	0	0	0	0	0	0		
	0	1	25	54	87	148	206	258	306	350	389	424	454	479	500	521	542	564	587	610	634	658	684	710	736		
	706	889	990	957	909	863	865	836	776	692	648	593	535	492	465	436	372	326	285	258	235	212	191	174	157		
	141	128	117	109	102	94	83	76	71	64	61	56	51	47	42	41	37	35	32	30	27	25	22	22	18		
RUN	9B	, SUBRUN 1				, DT=	0.05SECS(1ST 4 LINES)				THEN	0.50SECS(LAST 2 LINES)															
	0	0	0	0	0	0	0	0	0	0	0	0	0	0	0	0	0	0	0	0	0	0	0	0	0		
	0	0	0	0	0	0	0	0	0	0	0	0	0	0	0	0	0	0	0	0	0	0	0	0	0		
	0	0	0	0	0	0	0	0	0	0	0	0	0	0	0	0	0	0	0	0	0	0	0	0	0		
	0	0	0	0	0	0	0	0	0	0	0	0	0	0	0	0	0	0	0	0	0	0	0	0	0		
	224	455	712	836	954	980	941	947	903	780	669	576	505	417	348	298	250	211	178	149	131	116	105	96	89		
	83	77	72	67	63	60	57	54	53	50	48	46	44	43	41	40	37	36	34	33	30	28	28	27	25		
RUN	9B	, SUBRUN 2				, DT=	0.05SECS(1ST 4 LINES)				THEN	0.50SECS(LAST 2 LINES)															
	0	0	0	0	0	0	0	0	0	0	0	0	0	0	0	0	0	0	0	0	0	0	0	0	0		
	0	0	0	0	0	0	0	0	0	0	0	0	0	0	0	0	0	0	0	0	0	0	0	0	0		
	0	0	0	0	0	0	0	0	0	0	0	0	0	0	0	0	0	0	0	0	0	0	0	0	0		
	0	2	11	21	31	51	70	89	108	127	146	165	184	203	221	227	235	243	253	264	277	290	305	321	338		
	556	740	854	911	958	990	967	976	937	854	757	689	604	512	424	351	296	253	214	182	155	137	120	110	101		
	90	84	77	71	65	61	56	52	50	46	45	43	41	39	37	33	33	31	30	26	26	26	22	22	20		
RUN	9C	, SUBRUN 1				, DT=	0.05SECS(1ST 4 LINES)				THEN	0.50SECS(LAST 2 LINES)															
	0	0	0	0	0	0	0	0	0	0	0	0	0	0	0	0	0	0	0	0	0	0	0	0	0		
	0	0	0	0	0	0	0	0	0	0	0	0	0	0	0	0	0	0	0	0	0	0	0	0	0		
	0	0	0	0	0	0	0	0	0	0	0	0	0	0	0	0	0	0	0	0	0	0	0	0	0		
	34	57	83	112	145	161	177	193	209	224	240	256	272	288	304	324	344	364	384	405	425	446	467	488	509		
	747	871	945	988	952	833	795	770	724	671	595	534	477	446	416	400	368	337	304	262	231	205	186	168	153		
	140	123	120	110	100	92	85	77	74	69	64	59	56	52	49	46	42	39	38	34	33	29	29	29	26		
RUN	9C	, SUBRUN 2				, DT=	0.05SECS(1ST 4 LINES)				THEN	0.50SECS(LAST 2 LINES)															
	0	0	0	0	0	0	0	0	0	0	0	0	0	0	0	0	0	0	0	0	0	0	0	0	0		
	0	0	0	0	0	0	0	0	0	0	0	0	0	0	0	0	0	0	0	0	0	0	0	0	0		
	0	0	0	0	0	0	0	0	0	0	0	0	0	0	0	0	0	0	0	0	0	0	0	0	0		
	233	255	279	304	331	346	364	386	410	437	466	499	534	573	614	640	666	690	714	736	758	778	798	816	833		
	918	959	983	981	990	946	916	824	780	719	672	608	538	528	490	458	413	386	361	326	299	274	250	225	202		
	180	162	149	138	128	118	108	101	92	86	79	72	68	61	56	53	50	45	41	40	36	34	31	28	25		
RUN	9D	, SUBRUN 1				, DT=	0.05SECS(1ST 4 LINES)				THEN	0.50SECS(LAST 2 LINES)															
	0	0	0	0	0	0	0	0	0	0	0	0	0	0	0	0	0	0	0	0	0	0	0	0	0		
	0	0	0	0	0	0	0	0	0	0	0	0	0	0	0	0	0	0	0	0	0	0	0	0	0		
	0	0	0	0	0	0	0	0	0	0	0	0	0	0	0	0	0	0	0	0	0	0	0	0	0		
	226	264	305	351	401	437	470	501	530	556	580	602	621	638	653	682	709	734	756	777	794	810	823	834	843		
	867	941	987	984	939	863	852	836	773	701	673	643	573	538	469	434	401	375	349	305	271	253	234	220	203		
	188	179	166	144	135	131	122	111	99	90	85	77	68	62	59	53	49	46	42	37	33	31	27	25	24		
RUN	9D	, SUBRUN 2				, DT=	0.05SECS(1ST 4 LINES)				THEN	0.50SECS(LAST 2 LINES)															
	0	0	0	0	0	0	0	0	0	0	0	0	0	0	0	0	0	0	0	0	0	0	0	0	0		
	0	0	0	0	0	0	0	0	0	0	0	0	0	0	0	0	0	0	0	0	0	0	0	0	0		
	0	0	5	22	40	58	76	95	114	134	135	139	145	154	164	177	192	209	229	251	259	267	277	286	297		
	307	319	331	343	356	364	373	386	400	417	437	459	483	509	538	559	578	597	615	632	648	664	678	692	705		
	874	922	960	987	933	847	803	774	762	701	647	626	590	557	490	429	391	362	333	302	279	260	245	228	208		
	193	180	162	149	136	124	113	101	95	88	80	72	69	65	61	57	51	49	46	44	38	36	34	32	30		
RUN	9E	, SUBRUN 1				, DT=	0.05SECS(1ST 4 LINES)				THEN	0.50SECS(LAST 2 LINES)															
	0	0	0	0	0	0	0	0	0	0	0	0	0	0	0	0	0	0	0	0	0	0	0	0	0		
	0	0	0	0	0	0	0	0	0	0	0	0	0	0	0	0	0	0	0	0	0	0	0	0	0		
	0	0	0	0	0	0	0	0	0	0	0	0	0	0	0	0	0	0	0	0	0	0	0	0	0		
	480	511	541	571	600	643	682	715	744	767	785	799	807	811	810	810	810	810	811	811	812	812	813	814	814		
	862	937	967	963	924	847	767	729	711	667	559	508	494	448	410	391	379	363	338	306	281	265	252	234	217		
	201	183	165	150	140	132	122	114	106	98	91	85	76	72	67	63	60	55	52	47	45	42	39	36	34		
RUN	9E	, SUBRUN 2				, DT=	0.05SECS(1ST 4 LINES)				THEN	0.50SECS(LAST 2 LINES)															
	0	0	0	0	0	0	0	0	0	0	0	0	0	0	0	0	0	0	0	0	0	0	0	0	0		
	0	0	0	0	0	0	0	0	0	0	0	0	0	0	0	0	0	0	0	0	0	0	0	0	0		
	0	0	0	0	0	0	0	0	0	0	18	39	60	81	102	124	145	167	189	210	234	260	287	315	346		
	378	411	447	484	522	558	594	629	663	697	731	764	797	830	861	871	878	884	888	890	891	890	888	884	878		
	921	980	980	939	858	822	806	746	685	650	605	564	515	465	421	393	373	351	322	293	270	254	243	229	210		
	191	174	158	146	140	129	117	110	100	93	86	81	75	68	63	57	54	52	48	45	41	37	36	34	30		









Table A2 (continued)

RUN 17C , SUBRUN 1 , DT= 0.02SECS(1ST 4 LINES) THEN 0.20SECS(LAST 2 LINES)																													
0	0	0	0	0	0	0	0	0	0	0	0	0	0	0	0	0	0	0	0	0	0	0	0	0	0	0	0	0	
0	0	0	0	0	0	0	0	0	0	0	0	0	0	0	0	0	0	0	0	0	0	0	0	0	0	0	0	0	
0	0	0	0	0	0	0	0	0	0	0	0	0	0	0	0	0	0	0	0	0	0	0	0	0	0	0	0	0	
0	0	0	0	0	0	0	0	0	0	0	0	0	0	0	0	2	3	4	5	6	8	9	10	12					
97	300	486	673	956	973	908	762	591	494	454	381	324	259	210	177	149	127	109	97	86	76	69	64	60					
55	50	47	44	42	41	39	37	34	32	31	30	29	26	24	23	22	22	21	20	20	19	18	18	17					
RUN 17C , SUBRUN 2 , DT= 0.02SECS(1ST 4 LINES) THEN 0.20SECS(LAST 2 LINES)																													
0	0	0	0	0	0	0	0	0	0	0	0	0	0	0	0	0	0	0	0	0	0	0	0	0	0	0	0	0	
0	0	0	0	0	0	0	0	0	0	0	0	0	0	0	0	0	0	0	0	0	0	0	0	0	0	0	0	0	
0	0	0	0	0	0	0	0	0	0	0	0	0	0	0	0	0	0	0	0	0	0	0	0	0	0	0	0	0	
1	2	5	7	10	14	20	29	39	52	66	83	102	122	145	170	194	219	245	270	297	323	350	378	406					
666	750	937	979	990	937	844	739	729	656	646	614	521	458	395	340	292	250	215	187	164	144	127	114	104					
95	87	79	72	65	63	60	58	55	52	50	47	45	43	41	40	39	37	36	35	34	33	32	31	30					
RUN 17D , SUBRUN 1 , DT= 0.02SECS(1ST 4 LINES) THEN 0.20SECS(LAST 2 LINES)																													
0	0	0	0	0	0	0	0	0	0	0	0	0	0	0	0	0	0	0	0	0	0	0	0	0	0	0	0	0	
0	0	0	0	0	0	0	0	0	0	0	0	0	0	0	0	0	0	0	0	0	0	0	0	0	0	0	0	0	
0	0	0	0	0	0	0	0	0	0	0	0	0	0	0	0	0	0	0	0	0	0	0	0	0	0	0	0	0	
0	0	0	0	0	0	1	3	6	8	11	15	18	22	26	31	36	42	48	55	62	71	79	89	99	110				
204	353	432	581	849	951	809	684	550	456	400	330	267	212	172	148	127	109	96	86	79	73	68	63	58					
55	51	47	44	41	40	38	36	35	33	33	32	30	29	27	26	25	25	24	23	22	22	21	20	20					
RUN 17D , SUBRUN 2 , DT= 0.02SECS(1ST 4 LINES) THEN 0.20SECS(LAST 2 LINES)																													
0	0	0	0	0	0	0	0	0	0	0	0	0	0	0	0	0	0	0	0	0	0	0	0	0	0	0	0	0	
0	0	0	0	0	0	0	0	0	0	0	0	0	0	0	0	0	0	0	0	0	0	0	0	0	0	0	0	0	
0	0	0	0	0	0	0	0	0	0	0	0	0	0	0	0	0	0	0	0	0	0	0	0	0	0	0	0	0	
0	0	0	0	0	0	0	0	0	0	0	0	0	0	0	0	0	0	0	0	0	0	0	0	0	0	0	0	0	
59	229	391	630	919	970	987	834	689	536	451	383	306	246	204	165	132	107	88	76	64	55	47	41	38					
34	31	28	24	21	19	17	16	15	15	15	14	14	13	11	11	11	10	10	10	9	9	9	8	8					
RUN 17E , SUBRUN 1 , DT= 0.02SECS(1ST 4 LINES) THEN 0.20SECS(LAST 2 LINES)																													
0	0	0	0	0	0	0	0	0	0	0	0	0	0	0	0	0	0	0	0	0	0	0	0	0	0	0	0	0	
0	0	0	0	0	0	0	0	0	0	0	0	0	0	0	0	0	0	0	0	0	0	0	0	0	0	0	0	0	
0	0	0	0	0	0	0	0	0	0	0	0	0	0	0	0	0	0	0	0	0	0	0	0	0	0	0	0	0	
0	0	0	0	0	0	0	0	0	0	0	0	0	0	0	0	0	0	0	0	0	0	0	0	0	0	0	0	0	
24	28	33	38	44	51	59	67	74	82	89	97	104	111	118	120	127	138	155	176	201	232	267	307	352					
638	847	935	990	891	791	638	495	396	308	236	183	143	115	96	83	72	64	57	52	48	45	42	40	39					
39	38	38	37	36	30	26	24	22	22	20	19	17	15	13	12	12	12	11	11	10	10	10	9	9					
RUN 17E , SUBRUN 2 , DT= 0.02SECS(1ST 4 LINES) THEN 0.20SECS(LAST 2 LINES)																													
0	0	0	0	0	0	0	0	0	0	0	0	0	0	0	0	0	0	0	0	0	0	0	0	0	0	0	0	0	
0	0	0	0	0	0	0	0	0	0	0	0	0	0	0	0	0	0	0	0	0	0	0	0	0	0	0	0	0	
0	0	0	0	0	0	0	0	0	0	0	0	0	0	0	0	0	0	0	0	0	0	0	0	0	0	0	0	0	
0	0	0	0	0	0	1	2	4	7	10	13	16	20	25	30	37	44	52	61	70	79	88	98	109	119				
410	620	780	880	910	775	645	660	540	430	350	280	219	170	139	116	97	83	74	70	66	61	58	53	50					
45	41	38	35	33	31	30	29	28	28	24	21	20	19	20	19	18	18	17	17	16	16	15	15	14					
RUN 18A , SUBRUN , DT= 0.02SECS(1ST 4 LINES) THEN 0.20SECS(LAST 2 LINES)																													
0	0	0	0	0	0	0	0	0	0	0	0	0	0	0	0	0	0	0	0	0	0	0	0	0	0	0	0	0	
0	0	0	0	0	0	0	0	0	0	0	0	0	0	0	0	0	0	0	0	0	0	0	0	0	0	0	0	0	
0	0	0	0	0	0	0	0	0	0	0	0	0	0	0	0	0	0	0	0	0	0	0	0	0	0	0	0	0	
1	3	5	8	12	29	47	67	87	108	130	154	178	203	229	254	281	307	334	362	390	418	447	477	507					
748	857	941	989	977	977	977	893	796	676	585	506	438	382	338	307	279	252	227	205	178	155	135	120	108					
98	89	79	70	60	59	57	55	52	48	45	43	41	38	36	36	36	35	33	30	29	28	27	26	26					
RUN 19A , SUBRUN , DT= 0.02SECS(1ST 4 LINES) THEN 0.20SECS(LAST 2 LINES)																													
0	0	0	0	0	0	0	0	0	0	0	0	0	0	0	0	0	0	0	0	0	0	0	0	0	0	0	0	0	
0	0	0	0	0	0	0	0	0	0	0	0	0	0	0	0	0	0	0	0	0	0	0	0	0	0	0	0	0	
0	0	0	0	0	0	0	0	0	0	0	0	0	0	0	0	1	2	4	6	9	11	15	21	28	36				
46	58	71	85	101	114	130	149	170	194	220	249	280	314	351	386	421	454	486	517	547	576	604	630	656					
877	988	933	914	822	674	554	443	351	277	226	184	150	126	110	98	87	78	70	64	60	57	53	49	46					
41	38	35	33	32	30	29	28	26	25	24	23	22	21	20	19	18	17	16	16	15	14	14	13	12					

Table A2 (continued)

RUN 20A , SUBRUN 1 ,		DT=	0.02SECS(1ST 4 LINES)				THEN	0.20SECS(LAST 2 LINES)							
0	0	0	0	0	0	0	0	0	0	0	0	0	0	0	0
0	0	0	0	0	0	0	0	0	0	0	0	0	0	0	0
127	148	170	194	220	247	276	306	337	371	399	426	453	479	504	529
730	745	761	775	788	803	817	830	843	856	868	880	891	902	912	922
943	881	804	727	634	556	479	417	371	324	288	255	226	200	177	158
72	68	65	63	61	58	55	52	49	46	44	41	39	37	35	33
31	30	28	26	25	24	22	21	20	19	18	17	16	15	14	13
RUN 20A , SUBRUN 2 ,		DT=	0.02SECS(1ST 4 LINES)				THEN	0.20SECS(LAST 2 LINES)							
0	0	0	0	0	0	0	0	0	0	0	0	0	0	0	0
0	0	0	0	0	0	0	0	0	0	0	0	0	0	0	0
268	296	325	354	384	415	446	478	511	544	566	587	608	628	649	669
856	874	891	908	924	934	944	952	960	967	973	978	982	985	987	989
899	835	772	696	607	544	481	417	354	316	282	251	223	199	177	158
83	78	73	68	63	59	56	53	50	47	45	42	40	38	36	34
32	30	29	27	26	24	23	22	21	20	19	18	17	16	15	14
RUN 20B , SUBRUN 1 ,		DT=	0.02SECS(1ST 4 LINES)				THEN	0.20SECS(LAST 2 LINES)							
0	0	0	0	0	0	0	0	0	0	0	0	0	0	0	0
0	0	0	0	0	0	0	0	0	0	0	0	0	0	0	0
89	118	152	189	229	274	321	373	428	487	518	545	578	607	634	660
861	875	888	900	911	913	916	919	922	925	928	931	935	939	942	946
958	864	770	660	565	487	408	345	298	267	236	208	183	160	141	124
50	46	43	41	39	36	34	31	29	27	25	24	22	21	19	18
17	15	14	13	12	11	10	9	8	7	6	5	4	3	2	1
RUN 20B , SUBRUN 2 ,		DT=	0.02SECS(1ST 4 LINES)				THEN	0.20SECS(LAST 2 LINES)							
0	0	0	0	0	0	0	0	0	0	0	0	0	0	0	0
0	0	0	0	0	0	0	0	0	0	0	0	0	0	0	0
215	247	280	316	353	393	435	478	524	572	595	617	639	660	681	700
858	869	880	891	900	907	914	921	927	933	938	944	949	953	958	962
972	886	800	715	614	529	457	371	328	286	250	218	189	164	143	124
45	41	38	36	35	33	31	29	27	25	23	22	20	19	17	16
15	14	13	12	11	10	9	8	7	6	5	4	3	2	1	0
RUN 20C , SUBRUN 1 ,		DT=	0.02SECS(1ST 4 LINES)				THEN	0.20SECS(LAST 2 LINES)							
0	0	0	0	0	0	0	0	0	0	0	0	0	0	0	0
0	0	0	0	0	0	0	0	0	0	0	0	0	0	0	0
665	694	718	737	752	762	767	768	764	755	771	786	801	815	829	843
956	965	973	981	989	989	989	988	986	984	981	977	973	968	962	955
769	701	618	522	439	371	316	274	233	206	180	157	136	118	103	89
37	34	32	29	27	25	23	21	20	18	17	16	14	13	12	11
10	9	8	7	6	5	4	3	2	1	0	0	0	0	0	0
RUN 20C , SUBRUN 2 ,		DT=	0.02SECS(1ST 4 LINES)				THEN	0.20SECS(LAST 2 LINES)							
0	0	0	0	0	0	0	0	0	0	0	0	0	0	0	0
0	0	0	0	0	0	0	0	0	0	0	0	0	0	0	0
533	570	604	637	668	696	723	748	771	792	811	829	846	863	878	892
982	985	988	989	990	988	986	983	980	977	974	970	966	961	957	951
792	709	610	511	429	379	330	280	231	214	190	167	148	130	115	102
46	44	42	41	41	38	35	32	30	28	25	24	22	20	19	17
16	15	14	12	12	11	10	9	8	7	6	5	4	3	2	1
RUN 20D , SUBRUN 1 ,		DT=	0.02SECS(1ST 4 LINES)				THEN	0.20SECS(LAST 2 LINES)							
0	0	0	0	0	0	0	0	0	0	0	0	0	0	0	0
0	0	0	0	0	0	0	0	0	0	0	0	0	0	0	0
187	208	230	252	275	299	323	348	374	401	425	450	474	498	522	545
759	778	798	816	835	835	835	836	838	841	845	850	855	861	868	876
985	952	918	802	718	618	551	467	401	284	245	211	181	155	133	115
45	41	38	35	33	31	29	27	26	24	23	21	20	19	18	17
16	15	14	13	12	11	10	9	8	7	6	5	4	3	2	1
RUN 20D , SUBRUN 2 ,		DT=	0.02SECS(1ST 4 LINES)				THEN	0.20SECS(LAST 2 LINES)							
0	0	0	0	0	0	0	0	0	0	0	0	0	0	0	0
0	0	0	0	0	0	0	0	0	0	0	0	0	0	0	0
360	391	423	454	485	516	547	578	608	638	655	673	689	706	723	739
892	907	921	935	948	954	959	963	967	974	975	978	981	983	985	987
930	857	784	675	583	510	437	383	328	273	242	213	188	165	145	129
70	68	66	64	63	60	56	53	50	47	44	41	39	37	34	32
30	29	27	25	24	22	21	20	19	18	17	16	15	14	13	12
RUN 20E , SUBRUN 1 ,		DT=	0.02SECS(1ST 4 LINES)				THEN	0.20SECS(LAST 2 LINES)							
0	0	0	0	0	0	0	0	0	0	0	0	0	0	0	0
0	0	0	0	0	0	0	0	0	0	0	0	0	0	0	0
436	459	479	497	511	523	532	539	542	543	560	578	595	613	631	648
825	842	860	877	895	908	921	932	943	952	960	967	974	979	983	986
910	822	719	616	513	440	381	337	293	249	221	195	172	150	132	115
47	44	41	39	36	34	31	29	27	25	23	22	20	19	17	16
15	14	13	12	11	10	9	8	7	6	5	4	3	2	1	0
RUN 20E , SUBRUN 2 ,		DT=	0.02SECS(1ST 4 LINES)				THEN	0.20SECS(LAST 2 LINES)							
0	0	0	0	0	0	0	0	0	0	0	0	0	0	0	0
0	0	0	0	0	0	0	0	0	0	0	0	0	0	0	0
86	124	167	215	268	326	389	458	531	609	650	688	725	759	790	820
984	988	990	989	985	983	980	978	976	974	972	971	969	968	967	966
949	842	770	663	573	483	394	340	286	250	220	192	167	144	125	108
51	49	47	45	44	41	38	35	33	31	28	26	24	23	21	20
18	17	16	15	14	13	12	11	10	9	8	7	6	5	4	3



Table A2 (continued)

RUN 21A, SUBRUN 1					DT=	0.02SECS(1ST 4 LINES)					THEN	0.20SECS(LAST 2 LINES)										
0	0	0	0	0	0	0	0	0	0	0	0	0	0	0	0	0	0	0	0	0	0	0
0	0	0	0	0	0	0	0	0	0	0	0	0	0	0	0	0	0	0	0	0	0	0
0	0	0	0	0	9	21	36	54	75	137	196	251	303	351	395	436	473	506	536	561	584	605
657	670	682	691	699	688	685	692	708	733	765	809	860	920	990	959	929	901	873	846	820	795	771
593	540	479	426	347	285	233	192	160	139	117	98	83	72	64	57	51	46	41	37	35	32	30
26	24	23	22	21	20	19	18	17	15	15	14	14	13	13	12	12	12	11	11	10	10	9
RUN 21A, SUBRUN 2					DT=	0.02SECS(1ST 4 LINES)					THEN	0.20SECS(LAST 2 LINES)										
0	0	0	0	0	0	0	0	0	0	0	0	0	0	0	0	0	0	0	0	0	0	0
0	0	0	0	0	0	0	0	0	0	0	0	0	0	0	0	0	0	0	0	0	0	0
0	0	0	0	0	0	0	0	0	0	0	0	0	0	0	0	0	0	0	0	0	0	0
0	0	0	1	13	29	51	78	111	149	192	238	283	326	367	407	446	483	518	552	585	607	627
686	695	702	708	711	800	871	926	964	985	990	977	947	901	837	833	828	820	811	800	787	773	756
622	496	437	378	322	275	233	197	167	143	122	105	92	81	74	67	61	56	52	49	45	42	40
34	31	30	29	29	28	27	26	24	23	22	22	21	20	19	19	18	17	17	16	16	15	15
RUN 21B, SUBRUN 1					DT=	0.02SECS(1ST 4 LINES)					THEN	0.20SECS(LAST 2 LINES)										
0	0	0	0	0	0	0	0	0	0	0	0	0	0	0	0	0	0	0	0	0	0	0
0	0	0	0	0	0	0	0	0	0	0	0	0	0	0	0	0	0	0	0	0	0	0
0	0	0	0	0	0	0	0	0	0	0	0	0	0	0	0	0	0	0	0	0	0	0
0	0	0	0	0	0	0	0	0	0	0	0	0	0	0	0	0	0	0	0	0	0	0
70	93	119	147	179	213	251	291	334	380	436	487	533	574	609	640	665	685	700	710	690	681	682
750	794	849	914	990	947	911	881	857	839	827	821	821	827	839	826	814	803	792	781	772	763	754
602	520	441	401	329	277	231	193	161	136	119	104	92	82	75	69	63	58	54	50	46	44	42
37	34	32	30	28	29	28	28	27	25	24	24	23	22	21	20	20	19	18	18	17	17	16
RUN 21B, SUBRUN 2					DT=	0.02SECS(1ST 4 LINES)					THEN	0.20SECS(LAST 2 LINES)										
0	0	0	0	0	0	0	0	0	0	0	0	0	0	0	0	0	0	0	0	0	0	0
0	0	0	0	0	0	0	0	0	0	0	0	0	0	0	0	0	0	0	0	0	0	0
0	0	0	0	0	0	0	0	0	0	0	0	0	0	0	0	0	0	0	0	0	0	0
0	0	0	0	0	0	0	0	0	0	0	0	0	0	0	0	0	0	0	0	0	0	0
91	120	149	178	206	233	261	287	314	340	361	382	403	423	443	462	481	500	518	536	556	575	594
644	660	674	688	700	717	733	750	766	783	799	816	832	849	865	898	926	948	966	979	987	990	987
953	834	711	618	546	467	394	328	269	216	178	147	122	104	92	82	73	65	57	51	46	43	41
36	33	31	30	30	29	28	27	25	23	22	22	21	20	19	19	18	17	17	16	16	15	15
RUN 21C, SUBRUN 1					DT=	0.02SECS(1ST 4 LINES)					THEN	0.20SECS(LAST 2 LINES)										
0	0	0	0	0	0	0	0	0	0	0	0	0	0	0	0	0	0	0	0	0	0	0
0	0	0	0	0	0	0	0	0	0	0	0	0	0	0	0	0	0	0	0	0	0	0
0	0	0	0	0	0	0	0	0	0	0	0	0	0	0	0	0	0	0	0	0	0	0
0	0	0	0	0	0	0	0	0	0	0	0	0	0	0	0	0	0	0	0	0	0	0
32	42	57	75	97	122	151	184	221	261	293	325	355	385	413	440	467	492	516	540	559	577	595
644	659	673	687	700	706	717	732	752	776	804	837	874	916	961	974	983	988	990	987	980	970	955
852	725	607	544	455	374	307	253	212	185	161	140	121	105	92	82	73	66	62	59	54	50	46
38	36	34	33	32	32	31	29	28	26	25	24	23	22	21	20	19	18	18	17	16	16	15
RUN 21C, SUBRUN 2					DT=	0.02SECS(1ST 4 LINES)					THEN	0.20SECS(LAST 2 LINES)										
0	0	0	0	0	0	0	0	0	0	0	0	0	0	0	0	0	0	0	0	0	0	0
0	0	0	0	0	0	0	0	0	0	0	0	0	0	0	0	0	0	0	0	0	0	0
0	0	0	0	0	0	0	0	0	0	0	0	0	0	0	0	0	0	0	0	0	0	0
0	0	0	0	0	6	15	26	39	55	90	125	162	199	237	277	317	358	400	443	476	506	533
595	609	621	629	634	649	664	678	691	704	716	727	738	748	757	831	891	937	968	986	990	979	954
810	704	616	528	459	405	353	302	253	206	173	145	123	105	92	82	74	66	60	54	49	45	42
38	36	34	33	32	29	27	25	25	25	24	23	22	21	20	20	19	18	17	16	16	15	15
RUN 21D, SUBRUN 1					DT=	0.02SECS(1ST 4 LINES)					THEN	0.20SECS(LAST 2 LINES)										
0	0	0	0	0	0	0	0	0	0	0	0	0	0	0	0	0	0	0	0	0	0	0
0	0	0	0	0	0	0	0	0	0	0	0	0	0	0	0	0	0	0	0	0	0	0
0	0	0	0	0	0	0	0	0	0	0	0	0	0	0	0	0	0	0	0	0	0	0
0	0	0	0	0	3	9	15	23	33	64	96	129	164	198	234	271	309	347	386	430	469	504
587	606	622	633	641	665	688	710	731	751	771	789	807	824	840	835	834	838	845	856	871	891	914
906	862	729	652	571	472	389	321	269	232	194	163	136	115	99	85	74	65	58	53	48	44	41
32	30	29	28	27	25	23	21	19	18	17	17	16	15	14	14	13	12	12	11	11	10	10
RUN 21D, SUBRUN 2					DT=	0.02SECS(1ST 4 LINES)					THEN	0.20SECS(LAST 2 LINES)										
0	0	0	0	0	0	0	0	0	0	0	0	0	0	0	0	0	0	0	0	0	0	0
0	0	0	0	0	0	0	0	0	0	0	0	0	0	0	0	0	0	0	0	0	0	0
0	0	0	0	0	8	20	34	52	72	114	155	194	232	269	305	339	372	404	435	450	468	489
568	601	636	674	715	732	747	762	775	788	799	809	819	827	834	869	899	925	947	964	977	985	990
865	746	653	601	508	423	352	294	249	217	185	157	134	116	103	95	87	78	70	62	57	53	50
43	41	39	36	33	32	31	30	29	29	27	26	25	24	23	22	21	20	19	18	17	16	15
RUN 21E, SUBRUN 1					DT=	0.02SECS(1ST 4 LINES)					THEN	0.20SECS(LAST 2 LINES)										
0	0	0	0	0	0	0	0	0	0	0	0	0	0	0	0	0	0	0	0	0	0	0
0	0	0	0	0	0	0	0	0	0	0	0	0	0	0	0	0	0	0	0	0	0	0
0	0	0	0	0	0	0	0	0	0	0	0	0	0	0	0	0	0	0	0	0	0	0
0	0	0	0	0	0	0	0	0	0	0	0	0	0	0	0	0	0	0	0	0	0	0
271	303	336	370	405	442	477	508	537	563	587	607	625	640	653	636	630	635	652	680	719	770	832
880	673	474	398	354	280	219	168	130	103	86	72	61	52	46	40	35	30	27	24	22	20	18
14	13	12	11	9	8	7	7	6	6	6	6	5	5	5	5	4	4	4	4	4	3	3
RUN 21E, SUBRUN 2					DT=	0.02SECS(1ST 4 LINES)					THEN	0.20SECS(LAST 2 LINES)										
0	0	0	0	0	0	0	0	0	0	0	0	0	0	0	0	0	0	0	0	0	0	0
0	0	0	0	0	0	0	0	0	0	0	0	0	0	0	0	0	0	0	0	0	0	0
0	0	0	0	0	2	6	11	17	24	16	16	23	36	56	82	115	156	202	256	295	332	367
462	489	515	538	560	582	603	624	644	664	684	704	723	742	760	803	841	875	904	929	949	965	976
816	688	592	480	384	303	236	183	144	120	101	86	74	67	64	56	50	46	44	44	40	38	35
30	28	27	25	24	23	22	22	21	20	19	18	17	16	15	15	14	13	13	12	12	11	10

Table A2 (continued)

[illegible]





Table A3: (continued)

RUN	5B	SUBRUN 1				DT= 0.20SECS(1ST 4 LINES) THEN				2.00SECS(LAST 2 LINES)							
0	0	0	0	0	0	0	0	0	0	0	0	0	0	0	0	0	0
36	38	46	62	83	164	238	305	365	419	453	497	552	616	691	749	797	834
964	979	988	990	984	976	968	959	951	943	901	870	850	839	838	832	823	810
663	639	618	601	586	580	571	559	543	523	504	488	476	466	461	452	444	435
335	293	272	209	176	148	124	104	88	74	62	52	44	37	31	26	22	18
4	3	3	2	2	1	1	1	1	0	0	0	0	0	0	0	0	0
RUN	6B	SUBRUN 2				DT= 0.20SECS(1ST 4 LINES) THEN				2.00SECS(LAST 2 LINES)							
0	0	0	0	0	0	0	0	0	0	0	0	0	0	0	0	0	0
27	53	75	95	113	208	306	406	509	615	698	755	817	853	874	904	929	948
964	969	973	973	971	980	986	989	990	988	964	946	933	925	923	836	855	829
680	680	680	680	680	692	697	693	682	664	657	651	644	638	631	620	607	590
323	437	356	291	245	206	173	145	122	103	86	72	61	51	43	36	30	25
6	5	4	3	3	2	2	1	1	1	1	0	0	0	0	0	0	0
RUN	6C	SUBRUN 1				DT= 0.20SECS(1ST 4 LINES) THEN				2.00SECS(LAST 2 LINES)							
0	0	0	0	0	0	0	0	0	0	0	0	0	0	0	0	0	0
324	372	419	467	514	552	592	635	682	732	764	795	827	859	891	919	941	957
958	966	974	982	990	989	978	959	929	891	864	841	822	805	792	765	742	723
637	621	605	590	574	566	558	550	542	534	529	520	508	493	475	477	476	472
336	277	217	168	141	119	100	84	70	59	50	42	35	29	25	21	17	14
3	3	2	2	1	1	1	1	0	0	0	0	0	0	0	0	0	0
RUN	6C	SUBRUN 2				DT= 0.20SECS(1ST 4 LINES) THEN				2.00SECS(LAST 2 LINES)							
0	0	0	0	0	0	0	0	0	0	0	0	0	0	0	0	0	0
672	726	760	774	770	800	829	856	881	904	881	876	888	918	965	971	976	978
976	976	979	983	990	986	981	973	964	953	943	933	924	914	904	889	875	860
738	718	699	679	660	651	641	629	615	598	587	578	571	565	562	555	551	549
415	330	293	238	200	168	141	119	100	84	70	59	50	42	35	29	25	21
5	4	3	3	2	2	1	1	1	1	0	0	0	0	0	0	0	0
RUN	6D	SUBRUN 1				DT= 0.20SECS(1ST 4 LINES) THEN				2.00SECS(LAST 2 LINES)							
0	0	0	0	0	0	0	0	0	0	0	0	0	0	0	0	0	0
533	594	643	679	702	763	814	852	880	895	930	957	975	985	987	990	989	985
906	893	877	857	834	806	783	765	751	743	741	736	728	717	702	700	695	687
583	580	580	583	590	588	583	575	564	549	531	515	503	494	488	487	482	474
335	305	234	203	172	146	124	106	90	76	65	55	46	39	33	28	24	20
5	4	4	3	2	2	2	1	1	1	1	0	0	0	0	0	0	0
RUN	6D	SUBRUN 2				DT= 0.20SECS(1ST 4 LINES) THEN				2.00SECS(LAST 2 LINES)							
0	0	0	0	0	0	0	0	0	0	0	0	0	0	0	0	0	0
652	664	687	724	772	819	862	899	930	957	967	975	982	986	990	982	973	962
878	873	866	858	848	831	813	796	778	761	751	743	736	731	728	718	710	704
640	634	626	614	598	579	562	547	533	522	514	505	494	482	467	449	432	416
337	261	239	195	166	141	120	102	86	73	62	53	45	38	32	27	23	19
5	4	3	3	2	2	2	1	1	1	1	0	0	0	0	0	0	0
RUN	6E	SUBRUN 1				DT= 0.20SECS(1ST 4 LINES) THEN				2.00SECS(LAST 2 LINES)							
0	0	0	0	0	0	0	0	0	0	0	0	0	0	0	0	0	0
506	601	687	764	832	875	907	927	936	933	946	957	965	972	976	985	990	985
945	938	926	910	890	871	854	840	828	818	806	795	783	772	760	756	750	741
670	664	655	644	631	620	608	597	585	574	561	550	541	535	531	534	533	527
358	287	258	222	190	163	140	120	103	88	75	64	55	47	40	35	30	25
7	6	5	4	4	3	2	2	2	1	1	1	1	1	0	0	0	0
RUN	6E	SUBRUN 2				DT= 0.20SECS(1ST 4 LINES) THEN				2.00SECS(LAST 2 LINES)							
0	0	0	0	0	0	0	0	0	0	0	0	0	0	0	0	0	0
576	632	676	707	725	730	741	757	779	806	825	843	860	874	886	906	924	940
986	990	990	986	978	981	980	976	967	955	958	957	953	944	932	908	885	865
785	776	767	757	748	739	730	720	711	702	690	675	659	641	621	608	594	580
414	333	264	230	197	169	145	124	106	91	78	67	57	49	42	36	31	26
7	6	5	4	4	3	3	2	2	1	1	1	1	1	0	0	0	0

Table A3 (continued)

RUN 10B , SUBRUN 1 , DT=				0.10SECS(1ST 4 LINES)				THEN				1.00SECS(LAST 2 LINES)											
0	0	0	0	0	0	0	0	0	0	0	0	0	0	0	0	0	0	0	0	0	0		
0	0	0	0	0	0	0	0	0	10	29	54	84	121	163	219	275	330	384	438	490	542		
753	807	854	894	927	953	972	984	989	988	983	976	968	959	947	934	919	903	885	866	825	786		
652	623	597	572	550	526	504	481	459	438	416	396	375	355	336	321	306	292	278	264	251	239		
145	101	73	61	52	45	40	35	32	28	25	23	20	18	16	15	13	12	11	9	8	7		
5	4	4	3	3	3	2	2	2	2	1	1	1	1	1	1	1	0	0	0	0	0		
RUN 10B , SUBRUN 2 , DT=				0.10SECS(1ST 4 LINES)				THEN				1.00SECS(LAST 2 LINES)											
0	0	0	0	0	0	0	0	0	0	0	0	0	0	0	0	0	0	0	0	0	0		
0	0	0	0	0	0	0	0	0	0	33	78	134	201	280	340	398	454	508	560	609	657		
832	870	904	931	954	971	982	989	989	985	962	937	910	881	850	817	782	744	705	663	639	615		
513	486	459	432	404	387	370	353	337	321	306	291	276	262	248	202	173	163	170	197	241	304		
280	82	10	62	53	46	42	41	37	33	30	27	24	21	19	17	15	14	12	11	10	9		
6	5	4	4	3	3	3	2	2	2	2	1	1	1	1	1	1	0	0	0	0	0		
RUN 10C , SUBRUN 1 , DT=				0.10SECS(1ST 4 LINES)				THEN				1.00SECS(LAST 2 LINES)											
0	0	0	0	0	0	0	0	0	0	0	0	0	0	0	0	0	0	0	0	0	0		
8	20	35	53	74	107	145	188	236	289	348	412	481	555	635	720	793	855	905	944	970	986		
951	940	931	923	915	909	905	901	898	897	895	893	889	884	878	871	863	853	843	831	810	789		
724	711	700	690	682	682	680	674	665	654	639	622	601	577	551	529	509	490	473	457	443	431		
294	214	163	140	114	93	77	65	59	53	48	44	39	36	32	29	26	24	22	19	18	16		
11	9	9	8	7	6	6	5	4	4	4	3	3	3	2	2	2	2	1	1	1	1		
RUN 10C , SUBRUN 2 , DT=				0.10SECS(1ST 4 LINES)				THEN				1.00SECS(LAST 2 LINES)											
0	0	0	0	0	0	0	0	0	0	0	0	0	0	0	0	0	0	0	0	41	83		
263	311	360	410	461	505	550	595	641	687	733	780	827	875	922	938	952	963	972	979	983	986		
982	984	986	987	988	989	990	990	989	988	990	987	982	973	960	944	925	902	876	840	830	813		
745	728	711	695	678	660	643	626	609	593	577	562	546	532	517	511	504	496	488	487	471	462		
322	235	171	131	111	94	80	70	63	57	52	47	43	38	35	31	28	26	23	21	19	17		
11	10	9	8	8	7	6	5	5	4	4	4	3	3	2	2	2	2	2	1	1	1		
RUN 10D , SUBRUN 1 , DT=				0.10SECS(1ST 4 LINES)				THEN				1.00SECS(LAST 2 LINES)											
0	0	0	0	0	0	0	0	0	0	0	0	0	0	0	0	0	0	0	0	22	50		
217	273	334	401	474	574	663	741	808	864	909	942	964	976	976	981	984	987	989	990	989	987		
959	944	930	918	906	895	886	877	870	864	858	851	842	833	822	810	793	784	769	752	730	708		
640	628	616	607	599	591	582	574	566	557	549	541	532	524	515	505	495	487	480	474	469	465		
359	278	216	174	148	125	106	90	81	73	65	59	53	47	42	38	34	31	28	25	22	20		
13	11	10	9	8	7	7	6	5	5	4	4	3	3	2	2	2	2	1	1	1	1		
RUN 10D , SUBRUN 2 , DT=				0.10SECS(1ST 4 LINES)				THEN				1.00SECS(LAST 2 LINES)											
0	0	0	0	0	0	0	0	0	0	0	0	0	0	0	0	0	0	0	0	26	54		
186	224	263	304	348	388	430	474	520	568	618	669	723	778	835	869	899	924	945	963	976	984		
969	952	936	920	905	890	875	861	848	835	836	836	834	829	823	815	806	794	781	765	748	731		
669	655	641	627	614	609	603	596	588	580	570	559	548	535	522	503	485	469	454	440	428	418		
333	278	229	185	153	127	107	92	83	75	67	60	54	48	44	39	35	31	28	25	23	20		
13	12	11	9	8	7	7	6	5	5	4	4	3	3	3	2	2	2	1	1	1	1		
RUN 10E , SUBRUN 1 , DT=				0.10SECS(1ST 4 LINES)				THEN				1.00SECS(LAST 2 LINES)											
0	0	0	0	0	0	0	0	0	0	0	0	0	0	0	0	0	0	0	0	43	92		
325	393	466	542	623	632	644	660	679	702	729	760	794	831	872	903	937	960	976	986	989	987		
922	905	889	874	861	849	839	830	822	816	792	770	749	731	714	699	686	674	665	657	648	639		
603	594	585	575	566	562	557	550	542	532	521	509	496	481	464	458	451	444	437	430	424	417		
323	260	209	170	145	124	106	90	81	73	65	59	53	47	43	38	34	31	28	25	22	20		
13	11	10	9	8	7	7	6	5	5	4	4	3	3	2	2	2	2	1	1	1	1		
RUN 10E , SUBRUN 2 , DT=				0.10SECS(1ST 4 LINES)				THEN				1.00SECS(LAST 2 LINES)											
0	0	0	0	0	0	0	0	0	0	0	0	0	0	0	0	0	0	0	0	98	190		
482	537	585	626	659	698	734	768	800	829	857	882	904	925	943	958	969	979	985	989	990	988		
952	939	925	911	898	884	870	857	843	829	823	815	806	796	784	771	756	740	723	704	695	684		
633	618	603	586	568	551	535	519	503	488	474	460	446	433	420	408	398	389	381	375	370	366		
301	250	210	181	150	125	105	90	81	73	66	59	53	47	43	38	34	31	28	25	22	20		
13	11	10	9	8	7	7	6	5	5	4	4	3	3	3	2	2	2	1	1	1	1		



Table A3 (continued)

RUN 20B , SUBRUN 1 , DT=					0.02SECS(1ST 4 LINES)					THEN					0.20SECS(LAST 2 LINES)									
0	0	0	0	0	0	0	0	0	0	0	0	0	0	0	0	0	0	0	0	0				
0	0	0	0	0	0	0	0	0	0	0	0	0	0	0	13	28	44	61	80	100				
219	247	275	306	337	370	404	440	476	514	532	550	567	585	603	620	638	656	673	691	709				
797	815	833	850	868	885	901	915	928	940	951	960	968	975	980	985	988	989	990	989	986				
868	755	707	578	482	402	321	273	225	192	168	146	127	110	96	84	75	69	65	64	61				
45	41	38	35	32	30	28	26	24	23	22	20	19	18	17	16	15	14	13	12	11				
100	121	144	167	192	219	247	275	306	337	370	404	440	476	514	532	550	567	585	603	620				
709	726	744	762	779	797	815	833	850	868	885	901	915	928	940	951	960	968	975	980	985				
986	983	978	972	964	951	940	928	915	901	885	868	850	833	815	797	755	707	578	482	402				
61	57	54	51	48	45	41	38	35	32	30	28	26	24	23	22	20	19	18	17	16				
11	11	10	9	9	9	9	9	9	9	9	9	9	9	9	9	9	9	9	9	9				
RUN 20B , SUBRUN 2 , DT=					0.02SECS(1ST 4 LINES)					THEN					0.20SECS(LAST 2 LINES)									
0	0	0	0	0	0	0	0	0	0	0	0	0	0	0	0	0	0	0	0	0				
0	0	0	0	0	0	0	0	0	0	0	0	0	0	0	0	7	18	30	44	61				
204	236	269	305	343	382	424	469	515	563	585	605	626	647	667	687	706	726	745	764	783				
872	889	906	923	939	949	958	966	973	978	983	986	988	990	989	988	986	982	978	972	965				
814	714	588	513	426	350	300	263	213	187	165	146	128	113	100	89	80	74	70	68	64				
47	44	41	39	37	35	33	31	29	27	25	24	22	21	20	18	17	16	15	14	13				
79	100	123	148	175	204	236	269	305	343	382	424	469	515	563	585	605	626	647	667	687				
645	671	696	720	744	764	783	801	819	837	855	872	889	906	923	939	949	958	966	973	978				
965	957	948	938	927	914	901	889	872	855	837	819	801	783	764	744	720	696	671	645	619				
64	60	56	53	50	47	44	41	39	37	35	33	31	29	27	25	24	22	21	20	18				
13	12	12	11	10	9	9	9	9	9	9	9	9	9	9	9	9	9	9	9	9				
RUN 20C , SUBRUN 1 , DT=					0.02SECS(1ST 4 LINES)					THEN					0.20SECS(LAST 2 LINES)									
0	0	0	0	0	0	0	0	0	0	0	0	0	0	0	0	0	0	0	0	0				
0	0	0	0	0	0	1	3	5	7	9	12	15	18	22	26	37	49	61	74	87				
173	189	205	221	238	256	273	292	310	329	360	391	421	451	480	509	537	565	592	619	645				
768	790	813	835	856	873	889	904	918	930	941	952	960	968	975	980	984	987	989	990	989				
896	777	685	606	513	434	368	303	263	224	198	174	153	134	118	104	93	83	76	72	67				
49	46	44	41	39	36	34	32	29	27	26	24	22	21	19	18	17	16	14	13	13				
100	114	128	143	158	173	189	205	221	238	256	273	292	310	329	360	391	421	451	480	509				
645	671	696	720	744	768	790	813	835	856	873	889	904	918	930	941	952	960	968	975	980				
989	987	984	980	975	968	956	941	924	907	889	873	856	835	813	790	768	744	720	696	671				
67	63	59	56	52	49	46	44	41	39	36	34	32	29	27	26	24	22	21	19	18				
13	12	11	10	9	9	9	9	9	9	9	9	9	9	9	9	9	9	9	9	9				
RUN 20C , SUBRUN 2 , DT=					0.02SECS(1ST 4 LINES)					THEN					0.20SECS(LAST 2 LINES)									
0	0	0	0	0	0	0	0	0	0	0	0	0	0	0	0	0	0	0	0	0				
0	0	0	0	0	0	2	6	10	14	19	25	31	38	45	53	91	127	163	197	229				
395	417	439	458	477	494	509	523	536	548	564	581	599	616	634	651	669	688	706	724	743				
839	859	878	899	919	922	926	929	933	936	940	944	947	951	954	958	961	965	968	972	975				
901	848	707	618	512	424	353	300	247	212	187	165	146	129	114	102	93	86	81	79	76				
58	54	51	47	44	41	38	35	33	31	29	27	25	23	22	20	19	17	16	15	14				
260	290	318	345	371	395	417	439	458	477	494	509	523	536	548	564	581	599	616	634	651				
743	762	781	800	819	839	859	878	899	919	922	926	929	933	936	940	944	947	951	954	958				
975	979	982	986	990	989	987	984	980	975	968	956	941	924	907	889	873	856	835	813	790				
76	72	68	65	61	58	54	51	47	44	41	38	35	33	31	29	27	25	23	22	20				
14	13	12	11	11	10	9	9	9	9	9	9	9	9	9	9	9	9	9	9	9				
RUN 20D , SUBRUN 1 , DT=					0.02SECS(1ST 4 LINES)					THEN					0.20SECS(LAST 2 LINES)									
0	0	0	0	0	0	0	0	0	0	0	0	0	0	0	0	0	0	0	0	0				
0	0	0	0	0	0	0	1	3	4	6	7	9	11	14	16	40	65	90	116	142				
309	339	369	399	431	462	494	527	560	593	610	626	643	659	676	692	709	725	742	758	775				
857	874	890	907	923	937	949	959	968	975	981	985	988	990	989	988	985	980	974	967	958				
824	742	610	527	445	379	329	263	230	197	172	150	130	113	98	87	77	71	67	65	62				
46	42	39	36	32	30	28	26	25	23	21	20	18	17	16	15	14	13	12	11	10				
168	196	223	251	280	309	339	369	399	431	462	494	527	560	593	610	626	643	659	676	692				
775	791	808	824	841	857	874	890	907	923	937	949	959	968	975	981	985	988	990	989	988				
958	947	935	922	907	890	874	857	841	824	808	791	775	758	742	725	709	709	725	742	758				
62	59	56	52	49	46	42	39	36	32	30	28	26	25	23	21	20	18	17	16	15				
10	10	9	9	8	8	9	9	9	9	9	9	9	9	9	9	9	9	9	9	9				
RUN 20D , SUBRUN 2 , DT=					0.02SECS(1ST 4 LINES)					THEN					0.20SECS(LAST 2 LINES)									
0	0	0	0	0	0	0	0	0	0	0	0	0	0	0	0	0	0	0	0	0				
0	0	0	0	0	0	0	0	0	0	0	0	0	0	0	0	2	5	10	16	23				
94	110	127	146	166	187	210	234	259	285	329	372	413	452	489	525	558	591	621	650	676				
785	801	816	829	840	858	874	890	904	917	929	940	950	959	967	973	979	983	986	988	990				
935	840	776	650	554	475	396	301	269	221	194	169	146	127	110	97	86	78	73	71	65				
43	40	37	34	31	29	27	25	24	22	20	19	18	16	15	14	13	12	12	11	10				
676	702	725	747	766	785	801	816	829	840	858	874	890	904	917	929	940	950	959	967	973				
990	989	988	986	983	979	975	969	961	952	940	926	911	895	878	861	844	826	808	789	770				
65	60	56	51	47	43	40	37	34	31	29	27	25	24	22	20	19	18	16	15	14				
10	9	9	8	7	10	9	9	9	9	9	9	9	9	9	9	9	9	9	9	9				
RUN 20E , SUBRUN 1 , DT=					0.02SECS(1ST 4 LINES)					THEN					0.20SECS(LAST 2 LINES)									
0	0	0	0	0	0	0	0	0	0	0	0	0	0	0	0	0	0	0	0	0				
0	0	0	0	0	0	0	0	0	0	0	0	0	0	0	0	0	0	0	0	0				
86	111	140	171	205	241	281	324	369	418	453	488	521	553	584	614	643	671	698	723	748				
852	870	887	902	916	925	934	942	950	956	962	968	973	977	980	983	986	987	988	989	988				
964	820	723	643	514	434	369	305	257	225	196	171	148	129	112	98	87	79	74	72	66				
44	40	37	34	32	30	28	26	24	22	21	19	18	17	16	15	14	13	12	11	10				
748																								



Table A4: U-functions for drying air R.T.D.

RUN 1A SUBRUN 1 ,S=0 TO .2938E+00											
-U0=	0.00000	0.89000	1.69300	2.43420	3.11330	3.74780	4.34790	4.92200	5.47500	6.01300	6.53900
U1=	31.79000	28.83000	26.20000	24.02000	22.29000	20.96000	19.94000	19.16000	18.56000	18.08000	17.70000
U2=	103.90000	96.17000	82.25000	66.33000	51.61000	39.51000	30.20000	23.25000	18.13000	14.35000	11.54000
RUN 1A SUBRUN 2 ,S=0 TO .2553E+00											
-U0=	0.00000	0.84900	1.62600	2.34000	3.00350	3.62580	4.21490	4.77700	5.31600	5.83600	6.34100
U1=	34.82000	31.77000	29.12000	26.92000	25.13000	23.68000	22.51000	21.54000	20.73000	20.05000	19.47000
U2=	125.20000	112.20000	95.07000	77.87000	62.93000	50.92000	41.60000	34.44000	28.89000	24.54000	21.05000
RUN 1B SUBRUN 1 ,S=0 TO .3327E+00											
-U0=	0.00000	0.89900	1.71300	2.45310	3.13230	3.76170	4.35100	4.90700	5.43600	5.94100	6.42700
U1=	23.35000	25.69000	23.30000	21.27000	19.61000	18.27000	17.18000	16.28000	15.53000	14.89000	14.34000
U2=	82.39000	76.77000	66.59000	55.16000	44.76000	36.27000	29.70000	24.67000	20.81000	17.78000	15.35000
RUN 1C SUBRUN 1 ,S=0 TO .3318E+00											
-U0=	0.00000	0.90200	1.72100	2.46600	3.15030	3.78500	4.37970	4.94200	5.47700	5.99000	6.48500
U1=	28.52000	25.88000	23.50000	21.48000	19.82000	18.48000	17.40000	16.51000	15.78000	15.16000	14.64000
U2=	81.55000	76.40000	66.61000	55.33000	44.86000	36.190	29.41000	24.20000	20.20000	17.09000	14.64000
RUN 1D SUBRUN 1 ,S=0 TO .4144E+00											
-U0=	0.00000	0.91000	1.72200	2.44750	3.10300	3.70450	4.26500	4.79400	5.29900	5.78400	6.25400
U1=	23.21000	20.74000	18.48000	16.59000	15.11000	13.97000	13.11000	12.45000	11.93000	11.52000	11.18000
U2=	60.08000	57.95000	50.44000	40.64000	31.31000	23.75000	18.11000	14.05000	11.14000	9.03700	7.49300
RUN 1E SUBRUN 1 ,S=0 TO .4431E+00											
-U0=	0.00000	0.89500	1.69700	2.41570	3.06770	3.66660	4.22400	4.74900	5.24800	5.72600	6.18700
U1=	21.31000	19.11000	17.10000	15.41000	14.07000	13.01000	12.19000	11.53000	11.01000	10.58000	10.22000
U2=	50.63000	48.20000	41.91000	34.16000	26.90000	20.98000	16.48000	13.14000	10.66000	8.79900	7.37200
RUN 1E SUBRUN 2 ,S=0 TO .4097E+00											
-U0=	0.00000	0.94600	1.80000	2.56920	3.26470	3.89900	4.48300	5.02700	5.53700	6.02000	6.48000
U1=	24.23000	21.95000	19.77000	17.83000	16.18000	14.83000	13.73000	12.84000	12.10000	11.49000	10.98000
U2=	55.21000	55.13000	50.77000	43.88000	36.43000	29.70000	24.14000	19.74000	16.30000	13.60000	11.47000
RUN 2A SUBRUN 1 ,S=0 TO .2938E+00											
-U0=	0.00000	0.89000	1.69800	2.43420	3.11330	3.74780	4.34790	4.92200	5.47500	6.01300	6.53900
U1=	31.79000	28.83000	26.20000	24.02000	22.29000	20.96000	19.94000	19.16000	18.56000	18.08000	17.70000
U2=	103.90000	96.17000	82.25000	66.33000	51.61000	39.51000	30.20000	23.25000	18.13000	14.35000	11.54000
RUN 2A SUBRUN 2 ,S=0 TO .2553E+00											
-U0=	0.00000	0.84900	1.62600	2.34000	3.00350	3.62580	4.21490	4.77700	5.31600	5.83600	6.34100
U1=	34.82000	31.77000	29.12000	26.92000	25.13000	23.68000	22.51000	21.54000	20.73000	20.05000	19.47000
U2=	125.20000	112.20000	95.07000	77.87000	62.93000	50.92000	41.60000	34.44000	28.89000	24.54000	21.05000
RUN 2B SUBRUN 1 ,S=0 TO .3738E+00											
-U0=	0.00000	0.92300	1.75300	2.50290	3.18570	3.81570	4.40400	4.96000	5.49000	5.99800	6.48800
U1=	25.99000	23.42000	21.07000	19.09000	17.50000	16.25000	15.27000	14.49000	13.86000	13.34000	12.90000
U2=	69.61000	66.63000	58.22000	47.65000	37.66000	29.49000	18.67000	15.27000	12.71000	10.75000	9.00000
RUN 2C SUBRUN 1 ,S=0 TO .3784E+00											
-U0=	0.00000	0.92700	1.76000	2.51180	3.19470	3.82300	4.40800	4.95900	5.48300	5.98500	6.46800
U1=	25.75000	23.23000	20.89000	18.89000	17.26000	15.98000	14.98000	14.18000	13.53000	13.01000	12.56000
U2=	67.12000	65.16000	57.76000	47.85000	38.10000	29.92000	23.59000	18.86000	15.34000	12.70000	10.69000
RUN 2C SUBRUN 2 ,S=0 TO .3274E+00											
-U0=	0.00000	0.90900	1.73700	2.49210	3.18700	3.83270	4.43800	5.01200	5.55800	6.08200	6.58600
U1=	29.10000	26.49000	24.11000	22.09000	20.42000	19.07000	17.97000	17.07000	16.32000	15.68000	15.13000
U2=	81.56000	76.90000	67.45000	56.29000	45.79000	37.05000	30.22000	25.01000	21.06000	18.03000	15.67000
RUN 2D SUBRUN 1 ,S=0 TO .3555E+00											
-U0=	0.00000	0.90800	1.72800	2.46980	3.14610	3.76800	4.34600	4.88700	5.39700	5.88000	6.33900
U1=	26.84000	24.26000	21.91000	19.89000	18.21000	16.84000	15.71000	14.75000	13.94000	13.23000	12.61000
U2=	73.97000	70.20000	61.81000	51.83000	42.57000	34.98000	29.12000	24.68000	21.27000	18.58000	16.40000
RUN 2D SUBRUN 2 ,S=0 TO .4146E+00											
-U0=	0.00000	0.90500	1.71300	2.43470	3.08250	3.66870	4.20300	4.69400	5.14800	5.57000	5.96300
U1=	23.01000	20.63000	18.40000	16.46000	14.84000	13.48000	12.34000	11.37000	10.54000	9.81200	9.17900
U2=	57.99000	56.29000	50.47000	42.95000	35.78000	29.85000	25.23000	21.65000	18.76000	16.34000	14.23000
RUN 2E SUBRUN 1 ,S=0 TO .3776E+00											
-U0=	0.00000	0.90000	1.71000	2.44160	3.10990	3.72760	4.30600	4.85200	5.37400	5.87500	6.35800
U1=	25.08000	22.60000	20.36000	18.48000	16.98000	15.80000	14.87000	14.12000	13.52000	13.02000	12.60000
U2=	67.26000	63.39000	54.81000	44.63000	35.25000	27.65000	21.89000	17.62000	14.45000	12.06000	10.23000
RUN 2E SUBRUN 2 ,S=0 TO .3815E+00											
-U0=	0.00000	0.89200	1.69500	2.41990	3.08090	3.69100	4.26100	4.79800	5.30800	5.79700	6.26700
U1=	24.63000	22.17000	19.96000	18.11000	16.61000	15.42000	14.48000	13.71000	13.08000	12.56000	12.11000
U2=	66.15000	61.95000	53.50000	43.77000	34.88000	27.70000	22.21000	18.10000	15.01000	12.66000	10.83000
RUN 3A SUBRUN 1 ,S=0 TO .2889E+00											
-U0=	0.00000	0.78600	1.50400	2.16950	2.79460	3.38830	3.95800	4.50700	5.04100	5.56100	6.07300
U1=	28.51000	25.93000	23.88000	22.28000	21.05000	20.09000	19.34000	18.74000	18.25000	17.85000	17.51000
U2=	98.28000	80.14000	62.71000	48.33000	37.34000	29.18000	23.16000	18.68000	15.29000	12.69000	10.66000
RUN 4A SUBRUN 1 ,S=0 TO .4611E+00											
-U0=	0.00000	0.75200	1.42730	2.04550	2.62070	3.16330	3.68100	4.17800	4.65900	5.12600	5.58200
U1=	17.26000	15.41000	13.97000	12.90000	12.09000	11.47000	10.92000	10.60000	10.27000	9.99800	9.76100
U2=	44.70000	35.55000	26.90000	20.09000	15.18000	11.77000	9.38000	7.68300	6.44500	5.51700	4.80500

Table A4 (continued)

RUN 5A SUBRUN ,S=0 TO .4859E+00											
-U0=	0.00000	0.75400	1.43700	2.06700	2.65650	3.21510	3.74950	4.26500	4.76500	5.25100	5.72800
U1=	16.36000	14.72000	13.46000	12.51000	11.79000	11.23000	10.79000	10.43000	10.14000	9.90400	9.70000
U2=	37.67000	29.61000	22.49000	17.00000	13.00000	10.14000	8.07400	6.55600	5.41500	4.54000	3.85600
RUN 5B SUBRUN ,S=0 TO .6069E+00											
-U0=	0.00000	0.80600	1.51300	2.15640	2.73890	3.27900	3.78700	4.27000	4.73300	5.18000	5.61500
U1=	14.16000	12.45000	11.07000	10.01000	9.21600	8.61100	8.14600	7.78200	7.49200	7.25000	7.06100
U2=	30.46000	25.51000	19.94000	15.11000	11.39000	8.68900	6.74300	5.33200	4.29300	3.51400	2.92100
RUN 5C SUBRUN ,S=0 TO .6057E+00											
-U0=	0.00000	0.81100	1.52500	2.16110	2.73930	3.27350	3.77360	4.24700	4.69800	5.13100	5.54300
U1=	14.31000	12.52000	11.08000	9.98300	9.15100	8.51500	8.01700	7.61700	7.28300	7.01200	6.77700
U2=	31.87000	26.73000	20.83000	15.75000	11.94000	9.22700	7.32000	5.95600	4.95300	4.19400	3.60300
RUN 5D SUBRUN ,S=0 TO .5680E+00											
-U0=	0.00000	0.81200	1.52900	2.17060	2.75510	3.29610	3.80300	4.28400	4.74200	5.18300	5.60800
U1=	15.25000	13.40000	11.90000	10.75000	9.87400	9.20400	8.67800	8.25500	7.90600	7.61300	7.36100
U2=	35.30000	29.66000	23.19000	17.61000	13.39000	10.38000	8.25100	6.72700	5.60900	4.76700	4.11700
RUN 5E SUBRUN ,S=0 TO .6224E+00											
-U0=	0.00000	0.82500	1.54700	2.18760	2.76800	3.30320	3.80420	4.27900	4.73200	5.16800	5.59000
U1=	14.19000	12.37000	10.89000	9.76400	8.92700	8.29900	7.81900	7.44100	7.13700	6.88600	6.67600
U2=	31.47000	26.70000	20.79000	15.55000	11.58000	8.76200	6.79700	5.41100	4.41300	3.67500	3.11600
RUN 6A SUBRUN 1 ,S=0 TO .5009E+00											
-U0=	0.00000	0.70500	1.35120	1.95100	2.51520	3.05150	3.56500	4.06100	4.54200	5.01000	5.46800
U1=	14.79000	13.44000	12.39000	11.59000	10.96000	10.47000	10.07000	9.74000	9.46700	9.23600	9.03800
U2=	30.30000	23.66000	18.21000	14.09000	11.07000	8.84700	7.20200	5.95900	5.00300	4.25600	3.66300
RUN 6A SUBRUN 2 ,S=0 TO .4475E+00											
-U0=	0.00000	0.68100	1.30900	1.89670	2.45210	2.98120	3.48800	3.97700	4.44900	4.90600	5.35100
U1=	15.90000	14.57000	13.55000	12.74000	12.10000	11.57000	11.11000	10.72000	10.38000	10.07000	9.79600
U2=	33.80000	26.01000	20.14000	15.97000	13.03000	10.93000	9.36800	8.17700	7.23700	6.47200	5.83300
RUN 6B SUBRUN 1 ,S=0 TO .5186E+00											
-U0=	0.00000	0.77600	1.47150	2.10180	2.68070	3.21900	3.72400	4.20300	4.65900	5.09600	5.51600
U1=	15.86000	14.14000	12.73000	11.62000	10.74000	10.04000	9.47200	8.99900	8.59800	8.25300	7.95200
U2=	35.98000	30.14000	24.12000	19.00000	15.05000	12.12000	9.96600	8.36100	7.14400	6.20000	5.45200
RUN 6B SUBRUN 2 ,S=0 TO .5899E+00											
-U0=	0.00000	0.77000	1.45400	2.07160	2.63690	3.16240	3.65700	4.12700	4.57600	5.02400	5.42900
U1=	13.88000	12.28000	10.98000	9.98400	9.21700	8.62400	8.15700	7.78200	7.47600	7.22200	7.00900
U2=	29.72000	24.62000	19.29000	14.80000	11.38000	8.87500	7.05500	5.71300	4.70600	3.93300	3.33100
RUN 6C SUBRUN 1 ,S=0 TO .5276E+00											
-U0=	0.00000	0.73500	1.39100	1.98790	2.53880	3.05380	3.54000	4.00200	4.44400	4.86700	5.27400
U1=	14.79000	13.12000	11.83000	10.84000	10.08000	9.47100	8.97600	8.55600	8.19100	7.86600	7.57300
U2=	35.19000	27.97000	21.38000	16.16340	12.77000	10.30000	8.59300	7.38300	6.50000	5.83300	5.31200
RUN 6C SUBRUN 2 ,S=0 TO .6110E+00											
-U0=	0.00000	0.77900	1.46900	2.08840	2.65340	3.17650	3.66700	4.13000	4.57200	4.99600	5.40400
U1=	13.59000	11.97000	10.66000	9.65300	8.87600	8.27100	7.79000	7.39900	7.07300	6.79800	6.56200
U2=	28.85000	24.01000	18.83000	14.46000	11.16000	8.77400	7.05900	5.80900	4.87600	4.16300	3.60500
RUN 6D SUBRUN 1 ,S=0 TO .6536E+00											
-U0=	0.00000	0.77600	1.45560	2.05700	2.59760	3.09060	3.54500	3.96900	4.36600	4.74000	5.09400
U1=	12.72000	11.09000	9.74700	8.69700	7.87800	7.23000	6.70200	6.26300	5.89000	5.56800	5.28800
U2=	26.98000	22.86000	18.17000	14.13000	11.08000	8.89100	7.32500	6.17200	5.28800	4.58000	3.99200
RUN 6D SUBRUN 2 ,S=0 TO .5863E+00											
-U0=	0.00000	0.76800	1.44900	2.06310	2.62500	3.14670	3.63700	4.10100	4.54400	4.96900	5.38000
U1=	13.93000	12.30000	11.00000	9.99000	9.21300	8.60700	8.12300	7.72800	7.39900	7.12100	6.88300
U2=	30.35000	25.02000	19.55000	15.02000	11.63000	9.18700	7.42000	6.11900	5.13600	4.37300	3.76700
RUN 6E SUBRUN 1 ,S=0 TO .6771E+00											
-U0=	0.00000	0.80300	1.50200	2.11970	2.67640	3.21900	3.66600	4.11700	4.54800	4.96200	5.36200
U1=	12.73000	11.04000	9.66400	8.62500	7.85700	7.28400	6.84700	6.50400	6.23000	6.00600	5.81900
U2=	26.96000	22.84000	17.69000	13.15000	9.73800	7.33900	5.67300	4.49800	3.64700	3.01500	2.53200
RUN 6E SUBRUN 2 ,S=0 TO .6128E+00											
-U0=	0.00000	0.78400	1.47500	2.09410	2.65890	3.18280	3.67500	4.14300	4.59200	5.02400	5.44300
U1=	13.65000	11.98000	10.64000	9.61600	8.85100	8.27200	7.82300	7.46600	7.17600	6.93500	6.73200
U2=	29.58000	24.65000	19.10000	14.36000	10.80000	8.26900	6.48800	5.21800	4.29200	3.59900	3.06800
RUN 7A SUBRUN ,S=0 TO .5659E+00											
-U0=	0.00000	0.65300	1.25000	1.80500	2.32880	2.82810	3.30760	3.77100	4.21900	4.65600	5.08200
U1=	12.17000	10.99000	1.01400	9.50900	9.02300	8.63600	8.31800	8.05000	7.82100	7.62100	7.44600
U2=	24.44000	17.59000	12.84000	9.69200	7.60000	6.16300	5.13300	4.36500	3.77100	3.29900	2.91300
RUN 8A SUBRUN ,S=0 TO .6751E+00											
-U0=	0.00000	0.61100	1.17200	1.69470	2.18860	2.65970	3.11200	3.54900	3.97200	4.38400	4.78600
U1=	9.53100	8.64200	7.99600	7.51200	7.13500	6.83100	6.57900	6.36600	6.18300	6.02400	5.88400
U2=	0.15430	0.11140	0.82070	0.62740	0.49780	0.40740	0.34140	0.29130	0.25200	0.22040	0.19460
RUN 9A SUBRUN 1 ,S=0 TO .7567E+00											
-U0=	0.00000	0.63900	1.21240	1.73840	2.22940	2.69140	3.13240	3.55440	3.96240	4.35740	4.74140
U1=	8.96600	7.96300	7.22900	6.68600	6.27300	5.94900	5.68800	5.47200	5.29200	5.13900	5.00800
U2=	15.36000	11.30000	8.27500	6.20100	4.79600	3.82100	3.11800	2.59200	2.18400	1.86000	1.59800



Table A4 (continued)

RUN 10E SUBRUN 2 ,S=0 TO .1154E+01											
-U0=	0.00000	0.67200	1.24000	1.73510	2.18020	2.59020	2.97400	3.33900	3.68900	4.02600	4.35300
U1=	6.37800	5.31900	4.56500	4.04800	3.68300	3.43000	3.23800	3.09000	2.97100	2.87500	2.79400
U2=	10.54000	7.79200	5.38700	3.70100	2.61000	1.91100	1.45200	1.14000	0.92070	0.76120	0.64200
RUN 11A SUBRUN 1 ,S=0 TO .8529E+00											
-U0=	0.00000	0.59100	1.13300	1.64030	2.12190	2.58410	3.03100	3.46400	3.88700	4.30100	4.70600
U1=	7.31300	6.60900	6.12600	5.78100	5.52400	5.32100	5.15700	5.01800	4.90000	4.79600	4.70400
U2=	9.94300	6.77200	4.72500	3.45300	2.65100	2.12400	1.76000	1.49700	1.29800	1.14300	1.01900
RUN 13A SUBRUN 1 ,S=0 TO .1186E+01											
-U0=	0.00000	0.56250	1.07100	1.54190	1.98520	2.40710	2.81200	3.18200	3.58100	3.94900	4.30900
U1=	5.03700	4.48500	4.11000	3.84200	3.63900	3.47900	3.34800	3.23900	3.14600	3.06600	2.99600
U2=	5.66900	3.78100	2.63400	1.94300	1.50600	1.21200	1.00200	0.84560	0.72520	0.63050	0.55460
RUN 14A SUBRUN 1 ,S=0 TO .1433E+01											
-U0=	0.00000	0.56400	1.07520	1.55410	2.01040	2.45010	2.87700	3.29200	3.69900	4.09700	4.48900
U1=	4.17800	3.72300	3.44100	3.25500	3.12200	3.02000	2.93700	2.86800	2.80800	2.75700	2.71100
U2=	4.03200	2.45700	1.56600	1.08000	0.80490	0.63670	0.52510	0.44530	0.38470	0.33670	0.29750
RUN 14A SUBRUN 2 ,S=0 TO .1590E+01											
-U0=	0.00000	0.57320	1.06860	1.50660	1.89690	2.24330	2.54700	2.80900	3.03100	3.21600	3.36900
U1=	3.91500	3.33000	2.92000	2.59800	2.31400	2.04400	1.77800	1.52000	1.27600	1.05600	0.86480
U2=	4.43200	3.02400	2.23100	1.86600	1.72800	1.68500	1.65300	1.58600	1.46500	1.29900	1.10600
RUN 14B SUBRUN 1 ,S=0 TO .1248E+01											
-U0=	0.00000	0.55000	1.06800	1.56670	2.05220	2.52800	2.99610	3.45800	3.91300	4.36300	4.80800
U1=	4.56900	4.25700	4.06100	3.93700	3.85000	3.78100	3.72400	3.67400	3.62800	3.58500	3.54500
U2=	3.57400	2.01600	1.21800	0.81690	0.60930	0.45940	0.42790	0.38440	0.35390	0.33070	0.31210
RUN 14B SUBRUN 2 ,S=0 TO .1214E+01											
-U0=	0.00000	0.56400	1.08700	1.58610	2.06860	2.48550	3.00090	3.45400	3.90000	4.33900	4.77200
U1=	4.89200	4.44900	4.19400	4.03500	3.92400	3.83800	3.76700	3.70300	3.64600	3.59200	3.54100
U2=	4.80200	2.71100	1.61600	1.06700	0.70790	0.63780	0.55070	0.49580	0.45820	0.43060	0.40950
RUN 14C SUBRUN 1 ,S=0 TO .1244E+01											
-U0=	0.00000	0.54200	1.05500	1.54990	2.03020	2.49860	2.95570	3.40100	3.83400	4.25100	4.65100
U1=	4.51600	4.22400	4.04200	3.91400	3.81200	3.72000	3.62900	3.53100	3.42100	3.29100	3.13000
U2=	3.03400	1.80600	1.19100	0.89620	0.76600	0.72670	0.74850	0.82380	0.95700	1.15800	1.43500
RUN 14C SUBRUN 2 ,S=0 TO .1304E+01											
-U0=	0.00000	0.52900	1.03650	1.52990	2.01260	2.48640	2.95300	3.41200	3.86400	4.31100	4.75200
U1=	4.16800	3.96200	3.83200	3.73900	3.66500	3.60300	3.54700	3.49500	3.44700	3.40300	3.36100
U2=	2.02500	1.22200	0.82350	0.62280	0.51540	0.45230	0.41050	0.37920	0.35330	0.33040	0.30950
RUN 14D SUBRUN 1 ,S=0 TO .1295E+01											
-U0=	0.00000	0.53600	1.04680	1.54100	2.02330	2.49580	2.96000	3.41700	3.86600	4.30900	4.74500
U1=	4.28300	4.02800	3.87300	3.78700	3.68500	3.61600	3.55500	3.49800	3.44400	3.39300	3.34400
U2=	2.57100	1.49400	0.96360	0.70360	0.57130	0.49900	0.45520	0.42560	0.40340	0.38520	0.36940
RUN 14D SUBRUN 2 ,S=0 TO .1351E+01											
-U0=	0.00000	0.55200	1.06950	1.56730	2.05230	2.52770	2.99500	3.45500	3.90800	4.35500	4.79600
U1=	4.27900	3.93200	3.74600	3.63300	3.55300	3.48900	3.43200	3.38000	3.33200	3.28500	3.24100
U2=	3.51600	1.82300	1.03400	0.68140	0.52040	0.44170	0.39860	0.37130	0.35110	0.33410	0.31880
RUN 14E SUBRUN 1 ,S=0 TO .1345E+01											
-U0=	0.00000	0.54300	1.05050	1.53380	1.99960	2.45090	2.89000	3.31700	3.73400	4.14200	4.54100
U1=	4.22700	3.88400	3.67200	3.52400	3.40700	3.30700	3.21900	3.13900	3.06500	2.99800	2.93600
U2=	3.31000	1.95000	1.28500	0.96110	0.79270	0.69300	0.62420	0.56970	0.52240	0.47930	0.43910
RUN 14E SUBRUN 2 ,S=0 TO .1267E+01											
-U0=	0.00000	0.54900	1.06060	1.54750	2.01570	2.46850	2.90700	3.33300	3.74700	4.14800	4.53700
U1=	4.53200	4.16400	3.93100	3.76400	3.63200	3.51800	3.41300	3.31300	3.21600	3.12000	3.02400
U2=	3.68600	2.25800	1.51800	1.14800	0.95930	0.85990	0.80550	0.77530	0.76020	0.75600	0.76110
RUN 15A SUBRUN 1 ,S=0 TO .1447E+01											
-U0=	0.00000	0.54570	1.04480	1.51310	1.95930	2.38900	2.80400	3.20900	3.60300	3.99000	4.36900
U1=	3.98200	3.58500	3.32900	3.15100	3.01900	2.91500	2.83000	2.75900	2.69700	2.64300	2.59600
U2=	3.42800	2.16400	1.44700	1.04200	0.80070	0.64520	0.53740	0.45790	0.39650	0.34750	0.30740
RUN 16A SUBRUN 1 ,S=0 TO .1513E+01											
-U0=	0.00000	0.55960	1.07160	1.55350	2.01470	2.46000	2.89300	3.31500	3.72800	4.13300	4.53100
U1=	3.91000	3.51400	3.27000	3.10900	2.99100	2.89900	2.82300	2.75800	2.70100	2.65000	2.60400
U2=	3.34600	2.01200	1.28300	0.89380	0.67750	0.54760	0.46240	0.40170	0.35540	0.31820	0.28730
RUN 16A SUBRUN 2 ,S=0 TO .1563E+01											
-U0=	0.00000	0.55770	1.06530	1.54110	1.99500	2.43200	2.85700	-0.62400	3.67400	4.07000	4.45900
U1=	3.78400	3.38100	3.13200	2.96700	2.84700	2.75300	2.67700	2.61300	2.55800	2.51000	2.46700
U2=	3.27800	1.98900	1.27300	0.88660	0.66800	0.53380	0.44400	0.37900	0.32900	0.28890	0.25570
RUN 16B SUBRUN 1 ,S=0 TO .1512E+01											
-U0=	0.00000	0.562100	1.067600	1.535500	9.68200	10.10300	10.50800	10.90000	11.28000	11.65100	12.01400
U1=	3.96400	3.50400	3.20300	2.99600	2.84400	2.72700	2.63100	2.55200	2.48400	2.42500	2.37400
U2=	3.76700	2.42800	1.62200	1.15500	0.87460	0.69520	0.57250	0.48340	0.41580	0.36260	0.31960
RUN 16B SUBRUN 2 ,S=0 TO .1750E+01											
-U0=	0.00000	0.55840	1.05970	1.52430	1.96410	2.38410	2.79110	3.18510	3.57010	3.94710	4.31610
U1=	3.41200	3.00300	2.74600	2.57500	2.45300	2.36100	2.28700	2.22600	2.17400	2.13100	2.09200
U2=	2.93700	1.82500	1.17500	0.81150	0.60020	0.46890	0.38090	0.31790	0.27050	0.23330	0.20330

Table A4 (continued)

RUN 16C SUBRUN 1 ,S=0 TO .1601E+01											
-U0=	0.00000	0.54160	1.04390	1.51940	1.97550	2.41450	2.84050	3.25550	3.65950	4.05450	4.44150
U1=	3.54600	3.24200	3.04400	2.90200	2.79200	2.70200	2.62400	2.55500	2.49400	2.43900	2.39000
U2=	2.37300	1.50000	1.02600	0.76750	0.61740	0.52170	0.45440	0.40290	0.36110	0.32560	0.29480
RUN 16C SUBRUN 2 ,S=0 TO .1466E+01											
-U0=	0.00000	0.54490	1.05550	1.54400	2.01660	2.47660	2.92660	3.36860	3.80160	4.22760	4.64760
U1=	3.87700	3.58100	3.39700	3.27200	3.17800	3.10300	3.03800	2.98200	2.93100	2.88500	2.84300
U2=	2.57700	1.55500	1.01100	0.72540	0.56760	0.48800	0.41020	0.36440	0.32810	0.29780	0.27150
RUN 16D SUBRUN 1 ,S=0 TO .1484E+01											
-U0=	0.00000	0.53390	1.04260	1.53520	2.01590	2.48790	2.95090	3.40590	3.85490	4.29590	4.73190
U1=	3.71600	3.49800	3.36600	3.27600	3.20600	3.14700	3.09400	3.04500	2.99800	2.95500	2.91300
U2=	1.92500	1.10900	0.71380	0.52310	0.42740	0.37540	0.34360	0.32130	0.30360	0.28830	0.27420
RUN 16D SUBRUN 2 ,S=0 TO .1483E+01											
-U0=	0.00000	0.54710	1.06190	1.55640	2.03690	2.50490	2.96390	3.41290	3.85390	4.28590	4.71090
U1=	3.84300	3.56100	3.39300	3.28100	3.19600	3.12400	3.06000	3.00000	2.94300	2.88900	2.83800
U2=	2.48700	1.42800	0.90040	0.64530	0.51970	0.45410	0.41620	0.39100	0.37160	0.35500	0.33950
RUN 16E SUBRUN 1 ,S=0 TO .1532E+01											
-U0=	0.00000	0.54530	1.05810	1.55060	2.02830	2.49530	2.95330	3.40230	3.84330	4.27630	4.70330
U1=	3.70900	3.43500	3.27200	3.16300	3.08200	3.01500	2.95600	2.90300	2.85400	2.80800	2.76600
U2=	2.34500	1.34200	0.84340	0.59970	0.47580	0.40680	0.36340	0.33220	0.30720	0.28560	0.26630
RUN 16E SUBRUN 1 ,S=0 TO .1545E+00											
-U0=	0.00000	0.53430	1.03360	1.50820	1.96420	2.40520	2.83220	3.24720	3.65220	4.04820	4.43520
U1=	3.60700	3.33100	3.14500	3.00800	2.89900	2.80700	2.72700	2.65500	2.59100	2.53200	2.47900
U2=	2.22600	1.43400	1.01300	0.78160	0.64420	0.55410	0.48910	0.43860	0.39700	0.36160	0.33060
RUN 17A SUBRUN 1 ,S=0 TO .1779E+00											
-U0=	0.00000	0.54190	1.03790	1.50490	1.95190	2.38290	2.80090	3.20690	3.60390	3.99190	4.37190
U1=	3.22500	2.89600	2.69600	2.56200	2.46300	2.38300	2.31600	2.25700	2.20400	2.15700	2.11400
U2=	2.39900	1.40800	0.89540	0.63500	0.49390	0.40930	0.35290	0.31180	0.27970	0.25340	0.23120
RUN 17A SUBRUN 2 ,S=0 TO .1713E+01											
-U0=	0.00000	0.55230	1.05230	1.51930	1.96430	2.39330	2.81030	3.21630	3.61330	4.00230	4.38430
U1=	0.34450	3.04500	2.80700	2.65500	2.54800	2.46600	2.39900	0.23430	2.29400	2.25000	2.21100
U2=	0.30240	1.76500	1.08400	0.73020	0.53910	0.42710	0.35550	0.30590	0.26930	0.24100	0.21830
RUN 17B SUBRUN 1 ,S=0 TO .1682E+00											
-U0=	0.00000	0.53800	1.03300	1.50100	1.94900	2.38100	2.80100	-0.38550	3.61000	4.00200	4.38600
U1=	0.33760	3.05300	2.85200	2.71500	2.61400	2.53200	2.46400	0.24050	2.35300	2.30600	2.26400
U2=	0.24650	1.48200	0.96290	0.68890	0.53430	0.43890	0.37460	0.32830	0.29320	0.26560	0.24340
RUN 17B SUBRUN 2 ,S=0 TO .1833E+00											
-U0=	0.00000	0.53580	1.02080	1.47280	1.89980	2.30880	2.70080	-0.27170	3.44780	3.80580	4.15480
U1=	0.31070	2.76400	2.54500	2.39300	2.27700	2.18300	2.10400	0.20370	1.97800	1.92600	1.87900
U2=	0.23610	1.46300	0.97800	0.71580	0.56300	0.46470	0.39570	0.34360	0.30240	0.26870	0.24030
RUN 17C SUBRUN 1 ,S=0 TO .1753E+00											
-U0=	0.00000	0.54200	1.04800	1.53300	2.00400	2.46500	2.91800	3.36400	3.80300	4.23700	4.66500
U1=	3.24300	2.96800	2.81700	2.72300	2.65800	2.60600	2.56300	2.52400	2.48900	2.45600	2.42600
U2=	2.11900	1.13200	0.65670	0.43430	0.32560	0.26750	0.23290	0.20990	0.19290	0.17950	0.16830
RUN 17C SUBRUN 2 ,S=0 TO .1779E+01											
-U0=	0.00000	0.54030	1.03030	1.48830	1.92230	2.33830	2.74030	3.13030	3.51030	3.88030	4.24330
U1=	3.23300	2.87500	2.65100	2.49900	2.38600	2.29700	2.22400	2.16100	2.10800	2.06100	2.02100
U2=	2.57800	1.55700	1.01300	0.72420	0.55830	0.45250	0.37850	0.32300	0.27970	0.24480	0.21620
RUN 17D SUBRUN 1 ,S=0 TO .1807E+01											
-U0=	0.00000	0.54580	1.05180	1.53280	1.99880	2.45180	2.89480	3.32880	3.75380	4.16980	4.57880
U1=	3.19000	2.88700	2.72000	2.61600	2.54000	2.49700	2.42500	2.37500	2.32900	2.28400	2.24200
U2=	2.26600	1.20900	0.70540	0.47660	0.36990	0.31610	0.28560	0.26370	0.25090	0.23840	0.22710
RUN 17D SUBRUN 2 ,S=0 TO .1758E+01											
-U0=	0.00000	0.52200	1.02400	1.51400	1.99300	2.46600	2.93100	3.39100	3.84400	4.29300	4.73600
U1=	3.05700	2.90300	2.81400	2.75400	2.70700	2.66700	2.63000	2.59700	2.56600	2.53600	2.50800
U2=	1.18100	0.64210	0.40340	0.29620	0.24410	0.21550	0.19700	0.18350	0.17240	0.16280	0.15410
RUN 17E SUBRUN 1 ,S=0 TO .2207E+01											
-U0=	0.00000	0.53340	1.03590	1.52080	1.99330	2.45580	2.90880	3.35380	3.79180	4.22080	4.64380
U1=	2.52400	2.33200	2.23100	2.16700	2.11700	2.07400	2.03500	1.99800	1.96300	1.93000	1.89800
U2=	1.22000	0.60510	0.34940	0.24800	0.20570	0.18500	0.17220	0.16250	0.15410	0.14650	0.13950
RUN 17E SUBRUN 2 ,S=0 TO .1971E+01											
-U0=	0.00000	0.53530	1.03720	1.51940	1.98820	2.44700	2.89600	3.33800	3.77300	4.20100	4.62300
U1=	2.84500	2.61600	2.49000	2.41000	2.35100	2.30300	2.26100	2.22300	2.18800	2.15700	2.12700
U2=	1.58200	0.83380	0.49190	0.33900	0.26600	0.22640	0.20120	0.18290	0.16810	0.15570	0.14480
RUN 18A SUBRUN ,S=0 TO .1815E+01											
-U0=	0.00000	0.53460	1.01800	1.46830	1.89510	2.30400	2.69800	3.08100	3.45300	3.81600	4.17200
U1=	3.13500	2.78200	2.56000	2.40900	2.29800	2.21000	2.13800	2.07700	2.02500	1.97900	1.93900
U2=	2.46900	1.51200	0.98830	0.70390	0.53910	0.43480	0.36290	0.30990	0.26870	0.23560	0.20830
RUN 19A SUBRUN ,S=0 TO .2288E+01											
-U0=	0.00000	0.52920	1.01860	1.48470	1.93500	2.37300	2.80100	3.21900	3.63000	4.03300	4.43000
U1=	2.43900	2.20800	2.08000	1.99900	1.93900	1.89100	1.84900	1.81100	1.77800	1.74700	1.71900
U2=	1.37500	0.72640	0.43030	0.29720	0.23220	0.19560	0.17170	0.15400	0.13990	0.12800	0.11780

Table A4 (continued)

RUN 20A SUBRUN 1 ,S=0 TO .2861E+01											
-U0=	0.00000	0.54160	1.00830	1.43110	1.82440	2.19540	2.54840	2.88640	3.21140	3.52540	3.83040
U1=	2.08600	1.73700	1.54300	1.42100	1.33200	1.26300	1.20600	1.15800	1.11700	1.08200	1.05100
U2=	1.63700	0.88250	0.52010	0.35520	0.27020	0.21820	0.18190	0.15460	0.13310	0.11570	0.10140
RUN 20A SUBRUN 2 ,S=0 TO .3020E+01											
-U0=	0.00000	0.54100	0.99920	1.40980	1.78870	2.14370	2.48070	2.80270	3.11170	3.40970	3.69970
U1=	1.99400	1.62700	1.42600	1.30100	1.21200	1.14400	1.08900	1.04300	1.00500	0.97190	0.94370
U2=	1.63200	0.87290	0.50660	0.34080	0.25490	0.20210	0.16540	0.13810	0.11700	0.10020	0.08670
RUN 20B SUBRUN 1 ,S=0 TO .3115E+01											
-U0=	0.00000	0.52930	0.99630	1.42630	1.83040	2.21540	2.58440	2.94040	3.28640	3.62240	3.95040
U1=	1.84700	1.58000	1.43100	1.33500	1.26500	1.20900	1.16300	1.12500	1.09300	1.06600	1.04300
U2=	1.16600	0.61740	0.37060	0.25950	0.19930	0.16120	0.13300	0.11120	0.09388	0.07987	0.06845
RUN 20B SUBRUN 2 ,S=0 TO .3147E+01											
-U0=	0.00000	0.52480	0.99730	1.41050	1.80500	2.17700	2.53200	2.87100	3.19700	3.51300	3.82000
U1=	1.80800	1.55100	1.39900	1.29500	1.21600	1.15200	1.10000	1.05600	1.02000	0.98860	0.96200
U2=	1.08100	0.60700	0.38900	0.28450	0.22390	0.18230	0.15100	0.12650	0.10700	0.09130	0.07853
RUN 20C SUBRUN 1 ,S=0 TO .3823E+01											
-U0=	0.00000	0.51500	0.96270	1.36840	1.74460	2.09760	2.43260	2.75260	3.06160	3.36160	3.65360
U1=	1.47500	1.24300	1.10900	1.01800	0.95070	0.89800	0.85630	0.82260	0.79520	0.77270	0.75390
U2=	0.81620	0.44320	0.28060	0.20230	0.15500	0.12210	0.09767	0.07914	0.06483	0.05366	0.04486
RUN 20C SUBRUN 2 ,S=0 TO .3689E+01											
-U0=	0.00000	0.52010	0.96970	1.37820	1.75900	2.11800	2.46100	2.79100	3.11000	3.41900	3.72200
U1=	1.55300	1.29500	1.15500	1.06500	1.00000	0.95030	0.91030	0.87790	0.85130	0.82910	0.81060
U2=	0.96470	0.49510	0.29270	0.20290	0.15340	0.12070	0.09715	0.07936	0.06560	0.05479	0.04617
RUN 20D SUBRUN 1 ,S=0 TO .3003E+01											
-U0=	0.00000	0.52590	0.99620	1.42870	1.83170	2.21170	2.56970	2.91170	3.23870	3.55270	3.85670
U1=	1.88000	1.64400	1.49700	1.38800	1.30000	1.22700	1.16500	1.11200	1.06600	1.02800	0.99400
U2=	1.02800	0.59660	0.41030	0.32140	0.26620	0.22470	0.19080	0.16280	0.13950	0.12020	0.10420
RUN 20D SUBRUN 2 ,S=0 TO .3244E+01											
-U0=	0.00000	0.53260	0.99060	1.40440	1.78720	2.14720	2.48720	2.81320	3.12520	3.42620	3.71920
U1=	1.81200	1.50400	1.33400	1.22400	1.14200	1.07700	1.02500	0.98110	0.94490	0.91430	0.88830
U2=	1.29300	0.67890	0.40800	0.28770	0.22210	0.17870	0.14670	0.12200	0.10240	0.08668	0.07394
RUN 20E SUBRUN 1 ,S=0 TO .3338E+01											
-U0=	0.00000	0.52240	0.97730	1.38980	1.77140	2.12940	2.46840	2.78940	3.09840	3.39440	3.68140
U1=	1.71100	1.44600	1.29100	1.18600	1.10600	1.04100	0.98740	0.94270	0.90520	0.87360	0.00000
U2=	1.06200	0.58420	0.37040	0.27130	0.21470	0.17580	0.14610	0.12240	0.10300	0.08701	0.07371
RUN 20E SUBRUN 2 ,S=0 TO .3272E+01											
-U0=	0.00000	0.52650	0.99380	1.42590	1.83360	2.22160	2.59460	2.95560	3.30660	3.64960	3.98560
U1=	1.74400	1.50100	1.36700	1.27900	1.21300	1.16200	1.12100	1.08700	1.06000	1.03700	1.01800
U2=	1.02100	0.52860	0.32110	0.22810	0.17570	0.14000	0.11330	0.09270	0.07652	0.06373	0.05354
RUN 21A SUBRUN 1 ,S=0 TO .2981E+01											
-U0=	0.00000	0.51260	0.97510	1.40750	1.81930	2.21600	2.60000	2.97400	3.34000	3.69900	4.05200
U1=	1.84200	1.62000	1.49400	1.41200	1.35400	1.30800	1.27100	1.24100	1.21500	1.19300	1.17400
U2=	1.00200	0.54350	0.32980	0.22750	0.17150	0.13630	0.11170	0.09351	0.07952	0.06849	0.05962
RUN 21A SUBRUN 2 ,S=0 TO .3009E+01											
-U0=	0.00000	0.51700	0.97480	1.39900	1.80150	2.18840	2.56340	2.92840	3.28540	3.63540	3.97940
U1=	1.86500	1.60000	1.45600	1.36900	1.30900	1.26400	1.22900	1.19900	1.17400	1.15300	1.13400
U2=	1.19700	0.62860	0.35910	0.23430	0.16990	0.13200	0.10700	0.08935	0.07619	0.06603	0.05797
RUN 21B SUBRUN 1 ,S=0 TO .3143E+01											
-U0=	0.00000	0.51210	0.96230	1.37660	1.76740	2.14100	2.50100	2.85100	3.19100	3.52300	3.84800
U1=	1.77700	1.51100	1.36600	1.27700	1.21400	1.16600	1.12800	1.09600	1.06900	1.04600	1.02500
U2=	1.14700	0.60610	0.35120	0.23330	0.17200	0.13520	0.11050	0.09275	0.07933	0.06887	0.06050
RUN 21B SUBRUN 2 ,S=0 TO .2836E+01											
-U0=	0.00000	0.51090	0.96980	1.39430	1.79330	2.17190	2.53290	2.87890	3.21290	3.53590	3.84790
U1=	1.92800	1.69500	1.55000	1.44800	1.36800	1.30200	1.24600	1.19800	1.15600	1.11900	1.08600
U2=	1.06700	0.62750	0.41850	0.31440	0.25400	0.01320	0.18260	0.15840	0.13850	0.12180	0.10760
RUN 21C SUBRUN 1 ,S=0 TO .2872E+01											
-U0=	0.00000	0.51710	0.97700	1.40320	1.80550	2.19000	2.55900	2.91600	3.26200	3.59900	3.83700
U1=	1.94200	1.68300	1.53400	1.43800	1.36700	1.31100	1.26400	1.22300	1.18800	1.15700	1.13000
U2=	1.20600	0.66250	0.40370	0.28170	0.21730	0.17800	0.15090	0.13070	0.11470	0.10170	0.09080
RUN 21C SUBRUN 2 ,S=0 TO .2702E+01											
-U0=	0.00000	0.51850	0.98280	1.41410	1.82280	2.21490	2.59290	2.95890	3.31690	3.66590	4.00790
U1=	2.06300	1.80000	1.64800	1.55000	1.47800	1.42300	1.37700	1.33900	1.30700	1.27800	1.25400
U2=	1.29400	0.71830	0.44020	0.30480	0.23090	0.18490	0.15310	0.12960	0.11150	0.09718	0.08549
RUN 21D SUBRUN 1 ,S=0 TO .2661E+01											
-U0=	0.00000	0.51440	0.98160	1.41870	1.83430	2.23340	2.61840	2.99140	3.35440	3.70940	4.05640
U1=	2.05800	1.83000	1.69200	1.59900	1.52800	1.47100	1.42400	1.38400	1.34900	1.31800	1.29200
U2=	1.12700	0.64590	0.41510	0.30040	0.23560	0.19370	0.16350	0.14040	0.12190	0.10690	0.09430
RUN 21D SUBRUN 2 ,S=0 TO .2691E+01											
-U0=	0.00000	0.52100	0.98500	1.41600	1.82400	2.21460	2.59200	2.95820	3.31470	3.66310	4.00410
U1=	2.08400	1.81000	1.65300	1.55300	1.48200	1.42600	1.38000	1.34200	1.30900	1.28000	1.25500
U2=	1.35800	0.74870	0.45120	0.30810	0.23200	0.18590	0.15470	0.13180	0.11410	0.10000	0.08850

Table A4 (continued)

RUN 21E SUBRUN 1 ,S=0 TO .2869E+01											
-U0=	0.00000	0.51200	0.99550	1.46120	1.91370	2.35570	2.78870	3.21470	3.63270	4.04370	4.44970
U1=	1.85800	1.72600	1.65000	1.59900	1.55800	1.52500	1.49500	1.46900	1.44600	1.42400	1.40500
U2=	0.62900	0.33330	0.21040	0.15600	0.12740	0.10930	0.09624	0.08607	0.07779	0.07085	0.06490
RUN 21E SUBRUN 2 ,S=0 TO .2890E+01											
-U0=	0.00000	0.52180	1.00120	1.45680	1.89620	2.32280	2.73980	3.14680	3.54680	3.93880	4.32480
U1=	1.91900	1.71700	1.61100	1.54600	1.49800	1.45900	1.42500	1.39600	1.37000	1.34700	1.32500
U2=	0.98200	0.48440	0.27610	0.18940	0.14810	0.12410	0.10770	0.09523	0.08516	0.07677	0.06963
RUN 22A SUBRUN ,S=0 TO .3086E+01											
-U0=	0.00000	0.51140	0.98060	1.42380	1.84850	2.25750	2.65450	3.04150	3.41750	3.78650	4.14750
U1=	1.75700	1.57600	1.47300	1.40300	1.35000	1.30600	1.26800	1.23600	1.20700	1.18100	1.15800
U2=	0.79700	0.42620	0.26560	0.19350	0.15540	0.13110	0.11330	0.09933	0.08783	0.07816	0.06991
RUN 23A SUBRUN ,S=0 TO .3700E+01											
-U0=	0.00000	0.51880	0.96980	1.38650	1.78170	2.16070	2.52670	2.88170	3.22770	3.56670	3.89870
U1=	1.55200	1.28800	1.16400	1.09400	1.04400	1.00500	0.97380	0.94730	0.92490	0.90590	0.88960
U2=	1.04200	0.46600	0.23930	0.15470	0.11650	0.09394	0.07797	0.06560	0.05563	0.04747	0.04072
RUN 24A SUBRUN ,S=0 TO .3605E+01											
-U0=	0.00000	0.49500	0.94250	1.36190	1.76250	2.14940	2.52440	2.88940	3.24640	3.59640	3.94040
U1=	1.47000	1.29500	1.19700	1.13500	1.09000	1.05500	1.02600	1.00200	0.98040	0.96150	0.94460
U2=	0.65280	0.35270	0.20940	0.14260	0.10790	0.08718	0.07335	0.06333	0.05564	0.04950	0.04442
RUN 25A SUBRUN ,S=0 TO .4254E+01											
-U0=	0.00000	0.50070	0.97700	1.43130	1.86560	2.28160	2.68160	3.06760	3.44160	3.80460	4.15960
U1=	1.21000	1.14700	1.09300	1.04300	0.99840	0.95840	0.92340	0.89280	0.86620	0.84310	0.82300
U2=	0.16920	0.13290	0.12180	0.11160	0.10000	0.08814	0.07699	0.06698	0.05820	0.05062	0.04411
RUN 26A SUBRUN ,S=0 TO .5099E+01											
-U0=	0.00000	0.50100	0.97840	1.43360	1.86760	2.28460	2.68560	3.07360	3.45060	3.81860	4.17860
U1=	1.00800	0.95880	0.91380	0.87160	0.83380	0.80110	0.77330	0.74970	0.72970	0.71270	0.69830
U2=	0.10870	0.08994	0.08612	0.07882	0.06913	0.05926	0.05027	0.04252	0.03600	0.03060	0.02615
RUN 27A SUBRUN ,S=0 TO .5127E+01											
-U0=	0.00000	0.49960	0.96990	1.41790	1.84790	2.25990	-2.05610	3.04290	3.41790	3.78290	4.13990
U1=	1.01500	0.94180	0.89460	0.85500	0.82000	0.78950	0.76310	0.74050	0.72110	0.70450	0.69010
U2=	0.20210	0.10590	0.08268	0.07259	0.06379	0.05534	0.04761	0.04082	0.03500	0.03008	0.02595
RUN 28A SUBRUN ,S=0 TO .5046E+01											
-U0=	0.00000	0.49320	0.95180	1.38680	1.80240	2.20240	2.58840	2.96240	3.32540	3.67940	4.02640
U1=	1.02800	0.93720	0.88340	0.84220	0.80750	0.77780	0.75210	0.72990	0.71060	0.69380	0.67910
U2=	0.25540	0.12960	0.09064	0.07433	0.06349	0.05467	0.04723	0.04092	0.03560	0.03109	0.02727

Table A5: U-functions for atomising air R.T.D.

RUN 1B SUBRUN 1, S=0 TO .5350E+00											
-U0=	0.00000	0.85400	1.61380	2.29420	2.91260	3.48400	4.01800	4.52300	5.00500	5.46800	5.91600
U1=	16.96000	15.04000	13.40000	12.09000	11.03000	10.30000	9.69400	9.21400	8.82500	8.50200	8.22900
U2=	37.46000	33.59000	27.59000	21.54000	16.52000	12.74000	10.01000	8.03900	6.59900	5.52500	4.70600
RUN 1B SUBRUN 2, S=0 TO .4463E+00											
-U0=	0.00000	0.86500	1.64080	2.34070	2.97910	3.56900	4.12100	4.64300	5.14000	5.61800	6.08000
U1=	20.46000	18.34000	16.48000	14.94000	13.72000	12.76000	12.00000	11.40000	10.92000	10.51000	10.17000
U2=	49.22000	45.09000	38.21000	30.79000	24.27000	18.98000	15.01000	12.07000	9.88400	8.25100	7.01400
RUN 1C SUBRUN 1, S=0 TO .3524E+00											
-U0=	0.00000	0.87600	1.66900	2.39050	3.05410	3.67160	4.25240	4.80400	5.33100	5.83900	6.32900
U1=	26.13000	23.63000	21.42000	19.59000	18.13000	16.96000	16.03000	15.28000	14.66000	14.15000	13.71000
U2=	73.91000	67.50000	57.33000	46.52000	37.00000	29.40000	23.61000	19.26000	15.97000	13.44000	11.47000
RUN 1C SUBRUN 2, S=0 TO .1594E+01											
-U0=	0.00000	0.89340	1.59740	2.19340	2.74140	3.27040	3.79040	4.30840	4.82340	5.33640	5.84840
U1=	6.33000	4.92700	4.00000	3.54700	3.35800	3.28400	3.25300	3.23700	3.22700	3.21800	3.20800
U2=	9.44000	7.56800	4.12200	1.80400	0.72040	0.28710	0.12800	0.07477	0.06012	0.05850	0.06044
RUN 1D SUBRUN 1, S=0 TO .4050E+00											
-U0=	0.00000	0.90700	1.72500	2.46350	3.13750	3.75960	4.34000	4.88800	5.40900	5.90300	6.38900
U1=	23.57000	21.26000	19.16000	17.39000	15.95000	14.81000	13.90000	13.17000	12.58000	12.08000	11.67000
U2=	58.39000	55.16000	47.99000	39.47000	31.54000	25.05000	20.04000	16.25000	13.37000	11.17000	9.44100
RUN 1D SUBRUN 2, S=0 TO .3754E+00											
-U0=	0.00000	0.89800	1.70940	2.44600	3.12140	3.74800	4.33600	4.89300	5.42400	5.93400	6.42600
U1=	25.17000	22.72000	20.55000	18.75000	17.29000	16.14000	15.21000	14.47000	13.85000	13.34000	12.90000
U2=	67.35000	62.12000	53.09000	43.22000	34.44000	27.40000	22.04000	18.00000	14.94000	12.60000	10.76000
RUN 1E SUBRUN 1, S=0 TO .4538E+00											
-U0=	0.00000	0.95100	1.80570	2.57050	3.25560	3.87300	4.43400	4.94800	5.42300	5.86700	6.28500
U1=	22.02000	19.89000	17.81000	15.93000	14.31000	12.94000	11.81000	10.88000	10.11000	9.47800	8.95500
U2=	46.50000	46.92000	43.91000	38.75000	32.92000	27.40000	22.60000	18.59000	15.31000	12.65000	10.48000
RUN 1E SUBRUN 2, S=0 TO .3556E+00											
-U0=	0.00000	0.87600	1.66300	2.37580	3.02840	3.63470	4.20500	4.74700	5.26600	5.76700	6.25300
U1=	26.00000	23.34000	21.02000	19.13000	17.65000	16.50000	15.61000	14.90000	14.33000	13.86000	13.46000
U2=	77.90000	70.91000	59.34000	47.06000	36.48000	28.27000	22.22000	17.81000	14.59000	12.19000	10.37000
RUN 2B SUBRUN 1, S=0 TO .4022E+00											
-U0=	0.00000	0.93600	1.77800	2.53670	3.22610	3.86110	4.45400	5.01400	5.54800	6.06100	6.55800
U1=	24.49000	22.07000	19.84000	17.93000	16.41000	15.22000	14.30000	13.58000	13.00000	12.54000	12.15000
U2=	60.34000	58.68000	51.86000	42.61000	33.51000	25.92000	20.13000	15.88000	12.79000	10.53000	8.85600
RUN 2B SUBRUN 2, S=0 TO .3553E+00											
-U0=	0.00000	0.91500	1.74000	2.48800	3.17070	3.80160	4.39170	4.95000	5.48200	5.99300	6.48700
U1=	27.06000	24.46000	22.08000	20.07000	18.43000	17.14000	16.12000	15.31000	14.66000	14.13000	13.69000
U2=	74.42000	70.98000	62.23000	51.32000	40.88000	32.17000	25.41000	20.32000	16.51000	13.64000	11.45000
RUN 2C SUBRUN 1, S=0 TO .4438E+00											
-U0=	0.00000	0.89000	1.68400	2.39370	3.03740	3.62970	4.18300	4.70600	5.20500	5.68400	6.14700
U1=	21.21000	18.92000	16.87000	15.19000	13.87000	12.87000	12.09000	11.49000	11.01000	10.61000	10.28000
U2=	52.60000	49.60000	42.32000	33.68000	25.88000	19.76000	15.28000	12.09000	9.80700	8.15900	6.94400
RUN 2C SUBRUN 2, S=0 TO .3837E+00											
-U0=	0.00000	0.91900	1.74300	2.48300	3.15350	3.76790	4.33800	4.87200	5.37800	5.86000	6.32200
U1=	25.23000	22.68000	20.33000	18.32000	16.69000	15.39000	14.36000	13.53000	12.85000	12.29000	11.81000
U2=	67.17000	64.80000	57.19000	47.36000	37.92000	30.07000	24.01000	19.45000	16.02000	13.40000	11.37000
RUN 2D SUBRUN 1, S=0 TO .4071E+00											
-U0=	0.00000	0.90700	1.72040	2.45150	3.11530	3.72600	4.29500	4.83100	5.34100	5.82900	6.29800
U1=	23.50000	21.10000	18.91000	17.07000	15.60000	14.45000	13.54000	12.82000	12.24000	11.75000	11.34000
U2=	59.75000	57.11000	49.73000	40.55000	31.96000	25.00000	19.74000	15.87000	13.01000	10.87000	9.22100
RUN 2D SUBRUN 2, S=0 TO .4078E+00											
-U0=	0.00000	0.89600	1.69830	2.41970	3.07620	3.68300	4.25000	4.78800	5.30200	5.79600	6.27500
U1=	23.19000	20.78000	18.62000	16.83000	15.43000	14.35000	13.52000	12.87000	12.35000	11.93000	11.58000
U2=	60.40000	56.83000	48.61000	38.90000	30.09000	23.11000	17.93000	14.17000	11.44000	9.42400	7.91000
RUN 2E SUBRUN 1, S=0 TO .5486E+00											
-U0=	0.00000	0.91100	1.70900	2.40770	3.02670	3.58500	4.09800	4.57700	5.03000	5.46200	5.87700
U1=	17.67000	15.55000	13.59000	11.95000	10.68000	9.72500	9.01200	8.47100	8.05000	7.71400	7.44200
U2=	38.28000	37.93000	33.20000	26.48000	20.04000	14.95000	11.25000	8.64400	6.80800	5.48600	4.51100
RUN 2E SUBRUN 2, S=0 TO .3535E+00											
-U0=	0.00000	0.90100	1.71300	2.44900	3.12150	3.74400	4.32680	4.87800	5.40200	5.90500	6.38900
U1=	26.81000	24.19000	21.83000	19.85000	18.26000	17.00000	16.00000	15.19000	14.51000	13.94000	13.44000
U2=	75.93000	71.22000	61.52000	50.26000	39.96000	31.68000	25.44000	20.85000	17.49000	15.00000	13.13000
RUN 6B SUBRUN 1, S=0 TO .5663E+00											
-U0=	0.00000	0.74800	1.41310	2.01560	2.57220	3.09400	3.58900	4.06100	4.51500	4.95200	5.37500
U1=	14.10000	12.41000	11.13000	10.20000	9.49700	8.95900	8.52800	8.16900	7.86100	7.59000	7.34700
U2=	33.64000	26.10000	19.26000	14.18000	10.72000	8.43300	6.89700	5.83600	5.07600	4.51500	4.08700
RUN 6B SUBRUN 2, S=0 TO .5701E+00											
-U0=	0.00000	0.76300	1.43550	2.04070	2.59690	3.11710	3.61000	4.08200	4.53700	4.97800	5.40800
U1=	14.32000	12.52000	11.15000	10.14000	9.40900	8.86500	8.44900	8.12000	7.85400	7.63300	7.44700
U2=	35.03000	27.80000	20.60000	14.95000	10.98000	8.28200	6.44200	5.15600	4.23000	3.54400	3.02200



Table A5 (continued)

RUN 6C SUBRUN 1 ,S=0 TO .6317E+00										
-U0=	0.00000	0.74400	1.39750	1.98230	2.51590	3.01100	3.47600	3.91800	4.34000	4.74700
U1=	12.62000	11.00000	9.75000	8.81300	8.11500	7.58200	7.16500	6.83000	6.55400	6.32200
U2=	28.27000	22.68000	17.13000	12.73000	9.58400	7.40300	5.83200	4.79200	3.98700	3.37300
RUN 6C SUBRUN 2 ,S=0 TO .7270E+00										
-U0=	0.00000	0.79000	1.47500	2.07830	2.62040	3.11750	3.58080	4.01800	4.43600	4.83800
U1=	11.68000	10.09000	8.80700	7.83400	7.11600	6.58300	6.18100	5.87100	5.62700	5.43000
U2=	23.56000	19.93000	15.44000	11.47000	8.45800	6.32000	4.82200	3.76300	2.99900	2.43700
RUN 6D SUBRUN 1 ,S=0 TO .7329E+00										
-U0=	0.00000	0.76500	1.42600	2.00880	2.53250	3.01250	3.45930	3.88000	4.27900	4.66100
U1=	11.25000	9.67700	8.43300	7.50500	6.81900	6.30400	5.90400	5.58400	5.32100	5.09900
U2=	23.34000	19.30000	14.68000	10.83000	8.04400	6.14000	4.84300	3.93800	3.28300	2.79100
RUN 6D SUBRUN 2 ,S=0 TO .7900E+00										
-U0=	0.00000	0.76700	1.42400	1.99690	2.50680	2.97060	3.39980	3.80300	4.18500	4.55000
U1=	10.51000	8.96500	7.73200	6.81000	6.13300	5.63200	5.25200	4.95700	4.72200	4.53000
U2=	21.09000	17.68000	13.54000	9.96300	7.32000	5.48100	4.21100	3.31700	2.67100	2.19000
RUN 6E SUBRUN 1 ,S=0 TO .7027E+00										
-U0=	0.00000	0.76700	1.43200	2.01870	2.54900	3.03760	3.49500	3.92800	4.34200	4.74100
U1=	11.75000	10.13000	8.85300	7.90900	7.22000	6.71100	6.32400	6.02000	5.77300	5.56800
U2=	25.14000	20.69000	15.64000	11.42000	8.36100	6.26700	4.84800	3.87000	3.17800	2.67500
RUN 6E SUBRUN 2 ,S=0 TO .7308E+00										
-U0=	0.00000	0.80200	1.49400	2.09870	2.63610	3.12260	3.57060	3.98900	4.38300	4.75800
U1=	11.81000	10.18000	8.82300	7.76900	6.97300	6.37100	5.90800	5.54600	5.25600	5.01800
U2=	23.63000	20.61000	16.44000	12.52000	9.42600	7.17200	5.56500	4.41400	3.57600	2.95200
RUN 10B SUBRUN 1 ,S=0 TO .9104E+00										
-U0=	0.00000	0.57800	1.11550	1.62490	2.11450	2.58890	3.05100	3.50200	3.94400	4.37800
U1=	6.65800	6.09400	5.72900	5.47600	5.28800	5.13800	5.01300	4.90500	4.80900	4.72300
U2=	7.73800	4.90200	3.27800	2.36200	1.82600	1.49300	1.27000	1.11100	0.99090	0.89540
RUN 10B SUBRUN 2 ,S=0 TO .9562E+00										
-U0=	0.00000	0.60100	1.15460	1.67590	2.17350	2.65300	3.11800	3.57200	4.01600	4.45200
U1=	6.59400	6.00600	5.60300	5.31500	5.10100	4.93500	4.80200	4.69200	4.59900	4.51800
U2=	7.44400	5.03200	3.51700	2.56800	1.95500	1.54300	1.25700	1.05200	0.90190	0.78870
RUN 10C SUBRUN 1 ,S=0 TO .9613E+00										
-U0=	0.00000	0.61800	1.17030	1.67650	2.14900	2.59610	3.02310	3.43400	3.83100	4.21800
U1=	6.85200	6.04600	5.47900	5.07300	4.77100	4.53900	4.35300	4.20000	4.07300	3.96300
U2=	9.92300	6.99100	4.94100	3.60400	2.73300	2.14800	1.74000	1.44500	1.22500	1.05600
RUN 10C SUBRUN 2 ,S=0 TO .1083E+01										
-U0=	0.00000	0.62800	1.17900	1.67290	2.12550	2.54620	2.94180	3.31700	3.67500	4.02000
U1=	6.24000	5.40500	4.79800	4.35300	4.02000	3.76000	3.55300	3.38300	3.24000	3.11900
U2=	8.94200	6.56000	4.75900	3.52500	2.69500	2.12800	1.72600	1.43100	1.20900	1.03600
RUN 10D SUBRUN 1 ,S=0 TO .1131E+01										
-U0=	0.00000	0.66000	1.22780	1.73190	2.19110	2.61790	3.02100	3.40400	3.77300	4.12900
U1=	6.33600	5.38500	4.70800	4.23700	3.90300	3.65900	3.47200	3.32400	3.20300	3.10200
U2=	9.72700	7.12000	4.96400	3.47100	2.50100	1.87300	1.45800	1.17400	0.97250	0.82450
RUN 10D SUBRUN 2 ,S=0 TO .1075E+01										
-U0=	0.00000	0.65800	1.22720	1.73390	2.19630	2.62590	3.03000	3.41500	3.78300	4.13600
U1=	6.63100	5.66000	4.97100	4.48600	4.13600	3.87200	3.66400	3.49500	3.35300	3.23200
U2=	1.05000	7.62300	5.33800	3.79300	2.80000	2.15900	1.73000	1.43200	1.21400	1.05000
RUN 10E SUBRUN 1 ,S=0 TO .1147E+01										
-U0=	0.00000	0.65800	1.22130	1.71800	2.16840	2.58540	2.97740	3.35000	3.70700	4.05000
U1=	6.24800	5.27300	4.58200	4.10400	3.76500	3.51600	3.32500	3.17300	3.04800	2.94400
U2=	9.84200	7.17600	4.97700	3.47100	2.50500	1.88500	1.47500	1.19300	0.98960	0.83770
RUN 10E SUBRUN 2 ,S=0 TO .1190E+01										
-U0=	0.00000	0.65100	1.20490	1.69310	2.13530	2.54440	2.92850	3.29300	3.64200	3.97700
U1=	5.97600	5.05100	4.34600	3.88700	3.56300	3.32400	3.14000	2.99300	2.87300	2.77300
U2=	9.43900	6.74900	4.61500	3.20300	2.31500	1.74900	1.37200	1.10900	0.91670	0.77120
RUN 16B SUBRUN 1 ,S=0 TO .1428E+01										
-U0=	0.00000	0.56470	1.07510	1.54800	1.99590	2.42300	2.83400	3.23100	3.61700	3.99400
U1=	4.20300	3.74000	3.43100	3.21600	3.05500	2.93000	2.82800	2.74300	2.67000	2.60600
U2=	3.98000	2.61100	1.77900	1.28500	9.82500	7.86100	6.50400	5.51600	4.76300	4.16800
RUN 16B SUBRUN 2 ,S=0 TO .1372E+01										
-U0=	0.00000	0.56810	1.08080	1.55440	1.99920	2.42100	2.82500	3.21400	3.58900	3.95300
U1=	4.40400	3.91500	3.57900	3.33800	3.15400	3.00700	2.88500	2.78100	2.69000	2.61100
U2=	4.31500	2.92000	2.04700	1.51700	1.18700	0.96960	0.81710	0.70410	0.61650	0.54620
RUN 16C SUBRUN 1 ,S=0 TO .1514E+01										
-U0=	0.00000	0.54820	1.05590	1.53750	2.00060	2.45000	2.88700	3.31400	3.73300	4.14500
U1=	3.80100	3.46500	3.25600	3.11400	3.00800	2.92400	2.85400	2.79400	2.74100	2.69400
U2=	2.83600	1.71400	1.11300	0.79400	0.61410	0.50340	0.42840	0.37300	0.32940	0.29350
RUN 16C SUBRUN 2 ,S=0 TO .1459E+01										
-U0=	0.00000	0.55120	1.05960	1.54020	2.00090	2.44600	2.87800	3.29900	3.71000	4.11200
U1=	3.97200	3.60600	3.37600	3.21900	3.09900	3.00300	2.92100	2.84800	2.78400	2.72500
U2=	3.19100	1.94300	1.27600	0.92320	0.72650	0.60640	0.52560	0.46640	0.42020	0.38260

Table A5 (continued)

RUN 160 SUBRUN 1 ,S=0 TO .1621E+01											
-U0=	0.00000	0.54720	1.06090	1.55480	2.03490	2.50490	2.96590	3.41790	3.86290	4.30190	4.73390
U1=	3.52600	3.25300	3.09900	3.00100	2.92900	2.86900	2.81700	2.76900	2.72500	2.68400	2.64500
U2=	2.26200	1.22600	0.73460	0.50780	0.39910	0.34170	0.30690	0.28230	0.26260	0.24560	0.23020
RUN 160 SUBRUN 2 ,S=0 TO .1796E+01											
-U0=	0.00000	0.55500	1.07020	1.56300	2.04120	2.50800	2.96600	3.41500	3.85700	4.29100	4.71800
U1=	3.25500	2.95600	2.79700	2.70000	2.63000	2.57400	2.52400	2.48000	2.43800	2.40000	2.36400
U2=	2.28100	1.17900	0.66760	0.44360	0.34230	0.29130	0.26100	0.23950	0.22200	0.20670	0.19270
RUN 16E SUBRUN 1 ,S=0 TO .1892E+01											
-U0=	0.00000	0.54690	1.05380	1.53630	2.00150	2.45300	2.89200	3.32000	3.73800	4.14700	4.54800
U1=	3.04500	2.76400	2.60500	2.50000	2.41900	2.35100	2.29000	2.23500	2.18400	2.13800	2.09600
U2=	1.99700	1.08100	0.66040	0.47510	0.38750	0.33870	0.30540	0.27870	0.25540	0.23430	0.21490
RUN 16E SUBRUN 2 ,S=0 TO .1785E+01											
-U0=	0.00000	0.54020	1.04760	1.53480	2.00070	2.47000	2.92100	3.36500	3.80000	4.22800	4.64800
U1=	3.16400	2.91900	2.77900	2.68700	2.61700	2.55900	2.50700	2.46000	2.41700	2.37700	2.34000
U2=	1.84400	1.00600	0.61600	0.43840	0.35260	0.30540	0.27480	0.25170	0.23230	0.21520	0.19980
RUN 20B SUBRUN 1 ,S=0 TO .3455E+01											
-U0=	0.00000	0.52980	1.00320	1.44220	1.85580	2.24780	2.62280	2.98180	3.32880	3.66480	3.99080
U1=	1.65600	1.43600	1.31400	1.23000	1.16400	1.10800	1.06100	1.02100	0.98670	0.95680	0.93080
U2=	0.89530	0.44930	0.28110	0.21270	0.17460	0.14720	0.12550	0.10770	0.09292	0.08057	0.07022
RUN 20B SUBRUN 2 ,S=0 TO .3522E+01											
-U0=	0.00000	0.52970	0.99890	1.43350	1.84350	2.23550	2.61150	2.97450	3.32550	3.66750	4.00150
U1=	1.63700	1.40000	1.27600	1.19700	1.13700	1.08800	1.04800	1.01300	0.98400	0.95850	0.93620
U2=	0.95370	0.46320	0.26990	0.19190	0.15150	0.12510	0.10540	0.09007	0.07773	0.06765	0.05931
RUN 20C SUBRUN 1 ,S=0 TO .3213E+01											
-U0=	0.00000	0.52990	0.99820	1.42960	1.83490	2.21790	2.58290	2.93190	3.26590	3.58790	3.89890
U1=	1.79200	1.53400	1.39200	1.29800	1.22400	1.16300	1.11000	1.06300	1.02100	0.98320	0.94900
U2=	1.10700	0.57010	0.34710	0.25430	0.20700	0.17680	0.15480	0.13750	0.12350	0.11170	0.10160
RUN 20C SUBRUN 2 ,S=0 TO .3459E+01											
-U0=	0.00000	0.52970	0.99080	1.41010	1.79850	2.16250	2.50550	2.83150	3.14250	3.44050	3.72750
U1=	1.68000	1.41300	1.26500	1.16400	1.08500	1.02000	0.96540	0.91890	0.87920	0.84530	0.81610
U2=	1.06600	0.54710	0.33950	0.25330	0.20580	0.17230	0.14570	0.12400	0.10590	0.09082	0.07827
RUN 20D SUBRUN 1 ,S=0 TO .3546E+01											
-U0=	0.00000	0.52570	0.98940	1.41570	1.81540	2.19240	2.55240	2.89740	3.22940	3.55140	3.86240
U1=	1.61400	1.37800	1.24800	1.16100	1.09400	1.03900	0.99290	0.95390	0.92050	0.89150	0.86630
U2=	0.92650	0.47010	0.28900	0.21250	0.17020	0.14110	0.11910	0.10160	0.08755	0.07602	0.06649
RUN 20D SUBRUN 2 ,S=0 TO .3181E+01											
-U0=	0.00000	0.52980	1.00640	1.45080	1.87130	2.27330	2.65830	3.02930	3.38930	3.73830	4.07830
U1=	1.79000	1.56600	1.44100	1.35600	1.29000	1.23500	1.18800	1.14800	0.11130	1.31100	1.23120
U2=	0.97380	0.50110	0.31100	0.23120	0.18830	0.15900	0.13650	0.11840	0.10360	0.09137	0.08126
RUN 20E SUBRUN 1 ,S=0 TO .3181E+01											
-U0=	0.00000	0.52980	1.00640	1.45080	1.87130	2.27330	2.65830	3.02930	3.38930	3.73830	4.07830
U1=	1.79000	1.56600	1.44100	1.35600	1.29000	1.23500	1.18800	1.14800	1.11300	1.08200	1.05400
U2=	0.97380	0.50110	0.31100	0.23120	0.18830	0.15900	0.13650	0.11840	0.10360	0.09137	0.08126
RUN 20E SUBRUN 2 ,S=0 TO .3261E+01											
-U0=	0.00000	5.29100	10.03300	14.44900	6.73000	7.13000	7.51500	7.88700	8.24900	8.60100	8.94500
U1=	1.75000	1.52200	1.39700	1.31500	1.25300	1.20200	1.16000	1.12400	1.09300	1.06700	1.04400
U2=	0.97090	0.49310	0.29810	0.21560	0.17140	0.14170	0.11920	0.10130	0.08686	0.07499	0.06517

Table A6: Moment analysis of drying air R.T.D.

Run	$\bar{t}/s$	$\sigma^2$	Pe
5a	12.6	.051	38.9
b	11.0	.082	24.4
c	11.0	.082	24.4
d	11.5	.076	26.3
e	10.8	.086	23.4
9a	8.5	.168	11.9
b	8.6	.133	15.0
c	8.7	.175	11.4
d	8.7	.200	10.0
e	8.5	.225	8.9
14a	3.3	.080	25.0
b	4.1	.025	77.0
c	3.9	.024	89.0
d	3.8	.020	98.0
e	3.7	.040	49.8
17a	3.1	.174	11.5
b	3.0	.155	12.9
c	3.0	.144	13.9
d	2.9	.179	11.2
e	2.6	.114	17.5
21a	1.89	.40	5.05
b	1.89	.40	5.00
c	2.02	.37	5.35
d	2.05	.30	6.65
e	1.85	.148	13.5
24a	1.49	.36	5.53

- Note: (1) Notation follows chapter 3.  
 (2) See chapter 3 for operating conditions.  
 (3) Pe calculated from  $Pe = 2/\sigma^2$ .

Table A7: Transfer function analysis (A.D.P.F. and T.S.P.F. models)  
of drying air R.T.D.

Run No.	A.D.P.F.		T.S.P.F.			Run No.	A.D.P.F.		T.S.P.F.		
	$\tau/s$	Pe	n	$T_t/s$	$T_p/s$		$\tau/s$	Pe	n	$T_t/s$	$T_p/s$
1a	34.3	13.9	2.07	26.3	11.8	12a	5.43	14.3	2.06	2.86	2.44
b	29.7	12.4	3.52	24.3	7.0						
c	29.8	12.7	3.12	24.5	7.8	13a	4.92	11.0	1.79	2.87	2.01
d	25.0	9.6	1.73	28.1	7.6						
e	24.6	10.4	2.28	21.3	6.1	14a	3.99	13.6	1.44	1.82	2.07
						b	4.52	23.6	2.36	1.64	2.67
2a	34.3	13.9	2.07	26.3	11.8	c	4.22	30.5	4.02	1.72	2.26
b	27.6	11.3	2.44	24.4	7.8	d	4.11	28.4	5.50	1.98	3.94
c	28.9	12.2	2.90	25.0	7.7	e	4.23	19.2	2.47	1.46	3.93
d	28.5	11.4	4.98	24.9	3.7						
e	26.2	11.2	2.62	22.4	7.1	15a	3.84	13.7	1.60	1.87	1.90
3a	28.5	15.5	1.51	18.3	13.5	16a	3.67	15.2	1.76	1.69	1.86
						b	3.54	11.5	1.48	1.87	1.62
4a	17.3	12.0	1.82	11.1	6.84	c	3.58	19.7	2.62	1.71	1.77
						d	3.65	28.7	7.09	2.08	1.44
5a	16.3	13.5	1.59	10.4	7.21	e	3.54	21.8	3.71	1.84	1.59
b	14.7	9.3	1.61	12.8	4.87						
c	14.9	8.7	2.29	11.7	3.92	17a	3.17	14.0	2.17	1.54	1.48
d	15.9	9.1	2.32	12.3	4.30	b	3.11	13.5	2.35	1.67	1.34
e	14.9	8.3	1.82	12.6	4.30	c	3.09	17.8	2.05	1.37	1.62
						d	2.99	29.3	5.30	1.48	1.39
6a	15.2	15.4	2.80	9.7	5.8	e	2.56	25.9	6.02	1.33	1.13
b	15.3	10.0	2.60	11.9	4.1						
c	14.6	9.8	3.19	11.0	3.4	18a	3.01	11.7	1.75	1.59	1.34
d	14.1	8.4	3.19	11.8	2.6						
e	13.6	8.3	1.79	11.5	4.1	19a	2.31	18.9	2.78	1.05	1.16
7a	12.0	13.9	2.29	6.99	4.88	20a	1.92	6.9	1.86	1.24	0.58
						b	1.74	9.0	1.61	1.08	0.66
8a	9.4	13.5	2.27	5.54	3.79	c	1.44	7.4	1.16	0.97	0.55
						d	1.78	8.0	2.08	1.27	0.51
9a	9.0	10.6	1.72	5.84	3.47	e	1.65	8.7	1.49	1.07	0.62
b	9.2	16.2	2.77	5.17	3.85						
c	9.2	10.1	1.70	5.94	3.46	21a	1.73	14.8	1.11	0.80	0.90
d	9.2	8.4	1.92	6.58	2.84	b	1.76	9.4	1.98	1.06	0.65
e	8.8	7.9	1.45	6.31	3.03	c	1.89	10.4	1.84	1.03	0.80
						d	1.96	11.5	1.70	1.03	0.88
10a	7.2	10.9	1.09	4.54	3.35	e	1.80	20.9	2.27	0.76	0.98
b	7.3	17.1	2.29	3.78	3.42						
c	7.6	10.8	1.79	4.60	2.98	22a	1.67	14.8	2.29	0.87	0.76
d	7.0	6.2	1.31	5.67	2.10	23a	1.40	9.8	1.29	0.70	0.66
e	7.1	6.5	1.42	5.45	2.16	24a	1.38	12.4	1.61	0.64	0.68
						25a	1.22	17.5	2.70	0.80	0.47
11a	7.1	14.1	1.79	2.87	2.01	26a	1.02	17.2	1.73	0.61	0.48
						27a	.995	17.3	1.98	0.58	0.46
						28a	.993	15.4	2.19	0.58	0.43

Note: Notation follows chapter 3.

Table A8: Transfer-function analysis (A.D.P.F. and T.S.P.F. models) of atomising air R.T.D.

Run No.	A.D.P.F.		T.S.P.F.		
	$\tau/s$	Pe	n	$T_t$	$T_p$
1b	19.7	10.1	2.22	17.1	5.6
c	27.1	12.4	2.58	21.6	8.3
d	25.6	11.8	2.74	21.5	7.0
e	27.1	11.4	2.09	22.3	8.8
2b	27.4	11.4	2.22	25.6	8.2
c	24.9	10.1	2.45	22.8	6.3
d	24.8	10.5	2.22	22.6	7.1
e	28.2	11.8	2.97	22.9	7.3
6b	14.4	10.0	1.52	10.6	5.3
c	12.8	7.7	1.75	11.2	3.6
d	11.8	6.3	1.93	10.1	2.6
e	12.8	6.7	1.85	11.2	3.0
10b	6.4	18.1	2.20	2.91	3.43
c	6.5	8.9	1.90	4.40	2.14
d	6.5	6.9	2.83	4.64	1.91
e	6.3	6.1	1.54	4.56	1.75
16b	4.19	11.3	2.17	2.48	1.60
c	3.73	17.7	2.38	1.79	1.83
d	3.22	24.9	4.07	1.48	1.60
e	2.97	22.3	4.44	1.59	1.26
20b	1.55	10.6	2.15	0.97	0.56
c	1.65	8.5	3.35	1.25	0.34
d	1.61	10.4	2.37	1.04	0.54
e	1.57	10.4	1.67	0.95	0.63

- Note: (1) Run 1 done with nozzle no. 1;  
other runs done with nozzle no. 2.
- (2) Notation follows chapter 3.
- (3) Values given are average of 2 readings.

Table A9: Transfer-function analysis (D.B.M. and B.C.P.F. models)  
of drying air R.T.D.

Run	D.B.M. + Plug flow				Backflow cell + P.F.			
	1/k	$T_o/s$	$T_p/s$	$\tau/s$	n	b	$T_t/s$	$T_p/s$
1a	NA	-	-	-				
b	NA	-	-	-				
c	NA	-	-	-				
d	NA	-	-	-				
e	NA	-	-	-				
2a	NA	-	-	-				
b	NA	-	-	-				
c	NA	-	-	-				
d	NA	-	-	-				
e	NA	-	-	-				
6a	NA	-	-	-	3.69	+ .24	9.8	5.5
b	NA	-	-	-	2.44	- .12	11.0	4.2
c	NA	-	-	-	3.28	- .01	11.0	3.3
d	NA	-	-	-	3.18	- .03	11.3	2.6
e	NA	-	-	-	1.61	- .22	9.9	4.1
10a	9.6	13.4	3.20	9.13	1.10	- .07	4.09	3.33
b	2.05	3.07	2.86	7.11	2.74	+ .16	4.00	3.35
c	3.53	7.05	2.63	8.21	2.40	+ .25	5.10	2.81
d	NA	-	-	-	1.22	- .20	4.65	2.12
e	NA	-	-	-	1.52	- .05	5.00	2.11
16a	2.38	1.53	1.57	3.38				
b	4.01	1.69	1.43	3.47				
c	1.63	0.96	1.39	3.36				
d	1.10	0.30	0.22	3.40				
e	1.33	0.67	1.00	3.32				
20a	3.17	1.56	0.47	1.83	2.20	+ .26	1.38	0.56
b	3.66	1.62	0.56	1.82	1.57	- .04	1.11	0.67
c	7.38	2.61	0.47	1.79	1.00	- .16	0.86	0.57
d	2.85	1.48	0.38	1.87	1.80	- .07	1.23	0.54
e	3.88	1.62	0.51	1.75	1.21	- .14	0.99	0.65

Notes: (1) NA: not applicable.  
(2)  $T_t$  is total tank time.  
(3) Notation follows chapter 3.

Table A10: Output concentration curves for spray R.T.D.

SPRAY R.T.D. DATA FOR RUN A1 AT TIME INTERVALS DT= 0.513 (STARTING AT T=DT)

0	0	0	0	0	0	0	0	2	15	23	34	69	133	155	196	240	469	479	561
424	428	473	540	622	778	727	690	705	710	786	999	770	750	694	686	672	610	756	962
851	695	675	601	597	603	580	654	741	593	416	460	447	406	420	396	352	329	313	282
230	211	261	232	163	141	126	147	148	113	109	91	81	90	89	110	92	63	72	79
82	74	77	74	70	74	77	57	44											

SPRAY R.T.D. DATA FOR RUN A2 AT TIME INTERVALS DT= 0.513 (STARTING AT T=DT)

0	0	0	1	1	1	1	14	67	118	187	257	348	348	403	464	615	648	801	781
839	995	999	939	586	672	419	403	445	466	501	472	445	343	319	299	368	383	397	330
277	232	228	203	179	150	152	134	194	130	136	130	127	123	132	138	159	136	114	85
87	87																		

SPRAY R.T.D. DATA FOR RUN A3 AT TIME INTERVALS DT= 0.513 (STARTING AT T=DT)

0	0	96	669	378	921	989	921	775	756	436	756	999	756	552	378	455	203	300	271
339	213	271	213	223	184	223	106	145	106	145	106	213	145	87	116	77	193	87	67
96	58	58	38	58	58	29	29	29	27	12	11	18	2	0	9	0	0	1	4

SPRAY R.T.D. DATA FOR RUN B3 AT TIME INTERVALS DT= 0.513 (STARTING AT T=DT)

0	0	0	23	202	466	782	999	956	909	937	777	782	631	395	433	419	343	230	193
127	127	136	113	84	56	61	61	51	42	47	37	32	18	23	18				

SPRAY R.T.D. DATA FOR RUN C3 AT TIME INTERVALS DT= 0.513 (STARTING AT T=DT)

0	0	73	91	174	568	989	476	999	714	531	476	687	641	458	274	284	174	229	201
91	82	119	73	128	64	54	36	64	45	27	27	27	36	36					

SPRAY R.T.D. DATA FOR RUN D3 AT TIME INTERVALS DT= 0.355 (STARTING AT T=DT)

0	0	0	0	739	819	739	999	559	479	153	253	139	53	39	19	6	19	6	13
6	0	6	0																

SPRAY R.T.D. DATA FOR RUN E3 AT TIME INTERVALS DT= 0.209 (STARTING AT T=DT)

68	342	684	985	999	821	615	478	369	307	273	246	218	205	239	205	164	136	109	88
68	47	34	20	13															

Table A11: U-functions for spray R.T.D.

RUN A1 ,S=0 TO .4170E+00

-U0=	0.00000	0.78100	1.49700	2.15200	2.75600	3.31700	3.84100	4.33400	4.80300	5.24900	5.67700
U1=	19.69000	17.97000	16.41000	15.07000	13.93000	12.98000	12.18000	11.52000	10.96000	10.48000	10.06000
U2=	42.92000	39.58000	34.85000	29.74000	2.49400	2.07900	1.73700	14.61000	12.42000	10.67000	9.26800

RUN A2 ,S=0 TO .4995E+00

-U0=	0.00000	0.67700	1.29200	1.85600	2.38100	2.87300	3.33800	3.78100	4.20400	4.60900	4.99800
U1=	14.29000	12.88000	11.76000	10.87000	10.16000	9.57000	9.07800	8.65400	8.28200	7.95000	7.65000
U2=	30.90000	25.17000	19.99000	15.89000	12.86000	10.68000	9.10000	7.92700	7.02400	6.30400	5.70900

RUN A3 ,S=0 TO .1007E+01

-U0=	0.00000	0.61100	1.14300	1.61400	2.03900	2.42800	2.78900	3.12800	3.44700	3.75200	4.04300
U1=	6.53000	5.64400	4.95200	4.42600	4.02400	3.71200	3.46400	3.26200	3.09400	2.95200	2.83000
U2=	9.76900	7.80400	5.97600	4.54000	3.49400	2.74700	2.21100	1.81900	1.52600	1.30200	1.12800

RUN B3 ,S=0 TO .9972E+00

-U0=	0.00000	0.54700	1.05000	1.51900	1.96000	2.37900	2.77900	3.16300	3.53300	3.89100	4.23900
U1=	6.38000	5.83200	5.40200	5.06100	4.78600	4.55800	4.36500	4.20000	4.05600	3.92900	3.81600
U2=	6.90200	5.39100	4.24000	3.39700	2.78100	2.32600	1.98200	1.74100	1.50200	1.33100	1.18900

RUN C3 ,S=0 TO .9798E+00

-U0=	0.00000	0.56700	1.08300	1.55700	1.99800	2.41200	2.80300	3.17400	3.52800	3.86600	4.18900
U1=	6.10200	5.50600	5.03400	4.65800	4.35300	4.10000	3.88400	3.69500	3.52700	3.37500	3.23400
U2=	6.80100	5.40100	4.27600	3.43400	2.82100	2.37600	2.05100	1.81000	1.62900	1.49000	1.38000

RUN D3 ,S=0 TO .1787E+01

-U0=	0.00000	0.49200	0.96200	1.41300	1.84700	2.26900	2.67800	3.07700	3.46700	3.84900	4.22500
U1=	2.82500	2.88600	2.57100	2.47500	2.39300	2.32200	2.26000	2.20700	2.16000	2.11800	2.08200
U2=	0.86150	0.70350	0.58630	0.49670	0.42600	0.36860	0.32100	0.28090	0.24660	0.21710	0.19160

RUN E3 ,S=0 TO .2930E+01

-U0=	0.00000	0.44900	0.83500	1.17300	1.47900	1.75900	2.01900	2.26400	2.49500	2.71400	2.92300
U1=	1.67200	1.41300	1.22600	1.09300	0.99530	0.92040	0.86050	0.81070	0.76780	0.72990	0.69590
U2=	1.02400	0.74980	0.53440	0.38590	0.28900	0.22630	0.18510	0.15700	0.13700	0.12210	0.11070

Table A12: Moment analysis and transfer-function analysis  
(A.D.P.F. and T.S.P.F. models) of spray R.T.D.

Run	Moment Analysis			Transfer-function analysis				
				A.D.P.F.		T.S.P.F.		
	$\bar{t}/s$	$\sigma^2$	Pe	$\tau/s$	Pe	n	$T_t/s$	$T_p/s$
A1	12.0	0.037	54.8	20.5	11.8	3.76	17.4	4.1
A2	10.0	0.044	45.4	14.4	11.3	4.42	11.2	2.7
A3	4.96	0.125	16.0	6.92	5.7	2.15	5.64	1.28
B3	5.57	0.091	21.9	6.36	11.9	2.82	4.32	2.00
C3	5.10	0.095	21.0	6.16	9.7	4.76	5.12	7.52
D3	2.80	0.096	20.9	2.81	21.2	2.14	1.42	1.43
E3	1.71	0.387	5.17	1.74	3.96	2.15	1.32	0.23



APPENDIX BMISCELLANEOUS EXPERIMENTSContents

- I. DROP SIZES FROM PNEUMATIC ATOMISERS
1. Aims of experiment
  2. Theory
  3. Experimental details
  4. Results and discussion
- Notation
- References
- II. ATOMISER AIR-FLOW AREA AND AIR FLOWRATE MEASUREMENTS
1. Aims of experiment
  2. Theory
  3. Experimental details
  4. Results
- Notation
- References
- III. SUSPENDED DROPLET DRYING TESTS WITH A ZINC-OXIDE SLURRY
1. Aims of experiment
  2. Background and theory
  3. Experimental details
  4. Results
- Notation
- IV. AN ATTEMPTED SIMULTANEOUS MEASUREMENT OF EVAPORATION AND  
RESIDENCE TIME
1. Aim of experiment
  2. Background and theory
  3. Experimental details
  4. Results
- References

## APPENDIX B

### MISCELLANEOUS EXPERIMENTS

#### B.I DROP SIZES FROM PNEUMATIC ATOMISERS

##### B.I.1 Aims of experiments

Experiments were carried out in order to

- (1) Measure the mean drop size of a pneumatic atomiser at varying air and liquid rates, and check various predictive equations.
- (2) Find the shape of the drop-size spectrum.
- (3) Find the influence of the presence of an undissolved solid (zinc oxide) on the drop sizes.
- (4) Find the influence of the drying-air flow on the drop sizes.

##### B.I.2 Theory

Equations for predicting either the Sauter diameter  $D_{32}$  or the mass median diameter  $D_m$  of a spray from a pneumatic nozzle have been proposed by many workers and reviewed in references 2, 4, 6 and 7.

It appears from all these works that the variables governing the droplet sizes are: the viscosity, density and surface tension of each phase, the velocity or flow rate of each phase, the orifice diameters and configurations (i.e. internal or external mixing) of the nozzle.

The most commonly used drop-size distribution functions have been reviewed by Mugele and Evans (5). They are: the root-normal distribution, the log-normal distribution, the Nukiyama-Tasanawa distribution, and the Rosin-Rammler distribution. These and most other distribution equations proposed so far can be considered as particular cases of the following two groups:

- (1) Normal distributions, with the normally distributed variable being  $\sqrt{D}$ ,  $\ln D$  or  $\ln[aD/(D_{\max} - D)]$  (5).

- (2) Generalised Nukiyama-Tasanawa equations

$$\frac{dn}{dD} = aD^b \exp(-cD^d) \quad (B.1)$$

where  $n$  is the number of droplets with size below  $D$ . If  $b = 2$ , the

standard Nukiyama-Tasanawa equation is obtained. If  $b = 0$  and  $d = 1$ , one gets the log-number distribution. If  $b = d - 4$ , the Rosin-Rammler equation is obtained. Other authors have proposed  $b = d - 1$  (3,10) and  $b = 1, d = 2$  (Khragian and Mazin, as quoted in 1).

### B.I.3 Experimental details

The technique used for measuring drop sizes is to collect the droplets into a rectangular perspex cell (as described in chapter 4) with a 1 mm layer of Shell Carnea-69 oil, and to photograph them under a microscope. More details about the photographic technique can be found in chapter 4 and in references 9 and 11.

Nozzle No. 1 (table 1, chapter 1) was used. The nozzle was installed at the top of the spray drying chamber and the collecting cell placed 500 mm below it, about 20 mm below the point where the jet breaks up.

Eight runs were made with pure water as feed, at liquid rates ranging from 0.3 to 0.7 cm<sup>3</sup>/s. and atomising air rates ranging from 0.3-0.7 g/s. One run was made with a zinc-oxide slurry (30% solid by weight, viscosity = 0.005 N s/m<sup>2</sup>) at a liquid rate of 0.5 cm<sup>3</sup>/s and an atomising air rate of 1.3 g/s. One run was made with pure water at 0.5 cm<sup>3</sup>/s of liquid and 1.3 g/s of atomising air, with a drying-air velocity of 1.9 m/s in the drying chamber.

### B.I.4 Results and discussion

(1) Mean drop sizes: The measured Sauter mean diameters are shown in table 1. Also shown are the predicted values of  $D_{32}$  or  $D_m$  according to the equations of Nukiyama and Tasanawa, Wigg, Kim and Marshall, and Mugele. It can be seen that the Nukiyama-Tasanawa equation (8,7) for  $D_{32}$  gives the closest value, although it predicts that  $D_{32}$  is somewhat more sensitive to the flow rates than is the case.

(2) Size spectrum: Among the log-normal, root-normal, Nukiyama-Tasanawa and Rosin-Rammler distribution equations, the Nukiyama-Tasanawa equation fits the experimental spectrum best. The exponent  $d$  in equation 1 ranges from 0.35 to 0.60 for best fit (the best fit being measured by the correlation of a plot of  $\ln[(dn/dD)/D^2]$  vs  $D^d$ ), but a value of  $d \sim 0.5$  seems best for predicting the various mean diameters, although the other equations are also fairly good. Typical plots for various distribution equations are shown in figure 1, with the best fit value of  $d$ .

(3) Effect of undissolved solids:

The presence of fine (below 1  $\mu\text{m}$ ) zinc-oxide particles increases the viscosity of the feed from 0.001 to 0.005  $\text{N s/m}^2$  but does not seem to affect the mean drop size ( $D_{32} = 36 \mu\text{m}$  for pure water,  $= 37 \mu\text{m}$  for slurry), although the size distribution appears wider ( $d \approx 0.5$  for pure water,  $\approx 0.3$  for slurry). However, this result is somewhat inconclusive, due to the fact that the flow of slurry was not measured directly but was assumed to be the same as the flow of water under the same atomising conditions.

(4) Effect of external air flow:

When the external (drying) air velocity is increased from 0 to 1.9  $\text{m/s}$ , the Sauter mean diameter is decreased from 36 to 31.5  $\mu\text{m}$ . This is probably due to the turbulence in the external air flow breaking up the jet at an early stage, thus preventing recoalescence.

Table B.1

Measured and predicted mean diameters  
of droplets from a pneumatic nozzle

Air rate $/\text{g s}^{-1}$	Liquid rate $/\text{cm}^3 \text{s}^{-1}$	$D_{32}$ meas'd $/\mu\text{m}$	$D_{32}$ , N.T. $/\mu\text{m}$	$D_m$ , Wigg $/\mu\text{m}$	$D_m$ , K.M. $/\mu\text{m}$	$D_{32}$ , Mugele $/\mu\text{m}$
0.6	0.3	58	70	480	23	170
	0.47	66	92	-	-	-
1.05	0.47	-	38	240	12	115
	0.58	54	44	-	-	-
1.3	0.50	36	29	190	9.5	105
	0.65	45	32	-	-	-
1.75	0.50	35	21	124	8.3	90
	0.70	42	23	-	-	-

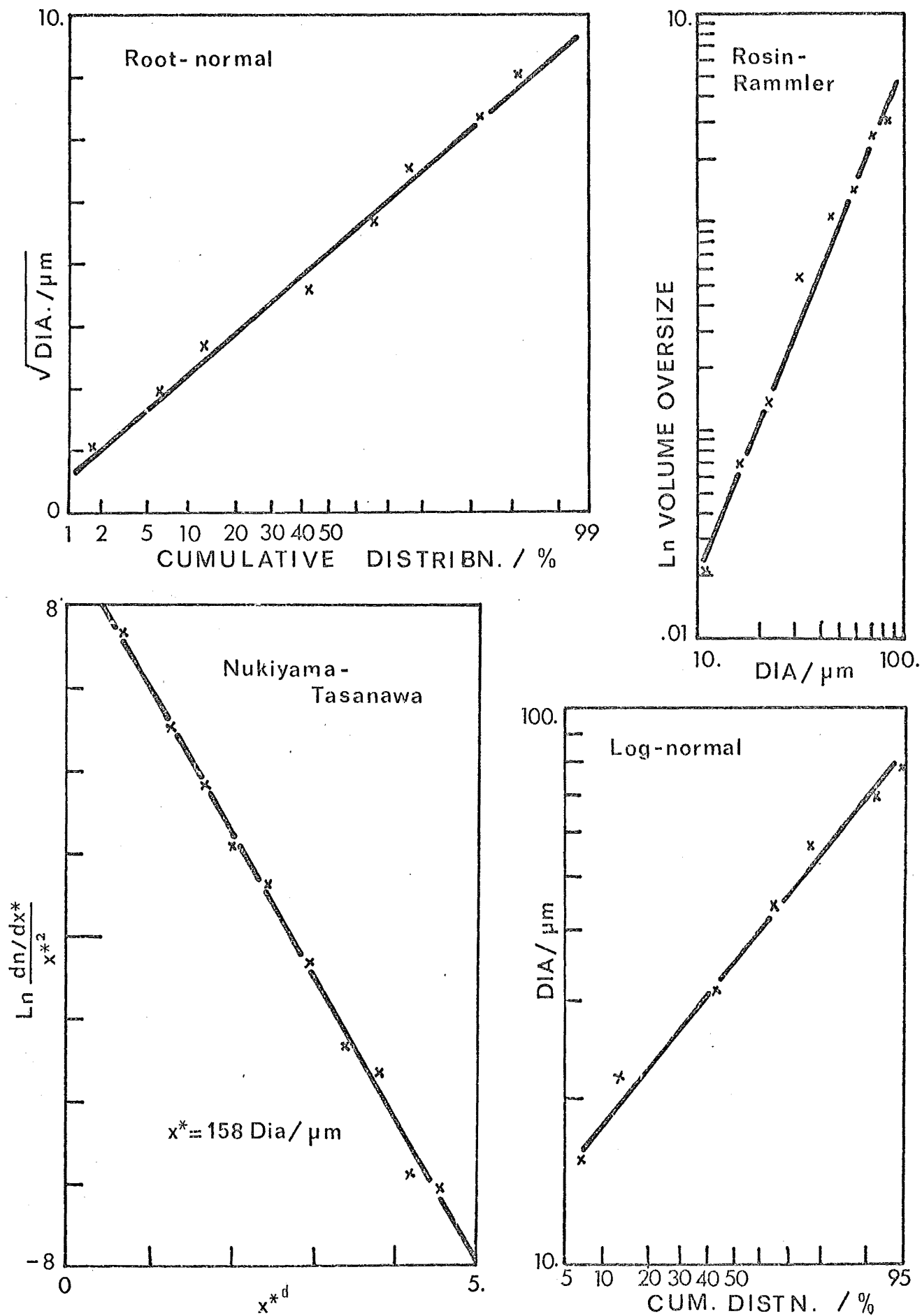


FIG. B1: DROP SIZE ANALYSES

Notation for appendix B.I:

a,b,c,d	constants in equation 1
D	droplet diameter [ m ]
$D_m$	mass-median droplet diameter [ m ]
$D_{max}$	maximum droplet diameter [ m ]
$D_{32}$	surface-volume or Sauter mean droplet diameter [ m ]
n	number of droplets with size below D [ - ]

References

- (1) Alonso J.R.F., Ph.D. Thesis, Dept of Industrial Science, University of Melbourne (1972)
- (2) Dombrowski N., article in "Biochemical and Biological Engineering Science", Blakebrough N., ed., vol. 2, Academic Press. N.Y. (1968)
- (3) Hopkins M.J., Eisenklam P., Chemeca '70 (1970) 91
- (4) Kim K.Y., Marshall W.R., A.I.Ch.E.J. 17 (1971) 575
- (5) Mugele R.A., Evans H.D., Ind. Eng. Chem. 43 (1951) 1317
- (6) Marshall W.R., "Atomisation and Spray Drying", Chem. Eng. Prog. Monograph Series 50 no.2 (1954)
- (7) Masters K., "Spray Drying", Leonard Hill, London (1972)
- (8) Nukiyama S., Tسانawa Y., Trans. Soc. Mech. Eng. Japan 5 no.18 (1938) 63
- (9) Robertson G.J., B.E. Project Report (1967), Dept of Chemical Engineering, University of Canterbury
- (10) Shapiro A.H., Erickson A.J., Trans. A.S.M.E. 79 (1957) 775
- (11) Son N.T., B.E. Project Report (1968), Dept of Chemical Engineering, University of Canterbury

## B.II ATOMISER AIR-FLOW AREA AND AIR FLOW RATE MEASUREMENTS

### B.II.1 Aim of experiment

Knowledge of the air-flow rate and air-flow area of the nozzle is essential for the prediction of drop sizes and the calculation of jet zone velocity, temperature, concentration and evaporation profiles (chapter 6). The manufacturer's values were found to be unreliable, so a direct measurement of flow rates was necessary.

### B.II.2 Theory

For the isentropic flow of an ideal gas through an orifice, the following equations apply (see, for example, reference 1):

$$\dot{m} = A \left\{ \frac{2k}{k-1} p_1 \rho_1 \left[ \left( \frac{p_2}{p_1} \right)^{2/k} - \left( \frac{p_2}{p_1} \right)^{(k+1)/k} \right] \right\}^{1/2} \quad (\text{B.2})$$

for  $\frac{p_2}{p_1} \geq \left( \frac{2}{k+1} \right)^{k/(k-1)}$

$$\dot{m} = A \left\{ k p_1 \rho_1 \left( \frac{2}{k+1} \right)^{(k+1)/(k-1)} \right\}^{1/2} \quad (\text{B.3})$$

for  $\frac{p_2}{p_1} \leq \left( \frac{2}{k+1} \right)^{k/(k-1)}$

where  $\dot{m}$  is the gas mass flow rate,  $A$  the orifice area,  $k$  the specific heat ratio of the gas,  $p_1$  and  $p_2$  the upstream and downstream absolute pressures, and  $\rho_1$  the upstream gas density. For a given downstream pressure  $p_2$ , since  $\rho_1$  is proportional to  $p_1$ , equation 3 predicts that the mass flow rate  $\dot{m}$  is directly proportional to the upstream absolute pressure  $p_1$ , provided that  $p_1$  exceeds a certain critical value:

$$p_c = p_2 \left( \frac{k+1}{2} \right)^{k/(k-1)} \quad (\text{B.4})$$

When the gas is air ( $k = 1.4$ ) discharging into the atmosphere ( $p_2 = 1.01 \times 10^5 \text{ Pa}$ ), equations 3 and 4 reduce to

$$\dot{m} = 2.45 \times 10^{-3} A p_1 \quad (\text{B.5})$$

in S.I. units, provided



$$p_1 \geq p_c = 1.9 \times 10^5 \text{ Pa} \quad (\text{B.6})$$

This equation can be used to calculate A from a plot of  $\dot{m}$  against  $p_1$ .

### B.II.3 Experimental details

Each nozzle was allowed to discharge, under a variable and controlled pressure obtained with a regulating valve, into a 20 litre flask. The flow from the flask to the atmosphere was measured with a rotameter. The liquid inlet to the nozzle was plugged.

### B.II.4 Results

For nozzles no. 1 and 2 (see table 1, chapter 1)  $\dot{m}$  is plotted against  $p_1$  in figure 2. The results agree well with the theory. From the slopes of the plots, the airflow areas of each nozzle can be calculated:

Nozzle 1:  $A = 1.4 \text{ mm}^2$  (manufacturer's value =  $0.81 \text{ mm}^2$ )

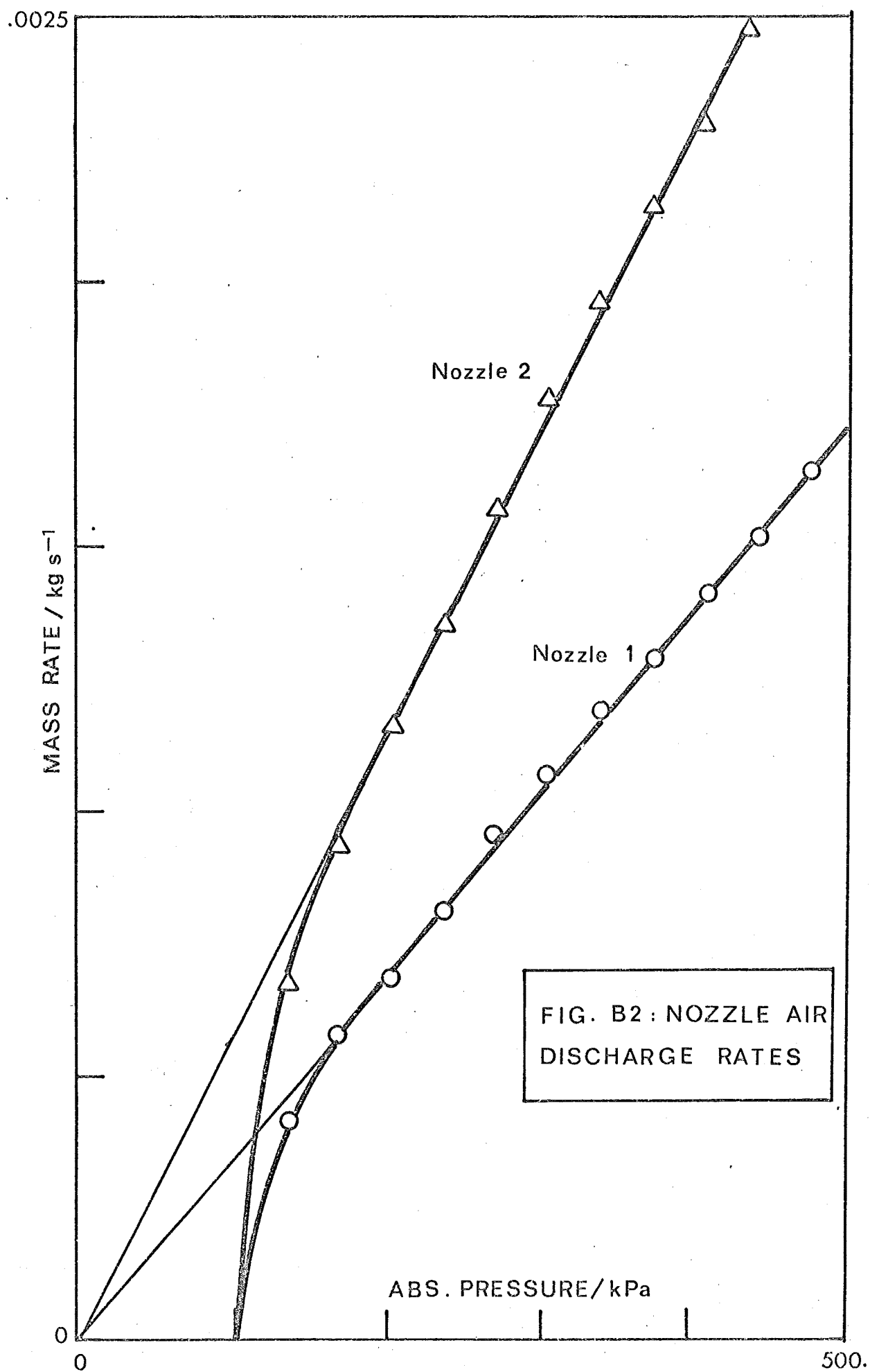
Nozzle 2:  $A = 2.3 \text{ mm}^2$  (manufacturer's value =  $1.2 \text{ mm}^2$ )

### Notation for appendix B.II

A	discharge area [ $\text{m}^2$ ]
k	constant pressure/constant volume specific heat ratio of gas [ - ]
$\dot{m}$	mass flow rate of gas [ $\text{kg/s}$ ]
$p_1$	upstream or atomising absolute pressure [ Pa ]
$p_2$	downstream or atmospheric absolute pressure [ Pa ]
$p_c$	critical pressure [ Pa ]
$\rho_1$	gas density at pressure $p_1$ [ $\text{kg/m}^3$ ]

### Reference

- (1) Bird R.B., Stewart W.E., Lightfoot E.N., "Transport Phenomena", J. Wiley & Sons, N.Y. (1960)



B.III    SUSPENDED DROPLET DRYING TESTS  
           WITH A ZINC OXIDE SLURRY

B.III.1    Aim of the experiment

(1) To investigate the process of shrinking and consolidation of drops of a zinc-oxide slurry.

(2) To find the relationship between the initial solid content and the final porosity for drops of the same material.

B.III.2    Background and theory

The mechanism of particle formation from evaporating droplets and its influence on the drying rate has been reviewed in chapter 5.

Consider a simple process where a drop containing either dissolved or very finely dispersed solid (particle diameter  $\ll$  drop diameter) at first shrinks freely as the liquid evaporates, then suddenly stops shrinking when a solid structure forms. The weight-volume plot of such a drop would have the shape shown in figure 3.

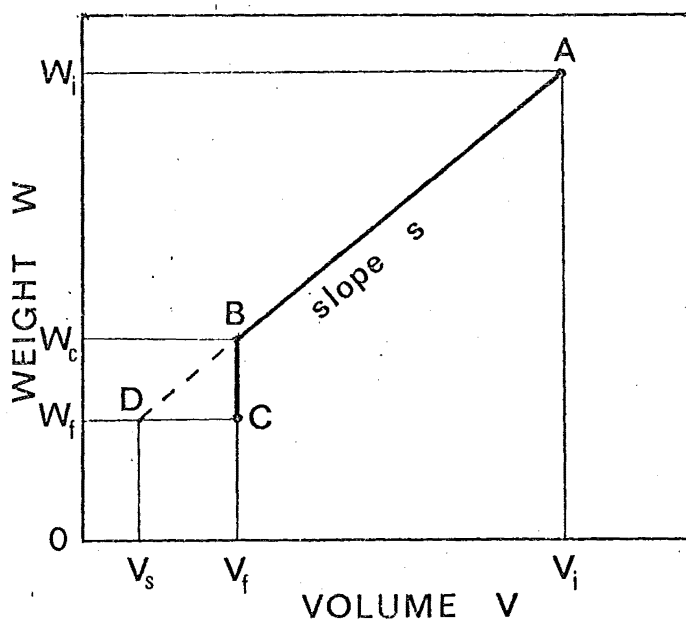


FIGURE B.3: TWO-PERIOD PARTICLE FORMATION

The point D ( $W_c, V_s$ ) on the graph represents the state of a hypothetical dry particle formed from the original drop with no voidage, since the shrinkage continues until the particle is completely dry. Hence  $V_s$  is the actual volume of solid in the droplet or particle, and the void fraction  $\epsilon_f$  of the dry particle is

$$\epsilon_f = \frac{V_f - V_s}{V_f} \quad (\text{B.7})$$

Similarly, it can be shown that the initial water volume fraction  $\epsilon_i$  is

$$\epsilon_i = \frac{V_i - V_s}{V_i} \quad (\text{B.8})$$

From equations 7 and 8 it is seen that both the weight and the volume scales in figure 3 can be in arbitrary unit (for example, weights can be expressed in terms of the deflection of a support), and the point  $W = 0$  is not required to be known.

By algebraic manipulation of equations 7 and 8, it can also be shown that

$$\epsilon_f = \frac{W_c - W_f}{sV_f} \quad (\text{B.9})$$

$$\epsilon_i = \left\{ 1 + \frac{W_c - W_f}{W_i - W_f} \left( \frac{1}{\epsilon_f} - 1 \right) \right\}^{-1} \quad (\text{B.10})$$

where  $W$  and  $V$  are in arbitrary units, and  $s$  is the slope of the  $W$ - $V$  curve in the shrinking period (if  $W$  and  $V$  are in consistent units,  $s = \rho_l$ , the liquid density).

### B.III.3 Experimental details

Drops of finely ground zinc-oxide slurry (ZnO particle size  $\leq 1 \mu\text{m}$ ) were suspended by means of a hypodermic syringe at the tip of a 30 to 40 mm section of 46-gauge (0.061 mm diameter) copper wire. Drop sizes varied from 0.8 to 2 mm diameter. The copper wire was clamped to a microscope mechanical stage mounted on a support in such a manner that fine horizontal and vertical displacements of the wire could be made.

Photographs of the drops were taken with a 35 mm camera fitted with a 1:3.5/35 lens at the end of a 200 mm extension bellow . Both camera and mechanical stage support were securely mounted on a common platform. Each drop was photographed under a floodlight against a dark background, at intervals of 1 minute. The drops were evaporating in quiescent air at room temperature and no attempt was made to control the evaporation conditions. The total change in wire deflection ranged from 10 to 40 mm.

A sevenfold magnification was obtained on the negative. The final enlargement gave a total magnification of about 50. Because the drop or particle shape was not completely spherical, the cross-section area of the drop was measured with a planimeter and from this the diameter could be calculated. For liquid droplets, symmetry about a vertical axis was assumed, while for elongated consolidated particles, symmetry about an axis parallel to the supporting wire was assumed (figure 4).

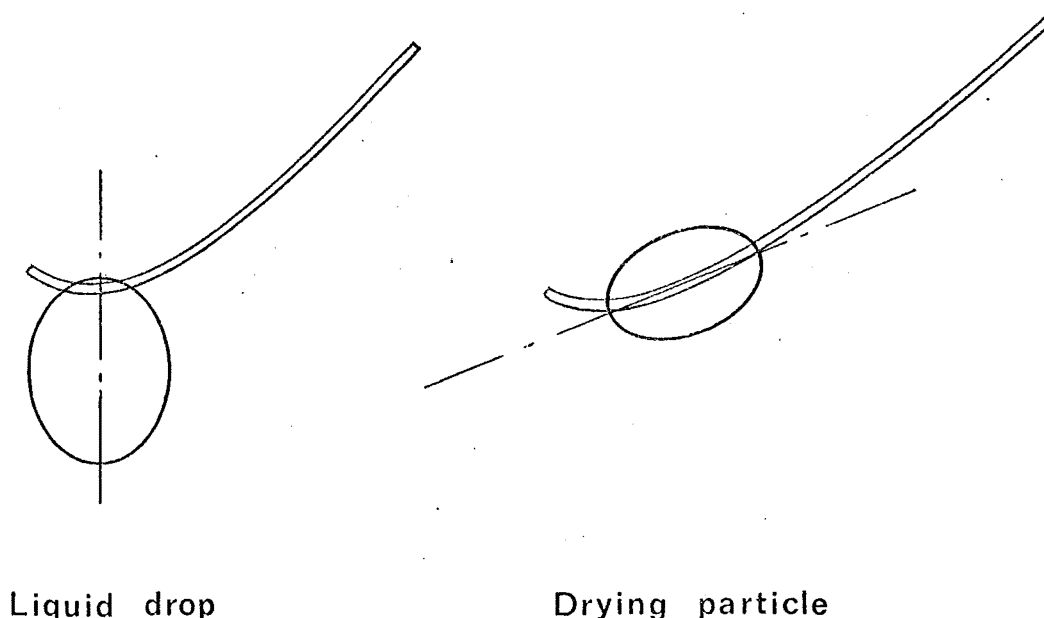


FIGURE B.4 : DEFORMATION OF SUSPENDED DROP & PARTICLE

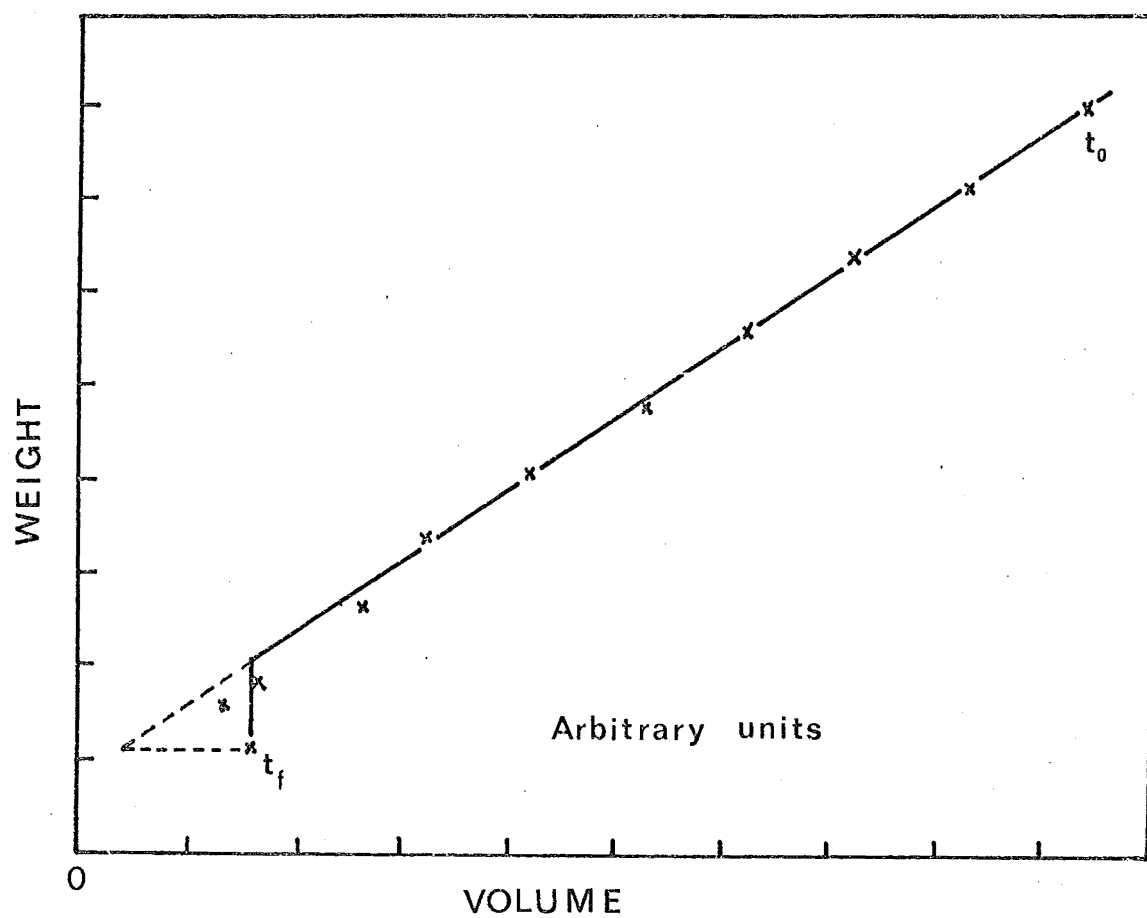


FIG. B5: WEIGHT-VOLUME PLOT FOR ZnO SLURRY

B.III.4 Results

A typical weight-volume graph for the zinc-oxide slurry is shown in figure 5. It can be seen that the simple two-period model holds fairly well, although the separation between the two periods is not quite sharp, indicating that some gradual consolidation takes place in the real situation. Also, some "over-shrinkage" occurs, the volume shrinking to below its final value  $V_f$  and then expanding again. This is probably due to the surface-tension forces exerted by the moisture when in the pendular (wedge-shaped) state between the particle of solids. These forces tend to pull the particles together (figure 6). Assuming that the mean ZnO particle diameter is  $1\text{ }\mu\text{m}$ , a force balance based on figure 6 showed that surface-tension forces can exert an equivalent pressure of up to  $2.4 \times 10^5$  Pa, or 2.4 atmospheres.

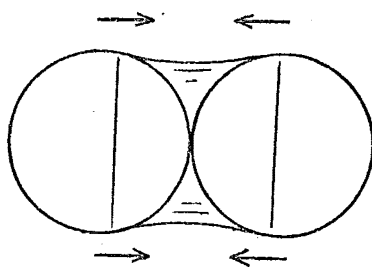


FIGURE B.6: SURFACE-TENSION FORCES EXERTED BY MOISTURE

The results of all runs have already been plotted as the final void fraction vs the initial liquid volume fraction in figure 3 of chapter 5.

Notation for appendix B.III

D	droplet or particle diameter [ m ]
s	slope of the weight-volume plot in the free shrinking period [ N/m <sup>3</sup> ]
V	drop or particle volume [ m <sup>3</sup> ]
W	drop or particle weight [ N ]
ε	liquid volume fraction or void fraction [ - ]

Subscripts:

c	critical, or consolidation
f	final, or dry particle
i	initial
s	solid



B.IV AN ATTEMPTED SIMULTANEOUS MEASUREMENT OF  
EVAPORATION AND RESIDENCE TIME

B.III.1 Aim of the experiment

To measure the degree of evaporation of droplets against their residence time in the spray drying chamber.

B.III.2 Background and theory

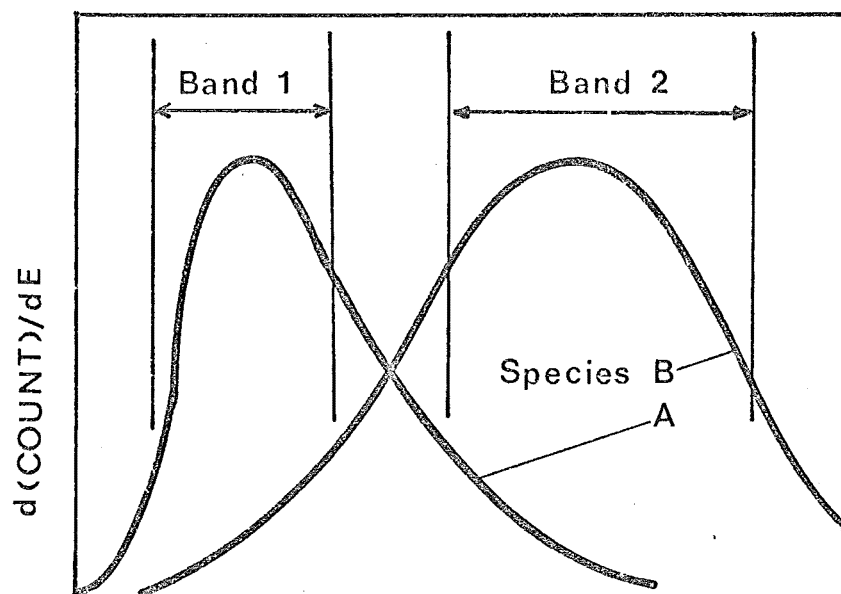
In chapter 6 of this thesis, we have seen that the spray residence time distribution has an important effect on the dryness of the product. If it was possible to know directly the evaporation as a function of residence time, this effect could be predicted and the performance of the spray dryer could be calculated with great accuracy.

The method whereby it was intended to measure these variables is by double-labelling the spray: a non-evaporating tracer can be used to measure residence times (as described in chapter 4), while a tracer evaporating with water can be used to measure evaporation.

The principle of double-label counting radioactive materials using a scintillation counter has been described by Bush (1). In scintillation counting, each radioactive species produces pulses with a specific energy spectrum (figure 7a). If counting is done within two energy bands, the ratio of the number of pulses counted in band 1 and band 2 will depend upon the species. Figure 7b gives a vectorial illustration of the method whereby the activities of two species can be measured simultaneously.

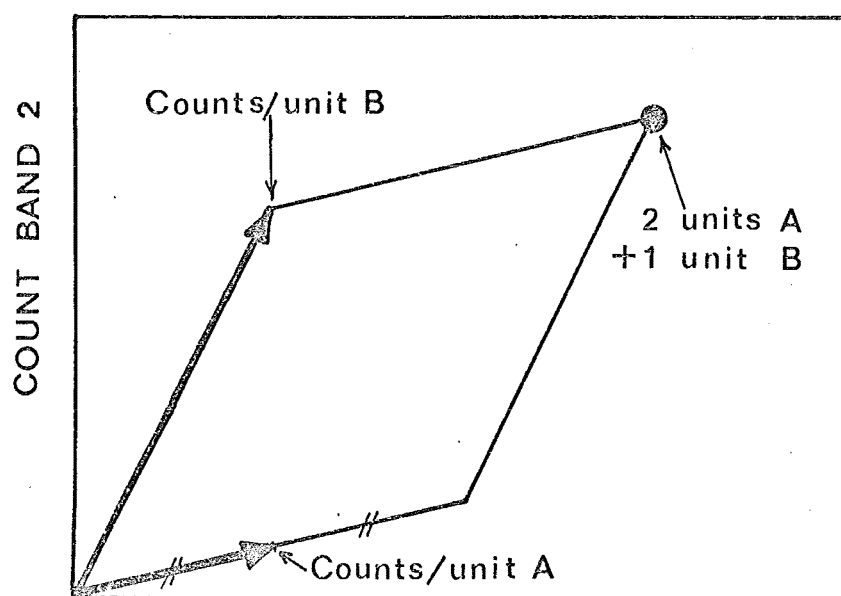
B.III.3 Experimental details

A saturated sodium-chloride solution was sprayed into the drying chamber. Tritium ( $^3\text{H}$ ) as  $\text{H}_2\text{O}$  was used to label the water, and  $^{14}\text{C}$  as  $\text{NaHCO}_3$  was used to label the salt. A pulse containing about 10  $\mu\text{C}$  of  $^{14}\text{C}$  and 50  $\mu\text{C}$  of  $^3\text{H}$  was injected into the nozzle at time 0.



ENERGY  $E$

(a)



COUNT BAND 1

(b)

FIG. B6: PRINCIPLE OF DOUBLE-LABEL COUNTING

The droplets were collected at the outlet of the spray dryer by a travelling droplet catcher as described in chapter 4. However, the collecting cells in this experiment were not covered with glass filter paper, but were filled with a collecting liquid and tightly wrapped around the side and at the bottom with thin, impervious P.T.F.E. tape. A small piece of brass was placed in each cell to facilitate the emptying of the cell.

Bench tests were carried out to find the best collecting liquid, i.e. one that would absorb the droplets or cover them so that evaporation from the cell is minimised. In these bench tests, both tracers were injected into cells filled with the collecting liquid being tested, and the activities were counted after various time intervals. Toluene, n-decane, a stable suspension of toluene-Triton X-100 - water (the liquid scintillant described in chapter 4) and a saturated lithium-chloride solution were tested; the last one was finally chosen.

After the droplets had been collected into the cells these were unwrapped, placed into counting vials, the vials were shaken and counted for both  $^3\text{H}$  and  $^{14}\text{C}$  as described before.

#### B.III.4 Results and discussion

Only one run was carried out, at operating conditions corresponding to those of the spray residence time distribution experiment, run A3 (chapter 4, table 1).

An entirely unexpected result showed up: instead of the  $^3\text{H}/^{14}\text{C}$  ratio decreasing with residence time (because tritium is evaporating while  $^{14}\text{C}$  is not), this ratio was found to increase with time and even exceed the ratio in the injected tracer pulse (figure 8).

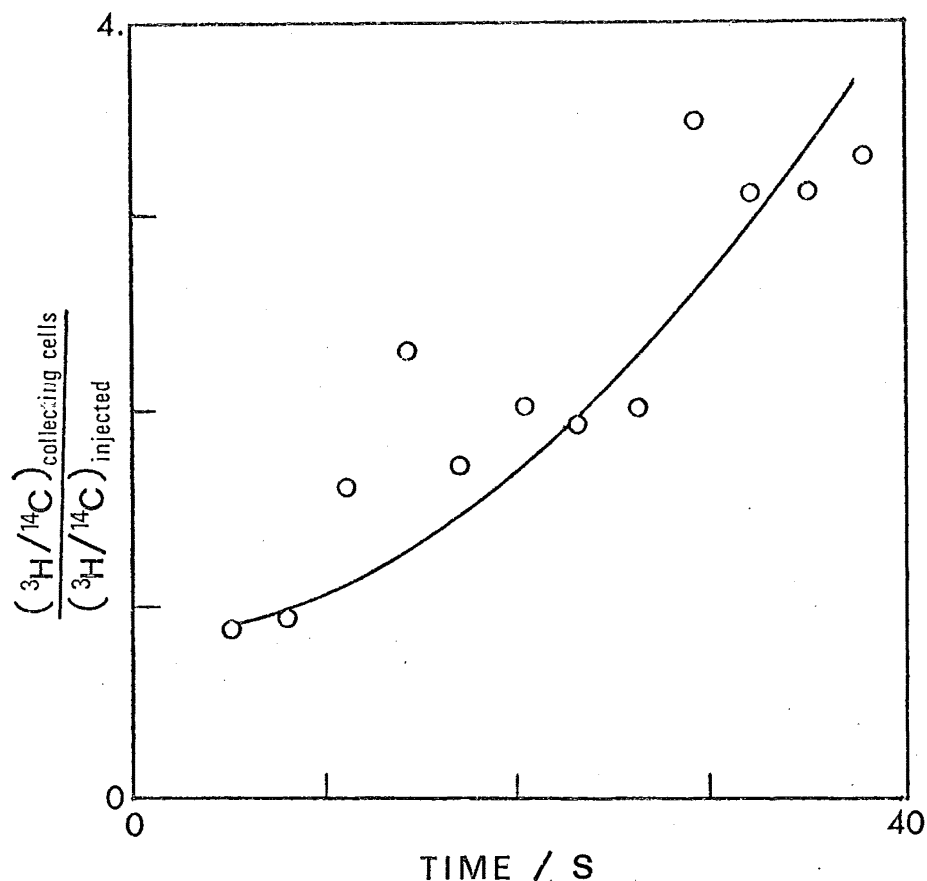


FIGURE B8: 'EVAPORATION' VS RESIDENCE TIME

The explanation for this phenomenon is that evaporation is not a one-way process but the net result of interchange of water molecules between the droplets and the air. Thus some tritiated water molecules were transferred from the droplets to the air, then re-entered droplets which had a higher residence time or which were injected into the drying chamber at a later time, thus increasing the  $^3\text{H}/^{14}\text{C}$  ratio.

This failure illustrates the need for careful theoretical investigation before starting any experiment.

#### Reference

- (1) Bush E.T., Anal. Chem. 36, 1082 (1964)

APPENDIX COPERATING PROCEDURES FOR THETWO-STAGE SPRAY DRYER

In the following sections valves identification numbers are shown on the flow diagram, Figure 3 of Chapter 1.

I. "COLD" RUN, AIR FLOW ONLY:I.1 - Preparation:

1. Fill in the operating sheet (Figure C1).
2. Check that no leak is present.
3. Isolate the two stages by ensuring that the rotary valve is in the "off" position, and close valve V7.
4. If the second stage is not required, close valves V3, V4 and V8 to isolate this stage.
5. If the second stage is required : open valves V3 and V4 full; ensure that the control valve CV2 is fully open and its actuator turned off; open valve V8 fully; close the butterfly valve V5 by lowering its lever, besides the cooler-scrubber.
6. Open valves V1 and/or V2 depending on the flowrate required.
7. Ensure that the pressure drops across the two pitot tubes (for the 100 mm main inlet pipe and for the 25.4 mm busbar box inlet pipe) are not excessive for the manometers used.
8. Set blower gearbox, according to the graph of Figure C3. Use third or fourth gear to avoid slow pulsations.
9. Fully open valve V14.
10. Set bypass valve V15 according to flowrate required. If inexperienced in using the spray dryer, open V15 fully, then close it slowly once blower has been started.

### I.2 - Turn-on Procedure:

1. Go through the check-list (Figure C2).
2. Turn the blower on.
3. Adjust valves V1 and/or V2 and/or V15 until the flowrate required for the first stage is obtained.
4. If the second stage is required : adjust valves V3, V4 and V8 until the flowrate required for the second stage is obtained.

### I.3 - Turn-off Procedure:

Turn the blower off.

## II. "HOT" RUN, AIR FLOW ONLY:

### II.1 - Preparation:

1. Go through the procedure described in Section I.1.
2. Set the control temperature of the steam heater on the temperature controller TC1.
3. Open the busbar box and connect the number (multiple of 3) of elements required. Check that all connectors are secure. Close busbar box.
4. If the second stage is required : set the temperature controller TC2.
5. Clean the psychrometer wet bulb and check their distilled water supply if required. CAUTION: The water level must be such that the wet bulb is just wet, not dry or overflowing.
6. Connect the required thermocouple terminals required to the 12-point recorder at the connecting board besides the control panel.
7. Ensure that the thermocouple cold junctions are at 0°C.

8. Ensure that the bleed valve V16 (for the probe of controller TC1) is fully open.

#### II.2 - Turn-on Procedure:

1. Go through check list.
2. Turn blower on.
3. Readjust the flow through the first stage as in Section I.2.
4. Readjust the flow through the second stage as in Section I.2.
5. Check the flow in the first stage.
6. Turn the temperature controllers on at the control panel.
7. Turn electric heater on if required.
8. Turn steam heater on very slowly by opening valve V12.
9. If required, turn the LiCl cells on.
10. If required, turn humidifying steam on by opening valves V9 and V11, and adjusting valves RV1 and V10.
11. Open the bleed valves associated with the humidity measuring devices H1, H2, H3, H4 until suitable flow rates are obtained (less than 0.5 m/s past the LiCl cells, at least 3 m/s past the psychometers). Ensure that the air temperature in the line from the column to the humidity measuring devices does not drop below the dew point.

#### II.3 - Turn-off Procedure:

1. Turn off electric heater.
2. Turn off heating steam.
3. Turn off humidifying steam.
4. When temperatures in system have dropped below 60°C, turn off blower.
5. Turn off the recorder and the LiCl cells.

### III. "HOT" RUN WITH SPRAYING OF FEED: (Using a two-fluid atomiser).

#### III.1 - Preparation:

1. Go through the procedure described in Section II.1.
2. Ensure that the proper nozzle is installed, the feed and the atomising air lines are connected, and the pressure equalising line is installed.
3. Ensure that a cyclone of the proper size is used as Cyclone 1. (see Chapter 1)
4. If the second stage is used : ensure that the rotary valve is clean, check that its speed is about 100-120 rpm, open fully valve V7 and close valve V6 , install a receiver under Cyclone 2. CAUTION: Dirt will cause leaks and damage the Rotary valve.
5. If the second stage is not used : install a product receiver at the base of Cyclone 1.
6. Check the working conditions of the pneumatic vibrators at the base of Cyclone 1 and at the bends of the second stage, the nozzle cleaner solenoid and its circuit, the intermittent valve V13 and its circuit, the air cooler for the solenoid of Valve V13.
7. If a high air rate (greater than 0.4 m/s in the drying chamber) is used, remove packing from the cooler scrubber.
8. Install filter bag if required.

#### III.2 - Turn-on Procedure:

1. Go through the procedure described in Section II.2.
2. Turn on the rotary valve.
3. Turn on the nozzle cleaner, the intermittent valve V13, the air cooler for the solenoid of V13, the pneumatic vibrators.



4. Turn on the cooler-scrubber water using a low flow rate (about 1 turn). CAUTION: Ensure that flow is not excessive, causing flooding of the plates in the cooler or flowback into Cyclone 1 and the rotary valve.
5. Turn on the atomising air and the feed pump, and adjust the feed rate.
6. Check temperatures and flowrates, and readjust if necessary.

### III.3 - Turn-off Procedure:

1. Turn off feed flow to nozzle. Turn off atomising air.
2. Turn off humidifying steam.
3. After twenty minutes, turn off heaters.
4. Turn off vibrator and intermittent valve V13. Turn off air cooler for V13.
5. Turn off rotary valve.
6. Turn off cooler-scrubber.
7. When temperatures in system have dropped to below 60°C, turn off blower.
8. Turn off recorder and LiCl cells.

# FIGURE C1

DATE:  
RUN:  
TIME ON:  
TIME OFF:

## SPRAY DRIER OP. SHEET

### NOZZLE

Dvs/ $\mu$ m:  
Nozzle No.:  
Air P/psig:  
Liq. head/in:  
Air rota/cm:  
Liq. rota/cm:  
Slurry concn/% solid:  
Mean final ptcle size/ $\mu$ m:  
Final density:  
Initial feed level:  
Final feed level:

### EVAPN CONDITIONS

$T_{air} - T_{wb}$  /  $^{\circ}$ C:  
Air humidity:  
 $T_{air}$  /  $^{\circ}$ C:  
 $T_{wb}$  /  $^{\circ}$ C:  
Time for 100% evap:  
99% evap:  
95% evap:

### ROTARY VALVE

Bottom rota rdg:  
Top rota rdg:  
Speed/rpm

### MANOMETERS

Busbars cooling pitot:  
Balance hot/cold air:  
Across 1st cyclone:  
Across 2nd cyclone:  
Across 2nd stage:  
Across cooler:

### 1ST STAGE AIR

$T$  /  $^{\circ}$ C:  
Humidity:  
 $Vel/m s^{-1}$   
Air Res. Time/s:  
Blower gear:  
Bypass:  
Butterfly valve:  
Pitot rdg/cm:  
Cyclone No.:

### 2ND STAGE AIR

No. of sections (3/1)  
Air rate, top rota rdg:  
Rate/kg  $s^{-1}$ :  
 $T$  control setting/ $^{\circ}$ C:  
 $T$  bottom/ $^{\circ}$ C:  
 $T$  top/ $^{\circ}$ C:  
 $Vel/m s^{-1}$ :  
Res. time/s:

### HEATERS

Final  $T$ / $^{\circ}$ C:  
Steam hter setting/ $^{\circ}$ C:  
Elec heater:  
 $T$  rise/ $^{\circ}$ C:  
Power/kW:  
No. elements:

### PRODUCT

Weight:  
Size:  
Moisture:

## FIGURE C2

### CHECK LIST

MANOMETERS: connected/isolated

12-PT RECORDER IDENTIFIED:

1/	2/	3/
4/	5/	6/
7/	8/	9/
10/	11/	12/

MAIN AIR STREAM:

Gearbox set:

Bypass set:

Main gate valve set:

Blower on:

Butterfly valve set:

Pitot tube read:

2ND STAGE:

No. of sections set:

Inlet valves set:

Outlet valve open/shut:

Rotameter read:

ROTARY VALVE:

Speed set:

Flows set:

Motor on:

12-POINT RECORDER:

Thermos filled:

Recorder on:

Date entered:

HEATING SYSTEM:

Modulating valves on:

Control temperatures set:

Steam on:

Elements set:

Busbar cooling air on/off:

Electric heater on:

HUMIDIFICATION

1st stage humidification steam on:

2nd stage humidification steam on:

LiCl cells on:

Hygrometers cleaned and filled:

AUXILIARY EQUIPMENT:

Cooler-scrubber on:

Cooling-water on:

Vibrator on:

Pulsing valve on:

"Hair dryer" on:

EQUILIBRIUM T REACHED

LINES CLEARED

NOZZLE:

Cleaner on/checked:

Initial feed level recorded:

P. equalising line on:

Stirrer on:

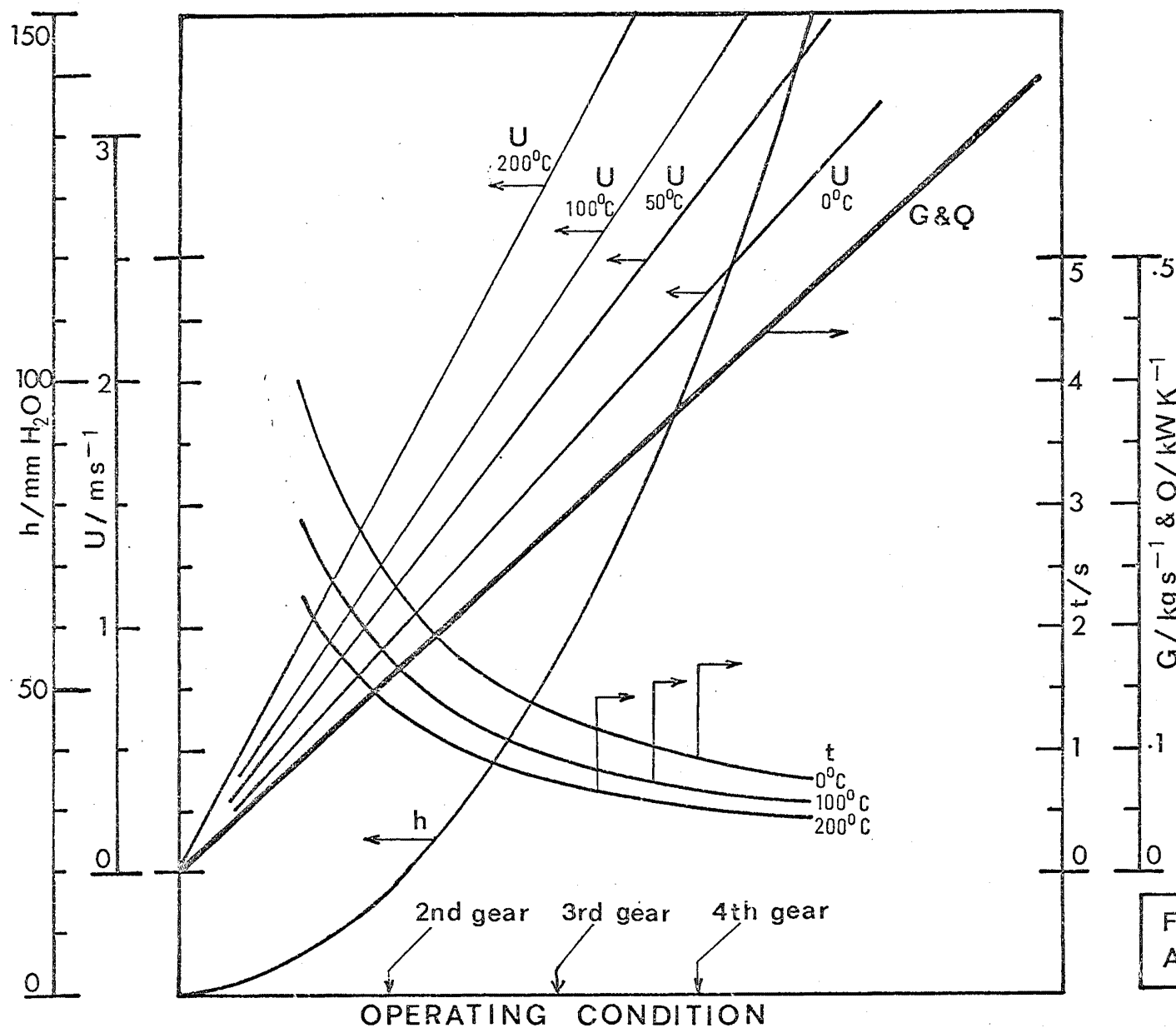
Air on:

Line opened, time:

TIME SPRAYING STOPPED:

FINAL FEED LEVEL RECORDED:

PRODUCT WEIGHED:



$h$  = 4" inlet Pitot tube reading

$G$  = mass air rate

$Q$  = heat required for 1 K raise

$U$  = air velocity in dryer

To find approximate settings, draw a vertical line through the desired operating condition.

FIG. C3 : SPRAY DRYER AIRFLOW SETTINGS

APPENDIX D

LISTING OF COMPUTER PROGRAM

FOR EVAPORATION CALCULATION

IN COCURRENT SPRAY DRYERS

```

C EVAPORATION IN COCURRENT SPRAYDRYER WITH PRESSURE OR PNEUMATIC NOZZLE 00002000
C VERSION 3 00003000
C EXTENSION OF PROG. OF 13-MAY-74 AND 27-JUN-75 00004000
C 00005000
C 00006000
C *****00007000
C 00008000
C THEORY 00009000
C 00010000
C 00011000
C ASSUME HYDRODYNAMIC PROFILE IS DIVIDED INTO 2 ZONES: 00012000
C 1/ JET ZONE,GOVERNED BY JET DYNAMICS,WHOSE MASS FLOW,VEL.,TEMP. AND 00013000
C HUMIDITY PROFILE IS CALC. IN SUBROUTINE "PROFIL" 00014000
C IN THIS ZONE MOMENTUM BALANCE IS NOT NEGL. FOR THE AIR 00015000
C THIS ZONE MAY INCLUDE A TRANSITION WHERE PROFILES CHANGE LINEARLY 00016000
C WITH DISTANCE FROM JET TO MAIN ZONE CHARACTERS 00017000
C 2/ MAIN ZONE,WHICH DEPENDS ON THE DRYER,WHOSE MASS FLOW ETC... 00018000
C PROFILE ARE CALC. IN SUBROUTINE "PROFII" 00019000
C AT START OF THIS ZONE ALL DROPLETS ARE AT SETTLING VEL. 00020000
C BY DEFAULT ASSUME A LINEAR TEMPERATURE PROFILE IN MAIN ZONE DUE TO 00021000
C WALL HEAT LOSS,IN THE ABSENCE OF EVAPORATION 00022000
C IN ADDITION A TRANSITION ZONE WITH LINEAR GRADIENTS MAY BE 00023000
C INSERTED BETWEEN THE PREVIOUS 2 ZONES 00024000
C 00025000
C NB BY CHANGING PROFIL&PROFII CAN ACCOMODATE ANY FLOW REGIME,HT LOSS... 00026000
C 00027000
C THE VELOCITY,TEMPERATURE & CONCENTRATION PROFILE IN A JET CAN BE 00028000
C FOUND IN ABRAHOVITCH,"THEORY OF TURBULENT JETS" 00029000
C THE EFFECTIVE TEMPERATURES,VELOCITIES ETC... IN A JET ARE CALCULATED 00030000
C IN THESIS 00031000
C ENTRAINMENT OF AIR INTO JET IS CALCULATED BY DAVIES 00032000
C 00033000
C EVAPORATION FROM DROPLETS FOLLOW RANZ & MARSHALL EQN 00034000
C  $NU=2+0.6*RE^{0.5}*PR^{0.5}$  00035000
C 00036000
C EFFECT OF MASS TRANSFER ON HEAT TR. GIVEN BY  $(1/(1+B))$  00037000
C WHERE  $B=SPEC.HT*TEMP.DIFFERENCE/LATENT HEAT$  00038000
C 00039000
C ASSUME THAT DROPLET EVAPORATION COMPRISES 2 PERIODS: 00040000
C 1ST PERIOD:DROPLET SHRINKS FREELY 00041000
C 2ND PERIOD:(AFTER WCRIT,ECRIT,DCRIT) CRUST FORMS,SHRINKING CEASAS 00042000
C DROPLET DENSITY FALLS 00043000
C 00044000
C STD DRAG CURVE IS APPROXIMATED SEGMENTWISE 00045000
C 00046000
C ADIABATIC-SATURATION TEMPERATURE&HUMIDITY OF EVAPORATING SOLUTION 00047000
C ARE CALCULATED IN SUBROUTINE WBULB 00048000
C 00049000
C EFFECT OF TURBULENCE:CALC. RELATIVE VEL. DUE TO TURBULENCE AS LEVIN & 00050000
C GLASTONBURY,THEN ADD VECTORIALLY TO MEAN REL.VEL.,FROM THIS COMBINED 00051000
C VEL FIND RE,DRAG,NUSSELT NO. 00052000
C 00053000
C APPROX. TERMINAL VEL AT START OF MAIN ZONE CALC FROM SMITH 00054000
C 00055000
C EFFECT OF RADIATION EITHER FOLLOWS TREATMENT IN THESIS(ASSUMING 00056000
C UNIFORM RADIATION) OR HOTTEL&COHEN TREATMENT(SEE DEFINITION OF RADCAL) 00057000
C 00058000
C 00059000
C 00060000
C CALCULATION METHOD 00061000
C 00062000
C 00063000
C AT EACH POINT IN SPACE,CALCULATE THE VELOCITIES AND EVAPORATIONS 00064000
C FOR EACH SIZE RANGE 00065000
C ADD UP OVER ALL SIZE RANGES 00066000
C FIND EFFECT ON AIR VELOCITY,TEMPERATURE AND HUMIDITY 00067000
C RECALCULATE SPRAY VELOCITY AND EVAPORATION BASED ON THE CORRECTED 00068000
C AIR CONDITIONS,ETC... UNTIL GET CONVERGENCE ("TEST" & "DAM"<.01) 00069000
C ITERATION IS ACCELERATED BY USING THE WIGHTING FACTORS H FOR 00070000
C EVAPORATION AND HV FOR SPRAY VELOCITY 00071000
C WHEN CONVERGENCE IS REACHED,GO ON TO THE NEXT POINT 00072000
C 00073000
C FOR DROPLET SURFACE TEMPERATURE,FILM TEMP.,FILM PROPERTIES,USE VALUES 00074000
C AT PREVIOUS POSITION 00075000
C FOR DROPLET SIZE&DENSITY,AIR TEMP.,AIR VEL.,CORRECT DURING ITERATIONS 00076000
C 00077000
C THE EQUATION OF MOTION EXPRESSES THE RATE OF CHANGE OF SQUARED 00078000
C VELOCITY OF EACH DROPLET WRT DISTANCE 00079000
C FOR VERY SMALL DROPLETS(TERMINAL REYNOLDS NO<1)ASSUME REL.VEL. IN 00080000
C MAIN ZONE FOLLOWS STOKES EQN 00081000
C THE EQN OF EVAPORATION EXPRESSES THE RATE OF CHANGE OF REL.EVAPORATN 00082000
C WRT DISTANCE 00083000
C 00084000
C RUNGE-KUTTA METHOD OF ORDER 4 IS USED IN SOLVING THE EQUATION OF 00085000
C MOTION AND EVAPORATION 00086000
C 00087000
C 00088000
C 00089000
C *****00090000
C 00091000

```

C	00092000
C NOTATION	00093000
C	00094000
C	00095000
C AK1,AL1,AK2,AL2...=INCREMENTS IN ESIZE(J)&W(J) FOR RUNGE-KUTTA	00096000
C AM=MEAN VEL. FOR WHOLE SPRAY AT A CERTAIN DISTANCE,M/S	00097000
C AMOLD=OLD AM,M/S	00098000
C AMSIZE(J)=LOCAL VELOCITY FOR J-TH SIZE RANGE,M/S	00099000
C NB:AM,AMSIZE INCLUDE THE MOMENTUM OF EVAPORATED LIQUID	00100000
C ANOZ:IF(ANOZ.GT.0.)PNEUMATIC NOZZLE,OTHERWISE PRESSURE NOZZLE	00101000
C ATP=INVERSE PARTICLE TIME CST,/S	00102000
C CORESQ=DRAG COEFT.*TERMINAL REYNOLDS NO. SQUARED	00103000
C CDRT=TERMINAL DRAG FROM SMITH	00104000
C CF=FEED SPECIFIC HEAT,J/KGK	00105000
C COEFF2=CONSTANT COEFFICIENT IN THE EVAPORATH EQN=6/HTLAT/WLIQ/DENSLO	00106000
C COND=CONDITION THAT(ITER.GT.16)	00107000
C COND1=CONDITION FOR CONVERGENCE	00108000
C CPGAS=AIR SPECIFIC HEAT,J/KG K	00109000
C CRAD=RADIATION FLUX TO DROP/(RADIOS-TWB**4),W/M2K2	00110000
C CS=ADIABATIC SATURATED AIR SPECIFIC HT,J/KGK	00111000
C CSJ(J)=SPECIFIC HEAT OF AIR+WATER VAPOUR AT DROP SURFACE,J/KG.K	00112000
C CSS=CSJ(J)	00113000
C DAM=RELATIVE CHANGE IN SPRAY MOMENTUM	00114000
C DCR(J)=CRUST FORMING DIAMETER,M	00115000
C DCRIT=CRUST FORMING DIAMETER,M	00116000
C DEN(J)=DROPLET DENSITY,KG/M3	00117000
C DENLIQ=DENSITY OF LIQUID IN FEED,KG/M3	00118000
C DENOLD(J)=VALUE OF DEN(J) AT PREVIOUS POSITION	00119000
C DENS=LOCAL AIR DENSITY,KG/S	00120000
C DENSL=DENSITY OF DROPLET BEING CONSIDERED,KG/M3	00121000
C DENSLO=INITIAL DROPLET DENSITY,KG/M3	00122000
C DENSOL=DENSITY OF SOLID IN FEED,KG/M3	00123000
C DER=DERIVATIVE OF SATURATION CURVE OF WATER,/K	00124000
C DHY=HYDRAULIC DIAMETER OF DRYER=4*VOL/WALL AREA,M	00125000
C DISTAN=DISTANCE FROM NOZZLE AT WHICH CALCULATIONS ARE TERMINATED,M	00126000
C DN=MATRIX OF NUMBER OF DROPLETS IN EACH SIZE RANGE	00127000
C DOLD(J)=VALUE OF D(J) AT PREVIOUS POSITION	00128000
C DRAG=SUBFUNCTION CALCULATING DRAG COEFFICIENT	00129000
C DVOL(J)=INITIAL VOLUME FRACTION OF J-TH SIZE RANGE	00130000
C DX1=DISTANCE INCREMENT IN JET ZONE,M	00131000
C DX2=DISTANCE INCREMENT IN MAIN ZONE,M	00132000
C DO=MATRIX OF VALUES OF INITIAL DROPLET DIAS FOR EACH SIZE RANGE,M	00133000
C D32(I)=SAUTER MEAN DIAMETER,M	00134000
C E(I)=FRACTION OF SPRAY EVAPORATED	00135000
C ECRIT=FRACTION EVAPORATION AT WHICH CRUST FORMS	00136000
C EMAX=MAX.POSSIBLE EVAPORATION	00137000
C EMIS=MEAN ABSORPTIVITY OR EMISSIVITY OF DROPLETS IN DRYER	00138000
C EMIW=EMISSIVITY OF WALL	00139000
C ESOLD(J)=OLD VALUE OF ESIZE(J)	00140000
C ESIZE(J)=FRACTION EVAPORATED FOR J-TH SIZE RANGE (LOCAL)	00141000
C EXC=EXTINCTION COEFFT FOR RADIATION INTO CLOUD=PROJECTED AREA OF DROPS	00142000
C PER UNIT VOL,/M	00143000
C EOO=TOTAL EVAPORATION TO DATE NOT DUE TO DROPLET OVERHEAT	00144000
C FAC=RELATIVE DRYING RATE AS COMPARED WITH DROPLET OF LIQUID SOLUTION	00145000
C FCL=EFFECTIVE ABSORPTIVITY OF CLOUD OF DROPLETS AS A WHOLE	00146000
C FCURVE=SUBFUNCTION TO CALC. FAC	00147000
C FE=FRACTION UNEVAPORATED FOR WHOLE SPRAY	00148000
C FSIZE=1-ESIZE(J)	00149000
C FO=LIQUID MASS FEED RATE,KG/S	00150000
C F1=SUBFUNCTION CALCULATING THE DERIVATIVE OF W(J) VS DISTANCE	00151000
C F2=SUBFUNCTION CALCULATING THE DERIV. OF ESIZE(J) VS DISTANCE	00152000
C G(I)=AIR MASS RATE INCLUDING ENTRAINED AIR,KG/S	00153000
C GEXT=MASS RATE OF EXTERNAL AIR FLOW,KG/S	00154000
C GO=ATOMISING AIR MASS RATE,KG/S	00155000
C HAJ=JET HALF ANGLE,DEG(DEFAULT VALUE=12.4)	00156000
C HCW=HTLAT*WLIQ/CF,K	00157000
C HRATIO=FO*WLIQ*HTLAT/CPGAS=TEMP. FALL CAUSED TO UNIT MASS RATE OF AIR	00158000
C BY TOTAL EVAPORATION OF FEED,K KG/S	00159000
C HTLAT=HEAT OF EVAPORATION OF LIQUID,J/KG	00160000
C I=INDEX REFERRING TO POSITION	00161000
C J=INDEX REFERRING TO SIZE RANGE	00162000
C JEV=NO. OF SIZE RANGES COMPLETELY EVAPORATED	00163000
C NPT=NUMBER OF POINTS IN SPACE CONSIDERED	00164000
C NP1=NO.OF PTS FROM ORIGIN TO XTRA INCLUSIVE	00165000
C NP2=NO.OF PTS FROM XTRA(EXCLUSIVE) TO XEND(INCLUSIVE)	00166000
C NP3=NO.OF PTS FROM ORIGIN TO XJET INCLUSIVE	00167000
C NSIZE=NO. OF SIZE RANGES(TO BE SUPPLIED BY "SPRAY")	00168000
C PRINT=DISTANCE INCREMENTS FOR PRINTOUT,JETZONE,M	00169000
C PRINT1=DISTANCE INCREMENTS FOR PRINTOUT,MAIN ZONE,M	00170000
C PROFIL=SUBROUTINE CALCULATING THE VELOCITY,TEMPERATURE ETC...	00171000
C PROFILE IN THE JET (& TRANSITION) ZONE	00172000
C PROF11=SUBROUTINE CALCULATING THE PROFILES IN THE MAIN ZONE	00173000
C QRCPI=1+RADIANT HT/CONVECTION HT	00174000
C RADCAL=PARAMETER IDENTIFYING METHOD OF RADIATION CALCN	00175000
C IF RADCAL=0.,NO RADIATION CALCULATION	00176000
C IF RADCAL<0.,ASSUME UNIFORM RADIATION&USE METHOD IN THESIS	00177000
C IF RADCAL.GT.0,USE HOTTEL&COHEN METHOD.WRAD(I),I=1,40 MUST THEN	00178000
C BE READ FROM CARDS	00179000
C RATE(J)=MEAN EVAPORATION RATE=ESIZE(J)/RTI(J),/S	00180000
C RCPI(J)=1+RADIANT HT/CONVECTION HT	00181000

C RJET=JET RADIUS,M	00182000
C RS=RELATIVE HUMIDITY OF AIR IN EQUIL. WITH EVAPORATING SOLUTION	00183000
C RTI(J)=REIDENCE TIME OF J-TH SIZE DROPLETS,S	00184000
C RTIME=A MEAN RESIDENCE TIME OF DROPLETS,S	00185000
C SE=DROPLET EVAPN RATE/EVAPN RATE WITH DROPLET OVERHEAT NEGLECTED	00186000
C SET=SPRAY EVAP RATE/EVAPN RATE WITH SPRAY OVERHEAT NEGLECTED	00187000
C SH=SHIELDING FACTOR FOR RADIATION FROM WALL TO DROPS	00188000
C SHA=HEAT CAPACITY OF ATOMISING AIR,J/K	00189000
C SHF=HEAT CAPACITY OF FEED,J/K	00190000
C SPRAY=SUBROUTINE CALCULATING THE DROPLET SIZE NUMBER DISTRIBUTN	00191000
C SQVRT=VRTSQ(J),M2/S2	00192000
C T(1)=JET AIR EFFECTIVE TEMP.,CORRECTED FOR EVAPORATION,DEG.K	00193000
C TAV=MEAN FILM TEMP. AROUND DROPLETS AT PREVIOUS POINT,DEG.K	00194000
C TDR(J)=DROPLET MEAN TEMPERATURE,K	00195000
C TEST=RELATIVE CHANGE IN EVAPORATH BW ITERATIONS	00196000
C TEXT=TEMPERATURE OF EXTERNAL AIRFLOW,DEG.K	00197000
C TF=FEED TEMPERATURE,K	00198000
C TFALL=FALL IN AIR TEMPERATURE DUE TO EVAPORATION,K	00199000
C THCOND=LOCAL AIR THERMAL CONDUCTIVITY,W/M K	00200000
C TINIT(1)=JET AIR EFFECTIVE TEMP. WITHOUT SPRAY,DEG.K	00201000
C TLOSS=DECREASE IN AIR TEMP.PER UNIT LENGTH DUE TO WALL LOSS,K/M	00202000
C TS(J)=TWB=SURFACE TEMP. OF DROPLET IF DROPLET HEAT NEGLECTED,K	00203000
C TUIH(1)=SQUARED TURBULENT VEL. OF AIR,M2/S2	00204000
C TUINO=TUIN AT TOP OF DRYER,M2/S2	00205000
C TUINI=TUIN AT BOTTOM OF DRYER,M2/S2	00206000
C TUSC(1)=LAGRANGIAN TIME SCALE OF TURBULENCE,S	00207000
C TUSCO=TUSC AT TOP OF DRYER,S	00208000
C TUSCI=TUSC AT BOTTOM OF DRYER,S	00209000
C TW=EQUILIBRIUM TEMPERATURE OF AIR&FEED EMERGING FROM NOZZLE,K	00210000
C TWA=MEAN RADIATING TEMP. OF WALL,K	00211000
C TSAVE = MASS AVERAGE OF THE SURFACE TEMPERATURES OF DROPLETS IN	00212000
C SPRAY,FOR PURPOSE OF CALC. THE FILM PROPERTIES,DEG.K	00213000
C TO=TEMPERATURE OF ATOMISING AIR,DEG.K	00214000
C TO WILL BE RECALC. TO GIVE HYGTROTHERMAL EQM WITH FEED	00215000
C VAIR(1)=AIR VEL. IN JET,CORRECTED FOR LOSS OF MOMENTUM TO SPRAY,M/S	00216000
C VELOUT=EMERGING LIQUID VELOCITY,M/S	00217000
C VDROPS=DROPLET VELOCITY AVERAGED OVER ALL SIZES,M/S	00218000
C VINI(1)=AIR VEL(EFFECTIVE) IN JET,WITHOUT SPRAY,M/S	00219000
C VISKIN=LOCAL AIR KINETIC VISCOSITY,M2/S	00220000
C VLIQ=INITIAL LIQ. VOL. FRACTION IN DROPS	00221000
C VRTSQ(J)=SQUARED REL.VEL. DUE TO TURBULENCE,M2/S2	00222000
C VO=VEL. OF ATOMISING AIR EMERGING FROM NOZZLE,M/S	00223000
C W(J)=SQUARED VELOCITY OF DRIplet,M2/S2	00224000
C WAGRAD=LOCAL AIR SQUARED VEL. GRADIENT	00225000
C WB=ADIABATIC-SATURATION TEMPERATURE OF EVAPORATING SOLUTION,K	00226000
C WBULB=SUBROUTINE CALCULATING ADIABATIC SATURATION TEMPERATURE &	00227000
C HUMIDITY,OR SATURATION HUMIDITY AT A GIVEN TEMPERATURE	00228000
C FOR A GIVEN EVAPORATING SOLUTION	00229000
C WLCRIT=WET BASIS MOISTURE CONTENT AT SOLIDIFICATION	00230000
C WLIQ=1-WSOL=INITIAL LIQ. MASS FRACTON	00231000
C WOLD(J)=OLD W(J),M2/S2	00232000
C WRAD(1)=RADIATION 'LEAVING FLUX DENSITY' AT PT 1,DEFINED BY HOTTEL ,	00233000
C ALSO CALLED RADIOSITY,W/M3 STERADIAN	00234000
C WSOL=MASS FRACTION SOLID IN INITIAL FEED,KG/KG	00235000
C X(1)=DISTANCE FROM NOZZLE,M	00236000
C XEND=TOTAL LENGTH CONSIDERED,M	00237000
C XJET=LENGTH OF JET ZONE(UP TO TRANSITION),M	00238000
C XTRA=LENGTH UP TO END OF TRANSITION ZONE,M	00239000
C Y(1)=EFFECTIVE HUMIDITY OF AIR IN JET,KG/KG	00240000
C YEXT=HUMIDITY OF EXTERNAL AIR FLOW,KG/KG	00241000
C YRISE=RISE IN AIR HUMIDITY DUE TO EVAPORATION,KG/KG	00242000
C YSAT=ADIABATIC SATURATION HUMIDITY OF WATER,KG/KG DRY AIR	00243000
C YSURF=SURFACE HUMIDITY OF DROPLETS,KG/KG DRY AIR	00244000
C YO=ATOMISING AIR HUMIDITY DRY BASIS,KG/KG	00245000
C YO WILL BE RECALC TO GIVE HYGTROTHERMAL EQM WITH FEED	00246000
C	00247000
C	00248000
C *****	00249000
C	00250000
C	00251000
C	00252000
C	00253000
C	00254000
LOGICAL COND,COND1	
DIMENSION VAIR(1001),D32(1001),E(1001),D(20),W(20),V(20),DVOL(20),	00255000
SAMSIZE(20),ESIZE(20),DN(20),DO(20),ESOLD(20),WOLD(20),DEN(20),	00256000
ST(1001),TS(20),DCR(20),VRTSQ(20),RCPI(20),CSJ(20),	00257000
SWRAD(1001),DSOLD(20),DENOLD(20),TDR(20),RTI(20),RATE(20)	00258000
COMMON/INIT/VINI(1001),YINIT(1001),G(1001),TINIT(1001),X(1001),	00259000
SRJET,VO,GO,TO,YO,FO,VEXT,GEXT,TEXT,YEXT,NP1,NP2,NPT,NP3	00260000
S,TUIN(1001),TUSC(1001),TUINO,TUINI,TUSCO,TUSCI,TLOSS,DENSF,HAJ	00261000
COMMON /VELEP/ DENSL0,WSOL,WLIQ,VLIQ,COEFF2,HTLAT,DENLIQ,ECRIT,	00262000
SDCRIT,TAIR, VA ,DENS,VISKIN,THCOND,TWB,DENSL,DINIT,DIA,RE,VELD ,	00263000
SCDRSQ,WAGRAD,SQVRT,CRAD,RADIOS,QRCPI,CSS	00264000
C	00265000
C	00266000
C	00267000
C	00268000
C	00269000
C	00270000
C	00271000



C		00272000
C		00273000
C		00274000
C	*****	00275000
C	INPUT INITIAL CONDITIONS	00276000
C	CARD 1:LAST 2 DATA OPTIONAL	00277000
C	CARD 3:FOR PNEUMATIC NOZZLE ONLY	00278000
C	CARD 5:LAST 4 DATA OPTIONAL(FOR CALC EFFECT OF TURBULENCE ONLY)	00279000
C	A FUNCTION FCURVE(AMOIST,D,RATE) MUST BE SUPPLIED TO CALC. RELATIVE	00280000
C	DRYING RATE	00281000
C	SUBR. SPRAY MUST SUPPLY INITIAL SIZES DO(J),NUMBER OF DROPLETS IN	00282000
C	EACH SIZE RANGE DN(J)(NON NORMALISED),NUMBER OF SIZE RANGES	00283000
C		00284000
C		00285000
C		00286000
1	FORMAT(8F10.0)	00287000
	READ(5,1)XJET,XTRA,DX1,XEND,DX2,PRINT1,PRINT2	00288000
	READ(5,1)ANOE,RJET,VELOUT,HAJ	00289000
	READ(5,1)VO,GO,TO,YO	00290000
	READ(5,1)FO,WSOL,DENSOL,DENLIQ,HTLAT,WLCRIT,CF,TF	00291000
	READ(5,1)RS	00292000
	READ(5,1)GEXT,TEXT,YEXT,VEXT,TLOSS	00293000
	READ(5,1)TUINO,TUINI,TUSCO,TUSCI	00294000
	READ(5,1)RADCAL,DHY,EXC,EMIS,EMIW,TWA	00295000
	IF(RADCAL.GT.0.)READ(5,1)(WRAD(1),I=1,1001)	00296000
	CALL SPRAY(00,0N,NSIZE)	00297000
		00298000
		00299000
C	END OF DATA INITIALISATION	00300000
C	*****	00301000
C		00302000
C		00303000
C		00304000
C		00305000
C		00306000
C		00307000
C		00308000
C		00309000
C		00310000
	PRINT 2 ,XJET,XTRA,XEND,DX1,DX2	00311000
	PRINT 12 ,ANOE,HAJ	00312000
	PRINT 22,RJET,VO,GO,TO,YO,FO,WSOL,DENSOL,DENLIQ,HTLAT,	00313000
	SWLCRIT,CF,TF,GEXT,TEXT,YEXT,VEXT,TLOSS	00314000
	PRINT 32 ,TUINO,TUINI,TUSCO,TUSCI,DHY,EXC,EMIS,EMIW,TWA,	00315000
	SRADCAL	00316000
	IF(PRINT1.EQ.0)PRINT1=DX1	00317000
	IF(PRINT2.EQ.0)PRINT2=DX2	00318000
	NP1=XTRA/DX1+1.1	00319000
	IF(NP1.GT.1001)NP1=1001	00320000
	NP2=(XEND-XTRA)/DX2+0.1	00321000
	IF(NP2.GT.1001-NP1)NP2=1001-NP1	00322000
	NPT=NP1+NP2	00323000
	NP3=XJET/DX1+1.1	00324000
	IF(NP3.GT.NP1)NP3=NP1	00325000
	WLIQ=1.-WSOL	00326000
	VLIQ=DENSOL*WLIQ	00327000
	VLIQ=VLIQ/(VLIQ+DENLIQ*WSOL)	00328000
	ECRIT=(1.-WLCRIT/WLIQ)/(1.-WLCRIT)	00329000
	DENSLO=WSOL/DENSOL+WLIQ/DENLIQ	00330000
	DENSLO=1./DENSLO	00331000
	DENSE=DENSLO	00332000
	COEFF2=6./HTLAT/WLIQ/DENSLO	00333000
	CPGAS=1.E3	00334000
	HRATIO=FO*WLIQ*HTLAT/CPGAS	00335000
	HCW=HTLAT*WLIQ/CF	00336000
	IF(ANOE.GT.0.)GOTO 10	00337000
	VO=VELOUT	00338000
	GO=0.	00339000
	TO=TF	00340000
10	CONTINUE	00341000
C	CALC VOLUME FRACTIONS IN SPRAY ,CRIT.DIAS AND INITIAL SAUTER DIA.	00342000
	SHRINK=(1.-ECRIT*VLIQ)**(1./3.)	00343000
	SUM2=0	00344000
	SUM3=0	00345000
	DO 20 J=1,NSIZE	00346000
	DVOL(J)=DN(J)*DO(J)**3	00347000
	VOL=VOL+DVOL(J)	00348000
	DD=DO(J)*DO(J)*DN(J)	00349000
	DDD=DD*DO(J)	00350000
	SUM2=SUM2+DD	00351000
	SUM3=SUM3+DDD	00352000
	DCR(J)=DO(J)*SHRINK	00353000
20	CONTINUE	00354000
	D32(1)=SUM3/SUM2	00355000
	DO 30 J=1,NSIZE	00356000
30	DVOL(J)=DVOL(J)/VOL	00357000
	IF(NP1.EQ.1)GOTO 50	00358000
	DO 40 I=2,NP1	00359000
40	X(I)=X(I-1)+DX1	00360000
	IF(NP2.EQ.0)GOTO 70	00361000

[illegible]

```

      NPRINT=PRINT1/0X1+.1
      DO 340 I=2,NPT
C
C  CALC AIR PROPERTIES IN FILM AROUND DROPLETS
      TAV=(T(I-1)+TSAVE)/2
      DENS = 1.293*273/TAV
      VISKIN = 1.488E-6*TAV**1.5/(TAV+122.1*EXP(-11.5/TAV))/DENS
      THCOND = 2.646E-3*TAV**1.5/(TAV+245.*EXP(-27.64/TAV))
      VAIR(I)=VINI(I)*T(I)/TINIT(I)
C
      IF(I.NE.NP1+1)GOTO 170
C
C  RESET PARAMETERS ,INITIAL CONDITNS & PRINT HEADINGS FOR MAIN ZONE
C
C
C
      IF(NP1.NE.1)PRINT 82
C
C  CALC RADIATION PARAMETERS
      IF(RADCAL.GE.0.)GOTO 140
      RADIOS=TWA**4.
      SH=1.
      IF(EXC.EQ.0.)GOTO 120
      DHYEXC=DHY*EXC
      SH=1./DHYEXC/EMIS
      IF(DHYEXC.GT.10.)GOTO 120
      BE=-ALOG(8./9./DHYEXC**2.*(1.-(1.+1.5*DHYEXC)*EXP(-1.5*DHYEXC)))
      EBE=EXP(-BE)
      EBE2=EXP(-BE/2.)
      FCL=EMIS*(1.-EBE)/(1.-(1.-EMIS)*(1.-EBE2))
      SH=1./EMIS/DHYEXC/(1./FCL+1./EMIW-1.)
120  CONTINUE
      CRAD =5.67E-8*SH*EMIS
140  CONTINUE
C
      PRINT 112
      IF(RADCAL.LT.0.)PRINT 242 ,FCL,SH,CRAD
      PRINT 72
      IF(NP1.EQ.1)PRINT 192,X(1),T(1),TSAVE,1.-E(1),VAIR(1),G(1),D32(1)
      DX=DX2
      NPRINT=PRINT2/0X2+.1
      IF(XJET.NE.XTRA)GOTO 150
      VINI(NP1)=VINI(NP1+1)
      YINIT(NP1)=YINIT(NP1+1)
      G(NP1)=G(NP1+1)
      TINIT(NP1)=TINIT(NP1+1)
      T(NP1)=TINIT(NP1)-E00*HRATIO/G(NP1)
      VAIR(NP1)=VINI(NP1)*T(NP1)/TINIT(NP1)
      YAIR = YINIT(NP1)+E(NP1)*FO*WLIQ/G(NP1)
150  CONTINUE
      DO 160 J=1,NSIZE
      IF(D(J).LE.0.)GOTO 160
C  AT START OF MAIN ZONE DROPLETS ARE APPROXLY AT TERMINAL VEL WRT AIR
C  CALC. TERMINAL VELOCITIES FROM SMITH
      CDRESQ=1.33*DEN(J)*9.8*D(J)**3/DENS/VIKIN/VIKIN
      IF((CDRESQ.GT.10.)AND.(XJET.NE.XTRA))GOTO 160
      CDRT=574./CDRESQ+32./CDRESQ**3.9+1./1.8+758/CDRESQ**3.6)
      IF(CDRESQ.LE.10.)CDRT=576./CDRESQ
      VTERM=SQRT(4.*D(J)*DEN(J)*9.8/3./DENS/CDRT)
      V(J)=VAIR(NP1)+VTERM
      W(J)=V(J)*V(J)
      WOLD(J)=W(J)
160  CONTINUE
C  FINISH RESETTNG FOR MAIN ZONE
170  CONTINUE
C
      IF(G(1).NE.0.)TFINIT=E00*HRATIO/G(1)
      TFM=TINIT(1)-TFINIT-WB
      IF(TFM.LT.0.)TFM=0.
      EMAX=E(1-1)+TFM*G(1)/HRATIO
      AHMAX=(G(1)*VINI(1)+FO*VELOUT)/(G(1)+FO)
C
      START ITERATING AT 1-TH PT -----
C
      DO 240 ITER=1,20
      COND=(ITER.GT.14).OR.(EMAX.LE.E(1-1))
      IF(RADCAL.GT.0.)RADIOS=WRAD(1)/5.67E-8
C
C  CALC SQUARED REL VEL DUE TO TURBULENCE
      DO 180 J=1,NSIZE
      IF(DSOLD(J).LE.0.)GOTO 180
      VRELAB=ABS(V(J)-VAIR(1-1))
      REY=VRELAB*DSOLD(J)/VIKIN
      CDR=DRAG(REY)
      ATP=3.*CDR*DENS*VRELAB/4./DSOLD(J)/DENOLD(J)
      VRTSQ(J)=TUIN(1-1)/(1.+ATP*TUSC(1-1))
180  CONTINUE
C
C  RECALC. AIR T, PROP & VEL PROFILE
      IF(1.LE.NP1.AND.ANOZ.GT.0.)VAIR(1)=VINI(1)-(AMAV-VELOUT)*FO/G(1)

```

```

00452000
00453000
00454000
00455000
00456000
00457000
00458000
00459000
00460000
00461000
00462000
00463000
00464000
00465000
00466000
00467000
00468000
00469000
00470000
00471000
00472000
00473000
00474000
00475000
00476000
00477000
00478000
00479000
00480000
00481000
00482000
00483000
00484000
00485000
00486000
00487000
00488000
00489000
00490000
00491000
00492000
00493000
00494000
00495000
00496000
00497000
00498000
00499000
00500000
00501000
00502000
00503000
00504000
00505000
00506000
00507000
00508000
00509000
00510000
00511000
00512000
00513000
00514000
00515000
00516000
00517000
00518000
00519000
00520000
00521000
00522000
00523000
00524000
00525000
00526000
00527000
00528000
00529000
00530000
00531000
00532000
00533000
00534000
00535000
00536000
00537000
00538000
00539000
00540000
00541000

```

	IF(G(1).NE.O.)TFALL=(EAV-E(I-1)+EOO)*HRATIO/G(1)	00542000
	T(I)=TINIT(I)-TFALL	00543000
	IF(T(I).LT.TSAVE )T(I)=TSAVE	00544000
	T1=T(I)	00545000
	E(I)=O.	00546000
	AM=O	00547000
C		00548000
C	CALC. EVAPN & MEAN VEL. OF EACH SIZE RANGE <<<<<<<<<<<<<<<<<<<<<<	00549000
	DO 220 J=1,N\$IZE	00550000
	IF(DSOLD(J).GT.O.)GOTO 190	00551000
	\$SIZE(J)=I.	00552000
	A\$SIZE(J) = VAIR(I)	00553000
	GOTO 210	00554000
190	CONTINUE	00555000
C	SOLVE DIFF.EQNS. WITH RUNGE-KUTTA METHOD ++++++	00556000
C	SET UP THE PARAMETERS OF THE D.E.	00557000
C		00558000
	CSS=\$J(J)	00559000
	SQRRT=\$RISQ(\$J)	00560000
	TWB=\$ (\$J)	00561000
	DGRIT=DGR(\$J)	00562000
	DINIT=\$D(\$J)	00563000
	V=\$VAIR(I-\$I)	00564000
	TAIR=\$(I-\$I)	00565000
	CDRESQ=100.	00566000
	IF((I.LE.HP1).AND.(ANOZ.GT.O.))GOTO 200	00567000
	CDRESQ=1.333*\$DEN(\$J)**9.8*\$D(\$J)**3/\$DENS/VISKIN/VISKIN	00568000
	IF(CDRESQ.GT.O.1)GOTO 200	00569000
C FOR SMALL PTCLES IN MAIN ZONE ASSUME COMPLETE ENTRAINMENT		00570000
	V1=\$VAIR(I)	00571000
	V2=\$VAIR(I-1)	00572000
	WAGRAD=(V1**V1-V2**V2)/DX	00573000
	W(\$J)=V2**V2	00574000
200	CONTINUE	00575000
C RUNGE-KUTTA 4-TH ORDER .		00576000
	AK1=DX*\$F1(W(\$J), \$SIZE(\$J))	00577000
	AL1=DX*\$F2(W(\$J), \$SIZE(\$J))	00578000
	IF(COND) AL1=O.	00579000
	V=\$VAIR(I-1)+VAIR(I))/2	00580000
	TAIR=\$(I-1)+(I))/2	00581000
	AK2=DX*\$F1(W(\$J)+AK1/2,\$SIZE(\$J)+AL1/2)	00582000
	AL2=DX*\$F2(W(\$J)+AK1/2,\$SIZE(\$J)+AL1/2)	00583000
	IF(COND) AL2=O.	00584000
	AK3=DX*\$F1(W(\$J)+AK2/2,\$SIZE(\$J)+AL2/2)	00585000
	AL3=DX*\$F2(W(\$J)+AK2/2,\$SIZE(\$J)+AL2/2)	00586000
	IF(COND) AL3=O.	00587000
	V=\$VAIR(I)	00588000
	TAIR=\$(I)	00589000
	AK4=DX*\$F1(W(\$J)+AK3,\$SIZE(\$J)+AL3)	00590000
	AL4=DX*\$F2(W(\$J)+AK3,\$SIZE(\$J)+AL3)	00591000
	IF(COND) AL4=O.	00592000
	W(\$J)=W(\$J)+(AK1+2*AK2+2*AK3+AK4)/6	00593000
	\$SIZE(\$J)\$SIZE(\$J)+(AL1+2*AL2+2*AL3+AL4)/6	00594000
		00595000
		00596000
C	END OF RUNGEKUTTA CALCULATION ++++++	00597000
C		00598000
C IF ITERATION DOESNT CONVERGE SET \$SIZE(J)=O.		00599000
C		00600000
	IF(\$SIZE(\$J).GT.I.\$SIZE(\$J)=I.	00601000
	IF(W(\$J).LE.O.)W(\$J)\$VAIR(I)*VAIR(I)	00602000
	V(\$J)=SQRT(W(\$J))	00603000
	RCP1(\$J)=QRCP1	00604000
	IF(\$SIZE(\$J).LT.ECRIT)D(\$J)=DINIT*(1.-VLIQ*\$SIZE(\$J))*(1./3.)	00605000
	IF(\$SIZE(\$J).GE.ECRIT)D(\$J)=DGR(\$J)	00606000
	EE=\$SIZE(\$J)*WLQ	00607000
C EE=RATIO MASS EVAPORATED/MAS(SOL+LIQ) REMAINING		00608000
	A\$SIZE(J) = V(\$J)*(1.-EE)+VAIR(I)*EE	00609000
210	CONTINUE	00610000
C		00611000
C TOTAL EVAPORATION AND SPRAY MOMENTUM/UNIT MASS FEED		00612000
	E(I)=E(I)+\$SIZE(J)*DVOL(J)	00613000
	A\$=A\$I+A\$SIZE(J)*DVOL(J)	00614000
220	CONTINUE	00615000
C		00616000
C FINISHED CONSIDERING J-TH SIZE RANGE <<<<<<<<<<<<<<<<<<<<<<		00617000
C		00618000
C WEIGHTING FACTORS TO ACCELERATE CONVERGENCE		00619000
	DENOM1=A\$MAX(A\$-A\$OLD-A\$AV	00620000
	IF(DENOM1.NE.O.) A\$AV=(A\$*A\$MAX-A\$AV*A\$OLD)/DENOM1	00621000
	DENOM=E\$AX+E(I)-E(I-1)-EAV	00622000
	IF(DENOM.NE.O.) EAV=(E(I)*E\$AX-EAV*(I-1))/DENOM	00623000
	IF(COND) EAV=E(I)	00624000
C		00625000
C TESTING FOR CONVERGENCE BY CONSIDERING THE CHANGE IN EVAPORN&MOM.		00626000
	DEV=EAV-E(I-1)	00627000
	TEST=E(I)-EAV	00628000
	TEST1=ABS(TEST)	00629000
	IF(DEV.EQ.O.) DEV=1.E-10	00630000
	TEST=TEST1/DEV	00631000

DAM=0.	00632000
IF((ANOZ.GT.0.).AND.(I.LE.NP3))DAM=ABS((AM-AMAV)/AM)	00633000
COND1=(TEST.LE.0.05).OR.(TEST1.LT.1.E-5)	00634000
COND1=COND1.AND.(E(I).LE.EMAX)	00635000
COND1=COND1.AND.(DAM.LE.0.05)	00636000
COND1=COND1.OR.(EMAX.LE.E(I-1))	00637000
IF(COND1)GOTO 250	00638000
C	00639000
C RESET EVAPORATNS & VELOCITIES BEFORE REPEATING THE CALCN.	00640000
IF(ITER.EQ.20) GO TO 240	00641000
DO 230 J=1,NSIZE	00642000
ESIZE(J)=ESOLD(J)	00643000
W(J)=WOLD(J)	00644000
D(J)=DSOLD(J)	00645000
230 CONTINUE	00646000
240 CONTINUE	00647000
C	00648000
C END OF ITERATIONS AT I-TH POINT -----	00649000
C	00650000
PRINT 122,X(I),TEST,E(I),DAM,AM,TSAVE,T(I)	00651000
250 CONTINUE	00652000
IF(E(I).GT.0.9999)GOTO 350	00653000
C	00654000
C CORRECT FOR INFLUENCE OF DROPLET OVERHEAT AS WELL AS SET UPPER	00655000
C LIMIT ON EVAPORATION	00656000
DEI=E(I)-E(I-1)	00657000
E00=E00+DEI	00658000
SET=1.	00659000
IF((E(I).EQ.E(I-1)).OR.(EMAX.EQ.E(I)))GOTO 280	00660000
SEMAX=(EMAX-E(I-1))/(E(I)-E(I-1))	00661000
E(I)=0.	00662000
DO 270 J=1,NSIZE	00663000
SE=1.	00664000
IF(TDR(J).LT.TS(J))GOTO 260	00665000
CALL WBULB(0.,0.,TDR(J),YDR,DUM1,CSDUM,RS,0.,-1)	00666000
IF(YSAT.NE.YAIR)SE=(YDR-YAIR)/(YSAT-YAIR)	00667000
IF(SE.GT.SEMAX)SE=SEMAX	00668000
IF(SE.LT.1.)SE=1.	00669000
DESIZE=ESIZE(J)-ESOLD(J)	00670000
SEMAX1=SEMAX	00671000
IF(DESIZE.GT.0.)SEMAX1=1.+(TDR(J)-TS(J)+1.)*(1.-WLIQ*ESIZE(J))/	00672000
SHCW/DESIZE	00673000
IF(SE.GT.SEMAX1)SE=SEMAX1	00674000
ESIZE(J)=ESOLD(J)+DESIZE*SE	00675000
260 CONTINUE	00676000
IF(ESIZE(J).GT.1.)ESIZE(J)=1.	00677000
IF(ESIZE(J).LT.ECRIT)D(J)=DO(J)*(1.-VLIQ*ESIZE(J))*(1./3.)	00678000
IF(ESIZE(J).GE.ECRIT)D(J)=DCR(J)	00679000
ANUM=1.-WLIQ*ESIZE(J)	00680000
IF((ESIZE(J).LT.ECRIT).AND.(VLIQ*ESIZE(J).NE.1.))	00681000
SDEN(J)=DENSLO*ANUM/(1.-VLIQ*ESIZE(J))	00682000
IF((ESIZE(J).GE.ECRIT).AND.(VLIQ*ECRIT.NE.1.))	00683000
SDEN(J)=DENSLO*ANUM/(1.-VLIQ*ECRIT)	00684000
E(I)=E(I)+ESIZE(J)*DVOL(J)	00685000
IF(T(I).EQ.TS(J))GOTO 270	00686000
IF(WLIQ*ESIZE(J).EQ.1.)GOTO 270	00687000
SEH=(T(I)-TDR(J))/(T(I)-TS(J))	00688000
DTR=HCW/(1.-WLIQ*ESIZE(J))*(SE-SEH)*(ESIZE(J)-ESOLD(J))	00689000
TDR(J)=TDR(J)-DTR	00690000
270 CONTINUE	00691000
SET=(E(I)-E(I-1))/DEI	00692000
280 CONTINUE	00693000
VDROPS=(AM-VAIR(I)*E(I)*WLIQ)/(1.-E(I)*WLIQ)	00694000
RTIME=RTIME+DX/VDROPS	00695000
C CALC. MEAN DIAMETER	00696000
SUM3=0	00697000
SUM2=0	00698000
DRTIME=0.	00699000
DO 290 J=1,NSIZE	00700000
IF(ESIZE(J).GT.0.9999)JEV=J	00701000
DRTI=DX/V(J)	00702000
RTI(J)=RTI(J)+DRTI	00703000
RATE(J)=ESIZE(J)/RTI(J)	00704000
DD=D(J)*D(J)*DH(J)	00705000
DDD=DD*D(J)	00706000
SUM2=SUM2+DD	00707000
SUM3=SUM3+DDD	00708000
290 CONTINUE	00709000
D32(I)=SUM3/SUM2	00710000
C	00711000
C SET UP CONDITIONS FOR NEXT POSITION	00712000
EAV=E(I)	00713000
AMOLD=AM	00714000
AMMAX=AM	00715000
YRISE=0.	00716000
TFALL=0.	00717000
IF(G(I).EQ.0.)GOTO 300	00718000
EVAP=E(I)*FO*WLIQ	00719000
YRISE=EVAP/G(I)	00720000
IF(G(I).NE.0.)TFALL=E00*HRATIO/G(I)	00721000

C		CONTINUE	00722000
		YAIR=YINIT(I)+YRISE	00723000
		T(1)=TINIT(I)-TFALL	00724000
		IF(1.LE.NP1.AND.ANOZ.GT.O.)VAIR(I)=VINI(I)-(AM-VELOUT)*FO/G(I)	00725000
C CALC.		DROPLET MOISTURE,WET BASIS,IN ORDER TO CALC SURF. TEMP.& DENSITY	00726000
		WBO=WB	00727000
		CALL WBULB(T(I),YAIR,WB,YSAT,DER,CS,KO,WBO,I)	00728000
		WBDEP=T(I)-WB	00729000
		DO 310 J=I,NSIZE	00730000
		IF(D(J).LE.O.)GOTO 310	00731000
		AMOIST=(1.-ESIZE(J))*WLIQ	00732000
		AMOIST=AMOIST/(AMOIST+WSQL)	00733000
		FAC=FURVE(AMOIST,D(J),RATE(J),WLIQ)	00734000
		YSURF=YINIT(I)+(YSAT-YINIT(I))*FAC	00735000
		CSJ(J)=YSURF*.189E3+(1.-YSURF)*1.E3	00736000
		TS(J)=T(I)-WBDEP*FAC	00737000
310 C		CONTINUE	00738000
		TSAVE=O	00739000
		ECOMP=1.-E(I)	00740000
		DO 320 J=I,NSIZE	00741000
		TSAVE=TSAVE+TS(J)*(1.-ESIZE(J))*DVOL(J)/ECOMP	00742000
		ESOLD(J)=ESIZE(J)	00743000
		WOLD(J)=W(J)	00744000
		DSOLD(J)=D(J)	00745000
		DEHOLD(J)=DEN(J)	00746000
320 C		CONTINUE	00747000
		IPRINT=MOD(I-1,NPRINT)*(I-NP1)*(I-NPT)	00748000
		FE=1.-E(I)	00749000
		IF(IPRINT.EQ.O)PRINT 192,X(I),T(I),TSAVE,FE,YAIR(I),G(I),D32(I),	00750000
		\$VDROPS,RTIME,YAIR,SET,JEV,ITER	00751000
		IPR1=MOD(I-1,10*NPRINT)	00752000
		IF(IPR1.NE.O)GOTO 330	00753000
		PRINT 132	00754000
		PRINT 142 ,(( TS(J)),J=1,NSIZE)	00755000
		PRINT 152 ,(( TDR(J)),J=1,NSIZE)	00756000
		PRINT 162 ,((1.-ESIZE(J)),J=1,NSIZE)	00757000
		PRINT 172 ,(( V(J)),J=1,NSIZE)	00758000
		PRINT 182 ,(( RTI(J)),J=1,NSIZE)	00759000
330 C		CONTINUE	00760000
		IF(1.EQ.NPT) GO TO 340	00761000
		E(I+1)=E(I)	00762000
		EAV=E(I)	00763000
		AMOLD=AM	00764000
		T(I+1)=TINIT(I+1)	00765000
		IF(G(I+1).NE.O.)T(I+1)=TINIT(I+1)-EOO* HRATIO/G(I+1)	00766000
C FINISHED CALCULATIONS FOR THIS POSITION-		&&&&&&&&&&&&&&&&&&&&&&&&&&&&&&&&	00767000
340 C		CONTINUE	00768000
			00769000
			00770000
			00771000
			00772000
350 C		CONTINUE	00773000
		IF(NP2.EQ.O)PRINT 82	00774000
		IF(NP2.NE.O)PRINT 202	00775000
		PRINT 212	00776000
		CALL PLOT1(E,NPT,O.,DX,O.,1.,5)	00777000
		PRINT 222	00778000
		CALL PLOT1(T,NPT,O.,DX,O.,0.,5)	00779000
		PRINT 232	00780000
		CALL PLOT1(D32,NPT,O.,DX,O.,0.,5)	00781000
		STOP	00782000
2		FORMAT('OXTRANS=',E10.3/' XTRA=',E10.3/' XEND=',E10.3/ \$' DX1=',E10.3/' DX2=',E10.3)	00783000 00784000
12		FORMAT('OANOZ=',E10.3/' HAJ=',E10.3 )	00785000
22		FORMAT('ORJET=',E10.3/' OVO=',E10.3/' GO=',E10.3 / 1' TO=',E10.3/' YO=',E10.3/' FO=',E10.3// 2' WSQL=',E10.3/' DENISOL=',E10.3/' DENLIQ=',E10.3/' HTLAT=',E10.3/ 3' WLCRIT=',E10.3/' CF=',E10.3/' TF=',E10.3/// GEXT=',E10.3/ 4' TEXT=',E10.3/' YEXT=',E10.3/' VEKT=',E10.3/ 5' TLOSS=',E10.3//) 32 FORMAT(' RS=',E10.3 / \$E10.3/// DHY=',E10.3/' EXC=',E10.3/' EMIS=',E10.3/' EMIW=',E10.3/OVERFLOW' \$' TVA=',E10.3/' RADCAL=',E10.3//))	00786000 00787000 00788000 00789000 00790000 00791000 00792000 00793000 00794000
42		FORMAT(' RSL=',E10.3)	00795000
52		FORMAT(' WSOL=',E10.3/' VLIIQ=',E10.3/' ECRII=',E10.3/' DENSLO=', \$E10.3/' COEFF2=',E10.3/' VELOUT=',E10.3/' SHRINK=',E10.3//))	00796000 00797000
62		FORMAT('OWARNING:DTW=',E10.3,'#####') 72 FORMAT('X',9X,'T',9X,'TSAVE FE',8X,'YAIR G',9X,'D32', \$7X,'VDROPS',4X,'RTIME',5X,'YAIR',6X,'SET',7X,'JEV ITER'/)	00798000 00799000 00800000
82		FORMAT('///// END OF JET ZONE ',50('*'))//)	00801000
102		FORMAT(' ISTART OF JET ZONE ',50('*'))//)	00802000
112		FORMAT(' IMAIN ZONE OF DRYER ',50('*'))//)	00803000
122		FORMAT('O##### NO CONVERG.:X,TEST,E,DAM,AM,TSAVE,T=',7E10.3)	00804000
132		FORMAT('O')	00805000
142		FORMAT(13X,'TS(J) = ',14F7.1)	00806000
152		FORMAT(13X,'TDR(J) = ',14F7.1)	00807000
162		FORMAT(13X,'FSIZE = ',14F7.4)	00808000
172		FORMAT(13X,'V(J) = ',14F7.2)	00809000
182		FORIAI(13X,'RTI(J) = ',14F7.2)	00810000
192		FORIAI(1X,11E10.3,215)	00811000

202	FORMAT('///// END OF MAIN ZONE ',50('*')//)	00812000
212	FORMAT('EVAPORATION VS DISTANCE'//)	00813000
222	FORMAT('EFFECTIVE AIR TEMPERATURE VS DISTANCE'//)	00814000
232	FORMAT('ISAUTER MEAN DIAMETER VS DISTANCE'//)	00815000
242	FORMAT('RADIATION PARAMETERS ****/' FCL='E10.3/' SH='E10.3/' CRAD='E10.3//)	00816000
	END	00817000
		00818000
	SUBROUTINE PROFIL(ANOZ)	00819000
C	SUB TO CALC INITIAL TEMP,VEL(AIR),ENTRAINMENT PROFILES	00820000
C	TO CALC ENTRAINMENT USE EQN BY DAVIES-REF G13	00821000
C	FOR ALL OTHERS USE ABRAHOVITCH(REF.WKBK8 P.128)	00822000
	COMMON/INIT/VINI(1001),YINI(1001),G(1001),TINIT(1001),X(1001),	00823000
	\$RJET,VO,GO,TO,YO,FO,VEXT,GEXT,TEXT,YEXT,NP1,NP2,NPT,NP3	00824000
	\$,TUIN(1001),TUSC(1001),TUINO,TUINI,TUSCO,TUSCI,TLOSS,DENSF,HAJ	00825000
	IF(NP1.EQ.1)RETURN	00826000
	HAJ=HAJ*.01745	00827000
	HR=TAN(HAJ)/TAN(.2164)	00828000
	IF(HR.EQ.0.)HR=1.	00829000
	IF(ANOZ.GT.0.)GOTO 60	00830000
		00831000
C	PROFILE FOR PRESSURE NOZZLE	00832000
	RJ2=RJET*RJET	00833000
	VDIF=(VO-VEXT)/HR	00834000
	VEQ=0.45*VDIF	00835000
	DTEQ=(TO-TEXT)/HR*.75	00836000
	DYEQ=(YO-YEXT)/HR*.75	00837000
	RHOG=1.293*273./TEXT	00838000
	AJ=DENSF/RHOG	00839000
	AJ1=SQRT(AJ)	00840000
	XO=RJET*(10.7*(1.73*AJ1-1.)-13.6*AJ1)	00841000
	BB=3.14159*2.*RJ2*RHOG*VEXT	00842000
	GCOEF=1.82*VDIF*RJ2*AJ*RHOG	00843000
	DO 70 I=1,NP3	00844000
	G(I)=0.	00845000
	VINI(I)=VO	00846000
	TINIT(I)=TO	00847000
	YINI(I)=YO	00848000
	IF(X(I).LE.XO)GOTO 70	00849000
	RS=RADJET(X(I),RJET,RHOG,DENSF)	00850000
	RRS=RS*RS	00851000
	AA=SQRT(1.+1.5*RRS/AJ)-1.	00852000
	G(I)=GCOEF*AA+BB*RRS	00853000
	G(I)=G(I)*HR	00854000
	IF(G(I).GT.GEXT)G(I)=GEXT	00855000
	RATIO=2.25*AJ/RRS*AA	00856000
	RATIO1=RATIO*0.73	00857000
	VINI(I)=VEQ*RATIO+VEXT	00858000
	TINIT(I)=DTEQ*RATIO1+TEXT	00859000
	YINI(I)=DYEQ*RATIO1+YEXT	00860000
70	CONTINUE	00861000
	GOTO 80	00862000
60	CONTINUE	00863000
C		00864000
C	PROFILE FOR PNEUMATIC NOZZLE	00865000
	AJ=1.+FO/GO	00866000
	AS=FO/(GO+FO)	00867000
	VEQ=.563*(VO-VEXT)/HR	00868000
	DTEQ=(TO-TEXT)/HR*.75	00869000
	DYEQ=(YO-YEXT)/HR*.75	00870000
	G(I)=GO	00871000
	TINIT(I)=TO	00872000
	VINI(I)=VEQ	00873000
	YINI(I)=YO	00874000
	DO 10 I=2,NP3	00875000
	G(I)=GO*(.115*X(I)/RJET-1.)	00876000
	G(I)=G(I)*HR	00877000
	IF(G(I).LE.GO)G(I)=GO	00878000
	IF(G(I).GT.GO+GEXT) G(I)=GO+GEXT	00879000
	VINI(I)=VEQ*12.4/(X(I)/RJET+12.4)+VEXT	00880000
	RATIO=0.73*(VINI(I)-VEXT)/VEQ	00881000
	DT=DTEQ*RATIO	00882000
	TINIT(I)=TEXT+DT	00883000
	DY=DYEQ*RATIO	00884000
	YINI(I)=YEXT+DY	00885000
10	CONTINUE	00886000
80	CONTINUE	00887000
	IF(NP1.EQ.NP3)GOTO 50	00888000
C	SET UP PROFILES FOR TRANSITION ZONE	00889000
	NDEL=NP1-NP3	00890000
	GGRAD=(G(NP1+1)-G(NP3))/NDEL	00891000
	VGRAD=(VINI(NP1+1)-VINI(NP3))/NDEL	00892000
	TGRAD=(TINIT(NP1+1)-TINIT(NP3))/NDEL	00893000
	YGRAD=(YINI(NP1+1)-YINI(NP3))/NDEL	00894000
	DO 30 I=NP3+1,NP1	00895000
	G(I)=G(I-1)+GGRAD	00896000
	VINI(I)=VINI(I-1)+VGRAD	00897000
	TINIT(I)=TINIT(I-1)+TGRAD	00898000
	YINI(I)=YINI(I-1)+YGRAD	00899000
30	CONTINUE	00900000
50	CONTINUE	00901000

	PRINT 12	00902000
12	FORMAT('OINITIAL PROFILES OF AIR STREAMS'/' X',2X,'TUIN',6X,	00903000
	\$ 'TUSC TINIT YINIT VINI G'/)	00904000
	DO 100 I=1,NPT,5	00905000
100	PRINT 2,X(I),TUIN(I),TUSC(I),TINIT(I),YINIT(I),VINI(I),G(I)	00906000
2	FORMAT(1X,9E10.3)	00907000
	END	00908000

	SUBROUTINE PROF11	00909000
	COMMON/INIT/VINI(1001),YINIT(1001),G(1001),TINIT(1001),X(1001),	00910000
	\$RJET,VO,GO,TO,YO,FO,VEXT,GEXT,TEXT,YEXT,NP1,NP2,NPT,NP3	00911000
	\$,TUIN(1001),TUSC(1001),TUINO,TUINI,TUSCO,TUSCI,TLOSS,DENSF,HAJ	00912000
	IF(NP2.EQ.0)RETURN	00913000
	GAM=GO+GEXT	00914000
	YAM=(YO*GO+YEXT*GEXT)/GAM	00915000
	TAM=(TO*GO+TEXT*GEXT)/GAM	00916000
	VAM=VEXT*GAM/GEXT	00917000
	TU=TUINO*TUINI*TUSCO*TUSCI	00918000
	IF(TU.EQ.0.)GOTO 20	00919000
	BI=1./TUINO	00920000
	AI=(1./TUINI-BI)/X(NPT)	00921000
	AS=(TUSCI-TUSCO)/X(NPT)	00922000
	BS=TUSCO	00923000
20	CONTINUE	00924000
	DO 10 I=1,NPT	00925000
	G(I)=GAM	00926000
	YINIT(I)=YAM	00927000
	TINIT(I)=TAM-TLOSS*X(I)	00928000
	VINI(I)=VAM*TINIT(I)/TEXT	00929000
	IF(TU.EQ.0.)GOTO 10	00930000
	TUIN(I)=1./(AI*X(I)+BI)	00931000
	TUSC(I)=AS*X(I)+BS	00932000
10	CONTINUE	00933000
	RETURN	00934000
	END	00935000

	FUNCTION F1(W,E)	00936000
	C DERIVATIVE OF DROPLET VELOCITY SQUARED WRT DISTANCE	00937000
	COMMON /VELEP/ DENSLO,WSOL,WLIQ,VLIQ,COEFF2,HTLAT,DENLIQ,ECRIT,	00938000
	\$DCRIT,TAIR,VAIR,DENS,VISKIN,THCOND,TWB,DENSL,DO,D,RE,V,CORESQ,	00939000
	\$WAGRAD,SQVRT,CRAD,RADIOS,QRCPI,CSS	00940000
	F1=WAGRAD	00941000
	IF(E.GT.1.)E=1.	00942000
	IF(VLIQ*E.GE.1.)RETURN	00943000
	C CALC. DIAMETER AND DENSITY	00944000
	IF(E.LT.ECRIT)GOTO 20	00945000
	D=DCRIT	00946000
	DENSL=DENSLO*(1.-WLIQ*E)/(1.-VLIQ*ECRIT)	00947000
	GOTO 30	00948000
20	D=DO*(1.-VLIQ*E)**(1./3.)	00949000
	DENSL=DENSLO*(1.-WLIQ*E)/(1.-VLIQ*E)	00950000
30	CONTINUE	00951000
	IF(D.LE.0.)RETURN	00952000
	C CALC. F1	00953000
	IF(W.LE.0)W=1.E-8	00954000
	V=SQRT(W)	00955000
	VREL=V-VAIR	00956000
	VRELAB=SQRT(VREL*VREL+SQVRT)	00957000
	RE=D*VRELAB/VISKIN	00958000
	CD=DRAG(RE)	00959000
	IF(CORESQ.GT.0.1)F1=-1.5*CD*DENS/D/DENSL*VREL*VRELAB*2*9.8	00960000
	RETURN	00961000
	END	00962000



```

FUNCTION F2(W,E)
C DERIVATIVE OF FRACTIONAL EVAPORATION WRT DISTANCE
COMMON /VELEP/ DENSLO,WSOL,WLIQ,VLIQ,COEFF2,HTLAT,DENLQ,ECRIT,
$OCRIT,TAIR,VAIR,DENS,VISKIN,THCOND,TWB,DENSL,DO,D,RE,V,CORESQ,
$WAGRAD,SQVRT,CRAD,RADIOS,QRCPI,CSS
C RE,D,V&DENSL HAVE BEEN CALCD BY F1 WHICH IS ALWAYS CALLED BEFORE F2
F2=0.
IF(E.GE.1.)RETURN
B=CSS*(TAIR-TWB)/HTLAT
A=1./(1.+B)
QC=(2.+53*SQRT(RE))*THCOND*(TAIR-TWB)/D*A
QR=CRAD*(RADIOS-TWB*.4)
QRCPI=1.
IF(QC,NE.0.)QRCPI=1.+QR/QC
IF(QC+QR,LE.0.)RETURN
F2=COEFF2*(QC+QR)*D*D/V/DO/DO/DO
RETURN
END

```

00963000  
00964000  
00965000  
00966000  
00967000  
00968000  
00969000  
00970000  
00971000  
00972000  
00973000  
00974000  
00975000  
00976000  
00977000  
00978000  
00979000  
00980000

```

FUNCTION DRAG(RE)
C APPROXIMATE TO STD DRAG CURVE, COMBINING EQNS BY SCHILLER&NAUMANN,
C BEARD&PRUPPACHER, CLIFF&GAUVIN-CORRECT TO 3PC.
IF(RE,EQ.0)RETURN
C=24./RE
DRAG=C
IF(RE,GT.0.4,AND,RE,LE.2.)DRAG=C*(1.+1*RE)
IF(RE,GT.2.)DRAG=C*(1.+15*RE*.687)+.42/(1.+4.25E4/RE**1.16)
RETURN
END

```

00981000  
00982000  
00983000  
00984000  
00985000  
00986000  
00987000  
00988000  
00989000  
00990000

```

SUBROUTINE PLOT1(Y,N,XO,DX,YMIN,YMAX,NSPACE)
C PLOT A POINT EVERY NSPACE VALUES
C DX*NSPACE=X-INCREMENTS BW PLOTTED POINTS
C Y=ARRAY TO BE PLOTTED
C XO=INITIAL X-VALUE
C IF YMIN & YMAX ARE UNKNOWN, SUPPLY THEM AS EQUAL NOS.
C N=NO. OF POINTS PLOTTED
DIMENSION Y(N)
IF(YMAX,GE,YMIN)GOTO 35
AA=YMIN
YMIN=YMAX
YMAX=AA
35 CONTINUE
IF((YMAX-YMIN),NE.0.)GO TO 70
YMAX=-1.E30
YMIN=+1.E30
DO 10 I=1,N
IF(Y(I),GT,YMAX)YMAX=Y(I)
10 IF(Y(I),LT,YMIN)YMIN=Y(I)
70 CONTINUE
REAL LINE(101),MINUS
DATA BLANK,PLUS,MINUS,BAR,PLT/1H,1H+,1H-,1H*,1H*/
X=XO
DO 2 I=1,101
LINE(I)=MINUS
2 IF(MOD(I-1,10),EQ.0) LINE(I)=PLUS
WRITE(6,3) YMIN,YMAX
3 FORMAT(15X,E15.5,80X,E15.5)
DY=(YMAX-YMIN)/100.
ITER=1
100 YY=Y(ITER)
IY=IFIX((YY-YMIN)/DY+0.5) + 1
IF(IY,LT,1,OR,IY,GT,101) GO TO 4
LINE(IY)=PLT
4 WRITE(6,5)LINE
5 FORMAT('+' /20X,101A1)
IF(MOD(LINES,10),EQ.0)WRITE(6,8)X
8 FORMAT('+' ,3X,E15.5)
LINES=LINES+1
IF(MOD(LINES,10),EQ.0) GO TO 9
DO 6 I=1,101
LINE(I)=BLANK
6 IF(MOD(I-1,10),EQ.0) LINE(I)=BAR
7 X=X+DX*NSPACE
ITER=ITER+NSPACE
IF(ITER,GT,N) RETURN
GO TO 100
9 DO 310 I=1,101
LINE(I)=MINUS
310 IF(MOD(I-1,10),EQ.0) LINE(I)=PLUS
GO TO 7
END

```

00991000  
00992000  
00993000  
00994000  
00995000  
00996000  
00997000  
00998000  
00999000  
01000000  
01001000  
01002000  
01003000  
01004000  
01005000  
01006000  
01007000  
01008000  
01009000  
01010000  
01011000  
01012000  
01013000  
01014000  
01015000  
01016000  
01017000  
01018000  
01019000  
01020000  
01021000  
01022000  
01023000  
01024000  
01025000  
01026000  
01027000  
01028000  
01029000  
01030000  
01031000  
01032000  
01033000  
01034000  
01035000  
01036000  
01037000  
01038000  
01039000  
01040000  
01041000  
01042000

```

SUBROUTINE SPRAY(D,DN,NSIZE)
DIMENSION D(20),DN(20)
C SUB TO READ SPRAY SIZE DISTN INTO MAIN PROG
C N-T DISTRIBUTION,DELTA=0.5
1 READ(5,1)NSIZE,DVS
FORMAT(12,8X,F10.0)
DDIA=DVS*2.5/NSIZE/0.94
C FACTOR 0.94 IS USED TO CORRECT FOR DIFFERENCE BW ANALYTICAL VALUE
C AND NUMERICALLY CALCD VALUE OF DVS
DO 20 I=1,NSIZE
20 D(I)=1*DDIA
B=SQRT(GAMMA(12.)/GAMMA(10.)/(DVS/0.94))
DO 10 I=1,NSIZE
X=D(I)
DN(I)=1.E15*X*X*EXP(-B*SQRT(X))
10 CONTINUE
PRINT 2
2 FORMAT('0SUBR. SPRAY RESULTS','ODIA NUMBER'/)
PRINT 22,((D(I),DN(I)),I=1,NSIZE)
22 FORMAT(1X,2E10.3)
PRINT 32,DVS
32 FORMAT(' D32=',E10.3//)
RETURN
END

```

```

01043000
01044000
01045000
01046000
01047000
01048000
01049000
01050000
01051000
01052000
01053000
01054000
01055000
01056000
01057000
01058000
01059000
01060000
01061000
01062000
01063000
01064000
01065000
01066000

```

```

FUNCTION FCURVE(AMOIST,D,RATE,AMOISO)
C RELATIVE DRYING RATE(AS COMPARED WITH DROPLET OF LIQUID)
C AMOIST=MOISTURE CONTENT WET BASIS
C D=DROPLET DIAMETER
C RATE=MEAN EVAPORATION RATE(DE/DT) UP TO THIS POINT
FCURVE=1.
AMOCR=AMOISO
XCR=AMOCR/(1.-AMOCR)
IF(AMOIST.GE.AMOCR)RETURN
X=AMOIST/(1.-AMOIST)
FCURVE=X/XCR
RETURN
END

```

```

01067000
01068000
01069000
01070000
01071000
01072000
01073000
01074000
01075000
01076000
01077000
01078000
01079000

```

```

SUBROUTINE WBULB(TA,YA,TS,YS,DER,CS,RS,TSO,INDEX)
C IF(INDEX.GT.0) SUBROUTINE CALC. ADIABATIC SATURATION TEMP. & HUMIDITY
C TS,YS FROM AIR CONDITIONS TA,YA
C IF(INDEX.LT.0) SUBROUTINE CALC SATURATION HUMIDITY YS FROM TS
C SUBR. ALSO RETURNS DER(DERIV. OF SATURATH CURVE)&CS(SATED AIR SP.HT)
C SATURATION CURVE GIVEN BY CURVE-FITTED RIEDEL-MILLER-PLANK EQN
C LOG(P)=A/TS+B+C*TS+D**2, TS=300-380K,P IN ATM
C CW=WATER VAPOUR SPEC. HT
C CA=AIR SPEC. HT
C HT=LATENT HT OF EVAPORATION
C RS=RELATIVE HUMIDITY OF AIR IN EQM WITH AQUOUS SOLUTION
C TSO=1ST ESTIMATE OF ADIABATIC SATURATION TEMP. OF SOLUTION
C
COMMON/WETBUL/A,B,C,D,D2,CA,CW,HT,ICNT
ICNT=ICNT+1
IF(ICNT.GT.1)GOTO 30
A=-.63488E4
B=22.536
C=-.019639
D=.13010E-4
D2=D*2.
CA=1.015E3
CW=1.89E3
HT=2.46E6
30 CONTINUE
IF(TSO.LT.273.)TSO=350.
IF(INDEX.GT.0)TS=TSO
DO 10 I=1,20
10
C CALC. SATURATION HUMIDITY

```

```

01080000
01081000
01082000
01083000
01084000
01085000
01086000
01087000
01088000
01089000
01090000
01091000
01092000
01093000
01094000
01095000
01096000
01097000
01098000
01099000
01100000
01101000
01102000
01103000
01104000
01105000
01106000
01107000
01108000
01109000

```

C	P=A/TS+B+(C+D*TS)*TS	01110000
	P=EXP(P)	01111000
	P=P*RS	01112000
	IF(P,LT,1.)GOTO 40	01113000
	DO 50 ITER=1,30	01114000
	TS=TS-5	01115000
	P=A/TS+B+(C+D*TS)*TS	01116000
	P=EXP(P)	01117000
	P=P*RS	01118000
	IF(P,LT,1.)GOTO 40	01119000
50	CONTINUE	01120000
40	CONTINUE	01121000
	YS=.622*P/(1.-P)	01122000
C	CALC. DERIVATIVE OF YS VS TS USING CHAIN RULE	01123000
C	DER=-A/TS/TS+C+D2*TS	01124000
	DER=DER*P	01125000
	DER=0.622 /((1.-P)/((1.-P)*DER	01126000
C	CALC THE ADIABATIC-SATURATION SLOPE	01127000
	CS=YS*CW+(1.-YS)*CA	01128000
	IF(INDEX,LT,0)RETURN	01129000
	SL=HT/CS	01130000
C	CALC. NEW APPROXIMATION	01131000
C	DTS=-(SL*(YS-YA)+(TS-TA))/(SL*DER+1.)	01132000
	TS=TS +DTS	01133000
	IF(TS,GT,500.)TS=500.	01134000
	IF(ABS(DTS).LE,0.02)RETURN	01135000
10	CONTINUE	01136000
	PRINT 2,TSO,TS	01137000
2	FORMAT(1 WARNING***SUB.WBULB DOESNT CONVERGE. TSO,TS=' ,2E10.3)	01138000
	RETURN	01139000
	END	01140000
		01141000
		01142000
		01143000

	FUNCTION RADJET(X,RO,RHOG,RHOL)	01144000
C	DIMLESS RAD. OF GAS JET INDUCED BY PRESSURE NOZZLE,R/RO	01145000
C	X=DIST. FROM ORIFICE	01146000
C	RHOG,RHOL=DENSITIES	01147000
C	AJ=RHOL/RHOG	01148000
C	XO=POSITION OF POLE	01149000
C	SUBSCRIPTS=DIMLESS	01150000
C	ST.SEGMENT APPROX. TO ABRAMOVITCH EQN. 12.318-ALSO WKBK 8P.174	01151000
C	XS=X/RO	01152000
	COMMON/RADJ/RS(501),XIS(501),XOS,ICALL	01153000
	ICALL=ICALL+1	01154000
	IF(ICALL,GT,1) GO TO 20	01155000
	AJ=RHOL/RHOG	01156000
	AJ1=SQRT(AJ)	01157000
	XOS=10.7*(1.73*AJ1-1.)-13.6*AJ1	01158000
	DLNR=(ALOG(1000.)-ALOG(3.))/500	01159000
	DO 10 I=1,501	01160000
	RS(I)=3.*EXP((I-1)*DLNR)	01161000
	AA=RS(I)/AJ1	01162000
	AB=AA*AA	01163000
	AC=SQRT(1.+1.48*AB)	01164000
	AD=RS(I)+AJ1*(ALOG(1.22*AA+AC)-0.25*ATAN	01165000
	\$ (1.28*AA*(AC-0.24)/(AC+0.31*AB)))	01166000
	XIS(I)=AD/0.22+XOS	01167000
10	CONTINUE	01168000
20	CONTINUE	01169000
	IF(XS,GT,XOS) GO TO 80	01170000
	RADJET=0.	01171000
	RETURN	01172000
80	CONTINUE	01173000
	IF(XS,GE,XIS(1)) GO TO 30	01174000
	RADJET=3*(XS-XOS)/(XIS(1)-XOS)	01175000
	RETURN	01176000
30	CONTINUE	01177000
	IF(XS,LE,XIS(501)) GO TO 40	01178000
	RADJET=0.22*(XS-XOS)	01179000
	RETURN	01180000
40	CONTINUE	01181000
	DO 50 I=1,501	01182000
	IF(XS,GT,XIS(I)) GO TO 60	01183000
50	CONTINUE	01184000
60	CONTINUE	01185000
	I=I+1	01186000
	D1=XIS(I)-XS	01187000
	D2=XS-XIS(I-1)	01188000
	RADJET=(RS(I)*D2+RS(I-1)*D1)/(D1+D2)	01189000
	RETURN	01190000
	END	01191000